

Intercellular Communication at the Neurovascular Unit:

The Effect of Astrocyte Secreted Factors on the Blood-Brain Barrier

A dissertation submitted for the degree of PhD by

Natalija Aleksejenko, B.A.

August 2026

Under the supervision of Dr. Janosch Heller, Prof. Phil Cummins and Dr. Keith Rochfort

School of Biotechnology,
Dublin City University,
Dublin 9,
Ireland

Declaration

I hereby certify that this material, which I now submit for assessment on the programme of study leading to the award of Doctor of Philosophy is entirely my own work, and that I have exercised reasonable care to ensure that the work is original and have conformed to the regulations on the use and declaration of Generative AI, and does not to the best of my knowledge breach any law of copyright, and has not been taken from the work of others save and to the extent that such work has been cited and acknowledged within the text of my work. I hereby certify that no Generative Artificial Intelligence (Gen AI) tools have been used in the creation of the thesis.

Signed: Natalija Aleksejenko

ID No.: 21262337

Date: 12/08/2026

Acknowledgements

First and foremost, I would like to thank my supervisors Dr. Janosch Heller, Prof. Phil Cummins, and Dr. Keith Rochfort, who provided me with this opportunity and without which this work would not have been possible. Your guidance and support has carried me throughout all the stages of writing this thesis. My deepest gratitude to all of you for your invaluable insights and advice during the last few years (and for providing a shoulder to cry on when things got tough). I wish your groups the best of luck in the future.

I would also like to extend my gratitude to Dr. Denise Harold for her part in the analysis of the raw sequencing files from Macrogen in Chapter 6 and additionally for her patience in guiding me through transcriptomic analysis.

Huge thanks to the members of the groups I was lucky enough to be part of: Toby and Niamh. Thank you for coming on coffee breaks with me when I thought I was going to lose my mind. It has been an absolute pleasure hearing about your topics, and I can only imagine your futures will be as bright as you are.

Thank you to my friends, both old and those I made at DCU. Your support has always meant the most to me. Thank you for letting me complain about the (literal) blood, sweat, and tears that have gone into this project and the times I didn't want to discuss it at all.

Last but not least, I want to thank my family for their endless support. Thank you for trying to understand what I was doing and encouraging me even when you didn't have a clue.

Table of Contents

Abbreviations VII
List of Figures X
List of Tables XII
Publications XIII
Abstract XIV
Chapter 1 : Introduction *15*
1.1 The Cerebrovasculature 16
1.1.1 The BBB 17
1.1.2 The Neurovascular Unit 25
1.2 Neuroinflammation 37
1.2.1 BBB breakdown 38
1.2.2 Microglia and Astrocytes in Neuroinflammation 38
1.3 EVs 39
1.3.1 History of EV Research 40
1.3.2 EV Subtypes 43
1.3.3 EV Nomenclature 49
1.3.4 EV Uptake 50
1.4 Astrocyte EVs in the brain 54
1.4.1 Physiological Roles 54
1.4.2 During neuroinflammation 55
1.5 Thesis Aims 57
Chapter 2 : Materials and Methods *60*
2.1 Materials 61
2.1.1 Reagents and Chemicals 61
2.1.2 Reagents and Chemicals used by Macrogen (South Korea) 64
2.1.3 Apparatus 64
2.1.4 Apparatus used by Macrogen (South Korea) 65
2.1.5 Preparations of stock buffer solutions 66
2.2 Methods 68
2.2.1 Culture and Maintenance of Primary Cells 68
2.2.2 Extracellular Vesicle Isolation 71
2.2.3 Cell Treatments 73
2.2.4 Cell Assays 76
2.2.5 RNA Isolation and Quantitative Polymerase Chain Reaction (qPCR) 79
2.2.6 Protein Isolation and Western Blotting 85
2.2.7 Transcriptomic Analysis 90

2.2.8 Statistical Analysis 91
Chapter 3:The Effect of Conditioned Media on HBMvEC Barrier Properties 93
3.1 Introduction 94
3.1.1 Chapter Aims 96
3.2 Results 98
3.2.1 Cell Characterisation 98
3.2.2 Effect of ACM on Endothelial Cell Barrier Properties 101
3.3 Discussion 114
Chapter 4 :Verification and Quantification of EV Isolation Methods 120
4.1 Introduction 121
4.1.1 Chapter Aims 124
4.2 Results 125
4.2.1 Comparison of EV methods 125
4.2.2 Verification of the ExtraPEG method 133
4.2.3 Optimisation of EV Yield using ExtraPEG isolation 137
4.3 Discussion 143
Chapter 5 :The Effect of Astrocyte-Derived EVs on HBMvEC Barrier Properties 150
5.1 Introduction 151
5.1.1 Chapter Aims 152
5.2 Results 153
5.2.1 Astrocyte-derived EVs affect HBMvEC permeability in a treatment orientation- and time- dependent manner 153
5.2.2 Astrocyte EVs decrease permeability of HBMvECs but do not affect tight junction expression levels 156
5.2.3 Astrocytes are inflamed by a cytokine cocktail but not LPS. 160
5.2.4 EVs derived from inflamed astrocytes increase permeability of HBMvECs. 165
5.3 Discussion 168
Chapter 6 :Transcriptomic Analysis of Astrocyte-Derived EV Treated HBMvECs 175
6.1 Introduction 176
6.1.1 Chapter Aims 177
6.2 Results 178
6.2.1 Primary human astrocyte-derived EVs do not seem to contain miRNA, likely due to negligible amounts of miRNA in their donor cells. 179
6.2.2 Astrocyte-derived EVs modify the transcriptome of HBMvECs 182
6.3 Discussion 194

Chapter 7 : Overall Discussion and Future Directions *199*
7.1 Overall Summary 200
7.2 Future Directions 201
Bibliography *205*
Appendix *301*

Abbreviations

AB	Apoptotic Body
ACM	Astrocyte Conditioned Media
AD	Alzheimer's Disease
AJ	Adherens Junction
ALIX	Alg-2-Interacting Protein X
AM	Astrocyte Media
ANG-1	Angiopoetin-1
ANOVA	Analysis Of Variance
APLN	Apelin
APS	Ammonium Persulfate
AQP4	Aquaporin 4
Aβ	B-Amyloid
BBB	Blood-Brain Barrier
BM	Basement Membrane
BSA	Bovine Serum Albumin
CBF	Cerebral Blood Flow
CCL2	C-C Motif Chemokine Ligand 2
CLCF1	Cardiotrophin-like Cytokine Factor 1
CLDN5	Claudin-5
CLEC14A	C-Type Lectin Domain Containing 14A
CNS	Central Nervous System
COL5A1	Collagen Type V Alpha 1
CSF	Cerebrospinal Fluid
Cx43	Connexin 43
DC	Differential Centrifugation
DEG	Differentially Expressed Gene
DEPC	Diethyl Pyrocarbonate
DGKZ	Diacylglycerol Kinase Zeta
DLS	Dynamic Light Scattering
EAE	Experimental Autoimmune Encephalitis
ECM	Endothelial Conditioned Media
EDTA	Ethylenediaminetetraacetic Acid
EHD2	EH Domain Containing 2
EM	Endothelial Media
EMT	Epithelial-Mesenchymal Transition
EndoMT	Endothelial-Mesenchymal Transition
ESCRT	Endosomal Sorting Complex Required For Transport
EV	Extracellular Vesicle
ExM	Extracellular Matrix
FBS	Foetal Bovine Serum
FGF-F	Fibroblast Growth Factor-2
FITC	Fluorescein Isothiocyanate
FZD8	Frizzled Class Receptor 8
GAPDH	Glyceraldehyde-3-Phosphate Dehydrogenase
GFAP	Glial Fibrillary Acidic Protein
HBMvECs	Human Brain Microvascular Endothelial Cells

HNSCC	Head And Neck Squamous-Cell Carcinoma Cells
HRP	Horseradish Peroxidase
Hsp70	Heat Shock Protein 70
HSPB1	Heat Shock Protein Family B 1
HUVEC	Human Umbilical Endothelial Cells
ICAM1	Intercellular Adhesion Molecule 1
ICH	Intracerebral Haemorrhage
IL1β	Interleukin-1 Beta
IL10	Interleukin-10
IL32	Interleukin-32
IL6	Interleukin-6
IL6ST	Interleukin 6 Cytokine Family Signal Transducer
ILV	Intraluminal Vesicle
ISEV	International Society of Extracellular Vesicles
ISF	Interstitial Fluid
ITGAV	Integrin Subunit Alpha V
JAK3	Janus Kinase 3
JAM	Junctional Adhesion Molecule
Kir4.1	Inwardly Rectifying Potassium Channel 4.1
LAMP1	Lysosomal-Associated Membrane Protein 1
lEV	Large Extracellular Vesicle
LIPG	Lipase G, Endothelial Type
LMNA	Lamin A/C
lncRNA	Long non-coding RNA
LPS	Lipopolysaccharide
MAN2A2	Mannosidase Alpha Class 2a Member 2
MAGuK	Membrane Associated Guanylate Kinase
MDCK	Madin-Darby Canine Kidney
MGP	Matrix Gla Protein
miRNA	Micro RNA
mOMECs	Monkey Ovarian Microvascular Endothelial Cells
MPS	Mononuclear Phagocyte System
mRNA	Messenger RNA
MS	Multiple Sclerosis
MV	Microvesicle
MVB	Multivesicular Body
MYRIP	Myosin Viia And Rab Interacting Protein
NBEAL2	Neurobeachin Like 2
NMDAR	N-methyl-D-aspartate receptor
NFKBIA	NF-κB Inhibitor Alpha
NK	Natural Killer
NTA	Nanoparticle Tracking Analysis
NTSR1	Neurotensin Receptor 1
NVEP	Non-Vesicular Extracellular Particles
NVU	Neurovascular Unit
OCLN	Occludin
OPC	Oligodendrocyte Precursor Cell
PBS	Phosphate Buffered Saline

PBS-T	Phosphate Buffered Saline- Tween
PC	Principal Component
PCA	Principal Component Analysis
PCR	Polymerase Chain Reaction
PDGF-B	Platelet Derived Growth Factor- B
PDZ	Postsynaptic Density 95/Disc-Large/Zona Occludens
PEG	Polyethylene Glycol
PFA	Paraformaldehyde
PKC	Protein Kinase C
POLR2J4	RNA Polymerase II Subunit J4
PTMS	Parathymosin
PVDF	Polyvinylidene Difluoride
RASA4CP	RAS p21 Protein Activator 4c
RIN	RNA Integrity Number
RIPA	Radioimmunoprecipitation Assay
RN7SL3	RNA Component Of Signal Recognition Particle 7SL3
ROS	Reactive Oxygen Species
SCARA3	Scavenger Receptor Class A Member 3
scRNAseq	Single Cell RNA Sequencing
SD	Standard Deviation
SDS	Sodium Dodecyl Sulfate
sEV	Small Extracellular Vesicle
SH3	Src Homology
Shh	Sonic Hedgehog
SNED1	Sushi, Nidogen And Egf Like Domains 1
snRNA	Small nuclear RNA
SOD2	Superoxide Dismutase 2
SSB	Sample Solubilisation Buffer
TAE	Tris-Acetate EDTA
TBI	Traumatic Brain Injury
TCIRG1	T-Cell Immune Regulator 1
TEMED	N,N,N’,N’-Tetramethylethylenediamine
TIMP2	Tissue Inhibitor of Metalloproteinases 2
TJ	Tight Junction
TNFAIP3	TNFα Induced Protein 3
TNFSF10	Tumour Necrosis Factor Superfamily Member 10
TNFα	Tumor Necrosis Factor Alpha
TSG101	Tumour Susceptibility Gene 101
VEGF	Vascular Endothelial Growth Factor
Vps	Vacuolar Protein Sorting
vWF	von Willebrand Factor
ZNF17	Zinc Finger Protein 17
ZNF587	Zinc Finger Protein 587
ZO	Zonula Occludens

List of Figures

Figure 1.1 An illustration of the anatomical and cellular structure of the blood-brain barrier. 17
Figure 1.2 Systemic trypan blue injections. 18
Figure 1.3 A schematic representation of the main tight junction and adherens junction proteins between two endothelial cells 19
Figure 1.4 An illustration of the structural and cellular components of the neurovascular unit 26
Figure 1.5 Schematic representation of the cargo of Extracellular Vesicles. 40
Figure 1.6 The first electron microscopy image of extracellular vesicle release. 42
Figure 1.7 Diagram illustrating different EV subtypes, their sizes, distinct cellular origins, and biogenesis pathways. 43
Figure 1.8 Mechanisms of EV uptake in the cell.. 52
Figure 1.9 A schematic representation of the overall hypothesis of this thesis. 58
Figure 2.1 A summary diagram for the preparation of conditioned media for treatment of cells. 74
Figure 2.2 Trans-Endothelial Permeability Assay.. 79
Figure 3.1 Cell characterization of astrocytes. 99
Figure 3.2 Cell characterization of HBMvECs. 100
Figure 3.3 Endothelial cell viability after incubation with EM (purple) or ECM (pink) 102
Figure 3.4 Endothelial cell viability after incubation with AM (gold) or ACM (green).104
Figure 3.5 Endothelial cell viability after basolateral incubation with astrocyte conditioned media 106
Figure 3.6 Permeability of HBMvECs after incubation with diluted astrocyte (conditioned) media. 108
Figure 3.7 TJ gene expression after incubation with diluted ACM. 110
Figure 3.8 Claudin-5 protein expression analysis in response to ACM 111
Figure 3.9 Occludin protein expression analysis in response to ACM 112
Figure 3.10 ZO-1 protein expression analysis in response to ACM 113
Figure 4.1 Flowchart summarising the Microvesicle Isolation method. 126
Figure 4.2 Flowchart summarising the Differential Centrifugation Isolation 127
Figure 4.3 Flowchart summarising the ExtraPEG Isolation method. 128
Figure 4.4 Comparison of MV, DC, and ExtraPEG methods to isolate ACM derived EVs (RNA) 129
Figure 4.5 DLS Analysis of the Average Size Distribution by Intensity of EVs isolated from ACM 130
Figure 4.6 Comparison of MV, DC, and ExtraPEG methods to isolate ECM derived EVs (RNA). 131
Figure 4.7 DLS Analysis of the Average Size Distribution by Intensity of EVs isolated from ECM 132
Figure 4.8 Verification of the ExtraPEG isolation method through western blot analysis of EV markers 135
Figure 4.9 Comparison of EV protein concentration isolated from unwashed and washed EV pellets 138
Figure 4.10 Comparison of EV RNA concentration isolated from unwashed and washed EV pellets 139
Figure 4.11 Average Size Distribution by Intensity. 141
Figure 4.12 Average Size Distribution by Intensity 142
Figure 5.1 Astrocyte derived EVs affect HBMvEC permeability in a treatment orientation - dependent manner 154

Figure 5.2 Astrocyte derived EVs affect HBMvEC permeability in a time-dependent manner..... 155
Figure 5.3 Illustration of AM and ACM derived EVs isolation. 156
Figure 5.4 Astrocyte derived EVs decrease HBMvEC permeability. 157
Figure 5.5 qPCR analysis in response to astrocyte derived EV treatment. 158
Figure 5.6 Protein expression analysis in response to astrocyte derived EV treatment .. 159
Figure 5.7 Gene expression analysis of astrocytes after LPS treatment 161
Figure 5.8 Gene expression comparison of astrocytes after treatment with LPS and cytokines using qPCR. 163
Figure 5.9 GFAP protein expression in astrocytes after cytokine treatment. 164
Figure 5.10 Dynamic Light Scattering Analysis of the Average Size Distribution by Intensity of EVs isolated from healthy and inflamed ACM..... 165
Figure 5.11 EVs derived from inflamed astrocytes increase HBMvEC permeability 166
Figure 5.12 Protein expression analysis in response to inflamed astrocyte derived EV treatment..... 167
Figure 6.1 Illustration of EV isolation from healthy and inflamed cells..... 178
Figure 6.2 Total RNA quality analysis of EVs isolated from healthy (A) and inflamed (B) astrocytes..... 180
Figure 6.3 Total RNA quality analysis of healthy (A) and inflamed (B) astrocytes. 181
Figure 6.4 PCA of gene expression data. 183
Figure 6.5 Volcano plot of differential gene expression of HBMvECs treated with vehicle control (PBS) vs. EVs isolated from inflamed astrocytes. 184
Figure 6.6 Gene ontology (GO) enrichment analysis of HBMvECs DEGs after treatment with inflamed EVs 193

List of Tables

Table 2.1 Primer Information (Obtained from Eurofins MWG Operon (Germany)) 64
Table 2.2: Preparation of Conditioned Media 73
Table 2.3: The preparation of conditioned media for apical treatment 77
Table 2.4: The preparation of conditioned media for abluminal treatment 78
Table 2.5: Components of the Reaction Mix used for cDNA synthesis. 81
Table 2.6: PCR reaction mixture 82
Table 2.7: PCR reaction method 82
Table 2.8: qPCR reaction mixture 83
Table 2.9: qPCR method 83
Table 2.10: SDS-PAGE resolving gel components. 87
Table 2.11: SDS-PAGE stacking gel components 87
Table 2.12: Primary Antibody Concentrations used in Immunoblotting 89
Table 2.13: Secondary Antibodies used in Immunoblotting 90
Table 4.1: CD63+ bands in the fractions derived from ECM and EM 136
Table 6.1: Genes downregulated in HBMvECs after treatment with inflamed EVs in comparison to control, in order of largest fold change 185
Table 6.2: Genes upregulated in HBMvECs after treatment with inflamed EVs in comparison to control, in order of largest fold change 189

Publications

Oral Publications

- An in vitro examination of astrocyte-derived EVs on a human brain microvascular endothelial cell model of the BBB. Presented at UK & Ireland Early Career BBB Symposium; 2025 July 17, TCD
- Extracellular Vesicle Driven Communication at the Blood-Brain Barrier. Presented at: BRS 15th Annual Research Day; 2024 April 18, DCU – **Awarded Best Research Talk**
- Astrocytic microRNA control of blood brain barrier breakdown in epilepsy. Presented at: IAS; 2023 March 28, Bertinoro, Italy.
- Analysing the Contents of Astrocyte and Endothelial Cell-derived Extracellular Vesicles. Presented at: 12th UK and Ireland Early Career BBB meeting; 2022 October 27; TCD
- Communication between Astrocytes and Endothelial Cells in Epilepsy. Presented at: Biology of Brain Disorders; 2022 Jun 15 - 17, TCD

Poster Publications

- Aleksejenko, N, Rochfort, KD, Cummins, PM, Heller, JP. Extracellular Vesicles: An Exploration into the Bi-directional Crosstalk of Endothelial Cells and Astrocytes at the Blood-Brain Barrier. Poster presented at: FENS 2024, Vienna
- Aleksejenko, N, Rochfort, KD, Cummins, PM, Heller, JP. Isolation and Analysis of Astrocyte and Endothelial Cell Derived Extracellular Vesicles. Poster presented at: BRS 14th Annual Research Day; 2023 April 20, DCU
- Aleksejenko, N., Rochfort, KD., Cummins, PM., Heller, JP. Optimization of Exosome Isolation from Astrocyte Conditioned Media. Poster presented at: BRS 13th Annual Research Day; 2022 May 27, DCU

Intracellular Communication at the Neurovascular Unit: The Effect of Astrocyte Secreted Factors on the Blood-Brain Barrier

Natalija Aleksejenko

Abstract

The properties of the blood-brain barrier are known to be maintained by endothelial cell interactions with astrocytes. Astrocytes secrete extracellular vesicles, important mediators of intercellular communication. Very few studies have explored the effect of astrocyte derived extracellular vesicles on barrier integrity. During neuroinflammation, barrier integrity decreases and astrocytes become reactive, reflected in the cargo of their secreted extracellular vesicles. This thesis investigated the effect of these astrocyte-derived extracellular vesicles on the barrier function of endothelial cells both in health and during neuroinflammation.

Astrocyte conditioned media generated from primary human astrocytes was used as a treatment on primary human brain microvascular endothelial cells. This conditioned media was able to attenuate the inherent detrimental effect of the base astrocyte media on endothelial cell viability and tight junction protein expression. This effect was hypothesized to be due to astrocyte-derived extracellular vesicles, necessitating their isolation to remove this confounding background effect.

Three isolation methods: differential centrifugation, microvesicle isolation and ExtraPEG, were compared. ExtraPEG was determined to be the optimal extracellular vesicle isolation method due to lower variation in isolated extracellular vesicle populations. Using this method, extracellular vesicles were isolated from healthy astrocytes. These vesicles were able to decrease barrier permeability in endothelial cells when treated basolaterally, but not through changes in tight junction gene or protein expression. However, treatment with inflamed astrocyte-derived extracellular vesicles, resulted in 10% increased barrier permeability. Inflamed extracellular vesicles were found to upregulate the expression of several inflammatory genes, including CCL2, in endothelial cells, as well as affecting the expression of genes involved in cell adhesion, cell migration, and protein localisation pathways. This reveals the contribution of astrocyte-derived extracellular vesicles to barrier maintenance and how this changes in pathology, as well as revealing several potential mechanisms that can be exploited in order to treat blood brain barrier dysfunction during neuroinflammation.

Chapter 1 :

Introduction

1.1 The Cerebrovasculature

Although the average adult human brain represents approximately 2% of body weight, it accounts for around 20% of the body's metabolic consumption (Clarke & Sokoloff, 1999; Y. Wang, Zhou, et al., 2025). This is not surprising as the brain requires a substantial amount of energy to maintain electrochemical gradients across neuronal membranes. It has been estimated that approximately 75% of the brain's calculated energy consumption is attributed to neuronal signalling, with the remaining energy allotted to basic cellular functions, such as molecule synthesis and organelle trafficking (Attwell & Laughlin, 2001; Harris et al., 2012).

Both the developing and adult brain receive the majority of their energy through the oxidation of glucose (McKenna et al., 2012; Solmonson et al., 2022). In addition to this, both glucose and oxygen are required for the synthesis of many important neurotransmitters (Gnegy, 2012; R. Han et al., 2021; Kotsyuba & Dyachuk, 2022). Interruptions to the brain's supply of glucose and oxygen can lead to cellular dysfunction and eventually cell death, with severe cases of hypoglycaemia (i.e., reduced availability of glucose) and hypoxia (i.e., reduced availability of oxygen) causing neurological damage and even death (Ribeiro et al., 2023). The brain is unable to synthesise or store substantial amounts of glucose. Therefore, the brain is critically dependant on a controlled and continuous supply of essential metabolites, which it receives from a vast network of blood vessels that permeate the brain tissue (Figure 1.1).

In particular, capillaries are thin-walled vessels, often constituting a single layer of endothelial cells, which allow for the efficient exchange of gases, nutrients, and waste products between the bloodstream and surrounding tissues. The total length of capillaries in an adult human brain is over 650 km, accounting for over 85% of cerebral blood vessels, with only around 40 μm separating adjacent capillaries (Zlokovic, 2008; Fu, 2018). This relatively short distance allows for rapid transport of small solutes from blood to the neuronal and glial cells in the brain tissue surrounding the microvessels.

However, in addition to oxygen and nutrients, blood also contains ions, molecules, cells, and pathogens that can interfere with the brain's highly controlled

microenvironment and impact its normal functioning (Daneman & Prat, 2015; Aborode et al., 2025). Therefore, unlike in the peripheral vasculature where there is relatively free small solute exchange, the influx and efflux of these substances is tightly regulated by a biological barrier that exists at the blood-to-brain interface, termed the blood-brain barrier (BBB) (Kiernan, 1996; B. Bell et al., 2023).

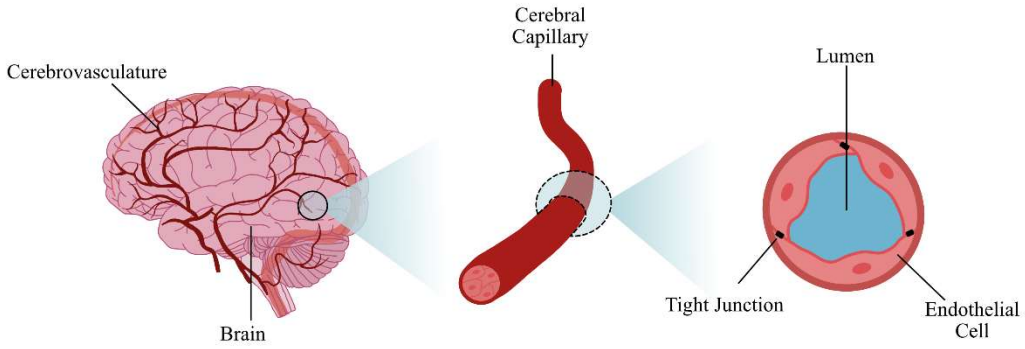


Figure 1.1 ***An illustration of the anatomical and cellular structure of the blood-brain barrier.*** *The left panel shows the cerebrovasculature embedded in brain tissue, highlighting a cerebral capillary, seen in the central magnified view, as the site of BBB function. The rightmost cross-section diagram details some of the cellular components of the BBB: the endothelial cells lining the lumen of the capillary, interconnected by tight junctions which restrict paracellular transport. Together these elements form a selective barrier that regulates the molecular exchange between the blood and the brain, maintaining the homeostasis of the brain. Figure created by author in Affinity Designer (version 1.10.6.1665).*

1.1.1 The BBB

1.1.1.1 History of the BBB

Early experiments by Paul Ehrlich had found that the injection of trypan blue, along with other dyes, intravenously stained all organs except the brain and spinal cord (Ehrlich, 1885 as reviewed in Liddelow, 2011) (Figure 1.2). Later, his student, Edwinn Goldmann, found that the injection of trypan blue directly into the brain had the converse result – the brain was stained but the body was not (Liddelow, 2011). These experiments demonstrated a clear compartmentalization between the brain and the rest of the body. However, it was not until the start of the 20th century that a physical barrier between the blood vessels and the rest of the central nervous system (CNS) was proposed by Lewandowsky after a set of experiments where cholic acids or sodium ferrocyanide were injected intravenously with no pharmacological effects on the nervous system. However, effects were seen after a

direct injection into the brain (Lewandowsky, 1900 as reviewed by Liddelow, 2011)
.



Figure 1.2 ***Systemic trypan blue injections.*** *A) A rat after injection with trypan blue (From Goldmann (1909)) B) The brain and spinal cord of a rat with trypan blue (From Goldmann (1913)).*

While Lewandowsky has often been credited with coining the term 'bluthirnschranke' or 'blood-brain barrier', he does not actually use this term in his original paper. In fact, the first use of the term "barrier" should be accredited to Stern and Gautier in their 1918 paper: *"La barrière qui s'oppose au passage dans le liquide céphalo-rachidien de substances circulant dans le sang présente des différences notables suivant les espèces animales"*(Stern & Gautier, 1918 as reviewed by Saunders et al., 2014). Stern and colleagues proposed two routes of entry into the brain, one through the choroid plexuses (the *"barrière hématoencéphalique"* (blood-brain barrier) (Stern & Gautier, 1921), which is now known as the blood-CSF barrier) and one directly through blood vessels (what is now deemed the BBB). Stern was the first to propose that this barrier was selective and provided a mechanism to control the brain's microenvironment (Stern, 1934 as reviewed by Saunders et al., 2014).

Even so, it was not until the late 1960s that the site of this barrier was discovered. Studies with horseradish peroxidase localized the BBB to protein complexes in between the endothelial cells that constitute the lumen of blood vessels (Reese &

Karnovsky, 1967), which was further confirmed by studying their electrical resistance (Crone & Olesen, 1982).

1.1.1.2 Junctional Complexes of the Blood-Brain Barrier

The BBB is established and maintained by junctional complexes between endothelial cells (Figure 1.3). These junctional complexes - adherens junctions (AJs) and tight junctions (TJs) - provide important adhesive contacts between endothelial and epithelial cells in a variety of tissue types. The expression of these TJ proteins between adjacent endothelial cells results in an obstruction to the paracellular pathways, limiting passive diffusion of certain molecules between the blood and the brain. Importantly, the formation of TJs requires cell-cell contacts initiated and maintained by AJs (Watabe-Uchida et al., 1998; Shigetomi et al., 2018).

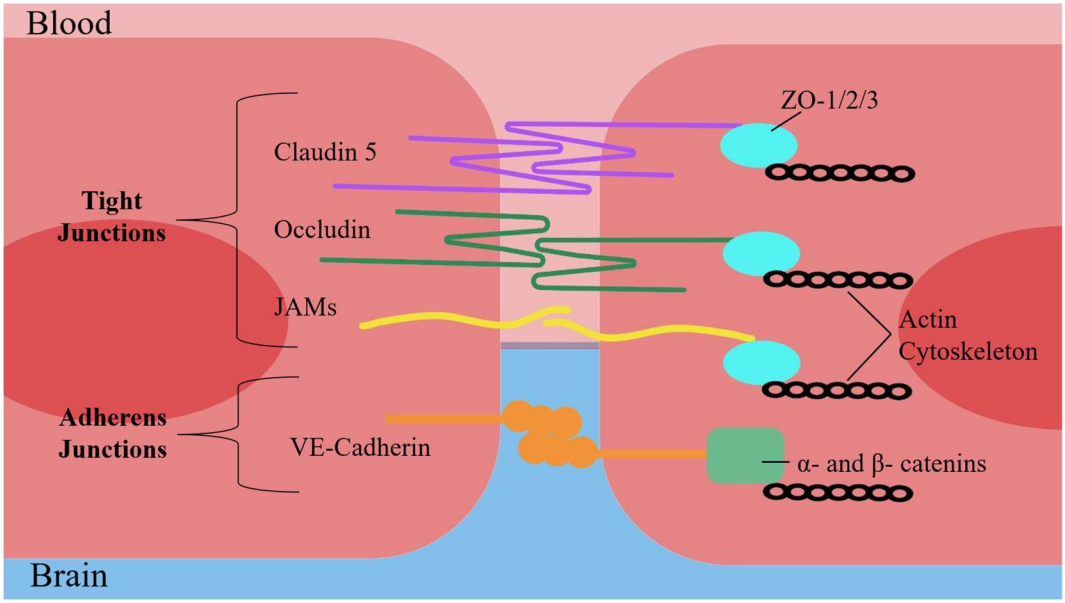


Figure 1.3 ***A schematic representation of the main tight junction and adherens junction proteins between two endothelial cells*** *showing the extracellular interaction between members of the claudin family, occludin and JAMs. These TJs are linked to the actin cytoskeleton by the ZO scaffolding proteins. VE-cadherin, a member of the adherens junction, is linked to the actin cytoskeleton by α- and β- catenins. Figure created by author in Affinity Designer (version 1.10.6.1665).*

The main proteins of AJs include members of the cadherin superfamily and the catenin family. The endothelial specific glycoprotein VE-cadherin is the core adhesion molecule that helps to promote vascular stability (Giampietro et al., 2012; Postma et al., 2025). Members of the catenin family, such as α-catenin and β-

catenin, connect VE-cadherin to the actin cytoskeleton. VE-cadherin also seems to play a role in the expression of TJ proteins, with VE-cadherin being able to upregulate claudin-5 gene expression (Taddei et al., 2008) and overexpression of VE-cadherin being able to rescue angiotensin II-induced inhibition and disordered distribution of ZO-1 (L. Liu et al., 2018). Another study also found that VE-cadherin was involved in a signalling pathway that modulated the phosphorylation state of occludin, thus being able to regulate barrier permeability (Walsh et al., 2011).

It is now known that TJs regulate the diffusion of components of the peripheral circulatory system into the CNS and vice versa in a size- and charge-specific manner. TJs consist of protein complexes spanning the intercellular cleft between adjacent cells and typically comprises of membrane linker proteins like occludin and claudins, as well as junctional adhesion molecules (JAMs), linked to cytoplasmic scaffolding and regulatory proteins such as the zonula occludens (ZO-1, ZO-2, ZO-3).

1.1.1.2.1 Occludin

Electron microscopy studies had revealed the presence of junctional complexes between epithelial cells (Farquhar & Palade, 1963). However, the components of these junctional complexes were not elucidated until 1993, when the first TJ protein, occludin, was discovered (Furuse et al., 1993). Occludin is a transmembrane phosphoprotein consisting of four transmembrane domains, two extracellular loops, and a cytoplasmic tail. Overexpression of occludin improves electrical resistance of Madin-Darby canine kidney (MDCK) cells (McCarthy et al., 1996). Importantly, several studies have shown that the phosphorylation state of occludin is related to the integrity of the BBB (DeMaio et al., 2006; Y.-S. Chen et al., 2007; Morgan et al., 2007; Rochfort et al., 2014; Goncalves et al., 2022; B. X. Huang et al., 2023).

Occludin is not required for TJ formation, however, as total deletion of occludin did not affect the viability of knockout mice nor the morphology of the TJs themselves (Saitou et al., 2000; Saito et al., 2021). Even so, several abnormalities, including chronic inflammation of tissues and calcification of the brain were noted in occludin knockout mice (Saitou et al., 2000). Several studies have also shown that occludin expression is downregulated after stroke, which leads to BBB breakdown (Y. Yang et al., 2007; W. Liu et al., 2009; J. Liu et al., 2012; C. Ren et al., 2015; Sugiyama et

al., 2023). This points to the importance of occludin in the stability of TJs and provides support for their role in barrier integrity.

1.1.1.2.2 Claudin-5

The tightness of each individual TJ is determined by the combination of claudins and mixing ratio of the claudins found at that TJ (Gonschior et al., 2022; Ogbu et al., 2025). In humans and mice, the claudins are a multigene family made up of over 20 members. They range from 21-28 kDa in size and consist of four transmembrane domains, two extracellular loops, a short cytoplasmic turn, and intracellular carboxy-and amino-terminal domains. Most claudins also contain a PDZ domain-binding motif at their C-terminal domain, allowing them to bind to scaffolding proteins, such as the ZO proteins.

At the BBB, claudin-5 is one of the most highly expressed TJ proteins. A notable study revealed that mouse claudin-5 knockouts allowed small molecules (<800 Da) but not larger molecules to cross the BBB (Nitta et al., 2003). Total deletion of the claudin-5 gene was found to be lethal with all knockout mice dying within 10 hours of birth (Nitta et al., 2003). However, TJs from these mice were not found to be morphologically different from normal mice, suggesting that other TJ proteins supplement TJ formation. Moreover, suppression of claudin-5 expression in adult mice results in seizures and death (Greene et al., 2022).

1.1.1.2.3 Other members of the Claudin family

The expression of other members of the claudin family at the BBB has been widely debated. Many early studies reporting the expression of claudin-1, claudin-3 and claudin-12 at the TJs of the BBB confirmed their presence through immunohistochemistry (Furuse, Fujita, et al., 1998; Liebner et al., 2000; Wolburg et al., 2003). However, multiple single-cell RNA sequencing (scRNAseq) transcriptomic studies have failed to demonstrate the expression of claudin-1 and claudin-3 in murine brain endothelial cells (L. He et al., 2018; Vanlandewijck et al., 2018).

Claudin-1 was the first member of the claudin family to be discovered (Furuse, Fujita, et al., 1998), and the introduction of its cDNA into mouse fibroblasts, which traditionally lack TJs, resulted in the organisation of claudin-1 proteins into the strand-like networks typical of TJs thus showing that claudin-1 was able to initiate TJ assembly, even in cell types typically lacking these protein complexes (Furuse,

Sasaki, et al., 1998). An early research paper found a relationship between downregulation of claudin-1 and an increase in endothelial permeability in the blood vessels of patients with glioblastoma multiforme (Liebner et al., 2000). However, a later paper was unable to detect claudin-1 localized to the TJs of brain endothelial cells in human and murine tissue (Wolburg et al., 2003). Claudin-1 knockout mice also died soon after birth, but this was linked to changes in TJ composition in the epidermis of these mice (Furuse et al., 2002).

A loss in BBB integrity was reported to accompany loss of claudin-3 at the BBB. Wolburg et al. (2003) found a selective loss of claudin-3 in inflamed vessels surrounded by infiltrating immune cells in a murine model of multiple sclerosis as well as in brain sections from human patients with glioblastoma multiforme. An *in vitro* study later found that at higher passage numbers (p31), the immortalised human brain endothelial cell line, hCMEC/D3, had reduced levels of claudin-3 in addition to a reduction in BBB properties in comparison to cells at a lower passage (p26) (Schrade et al., 2012). Although the researchers found this decrease in claudin-5 after only 5 passages, raising concerns of validating barrier properties in cell lines, this paper still corroborates other research showing that the BBB is disrupted with healthy aging (Elahy et al., 2015; Wen et al., 2020), with some evidence of fewer TJs (Bors et al., 2018). However, a more recent claudin-3 knockout study suggests that claudin-3 is not expressed at the BBB, as the BBB of knockout mice remained intact, with results suggesting that previous findings may be due to cross-reactivity of anti-claudin-3 antibodies with an unknown junctional antigen (Castro Dias, Coisne, Lazarevic, et al., 2019). Additionally, this study found that the absence of claudin-3 did not affect BBB integrity (Castro Dias, Coisne, Lazarevic, et al., 2019).

Claudin-12 is an unusual member of the claudin family as it lacks a PDZ binding domain. While studies have reported expression of this claudin in brain endothelial cells (Schrade et al., 2012; Akin-Kinay et al., 2025), claudin-12 was not detected at TJs in the BBB of LacZ reporter mice (Castro Dias, Coisne, Baden, et al., 2019). Recent scRNAseq transcriptomic analysis do show expression of *Cldn12* throughout the entire murine brain (Z. Yao et al., 2023). However, average reads for claudin-12 were found to be higher in smooth muscle cells in comparison to brain endothelial cells (L. He et al., 2018; Vanlandewijck et al., 2018). In humans,

claudin-12 is most prominently expressed in mature astrocytes and neurons (Y. Zhang et al., 2016) but is still expressed in endothelial cells. As these cells do not typically form tight junctions, this suggests that claudin-12 may play other important roles in the CNS but may not be involved in the formation of classical TJs.

In cerebral pathologies, TJ protein expression and BBB integrity is modified. Expression of claudins -1, -3 and -12 was upregulated in both human and murine ischemic tissue, while claudin-5 and occludin were downregulated at least 2-fold (Sladojevic et al., 2019). Ectopic expression of claudin-1 in the brain endothelial cells of a mouse model of MS resulted in significantly reduced BBB leakiness to a small molecular tracer (Hoechst dye) as well as to a large endogenous glycoprotein (fibronectin (~500-600 kDa)) (Pfeiffer et al., 2011).

In contrast, however, Berndt et al. (2019) found that expression of claudins-1, -3, -12, and occludin was downregulated in transient focal ischema in mice, while claudin-5 was upregulated. This study also found expression of other members of the claudin family (claudins -4, -11, -20 and -25) in endothelial cells of murine brain capillaries both at the mRNA and protein levels (Berndt et al., 2019). However, as previously mentioned, knockout studies have suggested these immunohistochemical results may be due to cross-reactivity of the anti-claudin antibodies with other TJ proteins found at the BBB, notably claudin-5, which is found at much higher expression levels in brain endothelial cells than other members of the claudin family. Overall, these studies suggest that the protein composition of TJs is altered in pathological conditions, where downregulation of claudin-5 potentially causes the incorporation of other compensatory members of the claudin family into TJs potentially resulting in changes to barrier integrity.

1.1.1.2.4 ZO-1 and other TJ members

The members of the ZO family, ZO-1 (225 kDa), ZO-2 (160 kDa), and ZO-3 (130 kDa) act as scaffolding proteins, linking other TJ proteins to the actin cytoskeleton (Umeda et al., 2006; Shimojima et al., 2008; Xiong et al., 2021). The ZO proteins are members of the membrane associated guanylate kinase (MAGuK) family and each contains 3 postsynaptic density 95/disc-large/zona occludens (PDZ) domains, a Src homology (SH3) domain, a GuK domain and an acidic domain at the C-terminus. The first of the PDZ domains has been found to bind to the C-terminus of

claudins (Itoh et al., 1999; Hiroaki et al., 2018). The C-terminus of JAMs contains a PDZ domain-binding motif, which has been found to interact with ZO-1 (Ebnet et al., 2000; Haas et al., 2020). Additionally, ZO-1 has been found to bind to the C-terminus of occludin via the unique-5 (U5) region between the SH3 and GuK domains (Fanning et al., 1998, 2007). ZO-1 is then able to anchor these TJ proteins to the actin cytoskeleton by a 28-residue sequence in its C-terminus region (Belardi et al., 2020; Fanning et al., 1998). Downregulation of ZO-1 results in damage to BBB integrity (Jiao et al., 2011; Branca et al., 2019)

Other notable proteins of the TJ complex include several JAMs, part of the immunoglobulin superfamily. JAMs consist of a single membrane-spanning domain, a short C-terminal tail, and an immunoglobulin G (IgG)-like extracellular domain, which mediates dimerization of JAM family members, contributing to binding between adjacent endothelial cells. While JAMs are not required for the formation of TJs, double knockout of JAM-A and claudin in MDCK cells results in abnormal localisation of ZO-1 and ZO-2 (Otani et al., 2019). Additionally, expression of JAM in Chinese hamster ovary cells resulted in localised recruitment of occludin to regions of cell contacts (Bazzoni et al., 2000).

1.1.2 The Neurovascular Unit

The barrier properties of the cerebral endothelial cells are not an inherent feature of these cells themselves. Early experiments by Stewart and Wiley revealed that the cerebral environment confers these properties onto endothelial cells, regardless of their origins (Stewart & Wiley, 1981). In these experiments, when avascular brain tissue from young quail embryos was transplanted into the coelomic cavity of chick embryos, the host endothelial cells that vascularised the neural tissue developed a competent BBB. Meanwhile, when avascular coelomic grafts from quail embryos were transplanted into the brains of embryonic chicks, the chick endothelial cells that vascularised these grafts were lacking these characteristics (Stewart & Wiley, 1981). Since then, studies have shown that barriergenesis in CNS endothelial cells is dependent on Wnt/β-catenin signaling (Liebner et al., 2008; Fetsko et al., 2023), activated by Wnt7 ligands, derived from neural progenitor cells (Eubelen et al., 2018) and from astrocytes in adulthood (Guérit et al., 2021; García-Velázquez et al., 2024).

The properties of the BBB are induced and maintained by the interactions of the endothelial cells with the basement membrane (BM) and the other cells of the brain: astrocytes, pericytes, neurons, oligodendrocytes, and microglia (Figure 1.4). Spatially, the endfeet of astrocytes almost completely ensheath capillaries (Mathiisen et al., 2010; Kubotera et al., 2019; Hösli et al., 2022). Pericytes are also found on the outside of capillaries, embedded in the BM. Endothelial cells, pericytes, and astrocytes all contribute proteins forming the layers of the BM (Sixt et al., 2001; Van Horssen et al., 2005; Turner et al., 2017). Additionally, it has been estimated that nearly every neuron has its own capillary (Zlokovic, 2005; Ventura-Antunes & Herculano-Houzel, 2022), with each neuron residing within 20 μm of a microvessel (Abbott et al., 2006; P. S. Tsai et al., 2009). This close relationship between the cells of the brain and the cerebral vasculature led to the concept of classifying them as a single functional unit, the neurovascular unit (NVU), formally introduced in 2001 (Iadecola, 2017; Alkayed & Cipolla, 2023).

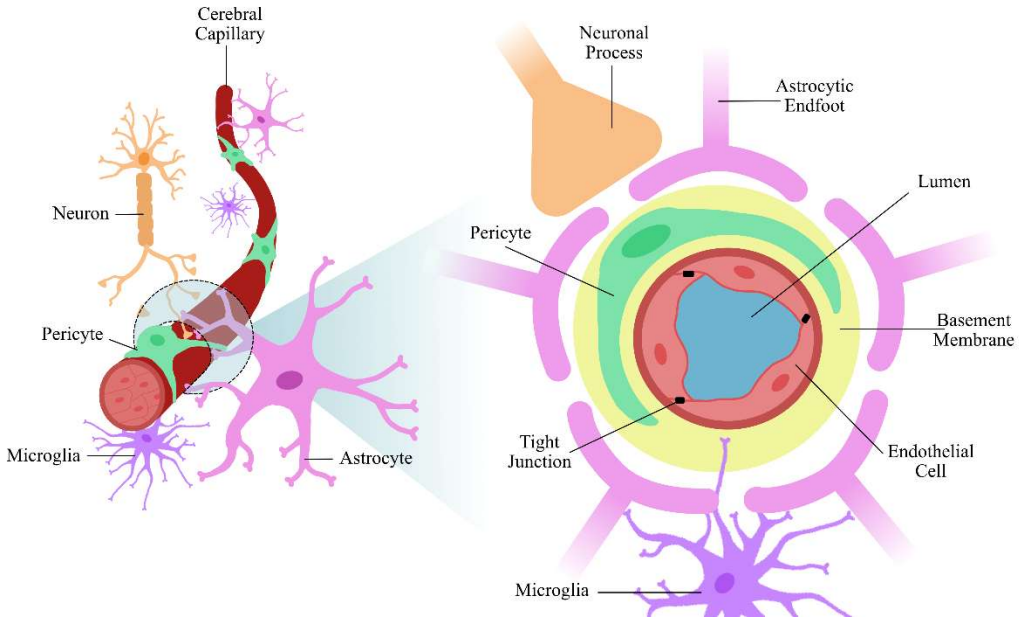


Figure 1.4 ***An illustration of the structural and cellular components of the neurovascular unit****. The left-hand side shows a cerebral capillary surrounded by a neuron, astrocytes, pericytes, and microglia. Astrocytic endfeet envelop the capillary, emphasizing their role in BBB maintenance and signalling. The right-hand side shows a magnified cross-section of the capillary, revealing the endothelial cells lining the lumen of the capillary, interconnected by tight junctions forming the selective barrier. The basal lamina surrounds the endothelium, with pericytes embedded between the endothelial layer and astrocyte endfeet. Neurons and microglia are shown in close proximity, highlighting their interactions with the BBB. Together, these components help to preserve the homeostasis of the CNS by regulating the molecular exchange between the blood and the brain. Figure created by author in Affinity Designer (version 1.10.6.1665).*

1.1.2.1 Pericytes

First discovered in the 19th century, pericytes are a type of mural cell that extends its processes along the abluminal surface of the cerebral microvasculature, usually stretching over multiple endothelial cells (Rouget, 1873, reviewed in Divecha et al., 2025). These cells have been found to be responsible for the vasoconstriction and vasodilation of the capillary during neurovascular coupling, with their constriction and relaxation being able to change the vessel diameter by up to 20% (Berthiaume et al., 2018; D. A. Hartmann et al., 2021). Pericyte phenotypes vary at different capillary locations, with differences in transcriptomes, morphologies, and contractile dynamics (Grant et al., 2019). A recent study, however, found that their transcriptomes may better reflect functional specialisations rather than their location (A. C. Yang et al., 2022; İş et al., 2024).

Pericyte densities also vary across different organs (Shepro & Morel, 1993; Helmbold et al., 2001; Nees et al., 2012). In comparison to the peripheral system, the CNS and retina show the highest densities of pericytes, with approximately one pericyte present for every three endothelial cells in the CNS and an equal number of pericytes to endothelial cells in the retina (Frank et al., 1987, 1990; Armulik et al., 2010; Mathiisen et al., 2010). With this high density, pericytes cover almost 100% of the capillary length, although their processes only cover a third of the circumference of the vessel (Mathiisen et al., 2010). These high densities in the CNS reflect the important functions pericytes play in the brain, including their role in supporting the BBB.

Pericytes are required for proper BBB formation. The onset of barrier function coincides with the recruitment of pericytes to the vasculature and blood vessel permeability is correlated with pericyte coverage of the vessel (R. D. Bell et al., 2010; Daneman et al., 2010). Mice lacking pericytes, either through global ablation or genetic manipulation, show an increase in vascular permeability (Armulik et al., 2010; Nikolakopoulou et al., 2019; Vazquez-Liebanas et al., 2022). Additionally, leukocytes were found to be able to infiltrate the CNS even under homeostatic conditions in pericyte-deficient mice, and the degree of leukocyte trafficking from the vasculature was inversely related to the extent of pericyte coverage of the blood vessel (O. Török et al., 2021). A more recent study, however, revealed that focal pericyte loss does not result in increased barrier permeability (Berthiaume et al., 2022). Recent evidence has also linked decreased TJ protein expression to pericyte dysfunction in several disease models (Y. Liu et al., 2021; W. Li et al., 2023; Yuan et al., 2023).

1.1.2.2 BM

In blood vessels, the BM, a unique form of extracellular matrix (ExM), ensheathes the basal face of endothelial cells. It provides support to cells and separates them from surrounding tissue (Halfter & Yip, 2014; D. Zhang et al., 2017; Sherwood, 2021). BMs also play important roles in mediating signals between cells and their surroundings (Nguyen-Ngoc et al., 2012; Randles et al., 2020). The ExM proteins collagen IV, laminin, nidogen, and proteoglycans tend to be core components of many BMs (LeBleu et al., 2007; Lennon & Sherwood, 2025). However, the protein

composition of BMs in the body varies greatly (Miner & Sanes, 1994; Miner et al., 1997; Jayadev et al., 2022).

In the brain, the BM surrounding the cerebral microvasculature is made up of two distinct ExM complexes known as the vascular and parenchymal BMs (Sixt et al., 2001; Hannocks et al., 2018). These are typically separated by pericytes but are physiologically indistinguishable in regions without pericytes. Still, these BMs differ in their protein composition with the vascular BM being comprised of proteins secreted by endothelial cells and pericytes while astrocytes contribute proteins to the parenchymal BM (Van Horssen et al., 2005; Turner et al., 2017). For example, these cells produce different laminin isoforms, with astrocytes predominantly producing laminin- α2β1γ1 (-211), and brain endothelial cells producing laminins- α4β1γ1 (-411) and -α5β1γ1 (-511) (Sorokin et al., 1997; Sixt et al., 2001).

The BM plays an important role in the formation and maintenance of the BBB. The addition of BMs in *in vitro* models of the BBB helps to increase barrier properties (Tilling et al., 1998; J.-W. Choi et al., 2023). For example, porcine brain endothelial cells grown on decellularized ECMs derived from porcine brain pericytes and astrocytes exhibited significantly increased electrical resistance measurements than those grown on non-brain cell derived ECM (C. Hartmann et al., 2007; Zobel et al., 2016).

Disrupting any of these BM proteins affects the vascular integrity of the cerebral blood vessels. Although complete knockout of *COL4A1* is embryonic lethal, loss of function of this collagen IV α-chain producing gene in endothelial cells and pericytes results in intracerebral haemorrhage (ICH) (Jeanne et al., 2015; Pöschl et al., 2004). Similarly, global knockout of most laminin subunits is lethal to the embryo (N. Smyth et al., 1998; Nguyen et al., 2002; Miner et al., 2004). Cell-specific knockout of laminin isoforms resulted in damage to the BBB, with loss of astrocytic laminin resulting in BBB breakdown and age-dependent ICH (Z.-L. Chen et al., 2013; Y. Yao et al., 2014). Loss of pericytic laminin had much milder effects, according to one study (Gautam et al., 2016). Here, the authors did find downregulation of TJ protein expression and BBB-breakdown but only in 10.7% of knockout mice that also developed hydrocephalus (Gautam et al., 2016). Knockout

studies of laminin-α2 and laminin- α5 also show that these subunits play a role in maintaining neurovascular integrity (Menezes et al., 2014; Nirwane et al., 2024).

1.1.2.3 Oligodendrocytes

Oligodendrocytes are mainly responsible for selectively coating neuronal axons with a myelin sheath which insulates the axon and improves the transmission of electrical impulses. Myelin also plays a role in memory consolidation (McKenzie et al., 2014; S. Pan et al., 2020; F. Wang et al., 2020). Oligodendrocytes arise from terminal differentiation of oligodendrocyte precursor cells (OPCs). OPCs persist in the CNS throughout life, unlike other progenitor cells, making up between 2-8% of the cells in the CNS (Raff et al., 1983; Dawson, 2003; Beiter et al., 2022). These cells can differentiate into mature oligodendrocytes and astrocytes (Suzuki et al., 2017; Y. He et al., 2021; Altunay et al., 2025). However, mature oligodendrocytes show very little turnover in the brain, suggesting that OPCs play other essential roles in the brain (Yeung et al., 2014; R. B. Tripathi et al., 2017).

OPCs have a close bidirectional relationship with the vasculature of the brain. During development in both mice and humans, OPCs migrate along the vasculature and then detach from it upon differentiating into mature oligodendrocytes (H.-H. Tsai et al., 2016; Y. Su et al., 2023). Another recent study, however, suggests that ~17% of mature oligodendrocytes remain in direct contact with blood vessels (Palhol et al., 2023). Additionally, one study found that OPCs were recruited to damaged regions by using the vasculature as a scaffold in a mouse model of stroke (Bonfanti et al., 2017).

Endothelial cells promote OPC survival, proliferation, and myelination (Arai & Lo, 2009; D. Ma et al., 2024; W. Wang et al., 2024). Vice versa, several studies have suggested that cells of the oligodendroglial lineage are able to promote angiogenesis (Yuen et al., 2014; Minocha et al., 2015) and modulate BBB integrity (Seo et al., 2014; Kimura et al., 2020). TGF-β1 secreted by OPCs was shown to decrease BBB permeability in endothelial cells (Seo et al., 2014). Both OPCs and oligodendrocytes were able to improve the BBB integrity of endothelial cells, albeit via different pathways (Kimura et al., 2020). Transplantation of OPCs into a mouse

model of brain ischemia improved BBB integrity and functional recovery (L. Wang et al., 2020).

In pathology, OPCs seem to drive breakdown of the barrier. OPCs treated with pro-inflammatory cytokines were found to secrete MMP9 which decreased ZO-1 protein expression and increased permeability in endothelial cells (Seo et al., 2013). In MS, in which both demyelination and BBB breakdown are common, OPCs have been found to cluster on the blood vessels in lesion areas with active inflammation, which disrupts the BBB by impairing TJs, leading to increased vascular permeability (Girolamo et al., 2019; J. Niu et al., 2019).

1.1.2.4 Neurons

A major component of the CNS, neurons process and transmit information to other cells through electrical and chemical signals. Neuronal activity has been correlated strongly with cerebral blood flow (CBF) (Silva et al., 2000; Longden et al., 2017; X. Gao et al., 2025). During vasodilation, the diameter of the vessel is increased, allowing more blood to flow through it. During vasoconstriction, the diameter of the vessel is decreased, slowing down blood flow. Neurons are able to induce vasodilation or vasoconstriction of the cerebrovasculature by two main mechanisms. Firstly, neuronal activity results in the release of neurotransmitters, which act on endothelial cells and mural cells (i.e. pericytes and vascular smooth muscle cells (which have a similar role to pericytes but are not found on the capillaries)) to regulate the diameter of blood vessels (Cauli et al., 2004; Hogan-Cann et al., 2019; D. Zhang et al., 2024). Secondly, neurons can also activate astrocytes, which then release vasoactive mediators that act on the vasculature to control CBF (Du et al., 2024; Isis Yonza et al., 2025).

In addition to this, several studies have also suggested that neurons also influence BBB integrity. The addition of neurons into a co-culture of endothelial cells and astrocytes was found to significantly improve barrier integrity in comparison to endothelial cells co-cultured with astrocytes alone (Schiera et al., 2005; Barberio et al., 2022). The levels of several junction proteins in endothelial cells also increased in the presence of neurons (Savettieri et al., 2000; L. Yang et al., 2024). Neurons, along with astrocytes, are important sources of Wnt ligands, which can activate the

Wnt pathway in endothelial cells (Stenman et al., 2008; Y. Wang et al., 2018; Ye et al., 2011). Several proteins involved in barrier function are downstream of Wnt, including claudin-5, which is upregulated by Wnt signalling, but also plasmalemma vesicle-associated protein (PLVAP), which is a marker of fenestrated vessels lacking a barrier and is downregulated by Wnt signalling (Y. Wang et al., 2019). Neuronal activity has been found to regulate the expression of several BBB-related genes, including claudin-5 and ZO-1, via endothelial cell circadian genes (Pulido et al., 2020).

1.1.2.5 Microglia

First defined in a series of papers by Pío del Río-Hortega in 1919 (Río-Hortega, 1919a, 1919b, 1919c, 1919d; translated and reviewed in Sierra et al., 2016), microglia act as the resident immune cells of the CNS. They continuously survey the brain by extending and retracting their long processes, allowing them to monitor changes in their microenvironment (Nimmerjahn et al., 2005; A. Y. Zhang et al., 2025) and maintain brain homeostasis by clearing waste and damaged cells via phagocytosis (Herzog et al., 2019; T. Yang et al., 2024). Additionally, their processes allow microglia to contact the other cells of the NVU, allowing them to sculpt neural circuits by pruning neuronal synapses and axons (Schafer et al., 2012; Y. Hu et al., 2024) and by promoting synapse formation (Miyamoto et al., 2016; Akiyoshi et al., 2018). Microglia have also been shown to play a role in neuronal regulation (Badimon et al., 2020; Y. He et al., 2023) and in the maintenance and regeneration of myelin (Hughes & Appel, 2020; Nemes-Baran et al., 2020; Djannatian et al., 2023).

Microglia are thought to originate from yolk sac-derived macrophages, which begin to colonise the brain during early development, prior to the formation of the BBB (Ginhoux et al., 2010; Swinnen et al., 2013; Paolicelli et al., 2022). These cells are known to migrate along the vasculature while colonizing the developing brain (Monier et al., 2007; Smolders et al., 2017). One study found that microglia remain in contact with areas of the vasculature lacking full ensheathment by astrocytic endfeet, regardless of age (Mondo et al., 2020). A recent study found that this association is guided by endothelial cells, which release ATP though PANX1, activating the P2RY12 receptor on microglia directing their positioning and

interactions with capillaries (Bisht et al., 2021). Microglia have been found to regulate capillary diameter, CBF, and vascular responsiveness (Mills et al., 2021; Császár et al., 2022). Although microglia display a close physical relationship with the vasculature, their role in maintaining BBB integrity is still being defined. One recent study found that ablation of microglia in the healthy adult brain did not affect the function or structure of the BBB (Profaci et al., 2024).

However, it seems that during insults to the brain, microglia are a double-edged sword as their effect on the BBB varies depending on their state. In response to stress and injury in the CNS, microglia become activated, associated with changes in their morphology and transcriptomes (Davalos et al., 2005; Bernier et al., 2019; Guvenek et al., 2024). This results in two broad categories of microglia: either pro-inflammatory (M1) or anti-inflammatory (M2) cells (Z. Zhang et al., 2017; C. Xing et al., 2018). M1 microglia induce inflammation and neurotoxicity by releasing inflammatory cytokines and chemokines. M2 microglia, on the other hand, are associated with neuroprotective effects, such as promoting neuronal regeneration (Batchelor et al., 1999; Narantuya et al., 2010). However, this binary model has increasingly become challenged as microglia appear to have a much broader range of activation states, influenced by signals from other cells in the NVU as well as the disease context and timing (Ransohoff, 2016; J. Qin et al., 2023)

Studies have found that the impact of microglia on the BBB during insults to the CNS is dependent on the activation state of the microglia. One study found that while unstimulated microglia promoted the expression of occludin and ZO-1 in endothelial cells, microglia stimulated with amyloid-β decreased expression of these TJ proteins and increased permeability in endothelial cells (Mehrabadi et al., 2017). Other studies have shown that this disruption to the integrity of the BBB results from the release of pro-inflammatory cytokines and reactive oxidative species released by activated microglia (Nishioku et al., 2010; Shigemoto-Mogami et al., 2018).

One study found that during adulthood microglia produce Platelet-Derived Growth Factor Subunit B (PDGF-B), which has been shown to play a part in pericyte recruitment and BBB development (Lindblom et al., 2003; L. C. D. Smyth et al., 2022), and the expression of this gene is upregulated in microglia during insults to

the BBB (Weng et al., 2024). Another study found that microglia express claudin-5 while contacting endothelial cells, in order to maintain BBB integrity during the early stages of systemic inflammation (Haruwaka et al., 2019). Yu et al., (2022) found that microglia protect BBB integrity by expressing miR-126a-5p in a murine model of multiple sclerosis. One recent study was able to restore BBB integrity in the ischemic brain by promoting the polarisation of M2-type microglia via the delivery of interleukin-10 mRNA loaded liquid nanoparticles (M. Gao et al., 2024).

1.1.2.6 Astrocytes

Astrocytes are the most abundant glial cell type in the mammalian nervous system (Azevedo et al., 2009; Von Bartheld et al., 2016; Stogsdill et al., 2023). Astrocytes were once classified simply into protoplasmic astrocytes, which are complex cells with many fine processes found in the grey matter, and fibrous astrocytes of the white matter, which are less complex and have less branching (Andriezen, 1893; Oberheim et al., 2012). The processes of these protoplasmic astrocytes can interact with the other cells of the NVU, further complementing the concept of the NVU as a singular functional unit. While these classes of astrocytes are still used today, further research has revealed that astrocytes are extremely heterogeneous, differing in morphology, function, calcium signalling activity and gliotransmitter release, both between and within brain regions and even within a single astrocyte's processes (De Ceglia et al., 2023; Bocchi et al., 2025).

Astrocytes contribute to the ionic, neurotransmitter and water homeostasis of the brain through the uptake of water and ions as well as through the removal and recycling of neurotransmitters (Bergami et al., 2008; Lichter-Konecki et al., 2008; Verkhratsky et al., 2020). Astrocytes also control the development of synapses (Allen & Eroglu, 2017; Y. Xie, Kuan, et al., 2022) and prune them through phagocytosis (Chung et al., 2013; J.-H. Lee et al., 2021). During an increase of neuronal activity, astrocytes provide metabolic substrates, such as lactate and glycogen, to the neuron, thus ensuring an adequate energy supply (L. Liu et al., 2017; Beard et al., 2022). A single astrocyte can wrap its processes around several different parts of multiple neurons in addition to ensheathing the blood vessels through a specialised cellular compartment known as the endfoot. After ablation of endfeet, astrocytes have been shown to actively position other endfeet in order to

directly contact the vasculature (Kubotera et al., 2019; Hösli et al., 2022). This strategic positioning of astrocytes in the brain allows them to regulate CBF in response to neuronal activity.

Astrocytes are thought to be involved in both the formation and the maintenance of the BBB (Stone et al., 2019). *In vitro* studies have shown that co-culture of astrocytes with endothelial cells improved barrier properties through increasing tight junction formation and organisation as well as decreasing permeability and/or increasing electrical resistance (Arthur et al., 1987; Barar et al., 2010; Baumann et al., 2021). Additionally, astrocytes secrete a range of factors that can decrease permeability of endothelial cells (Pellerin & Magistretti, 1994; Henneberger et al., 2010; Poskanzer & Yuste, 2016; De Ceglia et al., 2023). In fact, astrocytes are the primary source of Sonic Hedgehog (Shh) in the brain, which has been found to regulate the expression of several TJ proteins through the activation of the Shh pathway in endothelial cells (Alvarez et al., 2011; Zhen et al., 2018; Michinaga et al., 2021). The suppression of Shh release from astrocytes has been found to increase BBB permeability (Y. Wang et al., 2014; Allahyari et al., 2019). Astrocytes also secrete angiopoetin-1 (ANG-1), which plays a major role in vascular stabilisation and maturation (Nourhaghighi et al., 2003; Michinaga et al., 2020). ANG-1 has been found to counteract barrier disruption caused by vascular endothelial growth factor (VEGF) (Shen et al., 2011; Y. Zhou et al., 2022) and has been proposed to upregulate TJ expression levels after injury (Y. Xia et al., 2013; Siddiqui et al., 2015). In addition, astrocytes secrete retinoic acid, which has been shown to increase blood-brain barrier integrity and TJ gene expression through regulation of the WNT/β-catenin signalling pathway (Mizee et al., 2013; Lippmann et al., 2014; Bonney et al., 2018). Martinez-Lozada & Robinson (2020) found that astrocytes were able to increase expression of the Delta-like Notch ligand DLL4 in endothelial cells through the secretion of an unknown factor. In turn, both this ligand and DLL1 from endothelial cells activated notch signalling in astrocytes which increased the expression of the astrocytic glutamate transporters GLT-1 and GLAST, showcasing that bidirectional communication between astrocytes and endothelial cells was required for proper astrocyte maturation. Depleting astrocytes in adult murine brains resulted in both downregulated expression of ZO-1 and

increased permeability in vessels close to areas of astrocyte loss, indicating BBB damage (Heithoff et al., 2021).

Astrocytes play an integral role in health and disease. Depleting astrocytes in mice results in severe impairment of motor skills along with neuron cell loss (H.-H. Tsai et al., 2012; Schreiner et al., 2015). In pathological contexts, astrocytes undergo transcriptional, biochemical, and morphological changes, resulting in functional changes (Matusova et al., 2023; Zamanian et al., 2012). This can cause astrocytes to undergo a phenotypic shift called reactive astrogliosis (Escartin et al., 2021; Matusova et al., 2023). There is conflicting evidence on whether this phenotypic shift is neuroprotective or neurotoxic.

During injury, astrocytes become activated and migrate to the lesion area, forming part of a glial scar in order to minimize damage to the area (R. Zhang et al., 2018; Gong et al., 2023). However, reactive astrogliosis can also promote pathology by becoming neurotoxic, thus killing neurons and oligodendrocytes (Liddelow et al., 2017; Gomes et al., 2024). Astrogliosis can induce BBB breakdown (De Bock et al., 2022; H. Kim et al., 2022). However, astrocytes can also promote neuroinflammation by switching to a pro-inflammatory phenotype and facilitating vascular recovery (Williamson et al., 2021).

Based on gene expression, there seems to be 2 forms of activated astrocyte: A1, which are neurotoxic, and A2, which are neuroprotective (Liddelow & Barres, 2017; C. Wang & Li, 2023). Zamanian et al., (2012) found that 57 genes, including members of the complement system (C3 and Serping 1), and guanine nucleotide binding protein 2, were upregulated in LPS-induced A1 astrocytes, while 150 genes, including S100a10, pentraxin 3, and prokineticin-2, were upregulated in MCAO-induced A2 astrocytes. These have since been used as common markers for A1 and A2 astrocytes (Liddelow et al., 2017; T. Li et al., 2020; Fei et al., 2022). A1 and A2 astrocytes also differ morphologically, with C3+ A1 astrocytes being observed to have long dendrites both in vivo and in vitro, and S100a10+ A2 astrocytes showing hypertrophy and few dendrites (Zou et al., 2019). Additionally, another study also found that the upregulation of A1 markers and downregulation of A2 markers were accompanied by an increase in astrocyte cell volume, surface area, and filament length (Althammer et al., 2020).

A1 astrocytes have been noted to lose normal astrocytic functions, such as phagocytosing synapses (Liddelow et al., 2017). A1 astrocytes are also required for the cognitive impairments seen in a mouse model of perioperative neurocognitive disorders, as a lack of astrocyte activation also resulted in a lack of cognitive dysfunction (Li et al., 2020). A1 astrocytes also caused the death of several types of neurons (Liddelow et al., 2017; Hong et al., 2020). While the neurotoxic mechanisms behind this are largely unknown and seem to be complex, the genes upregulated in A1 astrocytes are known to be damaging to neurons, including C3, a central protein in the complement system (S. Hong et al., 2016; Zhu et al., 2024). C3 may also be a key signalling molecule in the crosstalk between astrocytes and microglia, as a deficiency of C3 in a mouse model of Alzheimer's disease reduced the number of M1 microglia and the amount of several pro-inflammatory cytokines, including TNF-α (Shi et al., 2017). Other studies have shown that A1 astrocyte-secreted C3, once cleaved to its active signalling form, C3a, interacts with its receptor on microglia (C3aR) and regulates microglial phagocytosis of synapses and neuroinflammation (Peng et al., 2025; Zhang et al., 2025). C3a/C3aR signalling has also been implicated as a driver for vascular inflammation and BBB dysfunction in endothelial cells (Propson et al., 2021). Additionally, higher serum levels of C3 have recently been correlated with increased BBB injury and worse clinical outcomes in patients with anti-N-methyl-D-aspartate receptor (NMDAR) encephalitis (J. Zhang et al., 2026).

There have not been as many studies on A2 astrocytes. Genes that were upregulated in A2 astrocytes including beneficial neurotrophic factors and inflammatory factors, such as CLCF1 (cardiotrophin-like cytokine factor 1), interleukin-6 (IL-6), interleukin-10 (IL-10), and thrombospondins, may promote neuronal survival and remodelling (Zamanian et al., 2012). A2 astrocytes have been shown to promote recovery through STAT3 signalling (Su et al., 2019; Chen et al., 2021), including attenuating BBB dysfunction in HIV-associated neurocognitive disorders (Lun et al., 2022) and in a mouse model of stroke (Geng et al., 2025).

Studies seem to indicate the presence of both during pathology (Z.-B. Ding et al., 2021; Jiwaji et al., 2022). However, other studies have found that A1 astrocytes are the predominant astrocytic subtype found in human post-mortem brains with

neurodegenerative diseases including AD (Liddelow et al., 2017; King et al., 2020) and as such, A1 astrocytes will be focused on in this thesis.

The activation of astrocytes is a major part of the brain's immune response. Although it was once considered to be an "immune privileged" site, the CNS is now known to have a complex response to injury and other factors that disturb the brain's homeostasis, similar to that of the periphery, known as neuroinflammation.

1.2 Neuroinflammation

Inflammation in the CNS is characterised by the activation of microglia and astrocytes and the release of cytokines, chemokines and reactive oxygen species, alone with other inflammation mediators (W. Zhang et al., 2023; Y. Chen et al., 2023). Neuroinflammation has a variety of causes, ranging from endogenous (e.g. genetic predisposition and protein aggregation) (Andrews et al., 2021; Mendiola et al., 2023) to environmental (e.g. exposure to toxins and diet) (H. Wei et al., 2023; Zou et al., 2023) in addition to both mental and physical illnesses (e.g. drug use and traumatic brain injury (TBI)) (Dunn et al., 2020; Cai et al., 2022; F. Xu et al., 2023). Inflammation in the peripheral system can also trigger inflammation in the CNS (Albaret et al., 2020; Matsushita et al., 2021).

The effect of neuroinflammation on the CNS is dependent on the duration and severity of immune signalling. Inflammation is important in maintaining homeostasis and plays a beneficial role in injury recovery and in pathogen removal (Russo & McGavern, 2015; Shao et al., 2023). However, prolonged or dysfunctional inflammation can cause damage to the blood-brain barrier, oxidative stress, loss of neuronal function, and inhibit regeneration, leading to the exacerbation of disease (Ophir et al., 2005; Malpetti et al., 2021; P. Wang, Jin, et al., 2023).

Neuroinflammation has been associated with multiple neurodegenerative disorders, such as Alzheimer's disease (AD) (Hou et al., 2021; Mi et al., 2023) and Parkinson's disease (Bido et al., 2024; Geng et al., 2023). Protein aggregates, a common feature of many neurodegenerative disorders, were once thought to induce neuroinflammation (Zeng et al., 2019; Hinkle et al., 2022). However, research has shown that neuroinflammation can also cause protein aggregation in earlier stages

(Gordon et al., 2018; W. Zhang et al., 2023). Additionally, neuroinflammation has been associated with psychiatric disorders such as depression (Z. Qin et al., 2023; D. Zhao et al., 2024) and schizophrenia (Allgäuer et al., 2023; Y. Zhu et al., 2025). In fact, neuroinflammation has been identified in almost all neurological disorders (reviewed in Gorji, 2022; Shi & Yong, 2025) and has also been associated with aging (G. L. Bowman et al., 2018; Schroer et al., 2023), showcasing the importance of understanding and targeting neuroinflammation.

1.2.1 BBB breakdown

One of the hallmarks of neuroinflammation is the breakdown of the BBB, which involves multiple physiological changes including differential expression of TJ proteins and a loss of adhesion between the TJs (Oikari et al., 2020; Sugiyama et al., 2023). This leads to the unregulated entry of molecules and cells through an increase in vascular permeability (Dickie et al., 2019; Wardlaw et al., 2009). This can result in the invasion of peripheral immune cells, resulting in exacerbation of neuroinflammation, and the disorder (Bartholomäus et al., 2009; Marchetti et al., 2022). These physiological changes to the BBB during neuroinflammation are predominantly a result of proinflammatory cytokines secreted by activated microglia and astrocytes (Takeshita et al., 2017; F. Guo et al., 2020).

1.2.2 Microglia and Astrocytes in Neuroinflammation

During neuroinflammation, microglia are activated, broadly into M1 or M2 microglia. A variety of stimuli can induce M1 microglial activation, including amyloid β (associated with AD) (S. Wang et al., 2012; Baik et al., 2019) and the activation of Toll-like receptors (Qie et al., 2020; Tannahill et al., 2013). This results in the production and secretion of pro-inflammatory cytokines such as TNFα and IL-1a (Honjoh et al., 2019; H. Yu et al., 2021) as well as reactive oxygen species (ROS) (Milton et al., 2008; O'Regan et al., 2021). Pro-inflammatory molecules produced by microglia has been found to then activate astrocytes (Liddelow et al., 2017).

Activated astrocytes are also a key source of chemokines, such as C-C motif ligand 2 (CCL2), and C-X-C chemokine ligand 8 (CXCL8), which been found to

contribute to the proinflammatory response, including BBB breakdown (Dimitrijevic et al., 2006; F. Guo et al., 2020; Cambier et al., 2023). Importantly, astrocytes have been found to package pro-inflammatory molecules in extracellular vesicles (EVs) (Goetzl et al., 2018; Rong et al., 2021). EVs from astrocytes have been found to play important roles in the brain (discussed in 1.4).

1.3 EVs

EVs are non-replicating nanoparticles enclosed by a phospholipid bilayer which are secreted by cells into their extracellular space. These contain a variety of signalling molecules and genetic information (Figure 1.5). Research has shown that almost all cells are capable of releasing EVs. Unsurprisingly, EVs have been found in many different types of biological fluid including blood (Karimi et al., 2018, 2022), urine (C.-Y. Chen et al., 2018; Khoo et al., 2024), sperm (X. Han et al., 2023; Y. Xie, Xu, et al., 2022), saliva (P. Han et al., 2023; Reseco et al., 2024), and breast milk (Bozack et al., 2022; L. Tong et al., 2023).

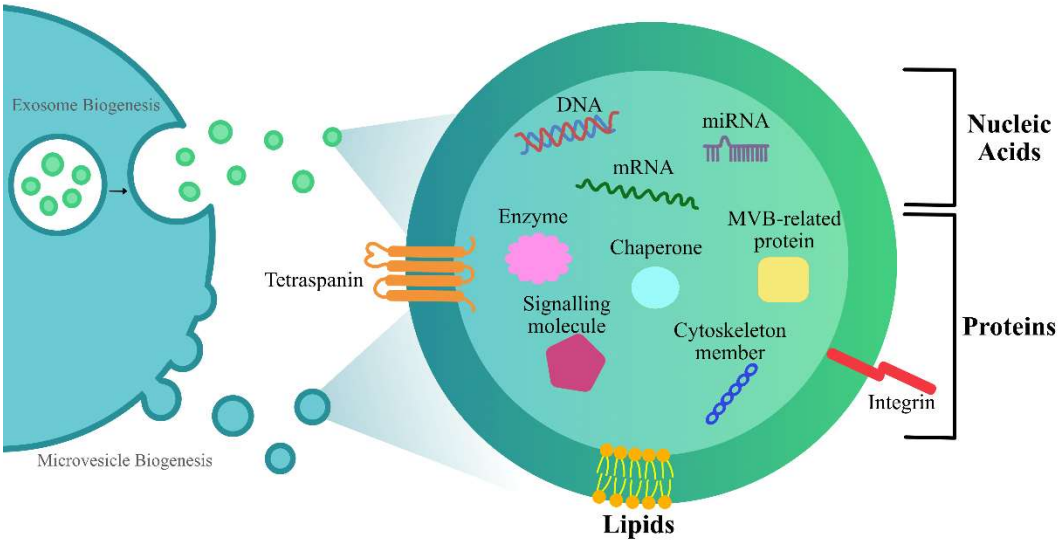


Figure 1.5 ***Schematic representation of the cargo of Extracellular Vesicles.*** *Extracellular vesicles encapsulate a variety of bioactive molecules including nucleic acids such as DNA, messenger RNA (mRNA), microRNA (miRNA); membrane-associated proteins such as tetraspanins and integrins; cytosolic proteins such as enzymes, chaperone proteins, multivesicular body (MVB)-related proteins, as well as proteins involved in signalling and members of the cytoskeleton; and lipids which shape vesicle architecture and influence EV uptake. This mixture mirrors the functional state of their donor cell and enables vesicles to act as potent mediators of intercellular communication. Figure created by author using Affinity Designer (v 1.10.6.1665).*

1.3.1 History of EV Research

When Chargaff and West isolated blood-clotting proteins from plasma using high-speed centrifugation, they described a fraction that had coagulant activity (Chargaff & West, 1946). They attributed this effect to a thromboplastic protein but suggested that this fraction could also contain "*a variety of minute breakdown products of blood corpuscles"*. This is thought to be the first suggestion towards the existence of EVs, although others have suggested that the origins of EV research align with studies of coagulation, which date back to the mid-1600s (Hargett & Bauer, 2013). Regardless, it was not until the late 1960s that Wolf was able to visualise lipid-rich particles isolated from platelet-free plasma using ultracentrifugation through electron microscopy (Wolf, 1967). These particles showed platelet-like activity, endorsing Chargaff and West's original study. Additionally, he found that there was an increase in these particles after storage of platelet-rich plasma and christened them "platelet dust". This was later revealed to be a major milestone in the history of EV research.

Others continued to research this “platelet dust”, now referred to as vesicles or microparticles, showing that these vesicles were not just fragments of the cell membrane and hinted at their potential significance in physiology. Webber & Johnson (1970) captured electron microscopy images of the thrombin-stimulated release of these vesicles by platelets. Additionally, they were shown to carry cargo, such as lipids, ATP and proteins (Crawford, 1971). Nunez et al., (1974) showed the presence of small vesicles (1-10 nm) within multivesicular bodies (MVB) close to the surface of the cell. They suggested that vesicles may be released upon the fusion of the MVB with the cell membrane.

However, it was not until almost a decade later that this hypothesis was fully substantiated by two research articles, published within a week of one another by the Stahl and Johnstone laboratories (Harding et al., 1983; Pan & Johnstone, 1983). Both were using reticulocyte maturation as a model. However, the Stahl lab was studying membrane trafficking while the Johnstone lab investigated the biochemistry of the plasma membrane. Both showed that the transferrin receptor is selectively removed through the formation of vesicles during the maturation of reticulocytes. Harding et al., (1983) proved the release of vesicles from MVBs upon their fusion with the plasma membrane through electron microscopy (Figure 1.6) thus showcasing the existence of a new intracellular sorting and trafficking pathway, and confirming the proposal of Nunez et al., (1974). Vesicles secreted by this pathway are now known as exosomes, as popularised by Johnstone et al., (1987) (Couch et al., 2021). This term was first proposed by Trams et al., (1981) in reference to vesicles produced by the outward budding of the plasma membrane (which are now referred to as microvesicles (MVs)).

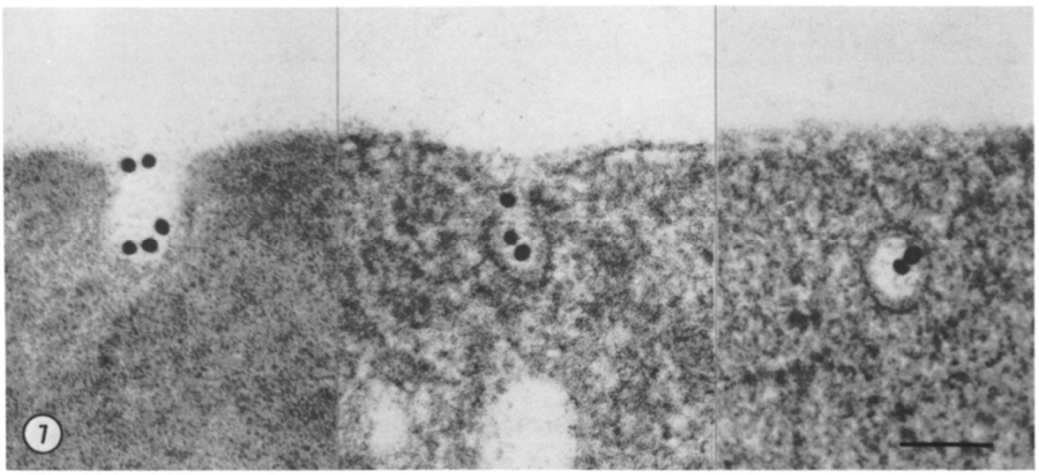


Figure 1.6 ***The first electron microscopy image of extracellular vesicle release****. This image shows the release of gold labelled transferrin-containing particles from the maturing reticulocyte via MVB fusion with the plasma membrane (Harding et al., 1983)*

At this point, EVs were thought to merely be a mechanism of discarding superfluous molecules (Johnstone et al., 1991), even though they were known to be enzymatically active (Johnstone et al., 1989; Fourcade et al., 1995). The first indication that EVs could play a functional role came in 1996, when Raposo et al., (1996) found that antigen-presenting vesicles released by B lymphocytes were capable of inducing T cell responses. This groundbreaking work captured the interest of researchers. A survey published by Roy et al., (2018) revealed that over 4000 articles were published in the decade following the turn of the millennium, over 4 times that which were published between 1985 – 2000. This interest was also further driven by the discovery that EVs were able to deliver their contents to other cells, horizontally transferring mRNA, microRNAs and proteins (Ratajczak et al., 2006; Valadi et al., 2007). This has led them to be known as key players in intercellular communication. EVs have been shown to play roles in cancers (S. Zhao et al., 2022; C. Yang et al., 2024) , inflammatory diseases (Kang et al., 2024; Hsu et al., 2025) and in neurological disorders (Ruan et al., 2021; P. Wang, Lan, et al., 2023). However, their contribution to both normal physiological conditions and to diseases is affected by the heterogeneity of EVs, as these particles vary in their molecular cargo, cellular origin and biological behaviour.

1.3.2 EV Subtypes

EVs differ in biogenesis, size, donor cell, cargo, and method of secretion, leading to heterogeneity among EVs released even by a single cell (Dechantsreiter et al., 2022; Nikoloff et al., 2021) (Figure 1.7). As such, EVs can be divided into several subtypes, of which microvesicles and exosomes have gained the most attention from researchers.

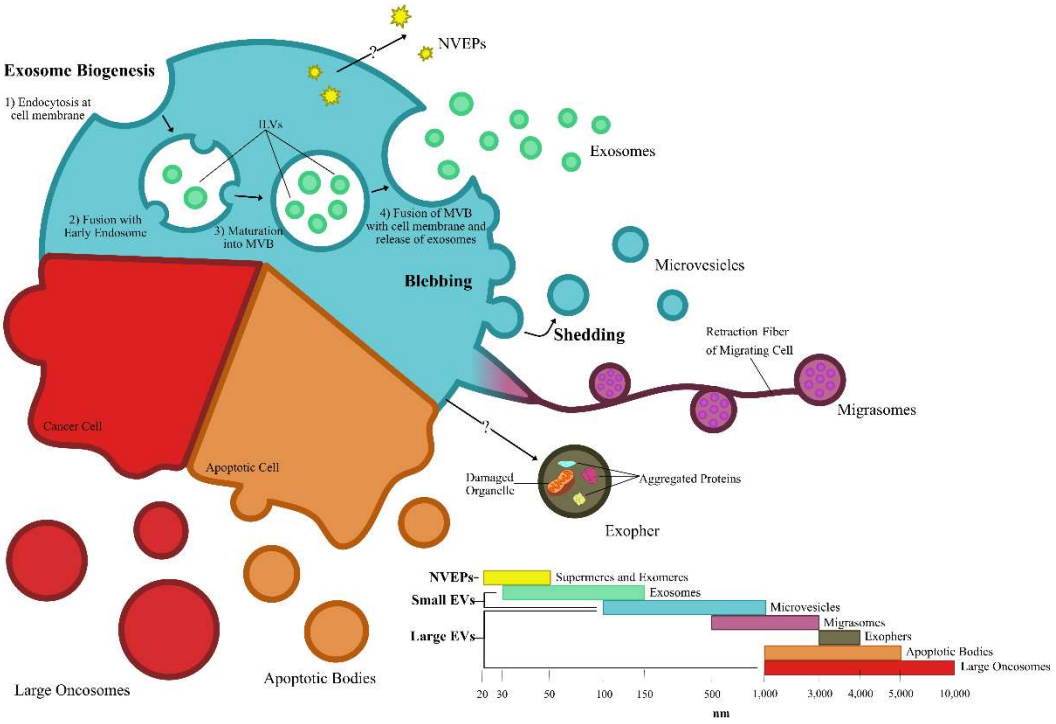


Figure 1.7 ***Diagram illustrating different EV subtypes, their sizes, distinct cellular origins, and biogenesis pathways.*** *The biogenesis and secretion pathways of the recently discovered non-vesicular nanoparticles, exomeres and supermeres, are still poorly understood. Exosomes originate within the endosomal system, forming as intraluminal vesicles (ILV) inside multivesicular bodies (MVB) that ultimately fuse with the plasma membrane, releasing these vesicles. Microvesicles are formed through outward budding of the plasma membrane. Exophers are large EVs, found to contain protein aggregates and damaged organelles, seem to also be formed through budding on the cell surface but can also remain connected to their cell of origin through a thin tubular membrane filament. Migrasomes develop on retraction fibres during cell migration, maturing into vesicular structures that are shed as the cell moves forward. Migrasomes also carry numerous smaller vesicles, leading to a "pomagrante-like" appearance. Apoptotic bodies are formed through membrane blebbing during late-stage apoptosis, producing large, heterogeneous vesicles containing nuclear fragments and organelles. Similarly to microvesicles, large oncosomes are also formed through budding of the plasma membrane. However, large oncosomes are unusually large vesicles that originate from cancer cells and are enriched in oncogenic cargo. A comparison of EV sizes is found in the bottom right corner. Figure created by author in Affinity Designer (version 1.10.6.1665).*

1.3.2.1 Microvesicles

MVs, sometimes referred to as microparticles or ectosomes, are formed through the outward blebbing of the cell membrane. Originally, these MVs were thought to be between 100 and 1000 nm in diameter (Santana et al., 2014; D. Yu et al., 2023). However, there is some evidence of smaller vesicles (30 - 120 nm) formed through blebbing (Jeppesen et al., 2019; Nabhan et al., 2012). Additionally, vesicles larger than 1000 nm, known as large oncosomes, have been noted to be released by cancer cells through a similar mechanism (Di Vizio et al., 2009; S. Zhang et al., 2022)

The underlying mechanisms of MV biogenesis have been less studied than exosomal biogenesis. Based on the existing literature, the outward budding of the membrane occurs due to localised redistribution of the protein and lipid components of the plasma membrane (Muralidharan-Chari et al., 2009; Shurer et al., 2019).

1.3.2.2 Exosomes

Exosomes, which range from 30-150 nm in diameter, have been the most well-studied type of extracellular vesicle (F. Wei et al., 2017; Welsh et al., 2024). Their biogenesis involves 4 general steps: endocytosis and cargo sorting, the formation of the MVB, the transportation of MVBs and the fusion of the MVB with the plasma membrane, which results in the secretion of exosomes. Firstly, extracellular macromolecules and proteins on the cell surface are packaged into endocytic vesicles following endocytosis. These vesicles fuse with early endosomes (Gorvel et al., 1991; Nagano et al., 2019). The cargo that the early endosome carries can undergo several fates. Cargo that is to be recycled will separate from the endosome to fuse with the Golgi network or the plasma membrane. Cargo that is not to be recycled will commit to the endosomal maturation pathway, eventually forming the late endosome. Additionally, regions of the endosomal membrane begin to bud inwards into the intraluminal space of the endosome, forming intraluminal vesicles (ILVs).

Late endosomes containing ILVs are known as MVBs. The cargo within ILVs of MVBs that fuse with the lysosome will be degraded. However, if the MVB fuses with the plasma membrane, these ILVs will be secreted into the extracellular space instead. At this point, these vesicles become known as exosomes. Consequently, future exosomes are dependent on ILV biogenesis, which is regulated mainly by the

endosomal sorting complex required for transport (ESCRT)-dependent machinery. However, other ILV biogenesis pathways which do not include the ESCRT protein complex have also been noted (Gurung et al., 2021; Kajimoto et al., 2013).

The ESCRT is a highly conserved multi-protein complex. In vertebrates, this machinery is composed of around 30 proteins, which assemble into several subcomplexes that are recruited to the endosomal membrane in a stepwise manner. These subcomplexes, known as ESCRT-0, I, II, and III) are composed of class E vacuolar protein sorting (Vps) proteins. ESCRT-0, I, and II each contain at least one ubiquitin-binding and one membrane binding subunit that allows them to recognise and retain ubiquitulated cargo at the endosomal membrane (Y. J. Lee et al., 2023; Mayers et al., 2011). As a result, these complexes are thought to be involved in cargo sorting. ESCRT-III, on the other hand, is thought to mediate the fission of the endosomal membrane. Unlike the components of the early endosomal sorting pathway, ESCRT-III only forms temporarily on endosomes. This complex forms helices that drive the invagination of the membrane, mediated by interations with ESCRT-II (Henne et al., 2012; Azad et al., 2023). The complex disasociates upon the binding of Vps4, an AAA-ATPase, resulting in the formation of a cargo-laden vesicle in the MVB. ESCRT-III and Vps4 can also be recruited by alternative mechanisms to sort cargo into vesicles. These are known as non canonical ESCRT-dependent pathways.

1.3.2.3 Apoptotic bodies

During apoptosis, the dying cell undergoes several morphological and biochemical changes (Cohen, 1997; Sorice, 2022). These include the condensation of chromatin, nuclear splitting, cell shrinkage, blebbing of the cell membrane, and ultimately, resulting in the packaging of the cellular content into vesicles. These vesicles released by apoptotic cells are known as apoptotic bodies (ABs). They are one of the largest types of EVs, ranging between 1 μm – 5 μm in diameter (Atkin-Smith et al., 2015; Y. Zhu et al., 2023). The formation of ABs is thought to be a protective mechanism, allowing damaged cell content to be removed in order to prevent toxins, stress signals, and degrading proteins from leaking to healthy cells (M. Li et al., 2024; Santavanond et al., 2021). ABs are eventually eliminated through phagocytosis.

1.3.2.4 Other Subtypes of EV

Although most studies have focused on exosomes and microvesicles, in addition to apoptotic bodies, other EV subtypes have been identified within the last two decades. Some, such as migrasomes and large oncosomes, are classified partially based on the donor cell type while others like exophers are also classified based on their biogenesis and size. Others still, like exomeres and supermeres, have been identified as non-vesicular extracellular particles (NVEPs) that are released by the cell.

1.3.2.4.1 Exomeres and Supermeres

NVEPs are a category of nanoparticles that lack a lipid bilayer membrane, but that contain full length transmembrane proteins. Lipoproteins, viral particles and vaults (large ribonucleoproteins with a hollow barrel-like structure that have been found to contain RNA (Kedersha & Rome, 1986; González-Álamos et al., 2024)) are considered to be NVEPs in addition to exomeres and supermeres. Exomeres were identified by H. Zhang et al., in 2018, when the researchers used asymmetric flow field-flow fractionation to further separate an initial EV pellet derived by a 100,000 x *g* ultracentrifugation in order to identify subtypes of EVs. During this, they found an abundant population of small (<50 nm) nanoparticles that did not have a membrane. These nanoparticles, which they termed “exomeres” contain a unique signature of cargo in comparison to the other subtypes of EVs identified, suggesting that these exomeres are not just fragments of exosomes or debris but unique particles in their own right (H. Zhang et al., 2018; Q. Zhang et al., 2019). One study found that specific miRNA levels were higher in exomeres than in exosomes, suggesting that there may be a sorting mechanism specifically loading exomeres with cargo (Noguchi et al., 2024). Like other EVs, exomeres can transfer their cargo to recipient cells (Noguchi et al., 2024; Q. Zhang et al., 2019), suggesting that they too, play an important role in intracellular communication.

Another NVEP type, supermeres, was discovered recently in the supernatant of isolated exomeres (Q. Zhang et al., 2021). These nanoparticles range between 22-32 nm in diameter and also show a different profile of cargo in comparison to exomeres and small EVs. miRNA-1246, for example, was found to be highly concentrated in supermeres (Tosar et al., 2022). Additionally, supermeres isolated from cetuximab-resistant cells can transfer resistance to cetuximab-sensitive cells.

This suggests that the secretion of these NVEP can influence the tumour microenvironment and contribute to disease progression.

Studies on both exomeres and supermeres are limited and not much is known about their biogenesis. However, the lack of typical exosomal markers, such as endosomal membrane proteins and proteins involved in the ESCRT complex, found in exomeres suggests that their biogenesis is distinct from the biogenesis of other EVs (H. Zhang et al., 2018). It has been speculated that that they may be directly secreted into the extracellular space.

1.3.2.4.2 Exophers

In 2017, the Driscoll lab found large EVs (~4 μm in diameter) released by adult neuronal cells in *C.elegans* (Melentijevic et al., 2017). These large EVs were termed "exophers" and were found to contain protein aggregates and damaged organelles, acting as a mechanism of waste removal by the cell (Melentijevic et al., 2017; Nicolás-Ávila et al., 2020). Since then, exophers produced by body wall muscle cells in *C. elegans* have also been shown to act as a nutrient source by transporting yolk proteins to newly formed oocytes (Turek et al., 2021). These large EVs are formed through budding on the cell surface, similarly to the formation of microvesicles. However, exophers can remain connected to the cell through a thin tubular membrane filament. Although the exact biogenesis of exopher formation is yet to be discerned, inhibition of autophagy genes disrupted exopher formation, suggesting that exopher biogenesis and autophagy are linked in some way (L.-H. Sun et al., 2024; Y. Yang et al., 2024).

1.3.2.4.3 Migrasomes

A novel EV type released by migrating cells was discovered by Ma et al., (2015). These migrasomes are large vesicles (500 nm – 3000 nm) that contain multiple smaller vesicles, giving them a "pomegranate"-like appearance. While integrins play a role in cell migration (Chastney et al., 2025), they also seem to promote the formation of migrasomes (D. Wu et al., 2017). Additionally, tetraspanin 4 and cholesterol are necessary for migrasome biogenesis (Y. Huang et al., 2019). These vesicles form by membrane swelling on retraction fibres, thin elongated structures that are pulled from the rear of the migrating cell as it moves forwards. Tetraspanin 4 is then recruited onto these swellings, which stabilizes the swelling as it grows in size and matures into a migrasome (Dharan et al., 2023). As the cell migrates

further, the retraction fibres break, releasing the migrasome into the extracellular space. The migrasome can be taken up by other cells or rupture, thus releasing its contents into the extracellular space. Like other EVs, the migrasome acts as a facilitator of intercellular communication (M. Zhu et al., 2021) and waste removal (Jiao et al., 2021). Interestingly, the cell can also deposit migrasomes in a specific location, where they can release signalling molecules that affect surrounding cells (D. Jiang et al., 2019). This has been shown to be important in embryogenesis, with impaired migrasome production affecting normal left-right asymmetry and being rescued by the injection of migrasomes from normal zebrafish embryos (D. Jiang et al., 2019).

1.3.2.4.4 Large Oncosomes

The term "oncosomes" was introduced in 2008, referring to any EV containing oncogenic cargo secreted by cancerous cells (Al-Nedawi et al., 2008). In the following year, a new subtype of EV derived from prostate cancer cells was identified (Di Vizio et al., 2009). These EVs were termed "large oncosomes" due to their uncommonly large size (ranging between 1 μm – 10 μm in diameter). Unlike oncosomes in general, large oncosomes are associated with the advanced stages of the disease, when the cells have acquired amoeboid characteristics (Di Vizio et al., 2012; Ciardiello et al., 2019). Similarly to other EVs, large oncosomes play an important role in cell-to-cell communication, especially in driving cancer progression (Minciacchi et al., 2017; S. Zhang et al., 2022).

1.3.3 EV Nomenclature

As seen throughout the history of EV research, these particles have been known by many names. This lack of consistency in the nomenclature has remained a key issue in this field, although this has improved in recent years. Roy et al., (2018) revealed that the most popular term used to refer to vesicles was “microparticles” (which can also refer to microparticles of iron oxide, often used as an imaging agent (Fouquet et al., 2022) and to synthesized drug delivery systems (Kállai-Szabó et al., 2024).

Even so, it is difficult to determine what researchers actually meant when using the term “exosome” (Gould & Raposo, 2013). Firstly, some used “exosomes” to refer to vesicles that are released by MVBs fusing with the plasma membrane. Others used this term to refer to all secreted vesicles that could have a physiological function. Others still used this term to refer to all vesicles isolated by differential centrifugation at 70,000 – 120,000 x g (Gould & Raposo, 2013).

In addition to this, researchers have also given a variety of names to EVs, mostly based on their function or the cell they are released from (e.g. “calcifying matrix vesicles” which are involved in the initiation of bone formation (Anderson, 1969), “tolerosomes” which induce immunological tolerance to dietary antigens (Karlsson et al., 2001) and “dexosomes” which are released by dendritic cells (Sakamoto et al., 2022).

The first meeting of the International Society for Extracellular Vesicles (ISEV) in 2012 attempted to address the issue of nomenclature but ultimately, researchers were unable to reach a consensus (Gould & Raposo, 2013). Regardless, the ISEV established guidelines in order to standardize terms in 2018, which were further updated in 2024 (Théry et al., 2018; Welsh et al., 2024). One of these was to push for the use of the generalised term “extracellular vesicles” in studies rather than the specification of subtype, in particular for exosomes and microparticles. This is due to several reasons. The classification of secreted EVs has historically been dependent on their size in addition to the expression of certain markers. However, there is an overlap in size between the largest of exosomes and the smallest of microparticles. In addition to this, while there are several classical protein markers associated with exosomes and MVs respectively, some “exosome” preparations have been positive for “microvesicle” markers and vice versa (Jeppesen et al.,

2019). Classical MV protein markers include the annexins A1 and A2 and flotillins. Classical exosomal markers include the tetraspanins CD9, CD63 and CD81, in addition to proteins associated with the ESCRT complex, namely tumour susceptibility gene 101 (TSG101) and ALG-2-interacting protein X (ALIX). In addition to this, not all exosomal and microvesicle preparations were found to be positive for their respective classical markers (Jeppesen et al., 2019).

Due to this overlap in size and this non-specificity of markers, distinguishing subtypes of EV is difficult. As a result, Théry et al., (2018) suggested that this distinction should not be made until their biogenesis has been confirmed through microscopy. Instead, the ISEV has pushed for the classification of EVs by size, with EVs with a diameter below 200 nm being classified as small EVs and EVs with a diameter over 200 nm being classified as medium/large EVs. This thesis will align with these guidelines.

1.3.4 EV Uptake

EVs are thought to contribute to intercellular communication in two ways. The first of these is by transmitting information to recipient cells through direct contact with receptors though their surface ligands, without the transfer of EV contents into the recipient cell. Several studies have found that EVs present ligands on their surface which are able to activate receptors on cells, thus activating signalling cascades (Raposo et al., 1996; Bitto et al., 2021). For example, cytotoxic T-cells and natural killer (NK) cells have been found to release EVs decorated with Fas ligand on their surface (Staufer et al., 2022). Upon the binding of the Fas ligand to receptors on the target cell, caspase-mediated apoptosis is initiated, showcasing a role of EVs in mediating apoptosis. This study also suggested that EVs are able to activate signalling pathways though concentrating ligand-receptor complexes to a small area on the cell membrane of the target cells, boosting receptor multimerization and signalling. A recent study also found that activated excitatory neurons were found to secrete EVs containing Notch1 and Notch2 proteins on their surface (Y.-Z. Wang et al., 2024). These were found to bind to Notch receptors on neurons, upon which the Notch pathway was activated but also resulting in the internalisation of the EV, therefore transferring its contents to the cell, the second mechanism.

The transfer of EV contents, including miRNA (Montecalvo et al., 2012; C.-Y. Kim et al., 2024), mRNA (J.-H. Wang et al., 2018; Y. Xing et al., 2023), mtDNA (Sansone et al., 2017; Puhm et al., 2019), lncRNA (X. Wu et al., 2021; Vilaça et al., 2024), proteins (S. Wu et al., 2021; Fujioka et al., 2025) and organelles (K. Xia et al., 2026), has been shown to affect the internal biological processes of the cell. EV internalisation is complex and can occur through various mechanisms. These have largely been sorted into two categories: 1) direct fusion of the EV and recipient cell and 2) endocytosis. The simplest method of EV uptake involves the direct fusion of the membrane of the EV and the plasma membrane of the recipient cell, allowing for the transfer of both membrane-associated and luminal constituents without the involvement of endocytic or lysosomal pathways (Montecalvo et al., 2012; Prada & Meldolesi, 2016). This process has been shown to be influenced by pH and membrane constitution (Morandi et al., 2022).

Nonetheless, EV uptake by recipient cells is more likely to occur via endocytosis (Costa Verdera et al., 2017; Hirosawa et al., 2025), with a variety of mechanisms including macropinocytosis, phagocytosis, lipid raft-mediated endocytosis, caveolin-mediated endocytosis and receptor-mediated endocytosis (also known as clathrin-mediated endocytosis) (Figure 1.8). These are briefly described below.

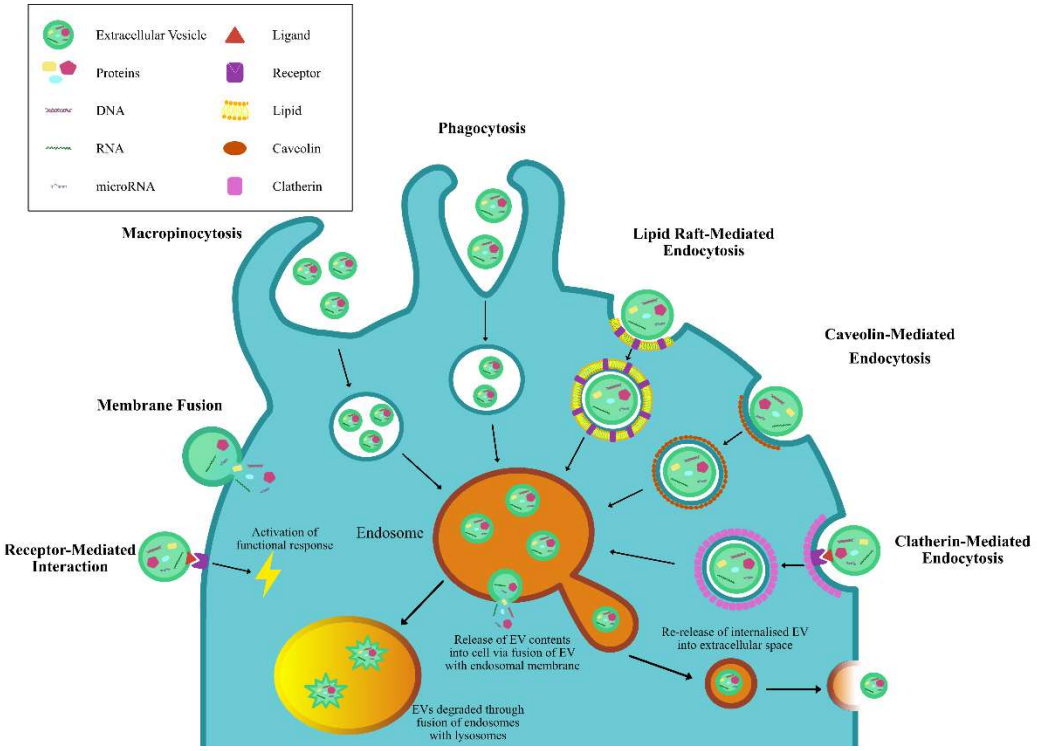


Figure 1.8 ***Mechanisms of EV uptake in the cell.*** *EVs can be internalised into a recipient cell by a variety of endocytic pathways, including micropinocytosis, phagocytosis, lipid – raft-, caveolin-, and clatherin-mediated endocytosis. Once EVs are internalised, they have been found to be localised in endosomes. The endosome can then go on to fuse with lysosomes where their contents, including EVs, are degraded. EVs can escape degradation by being recycled and re-released into the extracellular space or by fusing with the endosomal membrane, where their contents are released into the intercellular space. This release of their cargo can then result in phenotypic changes in the recipient cell. EVs do not have to be internalised in order to play a role in intercellular communication. Interactions between ligands found on the surface of EVs and receptors on the cell surface can result in the activation of signalling pathways. Additionally, EVs can fuse with the cell membrane, and release their contents into the intercellular space. Figure created by author in Affinity Designer (version 1.10.6.1665).*

Macropinocytosis, a form of non-selective fluid uptake by the cell which generates larger intracellular vesicles known as macropinosomes, is used to scavage macromolecules such as lipids and amino acids (reviewed in Wu et al., 2024 and Tu et al., 2025). Several studies have suggested that EVs may also enter cells through this mechanism (Costa Verdera et al., 2017; Brodeur et al., 2023; X. Lu et al., 2024). Phagocytosis has also been indicated as a mechanism by which EVs enter cells, primarily macrophages and other members of the mononuclear phagocyte system (MPS) (D. Feng et al., 2010; Mohning et al., 2018; Soni et al., 2022). However, other cell types have also been shown to phagocytose EVs, including vascular endothelial cells (X. Qin et al., 2022). Regardless, the MPS has been a considerable obstacle in the field of therapeutics, as EVs used to deliver

therapeutics are cleared quickly from the blood by its members (Matsumoto et al., 2020; Warashina et al., 2022). However, this process also depends on the characteristics of the EVs. For example, the presence of CD47 on the surface of EVs was found to inhibit their internalization via phagocytosis (Kamerkar et al., 2017; Y. Li et al., 2022).

Lipid rafts, micro-domains found in the plasma membrane which are enriched in cholesterol and glycosphingolipids (reviewed in Ouweneel et al., 2020), have been found to play vital roles in both vesicle formation and uptake (Escrevente et al., 2011; Sapoń et al., 2023). Two mechanisms of how rafts are involved in endocytosis have been suggested: firstly, that intracellular vesicle budding is triggered by enzymatic action on phospholipids and sphingolipids, resulting in changes in lipid shape (Trajkovic et al., 2008; Janas et al., 2015). Secondly, proteins and lipids found in these microdomains might interact with coat proteins, leading to budding and vesicle formation (Bonifacino & Glick, 2004; Sapoń et al., 2023). These lipid rafts are also involved in both caveolin-mediated endocytosis, where palmitoylated caveolin-1 binds to cholesterol in the lipid raft, causing the formation of caveola (Murata et al., 1995; Matthaeus et al., 2022).

Cell-specific EV internalisation occurs through receptor-mediated endocytosis, as both the EV and the recipient cell need to possess the right combination of ligand and receptor. For example, CD63+ EVs were found to be taken up by both neurons and astrocytes but CD63- EVs were specifically endocytosed by neurons alone (Laulagnier et al., 2018). This mechanism of endocytosis is also known as clathrin-mediated endocytosis, as during the internalisation of the EV from the surface into the cell, clathrin-coated vesicles are formed. After the receptor is stimulated by its ligand binding, clathrin is recruited to the site, forming a shallow indentation. As this indentation matures, it forms a spherical pit, coated with polymerised clathrin, which eventually invaginates completely, forming a vesicle that is cleaved from the membrane (Zimmer & Goepferich, 2023).

After uptake, internalised EVs have been found to co-localise with endosomes (Heusermann et al., 2016; Z. Yao et al., 2018). Upon maturing, endosomes are known to fuse with lysosomes, where these EVs are degraded (B. Tong et al., 2026). However, endosomal sorting can also result in the re-release of endocytic cargo,

with one study showing that internalised EVs can be re-released into the extracellular space by the recipient cell (O'Brien et al., 2022). Additionally, studies have shown that EVs are able to escape endosomes by fusing with the endosomal membrane, resulting the release of their contents into the cytoplasm of the recipient cell (Somiya & Kuroda, 2021; Morandi et al., 2022).

The accumulation of EVs in recipient cells therefore is determined by the rate of EV uptake, recycling and degradation. Studies exploring the quantitative rates of EV uptake are limited. However, reported EV uptake varies widely, from a low spontaneous rate (~1% at 1 hour) (Bonsergent et al., 2021) to ~6% (sEVs) and ~18% (lEVs) (Hirose et al., 2022). On the other hand, cargo release into the cytosol is dependent on EV fusion with the plasma membrane or endosomal membrane. Although EV uptake was limited in their study, Bonsergent et al., 2021 also reported that only ~30% of the internalised EVs delivered their cargo into the cytosol, suggesting that this is not a highly efficient process.

1.4 Astrocyte EVs in the brain

Regardless of subtype, EVs are known to carry genetic material, proteins, lipids and signalling nucleotides. Although the mechanisms of how cargo is sorted into EVs is still not fully understood, there is some evidence suggesting that cells specifically sort cargo into EVs. A landmark study published in 2007 showed that the mRNA contained within EVs from human and murine mast cells was translated in recipient cells (Valadi et al., 2007), proving that genetic information could be horizontally transferred from cell to cell. As such, studies have shown that EVs play important roles as mediators of intercellular communication. In particular, they are able to function over long distances and are able to modulate gene expression in distant cells. In the brain, communication between the cells of the NVU is fundamental for different biological processes such as brain development and maintenance of homeostasis (Faust et al., 2025; Marty-Lombardi et al., 2024). EVs derived from astrocytes have been recognised as a significant contributor to these processes.

1.4.1 Physiological Roles

Healthy astrocyte-derived EVs have been shown to play important roles in the CNS. Glial derived sEVs containing synapsin I were found to promote neurite growth and the survival of neurons upon treatment with hydrogen peroxide or oxygen-glucose deprivation (OGD) (Wang et al., 2011). Astrocyte EVs, but not EVs isolated from neurons or glioma, have also been found to promote the formation of dendritic spines and synapses in neurons through fibulin-2 mediated activation of TGF-β signalling (M. R. Patel & Weaver, 2021). Additionally, they have been found to promote neuronal postsynaptic function (Levy-Myers et al., 2023). EVs derived from young astrocytes were found to support oligodendrocyte differentiation (Willis et al., 2020).

EVs from astrocytes can carry growth factors such as vascular endothelial growth factor, which is known to regulate the permeability of endothelial cells (Proia et al., 2008; Upadhya, Zingg, et al., 2020). While EVs from neural progenitor cells, which can differentiate into neurons and glial cells, were found to have a beneficial effect on permeability (Zhang et al., 2021), the effects of astrocyte-derived EVs on the endothelial cells that make up the microvasculature of the brain has yet to be explored.

1.4.2 During neuroinflammation

The cargo of astrocyte EVs has been found to change during neuroinflammation (Chaudhuri et al., 2018; Goetzl et al., 2018). Astrocyte EVs have been found to play both protective and detrimental roles during disease.

1.4.2.1 Protective Roles of Astrocyte EVs during Neuroinflammation

Astrocyte EVs have been shown to be neuroprotective during acute cerebral injury, such as stroke. EVs isolated from astrocytes in an *in vitro* model of stroke (OGD) were able to attenuated neuronal death induced by OGD by downregulating inflammatory pathways (Deng et al., 2018; R. Sun et al., 2024; L. Xu et al., 2019).

Astrocyte EVs have also been shown to be protective during chronic neurological disorders. Astrocyte EVs were also able to attenuate neuronal death in an *in vivo* model of MS, experimental autoimmune encephalitis (EAE) (Pei et al., 2019). Astrocytes were found to package small heat shock protein αB-crystallin (CRYAB) into EVs during EAE, which downregulated pro-inflammatory cytokine expression

in astrocytes and microglial cells (Y. Guo et al., 2019). Modelling AD, astrocytes stimulated with amyloid β released EVs containing Hsp27, which was shown to interact with and potentially sequester amyloid β (Nafar et al., 2015). EVs from patients with neuromyelitis optica spectrum disorder (an autoimmune astrocytopathy) were found to contain increased levels of apolipoprotein E, which was suggested to be protective after injection of an APOE-mimic protein into a mouse model of this disorder resulting in alleviation of lesions, astrocyte loss, reactive microglial and demyelination (S. Jiang et al., 2024).

1.4.2.2 Detrimental Roles of Astrocyte EVs during Neuroinflammation

Upon exposure to inflammatory cytokines, astrocytes released EVs that were found to reduce neurite formation, diminish dendritic complexity and exacerbate neurodegeneration (Chaudhuri et al., 2018; Datta Chaudhuri et al., 2020). Additionally, astrocytes stimulated with LPS released EVs that enhanced the vulnerability of dopaminergic neurons to neurotoxins (S. Mao et al., 2015).

During disease, astrocyte-derived EVs seem to contribute to disease pathogenesis. Astrocytes carrying C9orf72 mutations (as a model of amyotrophic lateral sclerosis (ALS)) were found to release EVs that contributed to the degradation of motor neurons (Varcianna et al., 2019). Astrocyte-derived EVs isolated from patients with epilepsy were found to contain increased levels of TNFα and decreased levels of brain-derived neurotropic factors in comparison to controls, which the authors suggested may result in impaired neuroplasticity and increased inflammation. (S. Wang, Zhang, et al., 2025). Obesity-associated cognitive impairment can also be attributed to astrocyte-derived EVs which were found to contribute to synapse injury in the hippocampus (L. Wu et al., 2025)

Astrocytes are also able to amplify inflammation via the secretion of EVs, even in the peripheral system (Dickens et al., 2017). EVs released by ethanol-activated astrocytes have been found to increase inflammatory proteins in naïve neurons (Ibáñez et al., 2019). Additionally, astrocytes exposed to morphine have been found to shed EVs that activate TLR-7 in microglia and impair microglial phagocytosis (G. Hu et al., 2018; K. Liao et al., 2020) and contribute to pericyte loss at the BBB (K. Liao et al., 2022).

1.5 Thesis Aims

Although astrocytes and endothelial cells are in close proximity to each other, EV mediated communication remains essential for complex biological signalling. Firstly, EVs can carry a wide variety of molecules, which are protected from extracellular degradation by the lipid bilayer (Jeppesen et al., 2019; De Sousa et al., 2023). This allows for the activation of multiple different pathways in recipient cells, unlike when solitary ligands bind to single receptors. Additionally, and perhaps more importantly, EVs allow cells to communicate across long distances (Ofir-Birin et al., 2018; Gerwing et al., 2020). This is particularly relevant in disease, as EVs can be involved in the pathogenic mechanisms of disease progression, as seen by their role in cancer metastasis (Sun et al., 2022; Asao et al., 2023).

Neuroinflammation is a core hallmark of many neurological disorders, including Alzheimer's disease, stroke and depression (reviewed in Gorji, 2022; Shi & Yong, 2025), playing a crucial role in both injury and recovery. During disease, EVs released by cells in the CNS influence pathogenesis, development, and/or recovery through their role as mediators of communication (K. Liao et al., 2022; S. Wang, Zhang, et al., 2025). They have been shown to propagate neuroinflammation and neurodegeneration through the dissemination of toxic proteins and pro-inflammatory molecules (Prada et al., 2018; Scheld et al., 2026). However, studies exploring the effects of EVs on the BBB are limited. Neuronal EVs have been found to modulate the integrity of the BBB (B. Xu et al., 2017). Peripheral EVs have been found to drive neuroinflammation and BBB dysfunction after alcohol consumption (Togre et al., 2024). Although signalling from astrocytes is known to modulate barrier function and astrocytes, limited studies have explored the effect of astrocyte-derived EVs on BBB integrity, both physiologically and during disease. It is therefore hypothesised that EVs isolated from healthy astrocytes improve barrier function, while EVs derived from inflamed astrocytes increase permeability through changes in TJ expression levels (Figure 1.9).

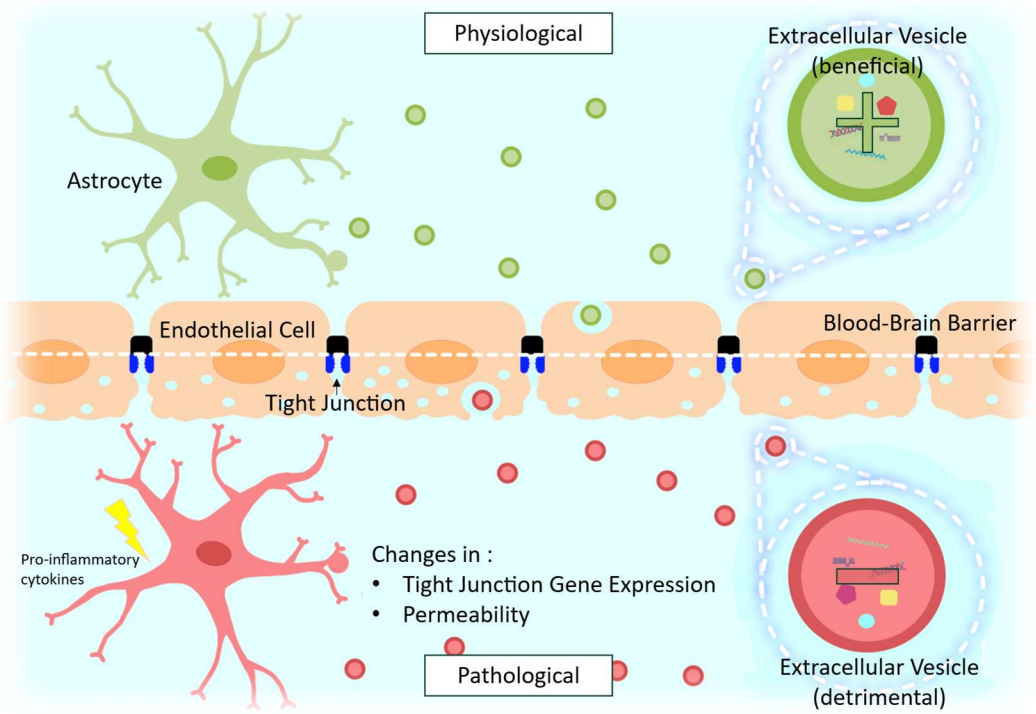


Figure 1.9 ***A schematic representation of the overall hypothesis of this thesis. Healthy*** *astrocytes release EVs containing cargo beneficial to the barrier function of endothelial cells. However, during neuroinflammation, activated astrocytes release EVs that negatively affect the barrier properties of endothelial cells. Figure created by author in Affinity Designer (version 1.10.6.1665).*

The core role of endothelial cells is to regulate vascular permeability, a function that is especially critical in the brain where they form the highly selective BBB. Dysfunction of the BBB has been implicated in many neurological disorders. Additionally, astrocytes have been shown to package miRNAs, which alter gene and protein expression levels, in EVs. As TJs form the main structural components of the paracellular barrier, measuring the mRNA and protein expression levels of the main TJ proteins after treatment with the full astrocyte secretome or astrocyte-derived EVs, could reveal how these treatments could affect the structural integrity of the BBB. In addition, permeability assays can capture the molecular passage of the cells after treatment, allowing for the exploration of how astrocytes could indirectly affect the functional integrity of the BBB.

Therefore, this project has the potential to provide insight into communication within the NVU, specifically by uncovering a novel mechanism by which astrocytes control BBB integrity and potentially, TJ gene and protein expression. Characterizing the physiological role of astrocyte-derived EVs in maintaining BBB

homeostasis may provide a foundation for the development of therapeutic strategies targeting BBB dysfunction, with the aim of preserving neurovascular stability in neurological disorders. Furthermore, these findings could enhance understanding of the mechanisms underlying the propagation of neuroinflammation within the CNS, potentially identifying novel therapeutic targets to attenuate or reverse inflammatory processes.

This thesis aims to explore the effects of EVs derived from primary human astrocytes on the paracellular barrier function of human primary brain microvascular endothelial cells. To do this, it has been planned to:

- Explore the effects of astrocyte conditioned media on the properties of endothelial cells, mainly viability, permeability and TJ gene and protein expression.
- Optimise a method of isolating EVs from conditioned media for use in future experiments.
- Explore the effect of astrocyte conditioned media derived EVs on the permeability of endothelial cells as well as their effects on TJ gene and protein expression.
- Explore the effect of EVs derived from inflamed astrocytes on the permeability of endothelial cells as well as their effects on TJ gene and protein expression.

Chapter 2 :
Materials and Methods

2.1 Materials

2.1.1 Reagents and Chemicals

Applied Biosystems (USA)	Catalogue No
High-Capacity cDNA Reverse Transcription Kit	4368814

Cell Signalling (USA)	Catalogue No
Anti-mouse IgG, HRP-linked antibody	7076S
Anti-rabbit IgG, HRP-linked antibody	7074S

Cell Systems Inc., (USA)	Catalogue No
Human Brain Microvascular Endothelial Cells (HBMvEC)	ACBRI 376

Gibco (UK)	Catalogue No
Distilled Water	15239-162
Dubecco's Phosphate Buffered Saline	14190-094
Human interleukin-1 alpha (IL-1α) Recombinant Protein	PHC0014
Penicillin Streptomycin	15140-122
Trypsin-EDTA (0.5%)	15400-054

Innoprot (Spain)	Catalogue No
Astrocyte Media Kit	P60101
Human Astrocytes	P10251

Invitrogen (USA)	Catalogue No
Diethyl Pyrocarbonate (DEPC) Treated Water, Pyrogen-free	46-2224
eBioscience™ Lipopolysaccharide (LPS) Solution (500X)	00-4976-93
SYBR®Safe DNA Gel Stain	S33102
TRIzol®	15596-018

Lifeline® Cell Technology (USA)	Catalogue No.
VascuLife® Basal Medium	LM-0002
VascuLife® EnGS-Mv LifeFactors Kit	LS-1035

Malvern Panalytical (UK)	Catalogue No.
Capillary Cuvettes	ZSU0003

Medguard Healthcare (Ireland)	Catalogue No.
BD Emerald 10 mL Syringe Luer Slip	307736

Millipore (USA)	Catalogue No.
Immobilin®- PSQ PVDF membrane, pore size: 0.2 µm	ISEQ00010
Immobilin® Forte Western HRP Substrate	WBLUF0100

Pierce Chemicals (UK)	Catalogue No.

BCA Protein Assay Kit	23225
Micro BCA Protein Assay Kit	23235

Promocell (Germany)	Catalogue No.
Cryo-SFM (Cryomedia)	C-29912

Roche Diagnostics (Switzerland)	Catalogue No.
cOmplete™, EDTA-free Protease Inhibitor Cocktail	4693132001
FastStart Essential DNA Green Master	57220100

Sigma-Aldrich (UK)	Catalogue No.
2-Mercaptoethanol	M6250
2-Propanol	33539
Acetone	34850
Acrylamide/Bis-acrylamide Solution	A3574
Agarose	A5093
Ammonium Persulfate	A9164
Bovine Serum Albumin (BSA)	A2153
Bromophenol Blue Sodium Salt	B6131
Chloroform	C2432
Complement Component 1q (C1q), Human	204876
Crystal Violet	C3886
Ethylenediaminetetraacetic Acid Disodium Salt Dihydrate (EDTA)	E5134
Ethyl Alcohol (Ethanol), pure 200 proof	E7023
Fluorescein Isothiocyanate-Dextran-40kDa (FITC-Dextran)	FD40S
Formaldehyde Solution	F8775
Glycerol	G6279
Glycine	G8898
HEPES	H4034
Methanol	34860
Poly-DL-lysine hydrobromide	P9011
Polyethylene Glycol (PEG) 6000	8.07491
Ponceau S Solution	P7170
Potassium Chloride	P9541
Potassium Phosphate Monobasic	P5379
Sodium Chloride	S3014
Sodium Deoxycholate	D6750
Sodium Dodecyl Sulfate (SDS)	L3771
Sodium Fluoride	S7920
Sodium Hydroxide	S8045
Sodium Orthovanadate	S6508
Sodium Phosphate Dibasic	S5136
Sucrose	S0389
Sterile Filtered Water	W3500
N,N,N’,N’-Tetramethylethylenediamine (TEMED)	T9281
Tris Acetate-EDTA Buffer	T9650
Triton™ X-100	X-100
Trizma® Hydrochloride (Tris HCL)	T3253
Tumor Necrosis Factor-α (TNFα), Human	T6674

Sarstedt (Germany)	Catalogue No
6 Well Plate	83.3920
6 Well Plate TC-Insert, pore size: 0.4 µm	83.3930.041
12 Well Plate	83.3921.300
12 Well Plate TC-Insert, pore size: 0.4 µm	83.3931.041
96 Well Plate	83.3924
96 Well LightCycler Plate, White (PCR)	72.1982.202
15 mL Screw Cap Tube	62.554.502
50 mL Screw Cap Tube	62.559.001
Biosphere SafeSeal Tube, 1.5 mL	72.706.200
Cell Scraper, 2-position blade	83.3950
CryoPure Tube 1.6 mL white	72.380
Multiply-Pro cup 0.2 mL, PP	72.737.002
Multiply-Pro cup 0.5 mL, PP	72.735.002
Pipette tip, 10 µl	70.3010
Pipette tip, 200 µl	70.3030
Pipette tip, 1000 µl	70.1181
qPCR film, transparent	95.1999
Serological 2 mL Pipette	86.1252.001
Serological 10 mL Pipette	86.1254.001
Syringe Filter, Filtropur S, PES, pore size: 0.2 µm	83.1826.001
Tissue Culture Dish 100, Standard	83.8902

Thermo Fisher Scientific (UK)	Catalogue No
GeneRuler™ 100 bp DNA Ladder Plus	SM0321
Nalgene™ Oak Ridge High-Speed PPCO Centrifuge Tubes, 30 mL	3119-0030
PageRuler Plus Prestained Protein Ladder	26619
Parafilm Wrap	PM992

vWR International Ltd. (UK)	Catalogue No
Tween®20	66368

Table 2.1 Primer Information (Obtained from Eurofins MWG Operon (Germany))

Target	Sequence	Product Size
Human GAPDH Forward (F)	5' – gag tca acg gat ttg gtc gt – 3'	238 bp
Human GAPDH Reverse (R)	5' – ttg att ttg gag gga tct cg – 3'	
Human GFAP F	5' – gaa gca gat gaa gcc acc ct – 3'	213 bp
Human GFAP R	5' – cat tgc ctc ata ctg cgt gc – 3'	
Human AQP4 F	5' – gcc atc att gga gca gga atc c – 3'	115 bp
Human AQP4 R	5' – act caa cca gga gac cat gac c – 3'	
Human Kir4.1 F	5' – gag tcc tga caa aag atg gtc gc – 3'	118 bp
Human Kir4.1 R	5' – agc ttg tag cgc cac tgc atg t – 3'	
Human Occludin F	5' – cct tca ccc cca tct gac ta – 3'	224 bp
Human Occludin R	5' – gca ggt gct ctt ttt gaa gg – 3'	
Human Claudin 5 F	5' – gag gcg tgc tct acc tgt tt – 3	240 bp
Human Claudin 5 R	5' – agt act tca cgg gga agc tg – 3'	
Human vWF F	5' – cca gat ttg cca ctg tga tg – 3'	220 bp
Human vWF R	5' – aaa ggc ctt cag cac ttc aa – 3'	

2.1.2 Reagents and Chemicals used by Macrogen (South Korea)

Illumina (USA)	Catalogue No
TruSeq Stranded Total RNA with Ribo-Zero H/M/R kit	RS-122-2201

Invitrogen (USA)	Catalogue No
Quant-it™ RiboGreen RNA Assay	R11490

Qiagen (Germany)	Catalogue No
RNeasy Mini Kit	74104

2.1.3 Apparatus

Block Heater	Stuart Scientific (UK)
BrightLine® Haemocytometer	Reichart (USA)
Centrifuge	Eppendorf, (UK)
Cryo-Freezing Container	Nalgene (USA)
Digital Disc Rotator	CliniSciences (France)
G: BOX Chemi-Luminescence Analysis System	Syngene (India)
HERACell CO_2 Incubator	Thermo Fisher (UK)
Holten Laminair Flow Cabinet	Thermo Fisher (UK)
LightCycler 96	Roche Diagnostics (Switzerland)
Low Volume Disposable Sizing Cell Holder	Malvern Panalytical (UK)
MiniAmpPlus Thermal Cycler	Applied Biosystems (USA)
Nanodrop 1000 Spectrophotometer	Thermo Fisher (UK)
Nikon Eclipse TS100 Microscope	Nikon (Japan)
Optima XL-80 Ultracentrifuge	Beckman Coulter (USA)
Orbital Shaker	Stuart Scientific (UK)
Pierce G2 Fast Blotter	Thermo Fisher (UK)
TECAN Infinite M200 Pro	Tecan (Switzerland)
Vortex	Stuart Scientific (UK)
Zetasizer Ultra	Malvern Panalytical (UK)

2.1.4 Apparatus used by Macrogen (South Korea)

Victor Nivo Multimode Microplate Reader	PerkinElmer (USA)
NovaSeq X	Illumina (USA)
4200 TapeStation System	Agilent (USA)

2.1.5 Preparations of stock buffer solutions

2.1.5.1 RNA Isolation and Quantitative Polymerase Chain Reaction

Agarose Gel Loading Buffer

Sucrose	40% (w/v)
Bromophenol Blue	0.25% (w/v)

2.1.5.2 SDS PAGE and Immunoblotting

Mild Stripping Buffer

Glycine	200 mM
SDS	3.5 mM
Tween 20	1% (v/v)

Components were dissolved in deionised water, and the pH of the solution was adjusted to 2.2 using HCl and NaOH, as required.

RIPA Cell Lysis Buffer Stock (1.28x)

HEPES, pH 7.5	64 mM
Sodium Chloride	192 mM
Triton X-100	1.28% (v/v)
Sodium Deoxycholate	0.64% (w/v)
SDS	0.128% (w/v)

RIPA Cell Lysis Buffer (1x)

1.28x RIPA Stock	1x
Sodium Fluoride	10 mM
EDTA, pH 8.0	5 mM
Sodium Phosphate	10 mM
Sodium Orthovanadate	1 mM
Protease Inhibitors	1x

Running Buffer (1x)

Tris-HCL, pH6.8	25 mM
Glycine	192 mM
SDS	0.1% (w/v)

Sample Solubilisation Buffer (SSB) (4x)

Tris-HCL, pH6.8	250 mM
SDS	8% (w/v)
Glycerol	40% (v/v)
2-Mercaptoethanol	4% (v/v)
Bromophenol Blue	0.008% (w/v)

Filter the solution using a 0.2 µm filter

Phosphate Buffered Saline (PBS), pH 7.4 (20x)

Sodium Chloride	16% (w/v)
Potassium Chloride	0.4% (w/v)
Sodium Phosphate Dibasic	2.88% (w/v)
Potassium Phosphate	0.48% (w/v)

Components were dissolved in deionised water and the pH of the solution was adjusted to 7.4 with HCl and NaOH, as required.

Transfer Buffer (1x)

Tris-HCL, pH6.8	25 mM
Glycine	192 mM
SDS	0.1 (w/v)
Methanol	20% (v/v)

2.2 Methods

2.2.1 Culture and Maintenance of Primary Cells

2.2.1.1 Human Astrocyte Culture

Human Astrocytes were isolated from post-mortem human brain tissue. Two vials of astrocytes were used. One was used for the generation of conditioned media for conditioned media experiments (Chapter 3) as well as for the optimisation of 1) EV isolation (Chapter 4) and 2) EV treatment (Chapter 5). The donor was a Caucasian male, aged 28, with no chronic disorders. The cause of death was acute myocardial infarction. The other vial was used for the generation of conditioned media from healthy and inflamed astrocytes (used in Chapter 5 and 6). Information regarding the donor is unknown. They were reported to test negative for HIV-1, HBV, HCV, and *Mycoplasma spp* by the company and were characterised via the expression of glial fibrillary acidic protein (GFAP) both by the company and prior to experimentation (see Section 2.2.1.1).

Cells were cultured on poly-DL-lysine coated (2 μg/cm^2) tissue grade plasticware as per manufacturer's guidelines. Poly-DL-lysine (2 μg/cm^2) was added to the culture dish the day before subculturing and left to incubate overnight at 37°C. This solution was removed, and the vessel washed once with sterile water prior to the addition of cells and growth medium.

Cells were grown in Astrocyte Medium. This media contains Astrocyte Growth Supplement (1%), Foetal Bovine Serum (FBS) (2%) and penicillin/streptomycin solution (1%). Cells were routinely cultured in tissue culture dishes (58.8 cm^2) for the generation of conditioned media. Cells were cultured in 6 well plates for experimental work. Cells were used between passages 2-5 and maintained in a humidified atmosphere of 5% CO_2/95% air at 37°C in a HERACell CO_2 Incubator.

2.2.1.2 Human Brain Microvascular Endothelial Cell (HBMvEC) Culture

HBMvECs are adherent cells which form a confluent, contact-inhibited monolayer over time. HBMvECs were isolated from a Caucasian male, aged 26, with no chronic conditions, who had died from acute myocardial infarction. These cells

were expanded in early passages in order to be used for the entire study. These cells were reported to test negative for the presence of *Mycoplasma spp.* and characterised via the expression of vWF.

Cells were cultured in VascuLife® Basal Medium supplemented with VascuLife® EnGS-Mv LifeFactors Kit and penicillin/streptomycin. The final constituents and their concentrations were: FBS (5%), L-Glutamine (10 mM), Ascorbic Acid (50 µg/mL), Heparin Sulfate (0.75 U/mL), Hydrocortisone Hemisuccinate (1 µg/mL), recombinant human Epidermal Growth Factor (rhEGF) (5 ng/mL), EndoGRO-LS Supplement (0.2%), Penicillin (100 U/mL) and Streptomycin (10 µg/mL). Cells were routinely cultured in tissue culture dishes (58.8 cm^2) for the generation of conditioned media. For experimental work, HBMvECs were cultured in 6-well and 12-well transwell inserts in 6-well and 12-well plates respectively, as well as directly in 96-well plates. Cells were used between passages 6-15 and maintained in a humidified atmosphere of 5% CO_2/95% air at 37°C in a HERACell CO_2 Incubator.

2.2.1.3 Subculturing of Cells

Cells were typically passaged between 70 - 90% confluency, confirmed through light microscopy. For astrocytes only, the plastic-ware was coated with Poly-DL-lysine (2 µg/cm^2) prior to seeding. Growth Medium and Trypsin/EDTA were pre-warmed to 37°C in a water bath.

For trypsinisation, the growth medium was removed, and the culture dish was washed briefly 1-2 times with sterile PBS to ensure the removal of any residual α1-antitrypsin, an inhibitor of trypsin found in serum. After washing, 2 mL of Trypsin/EDTA was added to the vessel and the vessel was placed in the incubator for 5-10 minutes. During this time, the cells were monitored until the majority had displayed a rounded morphology and had detached. An equal volume of growth media to Trypsin/EDTA was added to the dish to inhibit further trypsinization. The cell suspension was then centrifuged at 190 x *g* for 5 minutes. The supernatant was removed, and the cell pellet was resuspended in media. The cells were counted as described in Section 2.2.1.4 and either seeded to an appropriate density for experimental procedures (described in Section 2.2.4) or used for the propagation of

the cell line by being seeded at 5,000 cells/cm^2 (astrocytes) or 35,000 cells/cm^2 (HBMvECs).

2.2.1.4 Cell counting

Cell counts were performed using a haemocytometer prior to sub-culturing cells in order to ensure accurate reproducibility of experiments and to assess cell densities for sub-culturing and cryopreservation. 10 µL of the cell suspension was loaded into the haemocytometer chamber via capillary action. The number of cells was calculated as per the following equation:

$$\frac{Cell\ Number\ x\ 10^4\ (Conversion\ Factor)}{Number\ of\ Squares\ Counted} = Total\ cells/mL$$

2.2.1.5 Cryogenic preservation and recovery of cells

For long term storage, astrocytes and HBMvECs were preserved in a liquid nitrogen cryo-freezer unit. After trypsinization, cells were spun at 190 x *g* for 5 minutes. The supernatant was completely removed, and the pellet was resuspended in cryo-medium. Cell suspensions were placed in sterile CryoPure cryovials and stored in a Mr. Freeze® cryo-freezing container before being placed in a -80°C freezer. The Mr. Freeze® container ensured the cryovials were cooled at a rate of -1°C/min, minimizing cell damage during freezing. After 24 hours at -80 °C, the cryovials were transferred to a liquid nitrogen cryo-freezing container until further required.

For the recovery of cells, cryovials were warmed rapidly to 37°C in a water bath. Once fully thawed, the contents were quickly transferred to poly-DL-lysine coated (astrocytes only) 58.8 cm^2 dishes containing pre-warmed growth media. After 24 hours, the dishes were inspected via phase-contrast microscopy to inspect adherence and morphology of the cells. Following this, all growth media was aspirated, and the vessels were washed with sterile PBS to remove any residual DMSO. Fresh pre-warmed medium was then added to the cells.

2.2.2 Extracellular Vesicle Isolation

2.2.2.1 Generation of conditioned media

For both cell types, media was collected between 60 - 90% confluency. Briefly, media was conditioned on cells for up to 48 hours. Upon completion of the time course, this media was aspirated from the cells and replaced with fresh media. The incubated media was centrifuged at 1500 x *g* for 15 minutes before the supernatant was decanted into a new 50 mL tube. Conditioned media was stored at -20°C. Frozen media was thawed for approximately 2 hours at room temperature or overnight at 4°C before EV isolation. Three methods – microvesicle isolation (Section 2.2.2.2), differential centrifugation (Section 2.2.2.3), and ExtraPEG (Section 2.2.2.4) – were used to isolate EVs.

2.2.2.2 Protocol for Microvesicle Isolation

EVs were isolated using the microvesicle isolation method as applied in previous publications (F. A. Martin et al., 2014). Thawed media was centrifuged at 300 x *g* for 10 minutes. The resulting supernatant was decanted into a new falcon tube and centrifuged at 2500 x *g* for 20 minutes. The supernatant from this step was then transferred to an ultracentrifugation tube and centrifuged at 20,000 x *g* for 70 minutes using a Type 70 Ti Fixed-Angle Titanium Rotor. The resulting pellet at this step contained microvesicles and contaminating proteins. The supernatant was removed, and the pellet was washed by being resuspended in 1 mL of PBS, before being transferred to a microcentrifuge tube. This resuspension was then centrifuged at 17,000 x *g* for 70 minutes to isolate the washed EVs and the pellet resuspended in either PBS, TRIzol®, or RIPA buffer (see Section 2.1.5.2), depending on the downstream process.

2.2.2.3 Protocol for EV Isolation via Differential Centrifugation

The differential centrifugation method used was based on the protocol by Théry et al. (2006), with modifications. Briefly, thawed media was centrifuged at 300 x *g* for 10 minutes. The supernatant was decanted into a new falcon tube and centrifuged at 2000 x *g* for 20 minutes. The resulting supernatant was then transferred to an ultracentrifuge tube and centrifuged at 10,000 x *g* for 30 minutes using a Type 70

Ti Fixed-Angle Titanium Rotor. Next, the supernatant was transferred to a new ultracentrifuge tube, and one side of this tube was marked so that the pellet could be located. After a centrifugation step (maximum speed 50,000 x *g* for 70 minutes), the supernatant was discarded, and the pellet was resuspended in 1 mL of PBS. This pellet contained extracellular vesicles and contaminating proteins. The resuspension was transferred to a new ultracentrifuge tube and PBS was added to fill the tube to avoid tube collapse. This resuspension was then centrifuged at 50,000 x *g* for 70 minutes and the pellet resuspended in either PBS, TRIzol®, or RIPA buffer, depending on the downstream process

2.2.2.4 Protocol for EV isolation using ExtraPEG

The ExtraPEG method for isolating EVs was based on the protocol developed by Rider et al. (2016), with modifications. Briefly, thawed media was centrifuged at maximum speed on a benchtop centrifuge (3000 x *g*) for 45 minutes. The supernatant from this step was then syringe-filtered through a 0.20 µm filter into a new 50 mL tube. 50% polyethylene glycol-6000 (PEG) was added to the filtered supernatant so that the final concentration of PEG in the solution was 10%. 3.75 M NaCl was added to this solution (to a final concentration of 75 mM). The solution was inverted 3 - 4 times before being incubated at 4°C overnight (to a maximum of 16 hours). The solution was then centrifuged at 1500 x *g* for 30 minutes in a benchtop centrifuge. The wash step for this protocol involved resuspension of the pellet in 1 mL of 0.9% NaCl and centrifugation at maximum speed on an available centrifuge (17,000 x *g*) for 2 hours and 10 minutes. Depending on the downstream process, the pellet was resuspended in either PBS, TRIzol®, or RIPA buffer.

2.2.2.5 Zetasizer Ultra

The size range of isolated EVs was measured by using a Malvern Zetasizer Ultra. This instrument uses dynamic light scattering (DLS) to measure particle hydrodynamic diameter. DLS measures the fluctuations of small particle scattering over time to calculate particle size. Samples were measured using a low volume disposable sizing cell, which allows for low volume (3 µL minimum) samples to be read. A disposable capillary tube was dipped into the sample, and the sample was

drawn up through capillary action. The ends were then sealed with clay. The capillary was then placed into the Zetasizer.

2.2.3 Cell Treatments

2.2.3.1 Conditioned Media Treatments

Conditioned media (see Section 2.2.2.1) was used as a cell treatment. Non-conditioned media was used as control. This media was also incubated for 48 hours but without cells in the vessel. The conditioned media and controls are described in Table 2.2. Media was aspirated from the vessel upon completion of the time course and centrifuged at 1500 x *g* for 15 minutes. The supernatant was decanted into a new 50 mL falcon tube and stored at -20°C. Both were thawed at room temperature. Once thawed, media were diluted with fresh (i.e., straight out of the bottle) endothelial media so that the final concentrations of the conditioned media were 50% or used undiluted (100%). Figure 2.1 shows a summary of these steps. These were then warmed in a water bath to 37°C prior to use as treatment.

Table 2.2: Preparation of Conditioned Media

Conditioned Media	Media used	Cells
Astrocyte Conditioned Media (ACM)	Astrocyte Medium (Innoprot, Spain)	Astrocytes
Astrocyte Media (AM)	Astrocyte Medium (Innoprot, Spain)	-
Endothelial Conditioned Media (ECM)	Vascular Cell Basal Medium supplemented with Microvascular Endothelial Cell Growth – BBE (ATCC, USA)	HBMvECs
Endothelial Media (EM)	Vascular Cell Basal Medium supplemented with Microvascular Endothelial Cell Growth – BBE (ATCC, USA)	-
Fresh Endothelial Media (*used as a control and as a dilutant.)*	Vascular Cell Basal Medium supplemented with Microvascular Endothelial Cell Growth – BBE (ATCC, USA)	-

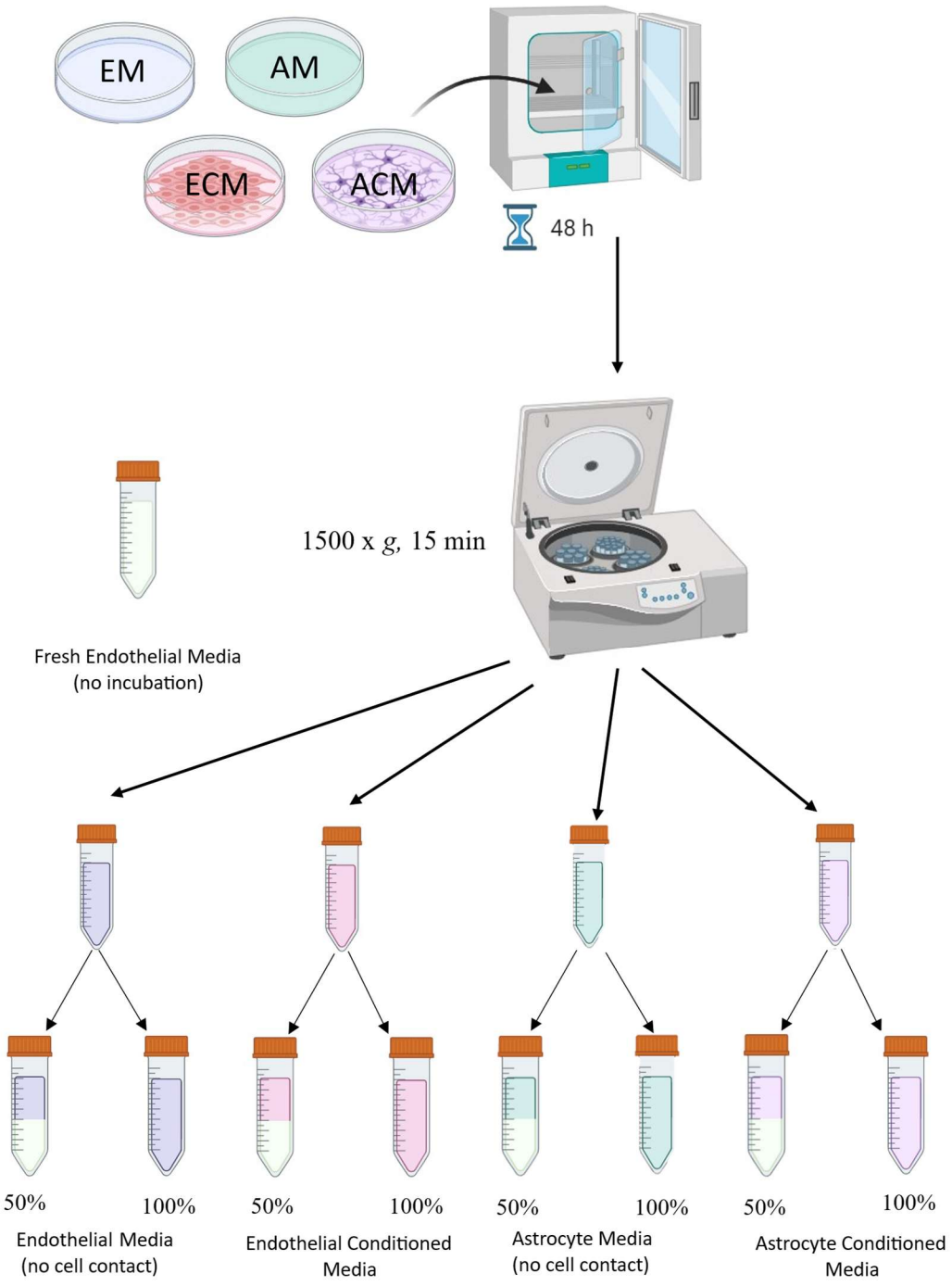


Figure 2.1 ***A summary diagram for the preparation of conditioned media for treatment of cells.*** *Both endothelial and astrocyte medias were incubated for 48 hours, with or without cells. Endothelial media incubated without cells is abbreviated as EM. Endothelial media incubated with cells (endothelial conditioned media) is abbreviated as ECM. Astrocyte media incubated without cells is abbreviated as AM. Astrocyte media incubated with cells (astrocyte conditioned media) is abbreviated as ACM. After completion of the incubation period, the supernatant(s) were removed and centrifuged at 1500 x g for 15 minutes. The conditioned media was then diluted with fresh endothelial media in a 1:1 ratio to produce 50% diluted media or used as is (100%). Figure created with Biorender.com and Powerpoint by author.*

2.2.3.2 EV treatment

For experiments involving EV treatment of endothelial cells, EVs were isolated from ACM using the ExtraPEG method as described in Section 2.2.2.4 on the day of treatment and resuspended in PBS. EVs were also isolated from AM as a non-conditioned control. Protein measurement was used as an indirect index of EV quantity.

Endothelial cells were seeded to confluency in the apical chamber of 12 well transwell inserts (2.5 x 10^5 cells per insert) and allowed to adhere for 24 hours. Prior to the addition of the treatment, the formation of a confluent monolayer on each transwell was verified by visual inspection using brightfield microscopy. The endothelial media was aspirated off, and the cells were washed briefly with PBS before the treatment was added.

For optimization experiments, EVs were diluted to the following concentrations: 6.25 or 12.5 μg/mL. Cells were treated with these concentrations of EVs and with an equivalent amount of PBS as a control for 6, 24 or 48 hours. These treatments were added either apically or basolaterally. Following incubation, the integrity of the barrier was explored through a trans-endothelial permeability assay as described below in Section 2.2.4.3.

Once the appropriate dose, incubation time, and direction of treatment were determined, cells were treated in this manner for all continuing experiments. Post-treatment, endothelial RNA and protein were harvested for analysis.

2.2.3.3 Astrocyte Inflammation

Astrocytes were inflamed using two stimulation methods: treatment with LPS (Tarassishin et al., 2014) and treatment with a cytokine cocktail (TNF-α (30 ng/mL), IL1α (3 ng/mL), and C1q (400 ng/mL)) (Liddelow et al., 2017). To determine the optimal dose of LPS, astrocytes were seeded at a concentration of 0.2 x 10^6 cells per well in 6 well plates and allowed to adhere overnight. The next day, the media was aspirated and the cells treated with two concentrations of LPS (100 ng/mL or 1000 ng/mL) or with PBS as a control for 24 hours. Upon completion of the timepoint, the cells were harvested for mRNA isolation to

conduct Real-Time PCR measurements of genes known to be expressed differently in inflamed astrocytes.

To determine the optimal inflammation method, astrocytes were seeded at a concentration of 0.2 x 10^6 cells per well in 6 well plates and allowed to adhere overnight. The next day, the media was aspirated and the cells treated with LPS (100 ng/mL), the cytokine cocktail, or PBS (1 µL/mL) as a control for 24 hours. The cells were then harvested for mRNA to conduct Real-Time PCR measurement of several genes known to be expressed differently in inflamed astrocytes.

For media conditioning, astrocytes were grown in 58.8 cm^2 dishes, with at least six dishes per condition. When cells were between 60-80% confluency, the media was aspirated. Each dish was then treated with 6mL of media containing the cytokine cocktail or control media containing the vehicle only (PBS (1 µL/mL)). The cells were incubated for 24 hours. Upon completion of the timepoint, media was collected and spun down at 1500 x *g* for 15 minutes in order to clear the media of cells and large debris. This cleared media was then frozen at -20°C until required.

2.2.4 Cell Assays

2.2.4.1 Adhesion Assay – Apical Treatments

In order to measure cell viability, the crystal violet assay was used (Feoktistova et al., 2016). HBMvECs were seeded at a concentration of 30,000 per well in 96 well plates and left overnight in an incubator. The next day, media was aspirated, and the cells briefly washed with PBS. Two hundred µL of treatment, made up as described in Table 2.3, was added to the wells in quintuplicate. Cells were treated for 6, 24 or 48 hours. Upon completion of the time course, the treatment was removed, and the cells washed with PBS. Formaldehyde (3.75%, 100 µL) was added to each well and left to incubate for 10 minutes at room temperature. Then, the formaldehyde was removed, and the cells were washed briefly once with PBS. PBS was then added to the wells and the plates stored at room temperature until the assay was carried out. This involved the removal of the PBS and the addition of a 5 mg/mL crystal violet solution (50 µL) to each well. The plate was allowed to incubate for 5 minutes at room temperature before being washed with deionized water until the water ran clear. The plates were then turned upside down and left to dry overnight. The next

day, 2% SDS (50 µL) was added to each well. The plate was left to incubate with gentle agitation for 30 minutes at room temperature. The absorbance was then read at 562 nm on a TECAN Infinite M200 Pro. Treated samples were compared against control cells (treated with fresh EM only)

Table 2.3: The preparation of conditioned media for apical treatment

	Treatments								
	Control	***EM***		***ECM***		***AM***		***ACM***	
Media (µL)		*50%*	*100%*	*50%*	*100%*	*50%*	*100%*	*50%*	*100%*
Fresh Endo Media	200	100	-	100	-	100	-	100	-
EM	-	100	200	-	-	-	-	-	-
ECM	-	-	-	100	200	-	-	-	-
AM	-	-	-	-	-	100	200	-	-
ACM	-	-	-	-	-	-	-	100	200
Total	*200*	*200*	*200*	*200*	*200*	*200*	*200*	*200*	*200*

2.2.4.2 Adhesion Assay – Basolateral Treatments

HBMvECs were seeded at a concentration of 0.5 x 10^6 cells in the upper (apical) chamber of sterile transwell inserts in a 6 well plate. Pre-warmed culture media was also added to the lower (basolateral) chamber. After the cells were allowed to adhere overnight, the media in the apical chamber was replaced with fresh culture media. Media in the basolateral chamber was removed, and treatments (as described in Table 2.4) were added. The cells were treated for 6, 24 or 48 hours. Upon completion of the time course, media in both chambers was removed, and the cells washed with PBS. Formaldehyde (3.75%, up to 1 mL) was added to both chambers, and the cells were left to incubate for 10 minutes at room temperature. Then, the formaldehyde was removed, and the cells were washed once with PBS. The transwell membrane was carefully removed from the transwell insert using a scalpel. The membrane was then stored in PBS at room temperature until the assay

was carried out. This involved the removal of the PBS and the addition of a 5 mg/mL crystal violet solution (500 µL) to each well. The plate was allowed to incubate for 5 minutes at room temperature before being washed with deionized water until the water ran clear. The membranes were then left to dry overnight. Once dry, 2% SDS (500 µL) was added to each well. The plate was left to incubate with gentle agitation for 30 minutes at room temperature. The absorbance was then read at 562 nm on a TECAN Infinite M200 Pro. Treated samples were compared against control cells (treated with fresh EM alone).

Table 2.4: The preparation of conditioned media for abluminal treatment

	Treatments				
	Control	***AM***		***ACM***	
Component (mL)		*50%*	*100%*	*50%*	*100%*
Fresh EM	2	1	-	1	-
AM	-	1	2	-	-
ACM	-	-	-	1	2
Total	*2*	*2*	*2*	*2*	*2*

2.2.4.3 Trans-Endothelial Cell Permeability Assay

HBMvECs were seeded at a concentration of 0.5 x 10^6 cells into the apical chamber of sterile transwell inserts in a 6 well plate. Pre-warmed culture media was also added to the lower chamber. After the cells were allowed to adhere overnight, the media in the apical chamber was replaced with fresh culture media. Media in the basolateral chamber was removed, and conditioned media treatments added (as described in Table 2.4). The cells were treated for 6, 24 or 48 hours. Upon completion of the time course, the treatment in the basolateral chamber was replaced with pre-warmed fresh growth media. FITC-dextran (40 kDa) in pre-warmed growth media (250 µg/mL) was added to the apical chamber. Twenty-eight µL was collected from the basolateral chambers at t = 0 and then every 30 minutes for the next 3 hours. These aliquots were diluted to 400 µL with fresh media before being plated in triplicate on a white 96 well microplate (100 µL). The plate was read using a TECAN Safire 2 fluorospectrometer, with excitation and emission

wavelengths of 490 and 520 nm, respectively, selected. Cell permeability was defined as the total basolateral-fluorescence at a given time point (0 - 180 minutes) expressed as a percentage of the total apical fluorescence at t=0 (Figure 2.2).

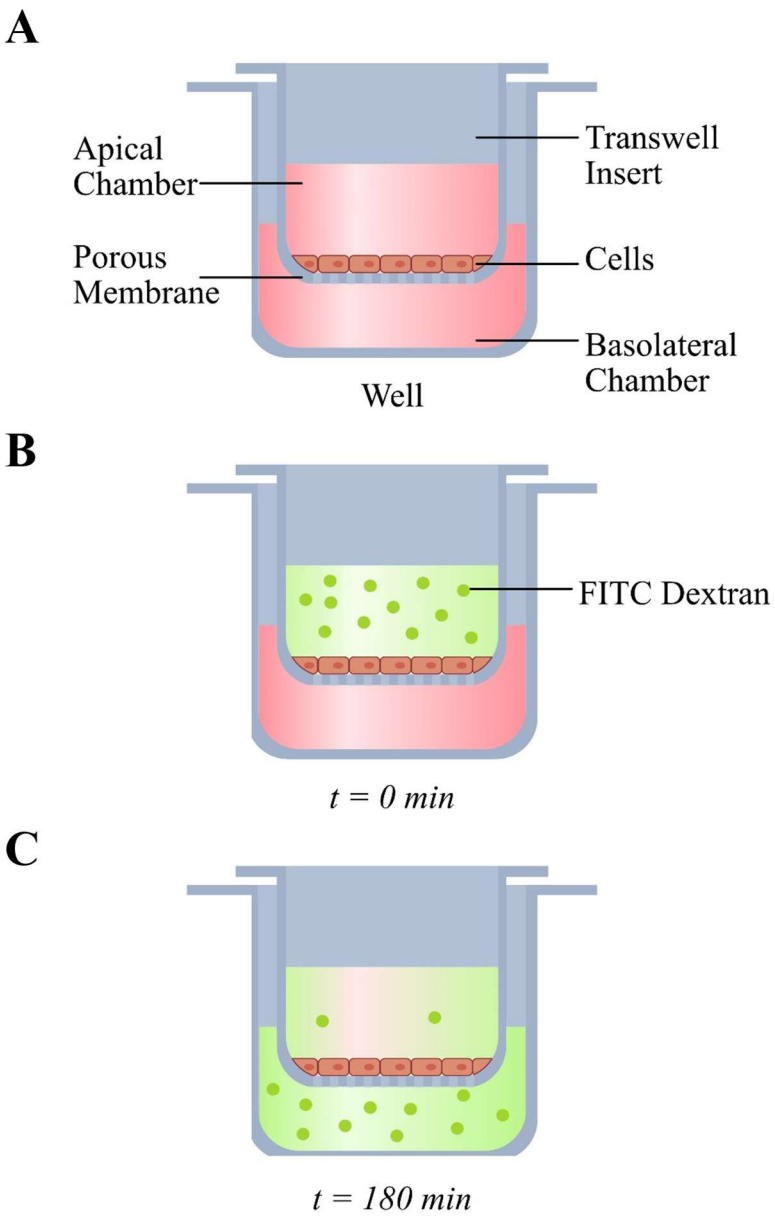


Figure 2.2 ***Trans-Endothelial Permeability Assay.*** *A) Cells were seeded equally across transwell inserts and left to adhere prior to treatment. B) FITC-dextran supplemented media replaced the media in the apical chamber. An aliquot of the media in the basolateral chamber is taken at t=0. C) At the end of the assay (t = 180 min), the amount of FITC-dextran in the basolateral chamber could be used as an indication of barrier strength. Figure created by author using Affinity Designer (v 1.10.6.1665).*

2.2.5 RNA Isolation and Quantitative Polymerase Chain Reaction (qPCR)

2.2.5.1 RNA Isolation

For cells, growth media was completely removed, and the cells were washed with PBS. TRIzol® was added (0.2 mL for 12 well transwell inserts, 0.5 mL for 6 well transwell inserts or 1 mL for petri dishes). Cells were scraped with a sterile cell scraper (Sarstedt) or pipette tip to aid sample homogenization. For EV pellets, the supernatant was completely removed and 0.2 mL TRIzol® was added. The pellet was then resuspended using a micropipette to ensure complete lysis of the sample.

Samples for Chapter 6 (Transcriptomic Analysis) were sent in TRIzol® and then processed by Macrogen (described in Section 2.2.7.1). The following method for TRIzol isolation was used for all routine qPCR experiments After sample homogenization, chloroform was added (0.2 mL per mL TRIzol®) and the tube inverted until the solution became opaque. After a 5 min incubation, the samples were spun at 12,000 x *g* for 10 min, separating the homogenate into three layers: the aqueous phase (containing RNA), the interphase (containing DNA), and the phenol phase (containing proteins). The aqueous phase was transferred to a new microcentrifuge tube and isopropanol (0.5 mL per mL TRIzol®) was added to allow the RNA to precipitate. This solution was incubated overnight at -20°C before being centrifuged at maximum speed (17,000 x *g*) at 4 °C for 30 minutes.

The resulting pellet was washed gently with ice-cold ethanol (75%) and centrifuged at 7,500 x *g* for 5 minutes. The supernatant was removed, and the pellet was allowed to air-dry for 5-10 minutes. An appropriate amount of DEPC-treated water was added to the RNA pellet (typically 10-20 µL for EV pellets and 50 µL for cell pellets) and heated to 60°C in a heat block for 10-15 minutes to homogenise the sample before quantification. The concentration and quality of RNA isolated was determined by using the NanoDrop™ One Spectrophotometer before storing at -80°C until required.

2.2.5.2 cDNA synthesis

cDNA was then synthesised using a High-Capacity cDNA Reverse Transcription Kit. This kit requires the addition of 200 ng – 1000 ng RNA. As such, isolated RNA was diluted to 20-100 ng/µL using DEPC-treated water. This was judged by the samples with the lowest concentration in each group. Ten µL of the diluted sample was added to 10 µL of reaction mix, the components of which are described below:

Table 2.5: Components of the Reaction Mix used for cDNA synthesis.

Component	Volume (per reaction) (µL)
10x RT Buffer	2
10x RT Random Primers	2
25x dNTP Mix	0.8
MultiScribe Reverse Transcriptase	1
Nuclease Free Water	4.2
Total Volume	*10*

Samples were mixed gently before being centrifuged briefly and being placed into a MiniAmpPlus Thermal Cycler and run at 25°C for 10 minutes, 37°C for 120 minutes and finally 85°C for 5 minutes. Samples were held at 4°C until retrieved.

cDNA products were then quantified on the NanoDrop™ to assess final working concentrations and purities of the samples. For qPCR (described in Section 2.2.5.5), an appropriate cDNA control was used in order to validate the experiment.

2.2.5.3 Primer Design

Primers were previously designed using Primer3 (https://primer3.ut.ee/) with parameters changed in accordance with standard rules of primer design and additional parameters implemented in the lab. Potential primer candidates were then verified *in silico* by BLAST (to check sequence homology and specificity) and mFold (to check for hairpin formations). Primers were then verified experimentally through benchtop PCR. Benchtop PCR was also used to optimise primer amplification conditions such as concentration and annealing temperatures. Primer efficiencies for each primer pair were calculated using standard curve analysis

generated via qPCR (see Section 2.2.5.6). Only primers that met the MIQE guidelines (Bustin et al., 2009, 2025) were used.

2.2.5.4 Benchtop PCR

For benchtop PCR, after Nanodrop™ analysis, cDNA products were diluted using RNase-free water to a final concentration of 500 ng/µL. Each reaction was set up in a 0.2 mL RNase-free PCR tube as follows:

Table 2.6: PCR reaction mixture

Component	**Volume (per reaction) (µL)**
Template cDNA (500 ng/µL)	2
Forward Primer (10 µM)	1
Reverse Primer (10 µM)	1
10x Reaction Buffer	2.5
dNTP (10 mM)	2
$MgCl_2$ (25 mM)	1.5
DreamTaq Polymerase (5 U/ µL)	0.2
RNase Free Water	14.8
Total Volume	*25*

Each tube was then placed into an MJ Mini Thermal Cycler and samples were subjected to the following reaction cycle:

Table 2.7: PCR reaction method

Step		**Temperature**	**Time**	**Cycle(s)**
Denaturing		95°C	5 minutes	1
Cycling	Denaturing	95°C	15 seconds	40 cycles
	Annealing	55-63°C	30 seconds	
	Extension	72°C	15 seconds	
Extension		72°C	5 minutes	1
Hold		4°C	∞	

Following this, agarose gel electrophoresis was performed as described in Section 2.2.5.7.

2.2.5.5 Quantitative Real-Time PCR

qPCR was carried out using a LightCycler® 96. Each reaction was set up in the well as follows:

Table 2.8: qPCR reaction mixture

Component	Volume (per reaction) (µL)
Template cDNA (500 ng/µL)	2
Nuclease Free Water	6
SYBR Green	10
Forward Primer (10 µM)	1
Reverse Primer (10 µM)	1
Total Volume	*20*

Samples were run in either duplicate or triplicate. Controls on the plate were set up as follows:

Component	Positive Control	No Template Control	Negative Control	Water Control
Cell cDNA	2	-	2	-
cDNA RT control	-	2	-	-
SYBR	10	10	-	-
GAPDH Primers	2	2	-	-
Water	6	6	18	20
Total	*20*	*20*	*20*	*20*

Once fully set up, the plate was sealed with an adhesive optical film. The plate was briefly spun and loaded onto the LightCycler® 96. The following method was applied:

Table 2.9: qPCR method

Step		Temperature	Time	Cycle(s)
Denaturing		95°C	5 minutes	1

Cycling	Denaturing	95°C	15 seconds	40
	Annealing	60°C	30 seconds	
	Extension	72°C	15 seconds	
Extension		72°C	5 minutes	1
Hold		4°C	∞	

The primer sequences used are described in Section 2.1.1. Changes in gene expression were then analysed according to the Comparative C_T method ($\Delta\Delta C_T$), as described by Livak and Schmittgen (2001). Glyceraldehyde 3-phosphate dehydrogenase (GAPDH) was used as an endogenous control in order to normalize C_T values. Melt curve analysis was also carried out to confirm single product formation and to rule out false positives as a result of primer dimerization and non-specific binding. Samples from qPCR were also visualized on 1% agarose gels as described in Section 2.2.5.7 below.

2.2.5.6 Primer Efficiency Curves

Primer efficiency curves were conducted by utilising the same reaction mixture as qPCR (Table 2.8) with a dilution of a PCR product, previously run with the same primer set, substituted in place of the cDNA. Briefly, a 1/1000 dilution of the PCR product is made using RNase-free water. Then, a 7-fold 1/10 serial dilution of this 1/1000 dilution was made, with 6.5 µL of each dilution substituting for the raw cDNA in each reaction mixture. A non-template control was used by making an additional reaction mixture with RNase-free water substituting the PCR product.

The reaction mixures were subjected to the same reaction temperature method as standard qPCR (Table 2.9) and the software programmed to plot the C_T values vs fluorescent signal (corresponding to the number of copies of the target genes). The following equation was used to calculate primer efficiency:

$$PCR\ effectinc = 10^{\frac{-1}{Slope}} - 1$$

According to MIQE guidelines, the efficiency of primer sets should be between 90 and 105% (Bustin et al., 2009, 2025).

2.2.5.7 Agarose Gel Analysis

Agarose gel electrophoresis was used as a quality control to visualize and assess mRNA and cDNA quality and purity as well as qPCR product sizes. Briefly, agarose was dissolved in Tris-acetate EDTA (TAE) buffer (40 mM Tris-Acetate pH 8.2, 1 mM EDTA) to make a 1% agarose mixture. The mixture was brought to a boil until the agarose had fully dissolved and the solution turned clear. Once cooled to 50-60°C, SYBR® Safe (1 µL per 10 mL of agarose) was added to the solution. 6x Agarose Gel Loading Buffer (see Section 2.1.5.1) was added to samples prior to loading. 10-20 µL of sample and 5-6 µL of 100 bp DNA Ladder were loaded. The gel was resolved at 100 V in 1X TAE buffer, for 60-90 minutes, until the tracking dye had been deemed to have resolved sufficiently. Bands were then visualised using a G: BOX fluorescence gel documentation and analysis system.

2.2.6 Protein Isolation and Western Blotting

2.2.6.1 Protein Isolation

Both cellular and EV proteins were isolated using 1x Radioimmunoprecipitation assay (RIPA) buffer (see Section 2.1.5.2), which was made up directly prior to isolation.

All media was removed from cells, and they were washed once briefly with PBS. RIPA buffer (1x, 200 µL (petri dish)/100 µL (6 well transwells)/50 µL (12 well transwells)) was added, and the cells left to incubate on ice for 10 minutes. Cells were then scraped off using a P200 tip. The cell suspension was transferred to a SafeSeal tube.

Post EV isolation (see Section 2.2.2), the EV pellet was resuspended in 1x RIPA Buffer (20-75 µL, depending on visual pellet size). The protein suspensions were rotated at 4°C for at least 1 hour. They were then centrifuged at 10,000 x *g* for 20 minutes at 4°C. The supernatant was aliquoted into new tubes and stored at -20°C.

2.2.6.2 Bicinchoninic Acid (BCA) Assay

Isolated proteins from cells were quantified using the Pierce™ BCA protein Assay Kit. Ten µL of samples and standards (0 - 2 mg/mL bovine serum albumin (BSA)) were loaded in triplicate to a clear, flat-bottomed 96-well plate. Two hundred µL

BCA working reagent (1:50 dilution of reagent B in reagent A) was added to each well before the plate was incubated at 37°C for 30 minutes in the dark.

Proteins from EV isolations were quantified using the Pierce™ MicroBCA protein Assay Kit, which has a working range of 0.5 – 20 µg/mL. 0.9% NaCl solution (150 µL) was added to each well before 2 µL of samples and standards (0-20 µg/mL BSA) were loaded in triplicate to a clear, flat-bottomed 96-well plate. Once 150 µL MicroBCA working reagent (25:25:1 reagent A: reagent B: reagent C) was added to each well, the plate was incubated at 37°C for 30 minutes in the dark. The plate was then read at 562 nm on a TECAN Infinite M200 Pro plate reader. The unknown protein concentrations were calculated using the standard curve.

2.2.6.3 Acetone Precipitation of Proteins

To precipitate out proteins from supernatants and to concentrate samples with low protein content, proteins were precipitated out using acetone with the addition of a pre-solubilisation step with NaOH, as published by Pérez-Rodriguez et al. (2020) with some modifications. Briefly, 10% (v/v) 0.2 M NaOH was added to the sample, and this solution was incubated for 2 minutes. Then, 4 times the sample volume of cold (-20°C) 80% (v/v) acetone was added. The sample was left to incubate overnight at -20°C. After centrifugation at 16,000 x *g* for 30 minutes, the supernatant was removed. The pellet was left to airdry for ~30 minutes at room temperature before resuspension in an appropriate amount of RIPA buffer (20 - 75 µL, dependent on pellet size).

2.2.6.4 Sodium Dodecyl Sulphate-Polyacrylamide Electrophoresis (SDS-PAGE)

Protein lysates were separated using SDS-PAGE according to the protocol of Laemmli (1970). Briefly, a 10% (v/v) polyacrylamide resolving gel was used throughout all experiments and was prepared as follows:

Table 2.10: SDS-PAGE resolving gel components.

Reagent	**10%**
Deionised Water	4 mL
1.5M Tris-HCl, pH 8.8	2.5 mL
Acrylamide, 30%	3.3 mL
10% SDS	100 µL
10% Ammonium Persulfate (APS)	50 µL
TEMED	5 µL
Total Volume	*10 mL*

Once the gel was set, a 4% stacking gel was prepared as described in Table 2.11.

Table 2.11: SDS-PAGE stacking gel components

Reagent	**4%**
Deionized Water	6 mL
0.5M Tris-HCl, pH 6.8	2.5 mL
Acrylamide, 30%	1.3 mL
10% SDS	100 µL
10% Ammonium Persulfate (APS)	100 µL
TEMED	10 µL
Total Volume	10 mL

The solution was poured on top of the polymerised resolving gel, followed immediately by the gel comb being inserted. If the gels were not to be used immediately, they were carefully wrapped in damp tissue and placed in the fridge for use the next day.

Post quantification using a BCA assay (see Section 2.2.6.2), protein lysates were diluted to 15 - 30 µg using deionised water. 4x Sample Solubilisation Buffer (SSB) (see Section 2.1.5.2) was added to each sample so that the final volume was 20 µL. Samples were denatured at 95°C for 5 minutes before being briefly centrifuged. The samples were loaded into the gel wells (~20 µL), alongside a protein ladder (~5/6 µL). Gels were run in Running Buffer (see Section 2.1.5.2) at 80V until proteins entered the resolving gel and then at 100V for 1.5-2 hours or until sufficient resolution was reached.

2.2.6.5 Electrophoretic Transfer

The proteins from the gel were transferred to a membrane using either a wet transfer technique or a semi-dry transferring system (Thermo Scientific Pierce G2 Fast Blotter). The gel was left to soak in transfer buffer (see Section 2.1.5.2) for at least 5 mins to remove any residual SDS that may be bound to the gel which could interfere with the protein transfer. Polyvinylidene Difluoride (PVDF) membrane was trimmed to the size of the gel and activated in methanol for 5-10 minutes, before being equilibrated in transfer buffer along with the filter paper.

For wet transfer, proteins were transferred overnight at a constant voltage of 50 V at 4°C. For semi-dry transfer, the standard semi-dry preprogrammed method was used (25V, 1 hour).

2.2.6.6 Ponceau S

Ponceau S was used to visualise successful transfer of proteins from the SDS-PAGE gel to the membrane. Briefly, 10-15 mL of Ponceau S stain was applied to the membrane under gentle agitation for ~ 5 minutes. The membrane was then washed with PBS-Tween 20 (PBS-T) (0.1%) until transferred bands (pink bands) were visible. At this point, the membrane was cut into manageable sections for the protein

of interest, if needed. The membrane was then further washed with PBS-T until the stain was removed entirely, and it was then used for immunoblotting.

2.2.6.7 Immunoblotting and imaging

The PVDF membrane was blocked in a 5% BSA solution, made up with PBS-T for 1 hour at room temperature. The membrane was then incubated with primary antibody (Table 2.12) in 1% BSA (in 0.1% PBS-T) overnight at 4°C. The following primary antibodies and dilutions were used:

Table 2.12: Primary Antibody Concentrations used in Immunoblotting

Target	Company	Host	Code	Concentration
Annexin V	Invitrogen	Rabbit	PA5-78784	1:1000
CD9	Genetex	Rabbit	GTX135296	1:1000
CD63	Genetex	Rabbit	GTX135220	1:1000
Claudin 5	Invitrogen	Mouse	35-2500	1:1000
GAPDH	Merch	Mouse	MAB374	1:500
GFAP	Genetex	Rabbit	GTX27260	1:10,000
Occludin	Invitrogen	Rabbit	40-4700	1:250
ZO-1	Invitrogen	Rabbit	61-7300	1:1000

The following day, the blots were washed with 0.1% PBS-T (3x, 5 minutes each). The blots were then incubated with the appropriate Horseradish Peroxidase (HRP)-conjugated secondary antibody (**Error! Reference source not found.**13) in 1% BSA-0.1% PBS-T for 2 hours at room temperature. Membranes were then washed with PBS-T (0.1%) (3x, 5 minutes each) followed by PBS (2x, 5 minutes each). Membranes were stored in deionised water until imaging. Proteins were detected using Immobilon® Forte Western HRP substrate and the G: BOX gel documentation system.

Table 2.13: Secondary Antibodies used in Immunoblotting

Target	Company	Host	Code	Concentration
Anti-mouse IgG, HRP-linked antibody	Cell Signalling	Horse	7076S	Dependent on primary antibody concentration
Anti-rabbit IgG, HRP-linked antibody	Cell Signalling	Goat	7074S	

2.2.6.8 Stripping and Reprobing

To conserve sample, western blots were stripped and reprobed for various proteins. First, the western blot was rinsed in deionised water in order to remove any remaining HRP substrate. Then, the membrane was incubated in mild stripping buffer (see Section 2.1.3.2) for 10-20 minutes. The membrane was then washed in 0.1% PBS- T (3x, 5 minutes each). After this, the membrane was reprobed as above, including being reblocked in 5% BSA.

2.2.7 Transcriptomic Analysis

2.2.7.1 RNA Sequencing

RNA extraction, quality assessment, library preparation and sequencing were performed by Macrogen (South Korea). Samples were sent in TRIzol® and RNA isolated by first separating the RNA, DNA, and protein phases using chloroform. After this, RNA was eluted from the upper aqueous phase using the RNeasy Mini Kit, following manufacturer instructions. Macrogen does not typically perform DNase digestion in order to remove potential genomic DNA contamination as the RNeasy kit efficiently removes the majority of contaminating DNA through its silica-membrane technology. RNA concentration was assessed using the Quant-it™ RiboGreen RNA Assay using the Victor Nivo Multimode Microplate Reader. RNA integrity was verified by using a 4200 TapeStation System. All samples had an RNA Integrity Number (RIN) > 9.5. The RIN, which ranges between 10 (intact RNA) and 1 (totally degraded RNA), is calculated by a software algorithm that explores multiple aspects of the electropherogram in order to determine the integrity of the sample (Schroeder et al., 2006; S. Li et al., 2024).

Libraries were prepared using a TruSeq Stranded Total RNA with Ribo-Zero H/M/R kit, according to manufacturer instructions and sequenced on an Illumina platform to generate 101 bp paired-end reads. Each sample yielded a minimum of 44 million reads.

2.2.7.2 Bioinformatic Models Employed to Analyse Data

Raw sequencing data (FASTQ) files were received from the sequencing provider. The sequence quality of these files was analysed using Falco (Galaxy Version 1.2.4+galaxy0) (Sena & Smith, 2022). MultiQC (Galaxy Version 1.27+galaxy4) was used to aggregate results into a generalised report (Ewels et al., 2016). Cutadapt (Galaxy Version 5.2+galaxy0) was used to improve quality by trimming adaptor sequences (M. Martin, 2011). Reads were then mapped to the human reference genome hg38 (GenBank Acquisition Number: GCA_000001405.15; Perez et al., 2025) and counted using RNA STAR (Galaxy Version 2.7.11b+galaxy0) (Dobin et al., 2013). Differential gene expression was analysed using edgeR (Robinson et al., 2010). Gene set enrichment analysis was performed using the Gene Ontology: Biological Processes gene set (The Gene Ontology Consortium et al., 2023) with goseq (Young et al., 2010).

2.2.8 Statistical Analysis

Statistical analysis and graphical representation of results were carried out and constructed using RStudio® (version 2023.6.1.524, R Foundation for Statistical Computing, Austria). Results were expressed as median ± standard deviation (SD). Welch's Two-Sample t-test was used for pairwise comparison. Analysis of variance (ANOVA) along with Tukey's HSD as a *post-hoc* test was used for multiple comparisons. Statistical tests used are described in the figure legends with significance defined as $P \leq 0.05$ for all tests. The number of biological replicates (n) used is stated in the figure legends.

qPCR results were quantified using Roche LightCycler® 96 System v1.1 software. $\Delta\Delta C_T$ was calculated by normalising treated samples against the average of the control samples. Protein expression levels were quantified by measuring the optical density of Western blots using Image Studio Lite v5.2 software using the method described in Stael et al., (2022). Briefly, the image was converted to greyscale and

lane profile plots were generated using the gel analysis tool in the software. These lane profile plots represent the relative density of each lane, with higher peaks representing darker bands. The size of each peak was measured with the wand tool, and the generated data was then used to calculate the relative density of both the loading control (GAPDH) and the protein of interest for each sample by normalising to the untreated control. The relative density of the samples were then scaled to the relative densities of the loading control in order to quantify the protein fold change.

Chapter 3 :

The Effect of Conditioned Media on HBMvEC Barrier Properties

3.1 Introduction

Astrocytes are intimately associated with the blood vessels of the CNS, essentially covering almost all of the endothelial abluminal surface through direct contact with their endfeet (Mathiisen et al., 2010; Hösli et al., 2022). This direct contact is particularly important for the structural development of the gliovascular interface as both of these cells contribute ExM proteins to the BM (Van Horssen et al., 2005; Turner et al., 2017). Both astrocytes and endothelial cells are also known to express connexin 43 (Cx43), a gap junction protein which allows adjacent cells to communicate directly (Zhang et al., 2020; Toychiev et al., 2021). Astrocyte-endothelial calcium signalling has been found to be communicated through these gap junction channels, and this have been speculated to play a role in blood flow regulation and other BBB-related functions(Simard et al., 2003; Schumacher et al., 2024). A recent study has found that over 1/5 of the astrocyte proteome is exclusively expressed in their endfeet processes, including several proteins that have previously been reported to be critical to the normal development and function of the BBB such as CD146 (J. Chen et al., 2017; D. Wang et al., 2020) and Reck (Ulrich et al., 2016; Cho et al., 2017) (Stokum et al., 2021). However, studies on whether these proteins are delivered through gap junctions or through an extracellular pathway are limited.

Astrocytes are potent secretory cells, releasing a variety of substances that contribute to the regulation of many aspects of the CNS (Pellerin & Magistretti, 1994; Henneberger et al., 2010; Poskanzer & Yuste, 2016; De Ceglia et al., 2023), including the vasculature (Howarth et al., 2017; D. Liu et al., 2024). In fact, astrocytes are known to release vasoactive mediators such as prostaglandin E2 (Rao et al., 2007; Forsberg et al., 2017; Perrot et al., 2020) and epoxyeicosatrienoic acids which act as vasodilators (C. Zhang & Harder, 2002; Nippert et al., 2022). In addition, astrocytes have been found to secrete proteins that improve barrier integrity in endothelial cells such as Wnt (Richards et al., 2015; Laksitorini et al., 2019; Guérit et al., 2021) and sonic hedgehog (Shh) (Alvarez et al., 2011; Zhen et al., 2018; Michinaga et al., 2021). However, they also secrete molecules that promote barrier permeabilisation like vascular endothelial growth factor (VEGF) (Argaw et al., 2012; S. Jiang et al., 2014; L. Wu et al., 2018). Therefore, astrocytes

are positioned to have significant influence over endothelial phenotype and behaviours. As such, this chapter aims to focus on the indirect signalling from astrocytes that may affect the integrity of the BBB, even in different regions.

Early studies of BBB function used *in vivo* animal models (Ehrlich, 1885; Lewandowsky, 1900). *In vivo* models provide highly physiologically relevant data as they capture the complexity of the entire system (A. Chen et al., 2024). However, the use of animals in studies can be expensive, and also requires experience and skills. Additionally, preclinical studies *in vivo* do not always translate successfully in clinical trials (Perrin, 2014; Mahalmani et al., 2022). Although the complexity of the NVU is difficult to replicate using *in vitro* systems, several models of translational value have been developed in order to study the BBB in a more cost-effective and ethical manner (reviewed in Jagtiani et al., 2022 and Soliman et al., 2025). One of the most popular systems is the transwell model, in which a semi-permeable membrane separates a chamber into two compartments to model the apical and basolateral sides of the BBB. Although it was initially developed in the early 1960's to study leukocyte chemotaxis (Boyden, 1962), the first use of transwells to model the BBB was reported in the 1980s (P. D. Bowman et al., 1983). In addition to its ease of use and availability, the transwell model also allows for co-culturing of different cell types, allowing for closer mimicking of the *in vivo* BBB (Strazza et al., 2016; W. Kim et al., 2022).

The BBB, however, exists in a dynamic 3D environment, influenced by blood flow shear stress (DeOre et al., 2022; Yates et al., 2025). As such, these 2D BBB models are oversimplified and static. Even in co-culture transwell models of the BBB, the distance between astrocytes and endothelial cells is greater than *in vivo* as the insert width is thicker than the BM in the CNS (Zakharova et al., 2021). The intercellular dynamics of the BBB *in vivo* can be better models through the use of 3D BBB models, such as hydrogel-based models, where hydrogels provide a 3D scaffold which can more accurately reflect the mechanical properties of the brain's ECM (Kurosawa et al., 2022; N. R. Singh et al., 2023). However, commonly used hydrogels, such as collagen I (Ahmad et al., 2011; Ruano-Salguero & Lee, 2018) and Matrigel (Kim et al., 2022; Bolden et al., 2023) do not accurately represent the microenvironment of the BBB (reviewed in Xu et al., 2019; Lennon & Sherwood, 2025).

Microfluidic BBB models, which range from simple single-cell flow circuits to more complex Organ-on-a-Chip or microphysiological systems, can simulate blood flow, thus introducing sheer stress into the system (Deosarkar et al., 2015; Kawakita et al., 2023). These systems, however, also fail to fully replicate the *in vivo* BBB microenvironment due to their artificial structure and organisation (W. Wei et al., 2023; Royse et al., 2024). 3D *in vitro* spheroid and organoid models are able to provide a more accurate representation of the *in vivo* BBB as direct cell-cell interactions are maintained and maximized in these models since cells are allowed to self-assemble in a low-attachment culture vessel or within an ECM gel (Dao et al., 2024; Paranjape et al., 2024). While 2D transwell models are simplistic, they were chosen as the BBB model due to the nature of this study, which aimed to get a basic understanding of how the astrocyte secretome affects the BBB.

Several studies have shown that the co-cultivation of astrocytes with brain and non-brain endothelial cells from various model organisms resulted in increased barrier function of these cells (Cecchelli et al., 1999; Kulczar et al., 2017; J. S. Park et al., 2023). These studies primarily focused on the effects of direct contact between endothelial cells and astrocytes. However, barrier activity has been found to increase both when astrocytes are in direct contact with the endothelial cells and when they are seeded at the bottom of the well, with no direct endothelial cell contact (Kulczar et al., 2017; Zamproni et al., 2025). Thus, direct contact is not necessary for astrocytes to affect endothelial cell properties.

Other studies have explored the effects of the astrocyte secretome on brain endothelial cells by using astrocyte conditioned media (ACM) (Arthur et al., 1987; Barar et al., 2010; Baumann et al., 2021). It can be noted, however, that studies using both primary human endothelial cells and primary human astrocytes are limited. To address this knowledge gap, this chapter specifically focuses on the effects of the secretome of primary human astrocytes on the barrier properties of primary human brain microvascular endothelial cells.

3.1.1 Chapter Aims

- To characterise both primary human brain astrocytes and primary human brain microvascular endothelial cells (HBMvECs)
- To explore the effect of primary human ACM on HBMvEC viability
- To explore the effect of primary human ACM on HBMvEC barrier function.
- To explore the effect of primary human ACM on TJ gene and protein expression of HBMvECs.

3.2 Results

3.2.1 Cell Characterisation

3.2.1.1 Human Primary Astrocytes

In order to obtain samples of the primary human astrocyte secretome, it was imperative to ensure our cells and the culturing regime provided samples that were of translational value. As such, human primary astrocytes obtained from a commercial source were first characterised in order to confirm appropriate marker expression of the cells (Figure 3.1). These cells were found to have a flat, spread-out morphology (Figure 3.1A), which is commonly found with quiescent astrocytes in 2D culture (Galland et al., 2019; Baldwin et al., 2024). Activated astrocytes in culture, on the other hand, become more elongated, extending their long processes (B. Liu et al., 2006). The common astrocytic biomarker GFAP was evaluated in order to assess the validity of these cells before media was collected. GFAP is an established component of astrocyte intermediate filaments and is a hallmark of reactive astrocytes (Escartin et al., 2021; De Bastiani et al., 2023). It has often been used to distinguish astrocytes from other glial cells (Cahoy et al., 2008; J.-M. Shi et al., 2023). Astrocytes were grown on coverslips and fixed in 4% paraformaldehyde (PFA) prior to the exploration of GFAP expression (Figure 3.1B). A low level expression of GFAP was seen in all cells, with the exception of higher expression in a marginal number of cells (not shown). Confluent astrocyte cultures (P2-P5) were harvested for mRNA isolation and revealed GFAP presence on the mRNA in these cells but not in endothelial cells (Figure 3.1C), further illustrating that the cells in culture are of astroglial lineage and express an astrocyte marker found *in vivo*.

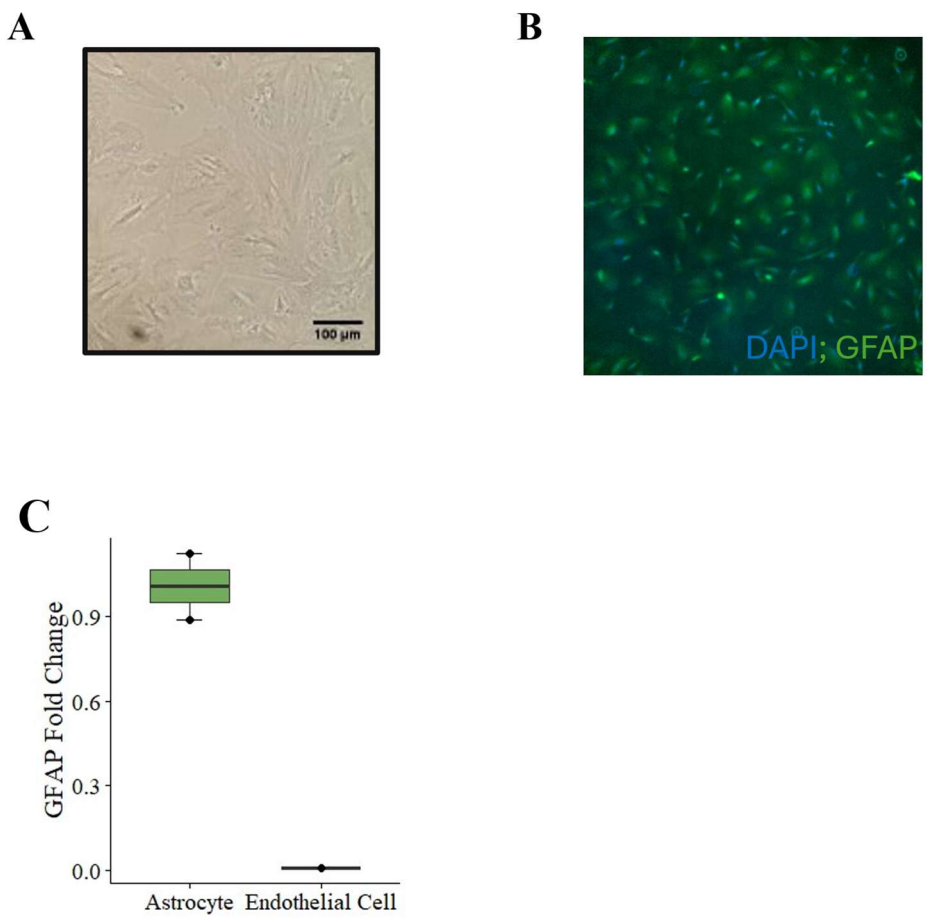


Figure 3.1 ***Cell characterization of astrocytes.*** *(A) shows a brightfield image of astrocyte morphology at passage 4 and 90% confluency using 4x magnification. B) shows the expression of GFAP in astrocytes at 10x magnification. C) shows the expression of GFAP mRNA in astrocytes but not in endothelial cells (n=2). Gene expression calculated using the* $\Delta\Delta C_T$ *method and normalised to the average* C_T *value of the astrocyte samples.*

3.2.1.2 HBMvECs

HBMvECs were characterised to demonstrate cell-specific marker expression (Figure 3.2). Although endothelial cells are typically associated with a cobblestone-like morphology, variability in their appearance has previously been observed (Rupnick et al., 1988; Ya & Bayraktutan, 2025), including the more spindle-shaped morphology developed by our cells seen in Figure 3.2A. A number of common biomarkers were also used to confirm the validity of these cells before routine experimentation. These were the TJ markers claudin-5 (CLDN5), occludin (OCLN) and ZO-1 (Stamatovic et al., 2016; Munji et al., 2019). Confluent HBMvECs were grown on transwell membranes before being fixed in 4% PFA and probed for ZO-

1 (Figure 3.2B). A mounting medium containing DAPI was used to mount the membrane onto a glass slide and to stain the nuclei of the cells. Confluent HBMvEC cultures (P6-P16) and astrocyte cultures (P2-P5) were also harvested for mRNA isolation. HBMvECs expressed CLDN5, OCLN and ZO-1 at higher levels in comparison to astrocytes. Together, these results illustrate that the cultured cells exhibit tight junction markers which confirms the cells to be specifically of brain endothelial cell lineage.

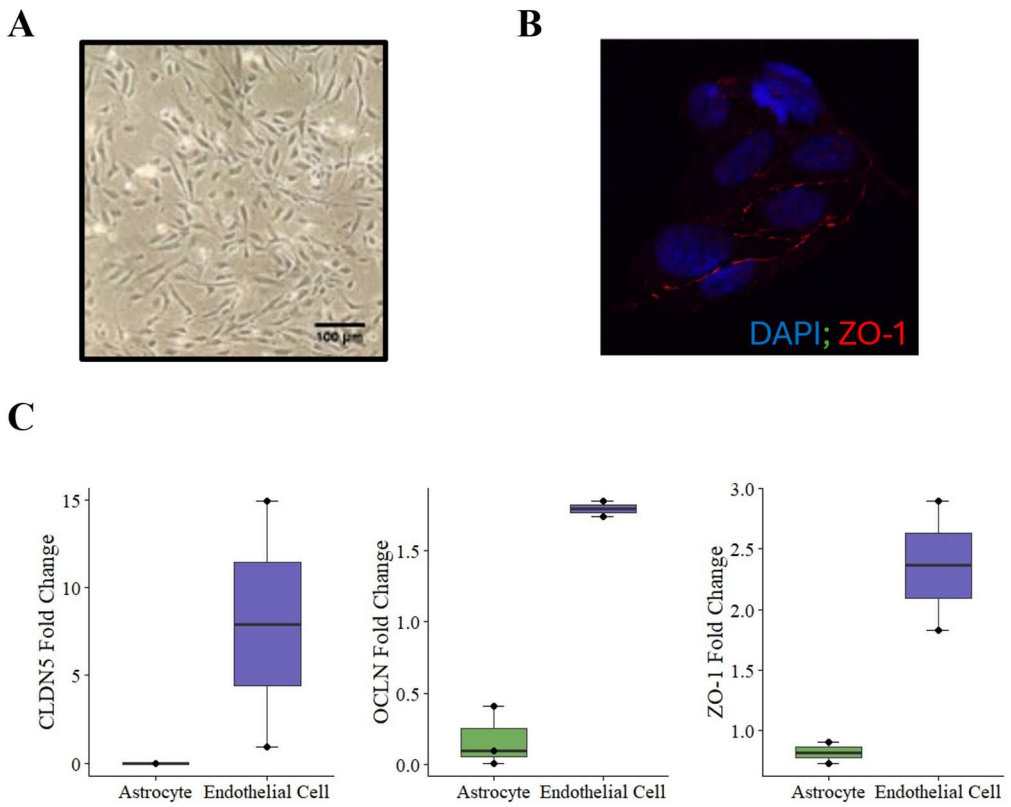


Figure 3.2 ***Cell characterization of HBMvECs.*** *(A) shows HBMvEC morphology at passage 12 and 70% confluency using 4x magnification. As these cells have not established a confluent monolayer, they are elongated and spindle-shaped which is typical of endothelial cells during active growth. In areas where the cells are closer together, they are beginning to exhibit the class "cobblestone" morphology associated with confluent endothelial cells. B) shows the location of the tight junction protein ZO-1 (red) at the periphery of the cells on transwell membrane using confocal microscopy at 40x. C) confirms the expression of claudin-5 (CLDN5) (right), occludin (OCLN) (centre) and ZO-1 (left) in these endothelial cells (blue) but minimal expression, if not none, in astrocytes (n=2).*

3.2.2 Effect of ACM on Endothelial Cell Barrier Properties

In order to discern the indirect effects of human primary astrocytes on the barrier properties of primary HBMvECs, astrocyte media (AM) was incubated on astrocytes for 48 hours to generate ACM. A 48-hour incubation period can result in the accumulation of toxic metabolite products released by the cells. This could therefore negatively affect cellular viability and barrier properties if used as a treatment. Therefore, to determine whether cells are reacting to metabolite toxicity, endothelial conditioned media (ECM) was generated by incubating endothelial media (EM) on endothelial cells for the same incubation period to be used as a control. Control media (AM and EM) were also incubated in the absence of cells for the same length of time to control for the baseline effects of media itself. ACM and ECM supernatants was collected and centrifuged at 1500 x *g* for 15 minutes to remove any dead cells or large molecules and then stored at -20°C until required. Frozen media was allowed to fully thaw at room temperature before being warmed to 37°C for experiments. Fresh media refers to media that has not been incubated nor come into contact with cells.

3.2.2.1 The Effect of ECM on Endothelial Cell Viability

Prior to exploring the effect of ACM on the barrier properties of HBMvECs, the viability of these cells after treatment with conditioned media was explored. Firstly, the effect of ECM itself on the viability of HBMvECs was investigated in order to identify any possible effect of toxic secreted endothelial waste products acting in an autocrine or paracrine manner on HBMvECs.

For these experiments, EM and ECM were used, either as is (100%) or diluted to 50% with an equal volume of fresh EM, i.e., media that had not been in contact with cells nor incubated (Figure 2.2). HBMvECs were seeded into 96 well plates and were treated with 50% EM, 50% ECM, 100% EM and 100% ECM in quintuplicate for 6, 24 and 48 hours. Upon completion of the timecourse, the cells were fixed with 3.5% PFA for 10 minutes. After fixation, cell viability was measured using a crystal violet assay (2.2.4.1). This assay relies on the principle that adherent cells detach from the plate during cell death. Results were normalised to cells that were

treated only with fresh EM on the plate. There was no significant difference in viability between EM and ECM, at any concentration or timepoint (Figure 3.3).

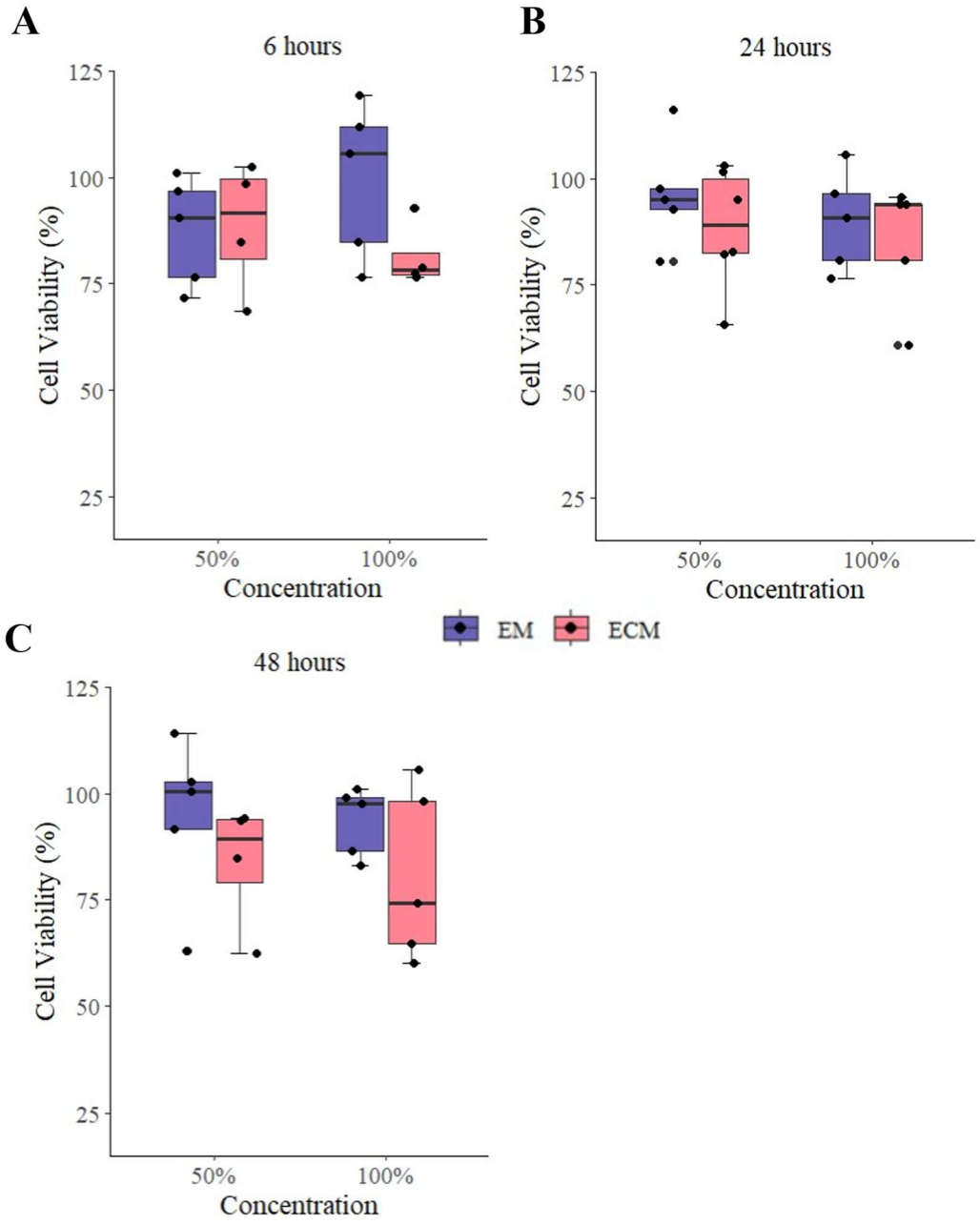


Figure 3.3 ***Endothelial cell viability after incubation with EM (purple) or ECM (pink)*** *for 6 (A), 24 (B), 48 (C) hours. One-way ANOVA analysis was performed for each timepoint in RStudio. n =5. Black dots signify individual data points.*

3.2.2.2 The Effect of ACM on Endothelial Cell Viability

As there was no significant change in viability of HBMvECs when treated with ECM, the effect of AM and ACM on the viability of these cells was subsequently explored to optimize treatment conditions for future experiments.

For this, AM and ACM were used, either as is (100%) or diluted to 50% with fresh EM (Figure 2.2). HBMvECs were seeded in 96 well plates and were then treated luminally in quintuplicate with 50% AM, 50% ACM, 100% AM and 100% ACM for 6, 24 and 48 hours. The viability of HBMvECs was measured as in 3.2.2.1.

While there seems to be a concentration-dependent decrease in viability for cells treated with AM and ACM, this decrease was not significant after 6 hours and 24 hours (Figure 3.4A, B). However, after 48 hours, there was a significant decrease in viability in cells that had been treated with 100% AM (49.2% ± 17.5%, $p = 0.008$), as well as in cells that had been treated with 100% ACM (49.2% ± 12.6%, $p = 0.0025$) in comparison to the control (Figure 3.4C). Importantly, there was no significant difference between undiluted AM and ACM. However, there was a significant difference in viability between 100% ACM and 50% ACM (49.2% ± 12.6% vs 96.5 ± 26.8% respectively, $p = 0.0285$).

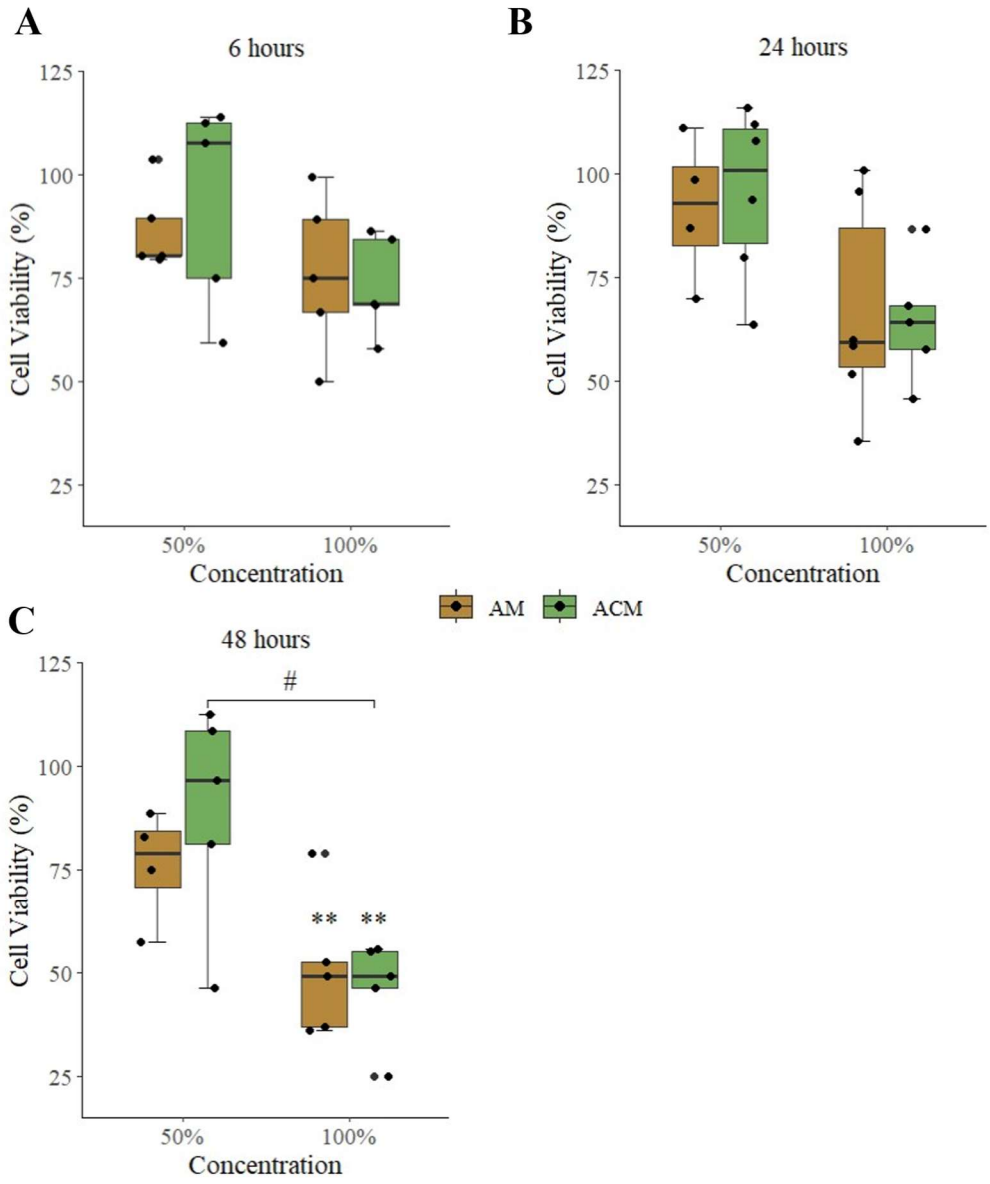


Figure 3.4 ***Endothelial cell viability after incubation with AM (gold) or ACM (green)*** *for 6 (A), 24 (B), 48 (C) hours. One-way ANOVA analysis was performed for each timepoint in RStudio. n =5. Black dots signify individual data points. ** $p < 0.01$ in comparison to control. # $p < 0.05$ between concentrations.*

Although there was a clear effect of ACM treatment on HBMvEC viability, treatment in 96 well plates does not accurately reflect the conditions of future planned experiments, where the cells will be grown in transwells and will therefore have more access to EM. Therefore, the effect of diluted and undiluted AM and ACM on the viability of HBMvECs under basolateral transwell exposure for 6, 24, and 48 hours was also explored. In this set of experiments, HBMvECs were seeded in the apical chamber of a transwell and allowed to adhere overnight. The media in the apical chamber was replaced with fresh EM. Treatments, as described in Table 2.3, were added to the basolateral chamber. Upon completion of the timecourse, the transwells were fixed in 3.5% PFA for 10 minutes. Cell viability was then measured using a crystal violet assay (2.2.4.2). Cell viabilities were normalised to the control: cells treated with fresh EM basolaterally.

Figure 3.5 shows that AM decreased HBMvEC viability in a time and concentration dependent manner. There was no significant difference in viability shown after 6 hours incubation with either AM or ACM, diluted or undiluted (Figure 3.5A). However, after 24 hours, viability decreased significantly upon treatment with undiluted AM (50.2% ± 12.8%, $p = 0.000526$) and undiluted ACM (44.2% ± 12.2%, $p = 0.001665$) (Figure 3.5B). Similar to results upon apical treatment of HBMvECs, there was no significant difference between undiluted AM and ACM. However, there was a significant difference in viability between 50% AM and 100% AM (83.5% ± 4.65% vs 50.2% ± 12.8% respectively, $p = 0.00869$) and between 50% ACM and 100% ACM (83.3% ± 5.79% vs 44.2% ± 12.2% respectively, $p = 0.0459$), suggesting that media concentration has a significant effect.

At 48 hours, the viability of cells treated with undiluted AM was significantly decreased in comparison to the control (21.1 ± 21.7% ($p = 0.00383$), (Figure 3.5C). Interestingly, although there was no significant difference in HBMvEC viability after incubation with either diluted AM or diluted and undiluted ACM, there was a significant decrease in HBMvEC viability after incubation with 100% ACM in comparison to 50% ACM (63.2% ± 12.4% vs 102% ± 26.6% respectively, $p = 0.0446$) as seen after 24 hour incubation. Additionally, the viability of HBMvECs treated with diluted ACM was significantly increased in comparison to those treated with diluted AM (56.6 % ± 4.04% vs 102% ± 26.6% respectively, $p = 0.0198$). This was also seen in HBMvECs treated with undiluted ACM and AM, although this was

not significant (63.2% ± 12.4% vs 21.1% ± 21.7%, p = 0.182). This was also seen at 6 hours (98.8% ± 14.2% vs 88.2% ± 10.7%) and 24 hours (50.2% ± 12.8% vs 44.2% ± 12.2%), although these were again not significantly. This suggests that ACM has a protective effect on HBMvEC viability.

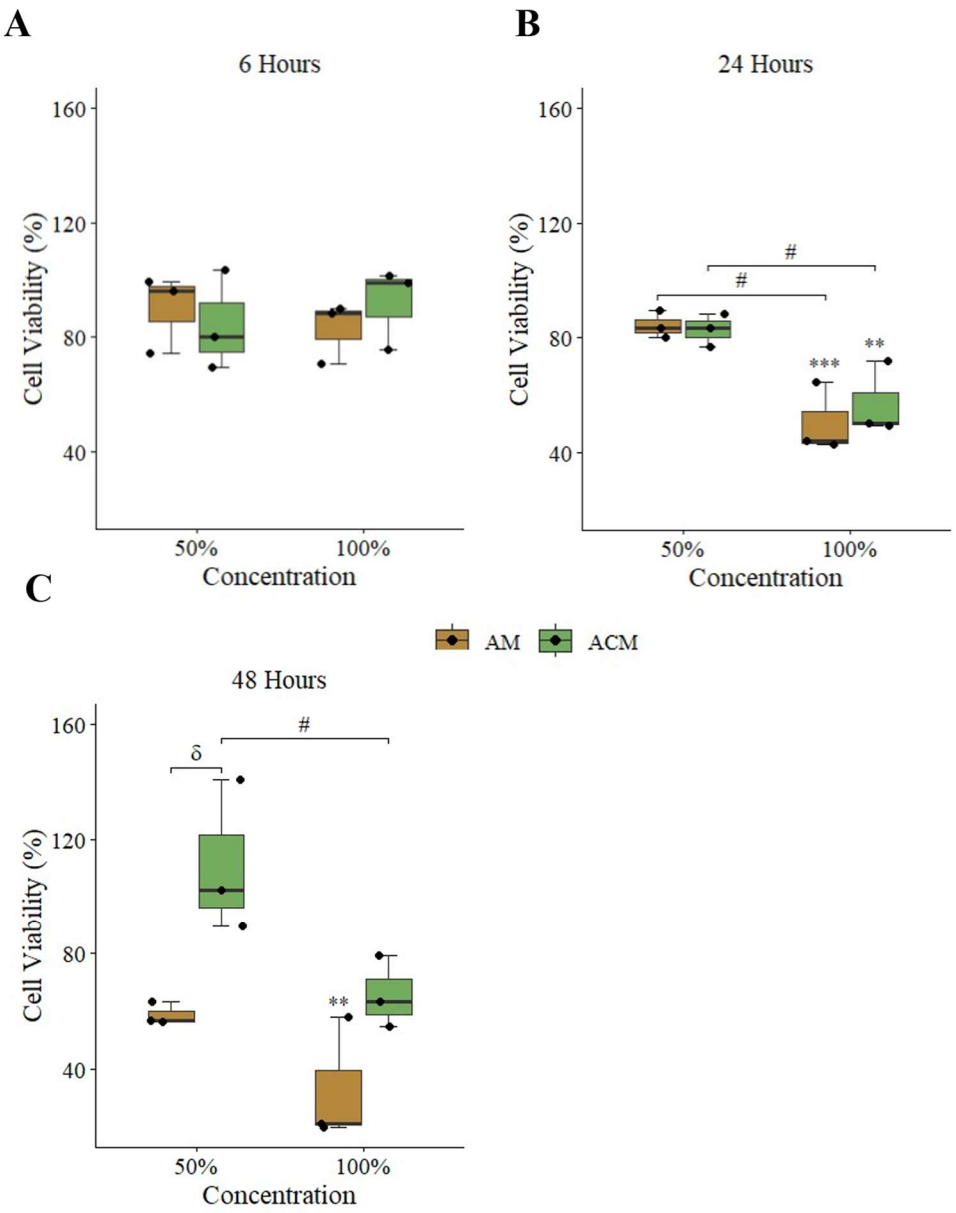


Figure 3.5 ***Endothelial cell viability after basolateral incubation with astrocyte conditioned media*** *for 6 (B), 24 (C), 48 (D) hours. A) describes the method of treatment. One-way ANOVA analysis was performed for each timepoint in RStudio. n =2. Black dots signify individual data points. ** p ≤ 0.01, *** p ≤ 0.001 compared to control. # p ≤ 0.005 compared between concentrations.* δ *p ≤ 0.01 compared between treatments.*

3.2.2.3 The Effect of ACM on HBMvEC Permeability

As treatment with undiluted AM and ACM resulted in significant decreases in HBMvEC viability (3.2.2.2), 50% AM and ACM were chosen for experiments looking at HBMvEC permeability. Endothelial cells were seeded onto a transwell and allowed to adhere overnight. The next day, the media was removed, and fresh endothelial media added to the apical chamber. Diluted (50%) ACM, Diluted (50%) AM control, or EM control was added to the basolateral chamber thereby better reflecting the spatial proximity of astrocytes to the basolateral surface of cerebral capillaries. Treatments were incubated for 6, 24, and 48 hours. After completion of the timecourse, media in the basolateral chambers was replaced with fresh endothelial media and 2 mL FITC-dextran (250 μg/mL, diluted in endothelial media) was added to each apical chamber. Samples of the media in the basolateral chamber were taken every half hour for 3 hours before the fluorescence was read at 535 nm. Fluorescence was normalised to control media and FITC-dextran.

There was no significant difference in the permeability of HBMvECs after 6 and 48 hours of incubation with diluted AM and ACM in comparison to the control (Figure 3.6A, C). After 24 hours of incubation, both cells that were treated with AM and ACM had increased permeability at the final time point although only cells treated with AM approached significance (1.27 ± 0.136, $p = 0.0867$ and 1.28 ± 0.195, $p = 0.127$, respectively) (Figure 3.6B). Although it seems that both HBMvECs treated with AM and ACM experience a decrease in permeability for the first half of the assay, there is no significant difference between the permeability of these cells to the control by the final timepoint ($t = 180$ mins).

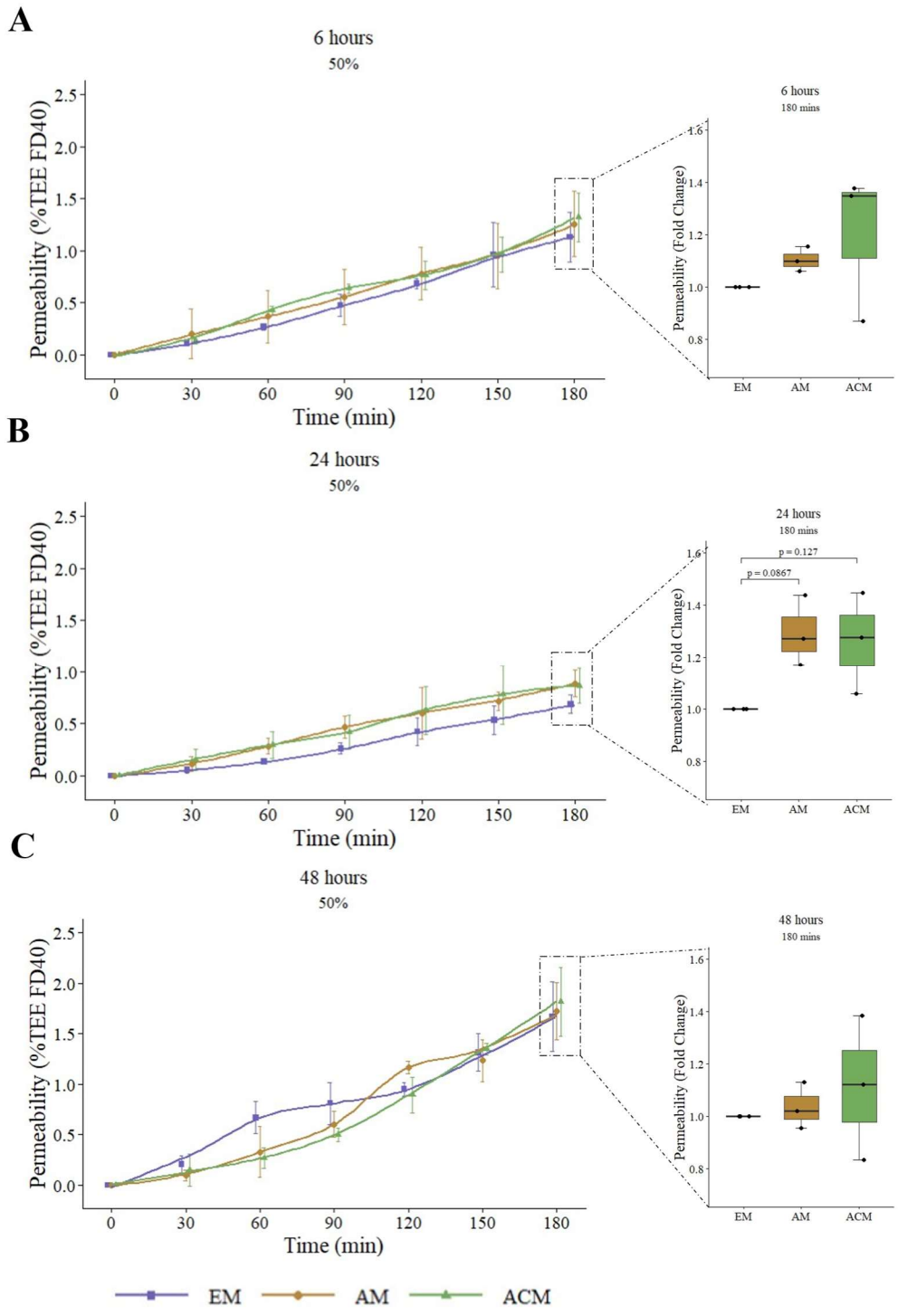


Figure 3.6 ***Permeability of HBMvECs after incubation with diluted astrocyte (conditioned) media*** *for 6 (A), 24 (B), and 48 (C) hours. Complete cell coverage was verified visually prior to treatment and prior to beginning of the assay. The line graphs (left) and histograms (right) show the change in permeability (%TEE FD40) between 0 – 180 mins and at a given timepoint (t = 180 mins), respectively. D) shows the permeation rate of each line graph. Results are averaged from n =3 independent experiments ± SD. Fold changes are shown normalised to EM control.*

3.2.2.4 The Effect of ACM on TJ Gene Expression Levels

Diluted (50%) ACM had no significant effect on HBMvEC permeability at any timepoint (Figure 3.7). However, as permeability assays focus on the overall integrity of the barrier, changes on the molecular level could be missed. Many members of the TJ protein families share similar functions, with the loss of a single protein compensated for by related homologs (Wada et al., 2013; Otani et al., 2019). Therefore, it was hypothesized that treatment with ACM may still cause an effect on the major proteins of the TJ complex. Therefore, the effect of ACM on the expression of claudin-5, occludin, and ZO-1 were explored on both the mRNA and protein levels.

For these experiments, endothelial cells were seeded onto a transwell and allowed to settle overnight. The next day, the media was removed, and fresh endothelial media added to the apical chamber. Diluted (50%) ACM, diluted (50%) AM control, or undiluted EM control was added to the basolateral chamber. Treatments were incubated for 6, 24, and 48 hours. After completion of the timecourse, cells were either lysed in TRIzol (for RNA isolation) or RIPA buffer (for protein isolation).

There were no statistically significant changes in CLDN-5, OCLN or ZO-1 gene expression after incubation with ACM at any time point (Figure 3.7)

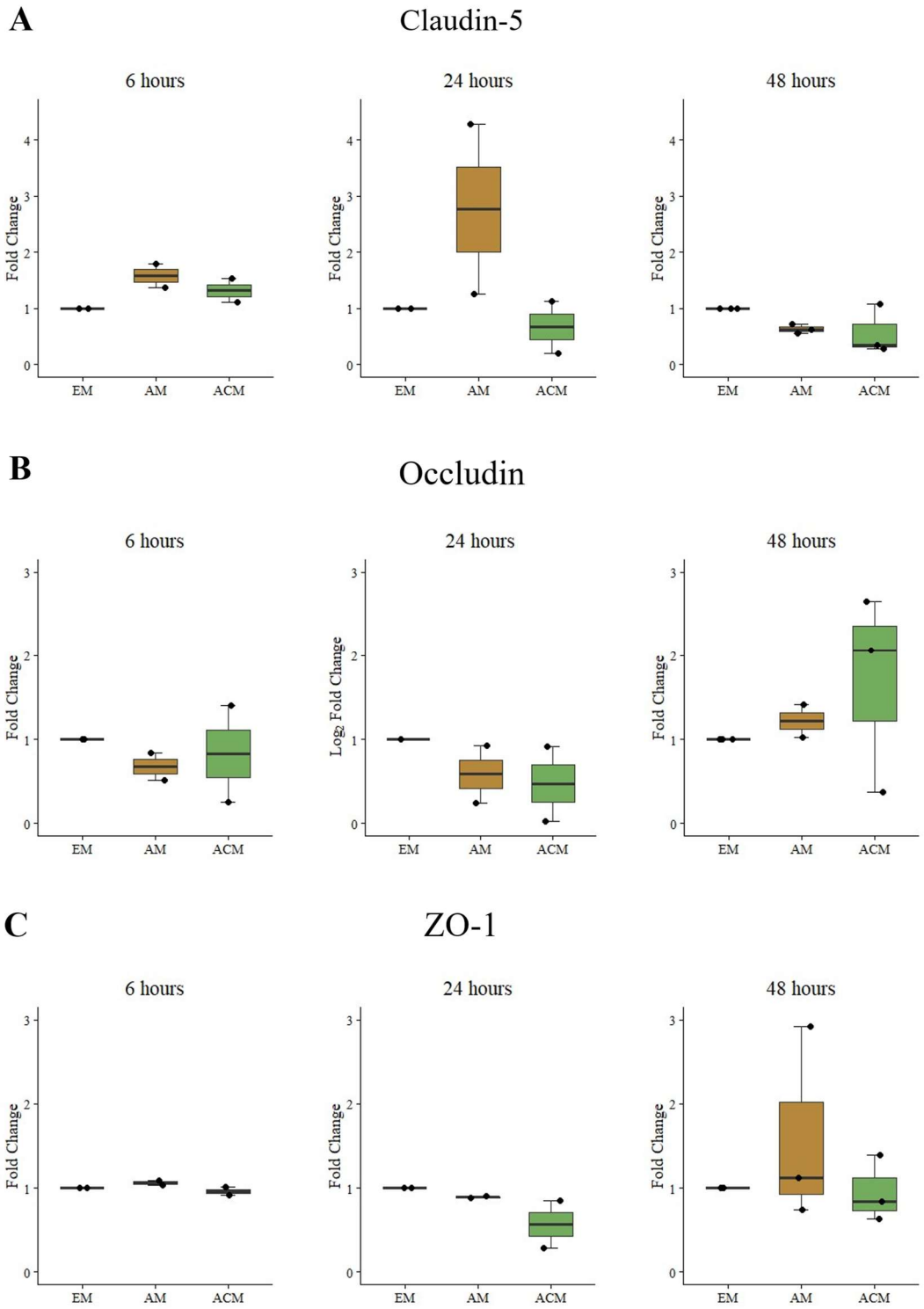


Figure 3.7 ***TJ gene expression after incubation with diluted ACM.*** *The expression of claudin-5 (A), occludin (B), and ZO-1 (C) were explored after 6 hours (left), 24 hours (middle), and 48 hours (right) incubation. Fold change values determined by qPCR. For 6 and 24 hours, n =2. For 48 hours, n = 3.*

On the protein level, there were no statistically significant differences in claudin- 5 protein expression at any timepoint (Figure 3.8). Trends indicated, however, that after 48 hours, this protein appeared to be down regulated by treatment with AM (-0.683±0.429, $p > 0.05$) while treatment with ACM seemed to attenuate protein expression (0.653±1.55, $p > 0.05$) in 2 out of 3 replicates (Figure 3.8C).

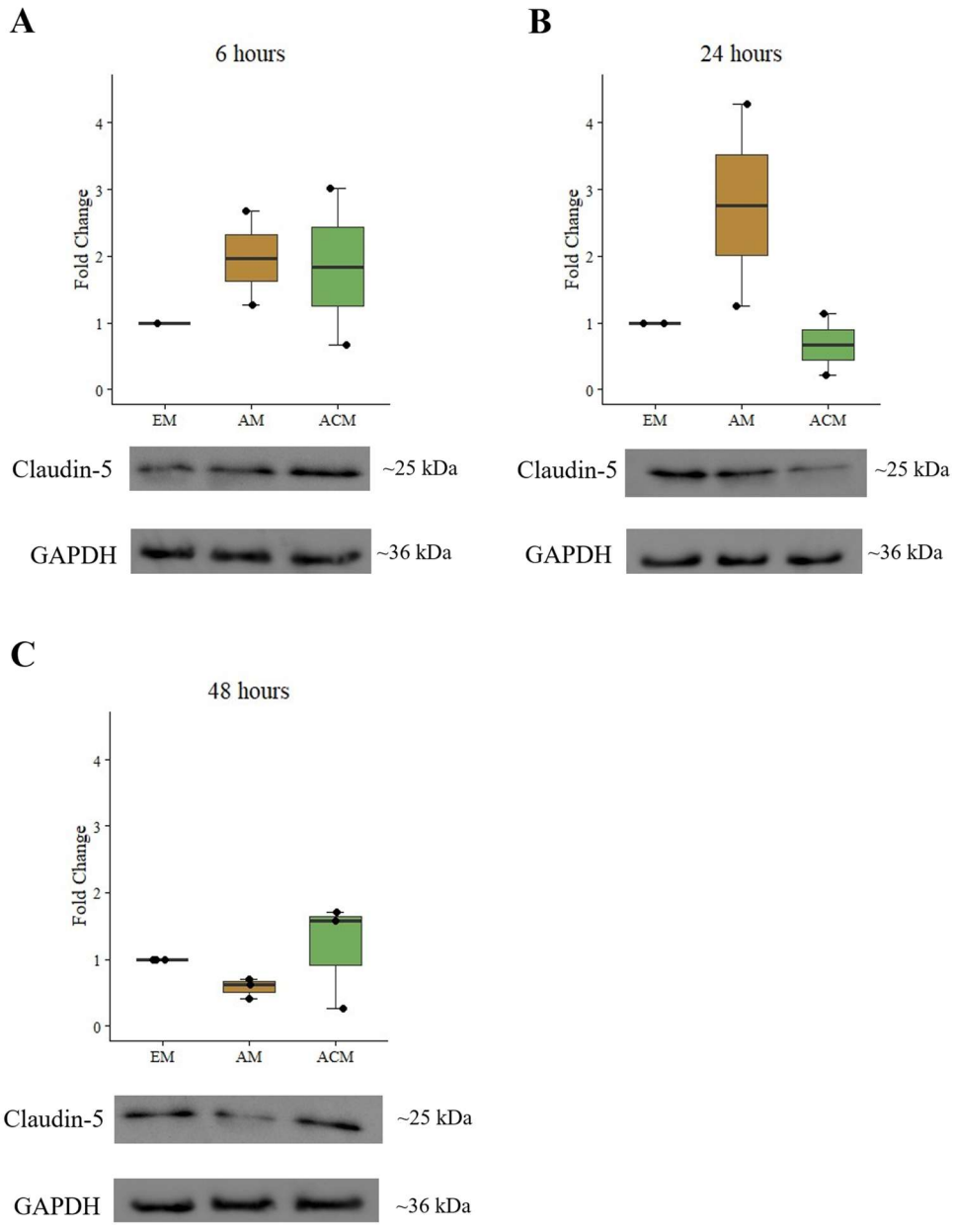


Figure 3.8 ***Claudin-5 protein expression analysis in response to ACM*** after 6 hours (A), 24 hours (B), and 48 hours (C). Black dots indicate individual data points. n = 2 (A, B). n =3(B, C). Data is presented as the median fold change ± SD. Data analysed using one-way ANOVA. Representative blots for claudin-5 at each time point are presented below each boxplot. GAPDH was used as a loading control.

There was no significant change in occludin gene expression levels after ACM treatment at any timepoint (Figure 3.9). However, AM treatment significantly reduced occludin protein expression levels after 48 hours of incubation (0.449 ± 0.127, p = 0.00537) (Figure 3.9C). Although only approaching significance, ACM seemed to attenuate this somewhat (0.775 ± 0.178, p = 0.0529).

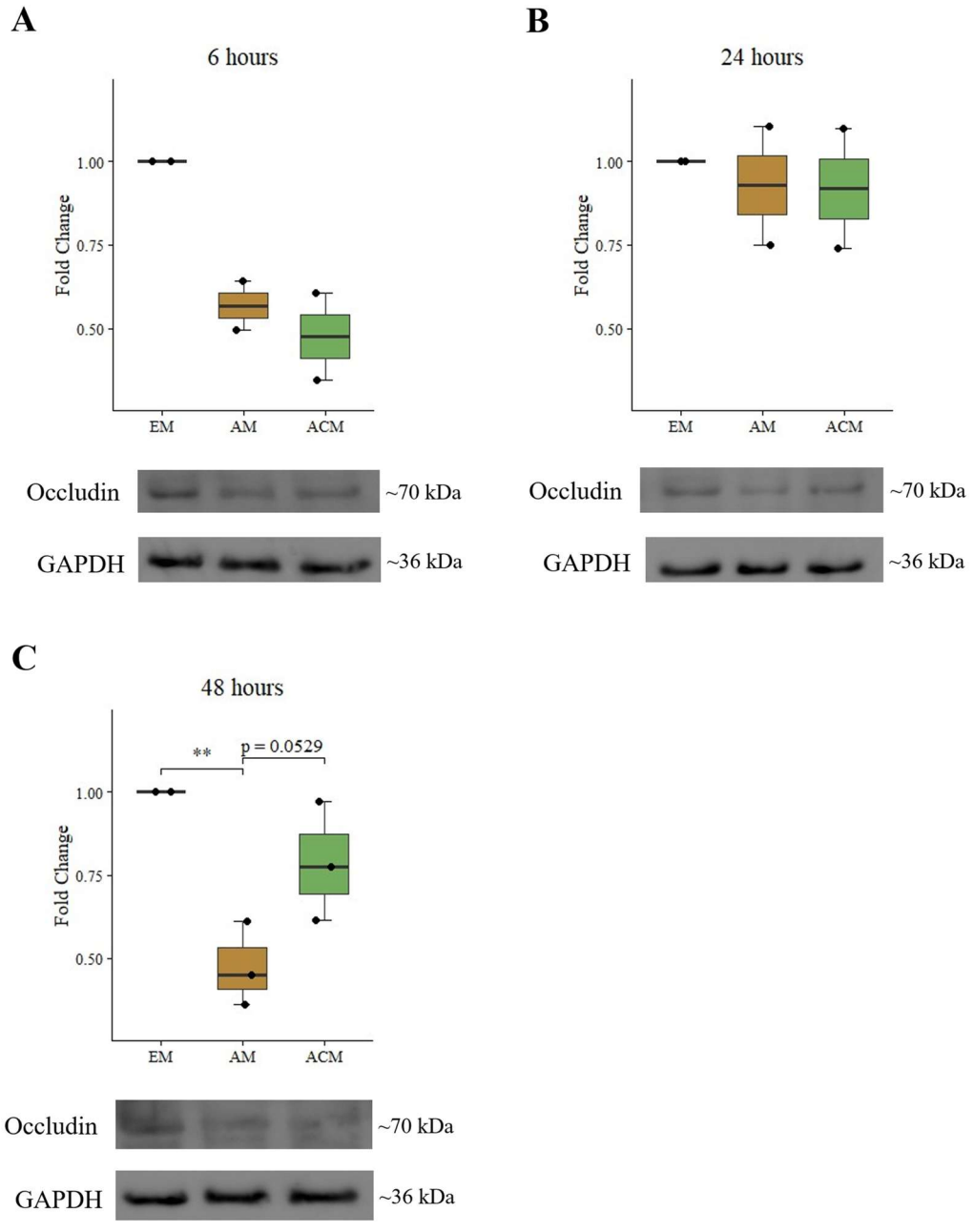


Figure 3.9 ***Occludin protein expression analysis in response to ACM*** after 6 hours (A), 24 hours (B), and 48 hours (C). Black dots indicate individual data points. n = 2 (A, B). n = 3(B, C). Data is presented as the median fold change ± SD. Data analysed using one-way ANOVA. Representative blots for occludin at each time point are presented below each boxplot. GAPDH was used as a loading control.

ZO-1 expression also remained statistically unchanged on the protein level at any timepoint (Figure 3.10).

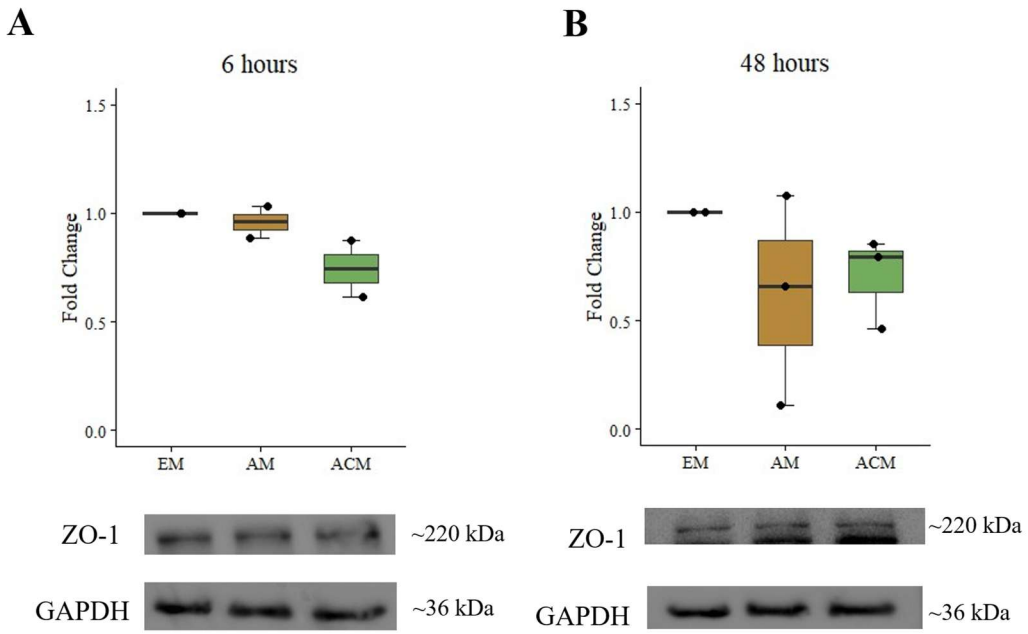


Figure 3.10 ***ZO-1 protein expression analysis in response to ACM*** after 6 hours (A) and 48 hours (B). Black dots indicate individual data points. n = 2 (A). n = 3 (B). Data is presented as the median fold change ± SD. Data analysed using one-way ANOVA. Representative blots for ZO-1 at each time point are presented below each boxplot. GAPDH was used as a loading control.

3.3 Discussion

This chapter examined the effects of ACM on the viability and BBB integrity of HBMvECs. As an initial step, the lineage of both primary astrocytes and HBMvECs were confirmed through the expression of several classical markers. Once the identity of these cells was confirmed, a bank of 48-hour conditioned media samples was prepared from both astrocyte and endothelial cell cultures maintained in standard culture conditions. The initial aim towards examining how the astrocyte-derived secretome influences HBMvEC phenotype required assessment of the impact of the secretome on HBMvEC viability with respect to concentration and time.

Although there was no significant change in HBMvEC viability after treatment with ECM, the viability of these cells decreased in a time and concentration-dependent manner upon apical treatment with both AM and ACM. This suggested that the chemical composition of the astrocyte base media itself has a detrimental effect on the viability of the cells, as diluting AM with EM resulted in an attenuation of this effect. Similar results were found upon basolateral exposure of HBMvECs to ACM. Studies looking at endothelial cell viability following ACM incubation are lacking in literature. However, Leopold et al., (2019) compared the effect of 7 purchasable endothelial culture media on key biological properties of primary human endothelial cells and found that viability varied widely. Since even some medias targeted for endothelial cell use resulted in poor viability, it is perhaps of no surprise that another media type would produce the same results.

Interestingly, after 48 hours of basolateral exposure, EM-diluted ACM significantly improved viability of HBMvECs in comparison to undiluted ACM. This suggests that the toxic effects of astrocytic media components on HBMvECs are being diluted. Furthermore, both diluted and undiluted ACM improved viability of HBMvECs in comparison to AM, pointing to the astrocyte secretome having a protective effect on the viability of HBMvECs and implying that the secretome of human brain astrocytes has a beneficial effect on these cells.

However, the crystal violet assay detects the maintained adherence of cells to the well as an indirect measure of viability (Mineiro et al., 2020; Gungor et al., 2026).

Therefore, these results may be attributed to AM and ACM affecting the adherence of HBMvECs but not viability. As a result, the adherence of cells after treatment with ACM was explored (Figure A.1, Appendix). There was no significant difference in the number of live cells found in the apical chamber after treatment with AM or ACM. If this treatment had affected adherence, then an increase in live cells would have been found. This result suggested that the results of the crystal violet assay are not due to changes in adherence but in viability. However, this could be further confirmed through the use of other assays that have been used to measure viability in endothelial cells such as PrestoBlue (Boncler et al., 2014; Luzak et al., 2022), MTT (F. Cheng et al., 2020; Parenti et al., 2026), and Cell Counting Kit-8 (CCK-8) (C. Song et al., 2024; Ryu et al., 2025).

By contrast, diluted ACM did not have a statistically significant effect on the integrity of the barrier at any timepoint. This contradicts other studies that have looked at the effect of ACM on endothelial cell permeability (Arthur et al., 1987; M. Török et al., 2003; Baumann et al., 2021). To overcome inter-species differences, this discussion will be limited to studies involving human endothelial cells and human-derived ACM. Siddharthan et al., (2007) found that static co-cultivation of primary human endothelial cells with ACM from human foetal astrocytes for 5 days was able to improve integrity of the BBB. The expression profile of astrocytes changes during development (Cahoy et al., 2008; Lattke et al., 2021), which may explain the contrasting results. However, Kuo & Lu (2011) also found that the barrier properties of primary human endothelial cells were improved upon long-term (14 days) treatment with diluted ACM from primary human astrocytes in the basolateral chamber, with increased electrical resistance and decreased permeability by 70%. Since the incubation time was much shorter in our study (i.e., up to 48 hours), this may explain the differences between results. By contrast, Guo et al., (2025) also found that ACM from human astrocytes was decreased permeability of HBMvECs, even after a shorter incubation period (3 days).

The aforementioned studies also used tracers of different sizes, varying from very small (>1kDa (Siddharthan et al., 2007; Kuo & Lu, 2011; Baumann et al., 2021)) to 66 kDa (Guo et al., 2025). Other studies used electrical resistance as a measurement of barrier integrity (M. Török et al., 2003; Kuo & Lu, 2011). In this

study, a fluorescent tracer (FITC-dextran) of 40 kDa was used, which could explain the contrasting results seen in comparison to these studies. FITC-dextran of 40 kDa is commonly used to explore the selective permeability of the BBB (Hoffmann et al., 2011; Greene et al., 2024). However, FITC-dextran is available in a variety of molecular weights, ranging from 0.4 kDa to 20,000 kDa (Sigma). 4 kDa and 70 kDa FITC-dextran are also used in BBB permeability assays (Hoffmann et al., 2011; Alves et al., 2019; Couto et al., 2019; J. Sun et al., 2022), in order to explore the permeability of the BBB to low and high molecular weight proteins, respectively. Due to material constraints, a decision was made to use a medium molecular weight FITC-dextran in order to capture an overview of the barrier's integrity. However, a limitation of this approach is a lack of insight into the integrity of the BBB to low and high molecular weight proteins in particular. Unlimited time and materials would have allowed for an exploration into the integrity of the barrier to both low and high molecular weight proteins. Additionally, while unavailable for this study, exploring the electrical resistance of HBMvECs would have allowed for a comprehensive analysis of the health of the TJs and barrier (Srinivasan et al., 2015; S. Shan et al., 2022).

Another rationale that could explain these contrasting results was that viability was significantly compromised upon HBMvEC exposure to both AM and ACM, likely due to a toxic effect of the astrocyte media composition on endothelial cells. Interestingly however, although viability decreased significantly upon treatment with AM, there was no significant difference in permeability between HBMvECs treated with AM and the control. This suggests that while both undiluted AM and ACM significantly decreased viability, the composition of the media itself may not be the cause of the significant increase in permeability. Additionally, this was not caused by changes in the adhesion of the cells as there was no significant difference in the amount of detached live cells found in the apical chambers of HBMvECs treated with undiluted AM or ACM (Figure A.1, Appendix). These results suggested that there may be an aspect of the astrocyte secretome that was able to modulate the barrier integrity of HBMvECs.

In further studies, the expression levels of the major TJ proteins were explored on both the mRNA and protein levels after HBMvEC incubation with diluted ACM. There were no statistically significant changes in claudin-5 gene expression at any

timepoint, although claudin-5 protein expression was observed to change, albeit not consistently, after 48 hours of incubation with ACM. In this respect, a study reported that primary human ACM had no effect on claudin-5 mRNA expression on a healthy human endothelial cell line after 6 hours of incubation (Stafford et al., 2022). An even earlier study, however, found that human ACM increases claudin-5 mRNA expression in brain endothelial cells after 24 hours (Alvarez et al., 2011). Y. Wang et al., (2014) found that claudin-5 protein levels increased in MBEC4 cells (a mouse brain capillary cell line) after incubation with undiluted mouse primary ACM for 24 hours. Another study also found that conditioned media from an immortalised astrocyte cell line, U251, was also able to increase claudin-5 protein levels in hCMEC/D3 cells after 6 days incubation, with media refreshed every 24 hours (L. Yang et al., 2024).

There were also no significant changes in occludin gene expression levels at any timepoint. In this respect, other studies on occludin expression after ACM treatment seem to be limited. However, Guo et al., (2025) found that ACM from human astrocytes was able to increase occludin mRNA expression in HBMvECs after 3 days incubation. Also in our studies, there appeared to be a significant decrease in occludin protein levels in HBMvECs incubated with AM which was attenuated by ACM after 48 hours, although no significant effect was observed at shorter timepoints. Another study also found that there was no significant change in occludin protein expression after a short period of incubation of the mouse brain endothelial cell line cerebEND with ACM derived from the rat glioma line, C6 (W. Neuhaus et al., 2014). However, Y. Wang et al., (2014) found that occludin protein levels increased in MBEC4 cells after incubation with mouse primary ACM for only 24 hours.

ZO-1 gene and protein expression remained consistent with control levels at all timepoints, in direct contrast to Siddharthan et al., (2007) who found that ZO-1 protein levels were increased upon treatment of primary human brain endothelial cells with ACM. Again, as Siddharthan et al., used foetal astrocytes, this increase in ZO-1 may be limited to a developmental stage of the astrocytes. Additionally, endothelial cells in this study were incubated with ACM for 5 days, a longer exposure time than that used in our study. Gardner et al., (1997) also found that 50% ACM was able to increase ZO-1 protein expression after only 3 days of

exposure. By contrast, Stafford et al., (2022), found that ZO-1 levels remain unchanged after 6 hours of incubation with ACM, which may suggest that changes to ZO-1 expression do occur but only after longer incubation times.

Interestingly, Zamproni et al., (2025) found that 103 genes were differently expressed in human endothelial cells cultivated with human astrocytes. Remarkably, however, these did not include claudin-5, occludin, or ZO-1. This contributes to the frequently contradicting results regarding TJ gene expression found across the literature. This variability could potentially be attributed to the differences in cells used, variations in the chemical composition of base media, and discrepancies in incubation times. One reoccurring aspect in these studies is that the same media used for conditioning was used for the maintenance of endothelial cells. This may have also played a role in the differences of our results. One paper found that the composition of medias resulted in variability of endothelial cell permeability of endothelial cells as well as in claudin-5 expression levels (Helms et al., 2010). Although this was a factor considered during experimental planning, there were concerns as to how the different composition of the media could affect the secretome of the astrocytes, as different culture media is known to result in differences in cellular properties (Combe & Sokolenko, 2021; J. Lee et al., 2025), including in astrocytes (Wolfes et al., 2017; Tsukuda et al., 2019).

Exploring the expression levels of TJ genes and proteins is an important initial step in understanding the underlying mechanism of BBB function as several studies have found a correlation between TJ expression levels and barrier function (McCarthy et al., 1996; Nitta et al., 2003; Jiao et al., 2011; Sugiyama et al., 2023). However, functional TJs rely on protein interactions between the transmembrane proteins at the cell periphery, which depends on the proper localisation of TJ proteins to the cell periphery. Gene and protein expression levels do not provide information about the location of these proteins in the cell and therefore only show an incomplete insight into the effect of ACM on TJs. Initially, plans were made into exploring the effect of ACM on the localisation of these TJ proteins and an attempt was made into staining of HBMvECs on transwell membranes. However, due to lack of antibody specification, issues with fixation in addition to a lack of time, as well as due to the confounding effect of the AM on HBMvECs, and seemingly

negligible effect of ACM on the integrity of BBB, other experiments were prioritised

In conclusion, although AM itself seemed to cause a decrease in viability, conditioned media attenuated this effect when cells were given access to endothelial media, regardless of whether ACM was diluted with EM itself or not, clearly indicating that ACM has a protective effect on HBMvECs. Similarly, incubation with AM resulted in a decrease in occludin protein levels but ACM was able to attenuate this effect Whilst there appeared to be no statistically significant change in permeability with either AM or ACM, the ACM did appear able to modulate claudin-5 protein levels following extended incubation times, albeit not statistically. This collective evidence indicates that there is some factor in ACM that does affect the barrier properties of HBMvECs. However, determining the exact component(s) is difficult due to the complexity of the astrocyte secretome (Matafora et al., 2023; J. Liu et al., 2025). The potentially toxic effects of the astrocytic base media chemical composition on the HBMvECs is also a confounding factor in these experiments.

Determining and isolating the beneficial factor(s) in ACM would allow us to explore their effects on the cells directly, without any confounding effects from the astrocyte media itself. Astrocytes have also been shown to release EVs as part of their secretome (Forró et al., 2024; Nieland et al., 2025). As EVs are mediators of cellular communication (J. Wang, Li, et al., 2022; Y. Yu et al., 2024), this may be one of the main secreted factors that is causing the increase in permeability and/or attenuating the effect that astrocyte media has on the viability of HBMvECs. The contents of EVs reflect the state of the donor cell (Hoshino et al., 2020; K. S. Lee et al., 2021) which may support the levels of statistical variability seen in some experimental results. Hence, the following chapters will now deal with EV isolation from conditioned media (Chapter 4) and their effect on the barrier function and TJ gene expression (Chapter 5) as well as on the transcriptome of HBMvECs (Chapter 6).

Chapter 4 : Verification and Quantification of EV Isolation Methods

4.1 Introduction

Intercellular communication is a key component of a variety of physiological functions (Ramilowski et al., 2015; X. Zhou et al., 2018; M. Tian et al., 2025). The importance of the cellular secretion and uptake of extracellular vesicles (EVs) in cell-cell communication has recently emerged (Irmer et al., 2023; T.-L. Liao et al., 2025), with EVs being consistently exchanged by different cells over short and long distances *in vivo* (Hoshino et al., 2015; Linxweiler et al., 2021). EVs are heterogeneous nanoparticles, containing cytosolic proteins and RNA, enclosed by a transmembrane protein-containing lipid bilayer.

The contents of these particles often reflect those of their donor cell, offering an insight into the state of their source (Tkach et al., 2017; O'Hara et al., 2020). As they can be found in practically all biological fluids, including blood (Abdelmohsen et al., 2023; Y. Ren et al., 2011), urine (Pisitkun et al., 2004; Filipović et al., 2024), and cerebral spinal fluid (Balusu et al., 2016; Gu et al., 2021), EVs have gathered much attention as a non-invasive biomarker for several diseases (A. Kumar et al., 2023; Z. Zhang et al., 2023; M. A. Kumar et al., 2024). For example, EV content differs significantly between head and neck squamous-cell carcinoma cells (HNSCC) and normal cells (Langevin et al., 2017; Theodoraki et al., 2021). In addition to this, EVs isolated from HNSCC patients who showed complete responses to treatment contained different proteins (Lim et al., 2019; Rodrigues-Junior et al., 2019), highlighting EVs not only as biomarkers of disease but their potential as predictors of therapeutic efficacy.

However, EVs also act as dynamic mediators of cellular communication by transferring their contents to recipient cells. This allows them to play important roles both physiologically (J. S. Choi et al., 2016; B. Li et al., 2020) and in disease progression (Cooks et al., 2018; S. Zhao et al., 2020). EVs have been shown to accumulate in multiple organs (Gupta et al., 2020; Liam-Or et al., 2024). As a result, discerning their effect on specific cell types is difficult *in vivo.* Therefore, using translational *in vitro* models allows for the isolation of EVs from one type of donor cell and the exploration of their effect on a particular recipient cell. Several studies have investigated EVs isolated from cell culture conditioned media *in vitro* in order to determine their properties (Silachev et al., 2019; Z. Wang et al., 2020) as well as

to study their therapeutic potential in pathological conditions (Jin et al., 2021; Turovsky et al., 2022).

Although several methods have been developed in order to isolate EVs both from biological sources and conditioned media, each of these methods has its own limitations. Research has shown that yield, purity, and preservation of the biophysical properties of isolated EVs depends on the method chosen (Nordin et al., 2015; Gámez-Valero et al., 2016; Brennan et al., 2020; Veerman et al., 2021; Suresh & Zhang, 2025). The gold standard for the isolation of exosomes has been through differential centrifugation (DC), which is the most commonly reported strategy (Gardiner et al., 2016; Konoshenko et al., 2018). First published by Johnstone et al. (1989), this method uses high centrifugal speeds (typically 100,000 -150,000 x *g*) in order to separate and purify EVs, following the removal of increasingly smaller debris through repeated centrifugation steps of increasing speeds. Repeated centrifugation can reduce the amount of non-EV particles that co-precipitate with the EVs. However, as a result, EVs can get lost or damaged, consequently reducing particle yield. As particle sizes have different sedimentation rates during centrifugation, larger particles like MVs can be isolated through centrifugation at a lower speed (14,000-20,000 x *g*) (F. A. Martin et al., 2014; Menck et al., 2017).

As DC requires access to high-speed centrifuges, polymer-based isolation methods, which require much lower centrifugation speeds, have become a more accessible option. Polyethylene glycol (PEG) is a polyether compound which is used to concentrate and purify viruses (Adams, 1973; Alexander et al., 2020). As viruses and EVs share similar biophysical properties, methods used to isolate viruses have been adapted in order to isolate EVs. Specifically, Rider et al (2016) developed a polymer-based EV isolation method using PEG (ExtraPEG) that has been routinely employed in EV research (Crewe et al., 2021; K. Yang et al., 2022; X. Xie et al., 2023). This method involves the overnight incubation of conditioned media with PEG, followed by a low-speed centrifugation step (1,500 - 2000 x *g*) in order to isolate the vesicles. The addition of highly hydrophilic polymers creates a hydrophobic micro-environment in the solution through their interaction with water molecules surrounding the EVs. This decreases the solubility of EVs and allows them to precipitate more easily with a lower speed centrifugation step as compared

to DC. Commercial polymer-based EV isolation reagents, such as ExoQuick™ (Systems Biosciences) and EXO-Prep™ (HansaBioMed), have also been widely used (C.-H. Lu et al., 2021; Y. Huang et al., 2022; Reseco et al., 2024). These are user-friendly and tend to result in higher yields in comparison to other methods (Tangwattanachuleeporn et al., 2022; Williams et al., 2023). However, one study found that RNA yield was lower using the ExoQuick™ kit in comparison to DC (Aziz et al., 2022). These also tend to be expensive whereas the ExtraPEG isolation method is comparatively cheaper and produces similar results. Polymer-based precipitation methods can result in high yields, but these can be of low purity due to coprecipitation of non-EV components. Additionally, remnants of the polymer may affect downstream processes, such as mass spectrometry (Coughlan et al., 2020).

In order for this body of research to investigate the biological influence of EVs, it was necessary to determine an effective method of isolating them from the sample matrix (i.e. cell culture media). As mentioned above, different isolation methods can affect the characteristics of the isolated EVs (Nordin et al., 2015; Gámez-Valero et al., 2016; Brennan et al., 2020; Veerman et al., 2021; Suresh & Zhang, 2025). This is particularly important given that different cell lines may require specific isolation methods for optimal EV isolation (Jeppesen et al., 2014; X. Xie et al., 2023). Therefore, it is essential to select a method that yields the optimum results in terms of both yield and purity for the specific cells used. As such, in this chapter it was endeavoured to isolate and characterise EVs released from both astrocytes and HBMvECs cells using both DC and PEG methods of EV isolation. Additionally, the effect of applying two different DC speeds (20,000 x *g* and 50,000 x *g*) was explored.

4.1.1 Chapter Aims

- To compare two different methods of isolating EVs derived from both astrocyte and endothelial cell conditioned media in terms of purity, heterogeneity, and absence of confounding factors with a view of selecting the best method.
- To optimise this isolation method with a view of maximising EV yield.
- To characterise the physical (size, heterogeneity) and molecular (protein) properties of the EV isolates.

4.2 Results

4.2.1 Comparison of EV methods

In order to compare three popular EV isolation methods, conditioned media was banked from both HBMvEC (ECM) and astrocyte (ACM) cultures. Large cells and cellular debris were removed from the media via centrifugation prior to storing of the supernatant at -20°C. EVs were isolated from batched media by following the methods below.

4.2.1.1 Microvesicle Isolation (MV)

For MV isolation, EVs were isolated using the method described in Section 2.2.2.2, based on a modification of the method previously published by Martin et al., (2014). Figure 4.1 summarises these steps.

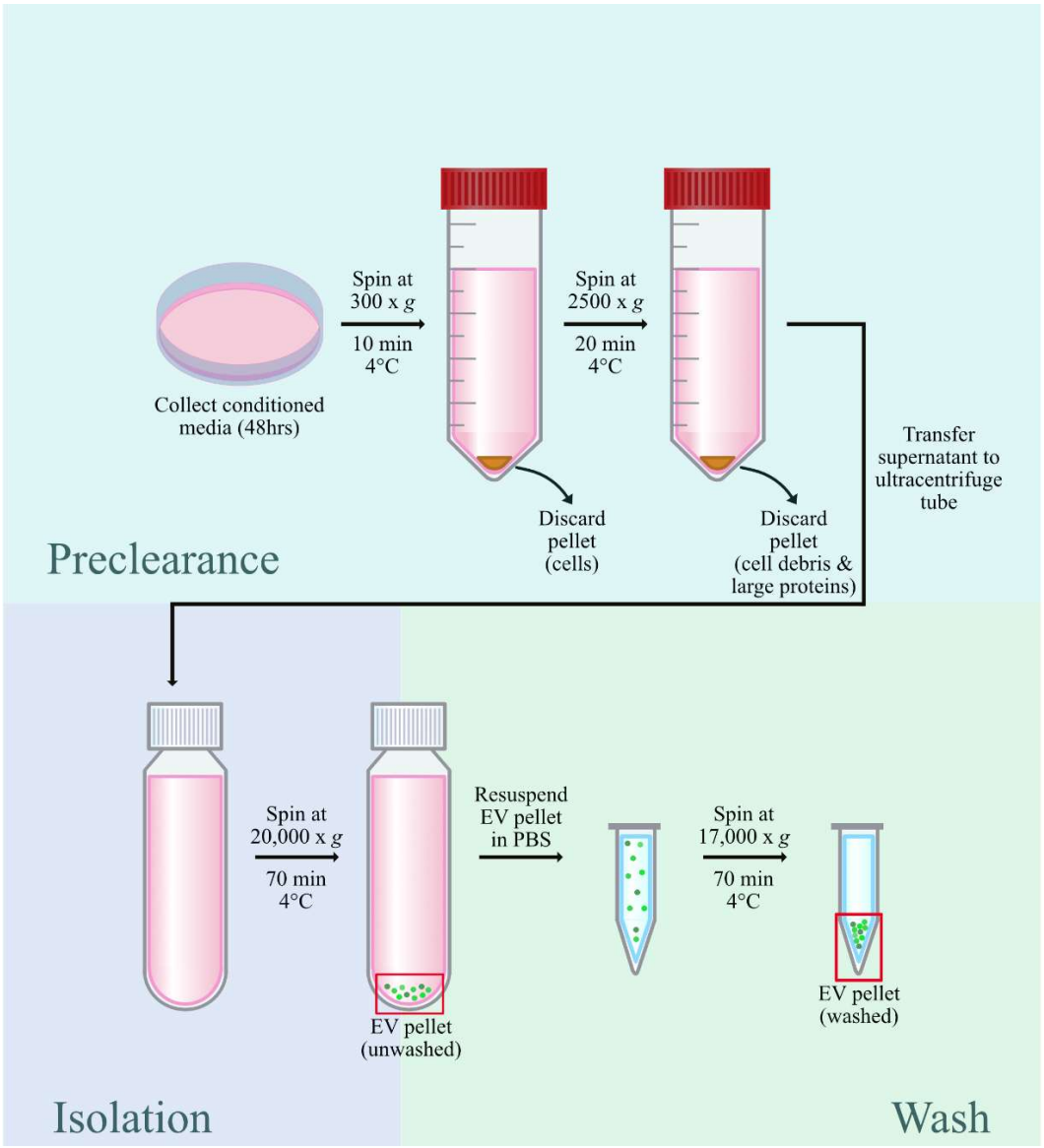


Figure 4.1 ***Flowchart summarising the Microvesicle Isolation method.*** *The stepwise removal of conditioned media constituents utilising centrifugal forces of increasing speeds and times. Following the removal of cells, cellular debris, proteins, etc, a spin at 20,000 x* g *results in an isolated pellet enriched in EVs. This pellet was resuspended in PBS to remove any unwanted co-precipitants and spun again. Figure created by author using Affinity Designer (v 1.10.6.1665).*

4.2.1.2 Differential Centrifugation (DC)

Based on the protocol of Théry et al. (2006), EVs were isolated using differential centrifugation as described in Section 2.2.2.3. The steps taken are summarised in a flowchart in Figure 4.2.

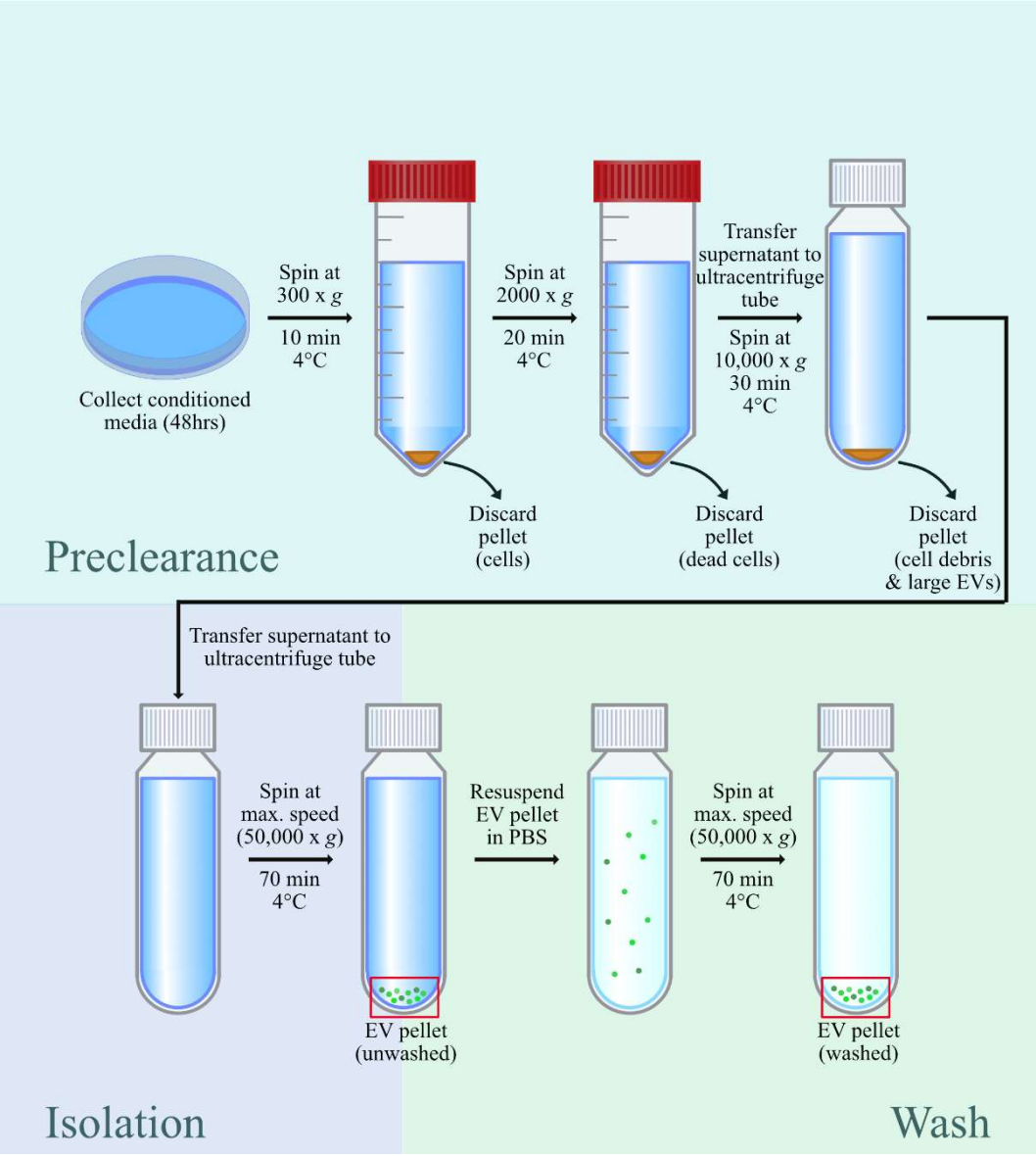


Figure 4.2 ***Flowchart summarising the Differential Centrifugation Isolation method.*** *This involves a series of centrifugations of increasing speeds and times before a spin at the maximum available speed for 70 minutes. The pellet from this step was resuspended in PBS and spun again at maximum speed to remove any contaminating proteins. The final washed pellet was then resuspended or lysed according to the downstream application. Figure created by author using Affinity Designer (v 1.10.6.1665).*

4.2.1.3 ExtraPEG

Unlike the two previous methods described above, ExtraPEG does not require an ultracentrifuge. EVs were isolated using the polymer-based isolation method based on the protocol developed by Rider et al. (2016), with modifications described in Section 2.2.2.4 and summarised in Figure 4.3.

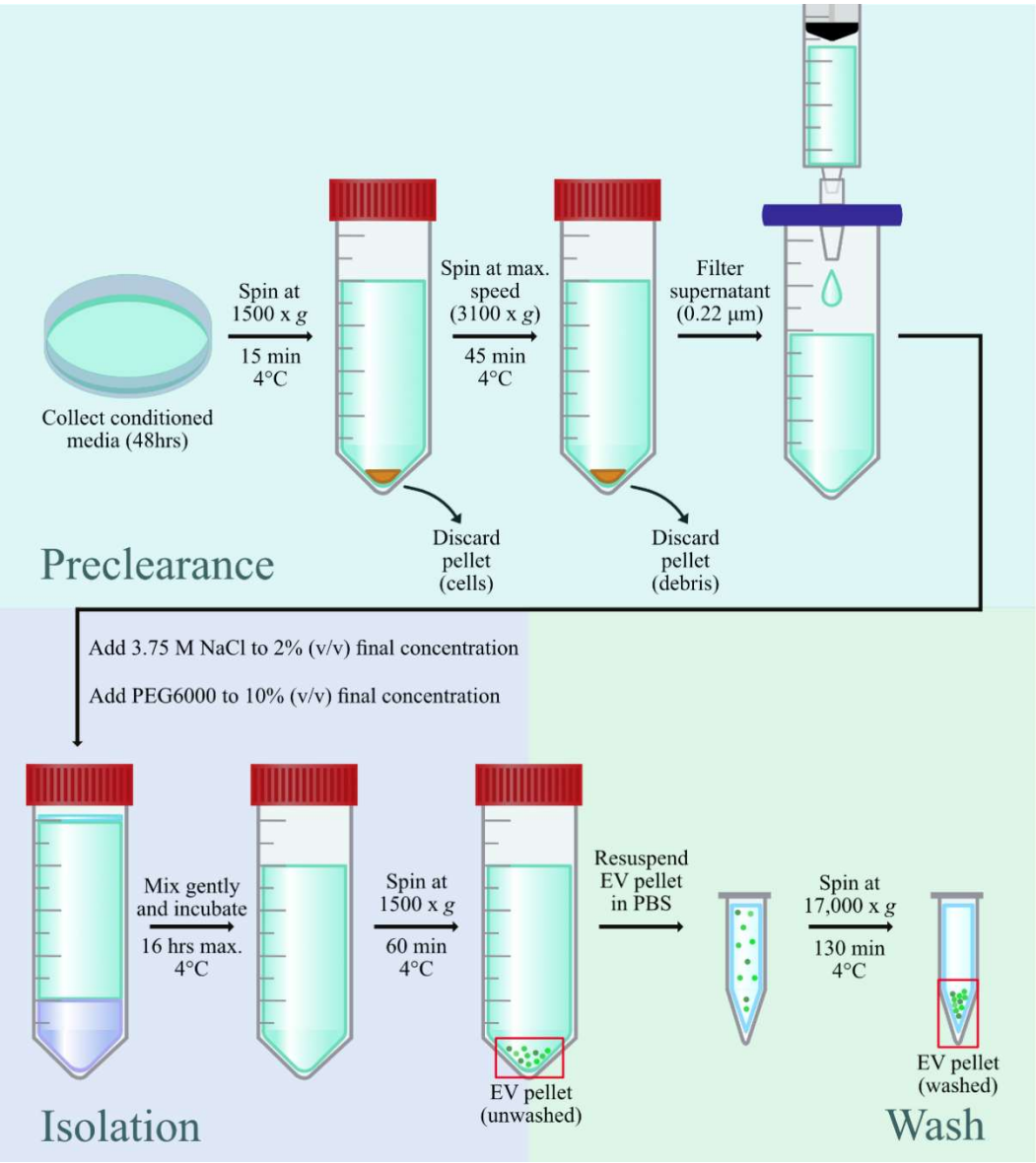


Figure 4.3 Flowchart summarising the ExtraPEG Isolation method*. This involves one spin post the pre-clearance step at maximum available speed. The resulting supernatant is then filtered before PEG and NaCl (3.75 M) are added. After an overnight incubation, the solution is spun at 1500 x g to isolate EVs. The resulting pellet can then be washed in 0.9% NaCl and spun at the maximum available speed. Both the unwashed and washed pellets are resuspended or lysed according to the downstream process. Figure created by author using Affinity Designer (v 1.10.6.1665).*

4.2.1.4 Comparison of Methods to Isolate ACM-derived EVs

EV pellets were isolated from media conditioned on astrocytes for 48 hours using the three different methods described above – MV, DC and ExtraPEG. The confluency of the astrocytes and the number of plates used were noted at the time of collection. All pellets were washed and either resuspended in PBS for size analysis or lysed in 200 µL TRIzol® and then frozen and stored at -80°C before further processing according to the method described in Section 2.2.5.1.

The total amount of RNA isolated was normalised to RNA isolated per 1,000,000 cells. This was calculated by using the confluency and the number of plates at the time of media collection in order to estimate the total number of cells generating EVs and account for differences in confluency upon media collection. There was no significant difference in ACM-derived EV RNA per 1,000,000 cells across all methods ($p = 0.69$) (Figure 4.4). MV isolation resulted in the lowest median yield of RNA per 1,000,000 cells (31.2 ± 64.8 ng). While DC isolation resulted in the highest median yield, there was a large amount of variability in yield (60.6 ± 64.4 ng). ExtraPEG isolation seemed to result in the most consistent isolation yield (49.1 ± 13.9 ng)

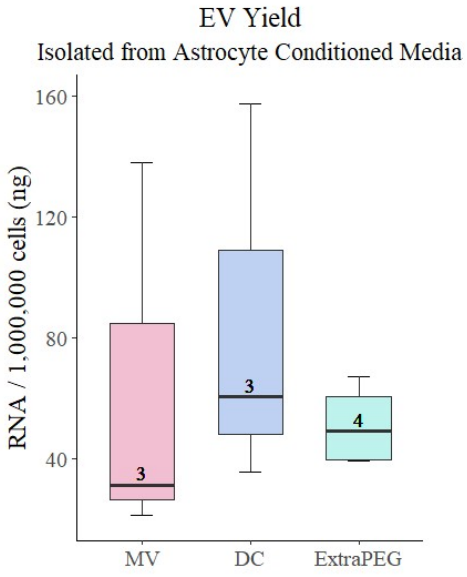


Figure 4.4 ***Comparison of MV, DC, and ExtraPEG methods to isolate ACM derived EVs (RNA)****. Results presented as the average amount of RNA (ng) isolated per 1,000,000 cells with the number of replicates ran per method denoted in the boxplot. Means compared using ANOVA. P = 0.690 (non-significant (ns)).*

The average size distribution of EV pellets was analysed using DLS (Figure 4.5). MV isolation yielded particles ranging between 60 nm and 1400 nm in size, with the majority of EVs isolated being around 488.7 nm. There was a secondary peak at 169.9 nm. Interestingly, particles isolated through the DC isolation method had a larger range of sizes, 60 nm to 1635 nm. However, the most frequent size of ACM-derived EVs isolated using this method was 420.2 nm, smaller than the majority of EVs isolated using the MV isolation method. There was a secondary peak of lEVs, of which the majority were 893.8 nm in size. The ExtraPEG method resulted in particles with a narrower spread in size distribution, with particles ranging from 60 nm to 900 nm. The most frequent size of particles isolated through this method was 197.6 nm.

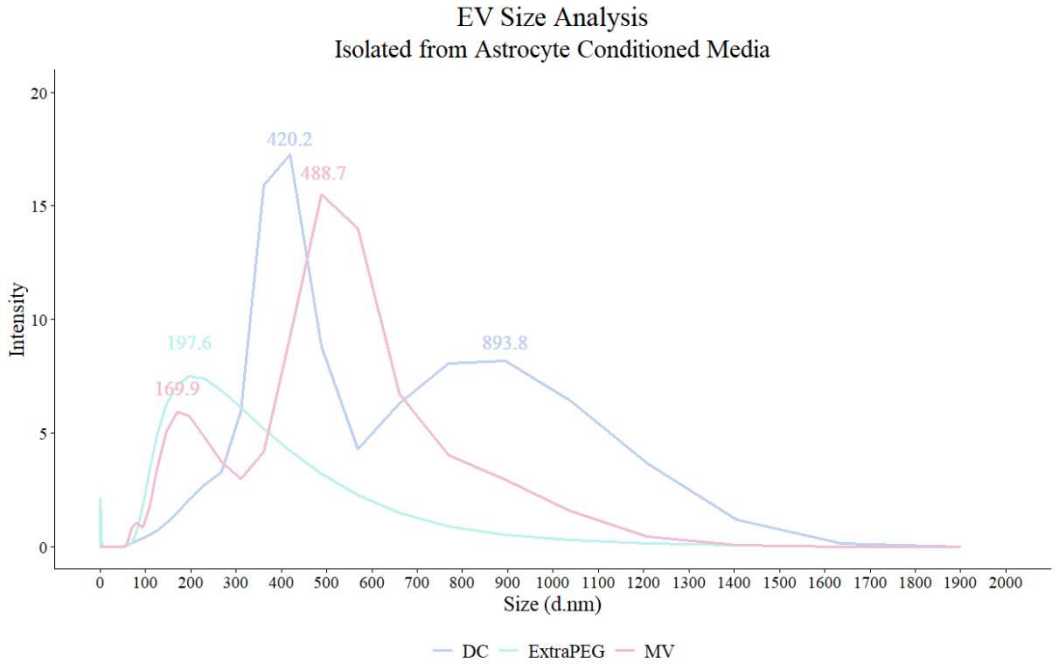


Figure 4.5 ***DLS Analysis of the Average Size Distribution by Intensity of EVs isolated from ACM*** *using Microvesicle (MV) Isolation, Differential Centrifugation Isolation (DC) and ExtraPEG isolation. Peak size (nm) denoted above peak. Intensity measures the percentage of EVs that fall under a particular size. Line graphs show the average of 3 isolations for each method.*

4.2.1.5 Comparison of Methods to Isolate Endothelial Conditioned Media Derived EVs

EV pellets were isolated from media conditioned on HBMvECs for 48 hours using the three different methods described above – MV, DC and ExtraPEG. The confluency of the endothelial cells and the number of plates used were noted at the time of collection. All pellets were washed and either resuspended in PBS or lysed in 200 µL TRIzol®. The latter were then frozen and stored at -80°C before further processing according to the method described in Section 2.2.5.1. The total amount of RNA isolated was normalised to RNA isolated per 1,000,000 cells, as in 4.2.1.4.

There was no significant difference in RNA isolated per 1,000,000 cells across all methods ($p = 0.687$) (Figure 4.6). ExtraPEG isolation resulted in the highest average amount of RNA per 1,000,000 cells isolated (36.2 ± 35.3 ng). Both MV and DC isolation resulted in similar amounts of RNA isolated (24.8 ± 19.7 ng and 26.1 ± 35.8 ng, respectively).

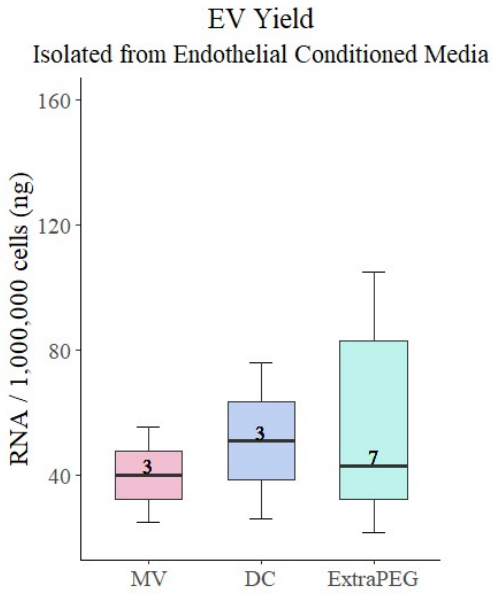


Figure 4.6 ***Comparison of MV, DC, and ExtraPEG methods to isolate ECM derived EVs (RNA).*** *Results presented as the average amount of RNA (ng) isolated per 1,000,000 cells with the number of replicates ran per method denoted in the boxplot. Means compared using ANOVA. P = 0.687.*

The average size distribution of EV pellets resuspended in HEPES/NaCl buffer was analysed by DLS (Figure 4.7). The size of particles isolated through MV isolation ranged between 50 nm and 2000 nm, peaking at 420.2 nm. Particles isolated through the DC isolation method had a narrower spread, falling between 100 nm and 1200 nm. The most frequent size of ECM-derived EVs isolated using this method was also 420.2 nm. However, there was also a secondary peak of lEVs, with the majority of these being 768.5 nm. Particles isolated through the ExtraPEG method had a narrower range, between 20 nm to 1040 nm, which the majority of EVs isolated through this method peaking at 229.8 nm.

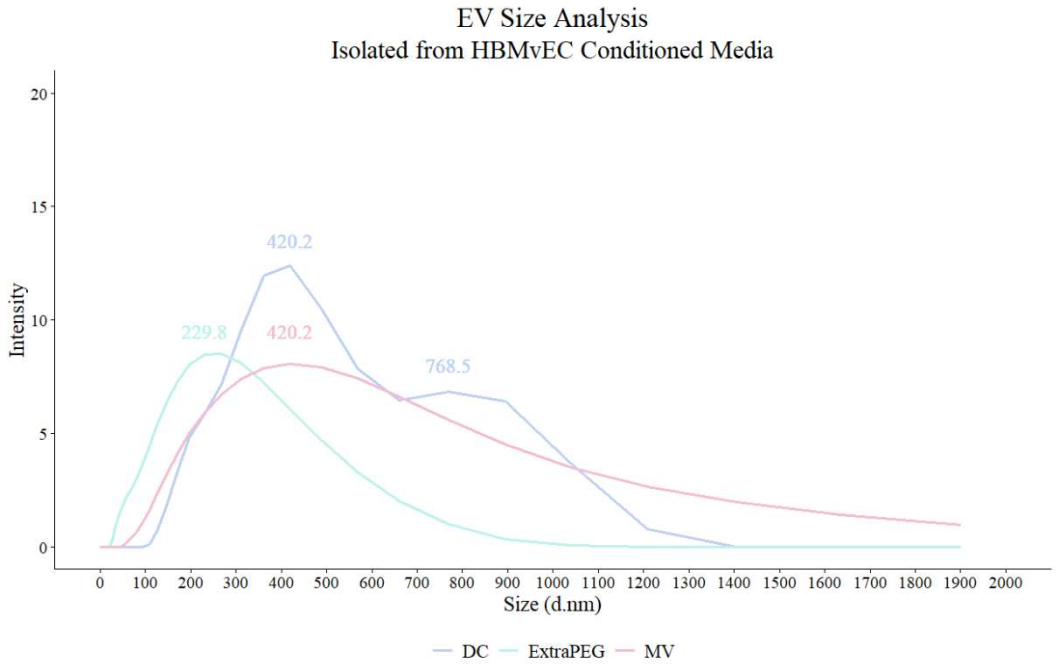


Figure 4.7 ***DLS Analysis of the Average Size Distribution by Intensity of EVs isolated from ECM*** *using Microvesicle (MV) Isolation, Differential Centrifugation Isolation (DC) and ExtraPEG isolation. Peak size (nm) denoted above peak. Intensity measures the percentage of EVs that fall under a particular size. Line graphs show the average of 3 isolations for each method.*

4.2.2 Verification of the ExtraPEG method

Due to the smaller heterogeneity of EV sizes, ExtraPEG isolation was found to be the most optimal EV isolation technique and was decided upon as the chosen isolation method. This method involves incubation with PEG and several centrifugation steps (Rider et al., 2016; S. Ma et al., 2025) with an added modification step of filtration as described above. To assess the effectiveness of EV isolation using this method, samples of the supernatants (distinguished as SX, where X is a number denoting where in the process the supernatant was generated) and pellets (distinguished as PX, where X is a number denoting where in the process the pellet was generated) were taken and used for protein analysis (Figure 4.8A). Briefly, a sample of the thawed media (S1) was taken before being centrifuged at maximum speed on a benchtop centrifuge (3000 x *g*) for 45 minutes. A sample of the supernatant was taken (S2) and the pellet resulting from the centrifugation was resuspended in PBS (P2). The remaining supernatant was then syringe-filtered through a 0.20 μm filter into a new 50 mL tube. A sample of the supernatant post-filtration was then taken (S3). PEG and NaCl were then added to the remaining supernatant, and the mixture was incubated overnight at 4°C. The solution was then centrifuged at 1500 x *g* for 30 minutes in a benchtop centrifuge. A sample of the supernatant was then taken (S4) and the remaining supernatant discarded. The pellet (containing unwashed EVs) was resuspended in PBS and a sample of this was taken (P4). This solution was centrifugation at maximum speed on an available centrifuge (17,000 x *g*) for 2 hours and 10 minutes. A sample of the supernatant (S5) was taken and the remaining supernatant discarded. The final pellet (containing washed EVs) was then resuspended in PBS (P5). This sequential sampling was used to assess the presence of EVs throughout the isolation process in order to confirm their accumulation in the final washed pellet. Additionally, this was used to identify any potential yield losses occurring throughout the process and critical points during the isolation process where adjustments could enhance EV recovery.

Proteins in these fractions were first concentrated using acetone protein precipitation. Although there was an attempt to repeat this with ACM-derived samples, the protein concentrations of these samples were too low, even after protein precipitation. Therefore, samples were run from ECM only. The presence

of two EV positive markers, CD63 and CD9, and an EV negative marker, Annexin V, in these fractions were explored through SDS-PAGE and western blotting. As FBS contains EVs (Benz & Moses, 1974; Pham et al., 2021), an endothelial cell media control was also incubated for the same length of time (48 hrs), without cells in the vessel. EM refers to endothelial cell media conditioned without exposure to cells. Additionally, whole cell endothelial proteins were loaded to confirm the specificity of EV-associated proteins, ensuring accurate characterisation. Twenty μL of sample were loaded per well. Samples were loaded between 0.1 – 0.4 μg/μL.

A strong CD9+ band was present in the P4 fraction derived from ECM (Figure 4.8B). Additionally, there was a much weaker band seen in P5. There were no other CD9+ bands found in any fraction derived from EM or in endothelial cells. Endothelial cells were positive for annexin V, with a large band seen at 35 kDa and smaller band visible at ~55 kDa. While the ECM derived S2 fraction was positive for annexin V, the media control was not. Only the P3 fraction of both medias was positive for this marker, with the later fractions showing no band. Table 4.1 describes the presence and sizes of CD63+ bands in both ECM and EM derived fractions.

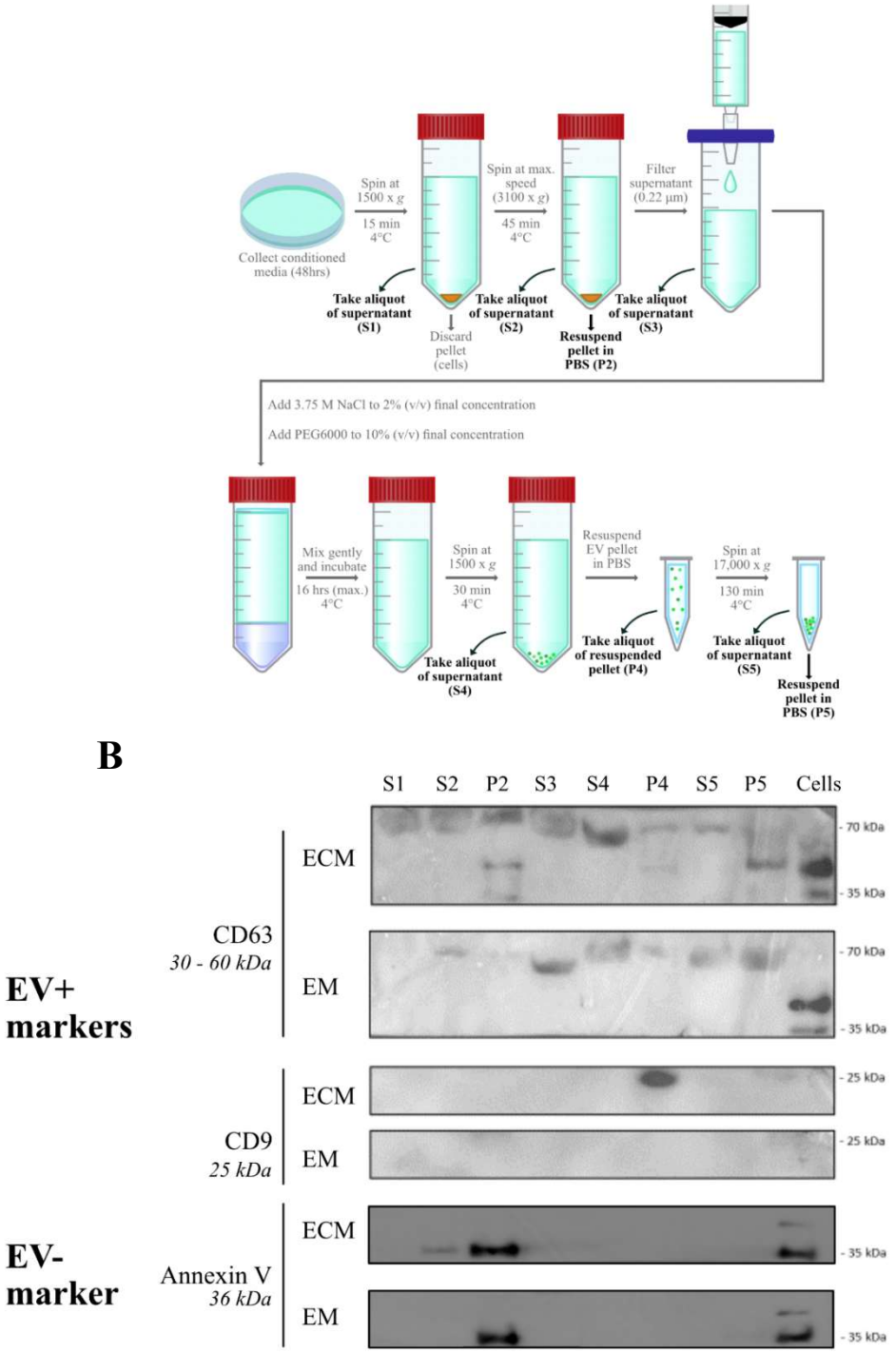


Figure 4.8 ***Verification of the ExtraPEG isolation method through western blot analysis of EV markers****, CD63 and CD9, at various points of the isolation process (A). (A) created by author (2025) using Affinity Designer (v 1.10.6.1665). Representative images of samples from endothelial cell medias (conditioned (ECM) and control (EM) (B)). Molecular weight according to company specifications indicated below protein name.*

Table 4.1: CD63+ bands in the fractions derived from ECM and EM

Fraction	Step in Isolation	Bands Present in ECM	Bands Present in EM
S1	Supernatant after initial clearance (1,500 x *g*; 15 min)	~70 kDa	
S2	Supernatant after cellular debris clearance (4,000 x *g*; 45 min)	~70 kDa	~70 kDa
P2	Pellet (Cellular debris)	~70 kDa **~55 kDa** **~35 kDa**	
S3	Supernatant after filtration	~70 kDa	~70 kDa
S4	Supernatant after incubation with PEG and EV isolation (1,500 x *g*; 30 min)	~70 kDa	~70 kDa
P4	Unwashed EV pellet	~70 kDa **~55 kDa** **~35 kDa**	~70 kDa
S5	Supernatant post EV wash step (17,000 x *g*; 130 mins)	~70 kDa	~70 kDa
P5	Washed EV pellet	~70 kDa **~55 kDa**	~70 kDa
Cells	EV Donor Cells	**~55 kDa** **~35 kDa**	

4.2.3 Optimisation of EV Yield using ExtraPEG isolation

4.2.3.1 Protein and RNA Yields from Unwashed EVs (P4) Are Higher Than Those from Washed EVs (P5)

The loss of signal in CD9 from P4 (unwashed EVs) to P5 (washed EVs) in the previous section indicated that a portion of the EVs were lost during the washing step. In order to verify this, protein and RNA yields were explored from unwashed and washed EVs isolated from both ACM and ECM, conditioned on astrocytes and HBMvECs, respectively, for 48 hours. Following the ExtraPEG protocol, the unwashed EV pellet (i.e. the pellet following the overnight incubation (1500 x *g*, 30 minutes)), was lysed in TRIzol® (for RNA isolation) or RIPA buffer (for protein isolation) ("unwashed" EVs) or washed by being resuspended in 0.9% NaCl and centrifuged (17,000 x *g*, 130 minutes). The pellet after centrifugation ("washed" EVs) was then lysed in TRIzol® or RIPA buffer. Both protein and RNA values were normalised per 1,000,000 cells, as described in Section 4.2.1.4.

There was a significant difference in protein concentration per 1,000,000 cells between unwashed and washed EV pellets derived from both astrocyte and endothelial cell conditioned media (Figure 4.9). The average amount of protein isolated from washed ACM-derived EVs was 0.488 ± 0.25 µg (Figure 4.9A). However, unwashed EVs had an average protein concentration of 33.048 ± 22.778 µg. Welch's Two Sample t-test revealed that there was a highly significant difference between these means ($p = 0.011$).

There was a similar result between unwashed and washed ECM-derived EVs (Figure 4.9B). The average amount of protein isolated from washed ECM-derived EVs was 10.217 ± 5.64 µg. However, unwashed EVs had an average protein concentration of 98.04 ± 22.78 µg. Welch's Two Sample t-test revealed that there was also a highly significant difference between these means ($p = 0.013$).

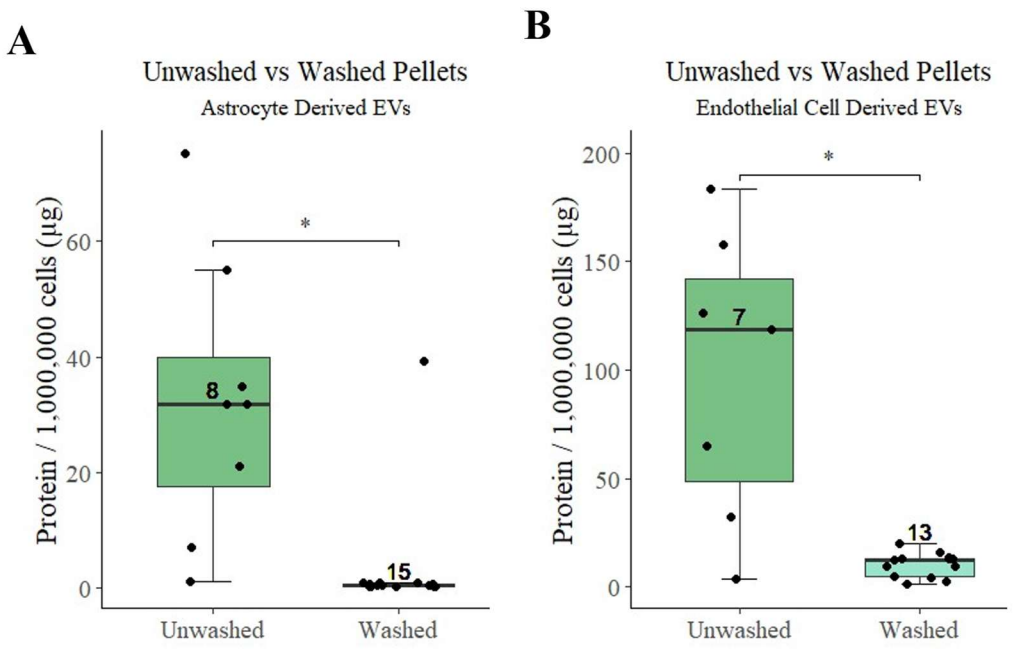


Figure 4.9 ***Comparison of EV protein concentration isolated from unwashed and washed EV pellets*** *derived from A) ACM and B) ECM. Results presented as average amount of protein (µg) isolated per 1,000,000 cells. Welch's Two Sample t-test was used to analyse this data. * $p < 0.05$*

A similar trend was observed in RNA isolated from both ACM- and ECM-derived EVs (Figure 4.10). The average amount of RNA isolated from washed ACM-derived EVs was 45.82 ± 10.85 ng. However, unwashed EVs had an average RNA isolation of 73.307 ± 8.65 ng. Welch's Two Sample t-test, however, revealed that the p value was above the cut-off value and was therefore not low enough to reject the null hypothesis.

Similarly, there was no significant difference between unwashed and washed ECM-derived EV RNA values. The average amount of RNA isolated from washed ECM-derived EVs was 50.64 ± 35.26 ng. Unwashed EVs had an average RNA concentration of 243.111 ± 112.91 ng. The p value approached significance (p = 0.0925) but was above the cut-off value to be able to reject the null hypothesis.

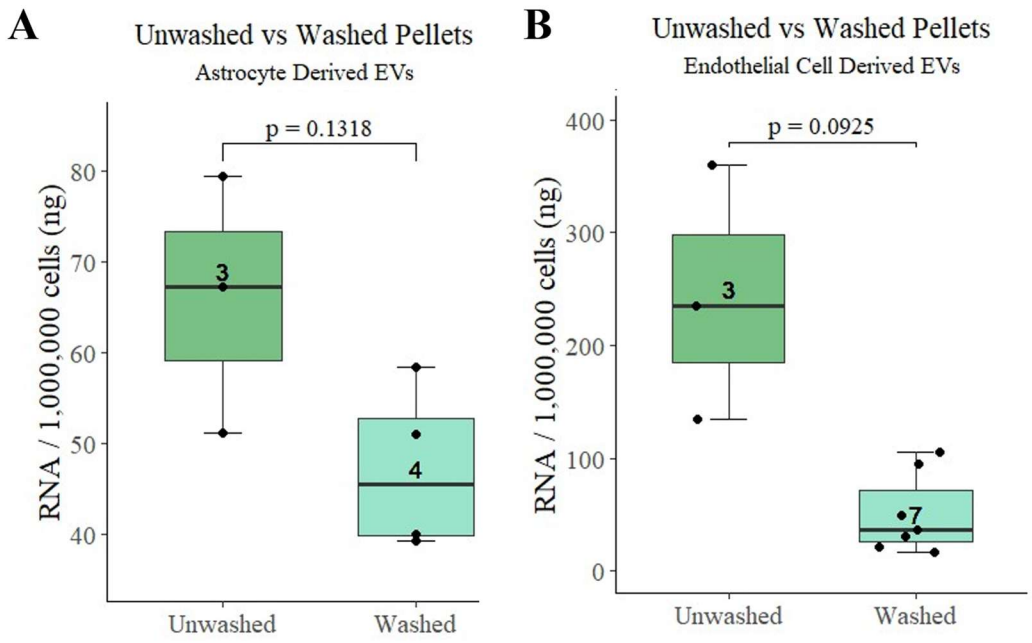


Figure 4.10 ***Comparison of EV RNA concentration isolated from unwashed and washed EV pellets*** *derived from A) ACM and B) ECM. Results presented as average amount of RNA (µg) isolated per 1,000,000 cells. Welch's Two Sample t-test was used to analyse this data. A) p value = 0.0594 B) p- value = 0.0925*

4.2.3.2 Size analysis of Unwashed vs Washed EVs

Although higher yields were obtained by removing the wash step, the size of EVs isolated using these needed to be verified. As a result, after ExtraPEG isolation of ACM- and ECM-derived EVs, unwashed EVs were resuspended in a 1 mL of PBS. 100 µL of this was kept (unwashed EVs) and the rest of the sample centrifuged at 17,000 x *g* for 130 mins. After centrifugation, the pellet (washed EVs) was resuspended in 200 µL PBS. The particle size distribution of both sample types was then analysed using DLS.

Size analysis revealed that the majority of unwashed ACM-derived EVs fell between 80 and 280 nm, with a peak at 162.6 nm (Figure 4.11A). There was also a small peak ranging between 18 and 51 nm, with 29.97 nm as the most common size of particles of this range. Again, washed ACM-derived EVs fell between 170 nm and 490 nm, with a peak at 276.9 nm (Figure 4.11B).

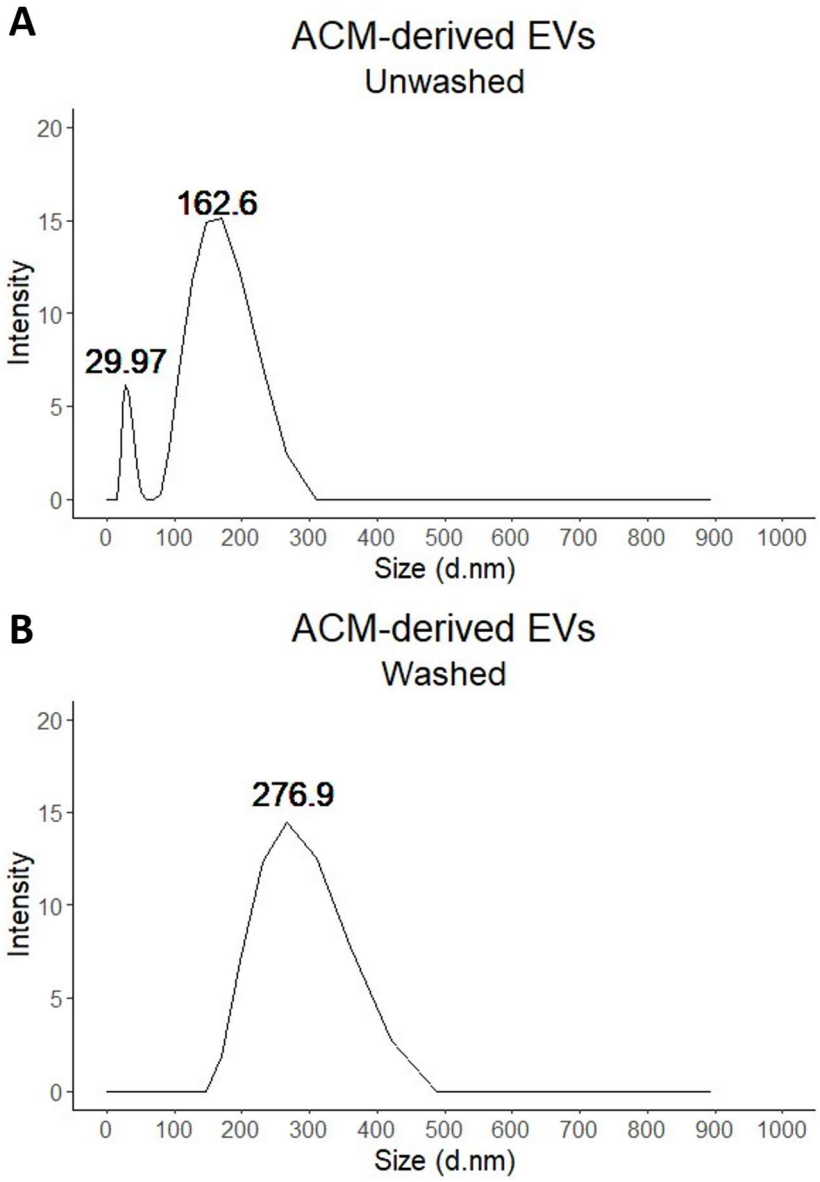


Figure 4.11 ***Average Size Distribution by Intensity*** *of A) Unwashed and B) Washed EVs derived from ACM, analysed using DLS. Peak size (nm) denoted above peak.*

Size analysis revealed that the majority of unwashed ECM-derived EVs fell between 108 and 770 nm, with a peak at 317.4 nm (Figure 4.12A). Again, there was also a small peak ranging between 24 and 108 nm, with 52.21 nm as the most common size of particles of this range. Washed ECM-derived EVs ranged between 20 nm to 1040 nm (Figure 4.12B). The most frequent size of these particles was 248.9 nm.

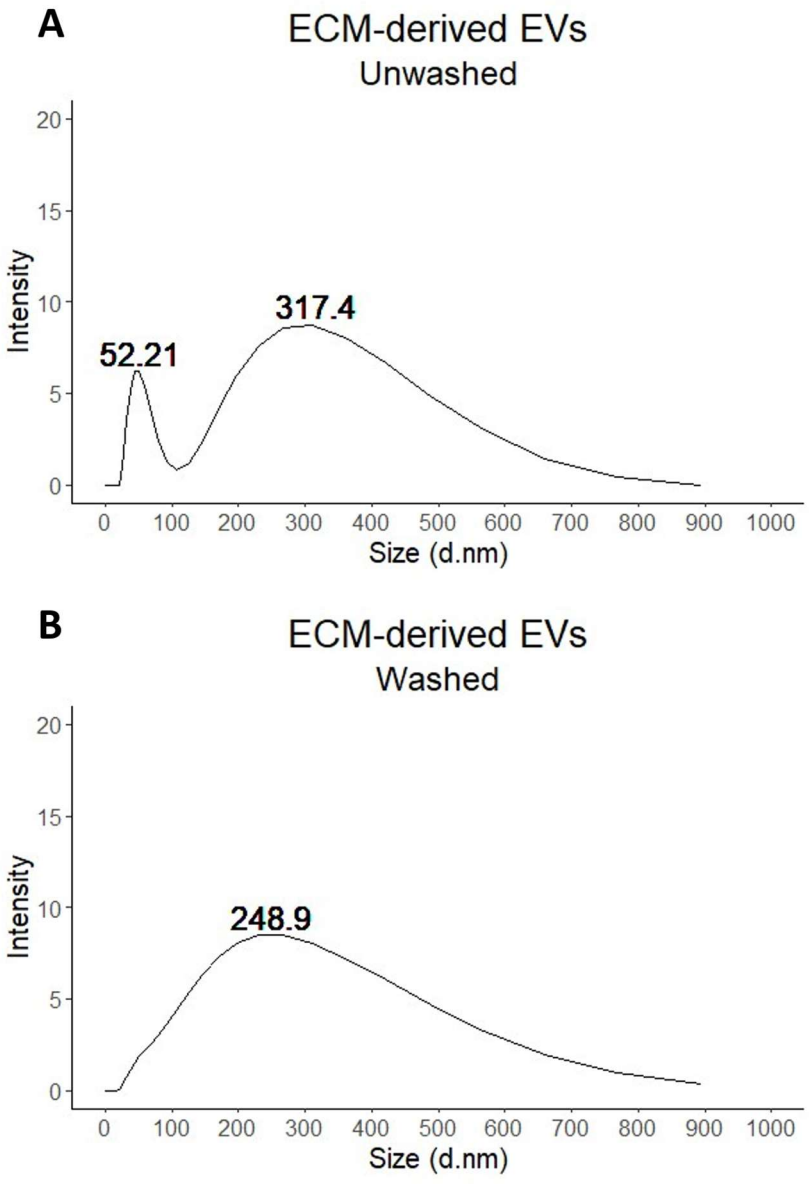


Figure 4.12 ***Average Size Distribution by Intensity*** *of A) Unwashed and B) Washed EVs derived from ECM, analysed using DLS. Peak size denoted (nm) above peak.*

4.3 Discussion

Results from chapter 3 indicated that there was a protective factor present in ACM that mediated HBMvEC viability and TJ gene expression. However, due to the negative effect of the unconditioned media on the survival of the endothelial cells as well as the complexity of the astrocyte secretome, it was decided that one key aspect of the secretome, specifically EVs, would be isolated and their effect on the BBB would be explored. EVs are key mediators in cell-cell communication, suggesting that they could potentially play a role in the astrocytic control of BBB integrity. They carry bioactive molecules that represent the molecular composition of the donor cell, allowing us to compare their effects in health and in disease.

In order to explore the effect of EVs on the BBB, isolation of EVs was required. As a result, this chapter focused on an exploration of three different EV isolation methods; namely MV isolation, DC isolation, and ExtraPEG isolation, in order to determine the most effective method(s) to isolate EVs from ACM and ECM. A reported 81% of all EV isolations up until 2016 used DC to isolate small EVs (sEVs (< 200 nm)) (Gardiner et al., 2016)**.** This is likely due to the affordability of the technique but requires the use of an ultracentrifuge. Additionally, the high speeds required (100,000 - 150,000 x *g*) can result in the impaired biological activity of EVs isolated using this method (Mol et al., 2017). LEVs (>200 nm), such as MVs, require much lower speeds. Polymer-based isolation methods, such as ExtraPEG, have been found to preserve the functionality of EVs (Z. Niu et al., 2017). This, along with the lack of need for specialised equipment, has grown their popularity among EV researchers. These isolation methods are commonly used but each varies in yield of EVs, depletion of contaminants, and labour-intensity (Brennan et al., 2020; Figueroa-Hall et al., 2025). As a result, the yield and size of EVs were compared amongst the three methods using both ACM and ECM. EVs were isolated from two conditioned media in order to assess each method's reproducibility.

EVs have been found to contain RNA (S. He, Liang, et al., 2023; Chitti et al., 2024), and as such, RNA yield was used as an indirect measurement of EV yield. With respect to EVs isolated from both cell types, there was variation in the amount of RNA isolated amongst the three methods and types of media as evidenced by high standard deviation values. Even EV populations released by individual cells tend to

be heterogeneous, varying in size and cargo (Nikoloff et al., 2021; Woo et al., 2025). Moreover, the RNA content of different classes of EVs varies (Jeppesen et al., 2019; Barranco et al., 2024). Following comparison of the isolates obtained from the three methods, there was no significant difference in RNA yield among the three. While RNA quantification is somewhat limited in its application to quantify EVs due to the variability of RNA populations between even the same subtype of EV and due to potential non-exosomal RNA contamination (Jeppesen et al., 2019; Gutiérrez García et al., 2020), it appeared that each method was as effective as the other. As such samples from each respective method were then analysed by using DLS to profile the samples more effectively.

Methods of measuring EV size such as DLS, are also able to give estimates of particle concentrations. However, this requires a minimal amount of 1 mL of sample. Our sample yields were too low and would have been too dilute if they were brought up to this minimum volume. Increasing the sample yields would have required considerably larger amounts of conditioned media, which was not feasible, for reasons of cost and practicality. However, Malvern Panalytical also offers a low volume sizing kit. This kit allows the use of much smaller volumes (as little as 3 μL) for size measurement alone.

As such, EV size was explored using this kit in order to determine the best method for EV isolation. DLS revealed that both MV and DC isolation yielded EVs of a greater wider size range than ExtraPEG for both types of media. Both MV and DC methods resulted in very heterogeneous populations of EVs, with the majority being part of the large EV class (>200 nm). The recommended speed for the isolation of EVs via centrifugation is between 100,000 and 150,000 x *g*. The maximum speed on the available ultracentrifuge is 50,000 x *g*, at least a 2-fold decrease in speed. As larger particles sediment more quickly and more readily at lower centrifugation speeds, using higher g-force (>100,000 x *g*) would allow for more efficient pelleting of small particles (<100 nm) in comparison to using 50,000 x *g*. Being unable to reach the speeds required for the sedimentation of these smaller particles is likely the reason behind the much higher range and peak sizes of EVs isolated through this method.

Only a few studies have analysed EVs which have been isolated using lower centrifugation speeds by DLS. Xu et al., (2015) isolated lEVs from the human colon carcinoma cell line, LIM1863 using a similar method but with a lower centrifugation step of 10,000 x *g*. They found that the majority of these EVs ranged between 450 and 1300 nm, with a peak around 650 nm. Patel et al., (2017) looked at the differences between EVs derived from pancreatic cancer cells treated with gemcitabine, a leading chemotherapy medication, or PBS. The average size of EVs isolated through a centrifugation step of 16,500 x *g*, which is closer to the speed used in this study, but for a shorter time (30 minutes) was over 800 nm. EVs from cells treated with gemcitabine were larger than those treated with the vehicle (883 nm vs 846.1 nm). However, Patel et al., (2017) do not describe the spread of EV sizes in their study. Therefore, our results are comparable to these published works and others, despite the modifications from the original protocols.

DC isolation is the gold standard for EV isolation and tends to isolate much smaller EVs. DC isolation resulted in a smaller size range than the MV isolation method. While the size ranges varied for the two types of conditioned media, the majority of EVs isolated were approximately the same size. However, lEVs isolated from ECM were smaller than those isolated from ACM. Xu et al., (2015) also isolated sEVs from LIM1863 conditioned media using an ultracentrifugation step of 100,000 x *g* for 1 hour. The majority of these EVs were between 50 - 80 nm, much smaller than those typically isolated with the methods that were used in this study. However, there was also a smaller secondary peak of EVs between 120 - 300 nm, similar to that which were observed in the isolate preparations from this study. Patel et al., (2017) also isolated sEVs from treated and untreated pancreatic cancer cells using an ultracentrifugation step of 120,000 x g for 2 hours. They found that the average size of treated sEVs was 124.8 nm and the average size of untreated sEVs was 103.6 nm. Again, the distribution of size of these was not reported. Kumar et al., (2018) isolated sEVs from a mixed culture of primary rat cerebrocortical neurons and astroglial cells using an ultracentrifugation step of 100,000 x g for 45 minutes. The isolated EVs were between 40 - 400 nm, with an average diameter of 137 - 149 nm. This is around 2x smaller than the average diameter of EVs isolated by the modified DC isolation method that was employed in this study. Mattera et al., (2020) isolated EVs from primary rat astrocytes using an ultracentrifugation

step of 100,000 x g for 70 min. The mean of EVs isolated at 4°C was 256 ± 22 nm, with a range of around 70 – 1000 nm. There is a large amount of variety between these published results, likely due to the variety of cell-conditioned media used. The average size and size range of our ACM-derived EVs are much closer to those of Mattera et al., (2020), who also used primary astrocytes. Mattera et al., (2020) also isolated EVs from Neuro-2A (a mouse neuroblastoma cell line) and OLN-93 (a rat oligodendroglioma cell line) conditioned media using the same method. They found that the average size of these EVs were 167 ± 24 nm and 182 ± 19 nm, respectively. This suggests that primary astrocytes produce larger EVs, which our results corroborate.

ExtraPEG isolation resulted in a much less varied population of EVs, with EVs isolated via this method being much smaller than those isolated via DC and MV. Thomas et al., (2022) isolated EVs from murine bone-marrow derived mesenchymal stromal cells using Exoquick-TC ULTRA, which is a commercial polymer-based EV isolation kit similar to ExtraPEG. Using this kit, the resulting EVs were between 200 - 1000 nm in diameter. Yue et al., (2019) isolated EVs from primary human umbilical endothelial cells (HUVECs) using a similar ExtraPEG method but with a final concentration of 12% PEG and higher centrifugation (12,000 x g for 1 hour). The majority of isolated EVs were around 100 nm in size but ranged between 10 and 1000 nm. This range is similar to the ECM-derived EVs isolated using ExtraPEG at a lower concentration of PEG and a lower centrifugation speed.

The ExtraPEG isolation features a filtration step that is intended to remove particles and aggregates larger than 200 nm. This means that only particles under 200 nm should remain in the supernatant prior to the addition of PEG. However, DLS analysis reveals that the majority of EVs isolated are larger than expected. This may be a result of improper resuspension of vesicle aggregates, as EVs are particularly prone to aggregation (Nizamudeen et al., 2021; S. Kim et al., 2025). While intensity size distribution is the best method for reporting DLS results, DLS analysis is skewed towards larger particles as these scatter more light, which can result in seemingly increased populations of larger particles. This could affect the peak mean sizes as well as the range (Khan et al., 2022).

While there was no significant difference between EV yield between the three isolation methods based on our approaches, ExtraPEG isolation resulted in a much less heterogeneous population of EVs, in contrast to MV and DC isolation. Additionally, RNA values did not differ much between ACM-derived EVs and ECM-derived EVs. Owing to the modifications required to both DC and MV isolation methods due to the limitations in centrifugation speeds available that may have impacted on the EV population profile, ExtraPEG was preferred as the method to use moving forward.

In addition to verifying the isolation of EVs by their size, EVs were also verified by confirming the presence of several proteins associated with EVs. Samples of the supernatants and pellets were taken throughout the isolation process in order to confirm the accumulation of EVs throughout the isolation process. The presence of two exosomal markers, CD9 and CD63 were explored in these fractions through western blot analysis. Both CD9 and CD63 are tetraspanin proteins which are enriched in EVs (Escola et al., 1998; Tognoli et al., 2023). CD63 regulates intracellular transport and localisation (Pols & Klumperman, 2009). CD63 is also highly expressed in microvascular endothelial cells and seems to play a role in fatty acid uptake (Tugues et al., 2013; Peche et al., 2023). While the predicted molecular weight of this tetraspanin is 25 kDa, western blotting experiments have demonstrated that the molecular weight ranges between 32-75 kDa, likely due to heavy N-linked glycosylation (Ageberg & Lindmark, 2003; Mathieu et al., 2021) which is known to cause gel smearing.

Interestingly, endothelial cells were positive for CD63 but seemed to be particularly enriched for a band of approximately 50 kDa. Signal for proteins around 60-70 kDa was visible in several fractions isolated from both ECM and EM, which could suggest that this a component of the unconditioned media itself rather than being released by endothelial cells. Only ECM pellet fractions were positive for bands at 35 and 55 kDa, corresponding with bands seen in the cell protein lane.

Annexin V is a protein that is typically associated with apoptotic cells. This protein binds to phosphatidylserine, a phospholipid that is transferred from the inner cell membrane to the outer cell membrane during apoptosis. Another subcategory of EVs, apoptotic bodies are released by dying cells in the final stage of apoptosis.

These apoptotic bodies are much larger than microvesicles or exosomes (up to 5000 nm) (L. Yu et al., 2023). The ExtraPEG isolation process effectively removes any larger EVs and cell debris from media using a centrifugation step and filtration step.

One of the limitations of this study was the consistently low yield of EVs from ACM. Supernatant fractions and pellets collected later in the isolation process had extremely low protein concentrations. While an attempt at verifying the presence of ACM-derived EVs was made, it may be that samples were simply too dilute for effective probing. Therefore, EVs may be present in the various fractions but outside the limits of detection. However, results from the aforementioned protein analysis of ECM EVs alone show the effectiveness of ExtraPEG in generating clean EV isolations.

The verification of the ExtraPEG method also revealed the presence of EV markers in the unwashed pellet fraction generated by the ExtraPEG method. The enrichment of CD9 particularly in the unwashed pellet inspired a thorough investigation into the effect of washing on the pellet. Many studies using EVs wash the isolated pellet in order to remove any contaminating proteins. However, several studies have recently published results featuring unwashed EVs from cell conditioned media (He et al., 2023; Li et al., 2023; Park et al., 2023; Skrika-Alexopoulos & Mark Smales, 2023).

There was a significant difference in protein concentration found between unwashed and washed EV pellets derived from both astrocytes and HBMvECs. This may be due to the fact that the unwashed pellet may contain both remaining PEG and contaminating proteins. PEG has been found to interfere with BCA results, with a false positive relationship between concentration and absorbance. However, this trend continued in RNA yield, with unwashed EVs from both astrocytes and HBMVECs resulting in higher amounts of RNA. These results were not significant although the p-values for these studies approached significance.

As previous results showed that washed EVs were much larger than expected, the size of the unwashed EVs was also explored. DLS size analysis results revealed a small peak under 60 nm in both unwashed ACM and ECM samples. These may be sEVs that are lost through the wash step, which also results in lower RNA and protein yields. This is likely due to the low speed used in pelleting the washed EVs,

17,000 x *g*, which may not be high enough upon the removal of PEG from the solution. This may explain the higher concentrations of both protein and RNA in the unwashed fractions as well as the presence of CD9 solely in the unwashed fraction derived from ECM and not in the washed.

Another factor that could potentially affect EV yield is storage at -20°C. Studies have shown that both the storage of freshly isolated EVs and the isolation of EVs from previously-stored biological samples may affect the properties of the vesicles (Jeyaram & Jay, 2018; Ahmadian et al., 2024). Although the ISEV had recommended preserving isolated EVs in PBS in siliconized vessels at -80 °C in 2013 (Witwer et al., 2013), their most recent guidelines do not provide standard recommendations for pre- and post-isolation storage as studies have reported conflicting effects on EV properties (Théry et al., 2018; Welsh et al., 2024). Studies exploring the effect of storage of conditioned cell media on EV properties are limited. However, one recent study found no significant difference in the number of EVs isolated from conditioned media collected from five mesenchymal stromal cell lines, stored at several different conditions, including room temperature, 4 °C, -20 °C and -80 °C (Wright et al., 2022). This was consistent with results suggesting that there was no significant difference in RNA amounts isolated from frozen and non-frozen ACM media (Figure A.2, Appendix). This indicates that EVs in conditioned media can be frozen at -20°C without decreasing particle concentration significantly.

In conclusion, a method for isolating EVs was determined and verified. During the verification of this isolation method, it was discovered that a significant population of sEVs is lost through the wash process. However, the effect of these EVs on cells is yet to be determined. The following chapter will focus on the effect of these astrocyte-derived EVs on the barrier properties of primary human endothelial cells. Due to the increased concentration of EVs in the unwashed fraction in comparison to the washed EV fraction, unwashed EVS will be used going forward.

Chapter 5 : The Effect of Astrocyte-Derived EVs on HBMvEC Barrier Properties

5.1 Introduction

Astrocytes have long been known as the secretory cells of the CNS, secreting a variety of gliotransmitters (Fukuyama et al., 2023; H. Li et al., 2025), neuromodulators (Vanacker et al., 2021), growth factors (Fernández-García et al., 2020), ExM proteins (Irala et al., 2024) and hormones (Torres et al., 2024). During neuroinflammation, a common hallmark of many CNS disorders, astrocytes promote inflammation in the CNS through the release of pro-inflammatory mediators (Rothhammer et al., 2016; Valentin-Torres et al., 2018; Wheeler et al., 2019).

In addition to these, astrocytes have also been shown to release EVs, under both physiological and pathological conditions (Chun et al., 2021; Tankov et al., 2024; L. Wu et al., 2025). Healthy astrocyte-derived EVs have been shown to play important roles in the CNS, including promoting neuronal survival and neurite outgrowth (Wang et al., 2011), promoting dendrite spine and synapse formation (M. R. Patel & Weaver, 2021), and promoting neuronal postsynaptic function (Levy-Myers et al., 2023). Additionally, astrocyte-derived EVs contain heat shock protein 70 (Hsp70), which displays a neuroprotective effect in the CNS (Taylor et al., 2007).

Although the relationship between astrocytes and the BBB has been well documented, studies looking at the effects of astrocyte-derived EVs on endothelial cells in brain are limited. Primary rat astrocyte EVs contain fibroblast growth factor-2 (FGF-2), which is known to maintain BBB integrity (Proia et al., 2008; B. Huang et al., 2012; Grabiec et al., 2016). Moreover, EVs from human iPSC-derived neural stem cells contain agrin, PTX3, hemopexin, and nidogen-1, which have all been also indicated as players involved in BBB integrity (Upadhya, Madhu, et al., 2020). Some of the most abundant proteins in EVs derived from astrocytes include fibronectin 1, collagens and TNFα induced protein 3 (TNFAIP3) (Chun et al., 2021). Astrocytes are known to secrete fibronectin 1 and collagens to support BBB integrity (Hirano et al., 2004). TNFAIP3 is a negative regulator of NF-κB signalling, potentially suggesting an anti-inflammatory role (Giordano et al., 2014; T. Kim et al., 2020). EVs from retinal astrocytes were able to suppress vessel leakage and angiogenesis in the retina of a mouse model of choroidal neovascularization (Hajrasouliha et al., 2013). Overall, these studies suggest that

healthy astrocytes may secrete EVs that can positively affect the BBB properties of endothelial cells.

EVs derived from inflamed astrocytes, on the other hand, are enriched with pro-inflammatory molecules, such as IL-6 and TNFα, and neurotoxic complement effector proteins, such as C1q, C4b, and complement factor B (Goetzl et al., 2018, 2020). Additionally, these pro-inflammatory EVs can be taken up by neurons, resulting in reduced neurite growth, dendritic complexity, neuronal activity and increased apoptosis (Chaudhuri et al., 2018; Datta Chaudhuri et al., 2020). The pro-inflammatory chemokine, CCL2, has been found to be encapsulated in EVs isolated from inflamed astrocytes (Rong et al., 2021). CCL2 has been found to increase BBB permeability, suggesting that reactive astrocytes could contribute to BBB breakdown during neuroinflammation (Dimitrijevic et al., 2006; F. Guo et al., 2020).

To our knowledge, no study has looked at the effect of primary human astrocyte-derived EVs on primary human brain microvascular endothelial cells, both physiologically and during neuroinflammation. This chapter explores the effect of astrocyte EVs on endothelial cells in order to determine whether they effect the barrier in a cell-state dependent manner.

5.1.1 Chapter Aims

- To optimise astrocyte-derived EVs treatments on endothelial cells by exploring dose, time and direction of treatment.
- To explore the effect of healthy astrocyte-derived EVs on endothelial cell permeability as well as tight junction gene and protein expression levels.
- To optimise a model of inflammation in astrocytes.
- To explore the effect of EVs isolated from inflamed astrocytes on endothelial cell permeability and tight junction protein expression levels.

5.2 Results

5.2.1 Astrocyte-derived EVs affect HBMvEC permeability in a treatment orientation- and time- dependent manner

Astrocyte EV treatments on HBMvECs were first optimised through analysis of endothelial barrier strength. HBMvECs were seeded to confluency in the apical chamber of a 12 well transwell insert. EVs were isolated from media on the day of treatment. Two concentrations of EVs were explored: 6.25 μg/mL and 12.5 μg/mL. Firstly, direction of treatment was explored by the addition of EVs into either the apical or basolateral chamber for 24 hours. Although not statistically significant, the orientation of treatment did affect barrier strength in a way that approached significance (Apical vs Basolateral, $p = 0.0556$) (Figure 5.1). There appears to be a dose-dependent decrease in barrier permeability in HBMvECs when treated basolaterally, although this was not found to be significant. However, there was no dose-dependent effect seen after apical treatment of EVs. As a result, HBMvECs were treated basolaterally in further studies.

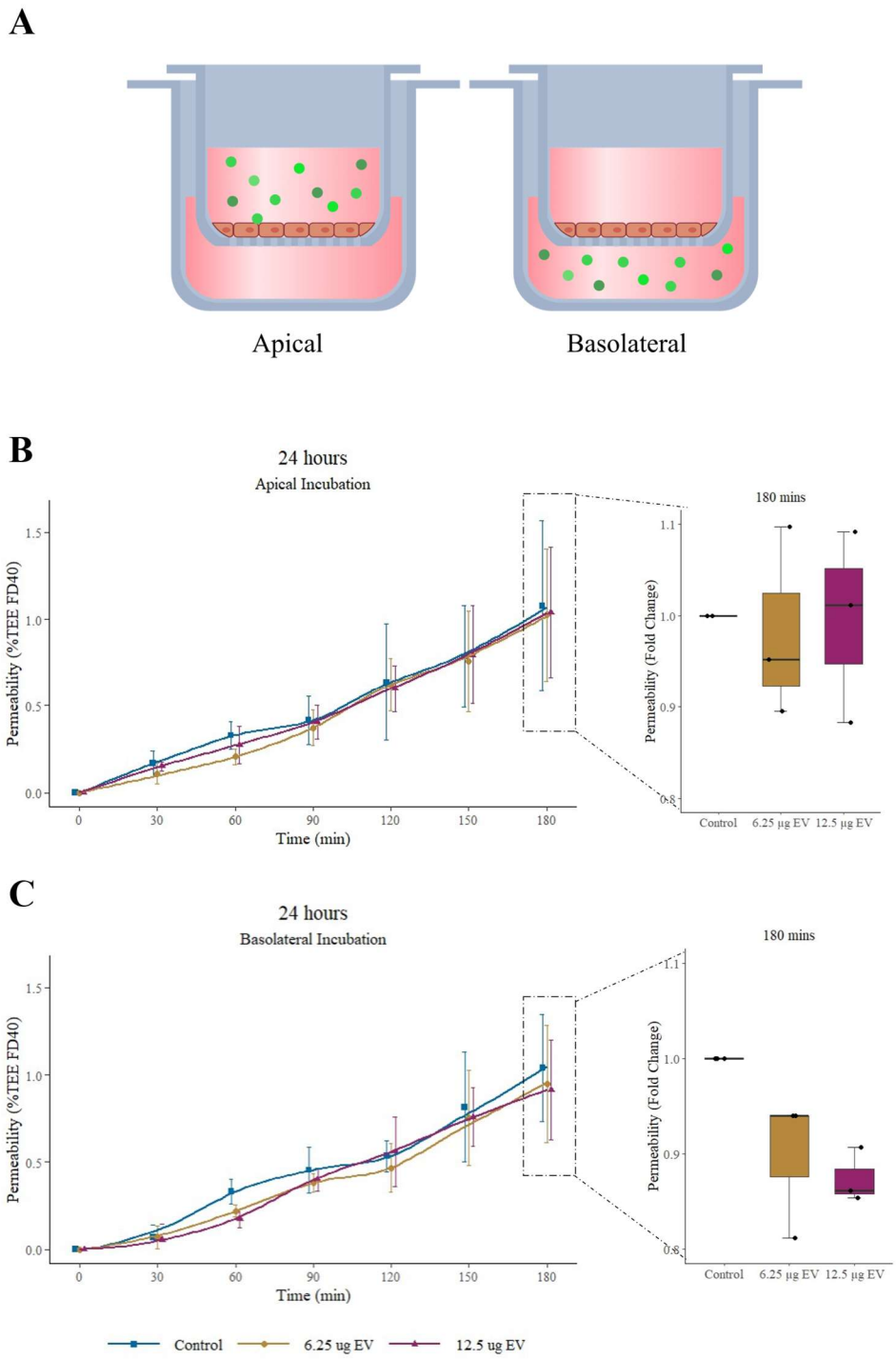


Figure 5.1 ***Astrocyte derived EVs affect HBMvEC permeability in a treatment orientation - dependent manner.*** *A) shows a graphical representation of the direction of treatment in transwells. B) shows the permeability (%TEE FD40) of endothelial cells after 24 hours of EV exposure apically over the course of the assay (0 – 180 mins) (LHS) and at 180 mins, with permeability fold changes normalised to the vehicle control (PBS). C) shows the permeability (%TEE FD40) of endothelial cells after 24 hours of basolateral EV exposure over the course of the assay (0 – 180 mins) (LHS) and at 180 mins, with permeability fold changes normalised to the vehicle control (PBS). Results are averaged from three independent experiments ± SD. Results were analysed using two-way ANOVA. Black dots indicate individual data points.*

The effect of a shorter (6 hour) and a longer (48 hour) incubation period was also considered (Figure 5.2). After 6 hours of incubation, there is a clear decrease in barrier permeability over the course of the assay although this does not seem to be dose dependent. This was not found to be significant. Additionally, there were no differences in barrier strength after 48 hours of incubation at either EV concentration. As a result, HBMvECs were incubated with the higher concentration of EVs for 24 hours in further experiments.

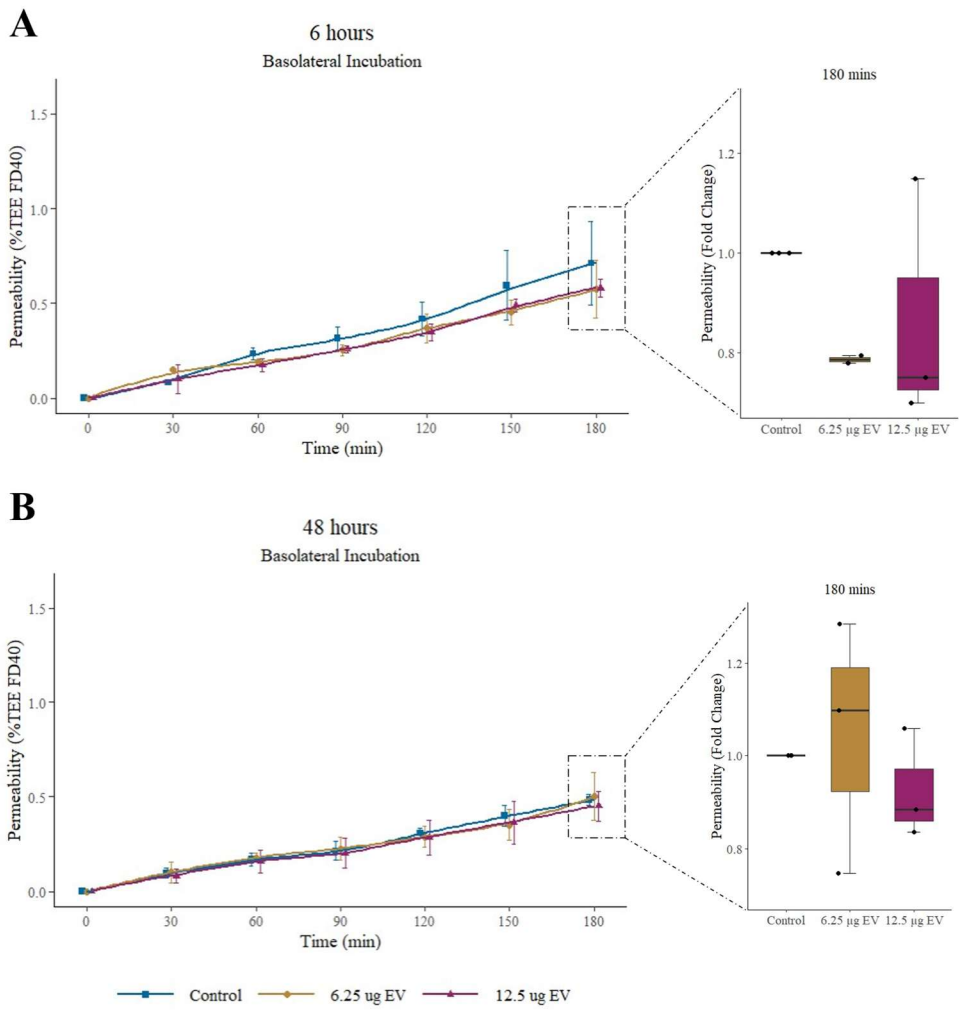


Figure 5.2 ***Astrocyte derived EVs affect HBMvEC permeability in a time-dependent manner***. *A) shows the permeability (%TEE FD40) of endothelial cells after 6 hours of basolateral EV exposure over the course of the assay (0 – 180 mins) (LHS) and at 180 mins, with permeability fold changes normalised to the vehicle control (PBS). B) shows the permeability (%TEE FD40) of endothelial cells after 48 hours of basolateral EV exposure over the course of the assay (0 – 180 mins) (LHS) and at 180 mins, with permeability fold changes normalised to the vehicle control (PBS). Results are averaged from three independent experiments ± SD. Results were analysed using two-way ANOVA. Black dots indicate individual data points.*

5.2.2 Astrocyte EVs decrease permeability of HBMvECs but do not affect tight junction expression levels

Following optimisation, the effect of astrocyte EVs on HBMvEC permeability was explored, accounting also for the effect of serum-derived EVs in the media itself. HBMvECs were exposed basolaterally to 12.5 µg EVs for 24 hours. These EVs were isolated using the ExtraPEG method, as described in Chapter 4, from media that had been conditioned on astrocytes for 48 hours (ACM EVs) or an incubation time- and media batch-matched control (AM EVs). Figure 5.3 briefly illustrates the acquisition of these EVs.

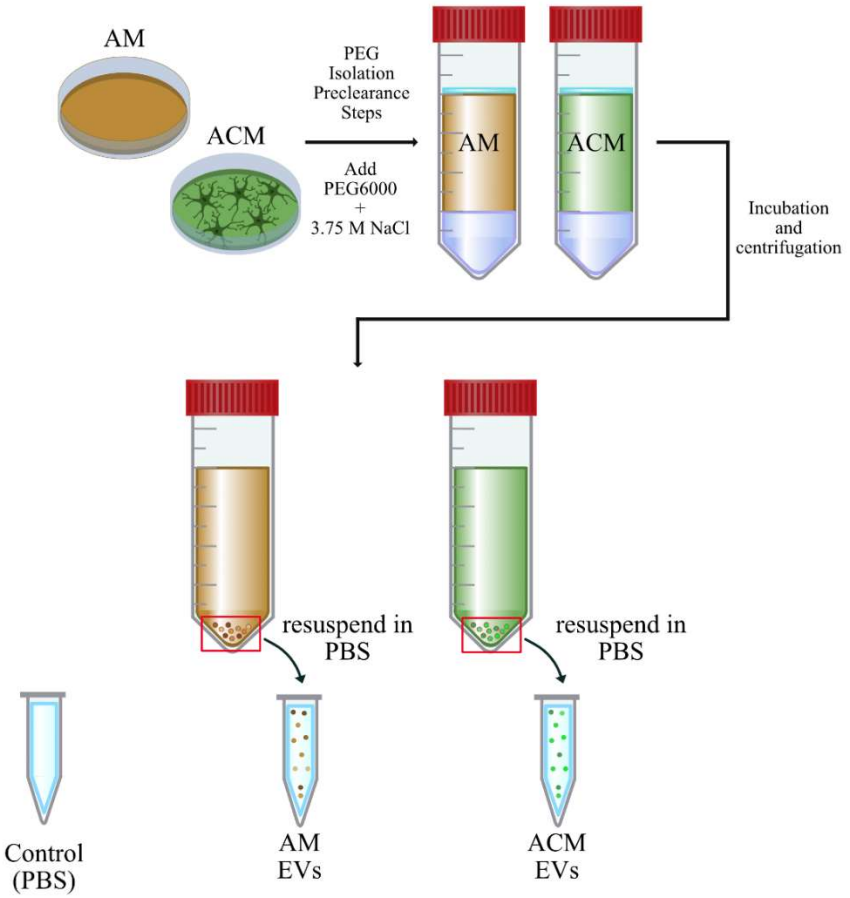


Figure 5.3 ***Illustration of AM and ACM derived EVs isolation.*** *After 48 hours of conditioning astrocyte media on cells (ACM) or without cells (AM), cell debris and larger proteins and microvesicles were cleared through preclearance steps as described in Chapter 4. 50% PEG6000 was added to a final concentration of 10% and 3.75M NaCl added to a final concentration of 2%. These medias were then incubated overnight and centrifuged at 1500 x g for 1 hour. The supernatant was collected (EV-depleted media), and the pellet was resuspended in 200 µL PBS.* Figure created by author using Affinity Designer (v 1.10.6.1665).

HBMvECs treated with ACM EVs had a significantly stronger barrier throughout the 3-hour permeability assay in comparison to both the control and cells treated with AM EVs (Control vs ACM EV, p = 0.00000446; AM EV vs ACM EV, p = 0.0292) (Figure 5.4A). It can be noted that when the final timepoint was normalised to the control, this decrease closely trended towards significance (0.679 ± 0.153, p = 0.0524) (Figure 5.4B). Nonetheless, this suggests that astrocyte-derived EVs are able to decrease barrier permeability.

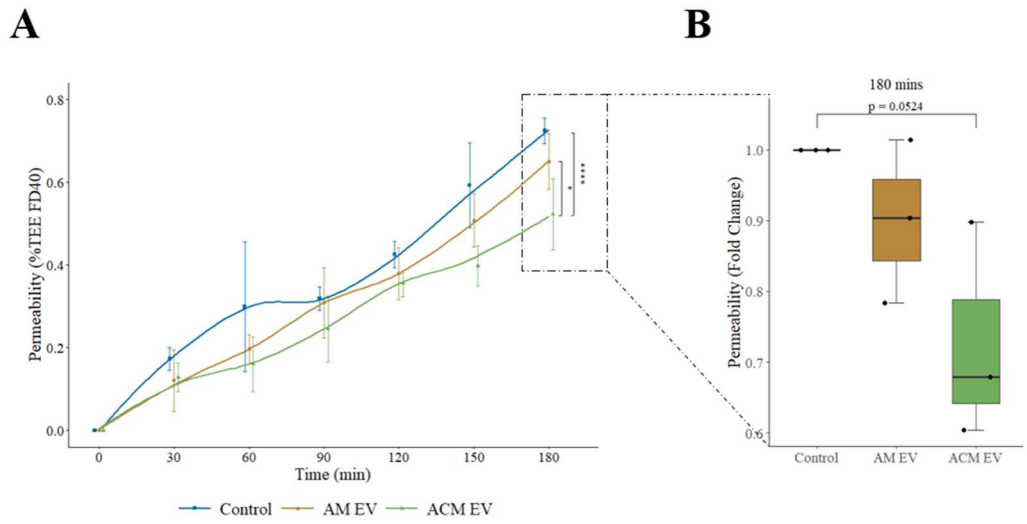


Figure 5.4 ***Astrocyte derived EVs decrease HBMvEC permeability.*** *A) shows the permeability (%TEE FD40) of endothelial cells after EV incubation over the course of the assay (0 – 180 mins). Results are averaged from three independent experiments ± SD. Results were analysed using two-way ANOVA. * p > 0.05, **** p > 0.0001 between treatments over the course of the assay. Boxes highlight the data used in B) the permeability (%TEE FD40) at the end of the assay (t = 180 mins). Fold changes are normalised to the vehicle control. Black dots show individual data points. Results analysed using one-way ANOVA.*

This decrease in barrier permeability does not appear to be due to changes in the gene expression of the major tight junction proteins: claudin-5, occludin, or ZO-1. There were no significant differences seen in levels of these after incubation with ACM EVs (Figure 5.5). There were also no significant differences seen in the expression of these proteins (Figure 5.6).

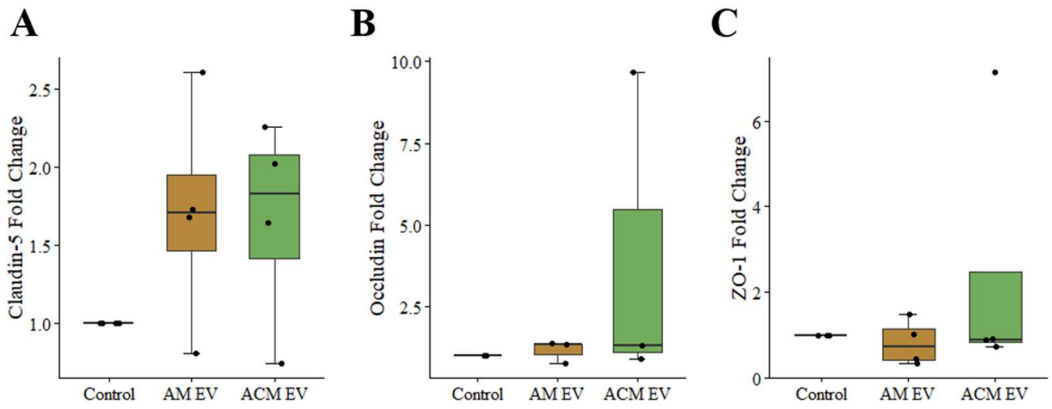


Figure 5.5 ***qPCR analysis in response to astrocyte derived EV treatment*** *of the tight junction genes claudin-5 (A), occludin (B), and ZO-1 (C). HBMvECs were treated basolaterally with ACM derived EVs or AM derived EVs for 24 hours. Black dots indicate individual data points. n = 4 (Claudin-5, ZO-1); n = 3 (Occludin). Data is presented as the median fold change ± SD. Gene expression calculated using the* $2^{-\Delta\Delta CT}$ *method and normalised to vehicle control. Data analysed using one-way ANOVA.*

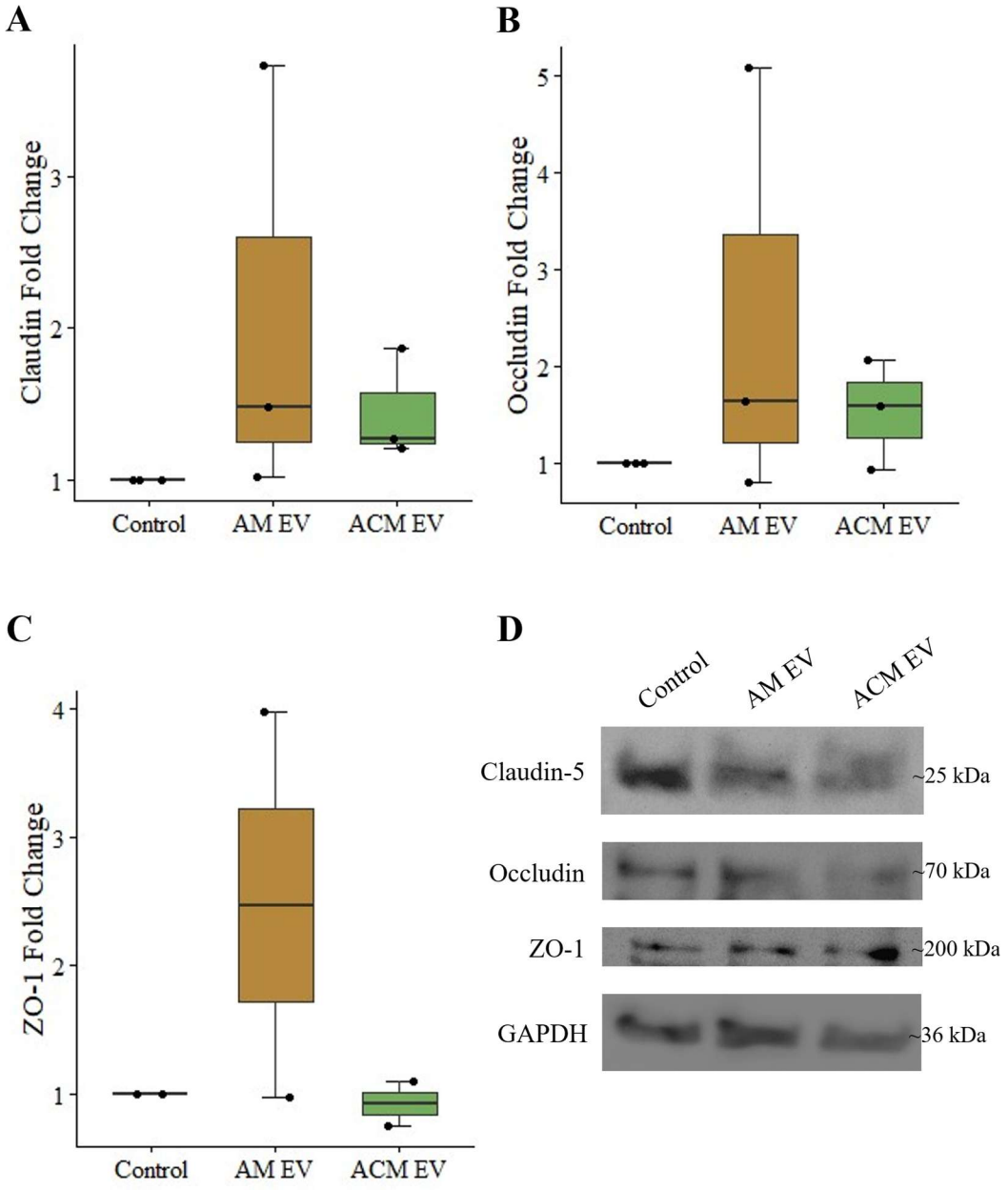


Figure 5.6 ***Protein expression analysis in response to astrocyte derived EV treatment*** *of the tight junction genes claudin-5 (A), occludin (B), and ZO-1 (C). HBMvECs were treated basolaterally with ACM derived EVs or AM derived EVs for 24 hours. Black dots indicate individual data points. n = 3 (A, B) Data analysed using one-way ANOVA. n = 2 (C). Data is presented as the median fold change ± SD. D) showcases representative blots for each TJ protein. GAPDH was used as a loading control.*

5.2.3 Astrocytes are inflamed by a cytokine cocktail but not LPS.

Two methods of inflammation were optimised prior to inflamed EV generation (Liddelow et al., 2017; Tarassishin et al., 2014). Firstly, astrocytes were exposed to two concentrations of lipopolysaccharide (LPS): 0.1 μg/mL and 1 μg/mL in order to determine the optimal concentration for further experiments. The gene expression levels of several genes known to be upregulated during neuroinflammation, namely c-c motif chemokine ligand 2 (CCL2), interleukin-1 beta (IL1β), interleukin-6 (IL6), tumour necrosis factor alpha (TNFα) and glial fibrillary acidic protein (GFAP), a marker of reactive astrocyte, were explored in order to determine the effect of LPS on the inflammatory status of astrocytes (Figure 5.7) There was no significant change in gene expression level in these genes after LPS treatment at either dose, although the gene expression of TNFα did approach significance at the higher LPS concentration in comparison to the control (3.31 ± 1.93, $p = 0.0963$). Due to the negligible changes in gene expression, the lower concentration of LPS was chosen for further experiments.

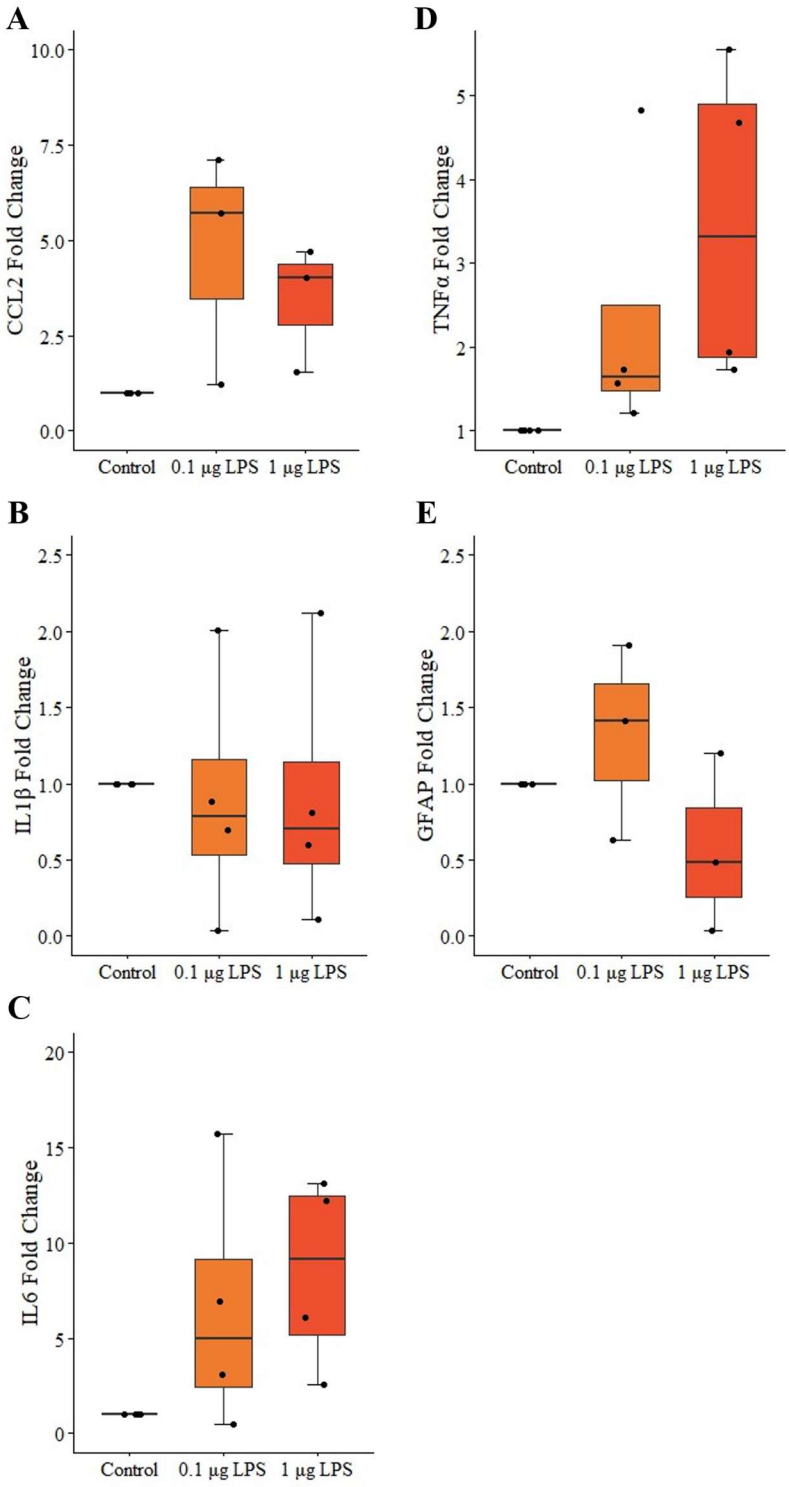


Figure 5.7 ***Gene expression analysis of astrocytes after LPS treatment using qPCR.*** *Several genes known to be upregulated after inflammation were quantified: CCL2 (A), IL-1β (B), IL6 (C), TNFα (D). Levels of GFAP (E) were also explored. Astrocytes were treated for 24 hours with PBS (Control) or LPS (0.1 µg/mL; 1 µg/mL) Black dots indicate individual data points. n = 3(A, E); n = 4 (B, C, D). Data is presented as the median fold change ± SD. Gene expression calculated using the* $2^{-\Delta\Delta CT}$ *method and normalised to vehicle control. Data analysed using one-way ANOVA.*

Although no significant change in the expression of genes associated with neuroinflammation was found when astrocytes were treated with LPS, a specific phenotype of neurotoxic reactive astrocytes has been able to be replicated in vitro through treatment with a cocktail of cytokines: TNFα, IL1α, and C1q (Liddelow et al., 2017; Barbar et al., 2020; Gomes et al., 2024). After astrocytes were exposed to these cytokines (TNFα (30 ng/mL), IL1α (3 ng/mL) and C1q (400 ng/mL)), the expression levels of these genes changed dramatically (Figure 5.8). CCL2 gene expression was increased by 25.3 ± 31.8 after cytokine treatment, although this only approached significance ($p = 0.0906$). Expression of IL6 increased to 69.6 ± 101 after cytokine treatment, again only approaching significance ($p = 0.0688$). IL1β expression was significantly upregulated after cytokine treatment, in comparison to the control (6.57 ± 5.41 vs 1, $p = 0.0406$) and in comparison to LPS treatment ((6.57 ± 5.41 vs 0.879 ± 0.712, $p = 0.046$). TNFα expression was also significantly upregulated after cytokine treatment, both in comparison to the control (33.4 ± 17.1 vs 1, $p = 0.006$) and in comparison to LPS treatment (3.20 ± 2.21, $p = 0.00967$). Although GFAP was downregulated after cytokine treatment, with expression lowering to 0.467 ± 0.143, this was not found to be significant.

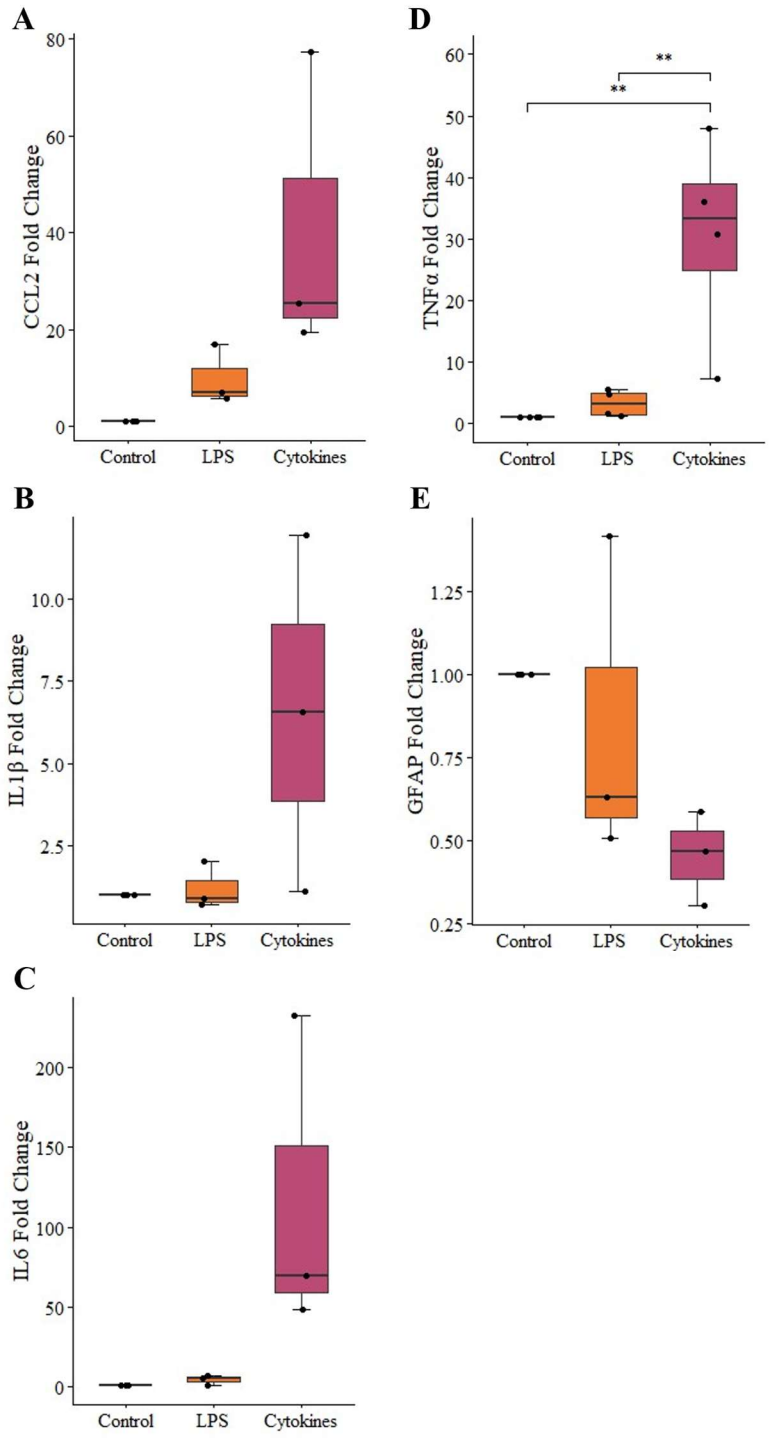


Figure 5.8 ***Gene expression comparison of astrocytes after treatment with LPS and cytokines using qPCR.*** *Several genes known to be upregulated after inflammation were quantified: CCL2 (A), IL-1β (B), IL6 (C), TNFα (D). Levels of GFAP (E) were also explored. Astrocytes were treated for 24 hours with PBS (Control), LPS (0.1 µg/mL), or cytokines (TNFα (30 ng/mL), IL1α (3 ng/mL), C1q (400 ng/mL)). Black dots indicate individual data points. n = 3(A, E); n =4 (B, C, D). Data is presented as the median fold change ± SD. Gene expression calculated using the* $2^{-\Delta\Delta CT}$ *method and normalised to vehicle control. Data analysed using one-way ANOVA.*

Interestingly, this downregulation of GFAP expression was also seen on the protein level (Figure 5.9). GFAP protein expression was decreased by ~30%, but this only approached significance (0.722 ± 0.239, p = 0.0803).

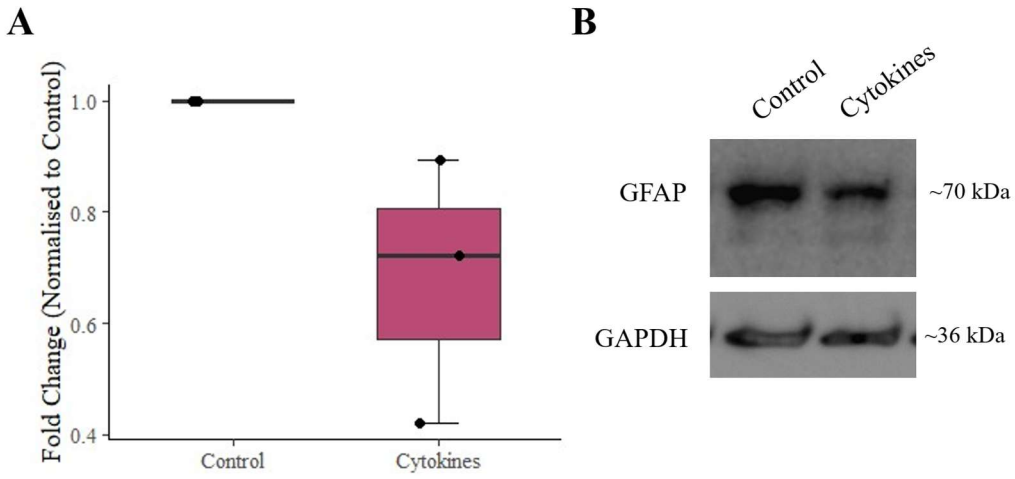


Figure 5.9 ***GFAP protein expression in astrocytes after cytokine treatment,*** *normalised to control. Astrocytes were treated with cytokines (TNFα (30 ng/mL), IL1α (3 ng/mL), C1q (400 ng/mL)) for 24 hours. Black dots indicate individual data points. n = 3 (A, B) Data analysed using one-way ANOVA. Data is presented as the median fold change ± SD. B) showcases a representative blot for GFAP. GAPDH was used as a loading control.*

5.2.4 EVs derived from inflamed astrocytes increase permeability of HBMvECs

Based on results from Section 5.2.3, astrocytes (at 70-90% confluency) were exposed to the cytokine storm (TNFα (30 ng/mL), IL1α (3 ng/mL), C1q (400 ng/mL)) for 24 hours. As a control, astrocytes were treated with an equal volume of PBS. Additionally, unconditioned media was incubated for 24 hours in order to isolate EVs indigenous to the media as a control (AM EVs). Upon completion of the timepoint, this media was collected and stored for a maximum of 6 months prior to EV isolation.

EVs were isolated from these medias using the ExtraPEG method, as described above and their size was analysed via dynamic light scattering (Figure 5.10). There was no visible difference in the size of EVs derived from inflamed astrocytes (EV_{INF}) in comparison to EVs derived from healthy astrocytes (EV_H). Both ranged in size from ~15 nm to ~650 nm, with a peak at 197.6 nm. However, the majority of small (<200 nm) EV_{INF} were larger than those of small EV_H (43.7 nm vs 32.3 nm).

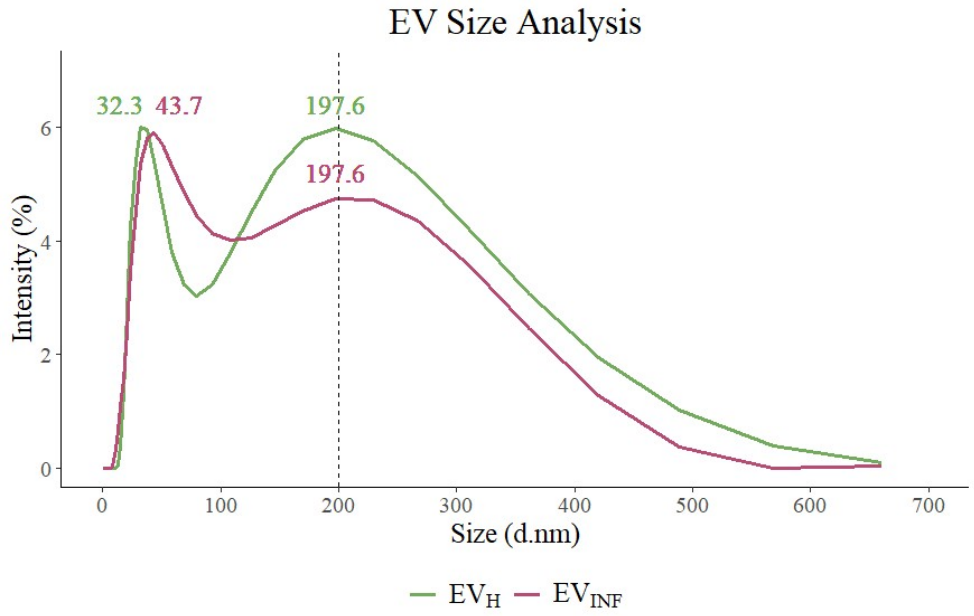


Figure 5.10 ***Dynamic Light Scattering Analysis of the Average Size Distribution by Intensity of EVs isolated from healthy and inflamed ACM.*** *Peak size denoted above peak. Intensity measures the percentage of EVs that fall under a particular size. Line graphs show the average of 3 isolations for each condition. As the medias were filtered prior to EV isolation, readings above 200 nm (denoted by the dashed line) are likely to be due to EV aggregation.*

The effect of these EVs on the barrier property of endothelial cells were then explored (Figure 5.11). As previously described, confluent HBMvECs grown in transwells were treated basolaterally with 12.5 µg/mL EVs for 24 hours.

As with previous results, endothelial cells treated with EVs derived from healthy astrocytes (EV_H) trended towards a ~10% decrease in permeability (0.913 ± 0.232). However, endothelial cells treated with EVs derived from inflamed astrocytes (EV_{INF}) showed a ~10% increase in permeability (1.11 + 0.0167). These results were found to be non-significant.

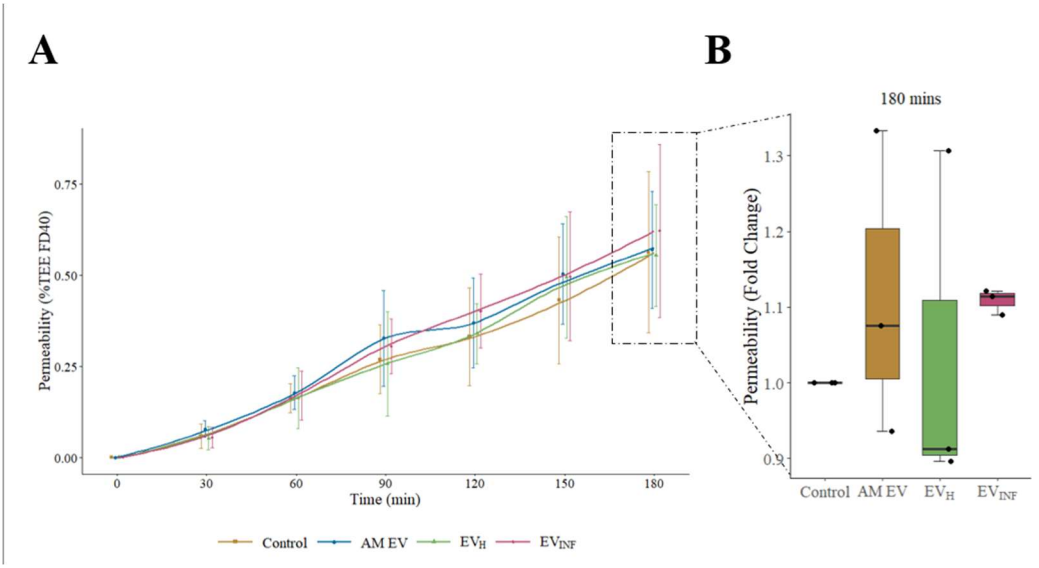


Figure 5.11 ***EVs derived from inflamed astrocytes increase HBMvEC permeability.*** *A) shows the permeability (%TEE FD40) of endothelial cells after EV incubation over the course of the assay (0 – 180 mins). Results are averaged from three independent experiments ± SD. Results were analysed using two-way ANOVA. Dashed box highlights the data used in B) the permeability (%TEE FD40) at the end of the assay (t = 180 mins). Fold changes are normalised to the vehicle control (Control). Black dots show individual data points. Results analysed using one-way ANOVA.*

The protein levels of claudin-5, occludin, and ZO-1 were then explored (Figure 5.12). Again, there were no significant results in claudin-5 protein levels after incubation with EVs isolated from both healthy and inflamed EVs. Interestingly, occludin expression after inflamed EV exposure seemed to increase over 2-fold (2.18 ± 0.329) while ZO-1 expression seemed to decrease after incubation with EVs derived from inflamed astrocytes in comparison to EVs derived from healthy astrocytes (0.609 ± 0.114 vs 1.13 ± 0.0867).

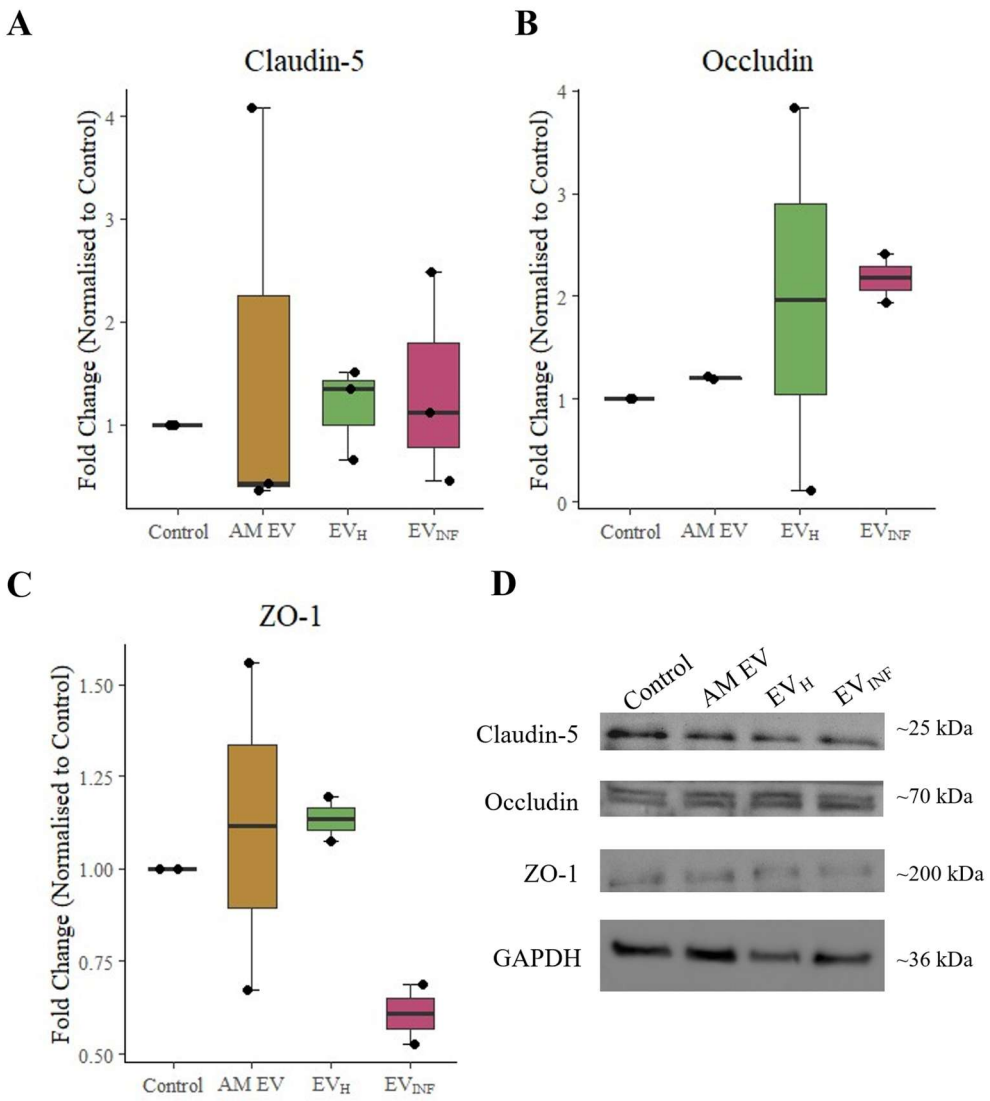


Figure 5.12 ***Protein expression analysis in response to inflamed astrocyte derived EV treatment*** *of the tight junction genes claudin-5 (A), occludin (B), and ZO-1 (C). HBMvECs were treated basolaterally with ACM derived EVs (healthy and inflamed) or AM derived EVs for 24 hours. Black dots indicate individual data points. n = 3 (A) Data analysed using one-way ANOVA. n = 2 (B, C). Data is presented as the median fold change ± SD. D) showcases representative blots for each TJ protein. GAPDH was used as a loading control.*

5.3 Discussion

This chapter showed that astrocyte-derived EVs appeared to strengthen the barrier properties of endothelial cells. Interestingly, basolateral but not apical exposure to EVs decreased HBMvEC barrier permeability. This reflects the spatial distribution of the cells *in vivo,* suggesting that the abluminal surface of endothelial cells plays a key role in mediating indirect communication with astrocytes. Several studies have shown that EV uptake is mediated via EV interactions with a variety of cell-surface proteins (Christianson et al., 2013; Svensson et al., 2013; Castro-Cruz et al., 2023), suggesting that the specific mechanism of EV uptake is dependent on both the EVs used and the recipient cells (Laulagnier et al., 2018). One study found that human epithelial cells also show an orientation preference for EV uptake (B. K. Singh et al., 2020). This study found that very few (~<1%) HEK-293T-derived EVs were taken up by these cells when treated apically. However, basolateral incubation resulted in more internalisation of these EVs (B. K. Singh et al., 2020). Epithelial cells are known to establish an apical-basal polarity through conserved polarity protein complexes (Kemphues et al., 1988; Bilder & Perrimon, 2000; Choi et al., 2019). Similarly, endothelial cells are also polarised along the apical-basolateral axis and exhibit asymmetric protein expression and function (Cornford & Hyman, 2005; Torcq et al., 2024). As EVs seemed to only strengthen the barrier upon basolateral treatment, this may suggest that the protein(s) or membrane receptor(s) that mediate astrocyte-derived EV interactions are localised to the abluminal side of the endothelial cell.

The most significant effect of EV treatment was seen after 24 hours incubation, with some strengthening of the barrier seen at 6 hours and no effect seen after 48-hour incubation, suggesting that astrocyte EVs are quickly taken up by the cells but do not result in long-term changes in endothelial cell barrier strength. Across the literature, EV treatment time tends to vary from short term (a few hours) exposure to several days of exposure (Y. Li et al., 2023; Forero et al., 2024; X. Liang et al., 2025). However, 24 hour treatment seems to have become a common incubation time for EV studies in endothelial cells (Durak-Kozica et al., 2018; Collado et al., 2024). Again, EV internalisation is dependent on both the cells involved in the secretion of the EVs and in the uptake of these secreted EVs. Additionally, dose can

affect treatment time as higher doses are internalised faster and therefore treatment time may be shortened (Jurgielewicz et al., 2020; Bonsergent et al., 2021; Hagey et al., 2023). As a result, the ISEV recommends performing dose-response and time-course studies (Welsh et al., 2024).

Healthy astrocyte-derived EVs were able to tighten the barrier of healthy endothelial cells significantly more than FBS-derived EVs. Tight junction protein complexes are the main contributors to barrier properties. However, astrocyte-derived EVs did not appear to significantly affect the gene or protein levels of the most studied tight junction proteins (claudin-5, occludin, and ZO-1). The scientific literature is quite mixed as to how these proteins may change in response to endothelial barrier-modifying stimuli. One study found that EVs derived from immortalised mouse astrocytes increased TEER values in hCMEC/D3 cells, an immortalised cerebral microvascular endothelial cell line but also found significant increases in the protein expression levels of claudin-5 (Kriaučiūnaitė et al., 2021). However, this study also found that levels of occludin or ZO-1 were unchanged in western blots after incubation with astrocyte-derived EVs. This contradiction in results could be caused by differing EV populations. In the aforementioned study, EVs were isolated from conditioned media from an immortalised mouse astrocyte line using differential centrifugation. The majority of these EVs isolated were 140 nm in diameter but ranged between ~60 – 500 nm in diameter, which differs from those isolated and described in chapter 4 of the current thesis. Additionally, these EVs were incubated on hCMEC/D3 cells for 4 days, rather than 24 hours. Regardless, transcriptomic analysis of endothelial cells after treatment with astrocyte-derived EVs could reveal more comprehensive transcriptional changes resulting in a stronger barrier other than changes in tight junction protein expression levels. Chen et al., (2020) found that EVs derived from an immortalised astrocyte cell line containing miR-195 could improve the stability of claudin-5 and ZO-1 protein expression and decreased BBB permeability of mouse cerebral endothelial cells by suppressing TJ degradation.

Results from several experiments in this study revealed pronounced variability across replicates. This was seen both in EVs isolated from AM and ACM. The cargo of EVs is known to depend on the state of the donor cell (J. S. Choi et al., 2016; K. Tripathi et al., 2023). In addition to this, there is high variability in the populations

of EVs released even by a single cell, including in their cargo (Dechantsreiter et al., 2022; Nikoloff et al., 2021). One study found that during herpes simplex virus 1 infection, HEL cells released EVs that had an overall pro-viral effect, a population of these were found to be antiviral (Dogrammatzis et al., 2021). This could suggest that variability seen in this study is due to the net effect of differences in the heterogeneous population of EVs released by astrocytes.

Treatment with cytokines, but not LPS, induced a neuroinflammatory response in astrocytes, as indicated by changes in several genes associated with reactivity in astrocytes. Although LPS is known to result in activation of astrocytes, particularly in model organisms (Xingi et al., 2023), this has been shown to be mediated by microglial activation in human models (Liddelow et al., 2017). LPS induces the production of cytokines via activation of toll-like receptor 4 (TLR4). Although human astrocytes express TLR4, unlike murine astrocytes, they lack CD14, a glycoprotein which presents LPS to the complex which results in the activation of intercellular signalling pathways (Tarassishin et al., 2014; J. Y. Park et al., 2017). As a result, LPS treatment alone does not result in significant changes in pro-inflammatory gene expression.

As expected, however, treatment with cytokines resulted in the upregulation of CCL2, IL1β, IL6 and TNFα, therefore confirming the production of activated astrocytes. Inflamed astrocytes produce CCL2, a chemokine which recruits immune cells to the CNS as well as continuing to activate glial cells (R. Y. Kim et al., 2014; Orchanian et al., 2024). IL1β is a pro-inflammatory cytokine upregulated in the brain after injury and is known as a marker of astrocyte activation (Baazm et al., 2021; Szpakowski et al., 2022; Gureev et al., 2024). Levels of IL-6 secreted by astrocytes are also increased after inflammation (Van Kralingen et al., 2013; Hyvärinen et al., 2019). IL-6 is a cytokine known to have both a neuroprotective and a detrimental effect on the brain (L. Sun et al., 2017; Pons-Espinal et al., 2024; C. Shan et al., 2024). TNFα, another pro-inflammatory cytokine, is also upregulated in activated astrocytes (Trindade et al., 2020; L. Wu et al., 2024).

Interestingly, GFAP expression was downregulated in the astrocytes used in this study after stimulation with cytokines. Typically, upregulation of GFAP is viewed as a marker of reactive astrocytes (Sofroniew, 2015; Pelkmans et al., 2024). The

paper that originally identified TNFα, IL-1α and C1q as promoting a neurotoxic astrocyte phenotype also found that GFAP was upregulated in astrocytes after treatment (Liddelow et al., 2017). However, the astrocytes used in that study were isolated from mice. Several studies focusing on human astrocytes have also seen a decrease in GFAP expression after stimulation with pro-inflammatory cytokines. Human iPSC-derived astrocytes co-stimulated with TNFα (10 ng/mL) and IL-1β (10 ng/mL) for 7 days showed ~8-fold decrease in both GFAP mRNA and protein levels (Hyvärinen et al., 2019). Astrocytes derived from human ReN cells also showed a decrease in GFAP mRNA expression after 24-hour exposure to TNFα (10 and 30 ng/mL) and IL-1β (30 ng/mL) (Pamies et al., 2021). This contributes to the growing awareness of moving beyond GFAP as a marker of reactive astrocytes.

While EVs isolated from healthy astrocytes were able to decrease permeability of HBMvECs, EVs isolated from inflamed cells appeared to marginally increase HBMvEC permeability. Similarly to previous results, there were no significant changes in claudin-5 or occludin expression on either the mRNA or protein levels. However, ZO-1 expression seemed to trend towards downregulation. Only two replicates were completed for this experiment and therefore at least one other replicate would be needed to confirm the significance of this. In the literature, studies exploring the effect of EVs from inflamed astrocytes are limited. A study focusing on the effects of EVs isolated from TNFα/IFNγ (10 ng/mL) stimulated hCMEC/D3 cells on healthy hCMEC/D3 cells showed a ~10% decrease in TEER values after 24 hours exposure (Hosseinkhani et al., 2023), suggesting that EVs isolated from inflamed cells in general damage BBB integrity. However, Kriaučiūnaitė et al., (2021) looked at the effect of EVs isolated from immortalised astrocytes from mouse model of Alzheimer's disease on endothelial cells. There were no significant changes in TEER values after exposure to these EVS, suggesting that these EVs had no effect on the barrier. However, these values were taken after a longer exposure time (4 days), potentially allowing damage to the barrier to repair itself. Interestingly, the protein levels of the tight junction genes in hCMEC/D3 cells followed the same trends as those observed in this chapter after exposure to these EVs. Levels of both claudin-5 and occludin remained unchanged although ZO-1 protein expression was also downregulated.

Gene expression analysis alone is not sufficient to assess barrier function. Barrier function depends on protein abundance and their proper assembly into functional junctions, which require further experimentation. Studies have shown that there is poor correlation between mRNA and protein expression levels (Schwanhäusser et al., 2011; Wang et al., 2019; reviewed in Samih et al., 2026), however one study has suggested that there is better correlation between mRNA and protein expression levels of differentially expressed genes (Koussounadis et al., 2015) and another has suggested that correlation efficiency can be improved by the introduction of a gene-specific RNA-to-protein conversion factor (Edfors et al., 2016). These studies suggest that gene expression and protein expression levels are not as poorly correlated as once thought. Protein expression alone is also not sufficient to assess barrier function. However, several studies have found a correlation between TJ expression and barrier function (McCarthy et al., 1996; Nitta et al., 2003; Jiao et al., 2011; Sugiyama et al., 2023). Therefore, exploring both gene and protein expression levels is an important initial step in understanding the underlying mechanisms of barrier function.

Given unlimited materials, protein localisation and post-translational modification levels could have also been explored which would have allowed for a more thorough exploration into the biochemical and biophysical mechanisms of barrier function after EV treatment. Phosphorylation of TJ proteins in particular is known to modulate barrier activity (Yamamoto et al., 2008; Murakami et al., 2012; K. Wang, Qu, et al., 2025). The effect on barrier integrity seen after EV treatment could potentially be due to effects on the phosphorylation of TJ proteins. Additionally, the expression levels members of the adherens junctions were not explored in this study. Adherens junctions also affect the permeability of the BBB (Steiner et al., 2014; C.-M. Chen et al., 2020). Future studies should be done to explore both TJ phosphorylation and the stability of adherens junctions after astrocyte-derived EV treatment to determine whether EVs modulate BBB integrity via changes to either of these.

While the majority of studies report that late-passage astrocytes are more reactive in comparison to early-passage astrocytes (M. Bang et al., 2021; W. Zhang et al., 2022; Pérez et al., 2024), the process of isolation may stress primary cells (reviewed in Berenyi, 2026). It has also been reported that astrocytes in culture are reactive in

comparison to quiescent *in vivo* astrocytes, due to being cultured in the presence of serum (Prah et al., 2019; White et al., 2024). As the cells used in this study were cultured in a serum-containing medium, this could mean that these cells were inherently reactive and therefore released EVs containing inflammatory cargo. Therefore, these results may not accurately reflect the impact of healthy astrocytes on endothelial cells *in vivo*. While this had been considered during experimental planning, a preliminary study revealed that these cells did not survive in serum-free media. Regardless, the use of serum-containing media is not uncommon in similar studies focusing on reactive astrocytes (S. Li et al., 2022; Cameron et al., 2024). While the use of the term "control astrocytes" may have described this cohort better, the use of "healthy astrocytes" ensures clarity in terms of treatments used.

In conclusion, astrocyte derived EVs are able to impact the barrier properties of endothelial cells. However, their impact depends on the condition of the cell upon media collection. EVs from healthy astrocytes tend to improve barrier function but not through any notable effect on TJ gene or protein expression levels. EVs from inflamed astrocytes, by contrast, tend to disrupt the barrier with some evidence of this resulting from decreased expression of ZO-1, suggesting potential instability of the TJ complex. As BBB dysfunction is a known hallmark of neuroinflammation, this points to a potential mechanism by which inflamed astrocytes destabilise the barrier, both locally and widespread across the brain.

While the TJs play a significant role in the integrity of the BBB, treatment with astrocyte-derived EVs in our study did not significantly affect their expression levels. However, other factors also affect BBB permeability, including inflammation (Haruwaka et al., 2019; Hilbrig et al., 2026). The dysregulation of several signalling molecules has been noted during neuroinflammation, including cytokines and MMPs, both of which are known causes of BBB leakage (J. Liu et al., 2012; A.-Q. Chen et al., 2019). Wnt signalling is also known as the master regulator of the BBB, as it is known to be involved in the activation of several BBB-related genes (Stenman et al., 2008; Guérit et al., 2021). EVs contain a variety of cargo and therefore, can affect multiple pathways in recipient cells. Therefore, in order to determine what effect EVs have on HBMvECs that may result in changes to barrier integrity, exploring the transcriptome of these cells post-treatment in

addition to the transcriptome of the EVs themselves could potentially identify affected pathways thus informing future experiments.

Chapter 6 : Transcriptomic Analysis of Astrocyte-Derived EV Treated HBMvECs

6.1 Introduction

As part of their cargo, EVs are known to carry different types of RNA, including both coding (mRNA) (Skog et al., 2008; H. Zong et al., 2023) and non-coding (e.g. long non-coding (lncRNA) (Gezer et al., 2014; X. Wei et al., 2022), microRNA (miRNA) (Valadi et al., 2007; X. Liu et al., 2023), and circular (circRNA) (C. Ding et al., 2021; Z. Pan et al., 2022)) RNA. Although the exact sorting mechanism(s) are yet to be determined, there is evidence that donor cells are able to selectively load cargo into EVs (Guduric-Fuchs et al., 2012; B. He et al., 2021). This cargo has been found to be biologically active, altering the behaviour of recipient cells and corroborating the role of EVs in intercellular communication (Valadi et al., 2007; G. Wang et al., 2023).

In particular, miRNAs are enriched in these vesicles in comparison to their donor cells (Goldie et al., 2014; Jeppesen et al., 2019; Sork et al., 2021). These non-coding small RNAs are typically around 20-25 nucleotides (nt) in length and act as regulators of gene expression (Hutvágner & Zamore, 2002; Mohamed et al., 2025). As a result, they are known to play roles in a variety of cellular function such as proliferation (Tao et al., 2019; M. Lu et al., 2023), differentiation (Hara et al., 2013; G. Zhang et al., 2022), and apoptosis (Dahiya & Atreya, 2021; Y. Ding et al., 2021). In addition, miRNAs have been shown to play roles in disease (Du et al., 2009; Peng et al., 2017; M.-L. Chen et al., 2021).

The miRNA transcriptome of EVs changes during disease (Banack et al., 2022; A. Kumar et al., 2023). Although one study found that EVs derived from healthy astrocytes contain miRNAs that regulate correct neuronal functions (Gordillo-Sampedro et al., 2024), astrocytes under inflammatory conditions were found to release EVs that were enriched in miRNAs that dampened the excitability of neurons (Chaudhuri et al., 2018). Another study found that EVs isolated from astrocytes in a model of TBI were found to promote mitochondrial dysfunction and apoptosis in neurons (Q. Hu et al., 2024).

Studies exploring the effect of astrocyte-derived EVs on other cells of the brain, including endothelial cells are limited. However, some studies have shown that EVs were able to induce changes in the transcriptome of endothelial cells (X. Li et al.,

2023; J.-J. Pan et al., 2024). Neuronal-derived EVs containing miR-132 were able to regulate the integrity of the BBB through the expression of VE-Cadherin (B. Xu et al., 2017). On the other hand, EVs from inflamed non-brain cells were found to drive inflammation in non-brain endothelial cells through the upregulation of several pro-inflammatory genes (F. Jiang et al., 2020). These studies reveal that EVs are capable of modulating the transcriptome of endothelial cells. As such, this chapter aims to discover the wider transcriptomic changes that occur in HBMvECs following treatment with EVs isolated from healthy and inflamed astrocytes, and whether these might explain the functional changes in these cells observed in chapter 5.

6.1.1 Chapter Aims

- To analyse the small RNA population of EVs isolated from healthy and inflamed astrocytes.
- To identify differentially expressed genes in HBMvECs treated with EVs derived from both healthy and inflamed astrocytes.
- To identify the cellular regulatory pathways these differentially expressed genes are putatively involved in.

6.2 Results

In order to analyse the miRNA transcriptomes of EVs from healthy (EV_H) and inflamed (EV_{INF}) astrocytes, EV_H and EV_{INF} were first isolated and lysed in TRIzol® (Figure 6.1). Healthy and inflamed astrocytes were also lysed in TRIzol® in order to allow for comparison between the miRNA transcriptomes of astrocytes and their corresponding EVs. These were then stored at -80°C prior to shipment to Macrogen (South Korea) where RNA extraction, quality assessment, library preparation, and sequencing were performed. Verification of miRNA isolation was performed by RNA size distribution analysis using the Bioanalyzer Small RNA chip run on the 2100 BioAnalyzer Instrument.

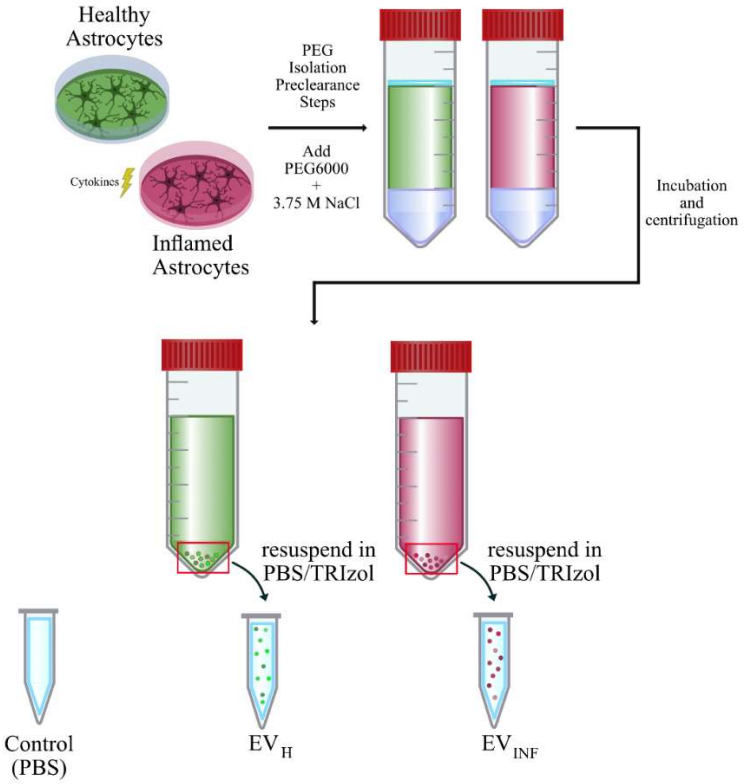


Figure 6.1 ***Illustration of EV isolation from healthy and inflamed cells.*** *After 24 hours of conditioning astrocyte media on healthy astrocytes or inflamed astrocytes, cell debris and larger proteins and microvesicles were cleared through preclearance steps as described in Chapter 4. 50% PEG6000 was added to a final concentration of 10% and 3.75M NaCl added to a final concentration of 2%. These medias were then incubated overnight and centrifuged at 1500 x g for 1 hour. The supernatant was then removed, and the pellet resuspended in TRIzol (for RNA isolation) or PBS (for cell treatment). Figure created by author using Affinity Designer (v 1.10.6.1665).*

6.2.1 Primary human astrocyte-derived EVs do not seem to contain miRNA, likely due to negligible amounts of miRNA in their donor cells.

Total RNA quality was assessed after RNA isolation. Figure 6.2A, B revealed that EVs carry a small quantity of a variety of RNAs with the majority of RNAs isolated being >200 nt, peaking at 117nt for EV_H (A(i)) and 119nt for EV_{INF} (B(i)). These small RNAs were then further resolved using a Bioanalyzer RNA Small RNA chip in order to determine the integrity and quantity of the small RNA populations prior to library preparation and sequencing (Figure 6.2A(ii), B(ii)). This revealed that there were no differences in small RNA populations between EV_H and EV_{INF}. The populations of small RNAs in these EVs were between 150-200 nt in size. Surprisingly, no peaks at around 20nt were seen, suggesting that these EVs carried very few, if any, EVs.

This was repeated on representative astrocyte cell samples. Again, Figure 6.3A, B reveals no changes in RNA populations between healthy (A) and inflamed (B) astrocytes. Although analysis of the small RNAs revealed many RNA populations that were not reflected in the small RNA transcriptome of EVs, these astrocytes again seemed to lack any substantial populations of miRNAs.

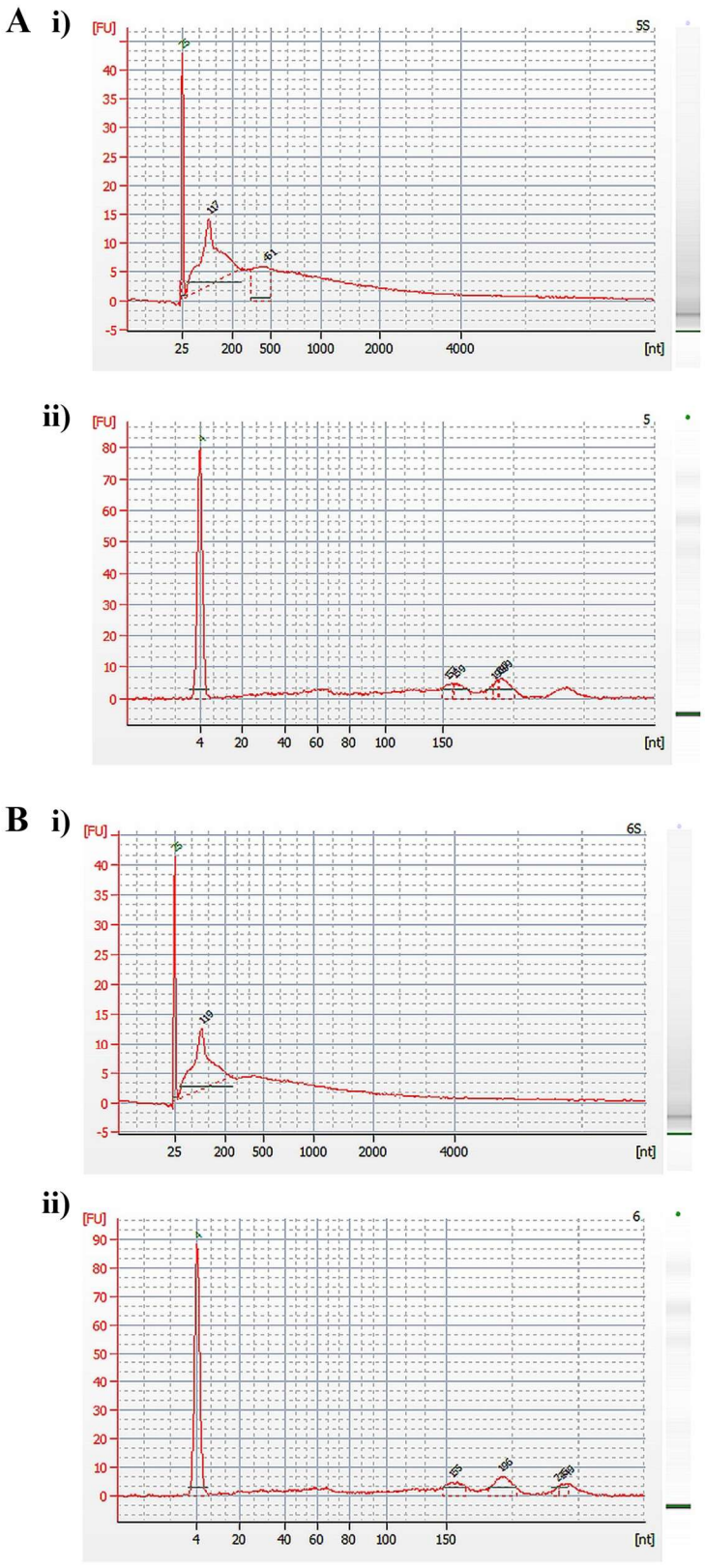


Figure 6.2 ***Total RNA quality analysis of EVs isolated from healthy (A) and inflamed (B) astrocytes*** *via BioAnalyser. Representative electropherograms and gel-like images from preparations using the RNA 6000 Pico Chip kit (i) and the Bioanalyzer RNA Small RNA chip (ii), run on the 2100 BioAnalyzer Instrument by Macrogen. n = 3.*

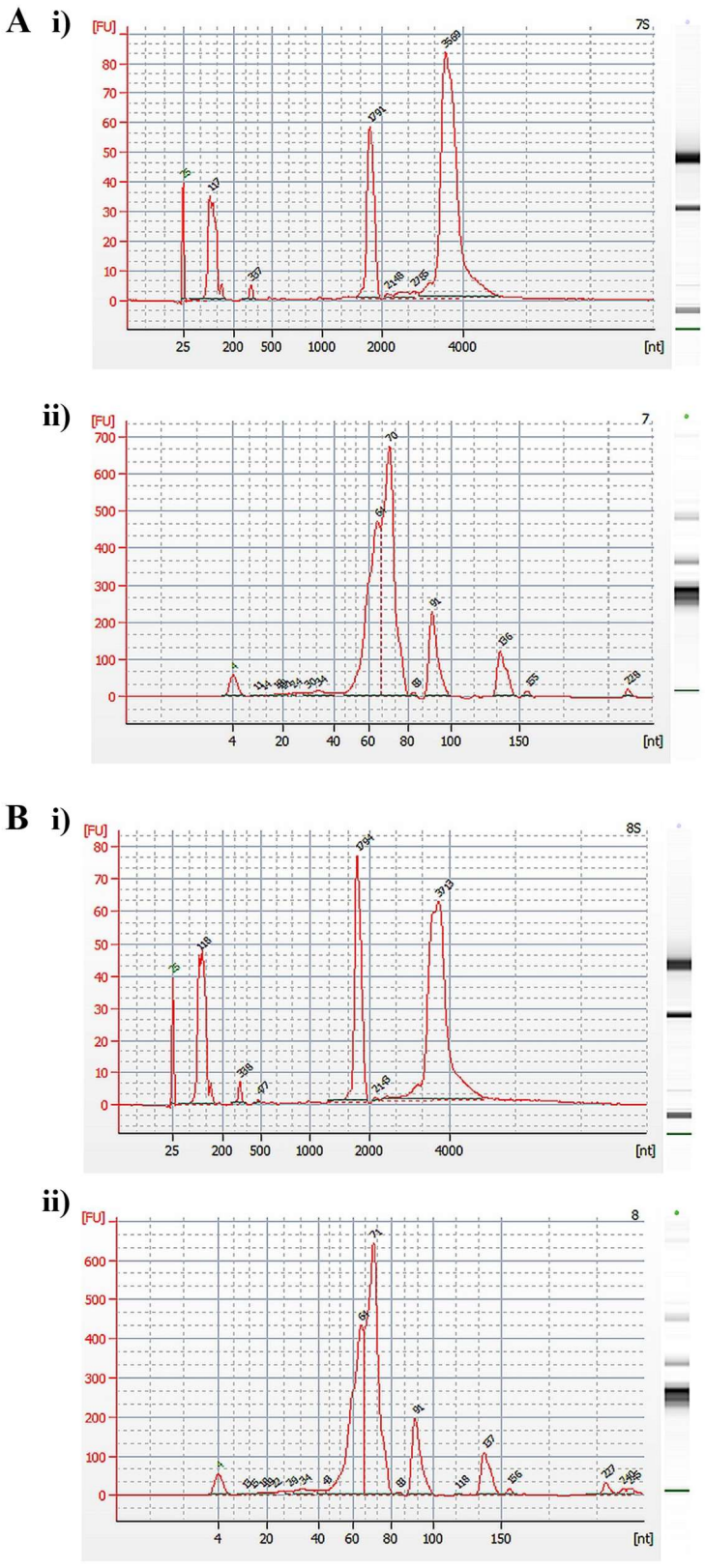


Figure 6.3 ***Total RNA quality analysis of healthy (A) and inflamed (B) astrocytes*** *via BioAnalyser. Representative electropherograms and gel-like images from preparations using the RNA 6000 Pico Chip kit (i) and the Bioanalyzer RNA Small RNA chip (ii), run on the 2100 BioAnalyzer Instrument by Macrogen. n = 3.*

6.2.2 Astrocyte-derived EVs modify the transcriptome of HBMvECs

Although astrocyte-derived EVs did not appear to contain miRNA, results from chapter 5 suggested that they were able to affect the permeability of HBMvECs. Moreover, whilst TJ genes appear unaffected, these EVs may have affected the expression of other endothelial genes indirectly impacting HBMvEC permeability. As such, the transcriptomes of HBMvECs after 24-hour treatment with PBS (control), EVH, and EVINF were analysed. Following completion of the treatments, HBMvECs were lysed in TRIzol®. These were then stored at -80°C prior to shipment to Macrogen (South Korea) where RNA extraction, quality assessment, library preparation, and sequencing were performed. Total RNA quality (Figure A.3, Appendix).and library quality (Figure A.4, Appendix). were assessed.

A principal component analysis (PCA) was first performed on normalised gene expression profiles of HBMvECs treated with PBS, EV_H, or EV_{INF} in order to explore variation in the dataset (Figure 6.4). The first two principal components explained 75% (PC1) and 22% (PC2) of the variance (Figure 6.4A). Rather than clustering according to treatment status, samples primarily clustered by experimental date, suggesting that the variance was mostly attributable to biological differences between stocks of HBMvECs used. However, one replicate (Rep1: Healthy EVs) varied widely from both cells treated on the same day and the second replicate. Removing healthy EVs from the analysis showed similar results, revealing a clear separation between replicates (Figure 6.4B). In this PCA, PC1 explained 96% of the variance. However, PC2 accounted for 3% of the variance and shows some similarity between HBMvECs treated with inflamed EVs. Based on these findings, the analysis will proceed focusing on the HBMvECs treated with control and EV_{INF} only, in order to find significant changes in the HBMvEC transcriptome after EV_{INF} treatment.

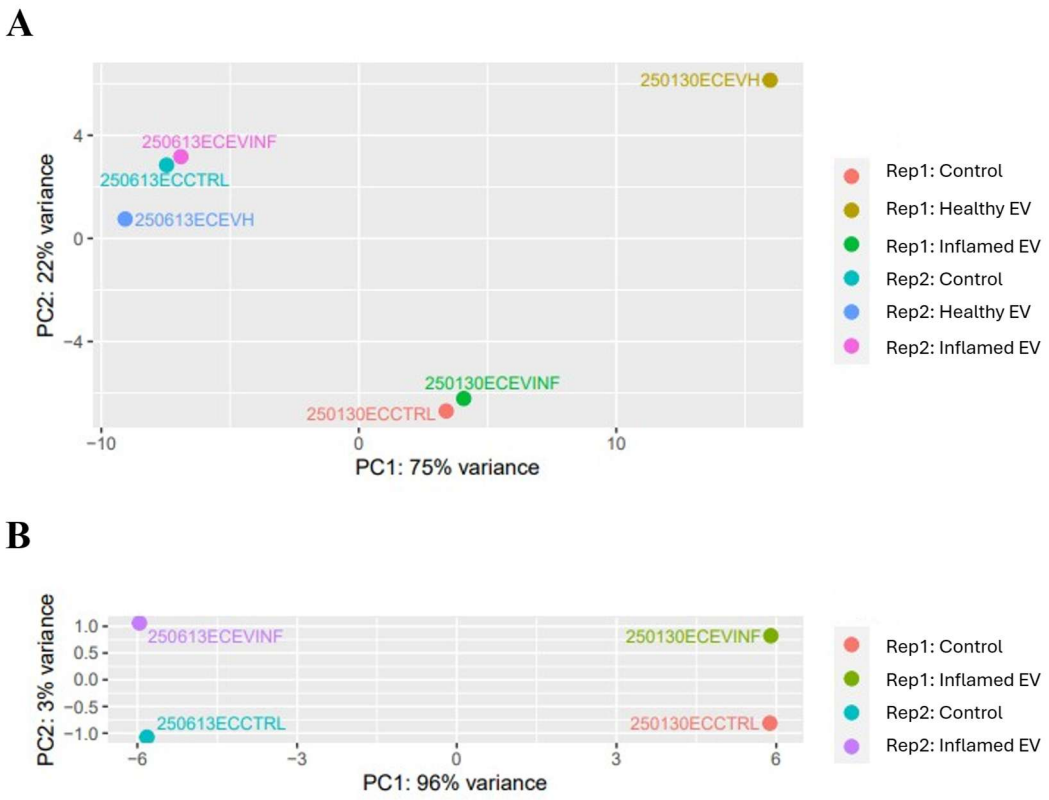


Figure 6.4 ***PCA of gene expression data***. *Each point represents one sample. A) shows data from HBMvECs treated with control (PBS), EVs from healthy astrocytes (Healthy EV), and inflamed astrocytes (Inflamed EVs). B) shows the variance of HBMvECs treated with control and inflamed EVs only. X-axis shows the first principal component. Y-axis shows the second principal component.*

In order to detect differentially expressed genes (DEGs) in HBMvECs treated with EV_{INF} in comparison to control, a pairwise comparison between these conditions was then performed using edgeR (Robinson et al., 2010; Y. Chen et al., 2025). Thirty four DEGs were identified (Figure 6.5). Of these, 19 genes were downregulated (listed in Table 6.1) and 15 genes were upregulated (listed in Table 6.2) in cells treated with inflamed EVs.

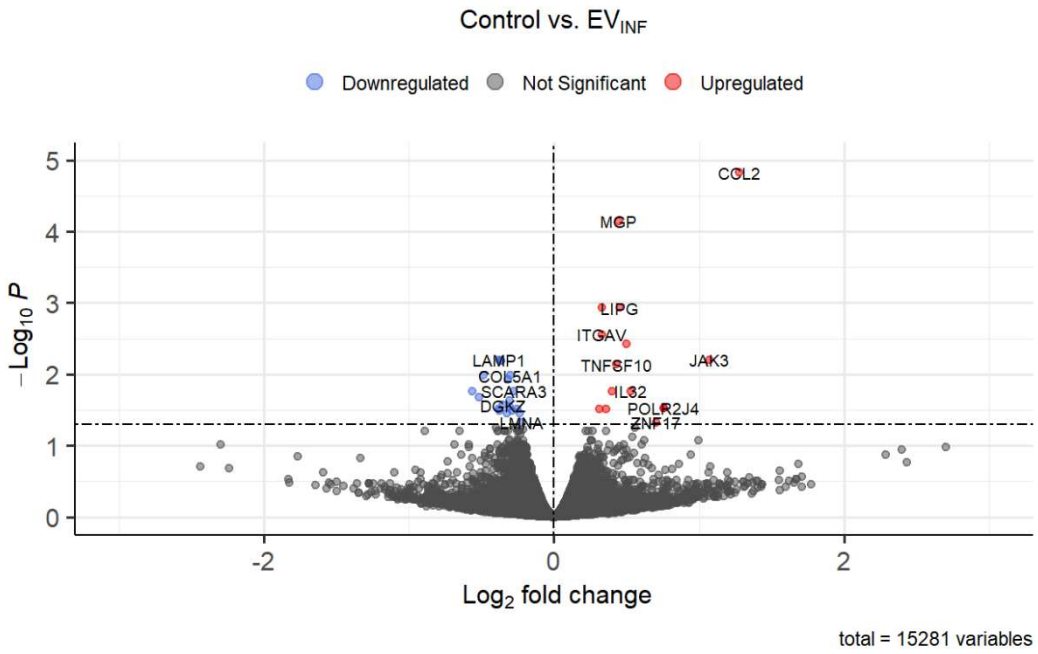


Figure 6.5 ***Volcano plot of differential gene expression of HBMvECs treated with vehicle control (PBS) vs. EVs isolated from inflamed astrocytes.*** *Each point represents the average value of one transcript in 2 replicate experiments. X-axis shows the log_2 fold change value. Y-axis shows the value of log_{10} (P value). The expression difference is considered significant for a non-zero log_2 fold change in gene expression (threshold denoted by vertical dashed line) and for a P value of ≤0.05 ($-log_{10}P$ of >1.3, denoted by horizontal dashed line). Genes that are considered significantly downregulated are coloured blue while those that are considered significantly upregulated are coloured red. Points that are grey are non-significant.*

Table 6.1: Genes downregulated in HBMvECs after treatment with inflamed EVs in comparison to control, in order of largest fold change

Gene Symbol	Gene Name	Log_2 Fold Change	P Value	Function
NTSR1	Neurotensin Receptor 1	-0.56034	0.017293	G-protein coupled receptor that binds to the neuropeptide neurotensin (Tanaka et al., 1990; Libanje et al., 2023). NTSR1 has recently been found to play a role in vascular remodelling (Z.-X. Wei et al., 2024).
FZD8	Frizzled Class Receptor 8	-0.51728	0.021004	A member of the Frizzled receptors for Wnt signalling proteins (S. Kumar et al., 2014; Murillo-Garzón et al., 2018).
TCIRG1	T-cell Immune Regulator 1	-0.48453	0.010332	Encodes the α3 isoform of the α subunit of the vacuolar ATPase proton pump, located primarily on lysosomes and regulates late phagosome-lysosomal fusion (Sun-Wada et al., 2009; Q. Chen et al., 2024). Mutations in this gene are associated with osteopetrosis (Frattini et al., 2000; Koçak et al., 2019).
MAN2A2	Mannosidase Alpha Class 2A Member 2	-0.38481	0.030319	Required for *N*-glycan trimming/maturation for proper post-translational modifications of proteins (Akama et al., 2006; Mahajan et al., 2023). A genome-wide association study has found genetic variability in this gene is associated with blood pressure (Buniello et al., 2019). This gene has also been found to be linked to ischemic stroke risk (Y. Liu et al., 2024).
LAMP1	Lysosomal-Associated Membrane Protein 1	-0.37619	0.006247	Highly abundant glycoprotein component typically associated with lysosomes (J. W. Chen et al., 1985; X.-T. Cheng et al., 2018) and involved in normal lysosomal function such as autophagy and exocytosis (Huynh et al., 2007; Yogalingam et al., 2008; Wilke et al., 2012; Chaudhry et al., 2022).

Continued on next page

Table 6.1 (continued)

Gene Symbol	Gene Name	Log_2 Fold Change	P Value	Function
PTMS	Parathymosin	-0.37444	0.032091	Has been shown to inhibit NF-κB transcriptional activity (Okamoto et al., 2016; Takami et al., 2023). Knockdown of PTMS has been shown to result in severe, age-related neurodegeneration (B. Yu et al., 2020; Jung et al., 2025).
APLN	Apelin	-0.36755	0.006569	A regulator of angiotensin-converting enzyme 2 (ACE2) which is known to regulate vascular tone (Tipnis et al., 2000; Z.-Z. Zhang et al., 2017; X.-T. Li et al., 2021). Apelin signalling has also been found to play important roles in maintaining cardiovascular homeostasis, including driving angiogenesis (Helker et al., 2020; Chang et al., 2021), increasing contractility (Kuba et al., 2007; Charo et al., 2009; Besserer-Offroy et al., 2018), and lowering blood pressure through its effects as a vasodilator (D. K. Lee et al., 2000; Japp et al., 2008; Schinzari et al., 2017)
SNED1	Sushi, Nidogen And EGF Like Domains 1	-0.36507	0.006569	Encodes for the ExM protein glycoprotein SNED1 (Barqué et al., 2021; Vallet et al., 2021).
DGKZ	Diacylglycerol Kinase Zeta	-0.35414	0.026969	Phosphorylates diacylglycerol (DAG), playing an important role in signalling (Bunting et al., 1996; Riese et al., 2011; Furuta et al., 2023).
MYRIP	Myosin VIIA And Rab Interacting Protein	-0.32378	0.035479	Regulates exocytosis of vWF by linking Rab27a and Myosin Va to the actin cytoskeleton (Nightingale et al., 2009; Rojo Pulido et al., 2011; Conte et al., 2016)
RN7SL3	RNA Component Of Signal Recognition Particle 7SL3	-0.3179	0.011888	Long, non-coding RNA component of the signal recognition particle complex which targets proteins to the endoplasmic reticulum (Regalia, 2002; Bujisic et al., 2025)

Continued on next page

Table 6.1 (continued)

Gene Symbol	Gene Name	Log_2 Fold Change	P Value	Function
NBEAL2	Neurobeachin Like 2	-0.30879	0.028149	Required for α-granule maturation and packaging of α-granule proteins (Kahr et al., 2013; Kat et al., 2023). Loss of function in this gene results in grey platelet syndrome (Albers et al., 2011; Posey et al., 2025)
EHD2	EH Domain Containing 2	-0.3039	0.023484	An ATPase that is a nuclear-cytoplasmic shuttle protein and inhibits gene transcription in the nucleus (Pekar et al., 2012; Torrino et al., 2018). Involved in several biological processes including endocytosis (Benjamin et al., 2011; Bar et al., 2014; Webb et al., 2022) and metabolism (S. Y. Park et al., 2004; Sackmann-Sala et al., 2014; M. Neuhaus et al., 2023)
COL5A1	Collagen Type V Alpha 1	-0.29786	0.010332	Encodes for the alpha 1 chain of the ExM protein collagen type V (Lebovitz et al., 1996; Kumskova et al., 2025)
HSPB1	Heat Shock Protein Family B 1 (also known as Hsp27)	-0.2875	0.032137	A member of the heat shock protein family which are primarily involved in maintaining homeostasis in the cell (Quraishe et al., 2008; R. Shan et al., 2021). Hsp27 chaperones the correct folding of proteins (Z. Liu et al., 2012; Selig et al., 2020) and in inhibiting apoptosis (X. Tian et al., 2016; Kennedy et al., 2017). Also has been shown to be neuroprotective during protein aggregation in the brain (King et al., 2009; Vicente Miranda et al., 2020)

Continued on next page

Table 6.1 (continued)

Gene Symbol	Gene Name	Log_2 Fold Change	P Value	Function
SCARA3	Scavenger Receptor Class A Member 3	-0.27536	0.017293	A member of the class A scavenger receptor family which mediates endocytosis by binding to and internalising a variety of targets (Arukuusk et al., 2013; Q. Song et al., 2021) and act as pattern recognition receptors of the innate immune system (Balla et al., 2009; J. He et al., 2014; Taban et al., 2022).
TIMP2	Tissue Inhibitor of Metalloproteinases 2	-0.25317	0.030319	An inhibitor of matrix metalloproteinases (MMPs), which are involved in degrading ExM proteins (Łukomska et al., 2020; Hayun et al., 2023)
CLEC14A	C-Type Lectin Domain Containing 14A	-0.23901	0.035479	Enriched in vascular endothelial cells and shown to play roles in cell-cell adhesion (Rho et al., 2011; Jang et al., 2017), migration (X. Zhuang et al., 2011; Ki et al., 2013), and angiogenesis (Mura et al., 2012; Y. Liao et al., 2024)
LMNA	Lamin A/C	-0.22533	0.047213	A nucleoskeletal intermediate filament that provides structural support to the cell nucleus, regulates gene expression (M. Singh et al., 2013; Bera & Sengupta, 2020) and plays a role in mechanotransduction (Lammerding et al., 2004; H. Liu et al., 2024). Mutations in this gene impair angiogenesis, potentially due to reduced NO production in cells (Bonello-Palot et al., 2014; Sayed et al., 2020; Gete et al., 2021) and result in cardiovascular complications in humans(Mosbah et al., 2020; J. Wang, Yu, et al., 2022).

Table 6.2: Genes upregulated in HBMvECs after treatment with inflamed EVs in comparison to control, in order of largest fold change

Gene Symbol	Gene Name	Log_2 Fold Change	P Value	Function
CCL2	C-C Motif Chemokine Ligand 2	1.277241	1.48E-05	A key inflammatory chemokine that regulates the recruitment of peripheral mononuclear cells (Strieter et al., 1989; Qian et al., 2011; Husain et al., 2025)
JAK3	Janus Kinase 3	1.072022	0.006247	A member of a family of non-receptor tyrosine kinases that play a crucial role in the immune system by mediating downstream cytokine signalling in the JAK-STAT pathway (Takahashi & Shirasaw, 1994; Macrì et al., 2023). JAK3 selectively associates with the cytokine receptor subunit γc, which is shared by several heteromeric cytokine receptors (Kirken et al., 1994; Dai et al., 2022). Mutations in JAK3 cause immune dysregulation (Thomis et al., 1995; Cornejo et al., 2009; Lahera et al., 2024).
POLR2J4	RNA Polymerase II Subunit J4 (Pseudogene)	0.754924	0.029789	lncRNA, acts as a miRNA sponge (Shpakovski et al., 2004; X. Lu et al., 2019). Regarded as an oncogene, promoting cancer cell proliferation and migration (Ji et al., 2024; M. Song et al., 2025)
RASA4CP	RAS p21 Protein Activator 4c (Pseudogene)	0.754924	0.029789	lncRNA, has been suggested as a biomarker for cervical cancer (W. Wu et al., 2019)
ZNF17	Zinc Finger Protein 17	0.706411	0.047269	Potentially involved in transcriptional regulation (GeneCards identifier GC19P057411). Mutations in ZNF17 result in ciliopathies (Castro-Sánchez et al., 2017) and have been identified in hepatocellular carcinoma (Kassem et al., 2024)

Continued on next page

Table 6.2 (continued)

Gene Symbol	Gene Name	Log_2 Fold Change	P Value	Function
IL32	Interleukin 32	0.529649	0.017293	A (mostly) proinflammatory cytokine that plays a role in a variety of inflammatory diseases (Shioya et al., 2007; Heinhuis et al., 2011; Q. Yao et al., 2019) and in immune response to viruses (Mesquita et al., 2016; Collister et al., 2019; Assou et al., 2023)
ICAM1	Intercellular Adhesion Molecule 1	0.497513	0.003781	Recruits leukocytes to sites of inflammation (Byeseda et al., 2009; Wiesolek et al., 2020)
LIPG	Lipase G, Endothelial Type	0.450942	0.001177	Plays a role in signal transduction by regulating high-density lipoprotein (HDL) cholesterol metabolism (Tatematsu et al., 2013; Ruff et al., 2021; Y. Wang, Huang, et al., 2025).
MGP	Matrix Gla Protein	0.448615	7.09E-05	A vitamin-K dependent protein that regulates vascular homeostasis via inhibition of vascular calcification (G. Luo et al., 1997; Malhotra et al., 2022)
TNFSF10	Tumour Necrosis Factor Superfamily Member 10 (also known as TRAIL)	0.429489	0.007268	Part of the tumour-immune system by inducing apoptosis in tumour cells (Wiley et al., 1995; De Wilt et al., 2024). Has been shown to inhibit VEGF-induced angiogenesis (Cantarella et al., 2006; Na et al., 2014)
ZNF587	Zinc Finger Protein 587	0.399428	0.017293	Upregulated in gastric cancer (J. Liu et al., 2021) and prostate cancer (T. Wu et al., 2022). Repressor of retroviral infection (Turelli et al., 2020; B. Yang et al., 2022)
SOD2	Superoxide Dismutase 2	0.357064	0.030319	A member of the superoxidase dismutase family which protect against oxidative stress by catalysing the dismutation of superoxide radicals in mitochondria (Lebovitz et al., 1996; Y.-S. Zhang et al., 2025).

Continued on next page

Table 6.2 (continued)

Gene Symbol	Gene Name	Log_2 Fold Change	P Value	Function
ITGAV	Integrin Subunit Alpha V	0.330863	0.002779	An RGD-recognizing integrin binding to the ExM forming cell-matrix adhesion complexes (Sims et al., 2000; Mariasoosai et al., 2024). Also associated with pro-inflammatory responses (X. Yao et al., 2023; Ghasempour et al., 2024)
IL6ST	Interleukin 6 Cytokine Family Signal Transducer (also known as GP130)	0.329807	0.001177	A shared signal transducing subunit for many cytokine receptor complexes in addition to IL-6 (Gearing et al., 1992; Jostock et al., 2001; Osman & Neamati, 2024)
NFKBIA	NF-κB Inhibitor Alpha	0.31008	0.030319	Regulates signalling by sequestering NF-κB in an inactive form in the cytoplasm (Baeuerle & Baltimore, 1988; Jacobs & Harrison, 1998; Fan et al., 2004; Palma et al., 2025)

The DEGs were then annotated using the Gene Ontology (GO) database, which allows for the determination of formally defined relationships between them. The GO classification system revealed that these genes could be classified into groups according to their biological processes (Figure 6.6). These DEGs were found to be enriched in several aspects affecting the vasculature, including blood vessel morphogenesis (which was found to have the lowest p-value), endothelial cell migration, regulation of vascular development, and artery development, as well as those affecting cell adhesion and migration. Additionally, several pathways relating to translation were enriched, including ribosome biogenesis, ribonucleoprotein biogenesis, cytoplasmic translation, rRNA processing, de novo post translational protein folding. Unsurprisingly, DEGs were also involved in the cytokine-mediated signalling pathway.

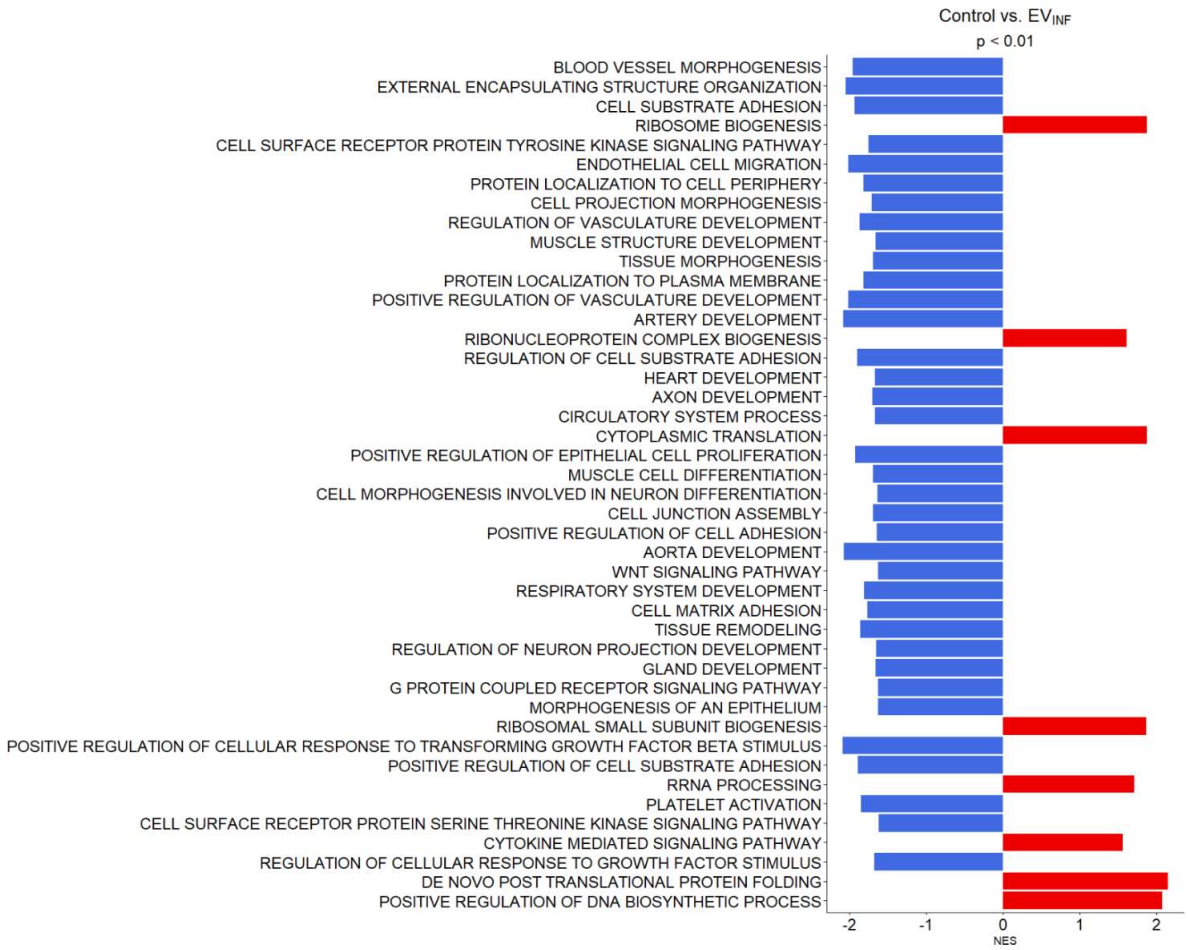


Figure 6.6 ***Gene ontology (GO) enrichment analysis of HBMvECs DEGs after treatment with inflamed EVs.*** *The x-axis displays the GO terms. The most significant pathways (p < 0.01) are shown, in order of significance. The y-axis shows the normalised enrichment score (NES). A positive NES score (red) indicates that the genes in that category are enriched at the "top" of the ranked list, typically corresponding to up-regulated genes. A negative NES score (blue) indicates that the genes involved in that pathway are enriched at the "bottom", typically corresponding to down-regulated genes*

6.3 Discussion

This chapter attempted to determine the changes in the miRNA transcriptome of EVs isolated from healthy and inflamed astrocyte and how they affected the transcriptome of HBMvECs treated with these EVs. Surprisingly, a lack of miRNA was found in the EVs isolated in this study, potentially due to the negligible population of miRNAs in the donor cells. miRNAs have been found both in astrocyte cultures (J. Chen et al., 2019; Gordillo-Sampedro et al., 2024) and in EVs derived from cultured astrocytes (Long et al., 2020; Q. Hu et al., 2024).) Additionally, several studies have shown that miRNAs delivered by astrocyte-derived EVs affect neuronal function (Varcianna et al., 2019; Q. Hu et al., 2024). One recent study has also provided evidence that IPSC-derived healthy astrocytes selectively load miRNAs into EVs (Gordillo-Sampedro et al., 2024). This corroborates that astrocyte- derived EVs should contain miRNAs. However, these studies focused on identifying the miRNAs present rather than the total quantity of miRNA. Therefore, the miRNA population of the cells used in this study may have been too low to be detected via Bioanalyzer, especially in comparison to the quantity of other RNAs present. In order to truly confirm the apparent absence of miRNA in these samples, sequencing of this RNA population should be performed.

Even seemingly lacking a notable amount of miRNA, these EVs induced a functional change in HBMvECs. While this could be due to other biologically active molecules in their cargo, there were several small RNA populations between 150 - 200 nt identified in these EVs. Small nuclear RNAs (snRNAs) range between 80 - 350 nt (Z. Lu & Matera, 2015). These form the small nuclear ribonucleoprotein complex, which is responsible for splicing of pre-mRNA into mature mRNA (Rogalska et al., 2024; Vorländer et al., 2024). These have been reported in EVs (Jeppesen et al., 2019) but no studies focusing on this subpopulation of RNA in EVs were found. Although lncRNAs present in EVs have demonstrated an effect in recipient cells (F. Liang et al., 2025; Meng et al., 2024), these RNAs are too short to be considered lncRNAs, which are typically >200 nt (Bu et al., 2012; Mattick et al., 2023).

Another possibility is that these RNAs could be fragments of mRNA. EVs have been found to contain fragments of mRNA ranging from 25 to 4,000 nt (Berardocco et al., 2017; Prieto-Vila et al., 2021), whereas intact mRNAs range from 400 to 12,000 nt in mammals (Ravasi et al., 2006; Miceli et al., 2024). These mRNA fragments have been shown to produce proteins upon delivery (Batagov & Kurochkin, 2013; Chiang et al., 2023), suggesting that these fragments are able to play a role in intercellular communication. However, sequencing of these fragments will be required to determine their identity and predict their function.

Both EV_H and EV_{INF} were able to induce changes in the transcriptome of endothelial cells. However, no significant DEGs were identified in cells treated with EV_H in comparison to control or in cells treated with EV_{INF} in comparison to cells treated with EV_H (Figure A. 5, Appendix). This is likely due to the high variability between replicates of cells treated with EV_H. One potential explanation for this variation could be due to the populations of RNAs isolated. The first replicate of HBMvECs treated with healthy EVs shows a much lower mRNA peak than other samples (Figure A. 4, Appendix). This could have potentially affected the available mRNAs, resulting in inflated reads and inaccurate analysis of gene expression data. Variation between samples were also seen in cells treated with EV_{INF} and control cells. All endothelial cells used in this experiment were derived from the same source and therefore there should not have been any biological variation between them. Similarly, all astrocytes used for the generation of conditioned media in this chapter were also derived from one donor. However, the same batch of media was used to generate ACM, while different batches of endothelial media were used for the passage and experimental procedures involving endothelial cells. This could account for some of the variability seen, as composition of media can result in variability of endothelial cell gene expression (Helms et al., 2010). Regardless, several DEGs and affected pathways were identified in cells treated with EV_{INF} in comparison to control and are discussed below.

Chapter 5 revealed that while EV_{INF} increased permeability in HBMvECs, they did not significantly affect TJ gene and protein expression levels. However, transcriptomic analysis of the DEGs and the pathways they are involved with have suggested several possible explanations for this increase in permeability.

Firstly, vascular inflammation has been associated with increased permeability of the BBB (Propson et al., 2021; Hermans et al., 2022). Several genes linked with inflammation were found to be upregulated in HBMvECs after treatment with EV_{INF}. These included *IL32*, which has been found to upregulate cytokine production in endothelial cells (Nold-Petry et al., 2009; Bunet et al., 2023) and *LIPG* which mediates inflammation by upregulating pro-inflammatory cytokines (Badellino et al., 2008; Riederer et al., 2011; C. Hong et al., 2021). In addition, the expression level of *JAK3* was found to be upregulated in our study. The JAK-STAT signalling pathway is known to promote neuroinflammation (H. Qin et al., 2016; H. Hong et al., 2024). Of particular note, H. Kim et al., (2022) showed that in an *in vivo* co-culture model, inflamed astrocytes were able to induce BBB dysfunction through the activation of STAT3. Overall, this suggests that EV_{INF} are able to induce inflammation in HBMvECs and potentially play a role in the pathogenesis of neuroinflammation in the CNS.

Neuroinflammation has been closely associated with increased oxidative stress (Heo et al., 2005; P. Zong et al., 2024). Several DEGs identified after EV_{INF} treatment have been linked to oxidative stress. *SCARA3*, found to be downregulated in our study, has been found to protect against oxidative stress (H. Han, 1998; Guadagno et al., 2017). This suggests that treatment with EV_{INF} results in increased levels of ROS, for which HBMvECs tries to compensate by upregulating *SOD2* expression, as seen in other studies (Z. Liu et al., 2014; K. Li et al., 2025). Excessive reactive oxygen species (ROS) are also known to contribute to cell dysfunction and to the breakdown of the BBB (Haileselassie et al., 2020; X. Zhao et al., 2024).

Additionally, several DEGs identified in our study have been shown to influence the permeability of endothelial cells. Firstly, *APLN,* which encodes for apelin, was found to be downregulated. While apelin did not show any effect on barriergenesis (Herdt et al., 2025), apelin-13 treatment was able to reduce BBB permeability in a mouse model of stroke (Chu et al., 2017). However, in diabetic patient testes, the blood-testes barrier is leaky and has been linked to a hyperactivated pathway involving apelin (K. Song et al., 2022). The gene encoding for Hsp27 was also downregulated in our study. Overexpression of this gene was found to have a protective effect on the BBB in models of ischemia (Leak et al., 2013; Y. Shi et al.,

2017) and during hypoxia (Halder et al., 2025). Interestingly, *CLEC14A* was found to be downregulated. One study found that knockout of *Clec14a* in otherwise healthy mice resulted in a decrease in BBB integrity, without any effect on the levels of claudin-5, occludin, or ZO-1 (Y. Kim et al., 2020).

CLEC14A has been identified as a promotor of endothelial cell migration and angiogenesis (Ki et al., 2013; Noy et al., 2016) and its overexpression was found to attenuate cell migration in a recent study (C. Su et al., 2019). Endothelial cells can acquire migratory properties in a process known as endothelial to mesenchymal transition (EndoMT), during which endothelial cells dedifferentiate into mesenchymal stem cells (Zeisberg et al., 2007; J. Zhuang et al., 2023). The integrity of the BBB is known to be disrupted during EndoMT (Derada Troletti et al., 2019; Y. Luo et al., 2022). Other DEGs identified in our study were also found to play roles in cell migration. *EHD2* was found to be downregulated in our study, which has been associated with migration in cancer (X. Yang et al., 2015; Guan et al., 2021). Similarly, *LMNA* depletion was found to increase cell mobility in fibroblasts (Corne et al., 2017). *LMNA* has been found to negatively regulate the expression of epithelial-mesenchymal transition (EMT) in cancer (C. Hu et al., 2022). The downregulation of *LAMP1* was found to also induce EMT in endometrial epithelial cells (Z. Zhou et al., 2022). Increased expression of *LAMP1* inhibited migration of renal cell carcinoma cells (X. Wang et al., 2024). Additionally, *LAMP1* has been found to affect the adhesion of cells to the ExM and basement membrane (Sawada et al., 1993; Z. Zhou et al., 2022). Other DEGs that have been found to affect cell adhesion were also identified in our study. Two genes that encode for ExM proteins were found to be downregulated, *SNED1* and *COL5A1*. *SNED1* was recently identified to mediate cell adhesion by interacting with integrins (Pally et al., 2025). Zebrafish *col5a1* mutants show spontaneous haemorrhage, showing that *COL5A1* plays a role in stabilizing blood vessels (Rajan et al., 2020).

In addition, GO analysis identified the protein localisation to the cell periphery pathway as significantly altered in HBMvECs after treatment with EV_{INF}. Interestingly, the pro-inflammatory cytokine CCL2 has been shown to cause the internalisation of TJ proteins from the cell border (Stamatovic et al., 2005; Dimitrijevic et al., 2006; Y. Yao & Tsirka, 2011; X. D. Mao et al., 2023). This was

found to occur through the activation of protein kinase C (PKC) (Stamatovic et al., 2006), which negatively regulates *DGKZ* (B. Luo et al., 2003; Ard et al., 2021). Additionally, Tang et al., (2023) found that TIMP1 was able to rescue the mislocalisation of junctional complexes in hypoxic mice. While *CCL2* was upregulated in our study, both *DGKZ* and *TIMP1* were downregulated, suggesting that the increased permeability of HBMvECs seen after EV_{INF} treatment may be a result of mislocalisation of the TJ proteins.

The adherens junctions (AJs) also play a role in barrier stability (Steiner et al., 2014; Kruse et al., 2019; Z. Zhang et al., 2024). Several DEGs affecting the stability of VE-cadherin, a major component of AJs were also identified. *TIMP1* is known to stabilise the localisation of VE-cadherin at the junction (Akahane et al., 2004; Tang et al., 2023). *TIMP1* was downregulated in our study, as was *NTSR1*, whose ligand, neurotensin, has been found to decrease permeability in monkey ovarian microvascular endothelial cells (mOMECs) via adherens junctions (Pearson et al., 2024). By contrast, *ITGAV*, which encodes the αv subunit, was found to be upregulated, activation of the integrin αvβ3 having previously been found to also disrupt the localisation of endothelial VE-cadherin (Alghisi et al., 2009; Nader & Kerrigan, 2022)**.** This suggests that EV_{INF} could influence the stability of VE-cadherin at the membrane and thus induce permeabilisation.

In conclusion, EV_{INF} may negatively affect the permeability of HBMvECs through several gene regulatory pathways – including upregulating cell migration and affecting cell adhesion by activating the EndoMT pathway. Similarly, the stability of the adherens junctions may also influence BBB integrity. Additionally, although TJ gene or protein expression were not affected by treatment with EV_{INF}, these proteins may have undergone posttranslational modification by phosphorylation to induce their relocalisation away from the HBMvEC peripheral space, which would increase permeability (Yamamoto et al., 2008; Murakami et al., 2012; K. Wang, Qu, et al., 2025). Further studies will be required in order to determine the true underlying cause of permeabilisation after EV_{INF} treatment.

Chapter 7 :

Overall Discussion and Future Directions

7.1 Overall Summary

The relationship between astrocytes and the BBB, along with other members of the NVU has been well documented (Abbott et al., 2006; Heithoff et al., 2021). Astrocytes are well known to aid in the formation and maintenance of the BBB (Araya et al., 2008; Zamproni et al., 2025). However, during neuroinflammation, astrocytes contribute to the breakdown of the barrier (H. Kim et al., 2022). EVs are well-known mediators of cell-cell communication (Valadi et al., 2007; Balusu et al., 2016). However, the role they play in the communication between astrocytes and the endothelial cells that line the microcerebral blood vessels and the maintenance of the barrier has been under researched. This thesis aimed to identify how the secretome of astrocytes affect the BBB both in health and during neuroinflammation.

This thesis has shown that the secretome of astrocytes is beneficial to endothelial cells (chapter 3 and 5). The complete astrocyte secretome was found to have protective effects on HBMvEC viability (chapter 3) and EVs isolated from healthy astrocytes was found to improve HBMvEC barrier integrity (chapter 5). Although the effects of astrocyte-derived EVs on endothelial cells are understudied, the astrocyte secretome has been known to decrease BBB permeability (Arthur et al., 1987; Barar et al., 2010; Baumann et al., 2021). EVs from other cell types have also been shown to improve barrier function (Brodeur et al., 2023; Hosseinkhani et al., 2023).

Although EVs isolated from healthy astrocytes were beneficial, EVs isolated from inflamed astrocytes increased barrier permeability and inflamed endothelial cells (Chapter 5 and 6). EVs from inflamed astrocytes have been shown to contribute to inflammation in other cells (G. Hu et al., 2018; Ibáñez et al., 2019; K. Liao et al., 2022). However, until now, the role they play in the loss of barrier integrity remained unclear. BBB breakdown is a hallmark of neuroinflammation (C.-Y. Chen et al., 2020; L. Zhang et al., 2022). Activated astrocytes have been known to cause BBB through increased expression of pro-inflammatory cytokines and other molecules (Dimitrijevic et al., 2006; F. Guo et al., 2020; H. Kim et al., 2022). However, EVs have now been implicated in the decrease of barrier integrity. This

is of particular importance considering that EVs are regarded as long-distance mediators of communication (C. Bang & Thum, 2012; Y. Feng et al., 2021). This could suggest that astrocyte EVs could contribute to a globalised inflammatory effect in the CNS.

7.2 Future Directions

This thesis has shown that astrocyte-derived EVs play a role in modulating the barrier but not through any effect on the expression levels of the TJs. Therefore, exploring the mechanism(s) behind the changes to BBB integrity are of great importance. Transcriptomic analysis of endothelial cells treated with EV_{INF} have shown several potential pathways affected by EV treatment (Chapter 6). These include the mislocalisation of TJs, potentially due to post-translational changes in addition to changes to cell adhesion and migration. Although the expression levels of TJ proteins were explored, post-translational modifications of these TJs were not. Post-translational modifications of TJ proteins have been shown to affect barrier integrity (Yamamoto et al., 2008; Murakami et al., 2012; K. Wang, Qu, et al., 2025). Additionally, during EndoMT, cell adhesion and migration changes, thus disrupting the barrier (Derada Troletti et al., 2019; Y. Luo et al., 2022). Therefore, exploring whether post-translational modifications are affected or whether the cells begin to undergo EndoMT could reveal more about the breakdown of the blood-brain barrier during neuroinflammation.

The main aim of this thesis was to explore the paracellular barrier function of endothelial cells after treatment with astrocyte-derived EVs. As such, permeability assays were the main functional assay used, specifically using a medium weight fluorescent tracer. However, as mentioned in chapter 3, the use of fluorescent tracers of other weights and TEER could have provided a better understanding of the impact these EVs have on the barrier integrity of endothelial cells. Additionally, immunocytochemical analysis of TJ proteins could have provided insight into the localisation of these proteins and could have provided an explanation into the changes in barrier integrity seen. Nevertheless, the physical yield of EVs from astrocytes was insufficient to conduct more assays, which was a key limitation of this thesis.

With a higher yield of EVs, it would have been possible to conduct additional functional assays to gain a more thorough understanding of the effect astrocyte-derived EVs in endothelial cells, beyond studying barrier integrity. As indicated by the transcriptomic study in Chapter 6, exploring the angiogenic properties of these cells after EV treatment through cell migration studies (e.g. scratch wound assay) and/or proliferation assays would have revealed whether astrocyte-derived EVs control this aspect of endothelial cells in either health or disease. Additionally, several endothelial inflammatory genes were upregulated after treatment with EVs isolated from inflamed astrocytes (Chapter 6). Therefore, exploring a key component of the endothelial inflammatory response through a leukocyte adhesion assay would confirm the propagation of inflammation through EV-mediated communication.

Although EVs are now known to play a role in BBB integrity, their contents remain a mystery. Although miRNAs found in EVs have been shown to play roles in the CNS, both in health and during disease pathogenesis (C.-Y. Chen et al., 2020; M.-L. Chen et al., 2021; K. Liao et al., 2022), our samples were not found to contain any meaningful populations. However, several longer small RNAs were found. Sequencing these could potentially provide information as to the mechanism behind the changes seen in BBB integrity. However, in addition to their transcriptome, EVs are known to carry proteins and other signalling molecules (Jeppesen et al., 2019; Abdelmohsen et al., 2023). Proteomic and lipidomic analysis of EV cargo would reveal the changes that occur during neuroinflammation but may also reveal the potential mechanisms by which the transcriptome of HBMvECs change after EV treatment.

Additionally, transcriptomic analysis of endothelial cells treated with EV_H was unsuccessful. Therefore, potential mechanisms behind the decrease in BBB permeability remain unknown. Repetition of this experiment could provide these answers. Several pathways linked to protein translation were upregulated after EV_{INF} treatment in Chapter 6. Whether this is a result of inflammation or related to treatment with EVs in general could be elucidated by this.

One potential limitation of this study was the use of FBS, due to both potential contamination of serum-derived vesicles in the isolation of astrocyte-derived EVs

as well as the potential activation of the "healthy" astrocyte cohort (Prah et al., 2019; White et al., 2024). While the first was managed with the use of unconditioned media as a control, more studies could have been conducted in order to confirm the health status of the astrocytes used to condition media. The media that was used was recommended by the company that provided the astrocytes. Additionally, the use of serum-containing media is not uncommon in similar studies focusing on reactive astrocytes (Li et al., 2022; Cameron et al., 2024). However, a non-serum containing media could have been used in order to avoid this issue, such as one supplemented with fibroblast growth factor 2 and epidermal growth factor which has been shown to maintain quiescent astrocytes *in vitro* (Prah et al., 2019).

In addition, had resources and time not been a limiting factor, several aspects of this study could have been improved. Firstly, while the use of DLS to measure EV size is not uncommon, the gold standard in the field is the use of nanoparticle tracking analysis (NTA), which allows for a more accurate measurement of EV size and concentration (Comfort et al., 2021; Y. Han et al., 2026). Although this had been explored, the machinery was unavailable due to its cost. However, this would have provided a much more accurate reading of the isolated particles and would have also allowed us to quantify particle concentration, which would have allowed for more accurate treatments. Secondly, using a 2D static transwell model of the BBB allowed for a preliminary exploration into the effect of astrocyte-derived EVs on endothelial cells. However, the BBB is influenced by shear stress introduced by blood flow (DeOre et al., 2022; Yates et al., 2025). Therefore, introducing shear stress into this static model would have reflected the *in vivo* environment more accurately and may have influenced results.

Another aspect that could have been explored was the uptake of EVs by endothelial cells and the potential receptors involved. Results from chapter 5 show that EVs affected barrier integrity in an orientation-dependent manner. This suggests that EVs are taken up via interactions with receptors found on the abluminal side of endothelial cells. An investigation into the particular receptor-ligand interaction could provide further insight into the EV-mediated communication between endothelial cells and astrocytes. In addition, this study could have been expanded to include a model of A2 astrocytes in order to explore how neuroprotective

astrocytes affect the integrity of the BBB and how the cargo of EVs released by these cells is affected by their state of reactivity.

Additionally, although an attempt had been made to identify changes in the cargo through transcriptomic analysis, this was unsuccessful prior to the completion of the thesis. Prioritising transcriptomic analysis earlier, in addition to proteomic and lipidomic analyses, would have allowed for a multi-omic characterisation of EV cargo dynamics during neuroinflammation. Although the changes in cargo identified through these approaches alongside their downstream effects would require substantial experimental validation, this would have revealed novel molecular targets. These insights could then inform the development of targeted EV therapeutics designed to attenuate neuroinflammation and enhance endothelial cell barrier integrity.

In summary, this thesis has shown that the astrocyte secretome plays a beneficial role in the biological properties of endothelial cells, at least in part due to astrocyte-derived EVs. The effects EVs play in endothelial cells depends greatly on the state of the donor cell. During neuroinflammation, astrocyte EVs contribute to the spread of inflammation by potentially upregulating pro-inflammatory genes and resulting in loss of BBB integrity.

Bibliography

Abbott, N. J., Rönnbäck, L., & Hansson, E. (2006). Astrocyte–endothelial interactions at the blood–brain barrier. Nature Reviews Neuroscience, 7(1), 41–53. https://doi.org/10.1038/nrn1824

Abdelmohsen, K., Herman, A. B., Carr, A. E., Henry-Smith, C. A., Rossi, M., Meng, Q., Yang, J., Tsitsipatis, D., Bangura, A., Munk, R., Martindale, J. L., Nogueras-Ortiz, C. J., Hao, J., Gong, Y., Liu, Y., Cui, C., Hartnell, L. M., Price, N. L., Ferrucci, L., … Gorospe, M. (2023). Survey of organ-derived small extracellular vesicles and particles (sEVPs) to identify selective protein markers in mouse serum. Journal of Extracellular Biology, 2(8), e106. https://doi.org/10.1002/jex2.106

Aborode, A. T., Adesola, R. O., Scott, G. Y., Adepoju, V. A., Akan, O. D., Ogunyemi, A., Adetunji, A. P.-G., Arogundade, F. Q., Somuah, D. K., Emmanuel, A. O., Ameh, B., Oluwaseun, I. S., Osu, A. I., Jonathan, V. C., Amadi, C. S., Oladayo, M. V., Matthew, A. F., Onifade, I. A., Fakorede, S., & Bakre, A. A. (2025). Role of Blood-Brain barrier in bacterial translocation. Neuroscience, 580, 99–114. https://doi.org/10.1016/j.neuroscience.2025.06.037

Adams, A. (1973). Concentration of Epstein-Barr Virus from Cell Culture Fluids with Polyethylene Glycol. Journal of General Virology, 20(3), 391–394. https://doi.org/10.1099/0022-1317-20-3-391

Ageberg, M., & Lindmark, A. (2003). Characterisation of the biosynthesis and processing of the neutrophil granule membrane protein CD63 in myeloid cells. Clinical & Laboratory Haematology, 25(5), 297–306. https://doi.org/10.1046/j.1365-2257.2003.00541.x

Ahmadian, S., Jafari, N., Tamadon, A., Ghaffarzadeh, A., Rahbarghazi, R., & Mahdipour, M. (2024). Different storage and freezing protocols for extracellular vesicles: A systematic review. Stem Cell Research & Therapy, 15(1), 453. https://doi.org/10.1186/s13287-024-04005-7

Akahane, T., Akahane, M., Shah, A., Connor, C. M., & Thorgeirsson, U. P. (2004). TIMP-1 inhibits microvascular endothelial cell migration by MMP-dependent and MMP-independent mechanisms. Experimental Cell Research, 301(2), 158–167. https://doi.org/10.1016/j.yexcr.2004.08.002

Akama, T. O., Nakagawa, H., Wong, N. K., Sutton-Smith, M., Dell, A., Morris, H. R., Nakayama, J., Nishimura, S.-I., Pai, A., Moremen, K. W., Marth, J. D., & Fukuda, M. N. (2006). Essential and mutually compensatory roles of α-mannosidase II and α-mannosidase IIx in N -glycan processing in vivo in mice. Proceedings of the National Academy of Sciences, 103(24), 8983–8988. https://doi.org/10.1073/pnas.0603248103

Akin-Kinay, F., Uzun, N., Kılınç, İ., & Kılıç, A. O. (2025). Tight Junction Proteins and Blood-brain Barrier Integrity in Pediatric Obsessive-compulsive Disorder: A Study on Claudin-5, Claudin-12, Occludin, Tricellulin, and Angulin-1. Clinical Psychopharmacology and Neuroscience, 23(3), 444–452. https://doi.org/10.9758/cpn.25.1293

Akiyoshi, R., Wake, H., Kato, D., Horiuchi, H., Ono, R., Ikegami, A., Haruwaka, K., Omori, T., Tachibana, Y., Moorhouse, A. J., & Nabekura, J. (2018). Microglia Enhance Synapse Activity to Promote Local Network Synchronization. Eneuro, 5(5), ENEURO.0088-18.2018. https://doi.org/10.1523/ENEURO.0088-18.2018

Albaret, G., Sifré, E., Floch, P., Laye, S., Aubert, A., Dubus, P., Azzi-Martin, L., Giese, A., Salles, N., Mégraud, F., Varon, C., Lehours, P., & Roubaud-Baudron, C. (2020). Alzheimer's Disease and Helicobacter pylori Infection: Inflammation from Stomach to Brain? Journal of Alzheimer's Disease, 73(2), 801–809. https://doi.org/10.3233/JAD-190496

Albers, C. A., Cvejic, A., Favier, R., Bouwmans, E. E., Alessi, M.-C., Bertone, P., Jordan, G., Kettleborough, R. N. W., Kiddle, G., Kostadima, M., Read, R. J., Sipos, B., Sivapalaratnam, S., Smethurst, P. A., Stephens, J., Voss, K., Nurden, A., Rendon, A., Nurden, P., & Ouwehand, W. H. (2011). Exome sequencing identifies NBEAL2 as the causative gene for gray platelet syndrome. Nature Genetics, 43(8), 735–737. https://doi.org/10.1038/ng.885

Alexander, M. R., Rootes, C. L., Van Vuren, P. J., & Stewart, C. R. (2020). Concentration of infectious SARS-CoV-2 by polyethylene glycol precipitation. Journal of Virological Methods, 286, 113977. https://doi.org/10.1016/j.jviromet.2020.113977

Alghisi, G. C., Ponsonnet, L., & Rüegg, C. (2009). The Integrin Antagonist Cilengitide Activates αVβ3, Disrupts VE-Cadherin Localization at Cell Junctions and Enhances Permeability in Endothelial Cells. PLoS ONE, 4(2), e4449. https://doi.org/10.1371/journal.pone.0004449

Alkayed, N. J., & Cipolla, M. J. (2023). The Ever-Evolving Concept of the Neurovascular Unit. Stroke, 54(8), 2178–2180. https://doi.org/10.1161/STROKEAHA.123.042705

Allahyari, R. V., Clark, K. L., Shepard, K. A., & Garcia, A. D. R. (2019). Sonic hedgehog signaling is negatively regulated in reactive astrocytes after forebrain stab injury. Scientific Reports, 9(1), 565. https://doi.org/10.1038/s41598-018-37555-x

Allen, N. J., & Eroglu, C. (2017). Cell Biology of Astrocyte-Synapse Interactions. Neuron, 96(3), 697–708. https://doi.org/10.1016/j.neuron.2017.09.056

Allgäuer, L., Cabungcal, J.-H., Yzydorczyk, C., Do, K. Q., & Dwir, D. (2023). Low protein-induced intrauterine growth restriction as a risk factor for schizophrenia phenotype in a rat model: Assessing the role of oxidative stress and neuroinflammation interaction. Translational Psychiatry, 13(1), 30. https://doi.org/10.1038/s41398-023-02322-8

Al-Nedawi, K., Meehan, B., Micallef, J., Lhotak, V., May, L., Guha, A., & Rak, J. (2008). Intercellular transfer of the oncogenic receptor EGFRvIII by microvesicles derived from tumour cells. Nature Cell Biology, 10(5), 619–624. https://doi.org/10.1038/ncb1725

Altunay, Z. M., Biswas, J., Cheung, H. W., Pijewski, R. S., Papile, L. E., Akinlaja, Y. O., Tang, A., Kresic, L. C., Schouw, A. D., Ugrak, M. V., Caro, K., Peña Palomino, P. A., Ressl, S., Nishiyama, A., Crocker, S. J., & Martinelli, D. C. (2025). C1ql1 expression in oligodendrocyte progenitor cells promotes oligodendrocyte differentiation. The FEBS Journal, 292(1), 52–74. https://doi.org/10.1111/febs.17256

Alvarez, J. I., Dodelet-Devillers, A., Kebir, H., Ifergan, I., Fabre, P. J., Terouz, S., Sabbagh, M., Wosik, K., Bourbonnière, L., Bernard, M., Van Horssen, J., De Vries, H. E., Charron, F., & Prat, A. (2011). The Hedgehog Pathway Promotes Blood-Brain Barrier Integrity and CNS Immune Quiescence. Science, 334(6063), 1727–1731. https://doi.org/10.1126/science.1206936

Alves, N. G., Yuan, S. Y., & Breslin, J. W. (2019). Sphingosine-1-phosphate protects against brain microvascular endothelial junctional protein disorganization and barrier dysfunction caused by alcohol. Microcirculation, 26(1), e12506. https://doi.org/10.1111/micc.12506

Anderson, H. C. (1969). VESICLES ASSOCIATED WITH CALCIFICATION IN THE MATRIX OF EPIPHYSEAL CARTILAGE. The Journal of Cell Biology, 41(1), 59–72. https://doi.org/10.1083/jcb.41.1.59

Andrews, S. J., Fulton-Howard, B., O'Reilly, P., Marcora, E., Goate, A. M., & collaborators of the Alzheimer's Disease Genetics Consortium. (2021). Causal Associations Between Modifiable Risk Factors and the Alzheimer's Phenome. Annals of Neurology, 89(1), 54–65. https://doi.org/10.1002/ana.25918

Andriezen, W. L. (1893). The Neuroglia Elements in the Human Brain. BMJ, 2(1700), 227–230. https://doi.org/10.1136/bmj.2.1700.227

Arai, K., & Lo, E. H. (2009). An Oligovascular Niche: Cerebral Endothelial Cells Promote the Survival and Proliferation of Oligodendrocyte Precursor Cells. The Journal of Neuroscience, 29(14), 4351–4355. https://doi.org/10.1523/JNEUROSCI.0035-09.2009

Araya, R., Kudo, M., Kawano, M., Ishii, K., Hashikawa, T., Iwasato, T., Itohara, S., Terasaki, T., Oohira, A., Mishina, Y., & Yamada, M. (2008). BMP signaling through BMPRIA in astrocytes is essential for proper cerebral angiogenesis and formation of the blood–brain-barrier. Molecular and Cellular Neuroscience, 38(3), 417–430. https://doi.org/10.1016/j.mcn.2008.04.003

Ard, R., Maillet, J.-C., Daher, E., Phan, M., Zinoviev, R., Parks, R. J., & Gee, S. H. (2021). PKCα-mediated phosphorylation of the diacylglycerol kinase ζ MARCKS domain switches cell migration modes by regulating interactions with Rac1 and RhoA. Journal of Biological Chemistry, 296, 100516. https://doi.org/10.1016/j.jbc.2021.100516

Argaw, A. T., Asp, L., Zhang, J., Navrazhina, K., Pham, T., Mariani, J. N., Mahase, S., Dutta, D. J., Seto, J., Kramer, E. G., Ferrara, N., Sofroniew, M. V., & John, G. R. (2012). Astrocyte-derived VEGF-A drives blood-brain barrier disruption in CNS inflammatory disease. Journal of Clinical Investigation, 122(7), 2454–2468. https://doi.org/10.1172/JCI60842

Armulik, A., Genové, G., Mäe, M., Nisancioglu, M. H., Wallgard, E., Niaudet, C., He, L., Norlin, J., Lindblom, P., Strittmatter, K., Johansson, B. R., & Betsholtz, C. (2010). Pericytes regulate the blood–brain barrier. Nature, 468(7323), 557–561. https://doi.org/10.1038/nature09522

Arthur, F. E., Shivers, R. R., & Bowman, P. D. (1987). Astrocyte-mediated induction of tight junctions in brain capillary endothelium: An efficient in vitro model. Developmental Brain Research, 36(1), 155–159. https://doi.org/10.1016/0165-3806(87)90075-7

Arukuusk, P., Pärnaste, L., Margus, H., Eriksson, N. K. J., Vasconcelos, L., Padari, K., Pooga, M., & Langel, Ü. (2013). Differential Endosomal Pathways for Radically Modified Peptide Vectors. Bioconjugate Chemistry, 24(10), 1721–1732. https://doi.org/10.1021/bc4002757

Assou, S., Ahmed, E., Morichon, L., Nasri, A., Foisset, F., Bourdais, C., Gros, N., Tieo, S., Petit, A., Vachier, I., Muriaux, D., Bourdin, A., & De Vos, J. (2023). The Transcriptome

Landscape of the In Vitro Human Airway Epithelium Response to SARS-CoV-2. International Journal of Molecular Sciences, 24(15), 12017. https://doi.org/10.3390/ijms241512017

Atkin-Smith, G. K., Tixeira, R., Paone, S., Mathivanan, S., Collins, C., Liem, M., Goodall, K. J., Ravichandran, K. S., Hulett, M. D., & Poon, I. K. H. (2015). A novel mechanism of generating extracellular vesicles during apoptosis via a beads-on-a-string membrane structure. Nature Communications, 6(1), 7439. https://doi.org/10.1038/ncomms8439

Attwell, D., & Laughlin, S. B. (2001). An Energy Budget for Signaling in the Grey Matter of the Brain. Journal of Cerebral Blood Flow & Metabolism, 21(10), 1133–1145. https://doi.org/10.1097/00004647-200110000-00001

Azad, K., Guilligay, D., Boscheron, C., Maity, S., De Franceschi, N., Sulbaran, G., Effantin, G., Wang, H., Kleman, J.-P., Bassereau, P., Schoehn, G., Roos, W. H., Desfosses, A., & Weissenhorn, W. (2023). Structural basis of CHMP2A–CHMP3 ESCRT-III polymer assembly and membrane cleavage. Nature Structural & Molecular Biology, 30(1), 81–90. https://doi.org/10.1038/s41594-022-00867-8

Azevedo, F. A. C., Carvalho, L. R. B., Grinberg, L. T., Farfel, J. M., Ferretti, R. E. L., Leite, R. E. P., Filho, W. J., Lent, R., & Herculano-Houzel, S. (2009). Equal numbers of neuronal and nonneuronal cells make the human brain an isometrically scaled-up primate brain. Journal of Comparative Neurology, 513(5), 532–541. https://doi.org/10.1002/cne.21974

Aziz, M. A., Seo, B., Hussaini, H. M., Hibma, M., & Rich, A. M. (2022). Comparing Two Methods for the Isolation of Exosomes. Journal of Nucleic Acids, 2022, 8648373. https://doi.org/10.1155/2022/8648373

Baazm, M., Behrens, V., Beyer, C., Nikoubashman, O., & Zendedel, A. (2021). Regulation of Inflammasomes by Application of Omega-3 Polyunsaturated Fatty Acids in a Spinal Cord Injury Model. Cells, 10(11), 3147. https://doi.org/10.3390/cells10113147

Badellino, K. O., Wolfe, M. L., Reilly, M. P., & Rader, D. J. (2008). Endothelial Lipase Is Increased In Vivo by Inflammation in Humans. Circulation, 117(5), 678–685. https://doi.org/10.1161/CIRCULATIONAHA.107.707349

Badimon, A., Strasburger, H. J., Ayata, P., Chen, X., Nair, A., Ikegami, A., Hwang, P., Chan, A. T., Graves, S. M., Uweru, J. O., Ledderose, C., Kutlu, M. G., Wheeler, M. A., Kahan, A., Ishikawa, M., Wang, Y.-C., Loh, Y.-H. E., Jiang, J. X., Surmeier, D. J., … Schaefer, A. (2020). Negative feedback control of neuronal activity by microglia. Nature, 586(7829), 417–423. https://doi.org/10.1038/s41586-020-2777-8

Baeuerle, P. A., & Baltimore, D. (1988). IκB: A Specific Inhibitor of the NF-κB Transcription Factor. Science, 242(4878), 540–546. https://doi.org/10.1126/science.3140380

Baik, S. H., Kang, S., Lee, W., Choi, H., Chung, S., Kim, J.-I., & Mook-Jung, I. (2019). A Breakdown in Metabolic Reprogramming Causes Microglia Dysfunction in Alzheimer's Disease. Cell Metabolism, 30(3), 493-507.e6. https://doi.org/10.1016/j.cmet.2019.06.005

Baldwin, K. T., Murai, K. K., & Khakh, B. S. (2024). Astrocyte morphology. Trends in Cell Biology, 34(7), 547–565. https://doi.org/10.1016/j.tcb.2023.09.006

Balla, B., Kósa, J. P., Kiss, J., Podani, J., Takács, I., Lazáry, Á., Nagy, Z., Bácsi, K., Speer, G., & Lakatos, P. (2009). Transcriptional profiling of immune system-related genes in postmenopausal osteoporotic versus non-osteoporotic human bone tissue. Clinical Immunology, 131(2), 354–359. https://doi.org/10.1016/j.clim.2009.01.004

Balusu, S., Van Wonterghem, E., De Rycke, R., Raemdonck, K., Stremersch, S., Gevaert, K., Brkic, M., Demeestere, D., Vanhooren, V., Hendrix, A., Libert, C., & Vandenbroucke, R. E. (2016). Identification of a novel mechanism of blood–brain communication during peripheral inflammation via choroid plexus-derived extracellular vesicles. EMBO Molecular Medicine, 8(10), 1162–1183. https://doi.org/10.15252/emmm.201606271

Banack, S. A., Dunlop, R. A., Stommel, E. W., Mehta, P., & Cox, P. A. (2022). miRNA extracted from extracellular vesicles is a robust biomarker of amyotrophic lateral sclerosis. Journal of the Neurological Sciences, 442, 120396. https://doi.org/10.1016/j.jns.2022.120396

Bang, C., & Thum, T. (2012). Exosomes: New players in cell–cell communication. The International Journal of Biochemistry & Cell Biology, 44(11), 2060–2064. https://doi.org/10.1016/j.biocel.2012.08.007

Bang, M., Gonzales, E. L., Shin, C. Y., & Kwon, K. J. (2021). Late Passage Cultivation Induces Aged Astrocyte Phenotypes in Rat Primary Cultured Cells. Biomolecules & Therapeutics, 29(2), 144–153. https://doi.org/10.4062/biomolther.2020.175

Bar, M., Schuster, S., Leibman, M., Ezer, R., & Avni, A. (2014). The function of EHD2 in endocytosis and defense signaling is affected by SUMO. Plant Molecular Biology, 84(4–5), 509–518. https://doi.org/10.1007/s11103-013-0148-7

Barar, J., Gumbleton, M., Asadi, M., & Omidi, Y. (2010). Barrier functionality and transport machineries of human ECV304 cells. Medical Science Monitor: International Medical Journal of Experimental and Clinical Research, 16(1), BR52-60.

Barberio, C., Withers, A., Mishra, Y., Couraud, P.-O., Romero, I. A., Weksler, B., & Owens, R. M. (2022). A human-derived neurovascular unit in vitro model to study the effects of cellular cross-talk and soluble factors on barrier integrity. Frontiers in Cellular Neuroscience, 16, 1065193. https://doi.org/10.3389/fncel.2022.1065193

Barqué, A., Jan, K., De La Fuente, E., Nicholas, C. L., Hynes, R. O., & Naba, A. (2021). Knockout of the gene encoding the extracellular matrix protein SNED1 results in early neonatal lethality and craniofacial malformations. Developmental Dynamics, 250(2), 274–294. https://doi.org/10.1002/dvdy.258

Bartholomäus, I., Kawakami, N., Odoardi, F., Schläger, C., Miljkovic, D., Ellwart, J. W., Klinkert, W. E. F., Flügel-Koch, C., Issekutz, T. B., Wekerle, H., & Flügel, A. (2009). Effector T cell interactions with meningeal vascular structures in nascent autoimmune CNS lesions. Nature, 462(7269), 94–98. https://doi.org/10.1038/nature08478

Batagov, A. O., & Kurochkin, I. V. (2013). Exosomes secreted by human cells transport largely mRNA fragments that are enriched in the 3′-untranslated regions. Biology Direct, 8(1), 12. https://doi.org/10.1186/1745-6150-8-12

Batchelor, P. E., Liberatore, G. T., Wong, J. Y. F., Porritt, M. J., Frerichs, F., Donnan, G. A., & Howells, D. W. (1999). Activated Macrophages and Microglia Induce Dopaminergic Sprouting in the Injured Striatum and Express Brain-Derived Neurotrophic Factor and Glial

Cell Line-Derived Neurotrophic Factor. The Journal of Neuroscience, 19(5), 1708–1716. https://doi.org/10.1523/JNEUROSCI.19-05-01708.1999

Baumann, J., Tsao, C.-C., Huang, S.-F., Gassmann, M., & Ogunshola, O. O. (2021). Astrocyte-specific hypoxia-inducible factor 1 (HIF-1) does not disrupt the endothelial barrier during hypoxia in vitro. Fluids and Barriers of the CNS, 18(1), 13. https://doi.org/10.1186/s12987-021-00247-2

Bazzoni, G., Martínez-Estrada, O. M., Orsenigo, F., Cordenonsi, M., Citi, S., & Dejana, E. (2000). Interaction of Junctional Adhesion Molecule with the Tight Junction Components ZO-1, Cingulin, and Occludin*. Journal of Biological Chemistry, 275(27), 20520–20526. https://doi.org/10.1074/jbc.M905251199

Beard, E., Lengacher, S., Dias, S., & Finsterwald, C. (2022). Astrocytes as Key Regulators of Brain Energy Metabolism: New Therapeutic Perspectives. Frontiers in Physiology, 12. https://doi.org/10.3389/fphys.2021.825816

Beiter, R. M., Rivet-Noor, C., Merchak, A. R., Bai, R., Johanson, D. M., Slogar, E., Sol-Church, K., Overall, C. C., & Gaultier, A. (2022). Evidence for oligodendrocyte progenitor cell heterogeneity in the adult mouse brain. Scientific Reports, 12(1), 12921. https://doi.org/10.1038/s41598-022-17081-7

Belardi, B., Hamkins-Indik, T., Harris, A. R., Kim, J., Xu, K., & Fletcher, D. A. (2020). A Weak Link with Actin Organizes Tight Junctions to Control Epithelial Permeability. Developmental Cell, 54(6), 792-804.e7. https://doi.org/10.1016/j.devcel.2020.07.022

Bell, B., Anzi, S., Sasson, E., & Ben-Zvi, A. (2023). Unique features of the arterial blood–brain barrier. Fluids and Barriers of the CNS, 20(1), 51. https://doi.org/10.1186/s12987-023-00450-3

Bell, R. D., Winkler, E. A., Sagare, A. P., Singh, I., LaRue, B., Deane, R., & Zlokovic, B. V. (2010). Pericytes Control Key Neurovascular Functions and Neuronal Phenotype in the Adult Brain and during Brain Aging. Neuron, 68(3), 409–427. https://doi.org/10.1016/j.neuron.2010.09.043

Benjamin, S., Weidberg, H., Rapaport, D., Pekar, O., Nudelman, M., Segal, D., Hirschberg, K., Katzav, S., Ehrlich, M., & Horowitz, M. (2011). EHD2 mediates trafficking from the plasma membrane by modulating Rac1 activity. Biochemical Journal, 439(3), 433–445. https://doi.org/10.1042/BJ20111010

Benz, E. W., & Moses, H. L. (1974). Brief Communication: Small, Virus-Like Particles Detected in Bovine Sera by Electron Microscopy2. JNCI: Journal of the National Cancer Institute, 52(6), 1931–1934. https://doi.org/10.1093/jnci/52.6.1931

Bera, M., & Sengupta, K. (2020). Nuclear filaments: Role in chromosomal positioning and gene expression. Nucleus, 11(1), 99–110. https://doi.org/10.1080/19491034.2020.1769445

Berardocco, M., Radeghieri, A., Busatto, S., Gallorini, M., Raggi, C., Gissi, C., D'Agnano, I., Bergese, P., Felsani, A., & Berardi, A. C. (2017). RNA-seq reveals distinctive RNA profiles of small extracellular vesicles from different human liver cancer cell lines. Oncotarget, 8(47), 82920–82939. https://doi.org/10.18632/oncotarget.20503

Berenyi, E. (2026). Primary Cell Isolation from Solid Tissues and Current Understanding for Their Application in Personalized Medicine and Drug Development. In J. Hahne (Ed.), Biochemistry (Vol. 71). IntechOpen. https://doi.org/10.5772/intechopen.1011997

Bergami, M., Santi, S., Formaggio, E., Cagnoli, C., Verderio, C., Blum, R., Berninger, B., Matteoli, M., & Canossa, M. (2008). Uptake and recycling of pro-BDNF for transmitter-induced secretion by cortical astrocytes. The Journal of Cell Biology, 183(2), 213–221. https://doi.org/10.1083/jcb.200806137

Berndt, P., Winkler, L., Cording, J., Breitkreuz-Korff, O., Rex, A., Dithmer, S., Rausch, V., Blasig, R., Richter, M., Sporbert, A., Wolburg, H., Blasig, I. E., & Haseloff, R. F. (2019). Tight junction proteins at the blood–brain barrier: Far more than claudin-5. Cellular and Molecular Life Sciences, 76(10), 1987–2002. https://doi.org/10.1007/s00018-019-03030-7

Bernier, L.-P., Bohlen, C. J., York, E. M., Choi, H. B., Kamyabi, A., Dissing-Olesen, L., Hefendehl, J. K., Collins, H. Y., Stevens, B., Barres, B. A., & MacVicar, B. A. (2019). Nanoscale Surveillance of the Brain by Microglia via cAMP-Regulated Filopodia. Cell Reports, 27(10), 2895-2908.e4. https://doi.org/10.1016/j.celrep.2019.05.010

Berthiaume, A.-A., Grant, R. I., McDowell, K. P., Underly, R. G., Hartmann, D. A., Levy, M., Bhat, N. R., & Shih, A. Y. (2018). Dynamic Remodeling of Pericytes In Vivo Maintains Capillary Coverage in the Adult Mouse Brain. Cell Reports, 22(1), 8–16. https://doi.org/10.1016/j.celrep.2017.12.016

Berthiaume, A.-A., Schmid, F., Stamenkovic, S., Coelho-Santos, V., Nielson, C. D., Weber, B., Majesky, M. W., & Shih, A. Y. (2022). Pericyte remodeling is deficient in the aged brain and contributes to impaired capillary flow and structure. Nature Communications, 13(1), 5912. https://doi.org/10.1038/s41467-022-33464-w

Besserer-Offroy, É., Bérubé, P., Côté, J., Murza, A., Longpré, J.-M., Dumaine, R., Lesur, O., Auger-Messier, M., Leduc, R., Marsault, É., & Sarret, P. (2018). The hypotensive effect of activated apelin receptor is correlated with β-arrestin recruitment. Pharmacological Research, 131, 7–16. https://doi.org/10.1016/j.phrs.2018.02.032

Bido, S., Nannoni, M., Muggeo, S., Gambarè, D., Ruffini, G., Bellini, E., Passeri, L., Iaia, S., Luoni, M., Provinciali, M., Giannelli, S. G., Giannese, F., Lazarevic, D., Gregori, S., & Broccoli, V. (2024). Microglia-specific IL-10 gene delivery inhibits neuroinflammation and neurodegeneration in a mouse model of Parkinson's disease. Science Translational Medicine, 16(761), eadm8563. https://doi.org/10.1126/scitranslmed.adm8563

Bisht, K., Okojie, K. A., Sharma, K., Lentferink, D. H., Sun, Y.-Y., Chen, H.-R., Uweru, J. O., Amancherla, S., Calcuttawala, Z., Campos-Salazar, A. B., Corliss, B., Jabbour, L., Benderoth, J., Friestad, B., Mills, W. A., Isakson, B. E., Tremblay, M.-È., Kuan, C.-Y., & Eyo, U. B. (2021). Capillary-associated microglia regulate vascular structure and function through PANX1-P2RY12 coupling in mice. Nature Communications, 12(1), 5289. https://doi.org/10.1038/s41467-021-25590-8

Bitto, N. J., Cheng, L., Johnston, E. L., Pathirana, R., Phan, T. K., Poon, I. K. H., O'Brien-Simpson, N. M., Hill, A. F., Stinear, T. P., & Kaparakis-Liaskos, M. (2021). Staphylococcus aureus membrane vesicles contain immunostimulatory DNA, RNA and peptidoglycan that activate innate immune receptors and induce autophagy. Journal of Extracellular Vesicles, 10(6), e12080. https://doi.org/10.1002/jev2.12080

Bocchi, R., Thorwirth, M., Simon-Ebert, T., Koupourtidou, C., Clavreul, S., Kolf, K., Della Vecchia, P., Bottes, S., Jessberger, S., Zhou, J., Wani, G., Pilz, G.-A., Ninkovic, J., Buffo, A., Sirko, S., Götz, M., & Fischer-Sternjak, J. (2025). Astrocyte heterogeneity reveals

region-specific astrogenesis in the white matter. Nature Neuroscience, 28(3), 457–469. https://doi.org/10.1038/s41593-025-01878-6

Boncler, M., Różalski, M., Krajewska, U., Podsędek, A., & Watala, C. (2014). Comparison of PrestoBlue and MTT assays of cellular viability in the assessment of anti-proliferative effects of plant extracts on human endothelial cells. Journal of Pharmacological and Toxicological Methods, 69(1), 9–16. https://doi.org/10.1016/j.vascn.2013.09.003

Bonello-Palot, N., Simoncini, S., Robert, S., Bourgeois, P., Sabatier, F., Levy, N., Dignat-George, F., & Badens, C. (2014). Prelamin A accumulation in endothelial cells induces premature senescence and functional impairment. Atherosclerosis, 237(1), 45–52. https://doi.org/10.1016/j.atherosclerosis.2014.08.036

Bonfanti, E., Gelosa, P., Fumagalli, M., Dimou, L., Viganò, F., Tremoli, E., Cimino, M., Sironi, L., & Abbracchio, M. P. (2017). The role of oligodendrocyte precursor cells expressing the GPR17 receptor in brain remodeling after stroke. Cell Death & Disease, 8(6), e2871–e2871. https://doi.org/10.1038/cddis.2017.256

Bonifacino, J. S., & Glick, B. S. (2004). The Mechanisms of Vesicle Budding and Fusion. Cell, 116(2), 153–166. https://doi.org/10.1016/S0092-8674(03)01079-1

Bonney, S., Dennison, B. J. C., Wendlandt, M., & Siegenthaler, J. A. (2018). Retinoic Acid Regulates Endothelial β-catenin Expression and Pericyte Numbers in the Developing Brain Vasculature. Frontiers in Cellular Neuroscience, 12, 476. https://doi.org/10.3389/fncel.2018.00476

Bonsergent, E., Grisard, E., Buchrieser, J., Schwartz, O., Théry, C., & Lavieu, G. (2021). Quantitative characterization of extracellular vesicle uptake and content delivery within mammalian cells. Nature Communications, 12(1), 1864. https://doi.org/10.1038/s41467-021-22126-y

Bonsergent, E., & Lavieu, G. (2019). Content release of extracellular vesicles in a cell-free extract. FEBS Letters, 593(15), 1983–1992. https://doi.org/10.1002/1873-3468.13472

Bowman, G. L., Dayon, L., Kirkland, R., Wojcik, J., Peyratout, G., Severin, I. C., Henry, H., Oikonomidi, A., Migliavacca, E., Bacher, M., & Popp, J. (2018). Blood-brain barrier breakdown, neuroinflammation, and cognitive decline in older adults. Alzheimer's & Dementia, 14(12), 1640–1650. https://doi.org/10.1016/j.jalz.2018.06.2857

Bowman, P. D., Ennis, S. R., Rarey, K. E., Lorris Betz, A., & Goldstein, G. W. (1983). Brain microvessel endothelial cells in tissue culture: A model for study of blood-brain barrier permeability. Annals of Neurology, 14(4), 396–402. https://doi.org/10.1002/ana.410140403

Bozack, A. K., Colicino, E., Rodosthenous, R. S., Bloomquist, T. R., Baccarelli, A. A., Wright, R. O., Wright, R. J., & Lee, A. G. (2022). Breast Milk-Derived Extracellular Vesicle Mirnas are Associated with Maternal Asthma and Atopy. Epigenomics, 14(12), 727–739. https://doi.org/10.2217/epi-2022-0090

Branca, J. J. V., Maresca, M., Morucci, G., Mello, T., Becatti, M., Pazzagli, L., Colzi, I., Gonnelli, C., Carrino, D., Paternostro, F., Nicoletti, C., Ghelardini, C., Gulisano, M., Di Cesare Mannelli, L., & Pacini, A. (2019). Effects of Cadmium on ZO-1 Tight Junction Integrity of the Blood Brain Barrier. International Journal of Molecular Sciences, 20(23), 6010. https://doi.org/10.3390/ijms20236010

Brennan, K., Martin, K., FitzGerald, S. P., O'Sullivan, J., Wu, Y., Blanco, A., Richardson, C., & Mc Gee, M. M. (2020). A comparison of methods for the isolation and separation of extracellular vesicles from protein and lipid particles in human serum. Scientific Reports, 10(1), 1039. https://doi.org/10.1038/s41598-020-57497-7

Brodeur, A., Migneault, F., Lanoie, M., Beillevaire, D., Turgeon, J., Karakeussian-Rimbaud, A., Thibodeau, N., Boilard, É., Dieudé, M., & Hébert, M.-J. (2023). Apoptotic exosome-like vesicles transfer specific and functional mRNAs to endothelial cells by phosphatidylserine-dependent macropinocytosis. Cell Death & Disease, 14(7), 449. https://doi.org/10.1038/s41419-023-05991-x

Bu, D., Yu, K., Sun, S., Xie, C., Skogerbo, G., Miao, R., Xiao, H., Liao, Q., Luo, H., Zhao, G., Zhao, H., Liu, Z., Liu, C., Chen, R., & Zhao, Y. (2012). NONCODE v3.0: Integrative annotation of long noncoding RNAs. Nucleic Acids Research, 40(D1), D210–D215. https://doi.org/10.1093/nar/gkr1175

Bujisic, B., Lee, H.-G., Xu, L., Weissbein, U., Rivera, C., Topisirovic, I., & Lee, J. T. (2025). 7SL RNA and signal recognition particle orchestrate a global cellular response to acute thermal stress. Nature Communications, 16(1), 1630. https://doi.org/10.1038/s41467-025-56351-6

Bunet, R., Roy-Cardinal, M.-H., Ramani, H., Cleret-Buhot, A., Durand, M., Chartrand-Lefebvre, C., Routy, J.-P., Thomas, R., Trottier, B., Ancuta, P., Hanna, D. B., Landay, A. L., Cloutier, G., Tremblay, C. L., & El-Far, M. (2023). Differential Impact of IL-32 Isoforms on the Functions of Coronary Artery Endothelial Cells: A Potential Link with Arterial Stiffness and Atherosclerosis. Viruses, 15(3), 700. https://doi.org/10.3390/v15030700

Buniello, A., MacArthur, J. A. L., Cerezo, M., Harris, L. W., Hayhurst, J., Malangone, C., McMahon, A., Morales, J., Mountjoy, E., Sollis, E., Suveges, D., Vrousgou, O., Whetzel, P. L., Amode, R., Guillen, J. A., Riat, H. S., Trevanion, S. J., Hall, P., Junkins, H., … Parkinson, H. (2019). The NHGRI-EBI GWAS Catalog of published genome-wide association studies, targeted arrays and summary statistics 2019. Nucleic Acids Research, 47(D1), D1005–D1012. https://doi.org/10.1093/nar/gky1120

Bunting, M., Tang, W., Zimmerman, G. A., McIntyre, T. M., & Prescott, S. M. (1996). Molecular cloning and characterization of a novel human diacylglycerol kinase zeta. The Journal of Biological Chemistry, 271(17), 10230–10236.

Bustin, S. A., Benes, V., Garson, J. A., Hellemans, J., Huggett, J., Kubista, M., Mueller, R., Nolan, T., Pfaffl, M. W., Shipley, G. L., Vandesompele, J., & Wittwer, C. T. (2009). The MIQE Guidelines: Minimum Information for Publication of Quantitative Real-Time PCR Experiments. Clinical Chemistry, 55(4), 611–622. https://doi.org/10.1373/clinchem.2008.112797

Bustin, S. A., Ruijter, J. M., Van Den Hoff, M. J. B., Kubista, M., Pfaffl, M. W., Shipley, G. L., Tran, N., Rödiger, S., Untergasser, A., Mueller, R., Nolan, T., Milavec, M., Burns, M. J., Huggett, J. F., Vandesompele, J., & Wittwer, C. T. (2025). MIQE 2.0: Revision of the Minimum Information for Publication of Quantitative Real-Time PCR Experiments Guidelines. Clinical Chemistry, 71(6), 634–651. https://doi.org/10.1093/clinchem/hvaf043

Byeseda, S. E., Burns, A. R., Dieffenbaugher, S., Rumbaut, R. E., Smith, C. W., & Li, Z. (2009). ICAM-1 Is Necessary for Epithelial Recruitment of γδ T Cells and Efficient

Corneal Wound Healing. The American Journal of Pathology, 175(2), 571–579. https://doi.org/10.2353/ajpath.2009.090112

Cahoy, J. D., Emery, B., Kaushal, A., Foo, L. C., Zamanian, J. L., Christopherson, K. S., Xing, Y., Lubischer, J. L., Krieg, P. A., Krupenko, S. A., Thompson, W. J., & Barres, B. A. (2008). A Transcriptome Database for Astrocytes, Neurons, and Oligodendrocytes: A New Resource for Understanding Brain Development and Function. The Journal of Neuroscience, 28(1), 264–278. https://doi.org/10.1523/JNEUROSCI.4178-07.2008

Cai, L., Gong, Q., Qi, L., Xu, T., Suo, Q., Li, X., Wang, W., Jing, Y., Yang, D., Xu, Z., Yuan, F., Tang, Y., Yang, G., Ding, J., Chen, H., & Tian, H. (2022). ACT001 attenuates microglia-mediated neuroinflammation after traumatic brain injury via inhibiting AKT/NFκB/NLRP3 pathway. Cell Communication and Signaling, 20(1), 56. https://doi.org/10.1186/s12964-022-00862-y

Cambier, S., Gouwy, M., & Proost, P. (2023). The chemokines CXCL8 and CXCL12: Molecular and functional properties, role in disease and efforts towards pharmacological intervention. Cellular & Molecular Immunology, 20(3), 217–251. https://doi.org/10.1038/s41423-023-00974-6

Cameron, E. G., Nahmou, M., Toth, A. B., Heo, L., Tanasa, B., Dalal, R., Yan, W., Nallagatla, P., Xia, X., Hay, S., Knasel, C., Stiles, T. L., Douglas, C., Atkins, M., Sun, C., Ashouri, M., Bian, M., Chang, K.-C., Russano, K., … Goldberg, J. L. (2024). A molecular switch for neuroprotective astrocyte reactivity. Nature, 626(7999), 574–582. https://doi.org/10.1038/s41586-023-06935-3

Cantarella, G., Risuglia, N., Dell'eva, R., Lempereur, L., Albini, A., Pennisi, G., Scoto, G. M., Noonan, D. N., & Bernardini, R. (2006). TRAIL inhibits angiogenesis stimulated by VEGF expression in human glioblastoma cells. British Journal of Cancer, 94(10), 1428–1435. https://doi.org/10.1038/sj.bjc.6603092

Castro Dias, M., Coisne, C., Baden, P., Enzmann, G., Garrett, L., Becker, L., Hölter, S. M., Hrabě De Angelis, M., Deutsch, U., Engelhardt, B., & German Mouse Clinic Consortium. (2019). Claudin-12 is not required for blood–brain barrier tight junction function. Fluids and Barriers of the CNS, 16(1), 30. https://doi.org/10.1186/s12987-019-0150-9

Castro Dias, M., Coisne, C., Lazarevic, I., Baden, P., Hata, M., Iwamoto, N., Francisco, D. M. F., Vanlandewijck, M., He, L., Baier, F. A., Stroka, D., Bruggmann, R., Lyck, R., Enzmann, G., Deutsch, U., Betsholtz, C., Furuse, M., Tsukita, S., & Engelhardt, B. (2019). Claudin-3-deficient C57BL/6J mice display intact brain barriers. Scientific Reports, 9(1), 203. https://doi.org/10.1038/s41598-018-36731-3

Castro-Cruz, M., Hyka, L., Daaboul, G., Leblanc, R., Meeussen, S., Lembo, F., Oris, A., Van Herck, L., Granjeaud, S., David, G., & Zimmermann, P. (2023). PDZ scaffolds regulate extracellular vesicle production, composition, and uptake. Proceedings of the National Academy of Sciences, 120(38). https://doi.org/10.1073/pnas.2310914120

Castro-Sánchez, S., Álvarez-Satta, M., Tohamy, M. A., Beltran, S., Derdak, S., & Valverde, D. (2017). Whole exome sequencing as a diagnostic tool for patients with ciliopathy-like phenotypes. PLOS ONE, 12(8), e0183081. https://doi.org/10.1371/journal.pone.0183081

Cauli, B., Tong, X.-K., Rancillac, A., Serluca, N., Lambolez, B., Rossier, J., & Hamel, E. (2004). Cortical GABA Interneurons in Neurovascular Coupling: Relays for Subcortical

Vasoactive Pathways. The Journal of Neuroscience, 24(41), 8940–8949. https://doi.org/10.1523/JNEUROSCI.3065-04.2004

Cecchelli, R., Dehouck, B., Descamps, L., Fenart, L., Buée-Scherrer, V., Duhem, C., Lundquist, S., Rentfel, M., Torpier, G., & Dehouck, M. P. (1999). In vitro model for evaluating drug transport across the blood–brain barrier. Advanced Drug Delivery Reviews, 36(2–3), 165–178. https://doi.org/10.1016/S0169-409X(98)00083-0

Chang, T.-K., Zhong, Y.-H., Liu, S.-C., Huang, C.-C., Tsai, C.-H., Lee, H.-P., Wang, S.-W., Hsu, C.-J., & Tang, C.-H. (2021). Apelin Promotes Endothelial Progenitor Cell Angiogenesis in Rheumatoid Arthritis Disease via the miR-525-5p/Angiopoietin-1 Pathway. Frontiers in Immunology, 12, 737990. https://doi.org/10.3389/fimmu.2021.737990

Chargaff, E., & West, R. (1946). The biological significance of the thromboplastic protein of blood. The Journal of Biological Chemistry, 166(1), 189–197.

Charo, D. N., Ho, M., Fajardo, G., Kawana, M., Kundu, R. K., Sheikh, A. Y., Finsterbach, T. P., Leeper, N. J., Ernst, K. V., Chen, M. M., Ho, Y. D., Chun, H. J., Bernstein, D., Ashley, E. A., & Quertermous, T. (2009). Endogenous regulation of cardiovascular function by apelin-APJ. American Journal of Physiology-Heart and Circulatory Physiology, 297(5), H1904–H1913. https://doi.org/10.1152/ajpheart.00686.2009

Chastney, M. R., Kaivola, J., Leppänen, V.-M., & Ivaska, J. (2025). The role and regulation of integrins in cell migration and invasion. Nature Reviews Molecular Cell Biology, 26(2), 147–167. https://doi.org/10.1038/s41580-024-00777-1

Chaudhry, N., Sica, M., Surabhi, S., Hernandez, D. S., Mesquita, A., Selimovic, A., Riaz, A., Lescat, L., Bai, H., MacIntosh, G. C., & Jenny, A. (2022). Lamp1 mediates lipid transport, but is dispensable for autophagy in Drosophila. Autophagy, 18(10), 2443–2458. https://doi.org/10.1080/15548627.2022.2038999

Chaudhuri, A. D., Dastgheyb, R. M., Yoo, S.-W., Trout, A., Talbot Jr, C. C., Hao, H., Witwer, K. W., & Haughey, N. J. (2018). TNFα and IL-1β modify the miRNA cargo of astrocyte shed extracellular vesicles to regulate neurotrophic signaling in neurons. Cell Death & Disease, 9(3), 363. https://doi.org/10.1038/s41419-018-0369-4

Chen, A., Volpato, G., Pong, A., Schofield, E., Huang, J., Qiu, Z., Paxinos, G., & Liang, H. (2024). The Blood-Brain Barrier in Both Humans and Rats: A Perspective From 3D Imaging. International Journal of Biomedical Imaging, 2024, 4482931. https://doi.org/10.1155/2024/4482931

Chen, A.-Q., Fang, Z., Chen, X.-L., Yang, S., Zhou, Y.-F., Mao, L., Xia, Y.-P., Jin, H.-J., Li, Y.-N., You, M.-F., Wang, X.-X., Lei, H., He, Q.-W., & Hu, B. (2019). Microglia-derived TNF-α mediates endothelial necroptosis aggravating blood brain–barrier disruption after ischemic stroke. Cell Death & Disease, 10(7), 487. https://doi.org/10.1038/s41419-019-1716-9

Chen, C.-M., Wu, M.-L., Ho, Y.-C., Gung, P.-Y., Tsai, M.-H., Orekhov, A. N., Sobenin, I. A., Lin, P., & Yet, S.-F. (2020). Exposure to Zinc Oxide Nanoparticles Disrupts Endothelial Tight and Adherens Junctions and Induces Pulmonary Inflammatory Cell Infiltration. International Journal of Molecular Sciences, 21(10), 3437. https://doi.org/10.3390/ijms21103437

Chen, C.-Y., Chao, Y.-M., Lin, H.-F., Chen, C.-J., Chen, C.-S., Yang, J.-L., Chan, J. Y. H., & Juo, S.-H. H. (2020). miR-195 reduces age-related blood–brain barrier leakage caused by thrombospondin-1-mediated selective autophagy. Aging Cell, 19(11), e13236. https://doi.org/10.1111/acel.13236

Chen, C.-Y., Rao, S.-S., Ren, L., Hu, X.-K., Tan, Y.-J., Hu, Y., Luo, J., Liu, Y.-W., Yin, H., Huang, J., Cao, J., Wang, Z.-X., Liu, Z.-Z., Liu, H.-M., Tang, S.-Y., Xu, R., & Xie, H. (2018). Exosomal DMBT1 from human urine-derived stem cells facilitates diabetic wound repair by promoting angiogenesis. Theranostics, 8(6), 1607–1623. https://doi.org/10.7150/thno.22958

Chen, J., Chen, T., Zhu, Y., Li, Y., Zhang, Y., Wang, Y., Li, X., Xie, X., Wang, J., Huang, M., Sun, X., & Ke, Y. (2019). circPTN sponges miR-145-5p/miR-330-5p to promote proliferation and stemness in glioma. Journal of Experimental & Clinical Cancer Research, 38(1), 398. https://doi.org/10.1186/s13046-019-1376-8

Chen, J., Luo, Y., Hui, H., Cai, T., Huang, H., Yang, F., Feng, J., Zhang, J., & Yan, X. (2017). CD146 coordinates brain endothelial cell–pericyte communication for blood–brain barrier development. Proceedings of the National Academy of Sciences, 114(36). https://doi.org/10.1073/pnas.1710848114

Chen, J. W., Murphy, T. L., Willingham, M. C., Pastan, I., & August, J. T. (1985). Identification of two lysosomal membrane glycoproteins. The Journal of Cell Biology, 101(1), 85–95. https://doi.org/10.1083/jcb.101.1.85

Chen, M.-L., Hong, C.-G., Yue, T., Li, H.-M., Duan, R., Hu, W.-B., Cao, J., Wang, Z.-X., Chen, C.-Y., Hu, X.-K., Wu, B., Liu, H.-M., Tan, Y.-J., Liu, J.-H., Luo, Z.-W., Zhang, Y., Rao, S.-S., Luo, M.-J., Yin, H., … Liu, Z.-Z. (2021). Inhibition of miR-331-3p and miR-9-5p ameliorates Alzheimer's disease by enhancing autophagy. Theranostics, 11(5), 2395–2409. https://doi.org/10.7150/thno.47408

Chen, Q., Kou, H., Demy, D. L., Liu, W., Li, J., Wen, Z., Herbomel, P., Huang, Z., Zhang, W., & Xu, J. (2024). The different roles of V-ATPase a subunits in phagocytosis/endocytosis and autophagy. Autophagy, 20(10), 2297–2313. https://doi.org/10.1080/15548627.2024.2366748

Chen, Y., Chen, L., Lun, A. T. L., Baldoni, P. L., & Smyth, G. K. (2025). edgeR v4: Powerful differential analysis of sequencing data with expanded functionality and improved support for small counts and larger datasets. Nucleic Acids Research, 53(2), gkaf018. https://doi.org/10.1093/nar/gkaf018

Chen, Y., Peng, F., Yang, C., Hou, H., Xing, Z., Chen, J., Liu, L., Peng, C., & Li, D. (2023). SIRT1 activation by 2,3,5,6-tetramethylpyrazine alleviates neuroinflammation via inhibiting M1 microglia polarization. Frontiers in Immunology, 14, 1206513. https://doi.org/10.3389/fimmu.2023.1206513

Chen, Y.-S., Chen, K.-H., Liu, C.-C., Lee, C.-T., Yang, C.-H., Chuang, K.-C., & Lin, C.-R. (2007). Propofol-induced vascular permeability change is related to the nitric oxide signaling pathway and occludin phosphorylation. Journal of Biomedical Science, 14(5), 629–636. https://doi.org/10.1007/s11373-007-9164-4

Chen, Z.-L., Yao, Y., Norris, E. H., Kruyer, A., Jno-Charles, O., Akhmerov, A., & Strickland, S. (2013). Ablation of astrocytic laminin impairs vascular smooth muscle cell

function and leads to hemorrhagic stroke. Journal of Cell Biology, 202(2), 381–395. https://doi.org/10.1083/jcb.201212032

Cheng, F., Chang, H., Yan, F., Yang, A., Liu, J., & Liu, Y. (2020). Agomelatine Attenuates Isoflurane-Induced Inflammation and Damage in Brain Endothelial Cells. Drug Design, Development and Therapy, 14, 5589–5598. https://doi.org/10.2147/DDDT.S281582

Cheng, X.-T., Xie, Y.-X., Zhou, B., Huang, N., Farfel-Becker, T., & Sheng, Z.-H. (2018). Characterization of LAMP1-labeled nondegradative lysosomal and endocytic compartments in neurons. Journal of Cell Biology, 217(9), 3127–3139. https://doi.org/10.1083/jcb.201711083

Chiang, C.-L., Ma, Y., Hou, Y.-C., Pan, J., Chen, S.-Y., Chien, M.-H., Zhang, Z.-X., Hsu, W.-H., Wang, X., Zhang, J., Li, H., Sun, L., Fallen, S., Lee, I., Chen, X.-Y., Chu, Y.-S., Zhang, C., Cheng, T.-S., Jiang, W., … James Lee, L. (2023). Dual targeted extracellular vesicles regulate oncogenic genes in advanced pancreatic cancer. Nature Communications, 14(1), 6692. https://doi.org/10.1038/s41467-023-42402-3

Chitti, S. V., Gummadi, S., Kang, T., Shahi, S., Marzan, A. L., Nedeva, C., Sanwlani, R., Bramich, K., Stewart, S., Petrovska, M., Sen, B., Ozkan, A., Akinfenwa, M., Fonseka, P., & Mathivanan, S. (2024). Vesiclepedia 2024: An extracellular vesicles and extracellular particles repository. Nucleic Acids Research, 52(D1), D1694–D1698. https://doi.org/10.1093/nar/gkad1007

Cho, C., Smallwood, P. M., & Nathans, J. (2017). Reck and Gpr124 Are Essential Receptor Cofactors for Wnt7a/Wnt7b-Specific Signaling in Mammalian CNS Angiogenesis and Blood-Brain Barrier Regulation. Neuron, 95(5), 1056-1073.e5. https://doi.org/10.1016/j.neuron.2017.07.031

Choi, J. S., Yoon, H. I., Lee, K. S., Choi, Y. C., Yang, S. H., Kim, I.-S., & Cho, Y. W. (2016). Exosomes from differentiating human skeletal muscle cells trigger myogenesis of stem cells and provide biochemical cues for skeletal muscle regeneration. Journal of Controlled Release, 222, 107–115. https://doi.org/10.1016/j.jconrel.2015.12.018

Choi, J.-W., Youn, J., Kim, D. S., & Park, T.-E. (2023). Human iPS-derived blood-brain barrier model exhibiting enhanced barrier properties empowered by engineered basement membrane. Biomaterials, 293, 121983. https://doi.org/10.1016/j.biomaterials.2022.121983

Christianson, H. C., Svensson, K. J., Van Kuppevelt, T. H., Li, J.-P., & Belting, M. (2013). Cancer cell exosomes depend on cell-surface heparan sulfate proteoglycans for their internalization and functional activity. Proceedings of the National Academy of Sciences, 110(43), 17380–17385. https://doi.org/10.1073/pnas.1304266110

Chu, H., Yang, X., Huang, C., Gao, Z., Tang, Y., & Dong, Q. (2017). Apelin-13 Protects against Ischemic Blood-Brain Barrier Damage through the Effects of Aquaporin-4. Cerebrovascular Diseases, 44(1–2), 10–25. https://doi.org/10.1159/000460261

Chun, C., Smith, A. S. T., Kim, H., Kamenz, D. S., Lee, J. H., Lee, J. B., Mack, D. L., Bothwell, M., Clelland, C. D., & Kim, D.-H. (2021). Astrocyte-derived extracellular vesicles enhance the survival and electrophysiological function of human cortical neurons in vitro. Biomaterials, 271, 120700. https://doi.org/10.1016/j.biomaterials.2021.120700

Chung, W.-S., Clarke, L. E., Wang, G. X., Stafford, B. K., Sher, A., Chakraborty, C., Joung, J., Foo, L. C., Thompson, A., Chen, C., Smith, S. J., & Barres, B. A. (2013). Astrocytes

mediate synapse elimination through MEGF10 and MERTK pathways. Nature, 504(7480), 394–400. https://doi.org/10.1038/nature12776

Ciardiello, C., Leone, A., Lanuti, P., Roca, M. S., Moccia, T., Minciacchi, V. R., Minopoli, M., Gigantino, V., De Cecio, R., Rippa, M., Petti, L., Capone, F., Vitagliano, C., Milone, M. R., Pucci, B., Lombardi, R., Iannelli, F., Di Gennaro, E., Bruzzese, F., … Budillon, A. (2019). Large oncosomes overexpressing integrin alpha-V promote prostate cancer adhesion and invasion via AKT activation. Journal of Experimental & Clinical Cancer Research, 38(1), 317. https://doi.org/10.1186/s13046-019-1317-6

Clarke, D. D., & Sokoloff, L. (1999). Circulation and energy metabolism. In G. J. Siegel, B. W. Agranoff, R. W. Albers, S. K. Fisher, & M. D. Uhler (Eds), Basic Neurochemistry: Molecular, cellular and medical aspects (6. ed, pp. 638–669). Lippincott Williams & Wilkins.

Cohen, G. M. (1997). Caspases: The executioners of apoptosis. Biochemical Journal, 326(1), 1–16. https://doi.org/10.1042/bj3260001

Collado, A., Humoud, R., Kontidou, E., Swaich, J., Yang, J., Mahdi, A., Tengbom, J., Zhou, Z., & Pernow, J. (2024). Increased endothelial cell uptake of erythrocyte-derived extracellular vesicles carrying arginase-1 induces endothelial dysfunction in type 2 diabetes. European Heart Journal, 45(Supplement_1), ehae666.3685. https://doi.org/10.1093/eurheartj/ehae666.3685

Collister, M., Rempel, J., Yang, J., Kaita, K., Raizman, Z., Gong, Y., & Minuk, G. (2019). Circulating and inducible IL-32α in chronic hepatitis C virus infection. Canadian Liver Journal, 2(1), 23–30. https://doi.org/10.3138/canlivj.2018-0003

Combe, M., & Sokolenko, S. (2021). Quantifying the impact of cell culture media on CHO cell growth and protein production. Biotechnology Advances, 50, 107761. https://doi.org/10.1016/j.biotechadv.2021.107761

Comfort, N., Cai, K., Bloomquist, T. R., Strait, M. D., Ferrante Jr., A. W., & Baccarelli, A. A. (2021). Nanoparticle Tracking Analysis for the Quantification and Size Determination of Extracellular Vesicles. Journal of Visualized Experiments, (169), 62447. https://doi.org/10.3791/62447

Conte, I. L., Hellen, N., Bierings, R., Mashanov, G. I., Manneville, J.-B., Kiskin, N. I., Hannah, M. J., Molloy, J. E., & Carter, T. (2016). Interaction between MyRIP and the actin cytoskeleton regulates Weibel–Palade body trafficking and exocytosis. Journal of Cell Science, 129(3), 592–603. https://doi.org/10.1242/jcs.178285

Cooks, T., Pateras, I. S., Jenkins, L. M., Patel, K. M., Robles, A. I., Morris, J., Forshew, T., Appella, E., Gorgoulis, V. G., & Harris, C. C. (2018). Mutant p53 cancers reprogram macrophages to tumor supporting macrophages via exosomal miR-1246. Nature Communications, 9(1), 771. https://doi.org/10.1038/s41467-018-03224-w

Corne, T. D. J., Sieprath, T., Vandenbussche, J., Mohammed, D., Te Lindert, M., Gevaert, K., Gabriele, S., Wolf, K., & De Vos, W. H. (2017). Deregulation of focal adhesion formation and cytoskeletal tension due to loss of A-type lamins. Cell Adhesion & Migration, 11(5–6), 447–463. https://doi.org/10.1080/19336918.2016.1247144

Cornejo, M. G., Kharas, M. G., Werneck, M. B., Bras, S. L., Moore, S. A., Ball, B., Beylot-Barry, M., Rodig, S. J., Aster, J. C., Lee, B. H., Cantor, H., Merlio, J.-P., Gilliland, D. G.,

& Mercher, T. (2009). Constitutive JAK3 activation induces lymphoproliferative syndromes in murine bone marrow transplantation models. Blood, 113(12), 2746–2754. https://doi.org/10.1182/blood-2008-06-164368

Costa Verdera, H., Gitz-Francois, J. J., Schiffelers, R. M., & Vader, P. (2017). Cellular uptake of extracellular vesicles is mediated by clathrin-independent endocytosis and macropinocytosis. Journal of Controlled Release, 266, 100–108. https://doi.org/10.1016/j.jconrel.2017.09.019

Couch, Y., Buzàs, E. I., Di Vizio, D., Gho, Y. S., Harrison, P., Hill, A. F., Lötvall, J., Raposo, G., Stahl, P. D., Théry, C., Witwer, K. W., & Carter, D. R. F. (2021). A brief history of nearly EV-erything—The rise and rise of extracellular vesicles. Journal of Extracellular Vesicles, 10(14), e12144. https://doi.org/10.1002/jev2.12144

Coughlan, C., Bruce, K. D., Burgy, O., Boyd, T. D., Michel, C. R., Garcia-Perez, J. E., Adame, V., Anton, P., Bettcher, B. M., Chial, H. J., Königshoff, M., Hsieh, E. W. Y., Graner, M., & Potter, H. (2020). Exosome Isolation by Ultracentrifugation and Precipitation and Techniques for Downstream Analyses. Current Protocols in Cell Biology, 88(1), e110. https://doi.org/10.1002/cpcb.110

Couto, M., Coelho-Santos, V., Santos, L., Fontes-Ribeiro, C., Silva, A. P., & Gomes, C. M. F. (2019). The interplay between glioblastoma and microglia cells leads to endothelial cell monolayer dysfunction via the interleukin-6-induced JAK2/STAT3 pathway. Journal of Cellular Physiology, 234(11), 19750–19760. https://doi.org/10.1002/jcp.28575

Crawford, N. (1971). The Presence of Contractile Proteins in Platelet Microparticles Isolated from Human and Animal Platelet-free Plasma. British Journal of Haematology, 21(1), 53–69. https://doi.org/10.1111/j.1365-2141.1971.tb03416.x

Crewe, C., Funcke, J.-B., Li, S., Joffin, N., Gliniak, C. M., Ghaben, A. L., An, Y. A., Sadek, H. A., Gordillo, R., Akgul, Y., Chen, S., Samovski, D., Fischer-Posovszky, P., Kusminski, C. M., Klein, S., & Scherer, P. E. (2021). Extracellular vesicle-based interorgan transport of mitochondria from energetically stressed adipocytes. Cell Metabolism, 33(9), 1853-1868.e11. https://doi.org/10.1016/j.cmet.2021.08.002

Crone, C., & Olesen, S. P. (1982). Electrical resistance of brain microvascular endothelium. Brain Research, 241(1), 49–55. https://doi.org/10.1016/0006-8993(82)91227-6

Császár, E., Lénárt, N., Cserép, C., Környei, Z., Fekete, R., Pósfai, B., Balázsfi, D., Hangya, B., Schwarcz, A. D., Szabadits, E., Szöllősi, D., Szigeti, K., Máthé, D., West, B. L., Sviatkó, K., Brás, A. R., Mariani, J.-C., Kliewer, A., Lenkei, Z., … Dénes, Á. (2022). Microglia modulate blood flow, neurovascular coupling, and hypoperfusion via purinergic actions. Journal of Experimental Medicine, 219(3), e20211071. https://doi.org/10.1084/jem.20211071

Dahiya, N., & Atreya, C. (2021). MiRNA-103b Downregulates ITGB3 and Mediates Apoptosis in Ex Vivo Stored Human Platelets. MicroRNA, 10(2), 123–129. https://doi.org/10.2174/2211536610666210604121854

Dai, Z., Sezin, T., Chang, Y., Lee, E. Y., Wang, E. H. C., & Christiano, A. M. (2022). Induction of T cell exhaustion by JAK1/3 inhibition in the treatment of alopecia areata. Frontiers in Immunology, 13, 955038. https://doi.org/10.3389/fimmu.2022.955038

Daneman, R., & Prat, A. (2015). The blood-brain barrier. Cold Spring Harbor Perspectives in Biology, 7(1), a020412. https://doi.org/10.1101/cshperspect.a020412

Daneman, R., Zhou, L., Kebede, A. A., & Barres, B. A. (2010). Pericytes are required for blood–brain barrier integrity during embryogenesis. Nature, 468(7323), 562–566. https://doi.org/10.1038/nature09513

Datta Chaudhuri, A., Dasgheyb, R. M., DeVine, L. R., Bi, H., Cole, R. N., & Haughey, N. J. (2020). Stimulus-dependent modifications in astrocyte-derived extracellular vesicle cargo regulate neuronal excitability. Glia, 68(1), 128–144. https://doi.org/10.1002/glia.23708

Davalos, D., Grutzendler, J., Yang, G., Kim, J. V., Zuo, Y., Jung, S., Littman, D. R., Dustin, M. L., & Gan, W.-B. (2005). ATP mediates rapid microglial response to local brain injury in vivo. Nature Neuroscience, 8(6), 752–758. https://doi.org/10.1038/nn1472

Dawson, M. (2003). NG2-expressing glial progenitor cells: An abundant and widespread population of cycling cells in the adult rat CNS. Molecular and Cellular Neuroscience, 24(2), 476–488. https://doi.org/10.1016/S1044-7431(03)00210-0

De Bastiani, M. A., Bellaver, B., Brum, W. S., Souza, D. G., Ferreira, P. C. L., Rocha, A. S., Povala, G., Ferrari-Souza, J. P., Benedet, A. L., Ashton, N. J., Karikari, T. K., Zetterberg, H., Blennow, K., Rosa-Neto, P., Pascoal, T. A., & Zimmer, E. R. (2023). Hippocampal GFAP-positive astrocyte responses to amyloid and tau pathologies. Brain, Behavior, and Immunity, 110, 175–184. https://doi.org/10.1016/j.bbi.2023.03.001

De Bock, M., De Smet, M., Verwaerde, S., Tahiri, H., Schumacher, S., Van Haver, V., Witschas, K., Steinhäuser, C., Rouach, N., Vandenbroucke, R. E., & Leybaert, L. (2022). Targeting gliovascular connexins prevents inflammatory blood-brain barrier leakage and astrogliosis. JCI Insight, 7(16), e135263. https://doi.org/10.1172/jci.insight.135263

De Ceglia, R., Ledonne, A., Litvin, D. G., Lind, B. L., Carriero, G., Latagliata, E. C., Bindocci, E., Di Castro, M. A., Savtchouk, I., Vitali, I., Ranjak, A., Congiu, M., Canonica, T., Wisden, W., Harris, K., Mameli, M., Mercuri, N., Telley, L., & Volterra, A. (2023). Specialized astrocytes mediate glutamatergic gliotransmission in the CNS. Nature, 622(7981), 120–129. https://doi.org/10.1038/s41586-023-06502-w

De Wilt, L., Sobocki, B. K., Jansen, G., Tabeian, H., De Jong, S., Peters, G. J., & Kruyt, F. (2024). Mechanisms underlying reversed TRAIL sensitivity in acquired bortezomib-resistant non-small cell lung cancer cells. Cancer Drug Resistance. https://doi.org/10.20517/cdr.2024.14

Dechantsreiter, S., Ambrose, A. R., Worboys, J. D., Lim, J. M. E., Liu, S., Shah, R., Montero, M. A., Quinn, A. M., Hussell, T., Tannahill, G. M., & Davis, D. M. (2022). Heterogeneity in extracellular vesicle secretion by single human macrophages revealed by super-resolution microscopy. Journal of Extracellular Vesicles, 11(4), e12215. https://doi.org/10.1002/jev2.12215

DeMaio, L., Rouhanizadeh, M., Reddy, S., Sevanian, A., Hwang, J., & Hsiai, T. K. (2006). Oxidized phospholipids mediate occludin expression and phosphorylation in vascular endothelial cells. American Journal of Physiology-Heart and Circulatory Physiology, 290(2), H674–H683. https://doi.org/10.1152/ajpheart.00554.2005

Deng, M., Xiao, H., Peng, H., Yuan, H., Xu, Y., Zhang, G., Tang, J., & Hu, Z. (2018). Preservation of neuronal functions by exosomes derived from different human neural cell types under ischemic conditions. European Journal of Neuroscience, 47(2), 150–157. https://doi.org/10.1111/ejn.13784

Deosarkar, S. P., Prabhakarpandian, B., Wang, B., Sheffield, J. B., Krynska, B., & Kiani, M. F. (2015). A Novel Dynamic Neonatal Blood-Brain Barrier on a Chip. PLOS ONE, 10(11), e0142725. https://doi.org/10.1371/journal.pone.0142725

Derada Troletti, C., Fontijn, R. D., Gowing, E., Charabati, M., Van Het Hof, B., Didouh, I., Van Der Pol, S. M. A., Geerts, D., Prat, A., Van Horssen, J., Kooij, G., & De Vries, H. E. (2019). Inflammation-induced endothelial to mesenchymal transition promotes brain endothelial cell dysfunction and occurs during multiple sclerosis pathophysiology. Cell Death & Disease, 10(2), 45. https://doi.org/10.1038/s41419-018-1294-2

Dharan, R., Huang, Y., Cheppali, S. K., Goren, S., Shendrik, P., Wang, W., Qiao, J., Kozlov, M. M., Yu, L., & Sorkin, R. (2023). Tetraspanin 4 stabilizes membrane swellings and facilitates their maturation into migrasomes. Nature Communications, 14(1), 1037. https://doi.org/10.1038/s41467-023-36596-9

Di Vizio, D., Kim, J., Hager, M. H., Morello, M., Yang, W., Lafargue, C. J., True, L. D., Rubin, M. A., Adam, R. M., Beroukhim, R., Demichelis, F., & Freeman, M. R. (2009). Oncosome formation in prostate cancer: Association with a region of frequent chromosomal deletion in metastatic disease. Cancer Research, 69(13), 5601–5609. https://doi.org/10.1158/0008-5472.CAN-08-3860

Di Vizio, D., Morello, M., Dudley, A. C., Schow, P. W., Adam, R. M., Morley, S., Mulholland, D., Rotinen, M., Hager, M. H., Insabato, L., Moses, M. A., Demichelis, F., Lisanti, M. P., Wu, H., Klagsbrun, M., Bhowmick, N. A., Rubin, M. A., D'Souza-Schorey, C., & Freeman, M. R. (2012). Large oncosomes in human prostate cancer tissues and in the circulation of mice with metastatic disease. The American Journal of Pathology, 181(5), 1573–1584. https://doi.org/10.1016/j.ajpath.2012.07.030

Dickens, A. M., Tovar-y-Romo, L. B., Yoo, S.-W., Trout, A. L., Bae, M., Kanmogne, M., Megra, B., Williams, D. W., Witwer, K. W., Gacias, M., Tabatadze, N., Cole, R. N., Casaccia, P., Berman, J. W., Anthony, D. C., & Haughey, N. J. (2017). Astrocyte-shed extracellular vesicles regulate the peripheral leukocyte response to inflammatory brain lesions. Science Signaling, 10(473), eaai7696. https://doi.org/10.1126/scisignal.aai7696

Dickie, B. R., Vandesquille, M., Ulloa, J., Boutin, H., Parkes, L. M., & Parker, G. J. M. (2019). Water-exchange MRI detects subtle blood-brain barrier breakdown in Alzheimer's disease rats. NeuroImage, 184, 349–358. https://doi.org/10.1016/j.neuroimage.2018.09.030

Dimitrijevic, O. B., Stamatovic, S. M., Keep, R. F., & Andjelkovic, A. V. (2006). Effects of the Chemokine CCL2 on Blood–Brain Barrier Permeability during Ischemia–Reperfusion Injury. Journal of Cerebral Blood Flow & Metabolism, 26(6), 797–810. https://doi.org/10.1038/sj.jcbfm.9600229

Ding, C., Yi, X., Chen, X., Wu, Z., You, H., Chen, X., Zhang, G., Sun, Y., Bu, X., Wu, X., Lin, Z., Gu, J., Lin, Y., & Kang, D. (2021). Warburg effect-promoted exosomal circ_0072083 releasing up-regulates NANGO expression through multiple pathways and

enhances temozolomide resistance in glioma. Journal of Experimental & Clinical Cancer Research, 40(1), 164. https://doi.org/10.1186/s13046-021-01942-6

Ding, Y., Ding, N., Zhang, Y., Xie, S., Huang, M., Ding, X., Dong, W., Zhang, Q., & Jiang, L. (2021). MicroRNA-222 Transferred From Semen Extracellular Vesicles Inhibits Sperm Apoptosis by Targeting BCL2L11. Frontiers in Cell and Developmental Biology, 9, 736864. https://doi.org/10.3389/fcell.2021.736864

Ding, Z.-B., Song, L.-J., Wang, Q., Kumar, G., Yan, Y.-Q., & Ma, C.-G. (2021). Astrocytes: A double-edged sword in neurodegenerative diseases. Neural Regeneration Research, 16(9), 1702–1710. https://doi.org/10.4103/1673-5374.306064

Divecha, Y. A., Rampes, S., Tromp, S., Boyanova, S. T., Fleckney, A., Fidanboylu, M., & Thomas, S. A. (2025). The microcirculation, the blood-brain barrier, and the neurovascular unit in health and Alzheimer disease: The aberrant pericyte is a central player. Pharmacological Reviews, 77(3), 100052. https://doi.org/10.1016/j.pharmr.2025.100052

Djannatian, M., Radha, S., Weikert, U., Safaiyan, S., Wrede, C., Deichsel, C., Kislinger, G., Rhomberg, A., Ruhwedel, T., Campbell, D. S., Van Ham, T., Schmid, B., Hegermann, J., Möbius, W., Schifferer, M., & Simons, M. (2023). Myelination generates aberrant ultrastructure that is resolved by microglia. Journal of Cell Biology, 222(3), e202204010. https://doi.org/10.1083/jcb.202204010

Dobin, A., Davis, C. A., Schlesinger, F., Drenkow, J., Zaleski, C., Jha, S., Batut, P., Chaisson, M., & Gingeras, T. R. (2013). STAR: Ultrafast universal RNA-seq aligner. Bioinformatics, 29(1), 15–21. https://doi.org/10.1093/bioinformatics/bts635

Dogrammatzis, C., Saleh, S., Deighan, C., & Kalamvoki, M. (2021). Diverse Populations of Extracellular Vesicles with Opposite Functions during Herpes Simplex Virus 1 Infection. Journal of Virology, 95(6), e02357-20. https://doi.org/10.1128/JVI.02357-20

Du, C., Liu, C., Kang, J., Zhao, G., Ye, Z., Huang, S., Li, Z., Wu, Z., & Pei, G. (2009). MicroRNA miR-326 regulates TH-17 differentiation and is associated with the pathogenesis of multiple sclerosis. Nature Immunology, 10(12), 1252–1259. https://doi.org/10.1038/ni.1798

Du, C., Park, K., Hua, Y., Liu, Y., Volkow, N. D., & Pan, Y. (2024). Astrocytes modulate cerebral blood flow and neuronal response to cocaine in prefrontal cortex. Molecular Psychiatry, 29(3), 820–834. https://doi.org/10.1038/s41380-023-02373-9

Dunn, G. A., Loftis, J. M., & Sullivan, E. L. (2020). Neuroinflammation in psychiatric disorders: An introductory primer. Pharmacology Biochemistry and Behavior, 196, 172981. https://doi.org/10.1016/j.pbb.2020.172981

Durak-Kozica, M., Baster, Z., Kubat, K., & Stępień, E. (2018). 3D visualization of extracellular vesicle uptake by endothelial cells. Cellular & Molecular Biology Letters, 23(1), 57. https://doi.org/10.1186/s11658-018-0123-z

Ebnet, K., Schulz, C. U., Meyer Zu Brickwedde, M.-K., Pendl, G. G., & Vestweber, D. (2000). Junctional Adhesion Molecule Interacts with the PDZ Domain-containing Proteins AF-6 and ZO-1. Journal of Biological Chemistry, 275(36), 27979–27988. https://doi.org/10.1074/jbc.M002363200

Ehrlich, P. (1885). Das Sauerstoff-Bedürfniss des Organismus: Eine farbenanalytische Studie. A. Hirschwald.

Escartin, C., Galea, E., Lakatos, A., O'Callaghan, J. P., Petzold, G. C., Serrano-Pozo, A., Steinhäuser, C., Volterra, A., Carmignoto, G., Agarwal, A., Allen, N. J., Araque, A., Barbeito, L., Barzilai, A., Bergles, D. E., Bonvento, G., Butt, A. M., Chen, W.-T., Cohen-Salmon, M., … Verkhratsky, A. (2021). Reactive astrocyte nomenclature, definitions, and future directions. Nature Neuroscience, 24(3), 312–325. https://doi.org/10.1038/s41593-020-00783-4

Escola, J.-M., Kleijmeer, M. J., Stoorvogel, W., Griffith, J. M., Yoshie, O., & Geuze, H. J. (1998). Selective Enrichment of Tetraspan Proteins on the Internal Vesicles of Multivesicular Endosomes and on Exosomes Secreted by Human B-lymphocytes. Journal of Biological Chemistry, 273(32), 20121–20127. https://doi.org/10.1074/jbc.273.32.20121

Escrevente, C., Keller, S., Altevogt, P., & Costa, J. (2011). Interaction and uptake of exosomes by ovarian cancer cells. BMC Cancer, 11(1), 108. https://doi.org/10.1186/1471-2407-11-108

Ewels, P., Magnusson, M., Lundin, S., & Käller, M. (2016). MultiQC: Summarize analysis results for multiple tools and samples in a single report. Bioinformatics, 32(19), 3047–3048. https://doi.org/10.1093/bioinformatics/btw354

Fan, C., Li, Q., Zhang, Y., Liu, X., Luo, M., Abbott, D., Zhou, W., & Engelhardt, J. F. (2004). IκBα and IκBβ possess injury context-specific functions that uniquely influence hepatic NF-κB induction and inflammation. Journal of Clinical Investigation, 113(5), 746–755. https://doi.org/10.1172/JCI17337

Fanning, A. S., Jameson, B. J., Jesaitis, L. A., & Anderson, J. M. (1998). The tight junction protein ZO-1 establishes a link between the transmembrane protein occludin and the actin cytoskeleton. The Journal of Biological Chemistry, 273(45), 29745–29753. https://doi.org/10.1074/jbc.273.45.29745

Fanning, A. S., Little, B. P., Rahner, C., Utepbergenov, D., Walther, Z., & Anderson, J. M. (2007). The Unique-5 and -6 Motifs of ZO-1 Regulate Tight Junction Strand Localization and Scaffolding Properties. Molecular Biology of the Cell, 18(3), 721–731. https://doi.org/10.1091/mbc.e06-08-0764

Farquhar, M. G., & Palade, G. E. (1963). JUNCTIONAL COMPLEXES IN VARIOUS EPITHELIA. Journal of Cell Biology, 17(2), 375–412. https://doi.org/10.1083/jcb.17.2.375

Faust, T. E., Lee, Y.-H., O'Connor, C. D., Boyle, M. A., Gunner, G., Durán-Laforet, V., Ferrari, L. L., Murphy, R. E., Badimon, A., Sakers, K., Eroglu, C., Ayata, P., Schaefer, A., & Schafer, D. P. (2025). Microglia-astrocyte crosstalk regulates synapse remodeling via Wnt signaling. Cell, 188(19), 5212-5230.e21. https://doi.org/10.1016/j.cell.2025.08.023

Fei, X., Dou, Y., Wang, L., Wu, X., Huan, Y., Wu, S., He, X., Lv, W., Wei, J., & Fei, Z. (2022). Homer1 promotes the conversion of A1 astrocytes to A2 astrocytes and improves the recovery of transgenic mice after intracerebral hemorrhage. Journal of Neuroinflammation, 19(1), 67. https://doi.org/10.1186/s12974-022-02428-8

Feng, D., Zhao, W.-L., Ye, Y.-Y., Bai, X.-C., Liu, R.-Q., Chang, L.-F., Zhou, Q., & Sui, S.-F. (2010). Cellular Internalization of Exosomes Occurs Through Phagocytosis. Traffic, 11(5), 675–687. https://doi.org/10.1111/j.1600-0854.2010.01041.x

Feng, Y., Zhong, X., Ni, H.-F., Wang, C., Tang, T.-T., Wang, L.-T., Song, K.-Y., Tang, R.-N., Liu, H., Liu, B.-C., & Lv, L.-L. (2021). Urinary small extracellular vesicles derived CCL21 mRNA as biomarker linked with pathogenesis for diabetic nephropathy. Journal of Translational Medicine, 19(1), 355. https://doi.org/10.1186/s12967-021-03030-x

Feoktistova, M., Geserick, P., & Leverkus, M. (2016). Crystal Violet Assay for Determining Viability of Cultured Cells. Cold Spring Harbor Protocols, 2016(4), pdb.prot087379. https://doi.org/10.1101/pdb.prot087379

Fernández-García, S., Sancho-Balsells, A., Longueville, S., Hervé, D., Gruart, A., Delgado-García, J. M., Alberch, J., & Giralt, A. (2020). Astrocytic BDNF and TrkB regulate severity and neuronal activity in mouse models of temporal lobe epilepsy. Cell Death & Disease, 11(6), 411. https://doi.org/10.1038/s41419-020-2615-9

Figueroa-Hall, L. K., Burrows, K., Alarbi, A. M., Hannafon, B. N., Hladik, C., Tan, C., Ramesh, R., Stewart, J. L., Risbrough, V. B., Paulus, M. P., & Teague, T. K. (2025). Comparison of Methods for Isolation and Characterization of Total and Astrocyte-Enriched Extracellular Vesicles From Human Serum and Plasma. Journal of Extracellular Biology, 4(2), e70035. https://doi.org/10.1002/jex2.70035

Filipović, L., Spasojević Savković, M., Prodanović, R., Matijašević Joković, S., Stevanović, S., Marco, A. de, Kosanović, M., Brajušković, G., & Popović, M. (2024). Urinary Extracellular Vesicles as a Readily Available Biomarker Source: A Simplified Stratification Method. International Journal of Molecular Sciences, 25(15), 8004. https://doi.org/10.3390/ijms25158004

Forero, A., Pipicelli, F., Moser, S., Baumann, N., Grätz, C., Gonzalez Pisfil, M., Pfaffl, M. W., Pütz, B., Kielkowski, P., Cernilogar, F. M., Maccarrone, G., Di Giaimo, R., & Cappello, S. (2024). Extracellular vesicle-mediated trafficking of molecular cues during human brain development. Cell Reports, 43(10), 114755. https://doi.org/10.1016/j.celrep.2024.114755

Forró, T., Manu, D. R., Barbu-Tudoran, L., & Bălașa, R. (2024). Astrocyte Dysfunction Reflected in Ischemia-Induced Astrocyte-Derived Extracellular Vesicles: A Pilot Study on Acute Ischemic Stroke Patients. International Journal of Molecular Sciences, 25(22), 12471. https://doi.org/10.3390/ijms252212471

Forsberg, D., Ringstedt, T., & Herlenius, E. (2017). Astrocytes release prostaglandin E2 to modify respiratory network activity. eLife, 6, e29566. https://doi.org/10.7554/eLife.29566

Fouquet, J. P., Sikpa, D., Lebel, R., Sibgatulin, R., Krämer, M., Herrmann, K.-H., Deistung, A., Tremblay, L., Reichenbach, J. R., & Lepage, M. (2022). Characterization of microparticles of iron oxide for magnetic resonance imaging. Magnetic Resonance Imaging, 92, 67–81. https://doi.org/10.1016/j.mri.2022.05.020

Fourcade, O., Simon, M. F., Viodé, C., Rugani, N., Leballe, F., Ragab, A., Fournié, B., Sarda, L., & Chap, H. (1995). Secretory phospholipase A2 generates the novel lipid mediator lysophosphatidic acid in membrane microvesicles shed from activated cells. Cell, 80(6), 919–927. https://doi.org/10.1016/0092-8674(95)90295-3

Frank, R. N., Durra, S., & Mancini, M. A. (1987). Pericyte Coverage is Greater in the Retinal Than in the Cerebral Capillaries of the Rat. Investigative Ophthalmology & Visual Science, 28(7), 1086–1091.

Frank, R. N., Turczyn, T. J., & Dos, A. (1990). Pericyte Coverage of Retinal and Cerebral Capillaries. Investigative Ophthalmology & Visual Science, 31, 999–1007.

Frattini, A., Orchard, P. J., Sobacchi, C., Giliani, S., Abinun, M., Mattsson, J. P., Keeling, D. J., Andersson, A.-K., Wallbrandt, P., Zecca, L., Notarangelo, L. D., Vezzoni, P., & Villa, A. (2000). Defects in TCIRG1 subunit of the vacuolar proton pump are responsible for a subset of human autosomal recessive osteopetrosis. Nature Genetics, 25(3), 343–346. https://doi.org/10.1038/77131

Fu, B. M. (2018). Transport Across the Blood-Brain Barrier. In B. M. Fu & N. T. Wright (Eds), Molecular, Cellular, and Tissue Engineering of the Vascular System (Vol. 1097, pp. 235–259). Springer International Publishing. https://doi.org/10.1007/978-3-319-96445-4_13

Fujioka, T., Nishimura, T., Kawana, H., Hirosawa, K. M., Yamakawa, R., Sapili, H., Oono-Yakura, K., Nakagawa, R., Inoue, T., Nureki, O., Suzuki, K. G. N., & Suetsugu, S. (2025). Efficient cellular transformation via protein delivery through the protrusion-derived extracellular vesicles. Nature Communications, 16(1), 10900. https://doi.org/10.1038/s41467-025-66351-1

Fukuyama, K., Motomura, E., & Okada, M. (2023). A Novel Gliotransmitter, L-β-Aminoisobutyric Acid, Contributes to Pathophysiology of Clinical Efficacies and Adverse Reactions of Clozapine. Biomolecules, 13(9), 1288. https://doi.org/10.3390/biom13091288

Furuse, M., Fujita, K., Hiiragi, T., Fujimoto, K., & Tsukita, S. (1998). Claudin-1 and -2: Novel Integral Membrane Proteins Localizing at Tight Junctions with No Sequence Similarity to Occludin. The Journal of Cell Biology, 141(7), 1539–1550. https://doi.org/10.1083/jcb.141.7.1539

Furuse, M., Hata, M., Furuse, K., Yoshida, Y., Haratake, A., Sugitani, Y., Noda, T., Kubo, A., & Tsukita, S. (2002). Claudin-based tight junctions are crucial for the mammalian epidermal barrier. The Journal of Cell Biology, 156(6), 1099–1111. https://doi.org/10.1083/jcb.200110122

Furuse, M., Hirase, T., Itoh, M., Nagafuchi, A., Yonemura, S., Tsukita, S., & Tsukita, S. (1993). Occludin: A novel integral membrane protein localizing at tight junctions. The Journal of Cell Biology, 123(6), 1777–1788. https://doi.org/10.1083/jcb.123.6.1777

Furuse, M., Sasaki, H., Fujimoto, K., & Tsukita, S. (1998). A Single Gene Product, Claudin-1 or -2, Reconstitutes Tight Junction Strands and Recruits Occludin in Fibroblasts. The Journal of Cell Biology, 143(2), 391–401. https://doi.org/10.1083/jcb.143.2.391

Furuta, M., Murakami, C., Numagami, Y., Suzuki, R., & Sakane, F. (2023). Diacylglycerol kinase ζ interacts with sphingomyelin synthase 1 and sphingomyelin synthase-related protein via different regions. FEBS Open Bio, 13(7), 1333–1345. https://doi.org/10.1002/2211-5463.13628

Galland, F., Seady, M., Taday, J., Smaili, S. S., Gonçalves, C. A., & Leite, M. C. (2019). Astrocyte culture models: Molecular and function characterization of primary culture, immortalized astrocytes and C6 glioma cells. Neurochemistry International, 131, 104538. https://doi.org/10.1016/j.neuint.2019.104538

Gámez-Valero, A., Monguió-Tortajada, M., Carreras-Planella, L., Franquesa, M., Beyer, K., & Borràs, F. E. (2016). Size-Exclusion Chromatography-based isolation minimally alters Extracellular Vesicles' characteristics compared to precipitating agents. Scientific Reports, 6(1), 33641. https://doi.org/10.1038/srep33641

Gao, M., Li, Y., Ho, W., Chen, C., Chen, Q., Li, F., Tang, M., Fan, Q., Wan, J., Yu, W., Xu, X., Li, P., & Zhang, X.-Q. (2024). Targeted mRNA Nanoparticles Ameliorate Blood–Brain Barrier Disruption Postischemic Stroke by Modulating Microglia Polarization. ACS Nano, 18(4), 3260–3275. https://doi.org/10.1021/acsnano.3c09817

Gao, X., Chen, X., Ye, M., Li, J.-L., Lu, N., Yao, D., Ci, B., Chen, F., Zheng, L., Yi, Y., Zhang, S., Bi, Z., Gao, X., Yue, Y., Li, T., Lin, J., Shi, Y.-C., Shi, K., Propson, N. E., … Ge, W. (2025). Reduction of neuronal activity mediated by blood-vessel regression in the adult brain. Nature Communications, 16(1), 5840. https://doi.org/10.1038/s41467-025-60308-0

Gardiner, C., Di Vizio, D., Sahoo, S., Théry, C., Witwer, K. W., Wauben, M., & Hill, A. F. (2016). Techniques used for the isolation and characterization of extracellular vesicles: Results of a worldwide survey. Journal of Extracellular Vesicles, 5(1), 32945. https://doi.org/10.3402/jev.v5.32945

Gardner, T. W., Lieth, E., Khin, S. A., Barber, A. J., Bonsall, D. J., Lesher, T., Rice, K., & Brennan, W. A., Jr. (1997). Astrocytes increase barrier properties and ZO-1 expression in retinal vascular endothelial cells. Investigative Ophthalmology & Visual Science, 38(11), 2423–2427.

Gautam, J., Zhang, X., & Yao, Y. (2016). The role of pericytic laminin in blood brain barrier integrity maintenance. Scientific Reports, 6(1), 36450. https://doi.org/10.1038/srep36450

Gearing, D. P., Comeau, M. R., Friend, D. J., Gimpel, S. D., Thut, C. J., McGourty, J., Brasher, K. K., King, J. A., Gillis, S., Mosley, B., Ziegler, S. F., & Cosman, D. (1992). The IL-6 Signal Transducer, gp130: An Pncostatin M Receptor and Affinity Converter for the LIF Receptor. Science, 255(5050), 1434–1437. https://doi.org/10.1126/science.1542794

Geng, L., Gao, W., Saiyin, H., Li, Y., Zeng, Y., Zhang, Z., Li, X., Liu, Z., Gao, Q., An, P., Jiang, N., Yu, X., Chen, X., Li, S., Chen, L., Lu, B., Li, A., Chen, G., Shen, Y., … Li, J. (2023). MLKL deficiency alleviates neuroinflammation and motor deficits in the α-synuclein transgenic mouse model of Parkinson's disease. Molecular Neurodegeneration, 18(1), 94. https://doi.org/10.1186/s13024-023-00686-5

Gete, Y. G., Koblan, L. W., Mao, X., Trappio, M., Mahadik, B., Fisher, J. P., Liu, D. R., & Cao, K. (2021). Mechanisms of angiogenic incompetence in Hutchinson–Gilford progeria via downregulation of endothelial NOS. Aging Cell, 20(7), e13388. https://doi.org/10.1111/acel.13388

Gezer, U., Özgür, E., Cetinkaya, M., Isin, M., & Dalay, N. (2014). Long non-coding RNAs with low expression levels in cells are enriched in secreted exosomes. Cell Biology International, 38(9), 1076–1079. https://doi.org/10.1002/cbin.10301

Ghasempour, S., Warner, N., Guan, R., Rodari, M. M., Ivanochko, D., Whittaker Hawkins, R., Marwaha, A., Nowak, J. K., Liang, Y., Mulder, D. J., Stallard, L., Li, M., Yu, D. D., Pluthero, F. G., Batura, V., Zhao, M., Siddiqui, I., Upton, J. E. M., Hulst, J. M., … Muise, A. M. (2024). Human ITGAV variants are associated with immune dysregulation, brain

abnormalities, and colitis. Journal of Experimental Medicine, 221(12), e20240546. https://doi.org/10.1084/jem.20240546

Giampietro, C., Taddei, A., Corada, M., Sarra-Ferraris, G. M., Alcalay, M., Cavallaro, U., Orsenigo, F., Lampugnani, M. G., & Dejana, E. (2012). Overlapping and divergent signaling pathways of N-cadherin and VE-cadherin in endothelial cells. Blood, 119(9), 2159–2170. https://doi.org/10.1182/blood-2011-09-381012

Ginhoux, F., Greter, M., Leboeuf, M., Nandi, S., See, P., Gokhan, S., Mehler, M. F., Conway, S. J., Ng, L. G., Stanley, E. R., Samokhvalov, I. M., & Merad, M. (2010). Fate Mapping Analysis Reveals That Adult Microglia Derive from Primitive Macrophages. Science, 330(6005), 841–845. https://doi.org/10.1126/science.1194637

Giordano, M., Roncagalli, R., Bourdely, P., Chasson, L., Buferne, M., Yamasaki, S., Beyaert, R., Van Loo, G., Auphan-Anezin, N., Schmitt-Verhulst, A.-M., & Verdeil, G. (2014). The tumor necrosis factor alpha-induced protein 3 (TNFAIP3, A20) imposes a brake on antitumor activity of CD8 T cells. Proceedings of the National Academy of Sciences, 111(30), 11115–11120. https://doi.org/10.1073/pnas.1406259111

Girolamo, F., Errede, M., Longo, G., Annese, T., Alias, C., Ferrara, G., Morando, S., Trojano, M., Kerlero De Rosbo, N., Uccelli, A., & Virgintino, D. (2019). Defining the role of NG2-expressing cells in experimental models of multiple sclerosis. A biofunctional analysis of the neurovascular unit in wild type and NG2 null mice. PLOS ONE, 14(3), e0213508. https://doi.org/10.1371/journal.pone.0213508

Gnegy, M. E. (2012). Catecholamines. In Basic Neurochemistry (pp. 283–299). Elsevier. https://doi.org/10.1016/B978-0-12-374947-5.00014-6

Goetzl, E. J., Schwartz, J. B., Abner, E. L., Jicha, G. A., & Kapogiannis, D. (2018). High complement levels in astrocyte-derived exosomes of Alzheimer disease. Annals of Neurology, 83(3), 544–552. https://doi.org/10.1002/ana.25172

Goetzl, E. J., Yaffe, K., Peltz, C. B., Ledreux, A., Gorgens, K., Davidson, B., Granholm, A., Mustapic, M., Kapogiannis, D., Tweedie, D., & Greig, N. H. (2020). Traumatic brain injury increases plasma astrocyte-derived exosome levels of neurotoxic complement proteins. The FASEB Journal, 34(2), 3359–3366. https://doi.org/10.1096/fj.201902842R

Goldie, B. J., Dun, M. D., Lin, M., Smith, N. D., Verrills, N. M., Dayas, C. V., & Cairns, M. J. (2014). Activity-associated miRNA are packaged in Map1b-enriched exosomes released from depolarized neurons. Nucleic Acids Research, 42(14), 9195–9208. https://doi.org/10.1093/nar/gku594

Gomes, C., Huang, K.-C., Harkin, J., Baker, A., Hughes, J. M., Pan, Y., Tutrow, K., VanderWall, K. B., Lavekar, S. S., Hernandez, M., Cummins, T. R., Canfield, S. G., & Meyer, J. S. (2024). Induction of astrocyte reactivity promotes neurodegeneration in human pluripotent stem cell models. Stem Cell Reports, 19(8), 1122–1136. https://doi.org/10.1016/j.stemcr.2024.07.002

Goncalves, A., Su, E. J., Muthusamy, A., Zeitelhofer, M., Torrente, D., Nilsson, I., Protzmann, J., Fredriksson, L., Eriksson, U., Antonetti, D. A., & Lawrence, D. A. (2022). Thrombolytic tPA-Induced Hemorrhagic Transformation of Ischemic Stroke is Mediated by PKCβ phosphorylation of Occludin. Blood, blood.2021014958. https://doi.org/10.1182/blood.2021014958

Gong, L., Gu, Y., Han, X., Luan, C., Liu, C., Wang, X., Sun, Y., Zheng, M., Fang, M., Yang, S., Xu, L., Sun, H., Yu, B., Gu, X., & Zhou, S. (2023). Spatiotemporal Dynamics of the Molecular Expression Pattern and Intercellular Interactions in the Glial Scar Response to Spinal Cord Injury. Neuroscience Bulletin, 39(2), 213–244. https://doi.org/10.1007/s12264-022-00897-8

Gonschior, H., Schmied, C., Van Der Veen, R. E., Eichhorst, J., Himmerkus, N., Piontek, J., Günzel, D., Bleich, M., Furuse, M., Haucke, V., & Lehmann, M. (2022). Nanoscale segregation of channel and barrier claudins enables paracellular ion flux. Nature Communications, 13(1), 4985. https://doi.org/10.1038/s41467-022-32533-4

González-Álamos, M., Guerra, P., & Verdaguer, N. (2024). Structure, Dynamics and Functional Implications of the Eukaryotic Vault Complex. In J. R. Harris & J. Marles-Wright (Eds), Macromolecular Protein Complexes V (Vol. 104, pp. 531–548). Springer International Publishing. https://doi.org/10.1007/978-3-031-58843-3_20

Gordillo-Sampedro, S., Antounians, L., Wei, W., Mufteev, M., Lendemeijer, B., Kushner, S. A., De Vrij, F. M. S., Zani, A., & Ellis, J. (2024). iPSC-derived healthy human astrocytes selectively load miRNAs targeting neuronal genes into extracellular vesicles. Molecular and Cellular Neuroscience, 129, 103933. https://doi.org/10.1016/j.mcn.2024.103933

Gordon, R., Albornoz, E. A., Christie, D. C., Langley, M. R., Kumar, V., Mantovani, S., Robertson, A. A. B., Butler, M. S., Rowe, D. B., O'Neill, L. A., Kanthasamy, A. G., Schroder, K., Cooper, M. A., & Woodruff, T. M. (2018). Inflammasome inhibition prevents α-synuclein pathology and dopaminergic neurodegeneration in mice. Science Translational Medicine, 10(465), eaah4066. https://doi.org/10.1126/scitranslmed.aah4066

Gorji, A. (2022). Neuroinflammation: The Pathogenic Mechanism of Neurological Disorders. International Journal of Molecular Sciences, 23(10), 5744. https://doi.org/10.3390/ijms23105744

Gorvel, J.-P., Chavrier, P., Zerial, M., & Gruenberg, J. (1991). Rab5 controls early endosome fusion in vitro. Cell, 64(5), 915–925. https://doi.org/10.1016/0092-8674(91)90316-Q

Gould, S. J., & Raposo, G. (2013). As we wait: Coping with an imperfect nomenclature for extracellular vesicles. Journal of Extracellular Vesicles, 2(1), 20389. https://doi.org/10.3402/jev.v2i0.20389

Grabiec, M., Hříbková, H., Vařecha, M., Střítecká, D., Hampl, A., Dvořák, P., & Sun, Y.-M. (2016). Stage-specific roles of FGF2 signaling in human neural development. Stem Cell Research, 17(2), 330–341. https://doi.org/10.1016/j.scr.2016.08.012

Grant, R. I., Hartmann, D. A., Underly, R. G., Berthiaume, A.-A., Bhat, N. R., & Shih, A. Y. (2019). Organizational hierarchy and structural diversity of microvascular pericytes in adult mouse cortex. Journal of Cerebral Blood Flow & Metabolism, 39(3), 411–425. https://doi.org/10.1177/0271678X17732229

Greene, C., Hanley, N., Reschke, C. R., Reddy, A., Mäe, M. A., Connolly, R., Behan, C., O'Keeffe, E., Bolger, I., Hudson, N., Delaney, C., Farrell, M. A., O'Brien, D. F., Cryan, J., Brett, F. M., Beausang, A., Betsholtz, C., Henshall, D. C., Doherty, C. P., & Campbell, M. (2022). Microvascular stabilization via blood-brain barrier regulation prevents seizure activity. Nature Communications, 13(1), 2003. https://doi.org/10.1038/s41467-022-29657-y

Greene, C., Rebergue, N., Fewell, G., Janigro, D., Godfrin, Y., Campbell, M., & Lemarchant, S. (2024). NX210c drug candidate peptide strengthens mouse and human blood-brain barriers. Fluids and Barriers of the CNS, 21(1), 76. https://doi.org/10.1186/s12987-024-00577-x

Gu, J., Jin, T., Li, Z., Chen, H., Xia, H., Xu, X., & Gui, Y. (2021). Exosomes expressing neuronal autoantigens induced immune response in antibody-positive autoimmune encephalitis. Molecular Immunology, 131, 164–170. https://doi.org/10.1016/j.molimm.2020.12.034

Guadagno, N. A., Moriconi, C., Licursi, V., D'Acunto, E., Nisi, P. S., Carucci, N., De Jaco, A., Cacci, E., Negri, R., Lupo, G., & Miranda, E. (2017). Neuroserpin polymers cause oxidative stress in a neuronal model of the dementia FENIB. Neurobiology of Disease, 103, 32–44. https://doi.org/10.1016/j.nbd.2017.03.010

Guan, C., Lu, C., Xiao, M., & Chen, W. (2021). EHD2 Overexpression Suppresses the Proliferation, Migration, and Invasion in Human Colon Cancer. Cancer Investigation, 1–13. https://doi.org/10.1080/07357907.2020.1870125

Guduric-Fuchs, J., O'Connor, A., Camp, B., O'Neill, C. L., Medina, R. J., & Simpson, D. A. (2012). Selective extracellular vesicle-mediated export of an overlapping set of microRNAs from multiple cell types. BMC Genomics, 13(1), 357. https://doi.org/10.1186/1471-2164-13-357

Guérit, S., Fidan, E., Macas, J., Czupalla, C. J., Figueiredo, R., Vijikumar, A., Yalcin, B. H., Thom, S., Winter, P., Gerhardt, H., Devraj, K., & Liebner, S. (2021). Astrocyte-derived Wnt growth factors are required for endothelial blood-brain barrier maintenance. Progress in Neurobiology, 199, 101937. https://doi.org/10.1016/j.pneurobio.2020.101937

Gungor, O., Ozel, R., Aysan, A., Seker, G., Ozdemir, E., Doganci, M. D., & Doganci, E. (2026). Silicon phthalocyanine-modified poly(lactic acid)/poly(ethylene glycol) biocomposites with selective antitumor and antibacterial activities. International Journal of Biological Macromolecules, 364, 152163. https://doi.org/10.1016/j.ijbiomac.2026.152163

Guo, F., Xu, D., Lin, Y., Wang, G., Wang, F., Gao, Q., Wei, Q., & Lei, S. (2020). Chemokine CCL2 contributes to BBB disruption via the p38 MAPK signaling pathway following acute intracerebral hemorrhage. The FASEB Journal, 34(1), 1872–1884. https://doi.org/10.1096/fj.201902203RR

Guo, S., Hamanaka, G., Zhang, F., Lee, J., Park, J. H., Li, W., Arai, K., & Lo, E. H. (2025). Effects of senescence on astrocyte to brain endothelial cell signaling. Neuroprotection, 3(3), 288–297. https://doi.org/10.1002/nep3.70013

Guo, Y., Liang, P., Lu, S., Chen, R., Yin, Y., & Zhou, J. (2019). Extracellular αB-crystallin modulates the inflammatory responses. Biochemical and Biophysical Research Communications, 508(1), 282–288. https://doi.org/10.1016/j.bbrc.2018.11.024

Gupta, D., Liang, X., Pavlova, S., Wiklander, O. P. B., Corso, G., Zhao, Y., Saher, O., Bost, J., Zickler, A. M., Piffko, A., Maire, C. L., Ricklefs, F. L., Gustafsson, O., Llorente, V. C., Gustafsson, M. O., Bostancioglu, R. B., Mamand, D. R., Hagey, D. W., Görgens, A., … El Andaloussi, S. (2020). Quantification of extracellular vesicles in vitro and in vivo using sensitive bioluminescence imaging. Journal of Extracellular Vesicles, 9(1), 1800222. https://doi.org/10.1080/20013078.2020.1800222

Gureev, A. P., Sadovnikova, I. S., Chernyshova, E. V., Tsvetkova, A. D., Babenkova, P. I., Nesterova, V. V., Krutskikh, E. P., Volodina, D. E., Samoylova, N. A., Andrianova, N. V., Silachev, D. N., & Plotnikov, E. Y. (2024). Beta-Hydroxybutyrate Mitigates Sensorimotor and Cognitive Impairments in a Photothrombosis-Induced Ischemic Stroke in Mice. International Journal of Molecular Sciences, 25(11), 5710. https://doi.org/10.3390/ijms25115710

Gurung, S., Perocheau, D., Touramanidou, L., & Baruteau, J. (2021). The exosome journey: From biogenesis to uptake and intracellular signalling. Cell Communication and Signaling, 19(1), 47. https://doi.org/10.1186/s12964-021-00730-1

Gutiérrez García, G., Galicia García, G., Zalapa Soto, J., Izquierdo Medina, A., Rotzinger-Rodríguez, M., Casas Aguilar, G. A., López Pacheco, C. P., Aguayo, Á., & Aguilar-Hernandez, M. M. (2020). Analysis of RNA yield in extracellular vesicles isolated by membrane affinity column and differential ultracentrifugation. PLOS ONE, 15(11), e0238545. https://doi.org/10.1371/journal.pone.0238545

Guvenek, A., Parikshak, N., Zamolodchikov, D., Gelfman, S., Moscati, A., Dobbyn, L., Stahl, E., Shuldiner, A., & Coppola, G. (2024). Transcriptional profiling in microglia across physiological and pathological states identifies a transcriptional module associated with neurodegeneration. Communications Biology, 7(1), 1168. https://doi.org/10.1038/s42003-024-06684-7

Haas, A. J., Zihni, C., Ruppel, A., Hartmann, C., Ebnet, K., Tada, M., Balda, M. S., & Matter, K. (2020). Interplay between Extracellular Matrix Stiffness and JAM-A Regulates Mechanical Load on ZO-1 and Tight Junction Assembly. Cell Reports, 32(3), 107924. https://doi.org/10.1016/j.celrep.2020.107924

Hagey, D. W., Ojansivu, M., Bostancioglu, B. R., Saher, O., Bost, J. P., Gustafsson, M. O., Gramignoli, R., Svahn, M., Gupta, D., Stevens, M. M., Görgens, A., & El Andaloussi, S. (2023). The cellular response to extracellular vesicles is dependent on their cell source and dose. Science Advances, 9(35). https://doi.org/10.1126/sciadv.adh1168

Haileselassie, B., Joshi, A. U., Minhas, P. S., Mukherjee, R., Andreasson, K. I., & Mochly-Rosen, D. (2020). Mitochondrial dysfunction mediated through dynamin-related protein 1 (Drp1) propagates impairment in blood brain barrier in septic encephalopathy. Journal of Neuroinflammation, 17(1), 36. https://doi.org/10.1186/s12974-019-1689-8

Hajrasouliha, A. R., Jiang, G., Lu, Q., Lu, H., Kaplan, H. J., Zhang, H.-G., & Shao, H. (2013). Exosomes from Retinal Astrocytes Contain Antiangiogenic Components That Inhibit Laser-induced Choroidal Neovascularization. Journal of Biological Chemistry, 288(39), 28058–28067. https://doi.org/10.1074/jbc.M113.470765

Halder, S. K., Delorme-Walker, V. D., & Milner, R. (2025). Endothelial αvβ3 integrin induction during hypoxia protects blood–brain barrier integrity. Proceedings of the National Academy of Sciences, 122(38), e2510931122. https://doi.org/10.1073/pnas.2510931122

Halfter, W., & Yip, J. (2014). An organizing function of basement membranes in the developing nervous system. Mechanisms of Development, 133, 1–10. https://doi.org/10.1016/j.mod.2014.07.003

Han, H. (1998). CSR, a scavenger receptor-like protein with a protective role against cellular damage causedby UV irradiation and oxidative stress. Human Molecular Genetics, 7(6), 1039–1046. https://doi.org/10.1093/hmg/7.6.1039

Han, P., Li, X., Wei, W., & Ivanovski, S. (2023). Saliva Diagnosis Using Small Extracellular Vesicles and Salivaomics. In G. J. Seymour, M. P. Cullinan, N. C. K. Heng, & P. R. Cooper (Eds), Oral Biology (Vol. 2588, pp. 25–39). Springer US. https://doi.org/10.1007/978-1-0716-2780-8_3

Han, R., Liang, J., & Zhou, B. (2021). Glucose Metabolic Dysfunction in Neurodegenerative Diseases—New Mechanistic Insights and the Potential of Hypoxia as a Prospective Therapy Targeting Metabolic Reprogramming. International Journal of Molecular Sciences, 22(11), 5887. https://doi.org/10.3390/ijms22115887

Han, X., Li, Y., Zong, Y., Li, D., Yuan, J., Yang, H., Ma, H., Ni, A., Wang, Y., Zhao, J., Chen, J., Ma, T., & Sun, Y. (2023). Extracellular vesicle-coupled miRNA profiles of chicken seminal plasma and their potential interaction with recipient cells. Poultry Science, 102(12), 103099. https://doi.org/10.1016/j.psj.2023.103099

Han, Y., Kim, M., Gerelkhuu, Z., Kwon, S. J., Bang, H., Ha, E., & Yoon, T. H. (2026). Establishing a standard workflow for fluorescence-based nanoparticle tracking analysis for the reliable quantification of extracellular vesicles. Methods, 254, 147–158. https://doi.org/10.1016/j.ymeth.2026.07.006

Hannocks, M.-J., Pizzo, M. E., Huppert, J., Deshpande, T., Abbott, N. J., Thorne, R. G., & Sorokin, L. (2018). Molecular characterization of perivascular drainage pathways in the murine brain. Journal of Cerebral Blood Flow & Metabolism, 38(4), 669–686. https://doi.org/10.1177/0271678X17749689

Hara, E. S., Ono, M., Eguchi, T., Kubota, S., Pham, H. T., Sonoyama, W., Tajima, S., Takigawa, M., Calderwood, S. K., & Kuboki, T. (2013). miRNA-720 Controls Stem Cell Phenotype, Proliferation and Differentiation of Human Dental Pulp Cells. PLoS ONE, 8(12), e83545. https://doi.org/10.1371/journal.pone.0083545

Harding, C., Heuser, J., & Stahl, P. (1983). Receptor-mediated endocytosis of transferrin and recycling of the transferrin receptor in rat reticulocytes. The Journal of Cell Biology, 97(2), 329–339. https://doi.org/10.1083/jcb.97.2.329

Hargett, L. A., & Bauer, N. N. (2013). On the Origin of Microparticles: From "Platelet Dust" to Mediators of Intercellular Communication. Pulmonary Circulation, 3(2), 329–340. https://doi.org/10.4103/2045-8932.114760

Harris, J. J., Jolivet, R., & Attwell, D. (2012). Synaptic Energy Use and Supply. Neuron, 75(5), 762–777. https://doi.org/10.1016/j.neuron.2012.08.019

Hartmann, C., Zozulya, A., Wegener, J., & Galla, H.-J. (2007). The impact of glia-derived extracellular matrices on the barrier function of cerebral endothelial cells: An in vitro study. Experimental Cell Research, 313(7), 1318–1325. https://doi.org/10.1016/j.yexcr.2007.01.024

Hartmann, D. A., Berthiaume, A.-A., Grant, R. I., Harrill, S. A., Koski, T., Tieu, T., McDowell, K. P., Faino, A. V., Kelly, A. L., & Shih, A. Y. (2021). Brain capillary pericytes exert a substantial but slow influence on blood flow. Nature Neuroscience, 24(5), 633–645. https://doi.org/10.1038/s41593-020-00793-2

Haruwaka, K., Ikegami, A., Tachibana, Y., Ohno, N., Konishi, H., Hashimoto, A., Matsumoto, M., Kato, D., Ono, R., Kiyama, H., Moorhouse, A. J., Nabekura, J., & Wake, H. (2019). Dual microglia effects on blood brain barrier permeability induced by systemic inflammation. Nature Communications, 10(1), 5816. https://doi.org/10.1038/s41467-019-13812-z

Hayun, H., Coban, M., Bhagat, A. K., Ozer, E., Alfonta, L., Caulfield, T. R., Radisky, E. S., & Papo, N. (2023). Utilizing genetic code expansion to modify N-TIMP2 specificity towards MMP-2, MMP-9, and MMP-14. Scientific Reports, 13(1), 5186. https://doi.org/10.1038/s41598-023-32019-3

He, B., Cai, Q., Qiao, L., Huang, C.-Y., Wang, S., Miao, W., Ha, T., Wang, Y., & Jin, H. (2021). RNA-binding proteins contribute to small RNA loading in plant extracellular vesicles. Nature Plants, 7(3), 342–352. https://doi.org/10.1038/s41477-021-00863-8

He, J., Liu, H., & Wu, C. (2014). Identification of SCARA3, SCARA5 and MARCO of class A scavenger receptor-like family in Pseudosciaena crocea. Fish & Shellfish Immunology, 41(2), 238–249. https://doi.org/10.1016/j.fsi.2014.07.037

He, L., Vanlandewijck, M., Mäe, M. A., Andrae, J., Ando, K., Del Gaudio, F., Nahar, K., Lebouvier, T., Laviña, B., Gouveia, L., Sun, Y., Raschperger, E., Segerstolpe, Å., Liu, J., Gustafsson, S., Räsänen, M., Zarb, Y., Mochizuki, N., Keller, A., … Betsholtz, C. (2018). Single-cell RNA sequencing of mouse brain and lung vascular and vessel-associated cell types. Scientific Data, 5(1), 180160. https://doi.org/10.1038/sdata.2018.160

He, S., Liang, J., Xue, G., Wang, Y., Zhao, Y., Liu, Z., Hao, X., Wei, Y., Chen, X., Wang, H., Kang, S., Wang, R., Zhao, Y., & Ye, X. (2023). RNA profiling of sEV (small extracellular vesicles)/exosomes reveals biomarkers and vascular endothelial dysplasia with moyamoya disease. Journal of Cerebral Blood Flow & Metabolism, 43(7), 1194–1205. https://doi.org/10.1177/0271678X231162184

He, S., Wang, Q., Chen, L., He, Y. J., Wang, X., & Qu, S. (2023). miR-100a-5p-enriched exosomes derived from mesenchymal stem cells enhance the anti-oxidant effect in a Parkinson's disease model via regulation of Nox4/ROS/Nrf2 signaling. Journal of Translational Medicine, 21(1), 747. https://doi.org/10.1186/s12967-023-04638-x

He, Y., An, J., Yin, J.-J., Miao, Q., Sui, R.-X., Han, Q.-X., Ding, Z.-B., Huang, J.-J., Ma, C.-G., & Xiao, B.-G. (2021). Ethyl Pyruvate–Derived Transdifferentiation of Astrocytes to Oligodendrogenesis in Cuprizone-Induced Demyelinating Model. Neurotherapeutics, 18(1), 488–502. https://doi.org/10.1007/s13311-020-00947-x

He, Y., Liu, T., He, Q., Ke, W., Li, X., Du, J., Deng, S., Shu, Z., Wu, J., Yang, B., Wang, Y., Mao, Y., Rao, Y., Shu, Y., & Peng, B. (2023). Microglia facilitate and stabilize the response to general anesthesia via modulating the neuronal network in a brain region-specific manner. eLife, 12, RP92252. https://doi.org/10.7554/eLife.92252

Heinhuis, B., Koenders, M. I., Van Riel, P. L., Van De Loo, F. A., Dinarello, C. A., Netea, M. G., Van Den Berg, W. B., & Joosten, L. A. B. (2011). Tumour necrosis factor alpha-driven IL-32 expression in rheumatoid arthritis synovial tissue amplifies an inflammatory cascade. Annals of the Rheumatic Diseases, 70(4), 660–667. https://doi.org/10.1136/ard.2010.139196

Heithoff, B. P., George, K. K., Phares, A. N., Zuidhoek, I. A., Munoz-Ballester, C., & Robel, S. (2021). Astrocytes are necessary for blood–brain barrier maintenance in the adult mouse brain. Glia, 69(2), 436–472. https://doi.org/10.1002/glia.23908

Helker, C. S., Eberlein, J., Wilhelm, K., Sugino, T., Malchow, J., Schuermann, A., Baumeister, S., Kwon, H.-B., Maischein, H.-M., Potente, M., Herzog, W., & Stainier, D. Y. (2020). Apelin signaling drives vascular endothelial cells toward a pro-angiogenic state. eLife, 9, e55589. https://doi.org/10.7554/eLife.55589

Helmbold, P., Wohlrab, J., Marsch, W. Ch., & Nayak, R. C. (2001). Human dermal pericytes express 3G5 ganglioside – A new approach for microvessel histology in the skin. Journal of Cutaneous Pathology, 28(4), 206–210. https://doi.org/10.1034/j.1600-0560.2001.028004206.x

Helms, H. C., Waagepetersen, H. S., Nielsen, C. U., & Brodin, B. (2010). Paracellular Tightness and Claudin-5 Expression is Increased in the BCEC/Astrocyte Blood–Brain Barrier Model by Increasing Media Buffer Capacity During Growth. The AAPS Journal, 12(4), 759–770. https://doi.org/10.1208/s12248-010-9237-6

Henne, W. M., Buchkovich, N. J., Zhao, Y., & Emr, S. D. (2012). The Endosomal Sorting Complex ESCRT-II Mediates the Assembly and Architecture of ESCRT-III Helices. Cell, 151(2), 356–371. https://doi.org/10.1016/j.cell.2012.08.039

Henneberger, C., Papouin, T., Oliet, S. H. R., & Rusakov, D. A. (2010). Long-term potentiation depends on release of d-serine from astrocytes. Nature, 463(7278), 232–236. https://doi.org/10.1038/nature08673

Heo, J. H., Han, S. W., & Lee, S. K. (2005). Free radicals as triggers of brain edema formation after stroke. Free Radical Biology and Medicine, 39(1), 51–70. https://doi.org/10.1016/j.freeradbiomed.2005.03.035

Herdt, L., Baumeister, S., Ravindra, J., Eberlein, J., & Helker, C. S. M. (2025). Apelin as a CNS-specific pathway for fenestrated capillary formation in the choroid plexus. Nature Communications, 16(1), 7729. https://doi.org/10.1038/s41467-025-63003-2

Hermans, D., Houben, E., Baeten, P., Slaets, H., Janssens, K., Hoeks, C., Hosseinkhani, B., Duran, G., Bormans, S., Gowing, E., Hoornaert, C., Beckers, L., Fung, W. K., Schroten, H., Ishikawa, H., Fraussen, J., Thoelen, R., De Vries, H. E., Kooij, G., … Broux, B. (2022). Oncostatin M triggers brain inflammation by compromising blood–brain barrier integrity. Acta Neuropathologica, 144(2), 259–281. https://doi.org/10.1007/s00401-022-02445-0

Herzog, C., Pons Garcia, L., Keatinge, M., Greenald, D., Moritz, C., Peri, F., & Herrgen, L. (2019). Rapid clearance of cellular debris by microglia limits secondary neuronal cell death after brain injury in vivo. Development, 146(9), dev174698. https://doi.org/10.1242/dev.174698

Heusermann, W., Hean, J., Trojer, D., Steib, E., Von Bueren, S., Graff-Meyer, A., Genoud, C., Martin, K., Pizzato, N., Voshol, J., Morrissey, D. V., Andaloussi, S. E. L., Wood, M. J., & Meisner-Kober, N. C. (2016). Exosomes surf on filopodia to enter cells at endocytic hot spots, traffic within endosomes, and are targeted to the ER. Journal of Cell Biology, 213(2), 173–184. https://doi.org/10.1083/jcb.201506084

Hilbrig, C. F., Baumann, B., Sievert, W., Halbgebauer, R., Huber-Lang, M., Beer, A. J., Rasche, V., & Löffler, J. (2026). Detection of inflammation-related blood–brain barrier

dysfunction using PET and MR imaging: A pilot study. Scientific Reports, 16(1), 12014. https://doi.org/10.1038/s41598-026-47352-6

Hinkle, J. T., Patel, J., Panicker, N., Karuppagounder, S. S., Biswas, D., Belingon, B., Chen, R., Brahmachari, S., Pletnikova, O., Troncoso, J. C., Dawson, V. L., & Dawson, T. M. (2022). STING mediates neurodegeneration and neuroinflammation in nigrostriatal α-synucleinopathy. Proceedings of the National Academy of Sciences, 119(15), e2118819119. https://doi.org/10.1073/pnas.2118819119

Hirano, S., Yonezawa, T., Hasegawa, H., Hattori, S., Greenhill, N. S., Davis, P. F., Sage, E. H., & Ninomiya, Y. (2004). Astrocytes express type VIII collagen during the repair process of brain cold injury. Biochemical and Biophysical Research Communications, 317(2), 437–443. https://doi.org/10.1016/j.bbrc.2004.03.049

Hiroaki, H., Satomura, K., Goda, N., Nakakura, Y., Hiranuma, M., Tenno, T., Hamada, D., & Ikegami, T. (2018). Spatial Overlap of Claudin- and Phosphatidylinositol Phosphate-Binding Sites on the First PDZ Domain of Zonula Occludens 1 Studied by NMR. Molecules, 23(10), 2465. https://doi.org/10.3390/molecules23102465

Hirosawa, K. M., Sato, Y., Kasai, R. S., Yamaguchi, E., Komura, N., Ando, H., Hoshino, A., Yokota, Y., & Suzuki, K. G. N. (2025). Uptake of small extracellular vesicles by recipient cells is facilitated by paracrine adhesion signaling. Nature Communications, 16(1), 2419. https://doi.org/10.1038/s41467-025-57617-9

Hirose, H., Hirai, Y., Sasaki, M., Sawa, H., & Futaki, S. (2022). Quantitative Analysis of Extracellular Vesicle Uptake and Fusion with Recipient Cells. Bioconjugate Chemistry, 33(10), 1852–1859. https://doi.org/10.1021/acs.bioconjchem.2c00307

Hoffmann, A., Bredno, J., Wendland, M., Derugin, N., Ohara, P., & Wintermark, M. (2011). High and Low Molecular Weight Fluorescein Isothiocyanate (FITC)-Dextrans to Assess Blood-Brain Barrier Disruption: Technical Considerations. Translational Stroke Research, 2(1), 106–111. https://doi.org/10.1007/s12975-010-0049-x

Hogan-Cann, A. D., Lu, P., & Anderson, C. M. (2019). Endothelial NMDA receptors mediate activity-dependent brain hemodynamic responses in mice. Proceedings of the National Academy of Sciences, 116(21), 10229–10231. https://doi.org/10.1073/pnas.1902647116

Hong, C., Deng, R., Wang, P., Lu, X., Zhao, X., Wang, X., Cai, R., & Lin, J. (2021). LIPG: An inflammation and cancer modulator. Cancer Gene Therapy, 28(1–2), 27–32. https://doi.org/10.1038/s41417-020-0188-5

Hong, H., Wang, Y., Menard, M., Buckley, J. A., Zhou, L., Volpicelli-Daley, L., Standaert, D. G., Qin, H., & Benveniste, E. N. (2024). Suppression of the JAK/STAT pathway inhibits neuroinflammation in the line 61-PFF mouse model of Parkinson's disease. Journal of Neuroinflammation, 21(1), 216. https://doi.org/10.1186/s12974-024-03210-8

Honjoh, K., Nakajima, H., Hirai, T., Watanabe, S., & Matsumine, A. (2019). Relationship of Inflammatory Cytokines From M1-Type Microglia/Macrophages at the Injured Site and Lumbar Enlargement With Neuropathic Pain After Spinal Cord Injury in the CCL21 Knockout (plt) Mouse. Frontiers in Cellular Neuroscience, 13, 525. https://doi.org/10.3389/fncel.2019.00525

Hoshino, A., Costa-Silva, B., Shen, T.-L., Rodrigues, G., Hashimoto, A., Tesic Mark, M., Molina, H., Kohsaka, S., Di Giannatale, A., Ceder, S., Singh, S., Williams, C., Soplop, N., Uryu, K., Pharmer, L., King, T., Bojmar, L., Davies, A. E., Ararso, Y., … Lyden, D. (2015). Tumour exosome integrins determine organotropic metastasis. Nature, 527(7578), 329–335. https://doi.org/10.1038/nature15756

Hoshino, A., Kim, H. S., Bojmar, L., Gyan, K. E., Cioffi, M., Hernandez, J., Zambirinis, C. P., Rodrigues, G., Molina, H., Heissel, S., Mark, M. T., Steiner, L., Benito-Martin, A., Lucotti, S., Di Giannatale, A., Offer, K., Nakajima, M., Williams, C., Nogués, L., … Lyden, D. (2020). Extracellular Vesicle and Particle Biomarkers Define Multiple Human Cancers. Cell, 182(4), 1044-1061.e18. https://doi.org/10.1016/j.cell.2020.07.009

Hösli, L., Zuend, M., Bredell, G., Zanker, H. S., Porto De Oliveira, C. E., Saab, A. S., & Weber, B. (2022). Direct vascular contact is a hallmark of cerebral astrocytes. Cell Reports, 39(1), 110599. https://doi.org/10.1016/j.celrep.2022.110599

Hosseinkhani, B., Duran, G., Hoeks, C., Hermans, D., Schepers, M., Baeten, P., Poelmans, J., Coenen, B., Bekar, K., Pintelon, I., Timmermans, J.-P., Vanmierlo, T., Michiels, L., Hellings, N., & Broux, B. (2023). Cerebral microvascular endothelial cell-derived extracellular vesicles regulate blood − brain barrier function. Fluids and Barriers of the CNS, 20(1), 95. https://doi.org/10.1186/s12987-023-00504-6

Hou, Y., Wei, Y., Lautrup, S., Yang, B., Wang, Y., Cordonnier, S., Mattson, M. P., Croteau, D. L., & Bohr, V. A. (2021). NAD^+ supplementation reduces neuroinflammation and cell senescence in a transgenic mouse model of Alzheimer's disease via cGAS–STING. Proceedings of the National Academy of Sciences, 118(37), e2011226118. https://doi.org/10.1073/pnas.2011226118

Howarth, C., Sutherland, B. A., Choi, H. B., Martin, C., Lind, B. L., Khennouf, L., LeDue, J. M., Pakan, J. M. P., Ko, R. W. Y., Ellis-Davies, G., Lauritzen, M., Sibson, N. R., Buchan, A. M., & MacVicar, B. A. (2017). A Critical Role for Astrocytes in Hypercapnic Vasodilation in Brain. The Journal of Neuroscience, 37(9), 2403–2414. https://doi.org/10.1523/JNEUROSCI.0005-16.2016

Hsu, A. Y., Huang, Q., Pi, X., Fu, J., Raghunathan, K., Ghimire, L., Balasubramanian, A., Xie, X., Yu, H., Loison, F., Haridas, V., Zha, J., Liu, F., Park, S., Bagale, K., Ren, Q., Fan, Y., Zheng, Y., Cancelas, J. A., … Luo, H. R. (2025). Neutrophil-derived vesicles control complement activation to facilitate inflammation resolution. Cell, 188(6), 1623-1641.e26. https://doi.org/10.1016/j.cell.2025.01.021

Hu, C., Zhou, A., Hu, X., Xiang, Y., Huang, M., Huang, J., Yang, D., & Tang, Y. (2022). LMNA Reduced Acquired Resistance to Erlotinib in NSCLC by Reversing the Epithelial–Mesenchymal Transition via the FGFR/MAPK/c-fos Signaling Pathway. International Journal of Molecular Sciences, 23(21), 13237. https://doi.org/10.3390/ijms232113237

Hu, G., Liao, K., Niu, F., Yang, L., Dallon, B. W., Callen, S., Tian, C., Shu, J., Cui, J., Sun, Z., Lyubchenko, Y. L., Ka, M., Chen, X.-M., & Buch, S. (2018). Astrocyte EV-Induced lincRNA-Cox2 Regulates Microglial Phagocytosis: Implications for Morphine-Mediated Neurodegeneration. Molecular Therapy Nucleic Acids, 13, 450–463. https://doi.org/10.1016/j.omtn.2018.09.019

Hu, Q., Wu, X., Guo, C., Wang, T., Guo, H., Wang, J., Wang, B., Cui, W., Bai, H., Zhou, J., Li, L., Han, L., Cao, L., Ge, S., Gao, G., Wang, T., Wu, Z., Guo, W., Qu, Y., … Liu, H.

(2024). Astrocyte–neuron crosstalk through extracellular vesicle-shuttled miRNA-382-5p promotes traumatic brain injury. Experimental & Molecular Medicine, 56(12), 2642–2658. https://doi.org/10.1038/s12276-024-01355-3

Hu, Y., Qi, H., Yang, J., Wang, F., Peng, X., Chen, X., & Zhu, X. (2024). Wogonin mitigates microglia-mediated synaptic over-pruning and cognitive impairment following epilepsy. Phytomedicine, 135, 156222. https://doi.org/10.1016/j.phymed.2024.156222

Huang, B., Krafft, P. R., Ma, Q., Rolland, W. B., Caner, B., Lekic, T., Manaenko, A., Le, M., Tang, J., & Zhang, J. H. (2012). Fibroblast growth factors preserve blood–brain barrier integrity through RhoA inhibition after intracerebral hemorrhage in mice. Neurobiology of Disease, 46(1), 204–214. https://doi.org/10.1016/j.nbd.2012.01.008

Huang, B. X., Chen, H., Joo, Y., Kwon, H.-S., Fu, C., Spector, A. A., & Kim, H.-Y. (2023). Interaction between GPR110 (ADGRF1) and tight junction protein occludin implicated in blood-brain barrier permeability. iScience, 26(4), 106550. https://doi.org/10.1016/j.isci.2023.106550

Huang, Y., Liu, Y., Huang, Q., Sun, S., Ji, Z., Huang, L., Li, Z., Huang, X., Deng, W., & Li, T. (2022). TMT-Based Quantitative Proteomics Analysis of Synovial Fluid-Derived Exosomes in Inflammatory Arthritis. Frontiers in Immunology, 13, 800902. https://doi.org/10.3389/fimmu.2022.800902

Huang, Y., Zucker, B., Zhang, S., Elias, S., Zhu, Y., Chen, H., Ding, T., Li, Y., Sun, Y., Lou, J., Kozlov, M. M., & Yu, L. (2019). Migrasome formation is mediated by assembly of micron-scale tetraspanin macrodomains. Nature Cell Biology, 21(8), 991–1002. https://doi.org/10.1038/s41556-019-0367-5

Hughes, A. N., & Appel, B. (2020). Microglia phagocytose myelin sheaths to modify developmental myelination. Nature Neuroscience, 23(9), 1055–1066. https://doi.org/10.1038/s41593-020-0654-2

Husain, M. A., Smith, R., Sorge, R. E., Kaimari, A., Si, Y., Hassan, A. Z., Guha, A., Smith, K. A., Cardozo, C. P., DeBerry, J. J., Andrabi, S. A., Nabors, L. B., Filippova, N., Webb, C. K., & King, P. H. (2025). Inhibition of the RNA Regulator HuR Mitigates Spinal Cord Injury by Potently Suppressing Post-Injury Neuroinflammation. The FASEB Journal, 39(9), e70588. https://doi.org/10.1096/fj.202500236R

Hutvágner, G., & Zamore, P. D. (2002). A microRNA in a Multiple-Turnover RNAi Enzyme Complex. Science, 297(5589), 2056–2060. https://doi.org/10.1126/science.1073827

Huynh, K. K., Eskelinen, E.-L., Scott, C. C., Malevanets, A., Saftig, P., & Grinstein, S. (2007). LAMP proteins are required for fusion of lysosomes with phagosomes. The EMBO Journal, 26(2), 313–324. https://doi.org/10.1038/sj.emboj.7601511

Hyvärinen, T., Hagman, S., Ristola, M., Sukki, L., Veijula, K., Kreutzer, J., Kallio, P., & Narkilahti, S. (2019). Co-stimulation with IL-1β and TNF-α induces an inflammatory reactive astrocyte phenotype with neurosupportive characteristics in a human pluripotent stem cell model system. Scientific Reports, 9(1), 16944. https://doi.org/10.1038/s41598-019-53414-9

Iadecola, C. (2017). The Neurovascular Unit Coming of Age: A Journey through Neurovascular Coupling in Health and Disease. Neuron, 96(1), 17–42. https://doi.org/10.1016/j.neuron.2017.07.030

Ibáñez, F., Montesinos, J., Ureña-Peralta, J. R., Guerri, C., & Pascual, M. (2019). TLR4 participates in the transmission of ethanol-induced neuroinflammation via astrocyte-derived extracellular vesicles. Journal of Neuroinflammation, 16(1), 136. https://doi.org/10.1186/s12974-019-1529-x

Irala, D., Wang, S., Sakers, K., Nagendren, L., Ulloa Severino, F. P., Bindu, D. S., Savage, J. T., & Eroglu, C. (2024). Astrocyte-secreted neurocan controls inhibitory synapse formation and function. Neuron, 112(10), 1657-1675.e10. https://doi.org/10.1016/j.neuron.2024.03.007

Irmer, B., Efing, J., Reitnauer, L. E., Angenendt, A., Heinrichs, S., Schubert, A., Schulz, M., Binder, C., Tio, J., Hansen, U., Geyer, C., Gerwing, M., Bleckmann, A., & Menck, K. (2023). Extracellular vesicle-associated tyrosine kinase-like orphan receptors ROR1 and ROR2 promote breast cancer progression. Cell Communication and Signaling, 21(1), 171. https://doi.org/10.1186/s12964-023-01186-1

İş, Ö., Wang, X., Reddy, J. S., Min, Y., Yilmaz, E., Bhattarai, P., Patel, T., Bergman, J., Quicksall, Z., Heckman, M. G., Tutor-New, F. Q., Can Demirdogen, B., White, L., Koga, S., Krause, V., Inoue, Y., Kanekiyo, T., Cosacak, M. I., Nelson, N., … Ertekin-Taner, N. (2024). Gliovascular transcriptional perturbations in Alzheimer's disease reveal molecular mechanisms of blood brain barrier dysfunction. Nature Communications, 15(1), 4758. https://doi.org/10.1038/s41467-024-48926-6

Isis Yonza, A. K., Tao, L., Zhang, X., Postnov, D., Kucharz, K., Lind, B., Asiminas, A., Han, A., Sonego, V., Kim, K., & Cai, C. (2025). Spatially and temporally mismatched blood flow and neuronal activity by high-intensity intracortical microstimulation. Brain Stimulation, 18(3), 885–896. https://doi.org/10.1016/j.brs.2025.04.015

Itoh, M., Furuse, M., Morita, K., Kubota, K., Saitou, M., & Tsukita, S. (1999). Direct Binding of Three Tight Junction-Associated Maguks, Zo-1, Zo-2, and Zo-3, with the Cooh Termini of Claudins. The Journal of Cell Biology, 147(6), 1351–1363. https://doi.org/10.1083/jcb.147.6.1351

Jacobs, M. D., & Harrison, S. C. (1998). Structure of an IκBα/NF-κB Complex. Cell, 95(6), 749–758. https://doi.org/10.1016/S0092-8674(00)81698-0

Jagtiani, E., Yeolekar, M., Naik, S., & Patravale, V. (2022). In vitro blood brain barrier models: An overview. Journal of Controlled Release, 343, 13–30. https://doi.org/10.1016/j.jconrel.2022.01.011

Janas, T., Janas, M. M., Sapoń, K., & Janas, T. (2015). Mechanisms of RNA loading into exosomes. FEBS Letters, 589(13), 1391–1398. https://doi.org/10.1016/j.febslet.2015.04.036

Jang, J., Kim, M. R., Kim, T.-K., Lee, W. R., Kim, J. H., Heo, K., & Lee, S. (2017). CLEC14a-HSP70-1A interaction regulates HSP70-1A-induced angiogenesis. Scientific Reports, 7(1), 10666. https://doi.org/10.1038/s41598-017-11118-y

Japp, A. G., Cruden, N. L., Amer, D. A. B., Li, V. K. Y., Goudie, E. B., Johnston, N. R., Sharma, S., Neilson, I., Webb, D. J., Megson, I. L., Flapan, A. D., & Newby, D. E. (2008).

Vascular Effects of Apelin In Vivo in Man. Journal of the American College of Cardiology, 52(11), 908–913. https://doi.org/10.1016/j.jacc.2008.06.013

Jayadev, R., Morais, M. R. P. T., Ellingford, J. M., Srinivasan, S., Naylor, R. W., Lawless, C., Li, A. S., Ingham, J. F., Hastie, E., Chi, Q., Fresquet, M., Koudis, N.-M., Thomas, H. B., O'Keefe, R. T., Williams, E., Adamson, A., Stuart, H. M., Banka, S., Smedley, D., … Lennon, R. (2022). A basement membrane discovery pipeline uncovers network complexity, regulators, and human disease associations. Science Advances, 8(20), eabn2265. https://doi.org/10.1126/sciadv.abn2265

Jeanne, M., Jorgensen, J., & Gould, D. B. (2015). Molecular and Genetic Analyses of Collagen Type IV Mutant Mouse Models of Spontaneous Intracerebral Hemorrhage Identify Mechanisms for Stroke Prevention. Circulation, 131(18), 1555–1565. https://doi.org/10.1161/CIRCULATIONAHA.114.013395

Jeppesen, D. K., Fenix, A. M., Franklin, J. L., Higginbotham, J. N., Zhang, Q., Zimmerman, L. J., Liebler, D. C., Ping, J., Liu, Q., Evans, R., Fissell, W. H., Patton, J. G., Rome, L. H., Burnette, D. T., & Coffey, R. J. (2019). Reassessment of Exosome Composition. Cell, 177(2), 428-445.e18. https://doi.org/10.1016/j.cell.2019.02.029

Jeppesen, D. K., Hvam, M. L., Primdahl-Bengtson, B., Boysen, A. T., Whitehead, B., Dyrskjøt, L., Ørntoft, T. F., Howard, K. A., & Ostenfeld, M. S. (2014). Comparative analysis of discrete exosome fractions obtained by differential centrifugation. Journal of Extracellular Vesicles, 3(1), 25011. https://doi.org/10.3402/jev.v3.25011

Jeyaram, A., & Jay, S. M. (2018). Preservation and Storage Stability of Extracellular Vesicles for Therapeutic Applications. The AAPS Journal, 20(1), 1. https://doi.org/10.1208/s12248-017-0160-y

Ji, Y., Chen, X., Liu, X., Huang, J., & Liu, P. (2024). lncRNA POLR2J4 Plays a Biomarker Role in Hepatitis B Virus-Related Hepatocellular Carcinoma Through Regulating miR-214-3p. Turkish Journal of Gastroenterology, 35(10), 787–794. https://doi.org/10.5152/tjg.2024.24150

Jiang, D., Jiang, Z., Lu, D., Wang, X., Liang, H., Zhang, J., Meng, Y., Li, Y., Wu, D., Huang, Y., Chen, Y., Deng, H., Wu, Q., Xiong, J., Meng, A., & Yu, L. (2019). Migrasomes provide regional cues for organ morphogenesis during zebrafish gastrulation. Nature Cell Biology, 21(8), 966–977. https://doi.org/10.1038/s41556-019-0358-6

Jiang, F., Chen, Q., Wang, W., Ling, Y., Yan, Y., & Xia, P. (2020). Hepatocyte-derived extracellular vesicles promote endothelial inflammation and atherogenesis via microRNA-1. Journal of Hepatology, 72(1), 156–166. https://doi.org/10.1016/j.jhep.2019.09.014

Jiang, S., Li, X., Li, Y., Chang, Z., Yuan, M., Zhang, Y., Zhu, H., Xiu, Y., Cong, H., Yin, L., Yu, Z.-W., Fan, J., He, W., Shi, K., Tian, D.-C., Zhang, J., Verkhratsky, A., Jin, W.-N., & Shi, F.-D. (2024). APOE from patient-derived astrocytic extracellular vesicles alleviates neuromyelitis optica spectrum disorder in a mouse model. Science Translational Medicine, 16(736), eadg5116. https://doi.org/10.1126/scitranslmed.adg5116

Jiang, S., Xia, R., Jiang, Y., Wang, L., & Gao, F. (2014). Vascular Endothelial Growth Factors Enhance the Permeability of the Mouse Blood-brain Barrier. PLoS ONE, 9(2), e86407. https://doi.org/10.1371/journal.pone.0086407

Jiao, H., Jiang, D., Hu, X., Du, W., Ji, L., Yang, Y., Li, X., Sho, T., Wang, X., Li, Y., Wu, Y.-T., Wei, Y.-H., Hu, X., & Yu, L. (2021). Mitocytosis, a migrasome-mediated mitochondrial quality-control process. Cell, 184(11), 2896-2910.e13. https://doi.org/10.1016/j.cell.2021.04.027

Jiao, H., Wang, Z., Liu, Y., Wang, P., & Xue, Y. (2011). Specific Role of Tight Junction Proteins Claudin-5, Occludin, and ZO-1 of the Blood–Brain Barrier in a Focal Cerebral Ischemic Insult. Journal of Molecular Neuroscience, 44(2), 130–139. https://doi.org/10.1007/s12031-011-9496-4

Jin, Y., Xu, M., Zhu, H., Dong, C., Ji, J., Liu, Y., Deng, A., & Gu, Z. (2021). Therapeutic effects of bone marrow mesenchymal stem cells-derived exosomes on osteoarthritis. Journal of Cellular and Molecular Medicine, 25(19), 9281–9294. https://doi.org/10.1111/jcmm.16860

Jiwaji, Z., Tiwari, S. S., Avilés-Reyes, R. X., Hooley, M., Hampton, D., Torvell, M., Johnson, D. A., McQueen, J., Baxter, P., Sabari-Sankar, K., Qiu, J., He, X., Fowler, J., Febery, J., Gregory, J., Rose, J., Tulloch, J., Loan, J., Story, D., … Hardingham, G. E. (2022). Reactive astrocytes acquire neuroprotective as well as deleterious signatures in response to Tau and Aß pathology. Nature Communications, 13(1), 135. https://doi.org/10.1038/s41467-021-27702-w

Johnstone, R. M., Adam, M., Hammond, J. R., Orr, L., & Turbide, C. (1987). Vesicle formation during reticulocyte maturation. Association of plasma membrane activities with released vesicles (exosomes). The Journal of Biological Chemistry, 262(19), 9412–9420.

Johnstone, R. M., Bianchini, A., & Teng, K. (1989). Reticulocyte maturation and exosome release: Transferrin receptor containing exosomes shows multiple plasma membrane functions. Blood, 74(5), 1844–1851.

Johnstone, R. M., Mathew, A., Mason, A. B., & Teng, K. (1991). Exosome formation during maturation of mammalian and avian reticulocytes: Evidence that exosome release is a major route for externalization of obsolete membrane proteins. Journal of Cellular Physiology, 147(1), 27–36. https://doi.org/10.1002/jcp.1041470105

Jostock, T., Müllberg, J., Özbek, S., Atreya, R., Blinn, G., Voltz, N., Fischer, M., Neurath, M. F., & Rose-John, S. (2001). Soluble gp130 is the natural inhibitor of soluble interleukin-6 receptor transsignaling responses. European Journal of Biochemistry, 268(1), 160–167. https://doi.org/10.1046/j.1432-1327.2001.01867.x

Jung, H.-G., Yu, B., Choi, Y., Go, G., Zhang, Q., Tang, Y., Kim, M. W., & Cai, D. (2025). Control of aging-associated neurodegeneration via hypothalamic extracellular vesicles containing parathymosin. Cell Reports, 44(11), 116561. https://doi.org/10.1016/j.celrep.2025.116561

Jurgielewicz, B. J., Yao, Y., & Stice, S. L. (2020). Kinetics and Specificity of HEK293T Extracellular Vesicle Uptake using Imaging Flow Cytometry. Nanoscale Research Letters, 15(1). https://doi.org/10.1186/s11671-020-03399-6

Kahr, W. H. A., Lo, R. W., Li, L., Pluthero, F. G., Christensen, H., Ni, R., Vaezzadeh, N., Hawkins, C. E., Weyrich, A. S., Di Paola, J., Landolt-Marticorena, C., & Gross, P. L. (2013). Abnormal megakaryocyte development and platelet function in Nbeal2−/− mice. Blood, 122(19), 3349–3358. https://doi.org/10.1182/blood-2013-04-499491

Kajimoto, T., Okada, T., Miya, S., Zhang, L., & Nakamura, S. (2013). Ongoing activation of sphingosine 1-phosphate receptors mediates maturation of exosomal multivesicular endosomes. Nature Communications, 4(1), 2712. https://doi.org/10.1038/ncomms3712

Kállai-Szabó, N., Farkas, D., Lengyel, M., Basa, B., Fleck, C., & Antal, I. (2024). Microparticles and multi-unit systems for advanced drug delivery. European Journal of Pharmaceutical Sciences, 194, 106704. https://doi.org/10.1016/j.ejps.2024.106704

Kamerkar, S., LeBleu, V. S., Sugimoto, H., Yang, S., Ruivo, C. F., Melo, S. A., Lee, J. J., & Kalluri, R. (2017). Exosomes facilitate therapeutic targeting of oncogenic KRAS in pancreatic cancer. Nature, 546(7659), 498–503. https://doi.org/10.1038/nature22341

Kang, H., Liu, T., Wang, Y., Bai, W., Luo, Y., & Wang, J. (2024). Neutrophil–macrophage communication via extracellular vesicle transfer promotes itaconate accumulation and ameliorates cytokine storm syndrome. Cellular & Molecular Immunology, 21(7), 689–706. https://doi.org/10.1038/s41423-024-01174-6

Karimi, N., Cvjetkovic, A., Jang, S. C., Crescitelli, R., Hosseinpour Feizi, M. A., Nieuwland, R., Lötvall, J., & Lässer, C. (2018). Detailed analysis of the plasma extracellular vesicle proteome after separation from lipoproteins. Cellular and Molecular Life Sciences, 75(15), 2873–2886. https://doi.org/10.1007/s00018-018-2773-4

Karimi, N., Dalirfardouei, R., Dias, T., Lötvall, J., & Lässer, C. (2022). Tetraspanins distinguish separate extracellular vesicle subpopulations in human serum and plasma – Contributions of platelet extracellular vesicles in plasma samples. Journal of Extracellular Vesicles, 11(5), e12213. https://doi.org/10.1002/jev2.12213

Karlsson, M., Lundin, S., Dahlgren, U., Kahu, H., Pettersson, I., & Telemo, E. (2001). 'Tolerosomes' are produced by intestinal epithelial cells. European Journal of Immunology, 31(10), 2892–2900. https://doi.org/10.1002/1521-4141(2001010)31:10%3C2892::AID-IMMU2892%3E3.0.CO;2-I

Kassem, P. H., Montasser, I. F., Mahmoud, R. M., Ghorab, R. A., AbdelHakam, D. A., Fathi, M. E. S. A., Wahed, M. A. A., Mohey, K., Ibrahim, M., Hadidi, M. E., Masssoud, Y. M., Salah, M., Abugable, A., Bahaa, M., Khamisy, S. E., & Meteini, M. E. (2024). Genomic landscape of hepatocellular carcinoma in Egyptian patients by whole exome sequencing. BMC Medical Genomics, 17(1), 202. https://doi.org/10.1186/s12920-024-01965-w

Kat, M., Van Moort, I., Bürgisser, P. E., Kuijpers, T. W., Hofman, M., Favier, M., Favier, R., Margadant, C., Voorberg, J., & Bierings, R. (2023). Mutations in Neurobeachin-like 2 do not impact Weibel-Palade body biogenesis and von Willebrand factor secretion in gray platelet syndrome Endothelial Colony Forming Cells. Research and Practice in Thrombosis and Haemostasis, 7(2), 100086. https://doi.org/10.1016/j.rpth.2023.100086

Kawakita, S., Li, S., Nguyen, H. T., Maity, S., Haghniaz, R., Bahari, J., Yu, N., Mandal, K., Bandaru, P., Mou, L., Ermis, M., Khalil, E., Khosravi, S., Peirsman, A., Nasiri, R., Adachi, A., Nakayama, A., Bell, R., Zhu, Y., … Khademhosseini, A. (2023). Rapid integration of screen-printed electrodes into thermoplastic organ-on-a-chip devices for real-time monitoring of trans-endothelial electrical resistance. Biomedical Microdevices, 25(4), 37. https://doi.org/10.1007/s10544-023-00669-9

Kedersha, N. L., & Rome, L. H. (1986). Isolation and characterization of a novel ribonucleoprotein particle: Large structures contain a single species of small RNA. The Journal of Cell Biology, 103(3), 699–709. https://doi.org/10.1083/jcb.103.3.699

Kennedy, D., Mnich, K., Oommen, D., Chakravarthy, R., Almeida-Souza, L., Krols, M., Saveljeva, S., Doyle, K., Gupta, S., Timmerman, V., Janssens, S., Gorman, A. M., & Samali, A. (2017). HSPB1 facilitates ERK-mediated phosphorylation and degradation of BIM to attenuate endoplasmic reticulum stress-induced apoptosis. Cell Death & Disease, 8(8), e3026–e3026. https://doi.org/10.1038/cddis.2017.408

Khoo, A., Govindarajan, M., Qiu, Z., Liu, L. Y., Ignatchenko, V., Waas, M., Macklin, A., Keszei, A., Neu, S., Main, B. P., Yang, L., Lance, R. S., Downes, M. R., Semmes, O. J., Vesprini, D., Liu, S. K., Nyalwidhe, J. O., Boutros, P. C., & Kislinger, T. (2024). Prostate cancer reshapes the secreted and extracellular vesicle urinary proteomes. Nature Communications, 15(1), 5069. https://doi.org/10.1038/s41467-024-49424-5

Ki, M. K., Jeoung, M. H., Choi, J. R., Rho, S.-S., Kwon, Y.-G., Shim, H., Chung, J., Hong, H. J., Song, B. D., & Lee, S. (2013). Human antibodies targeting the C-type lectin-like domain of the tumor endothelial cell marker clec14a regulate angiogenic properties in vitro. Oncogene, 32(48), 5449–5457. https://doi.org/10.1038/onc.2013.156

Kiernan, J. A. (1996). Vascular permeability in the peripheral autonomic and somatic nervous systems: Controversial aspects and comparisons with the blood-brain barrier. Microscopy Research and Technique, 35(2), 122–136. https://doi.org/10.1002/(SICI)1097-0029(19961001)35:2%3C122::AID-JEMT3%3E3.0.CO;2-S

Kim, C.-Y., Lee, K.-H., Son, K. H., Shin, T.-J., & Cho, J.-Y. (2024). Extracellular vesicle-mediated transfer of miRNA-1 from primary tumors represses the growth of distant metastases. Experimental & Molecular Medicine, 56(3), 734–746. https://doi.org/10.1038/s12276-024-01181-7

Kim, H., Leng, K., Park, J., Sorets, A. G., Kim, S., Shostak, A., Embalabala, R. J., Mlouk, K., Katdare, K. A., Rose, I. V. L., Sturgeon, S. M., Neal, E. H., Ao, Y., Wang, S., Sofroniew, M. V., Brunger, J. M., McMahon, D. G., Schrag, M. S., Kampmann, M., & Lippmann, E. S. (2022). Reactive astrocytes transduce inflammation in a blood-brain barrier model through a TNF-STAT3 signaling axis and secretion of alpha 1-antichymotrypsin. Nature Communications, 13(1), 6581. https://doi.org/10.1038/s41467-022-34412-4

Kim, R. Y., Hoffman, A. S., Itoh, N., Ao, Y., Spence, R., Sofroniew, M. V., & Voskuhl, R. R. (2014). Astrocyte CCL2 sustains immune cell infiltration in chronic experimental autoimmune encephalomyelitis. Journal of Neuroimmunology, 274(1–2), 53–61. https://doi.org/10.1016/j.jneuroim.2014.06.009

Kim, S., Oh, I., Kim, J., Lee, N., Go, J., Jin, Y., Kim, W. J., & Lee, H. (2025). Efficient dispersion of aggregated extracellular vesicles: A comparative study of water-bath sonication and regular pipetting. Scientific Reports, 15(1), 25261. https://doi.org/10.1038/s41598-025-10050-w

Kim, T., Bae, S.-C., & Kang, C. (2020). Synergistic activation of NF-κB by TNFAIP3 (A20) reduction and UBE2L3 (UBCH7) augment that synergistically elevate lupus risk. Arthritis Research & Therapy, 22(1), 93. https://doi.org/10.1186/s13075-020-02181-4

Kim, W., Kim, J., Lee, S.-Y., Kim, H.-M., Joo, K. M., & Nam, D.-H. (2022). Simplified in vitro 3D co-culture-based blood-brain barrier model using transwell. Biochemical and Biophysical Research Communications, 620, 63–68. https://doi.org/10.1016/j.bbrc.2022.06.083

Kim, Y., Lee, S., Zhang, H., Lee, S., Kim, H., Kim, Y., Won, M.-H., Kim, Y.-M., & Kwon, Y.-G. (2020). CLEC14A deficiency exacerbates neuronal loss by increasing blood-brain barrier permeability and inflammation. Journal of Neuroinflammation, 17(1), 48. https://doi.org/10.1186/s12974-020-1727-6

Kimura, I., Dohgu, S., Takata, F., Matsumoto, J., Watanabe, T., Iwao, T., Yamauchi, A., & Kataoka, Y. (2020). Oligodendrocytes upregulate blood-brain barrier function through mechanisms other than the PDGF-BB/PDGFRα pathway in the barrier-tightening effect of oligodendrocyte progenitor cells. Neuroscience Letters, 715, 134594. https://doi.org/10.1016/j.neulet.2019.134594

King, M., Nafar, F., Clarke, J., & Mearow, K. (2009). The small heat shock protein Hsp27 protects cortical neurons against the toxic effects of β-amyloid peptide. Journal of Neuroscience Research, 87(14), 3161–3175. https://doi.org/10.1002/jnr.22145

Kirken, R. A., Rui, H., Malabarba, M. G., & Farrar, W. L. (1994). Identification of interleukin-2 receptor-associated tyrosine kinase p116 as novel leukocyte-specific Janus kinase. Journal of Biological Chemistry, 269(29), 19136–19141. https://doi.org/10.1016/S0021-9258(17)32285-8

Koçak, G., Güzel, B. N., Mıhçı, E., Küpesiz, O. A., Yalçın, K., & Manguoğlu, A. E. (2019). TCIRG1 and SNX10 gene mutations in the patients with autosomal recessive osteopetrosis. Gene, 702, 83–88. https://doi.org/10.1016/j.gene.2019.02.088

Konoshenko, M. Yu., Lekchnov, E. A., Vlassov, A. V., & Laktionov, P. P. (2018). Isolation of Extracellular Vesicles: General Methodologies and Latest Trends. BioMed Research International, 2018, 1–27. https://doi.org/10.1155/2018/8545347

Kotsyuba, E., & Dyachuk, V. (2022). Effect of Air Exposure-Induced Hypoxia on Neurotransmitters and Neurotransmission Enzymes in Ganglia of the Scallop Azumapecten farreri. International Journal of Molecular Sciences, 23(4), 2027. https://doi.org/10.3390/ijms23042027

Kriaučiūnaitė, K., Kaušylė, A., Pajarskienė, J., Tunaitis, V., Lim, D., Verkhratsky, A., & Pivoriūnas, A. (2021). Immortalised Hippocampal Astrocytes from 3xTG-AD Mice Fail to Support BBB Integrity In Vitro: Role of Extracellular Vesicles in Glial-Endothelial Communication. Cellular and Molecular Neurobiology, 41(3), 551–562. https://doi.org/10.1007/s10571-020-00871-w

Kruse, K., Lee, Q. S., Sun, Y., Klomp, J., Yang, X., Huang, F., Sun, M. Y., Zhao, S., Hong, Z., Vogel, S. M., Shin, J.-W., Leckband, D. E., Tai, L. M., Malik, A. B., & Komarova, Y. A. (2019). N-cadherin signaling via Trio assembles adherens junctions to restrict endothelial permeability. Journal of Cell Biology, 218(1), 299–316. https://doi.org/10.1083/jcb.201802076

Kuba, K., Zhang, L., Imai, Y., Arab, S., Chen, M., Maekawa, Y., Leschnik, M., Leibbrandt, A., Markovic, M., Schwaighofer, J., Beetz, N., Musialek, R., Neely, G. G., Komnenovic, V., Kolm, U., Metzler, B., Ricci, R., Hara, H., Meixner, A., … Penninger, J. M. (2007). Impaired Heart Contractility in Apelin Gene–Deficient Mice Associated With Aging and

Pressure Overload. Circulation Research, 101(4). https://doi.org/10.1161/CIRCRESAHA.107.158659

Kubotera, H., Ikeshima-Kataoka, H., Hatashita, Y., Allegra Mascaro, A. L., Pavone, F. S., & Inoue, T. (2019). Astrocytic endfeet re-cover blood vessels after removal by laser ablation. Scientific Reports, 9(1), 1263. https://doi.org/10.1038/s41598-018-37419-4

Kulczar, C., Lubin, K. E., Lefebvre, S., Miller, D. W., & Knipp, G. T. (2017). Development of a direct contact astrocyte-human cerebral microvessel endothelial cells blood–brain barrier coculture model. Journal of Pharmacy and Pharmacology, 69(12), 1684–1696. https://doi.org/10.1111/jphp.12803

Kumar, A., Su, Y., Sharma, M., Singh, S., Kim, S., Peavey, J. J., Suerken, C. K., Lockhart, S. N., Whitlow, C. T., Craft, S., Hughes, T. M., & Deep, G. (2023). MicroRNA expression in extracellular vesicles as a novel blood-based biomarker for Alzheimer's disease. Alzheimer's & Dementia, 19(11), 4952–4966. https://doi.org/10.1002/alz.13055

Kumar, D., Manek, R., Raghavan, V., & Wang, K. K. (2018). Protein Characterization of Extracellular Microvesicles/Exosomes Released from Cytotoxin-Challenged Rat Cerebrocortical Mixed Culture and Mouse N2a Cells. Molecular Neurobiology, 55(3), 2112–2124. https://doi.org/10.1007/s12035-017-0474-x

Kumar, M. A., Baba, S. K., Sadida, H. Q., Marzooqi, S. Al., Jerobin, J., Altemani, F. H., Algehainy, N., Alanazi, M. A., Abou-Samra, A.-B., Kumar, R., Al-Shabeeb Akil, A. S., Macha, M. A., Mir, R., & Bhat, A. A. (2024). Extracellular vesicles as tools and targets in therapy for diseases. Signal Transduction and Targeted Therapy, 9(1), 27. https://doi.org/10.1038/s41392-024-01735-1

Kumar, S., Žigman, M., Patel, T. R., Trageser, B., Gross, J. C., Rahm, K., Boutros, M., Gradl, D., Steinbeisser, H., Holstein, T., Stetefeld, J., & Özbek, S. (2014). Molecular dissection of Wnt3a-Frizzled8 interaction reveals essential and modulatory determinants of Wnt signaling activity. BMC Biology, 12(1), 44. https://doi.org/10.1186/1741-7007-12-44

Kumskova, M., Flora, G. D., Nayak, M. K., Budnik, I., Jain, A., Patel, R. B., Jha, A. B., Ghatge, M., Chauhan, N., Michael, J. V., McKenzie, S. E., Sharathkumar, A., Staber, J. M., Lentz, S. R., & Chauhan, A. (2025). Platelet defects in patients and mice with Ehlers-Danlos syndrome. Blood Journal, blood.2025029912. https://doi.org/10.1182/blood.2025029912

Kuo, Y.-C., & Lu, C.-H. (2011). Effect of human astrocytes on the characteristics of human brain-microvascular endothelial cells in the blood–brain barrier. Colloids and Surfaces B: Biointerfaces, 86(1), 225–231. https://doi.org/10.1016/j.colsurfb.2011.04.005

Kurosawa, T., Sako, D., Tega, Y., Debori, Y., Tomihara, Y., Aoyama, K., Kubo, Y., Amano, N., & Deguchi, Y. (2022). Construction and Functional Evaluation of a Three-Dimensional Blood–Brain Barrier Model Equipped With Human Induced Pluripotent Stem Cell-Derived Brain Microvascular Endothelial Cells. Pharmaceutical Research, 39(7), 1535–1547. https://doi.org/10.1007/s11095-022-03249-3

Laemmli, U. K. (1970). Cleavage of Structural Proteins during the Assembly of the Head of Bacteriophage T4. Nature, 227(5259), 680–685. https://doi.org/10.1038/227680a0

Lahera, A., Vela-Martín, L., Fernández-Navarro, P., Llamas, P., López-Lorenzo, J. L., Cornago, J., Santos, J., Fernández-Piqueras, J., & Villa-Morales, M. (2024). The JAK3^{Q988P}

mutation reveals oncogenic potential and resistance to ruxolitinib. Molecular Carcinogenesis, 63(1), 5–10. https://doi.org/10.1002/mc.23632

Laksitorini, M. D., Yathindranath, V., Xiong, W., Hombach-Klonisch, S., & Miller, D. W. (2019). Modulation of Wnt/β-catenin signaling promotes blood-brain barrier phenotype in cultured brain endothelial cells. Scientific Reports, 9(1), 19718. https://doi.org/10.1038/s41598-019-56075-w

Lammerding, J., Schulze, P. C., Takahashi, T., Kozlov, S., Sullivan, T., Kamm, R. D., Stewart, C. L., & Lee, R. T. (2004). Lamin A/C deficiency causes defective nuclear mechanics and mechanotransduction. Journal of Clinical Investigation, 113(3), 370–378. https://doi.org/10.1172/JCI200419670

Langevin, S., Kuhnell, D., Parry, T., Biesiada, J., Huang, S., Wise-Draper, T., Casper, K., Zhang, X., Medvedovic, M., & Kasper, S. (2017). Comprehensive microRNA-sequencing of exosomes derived from head and neck carcinoma cells in vitro reveals common secretion profiles and potential utility as salivary biomarkers. Oncotarget, 8(47), 82459–82474. https://doi.org/10.18632/oncotarget.19614

Lattke, M., Goldstone, R., Ellis, J. K., Boeing, S., Jurado-Arjona, J., Marichal, N., MacRae, J. I., Berninger, B., & Guillemot, F. (2021). Extensive transcriptional and chromatin changes underlie astrocyte maturation in vivo and in culture. Nature Communications, 12(1), 4335. https://doi.org/10.1038/s41467-021-24624-5

Laulagnier, K., Javalet, C., Hemming, F. J., Chivet, M., Lachenal, G., Blot, B., Chatellard, C., & Sadoul, R. (2018). Amyloid precursor protein products concentrate in a subset of exosomes specifically endocytosed by neurons. Cellular and Molecular Life Sciences, 75(4), 757–773. https://doi.org/10.1007/s00018-017-2664-0

Leak, R. K., Zhang, L., Stetler, R. A., Weng, Z., Li, P., Atkins, G. B., Gao, Y., & Chen, J. (2013). HSP27 Protects the Blood-Brain Barrier Against Ischemia-Induced Loss of Integrity. CNS & Neurological Disorders - Drug Targets, 12(3), 325–337. https://doi.org/10.2174/1871527311312030006

LeBleu, V. S., MacDonald, B., & Kalluri, R. (2007). Structure and Function of Basement Membranes. Experimental Biology and Medicine, 232(9), 1121–1129. https://doi.org/10.3181/0703-MR-72

Lebovitz, R. M., Zhang, H., Vogel, H., Cartwright, J., Dionne, L., Lu, N., Huang, S., & Matzuk, M. M. (1996). Neurodegeneration, myocardial injury, and perinatal death in mitochondrial superoxide dismutase-deficient mice. Proceedings of the National Academy of Sciences, 93(18), 9782–9787. https://doi.org/10.1073/pnas.93.18.9782

Lee, D. K., Cheng, R., Nguyen, T., Fan, T., Kariyawasam, A. P., Liu, Y., Osmond, D. H., George, S. R., & O'Dowd, B. F. (2000). Characterization of Apelin, the Ligand for the APJ Receptor. Journal of Neurochemistry, 74(1), 34–41. https://doi.org/10.1046/j.1471-4159.2000.0740034.x

Lee, J., Ortega-Rodriguez, U., Madhavarao, C. N., Ju, T., O'Connor, T., Ashraf, M., & Yoon, S. (2025). Effect of different cell culture media on the production and glycosylation of a monoclonal antibody from a CHO cell line. Cytotechnology, 77(3), 81. https://doi.org/10.1007/s10616-025-00733-7

Lee, J.-H., Kim, J., Noh, S., Lee, H., Lee, S. Y., Mun, J. Y., Park, H., & Chung, W.-S. (2021). Astrocytes phagocytose adult hippocampal synapses for circuit homeostasis. Nature, (590), 612–617. https://doi.org/10.1038/s41586-020-03060-3

Lee, K. S., Lee, J., Kim, H. K., Yeom, S. H., Woo, C. H., Jung, Y. J., Yun, Y. E., Park, S. Y., Han, J., Kim, E., Sul, J. H., Jung, J. M., Park, J. H., Choi, J. S., Cho, Y. W., & Jo, D. (2021). Extracellular vesicles from adipose tissue-derived stem cells alleviate osteoporosis through osteoprotegerin and miR-21-5p. Journal of Extracellular Vesicles, 10(12), e12152. https://doi.org/10.1002/jev2.12152

Lee, Y. J., Shin, K. J., Jang, H.-J., Ryu, J.-S., Lee, C. Y., Yoon, J. H., Seo, J. K., Park, S., Lee, S., Je, A. R., Huh, Y. H., Kong, S.-Y., Kwon, T., Suh, P.-G., & Chae, Y. C. (2023). GPR143 controls ESCRT-dependent exosome biogenesis and promotes cancer metastasis. Developmental Cell, 58(4), 320-334.e8. https://doi.org/10.1016/j.devcel.2023.01.006

Lennon, R., & Sherwood, D. R. (2025). Basement membranes at a glance. Journal of Cell Science, 138(17), jcs263947. https://doi.org/10.1242/jcs.263947

Leopold, B., Strutz, J., Weiß, E., Gindlhuber, J., Birner-Gruenberger, R., Hackl, H., Appel, H. M., Cvitic, S., & Hiden, U. (2019). Outgrowth, proliferation, viability, angiogenesis and phenotype of primary human endothelial cells in different purchasable endothelial culture media: Feed wisely. Histochemistry and Cell Biology, 152(5), 377–390. https://doi.org/10.1007/s00418-019-01815-2

Levy-Myers, R., Daudelin, D., Na, C. H., & Sockanathan, S. (2023). An independent regulator of global release pathways in astrocytes generates a subtype of extracellular vesicles required for postsynaptic function. Science Advances, 9(25). https://doi.org/10.1126/sciadv.adg2067

Lewandowsky, M. (1900). Zur lehre der cerebrospinal flüssigkeit. Z Klinische Medizin, (40), 480–490.

Li, B., Zang, G., Zhong, W., Chen, R., Zhang, Y., Yang, P., & Yan, J. (2020). Activation of CD137 signaling promotes neointimal formation by attenuating TET2 and transferrring from endothelial cell-derived exosomes to vascular smooth muscle cells. Biomedicine & Pharmacotherapy, 121, 109593. https://doi.org/10.1016/j.biopha.2019.109593

Li, H., Zhao, Y., Dai, R., Geng, P., Weng, D., Wu, W., Yu, F., Lin, R., Wu, Z., Li, Y., & Luo, M. (2025). Astrocytes release ATP/ADP and glutamate in flashes via vesicular exocytosis. Molecular Psychiatry, 30(6), 2475–2489. https://doi.org/10.1038/s41380-024-02851-8

Li, K., Wang, S., Li, J., Wang, L., Zhang, Q., Hou, L., Yu, X., Liu, Z., Lv, T., & Shang, L. (2025). Low shear stress induces vascular endothelial cells apoptosis via miR-330 /SOD2 /HSP70 signaling pathway. Experimental Cell Research, 445(1), 114410. https://doi.org/10.1016/j.yexcr.2025.114410

Li, M., Tang, Q., Liao, C., Wang, Z., Zhang, S., Liang, Q., Liang, C., Liu, X., Zhang, J., Tian, W., & Liao, L. (2024). Extracellular vesicles from apoptotic BMSCs ameliorate osteoporosis via transporting regenerative signals. Theranostics, 14(9), 3583–3602. https://doi.org/10.7150/thno.96174

Li, S., Fang, Y., Zhang, Y., Song, M., Zhang, X., Ding, X., Yao, H., Chen, M., Sun, Y., Ding, J., Wang, Q., Lu, M., Wu, G., & Hu, G. (2022). Microglial NLRP3 inflammasome

activates neurotoxic astrocytes in depression-like mice. Cell Reports, 41(4), 111532. https://doi.org/10.1016/j.celrep.2022.111532

Li, S., Liu, J., Zhao, M., Su, Y., Cong, B., & Wang, Z. (2024). RNA quality score evaluation: A preliminary study of RNA integrity number (RIN) and RNA integrity and quality number (RNA IQ). Forensic Science International, 357, 111976. https://doi.org/10.1016/j.forsciint.2024.111976

Li, S., Zhang, S., Chen, Z., Zhang, X., Ou, R., Wei, S., Liu, Y., Xu, Y., Chen, K., Chen, Z., & Shu, X. (2023). How to process synovial fluid samples of gouty arthritis and extract its exosomes for subsequent cytokine analysis. Medicine, 102(31), e34552. https://doi.org/10.1097/MD.0000000000034552

Li, T., Liu, T., Chen, X., Li, L., Feng, M., Zhang, Y., Wan, L., Zhang, C., & Yao, W. (2020). Microglia induce the transformation of A1/A2 reactive astrocytes via the CXCR7/PI3K/Akt pathway in chronic post-surgical pain. Journal of Neuroinflammation, 17(1), 211. https://doi.org/10.1186/s12974-020-01891-5

Li, W., Niu, X., Dai, Y., Wu, X., Li, J., & Sheng, W. (2023). Rnf-213 Knockout Induces Pericyte Reduction and Blood-Brain Barrier Impairment in Mouse. Molecular Neurobiology, 60(11), 6188–6200. https://doi.org/10.1007/s12035-023-03480-y

Li, X., Cao, Y., Xu, X., Wang, C., Ni, Q., Lv, X., Yang, C., Zhang, Z., Qi, X., & Song, G. (2023). Sleep Deprivation Promotes Endothelial Inflammation and Atherogenesis by Reducing Exosomal miR-182-5p. Arteriosclerosis, Thrombosis, and Vascular Biology, 43(6), 995–1014. https://doi.org/10.1161/ATVBAHA.123.319026

Li, X.-T., Zhang, M.-W., Zhang, Z.-Z., Cao, Y.-D., Liu, X.-Y., Miao, R., Xu, Y., Song, X.-F., Song, J.-W., Liu, Y., Xu, Y.-L., Li, J., Dong, Y., & Zhong, J.-C. (2021). Abnormal apelin-ACE2 and SGLT2 signaling contribute to adverse cardiorenal injury in patients with COVID-19. International Journal of Cardiology, 336, 123–129. https://doi.org/10.1016/j.ijcard.2021.05.029

Li, Y., Liu, B., Zhao, T., Quan, X., Han, Y., Cheng, Y., Chen, Y., Shen, X., Zheng, Y., & Zhao, Y. (2023). Comparative study of extracellular vesicles derived from mesenchymal stem cells and brain endothelial cells attenuating blood–brain barrier permeability via regulating Caveolin-1-dependent ZO-1 and Claudin-5 endocytosis in acute ischemic stroke. Journal of Nanobiotechnology, 21(1). https://doi.org/10.1186/s12951-023-01828-z

Li, Y., Wu, Y., Federzoni, E. A., Wang, X., Dharmawan, A., Hu, X., Wang, H., Hawley, R. J., Stevens, S., Sykes, M., & Yang, Y.-G. (2022). CD47 cross-dressing by extracellular vesicles expressing CD47 inhibits phagocytosis without transmitting cell death signals. eLife, 11, e73677. https://doi.org/10.7554/eLife.73677

Liam-Or, R., Faruqu, F. N., Walters, A., Han, S., Xu, L., Wang, J. T.-W., Oberlaender, J., Sanchez-Fueyo, A., Lombardi, G., Dazzi, F., Mailaender, V., & Al-Jamal, K. T. (2024). Cellular uptake and in vivo distribution of mesenchymal-stem-cell-derived extracellular vesicles are protein corona dependent. Nature Nanotechnology, 19(6), 846–855. https://doi.org/10.1038/s41565-023-01585-y

Liang, F., Huang, N., Tian, Y., Fang, Y., Huang, C., Qiu, B., Lu, T., Zheng, L., Cheng, J., Zhu, B., & Zhao, J. (2025). Extracellular vesicle-derived lncRNA VIM-AS1 promotes diabetic wound healing by promoting glycolysis and alleviating cellular senescence. Stem Cell Research & Therapy, 16(1), 341. https://doi.org/10.1186/s13287-025-04451-x

Liang, X., Gupta, D., Xie, J., Van Wonterghem, E., Van Hoecke, L., Hean, J., Niu, Z., Ghaeidamini, M., Wiklander, O. P. B., Zheng, W., Wiklander, R. J., He, R., Mamand, D. R., Bost, J., Zhou, G., Zhou, H., Roudi, S., Estupiñán, H. Y., Rädler, J., … El Andaloussi, S. (2025). Engineering of extracellular vesicles for efficient intracellular delivery of multimodal therapeutics including genome editors. Nature Communications, 16(1), 4028. https://doi.org/10.1038/s41467-025-59377-y

Liao, K., Niu, F., Hu, G., & Buch, S. (2022). Morphine-mediated release of astrocyte-derived extracellular vesicle miR-23a induces loss of pericyte coverage at the blood-brain barrier: Implications for neuroinflammation. Frontiers in Cell and Developmental Biology, 10, 984375. https://doi.org/10.3389/fcell.2022.984375

Liao, K., Niu, F., Hu, G., Yang, L., Dallon, B., Villarreal, D., & Buch, S. (2020). Morphine-mediated release of miR-138 in astrocyte-derived extracellular vesicles promotes microglial activation. Journal of Extracellular Vesicles, 10(1), e12027. https://doi.org/10.1002/jev2.12027

Liao, T.-L., Chen, D.-Y., Hsieh, S.-L., Yang, Y.-Y., Chen, Y.-M., Tang, K.-T., Chang, C.-H., & Yang, S.-S. (2025). Platelet-derived mitochondria regulate lipid metabolism in nonalcoholic steatohepatitis through extracellular vesicles. Hepatology, 82(3), 722–738. https://doi.org/10.1097/HEP.0000000000001149

Liao, Y., Wu, N., Guo, L., & Yang, D. (2024). CLEC14A facilitates angiogenesis and alleviates inflammation in diabetic wound healing. Life Sciences, 358, 123176. https://doi.org/10.1016/j.lfs.2024.123176

Libanje, F., Delille, R., Young, P. A., Rolland, S., Meyer-Losic, F., Lewkowicz, E., & Klinz, S. (2023). NTSR1 glycosylation and MMP dependent cleavage generate three distinct forms of the protein. Scientific Reports, 13(1), 4663. https://doi.org/10.1038/s41598-023-31790-7

Lichter-Konecki, U., Mangin, J. M., Gordish-dressman, H., Hoffman, E. P., & Gallo, V. (2008). Gene expression profiling of astrocytes from hyperammonemic mice reveals altered pathways for water and potassium homeostasis in vivo. Glia, 56(4), 365–377. https://doi.org/10.1002/glia.20624

Liddelow, S. A. (2011). Fluids and barriers of the CNS: A historical viewpoint. Fluids and Barriers of the CNS, 8(1), 2. https://doi.org/10.1186/2045-8118-8-2

Liddelow, S. A., & Barres, B. A. (2017). Reactive Astrocytes: Production, Function, and Therapeutic Potential. Immunity, 46(6), 957–967. https://doi.org/10.1016/j.immuni.2017.06.006

Liddelow, S. A., Guttenplan, K. A., Clarke, L. E., Bennett, F. C., Bohlen, C. J., Schirmer, L., Bennett, M. L., Münch, A. E., Chung, W.-S., Peterson, T. C., Wilton, D. K., Frouin, A., Napier, B. A., Panicker, N., Kumar, M., Buckwalter, M. S., Rowitch, D. H., Dawson, V. L., Dawson, T. M., … Barres, B. A. (2017). Neurotoxic reactive astrocytes are induced by activated microglia. Nature, 541(7638), 481–487. https://doi.org/10.1038/nature21029

Liebner, S., Fischmann, A., Rascher, G., Duffner, F., Grote, E.-H., Kalbacher, H., & Wolburg, H. (2000). Claudin-1 and claudin-5 expression and tight junction morphology are altered in blood vessels of human glioblastoma multiforme. Acta Neuropathologica, 100(3), 323–331. https://doi.org/10.1007/s004010000180

Lim, S. M., Cho, S. H., Hwang, I. G., Choi, J. W., Chang, H., Ahn, M.-J., Park, K. U., Kim, J.-W., Ko, Y. H., Ahn, H. K., Cho, B. C., Nam, B.-H., Chun, S. H., Hong, J. H., Kwon, J. H., Choi, J. G., Kang, E. J., Yun, T., Lee, K.-W., … Kim, H. R. (2019). Investigating the Feasibility of Targeted Next-Generation Sequencing to Guide the Treatment of Head and Neck Squamous Cell Carcinoma. Cancer Research and Treatment, 51(1), 300–312. https://doi.org/10.4143/crt.2018.012

Lindblom, P., Gerhardt, H., Liebner, S., Abramsson, A., Enge, M., Hellström, M., Bäckström, G., Fredriksson, S., Landegren, U., Nyström, H. C., Bergström, G., Dejana, E., Östman, A., Lindahl, P., & Betsholtz, C. (2003). Endothelial PDGF-B retention is required for proper investment of pericytes in the microvessel wall. Genes & Development, 17(15), 1835–1840. https://doi.org/10.1101/gad.266803

Linxweiler, J., Kolbinger, A., Himbert, D., Zeuschner, P., Saar, M., Stöckle, M., & Junker, K. (2021). Organ-Specific Uptake of Extracellular Vesicles Secreted by Urological Cancer Cells. Cancers, 13(19), 4937. https://doi.org/10.3390/cancers13194937

Lippmann, E. S., Al-Ahmad, A., Azarin, S. M., Palecek, S. P., & Shusta, E. V. (2014). A retinoic acid-enhanced, multicellular human blood-brain barrier model derived from stem cell sources. Scientific Reports, 4(1), 4160. https://doi.org/10.1038/srep04160

Liu, B., Chen, H., Johns, T. G., & Neufeld, A. H. (2006). Epidermal Growth Factor Receptor Activation: An Upstream Signal for Transition of Quiescent Astrocytes into Reactive Astrocytes after Neural Injury. The Journal of Neuroscience, 26(28), 7532–7540. https://doi.org/10.1523/JNEUROSCI.1004-06.2006

Liu, D., Liao, P., Li, H., Tong, S., Wang, B., Lu, Y., Gao, Y., Huang, Y., Zhou, H., Shi, L., Papadimitriou, J., Zong, Y., Yuan, J., Chen, P., Chen, Z., Ding, P., Zheng, Y., Zhang, C., Zheng, M., & Gao, J. (2024). Regulation of blood-brain barrier integrity by Dmp1 - expressing astrocytes through mitochondrial transfer. Science Advances, 10(26), eadk2913. https://doi.org/10.1126/sciadv.adk2913

Liu, H., Liu, X., Luo, S., Ma, R., Ge, W., Meng, S., & Gao, Y. (2024). Lamin A/C mediates microglial activation by modulating cell proliferation and immune response. Journal of Neuroscience Research, 102(1), e25263. https://doi.org/10.1002/jnr.25263

Liu, J., Gao, J., Guo, L., Ma, G., Guan, M., Xia, C., He, J., Yang, Y., Wu, Y., Xu, J., Xiong, L., Yu, C., Pei, G., Zhao, J., He, J., Zhang, Y., & Wang, W. (2025). Astrocyte Secretome Profiling via Biorthogonal Labeling Unveils Novel Factors Relevant to Neurodegenerative Diseases. Glia, 73(12), 2483–2498. https://doi.org/10.1002/glia.70079

Liu, J., Jin, X., Liu, K. J., & Liu, W. (2012). Matrix Metalloproteinase-2-Mediated Occludin Degradation and Caveolin-1-Mediated Claudin-5 Redistribution Contribute to Blood–Brain Barrier Damage in Early Ischemic Stroke Stage. The Journal of Neuroscience, 32(9), 3044. https://doi.org/10.1523/JNEUROSCI.6409-11.2012

Liu, J., Yan, S., Hu, J., Ding, D., Liu, Y., Li, X., Pan, H. S., Liu, G., Wu, B., & Liu, Y. (2021). MiRNA-4537 functions as a tumor suppressor in gastric cancer and increases the radiosensitivity of gastric cancer cells. Bioengineered, 12(1), 8457–8467. https://doi.org/10.1080/21655979.2021.1982843

Liu, L., MacKenzie, K. R., Putluri, N., Maletić-Savatić, M., & Bellen, H. J. (2017). The Glia-Neuron Lactate Shuttle and Elevated ROS Promote Lipid Synthesis in Neurons and

Lipid Droplet Accumulation in Glia via APOE/D. Cell Metabolism, 26(5), 719-737.e6. https://doi.org/10.1016/j.cmet.2017.08.024

Liu, L., Meng, L., Zhang, P., Lin, H., Chi, J., Peng, F., & Guo, H. (2018). Angiotensin II inhibits the protein expression of ZO-1 in vascular endothelial cells by downregulating VE-cadherin. Molecular Medicine Reports. https://doi.org/10.3892/mmr.2018.8991

Liu, W., Hendren, J., Qin, X.-J., Shen, J., & Liu, K. J. (2009). Normobaric hyperoxia attenuates early blood-brain barrier disruption by inhibiting MMP-9-mediated occludin degradation in focal cerebral ischemia. Journal of Neurochemistry, 108(3), 811–820. https://doi.org/10.1111/j.1471-4159.2008.05821.x

Liu, X., Chen, C., Jiang, Y., Wan, M., Jiao, B., Liao, X., Rao, S., Hong, C., Yang, Q., Zhu, Y., Liu, Q., Luo, Z., Duan, R., Wang, Y., Tan, Y., Cao, J., Liu, Z., Wang, Z., Xie, H., & Shen, L. (2023). Brain-derived extracellular vesicles promote bone-fat imbalance in Alzheimer's disease. International Journal of Biological Sciences, 19(8), 2409–2427. https://doi.org/10.7150/ijbs.79461

Liu, Y., Wang, W., Cui, X., Lyu, J., & Xie, Y. (2024). Exploring Genetic Associations of 3 Types of Risk Factors With Ischemic Stroke: An Integrated Bioinformatics Study. Stroke, 55(6), 1619–1628. https://doi.org/10.1161/STROKEAHA.123.044424

Liu, Y., Zhang, H., Wang, S., Guo, Y., Fang, X., Zheng, B., Gao, W., Yu, H., Chen, Z., Roman, R. J., & Fan, F. (2021). Reduced pericyte and tight junction coverage in old diabetic rats are associated with hyperglycemia-induced cerebrovascular pericyte dysfunction. American Journal of Physiology-Heart and Circulatory Physiology, 320(2), H549–H562. https://doi.org/10.1152/ajpheart.00726.2020

Liu, Z., Gou, Y., Zhang, H., Zuo, H., Zhang, H., Liu, Z., & Yao, D. (2014). Estradiol improves cardiovascular function through up-regulation of SOD2 on vascular wall. Redox Biology, 3, 88–99. https://doi.org/10.1016/j.redox.2014.11.001

Liu, Z., Xi, D., Kang, M., Guo, X., & Xu, B. (2012). Molecular cloning and characterization of Hsp27.6: The first reported small heat shock protein from Apis cerana cerana. Cell Stress and Chaperones, 17(5), 539–551. https://doi.org/10.1007/s12192-012-0330-x

Livak, K. J., & Schmittgen, T. D. (2001). Analysis of Relative Gene Expression Data Using Real-Time Quantitative PCR and the 2−ΔΔCT Method. Methods, 25(4), 402–408. https://doi.org/10.1006/meth.2001.1262

Long, X., Yao, X., Jiang, Q., Yang, Y., He, X., Tian, W., Zhao, K., & Zhang, H. (2020). Astrocyte-derived exosomes enriched with miR-873a-5p inhibit neuroinflammation via microglia phenotype modulation after traumatic brain injury. Journal of Neuroinflammation, 17(1), 89. https://doi.org/10.1186/s12974-020-01761-0

Longden, T. A., Dabertrand, F., Koide, M., Gonzales, A. L., Tykocki, N. R., Brayden, J. E., Hill-Eubanks, D., & Nelson, M. T. (2017). Capillary K+-sensing initiates retrograde hyperpolarization to increase local cerebral blood flow. Nature Neuroscience, 20(5), 717–726. https://doi.org/10.1038/nn.4533

Lu, C.-H., Chen, Y.-A., Ke, C.-C., Chiu, S.-J., Chen, C.-C., Hsieh, Y.-J., Yang, B.-H., & Liu, R.-S. (2021). Preclinical Characterization and In Vivo Imaging of 111In-Labeled Mesenchymal Stem Cell–Derived Extracellular Vesicles. Molecular Imaging and Biology, 23(3), 361–371. https://doi.org/10.1007/s11307-020-01562-0

Lu, M., Lu, F., Liao, C., Guo, Y., Mao, C., Lai, Y., Chen, X., & Chen, W. (2023). High throughput miRNA sequencing and bioinformatics analysis identify the mesenchymal cell proliferation and apoptosis related miRNAs during fetal mice palate development. The Journal of Gene Medicine, 25(9), e3531. https://doi.org/10.1002/jgm.3531

Lu, X., Song, Z., Hao, J., Kong, X., Yuan, W., Shen, Y., Zhang, C., Yang, J., Yu, P., Qian, Y., Zhang, G., Feng, H., Wang, J., Cai, Z., & Cai, Z. (2024). Proton pump inhibitors enhance macropinocytosis-mediated extracellular vesicle endocytosis by inducing membrane v-ATPase assembly. Journal of Extracellular Vesicles, 13(4), e12426. https://doi.org/10.1002/jev2.12426

Lu, X., Yu, Y., Liao, F., & Tan, S. (2019). Homo Sapiens Circular RNA 0079993 (hsa_circ_0079993) of the POLR2J4 Gene Acts as an Oncogene in Colorectal Cancer Through the microRNA-203a-3p.1 and CREB1 Axis. Medical Science Monitor, 25, 6872–6883. https://doi.org/10.12659/MSM.916064

Lu, Z., & Matera, A. G. (2015). Developmental Analysis of Spliceosomal snRNA Isoform Expression. G3 Genes|Genomes|Genetics, 5(1), 103–110. https://doi.org/10.1534/g3.114.015735

Łukomska, A., Baranowska-Bosiacka, I., Dec, K., Pilutin, A., Tarnowski, M., Jakubczyk, K., Żwierełło, W., Skórka-Majewicz, M., Chlubek, D., & Gutowska, I. (2020). Changes in Gene and Protein Expression of Metalloproteinase-2 and -9 and Their Inhibitors TIMP2 and TIMP3 in Different Parts of Fluoride-Exposed Rat Brain. International Journal of Molecular Sciences, 22(1), 391. https://doi.org/10.3390/ijms22010391

Luo, B., Prescott, S. M., & Topham, M. K. (2003). Protein Kinase Cα Phosphorylates and Negatively Regulates Diacylglycerol Kinase ζ. Journal of Biological Chemistry, 278(41), 39542–39547. https://doi.org/10.1074/jbc.M307153200

Luo, G., Ducy, P., McKee, M. D., Pinero, G. J., Loyer, E., Behringer, R. R., & Karsenty, G. (1997). Spontaneous calcification of arteries and cartilage in mice lacking matrix GLA protein. Nature, 386(6620), 78–81. https://doi.org/10.1038/386078a0

Luo, Y., Yang, H., Wan, Y., Yang, S., Wu, J., Chen, S., Li, Y., Jin, H., He, Q., Zhu, D.-Y., Zhou, Y., & Hu, B. (2022). Endothelial ETS1 inhibition exacerbate blood–brain barrier dysfunction in multiple sclerosis through inducing endothelial-to-mesenchymal transition. Cell Death & Disease, 13(5), 462. https://doi.org/10.1038/s41419-022-04888-5

Luzak, B., Siarkiewicz, P., & Boncler, M. (2022). An evaluation of a new high-sensitivity PrestoBlue assay for measuring cell viability and drug cytotoxicity using EA.hy926 endothelial cells. Toxicology in Vitro: An International Journal Published in Association with BIBRA, 83, 105407. https://doi.org/10.1016/j.tiv.2022.105407

Ma, D., Zhang, H., Yin, L., Xu, H., Wu, L., Shaji, R., Rezai, F., Mulla, A., Kaur, S., Tan, S., Kysela, B., Wang, Y., Chen, Z., Zhao, C., & Gu, Y. (2024). Human IPSC -derived endothelial cells promote CNS remyelination via BDNF and MTORC1 pathway. Glia, 72(1), 133–155. https://doi.org/10.1002/glia.24466

Ma, L., Li, Y., Peng, J., Wu, D., Zhao, X., Cui, Y., Chen, L., Yan, X., Du, Y., & Yu, L. (2015). Discovery of the migrasome, an organelle mediating release of cytoplasmic contents during cell migration. Cell Research, 25(1), 24–38. https://doi.org/10.1038/cr.2014.135

Ma, S., Ene, J., McGarraugh, C., Ma, S., Esmonde, C., Liu, Y., & Li, Y. (2025). Extracellular Vesicle Secretion from 3D Culture of Human Adipose-Derived Mesenchymal Stem Cells in Scalable Bioreactors. Bioengineering, 12(9), 933. https://doi.org/10.3390/bioengineering12090933

Macrì, F., Vigorito, I., Castiglione, S., Faggiano, S., Casaburo, M., Fanotti, N., Piacentini, L., Vigetti, D., Vinci, M. C., & Raucci, A. (2023). High Phosphate-Induced JAK-STAT Signalling Sustains Vascular Smooth Muscle Cell Inflammation and Limits Calcification. Biomolecules, 14(1), 29. https://doi.org/10.3390/biom14010029

Mahajan, S., Ng, B. G., AlAbdi, L., Earnest, P. D. J., Sosicka, P., Patel, N., Helaby, R., Abdulwahab, F., He, M., Alkuraya, F. S., & Freeze, H. H. (2023). Homozygous truncating variant in MAN2A2 causes a novel congenital disorder of glycosylation with neurological involvement. Journal of Medical Genetics, 60(7), 627–635. https://doi.org/10.1136/jmg-2022-108821

Mahalmani, V., Sinha, S., Prakash, A., & Medhi, B. (2022). Translational research: Bridging the gap between preclinical and clinical research. Indian Journal of Pharmacology, 54(6), 393–396. https://doi.org/10.4103/ijp.ijp_860_22

Malhotra, R., Nicholson, C. J., Wang, D., Bhambhani, V., Paniagua, S., Slocum, C., Sigurslid, H. H., Lino Cardenas, C. L., Li, R., Boerboom, S. L., Chen, Y.-C., Hwang, S.-J., Yao, C., Ichinose, F., Bloch, D. B., Lindsay, M. E., Lewis, G. D., Aragam, J. R., Hoffmann, U., … Ho, J. E. (2022). Matrix Gla Protein Levels Are Associated With Arterial Stiffness and Incident Heart Failure With Preserved Ejection Fraction. Arteriosclerosis, Thrombosis, and Vascular Biology, 42(2). https://doi.org/10.1161/ATVBAHA.121.316664

Malpetti, M., Passamonti, L., Jones, P. S., Street, D., Rittman, T., Fryer, T. D., Hong, Y. T., Vàsquez Rodriguez, P., Bevan-Jones, W. R., Aigbirhio, F. I., O'Brien, J. T., & Rowe, J. B. (2021). Neuroinflammation predicts disease progression in progressive supranuclear palsy. Journal of Neurology, Neurosurgery & Psychiatry, 92(7), 769–775. https://doi.org/10.1136/jnnp-2020-325549

Mao, S., Sun, Q., Xiao, H., Zhang, C., & Li, L. (2015). Secreted miR-34a in astrocytic shedding vesicles enhanced the vulnerability of dopaminergic neurons to neurotoxins by targeting Bcl-2. Protein & Cell, 6(7), 529–540. https://doi.org/10.1007/s13238-015-0168-y

Mao, X. D., Min, S. N., Zhu, M. Q., He, L., Zhang, Y., Li, J. W., Tian, Y. X., Yu, G. Y., Wu, L. L., & Cong, X. (2023). The Role of Endothelial Barrier Function in the Fibrosis of Salivary Gland. Journal of Dental Research, 102(1), 82–92. https://doi.org/10.1177/00220345221118508

Marchetti, L., Francisco, D., Soldati, S., Haghayegh Jahromi, N., Barcos, S., Gruber, I., Pareja, J. R., Thiriot, A., Von Andrian, U., Deutsch, U., Lyck, R., Bruggmann, R., & Engelhardt, B. (2022). ACKR1 favors transcellular over paracellular T-cell diapedesis across the blood-brain barrier in neuroinflammation in vitro. European Journal of Immunology, 52(1), 161–177. https://doi.org/10.1002/eji.202149238

Mariasoosai, C., Bose, S., & Natesan, S. (2024). Structural insights into the molecular recognition of integrin αVβ3 by RGD-containing ligands: The role of the specificity-determining loop (SDL). Biophysics. https://doi.org/10.1101/2024.09.23.614545

Martin, F. A., McLoughlin, A., Rochfort, K. D., Davenport, C., Murphy, R. P., & Cummins, P. M. (2014). Regulation of Thrombomodulin Expression and Release in Human Aortic Endothelial Cells by Cyclic Strain. PLoS ONE, 9(9), e108254. https://doi.org/10.1371/journal.pone.0108254

Martin, M. (2011). Cutadapt removes adapter sequences from high-throughput sequencing reads. EMBnet.Journal, 17(1), 10. https://doi.org/10.14806/ej.17.1.200

Martinez-Lozada, Z., & Robinson, M. B. (2020). Reciprocal communication between astrocytes and endothelial cells is required for astrocytic glutamate transporter 1 (GLT-1) expression. Neurochemistry International, 139, 104787. https://doi.org/10.1016/j.neuint.2020.104787

Marty-Lombardi, S., Lu, S., Ambroziak, W., Schrenk-Siemens, K., Wang, J., DePaoli-Roach, A. A., Hagenston, A. M., Wende, H., Tappe-Theodor, A., Simonetti, M., Bading, H., Okun, J. G., Kuner, R., Fleming, T., & Siemens, J. (2024). Neuron–astrocyte metabolic coupling facilitates spinal plasticity and maintenance of inflammatory pain. Nature Metabolism, 6(3), 494–513. https://doi.org/10.1038/s42255-024-01001-2

Matafora, V., Gorb, A., Yang, F., Noble, W., Bachi, A., Perez-Nievas, B. G., & Jimenez-Sanchez, M. (2023). Proteomics of the astrocyte secretome reveals changes in their response to soluble oligomeric Aβ. Journal of Neurochemistry, 166(2), 346–366. https://doi.org/10.1111/jnc.15875

Mathieu, M., Névo, N., Jouve, M., Valenzuela, J. I., Maurin, M., Verweij, F. J., Palmulli, R., Lankar, D., Dingli, F., Loew, D., Rubinstein, E., Boncompain, G., Perez, F., & Théry, C. (2021). Specificities of exosome versus small ectosome secretion revealed by live intracellular tracking of CD63 and CD9. Nature Communications, 12(1), 4389. https://doi.org/10.1038/s41467-021-24384-2

Mathiisen, T. M., Lehre, K. P., Danbolt, N. C., & Ottersen, O. P. (2010). The perivascular astroglial sheath provides a complete covering of the brain microvessels: An electron microscopic 3D reconstruction. Glia, 58(9), 1094–1103. https://doi.org/10.1002/glia.20990

Matsumoto, A., Takahashi, Y., Chang, H., Wu, Y., Yamamoto, A., Ishihama, Y., & Takakura, Y. (2020). Blood concentrations of small extracellular vesicles are determined by a balance between abundant secretion and rapid clearance. Journal of Extracellular Vesicles, 9(1), 1696517. https://doi.org/10.1080/20013078.2019.1696517

Matsushita, T., Otani, K., Oto, Y., Takahashi, Y., Kurosaka, D., & Kato, F. (2021). Sustained microglial activation in the area postrema of collagen-induced arthritis mice. Arthritis Research & Therapy, 23(1), 273. https://doi.org/10.1186/s13075-021-02657-x

Mattera, V. S., Pereyra Gerber, P., Glisoni, R., Ostrowski, M., Verstraeten, S. V., Pasquini, J. M., & Correale, J. D. (2020). Extracellular vesicles containing the transferrin receptor as nanocarriers of apotransferrin. Journal of Neurochemistry, 155(3), 327–338. https://doi.org/10.1111/jnc.15019

Matthaeus, C., Sochacki, K. A., Dickey, A. M., Puchkov, D., Haucke, V., Lehmann, M., & Taraska, J. W. (2022). The molecular organization of differentially curved caveolae indicates bendable structural units at the plasma membrane. Nature Communications, 13(1), 7234. https://doi.org/10.1038/s41467-022-34958-3

Mattick, J. S., Amaral, P. P., Carninci, P., Carpenter, S., Chang, H. Y., Chen, L.-L., Chen, R., Dean, C., Dinger, M. E., Fitzgerald, K. A., Gingeras, T. R., Guttman, M., Hirose, T., Huarte, M., Johnson, R., Kanduri, C., Kapranov, P., Lawrence, J. B., Lee, J. T., … Wu, M. (2023). Long non-coding RNAs: Definitions, functions, challenges and recommendations. Nature Reviews Molecular Cell Biology, 24(6), 430–447. https://doi.org/10.1038/s41580-022-00566-8

Matusova, Z., Hol, E. M., Pekny, M., Kubista, M., & Valihrach, L. (2023). Reactive astrogliosis in the era of single-cell transcriptomics. Frontiers in Cellular Neuroscience, 17, 1173200. https://doi.org/10.3389/fncel.2023.1173200

Mayers, J. R., Fyfe, I., Schuh, A. L., Chapman, E. R., Edwardson, J. M., & Audhya, A. (2011). ESCRT-0 Assembles as a Heterotetrameric Complex on Membranes and Binds Multiple Ubiquitinylated Cargoes Simultaneously. Journal of Biological Chemistry, 286(11), 9636–9645. https://doi.org/10.1074/jbc.M110.185363

McCarthy, K. M., Skare, I. B., Stankewich, M. C., Furuse, M., Tsukita, S., Rogers, R. A., Lynch, R. D., & Schneeberger, E. E. (1996). Occludin is a functional component of the tight junction. Journal of Cell Science, 109(9), 2287–2298. https://doi.org/10.1242/jcs.109.9.2287

McKenna, M. C., Dienel, G. A., Sonnewald, U., Waagepetersen, H. S., & Schousboe, A. (2012). Energy Metabolism of the Brain. In Basic Neurochemistry (pp. 200–231). Elsevier. https://doi.org/10.1016/B978-0-12-374947-5.00011-0

McKenzie, I. A., Ohayon, D., Li, H., Paes De Faria, J., Emery, B., Tohyama, K., & Richardson, W. D. (2014). Motor skill learning requires active central myelination. Science, 346(6207), 318–322. https://doi.org/10.1126/science.1254960

Mehrabadi, A. R., Korolainen, M. A., Odero, G., Miller, D. W., & Kauppinen, T. M. (2017). Poly(ADP-ribose) polymerase-1 regulates microglia mediated decrease of endothelial tight junction integrity. Neurochemistry International, 108, 266–271. https://doi.org/10.1016/j.neuint.2017.04.014

Melentijevic, I., Toth, M. L., Arnold, M. L., Guasp, R. J., Harinath, G., Nguyen, K. C., Taub, D., Parker, J. A., Neri, C., Gabel, C. V., Hall, D. H., & Driscoll, M. (2017). C. elegans neurons jettison protein aggregates and mitochondria under neurotoxic stress. Nature, 542(7641), 367–371. https://doi.org/10.1038/nature21362

Menck, K., Bleckmann, A., Schulz, M., Ries, L., & Binder, C. (2017). Isolation and Characterization of Microvesicles from Peripheral Blood. Journal of Visualized Experiments, (119), 55057. https://doi.org/10.3791/55057

Mendiola, A. S., Yan, Z., Dixit, K., Johnson, J. R., Bouhaddou, M., Meyer-Franke, A., Shin, M.-G., Yong, Y., Agrawal, A., MacDonald, E., Muthukumar, G., Pearce, C., Arun, N., Cabriga, B., Meza-Acevedo, R., Alzamora, M. D. P. S., Zamvil, S. S., Pico, A. R., Ryu, J. K., … Akassoglou, K. (2023). Defining blood-induced microglia functions in neurodegeneration through multiomic profiling. Nature Immunology, 24(7), 1173–1187. https://doi.org/10.1038/s41590-023-01522-0

Menezes, M. J., McClenahan, F. K., Leiton, C. V., Aranmolate, A., Shan, X., & Colognato, H. (2014). The Extracellular Matrix Protein Laminin α2 Regulates the Maturation and Function of the Blood–Brain Barrier. The Journal of Neuroscience, 34(46), 15260–15280. https://doi.org/10.1523/JNEUROSCI.3678-13.2014

Meng, Z., Zhang, R., Wu, X., Piao, Z., Zhang, M., & Jin, T. (2024). LncRNA HAGLROS promotes breast cancer evolution through miR-135b-3p/COL10A1 axis and exosome-mediated macrophage M2 polarization. Cell Death & Disease, 15(8), 633. https://doi.org/10.1038/s41419-024-07020-x

Mesquita, P. M. M., Preston-Hurlburt, P., Keller, M. J., Vudattu, N., Espinoza, L., Altrich, M., Anastos, K., Herold, K. C., & Herold, B. C. (2016). Role of IL-32 in HIV Reactivation and its Link to HIV-HSV Coinfection. Journal of Infectious Diseases, jiw612. https://doi.org/10.1093/infdis/jiw612

Mi, Y., Qi, G., Vitali, F., Shang, Y., Raikes, A. C., Wang, T., Jin, Y., Brinton, R. D., Gu, H., & Yin, F. (2023). Loss of fatty acid degradation by astrocytic mitochondria triggers neuroinflammation and neurodegeneration. Nature Metabolism, 5(3), 445–465. https://doi.org/10.1038/s42255-023-00756-4

Miceli, R. T., Chen, T., Nose, Y., Tichkule, S., Brown, B., Fullard, J. F., Saulsbury, M. D., Heyliger, S. O., Gnjatic, S., Kyprianou, N., Cordon-Cardo, C., Sahoo, S., Taioli, E., Roussos, P., Stolovitzky, G., Gonzalez-Kozlova, E., & Dogra, N. (2024). Extracellular vesicles, RNA sequencing, and bioinformatic analyses: Challenges, solutions, and recommendations. Journal of Extracellular Vesicles, 13(12), e70005. https://doi.org/10.1002/jev2.70005

Michinaga, S., Inoue, A., Sonoda, K., Mizuguchi, H., & Koyama, Y. (2021). Down-regulation of astrocytic sonic hedgehog by activation of endothelin ETB receptors: Involvement in traumatic brain injury-induced disruption of blood brain barrier in a mouse model. Neurochemistry International, 146, 105042. https://doi.org/10.1016/j.neuint.2021.105042

Michinaga, S., Tanabe, A., Nakaya, R., Fukutome, C., Inoue, A., Iwane, A., Minato, Y., Tujiuchi, Y., Miyake, D., Mizuguchi, H., & Koyama, Y. (2020). Angiopoietin-1/Tie-2 signal after focal traumatic brain injury is potentiated by BQ788, an ET_B receptor antagonist, in the mouse cerebrum: Involvement in recovery of blood–brain barrier function. Journal of Neurochemistry, 154(3), 330–348. https://doi.org/10.1111/jnc.14957

Mills, S. A., Jobling, A. I., Dixon, M. A., Bui, B. V., Vessey, K. A., Phipps, J. A., Greferath, U., Venables, G., Wong, V. H. Y., Wong, C. H. Y., He, Z., Hui, F., Young, J. C., Tonc, J., Ivanova, E., Sagdullaev, B. T., & Fletcher, E. L. (2021). Fractalkine-induced microglial vasoregulation occurs within the retina and is altered early in diabetic retinopathy. Proceedings of the National Academy of Sciences, 118(51), e2112561118. https://doi.org/10.1073/pnas.2112561118

Milton, R. H., Abeti, R., Averaimo, S., DeBiasi, S., Vitellaro, L., Jiang, L., Curmi, P. M. G., Breit, S. N., Duchen, M. R., & Mazzanti, M. (2008). CLIC1 Function Is Required for β-Amyloid-Induced Generation of Reactive Oxygen Species by Microglia. The Journal of Neuroscience, 28(45), 11488–11499. https://doi.org/10.1523/JNEUROSCI.2431-08.2008

Minciacchi, V. R., Spinelli, C., Reis-Sobreiro, M., Cavallini, L., You, S., Zandian, M., Li, X., Mishra, R., Chiarugi, P., Adam, R. M., Posadas, E. M., Viglietto, G., Freeman, M. R., Cocucci, E., Bhowmick, N. A., & Di Vizio, D. (2017). MYC Mediates Large Oncosome-Induced Fibroblast Reprogramming in Prostate Cancer. Cancer Research, 77(9), 2306–2317. https://doi.org/10.1158/0008-5472.CAN-16-2942

Mineiro, M. F., Patricio, E. de S., Peixoto, Á. S., Araujo, T. L. S., da Silva, R. P., Moretti, A. I. S., Lima, F. S., Laurindo, F. R. M., & Meotti, F. C. (2020). Urate hydroperoxide oxidizes endothelial cell surface protein disulfide isomerase-A1 and impairs adherence. Biochimica et Biophysica Acta (BBA) - General Subjects, 1864(3), 129481.

Miner, J. H., Li, C., Mudd, J. L., Go, G., & Sutherland, A. E. (2004). Compositional and structural requirements for laminin and basement membranes during mouse embryo implantation and gastrulation. Development, 131(10), 2247–2256. https://doi.org/10.1242/dev.01112

Miner, J. H., Patton, B. L., Lentz, S. I., Gilbert, D. J., Snider, W. D., Jenkins, N. A., Copeland, N. G., & Sanes, J. R. (1997). The Laminin α Chains: Expression, Developmental Transitions, and Chromosomal Locations of α1-5, Identification of Heterotrimeric Laminins 8–11, and Cloning of a Novel α3 Isoform. The Journal of Cell Biology, 137(3), 685–701. https://doi.org/10.1083/jcb.137.3.685

Miner, J. H., & Sanes, J. R. (1994). Collagen IV alpha 3, alpha 4, and alpha 5 chains in rodent basal laminae: Sequence, distribution, association with laminins, and developmental switches. The Journal of Cell Biology, 127(3), 879–891. https://doi.org/10.1083/jcb.127.3.879

Minocha, S., Valloton, D., Brunet, I., Eichmann, A., Hornung, J.-P., & Lebrand, C. (2015). NG2 glia are required for vessel network formation during embryonic development. eLife, 4, e09102. https://doi.org/10.7554/eLife.09102

Miyamoto, A., Wake, H., Ishikawa, A. W., Eto, K., Shibata, K., Murakoshi, H., Koizumi, S., Moorhouse, A. J., Yoshimura, Y., & Nabekura, J. (2016). Microglia contact induces synapse formation in developing somatosensory cortex. Nature Communications, 7(1), 12540. https://doi.org/10.1038/ncomms12540

Mizee, M. R., Wooldrik, D., Lakeman, K. A. M., Van Het Hof, B., Drexhage, J. A. R., Geerts, D., Bugiani, M., Aronica, E., Mebius, R. E., Prat, A., De Vries, H. E., & Reijerkerk, A. (2013). Retinoic Acid Induces Blood–Brain Barrier Development. The Journal of Neuroscience, 33(4), 1660–1671. https://doi.org/10.1523/JNEUROSCI.1338-12.2013

Mohamed, A. A., Wang, P. Y., Bartel, D. P., & Vos, S. M. (2025). The structural basis for RNA slicing by human Argonaute2. Cell Reports, 44(1), 115166. https://doi.org/10.1016/j.celrep.2024.115166

Mohning, M. P., Thomas, S. M., Barthel, L., Mould, K. J., McCubbrey, A. L., Frasch, S. C., Bratton, D. L., Henson, P. M., & Janssen, W. J. (2018). Phagocytosis of microparticles by alveolar macrophages during acute lung injury requires MerTK. American Journal of Physiology-Lung Cellular and Molecular Physiology, 314(1), L69–L82. https://doi.org/10.1152/ajplung.00058.2017

Mol, E. A., Goumans, M.-J., Doevendans, P. A., Sluijter, J. P. G., & Vader, P. (2017). Higher functionality of extracellular vesicles isolated using size-exclusion chromatography compared to ultracentrifugation. Nanomedicine: Nanotechnology, Biology and Medicine, 13(6), 2061–2065. https://doi.org/10.1016/j.nano.2017.03.011

Mondo, E., Becker, S. C., Kautzman, A. G., Schifferer, M., Baer, C. E., Chen, J., Huang, E. J., Simons, M., & Schafer, D. P. (2020). A Developmental Analysis of Juxtavascular Microglia Dynamics and Interactions with the Vasculature. The Journal of Neuroscience, 40(34), 6503–6521. https://doi.org/10.1523/JNEUROSCI.3006-19.2020

Monier, A., Adle-Biassette, H., Delezoide, A.-L., Evrard, P., Gressens, P., & Verney, C. (2007). Entry and Distribution of Microglial Cells in Human Embryonic and Fetal Cerebral Cortex: Journal of Neuropathology and Experimental Neurology, 66(5), 372–382. https://doi.org/10.1097/nen.0b013e3180517b46

Montecalvo, A., Larregina, A. T., Shufesky, W. J., Beer Stolz, D., Sullivan, M. L. G., Karlsson, J. M., Baty, C. J., Gibson, G. A., Erdos, G., Wang, Z., Milosevic, J., Tkacheva, O. A., Divito, S. J., Jordan, R., Lyons-Weiler, J., Watkins, S. C., & Morelli, A. E. (2012). Mechanism of transfer of functional microRNAs between mouse dendritic cells via exosomes. Blood, 119(3), 756–766. https://doi.org/10.1182/blood-2011-02-338004

Morandi, M. I., Busko, P., Ozer-Partuk, E., Khan, S., Zarfati, G., Elbaz-Alon, Y., Abou Karam, P., Napso Shogan, T., Ginini, L., Gil, Z., Regev-Rudzki, N., & Avinoam, O. (2022). Extracellular vesicle fusion visualized by cryo-electron microscopy. PNAS Nexus, 1(4), pgac156. https://doi.org/10.1093/pnasnexus/pgac156

Morgan, L., Shah, B., Rivers, L. E., Barden, L., Groom, A. J., Chung, R., Higazi, D., Desmond, H., Smith, T., & Staddon, J. M. (2007). Inflammation and dephosphorylation of the tight junction protein occludin in an experimental model of multiple sclerosis. Neuroscience, 147(3), 664–673. https://doi.org/10.1016/j.neuroscience.2007.04.051

Mosbah, H., Vatier, C., Boccara, F., Jéru, I., Lascols, O., Vantyghem, M.-C., Fève, B., Donadille, B., Sarrazin, E., Benabbou, S., Inamo, J., Ederhy, S., Cohen, A., Neraud, B., Richard, P., Picard, F., Christin-Maitre, S., Redheuil, A., Wahbi, K., & Vigouroux, C. (2020). Looking at New Unexpected Disease Targets in LMNA-Linked Lipodystrophies in the Light of Complex Cardiovascular Phenotypes: Implications for Clinical Practice. Cells, 9(3), 765. https://doi.org/10.3390/cells9030765

Munji, R. N., Soung, A. L., Weiner, G. A., Sohet, F., Semple, B. D., Trivedi, A., Gimlin, K., Kotoda, M., Korai, M., Aydin, S., Batugal, A., Cabangcala, A. C., Schupp, P. G., Oldham, M. C., Hashimoto, T., Noble-Haeusslein, L. J., & Daneman, R. (2019). Profiling the mouse brain endothelial transcriptome in health and disease models reveals a core blood–brain barrier dysfunction module. Nature Neuroscience, 22(11), 1892–1902. https://doi.org/10.1038/s41593-019-0497-x

Mura, M., Swain, R. K., Zhuang, X., Vorschmitt, H., Reynolds, G., Durant, S., Beesley, J. F. J., Herbert, J. M. J., Sheldon, H., Andre, M., Sanderson, S., Glen, K., Luu, N.-T., McGettrick, H. M., Antczak, P., Falciani, F., Nash, G. B., Nagy, Z. S., & Bicknell, R. (2012). Identification and angiogenic role of the novel tumor endothelial marker CLEC14A. Oncogene, 31(3), 293–305. https://doi.org/10.1038/onc.2011.233

Murakami, T., Frey, T., Lin, C., & Antonetti, D. A. (2012). Protein kinase cβ phosphorylates occludin regulating tight junction trafficking in vascular endothelial growth factor-induced permeability in vivo. Diabetes, 61(6), 1573–1583. https://doi.org/10.2337/db11-1367

Muralidharan-Chari, V., Clancy, J., Plou, C., Romao, M., Chavrier, P., Raposo, G., & D'Souza-Schorey, C. (2009). ARF6-Regulated Shedding of Tumor Cell-Derived Plasma Membrane Microvesicles. Current Biology, 19(22), 1875–1885. https://doi.org/10.1016/j.cub.2009.09.059

Murata, M., Peränen, J., Schreiner, R., Wieland, F., Kurzchalia, T. V., & Simons, K. (1995). VIP21/caveolin is a cholesterol-binding protein. Proceedings of the National Academy of Sciences, 92(22), 10339–10343. https://doi.org/10.1073/pnas.92.22.10339

Murillo-Garzón, V., Gorroño-Etxebarria, I., Åkerfelt, M., Puustinen, M. C., Sistonen, L., Nees, M., Carton, J., Waxman, J., & Kypta, R. M. (2018). Frizzled-8 integrates Wnt-11 and transforming growth factor-β signaling in prostate cancer. Nature Communications, 9(1), 1747. https://doi.org/10.1038/s41467-018-04042-w

Na, H.-J., Hwang, J.-Y., Lee, K.-S., Choi, Y. K., Choe, J., Kim, J.-Y., Moon, H.-E., Kim, K.-W., Koh, G. Y., Lee, H., Jeoung, D., Won, M.-H., Ha, K.-S., Kwon, Y.-G., & Kim, Y.-M. (2014). TRAIL negatively regulates VEGF-induced angiogenesis via caspase-8-mediated enzymatic and non-enzymatic functions. Angiogenesis, 17(1), 179–194. https://doi.org/10.1007/s10456-013-9387-0

Nabhan, J. F., Hu, R., Oh, R. S., Cohen, S. N., & Lu, Q. (2012). Formation and release of arrestin domain-containing protein 1-mediated microvesicles (ARMMs) at plasma membrane by recruitment of TSG101 protein. Proceedings of the National Academy of Sciences, 109(11), 4146–4151. https://doi.org/10.1073/pnas.1200448109

Nader, D., & Kerrigan, S. W. (2022). Molecular Cross-Talk between Integrins and Cadherins Leads to a Loss of Vascular Barrier Integrity during SARS-CoV-2 Infection. Viruses, 14(5), 891. https://doi.org/10.3390/v14050891

Nafar, F., Williams, J. B., & Mearow, K. M. (2015). Astrocytes Release HspB1 in Response to Amyloid-β Exposure in vitro. Journal of Alzheimer's Disease, 49(1), 251–263. https://doi.org/10.3233/JAD-150317

Nagano, M., Toshima, J. Y., Siekhaus, D. E., & Toshima, J. (2019). Rab5-mediated endosome formation is regulated at the trans-Golgi network. Communications Biology, 2(1), 419. https://doi.org/10.1038/s42003-019-0670-5

Narantuya, D., Nagai, A., Sheikh, A. Md., Masuda, J., Kobayashi, S., Yamaguchi, S., & Kim, S. U. (2010). Human Microglia Transplanted in Rat Focal Ischemia Brain Induce Neuroprotection and Behavioral Improvement. PLoS ONE, 5(7), e11746. https://doi.org/10.1371/journal.pone.0011746

Nees, S., Weiss, D. R., Senftl, A., Knott, M., Förch, S., Schnurr, M., Weyrich, P., & Juchem, G. (2012). Isolation, bulk cultivation, and characterization of coronary microvascular pericytes: The second most frequent myocardial cell type in vitro. American Journal of Physiology-Heart and Circulatory Physiology, 302(1), H69–H84. https://doi.org/10.1152/ajpheart.00359.2011

Nemes-Baran, A. D., White, D. R., & DeSilva, T. M. (2020). Fractalkine-Dependent Microglial Pruning of Viable Oligodendrocyte Progenitor Cells Regulates Myelination. Cell Reports, 32(7), 108047. https://doi.org/10.1016/j.celrep.2020.108047

Neuhaus, M., Fryklund, C., Taylor, H., Borreguero-Muñoz, A., Kopietz, F., Ardalani, H., Rogova, O., Stirrat, L., Bremner, S. K., Spégel, P., Bryant, N. J., Gould, G. W., & Stenkula, K. G. (2023). EHD2 regulates plasma membrane integrity and downstream insulin receptor signaling events. Molecular Biology of the Cell, 34(12), ar124. https://doi.org/10.1091/mbc.E23-03-0078

Neuhaus, W., Gaiser, F., Mahringer, A., Franz, J., RiethmÃ¼ller, C., & FÃ¶rster, C. (2014). The pivotal role of astrocytes in an in vitro stroke model of the blood-brain barrier. Frontiers in Cellular Neuroscience, 8. https://doi.org/10.3389/fncel.2014.00352

Nguyen, N. M., Miner, J. H., Pierce, R. A., & Senior, R. M. (2002). Laminin α5 Is Required for Lobar Septation and Visceral Pleural Basement Membrane Formation in the Developing Mouse Lung. Developmental Biology, 246(2), 231–244. https://doi.org/10.1006/dbio.2002.0658

Nguyen-Ngoc, K.-V., Cheung, K. J., Brenot, A., Shamir, E. R., Gray, R. S., Hines, W. C., Yaswen, P., Werb, Z., & Ewald, A. J. (2012). ECM microenvironment regulates collective migration and local dissemination in normal and malignant mammary epithelium. Proceedings of the National Academy of Sciences, 109(39). https://doi.org/10.1073/pnas.1212834109

Nicolás-Ávila, J. A., Lechuga-Vieco, A. V., Esteban-Martínez, L., Sánchez-Díaz, M., Díaz-García, E., Santiago, D. J., Rubio-Ponce, A., Li, J. L., Balachander, A., Quintana, J. A., Martínez-de-Mena, R., Castejón-Vega, B., Pun-García, A., Través, P. G., Bonzón-Kulichenko, E., García-Marqués, F., Cussó, L., A-González, N., González-Guerra, A., … Hidalgo, A. (2020). A Network of Macrophages Supports Mitochondrial Homeostasis in the Heart. Cell, 183(1), 94-109.e23. https://doi.org/10.1016/j.cell.2020.08.031

Nieland, L., Haidar, E. A., Rufino-Ramos, D., Prabhakar, S., Samaha, Y., Breyne, K., Fordjour, F. K., Das, S., Broekman, M. L. D., Gould, S., Breakefield, X. O., & Abels, E. R. (2025). AstroGreen transgenic mouse illuminates the trafficking of astrocyte-derived extracellular vesicles. Molecular and Cellular Neuroscience, 135, 104051. https://doi.org/10.1016/j.mcn.2025.104051

Nightingale, T. D., Pattni, K., Hume, A. N., Seabra, M. C., & Cutler, D. F. (2009). Rab27a and MyRIP regulate the amount and multimeric state of VWF released from endothelial cells. Blood, 113(20), 5010–5018. https://doi.org/10.1182/blood-2008-09-181206

Nikolakopoulou, A. M., Montagne, A., Kisler, K., Dai, Z., Wang, Y., Huuskonen, M. T., Sagare, A. P., Lazic, D., Sweeney, M. D., Kong, P., Wang, M., Owens, N. C., Lawson, E. J., Xie, X., Zhao, Z., & Zlokovic, B. V. (2019). Pericyte loss leads to circulatory failure and pleiotrophin depletion causing neuron loss. Nature Neuroscience, 22(7), 1089–1098. https://doi.org/10.1038/s41593-019-0434-z

Nikoloff, J. M., Saucedo-Espinosa, M. A., Kling, A., & Dittrich, P. S. (2021). Identifying extracellular vesicle populations from single cells. Proceedings of the National Academy of Sciences, 118(38), e2106630118. https://doi.org/10.1073/pnas.2106630118

Nimmerjahn, A., Kirchhoff, F., & Helmchen, F. (2005). Resting Microglial Cells Are Highly Dynamic Surveillants of Brain Parenchyma in Vivo. Science, 308(5726), 1314–1318. https://doi.org/10.1126/science.1110647

Nippert, A. R., Chiang, P.-P., Del Franco, A. P., & Newman, E. A. (2022). Astrocyte regulation of cerebral blood flow during hypoglycemia. Journal of Cerebral Blood Flow & Metabolism, 42(8), 1534–1546. https://doi.org/10.1177/0271678X221089091

Nirwane, A., Kang, M., Adithan, A., Maharaj, V., Nguyen, F., Santaella Aguilar, E., Nasrollahi, A., & Yao, Y. (2024). Endothelial and mural laminin-α5 contributes to neurovascular integrity maintenance. Fluids and Barriers of the CNS, 21(1), 18. https://doi.org/10.1186/s12987-024-00521-z

Nishioku, T., Matsumoto, J., Dohgu, S., Sumi, N., Miyao, K., Takata, F., Shuto, H., Yamauchi, A., & Kataoka, Y. (2010). Tumor Necrosis Factor-α Mediates the Blood–Brain Barrier Dysfunction Induced by Activated Microglia in Mouse Brain Microvascular Endothelial Cells. Journal of Pharmacological Sciences, 112(2), 251–254. https://doi.org/10.1254/jphs.09292SC

Nitta, T., Hata, M., Gotoh, S., Seo, Y., Sasaki, H., Hashimoto, N., Furuse, M., & Tsukita, S. (2003). Size-selective loosening of the blood-brain barrier in claudin-5–deficient mice. The Journal of Cell Biology, 161(3), 653–660. https://doi.org/10.1083/jcb.200302070

Niu, J., Tsai, H.-H., Hoi, K. K., Huang, N., Yu, G., Kim, K., Baranzini, S. E., Xiao, L., Chan, J. R., & Fancy, S. P. J. (2019). Aberrant oligodendroglial–vascular interactions disrupt the blood–brain barrier, triggering CNS inflammation. Nature Neuroscience, 22(5), 709–718. https://doi.org/10.1038/s41593-019-0369-4

Niu, Z., Pang, R. T. K., Liu, W., Li, Q., Cheng, R., & Yeung, W. S. B. (2017). Polymer-based precipitation preserves biological activities of extracellular vesicles from an endometrial cell line. PloS One, 12(10), e0186534. https://doi.org/10.1371/journal.pone.0186534

Nizamudeen, Z. A., Xerri, R., Parmenter, C., Suain, K., Markus, R., Chakrabarti, L., & Sottile, V. (2021). Low-Power Sonication Can Alter Extracellular Vesicle Size and Properties. Cells, 10(9), 2413. https://doi.org/10.3390/cells10092413

Noguchi, S., Tozawa, S., Sakurai, T., Ohkuchi, A., Takahashi, H., Fujiwara, H., & Takizawa, T. (2024). BeWo exomeres are enriched for bioactive extracellular placenta-specific C19MC miRNAs. Journal of Reproductive Immunology, 161, 104187. https://doi.org/10.1016/j.jri.2023.104187

Nold-Petry, C. A., Nold, M. F., Zepp, J. A., Kim, S.-H., Voelkel, N. F., & Dinarello, C. A. (2009). IL-32–dependent effects of IL-1β on endothelial cell functions. Proceedings of the National Academy of Sciences, 106(10), 3883–3888. https://doi.org/10.1073/pnas.0813334106

Nordin, J. Z., Lee, Y., Vader, P., Mäger, I., Johansson, H. J., Heusermann, W., Wiklander, O. P. B., Hällbrink, M., Seow, Y., Bultema, J. J., Gilthorpe, J., Davies, T., Fairchild, P. J., Gabrielsson, S., Meisner-Kober, N. C., Lehtiö, J., Smith, C. I. E., Wood, M. J. A., & Andaloussi, S. E. (2015). Ultrafiltration with size-exclusion liquid chromatography for high yield isolation of extracellular vesicles preserving intact biophysical and functional properties. Nanomedicine: Nanotechnology, Biology and Medicine, 11(4), 879–883. https://doi.org/10.1016/j.nano.2015.01.003

Nourhaghighi, N., Teichert-Kuliszewska, K., Davis, J., Stewart, D. J., & Nag, S. (2003). Altered Expression of Angiopoietins During Blood-Brain Barrier Breakdown and Angiogenesis. Laboratory Investigation, 83(8), 1211–1222. https://doi.org/10.1097/01.LAB.0000082383.40635.FE

Noy, P. J., Swain, R. K., Khan, K., Lodhia, P., & Bicknell, R. (2016). Sprouting angiogenesis is regulated by shedding of the C-type lectin family 14, member A (CLEC14A) ectodomain, catalyzed by rhomboid-like 2 protein (RHBDL2). The FASEB Journal, 30(6), 2311–2323. https://doi.org/10.1096/fj.201500122R

Nunez, E. A., Wallis, J., & Gershon, M. D. (1974). Secretory processes in follicular cells of the bat thyroid. III. The occurrence of extracellular vesicles and colloid droplets during

arousal from hibernation. American Journal of Anatomy, 141(2), 179–201. https://doi.org/10.1002/aja.1001410203

Oberheim, N. A., Goldman, S. A., & Nedergaard, M. (2012). Heterogeneity of Astrocytic Form and Function. In R. Milner (Ed.), Astrocytes (Vol. 814, pp. 23–45). Humana Press. https://doi.org/10.1007/978-1-61779-452-0_3

O'Brien, K., Ughetto, S., Mahjoum, S., Nair, A. V., & Breakefield, X. O. (2022). Uptake, functionality, and re-release of extracellular vesicle-encapsulated cargo. Cell Reports, 39(2), 110651. https://doi.org/10.1016/j.celrep.2022.110651

Ogbu, C. P., De Las Alas, M., Mandriota, A. M., Liu, X., Kapoor, S., Choudhury, J., Ruma, Y. N., Goodman, M. C., Sanders, C. R., Gonen, T., Kossiakoff, A. A., Duffey, M. E., & Vecchio, A. J. (2025). Biophysical basis of tight junction barrier modulation by a pan-claudin-binding molecule. PNAS Nexus, 4(6), pgaf189. https://doi.org/10.1093/pnasnexus/pgaf189

O'Hara, B. A., Morris-Love, J., Gee, G. V., Haley, S. A., & Atwood, W. J. (2020). JC Virus infected choroid plexus epithelial cells produce extracellular vesicles that infect glial cells independently of the virus attachment receptor. PLOS Pathogens, 16(3), e1008371. https://doi.org/10.1371/journal.ppat.1008371

Oikari, L. E., Pandit, R., Stewart, R., Cuní-López, C., Quek, H., Sutharsan, R., Rantanen, L. M., Oksanen, M., Lehtonen, S., De Boer, C. M., Polo, J. M., Götz, J., Koistinaho, J., & White, A. R. (2020). Altered Brain Endothelial Cell Phenotype from a Familial Alzheimer Mutation and Its Potential Implications for Amyloid Clearance and Drug Delivery. Stem Cell Reports, 14(5), 924–939. https://doi.org/10.1016/j.stemcr.2020.03.011

Okamoto, K., Hirata-Tsuchiya, S., Kitamura, C., Omoteyama, K., Sato, T., Arito, M., Kurokawa, M. S., Suematsu, N., & Kato, T. (2016). A Small Nuclear Acidic Protein (MTI-II, Zn^{2+} Binding Protein, Parathymosin) That Inhibits Transcriptional Activity of NF-κB and Its Potential Application to Antiinflammatory Drugs. Endocrinology, 157(12), 4973–4986. https://doi.org/10.1210/en.2016-1746

Ophir, G., Amariglio, N., Jacob-Hirsch, J., Elkon, R., Rechavi, G., & Michaelson, D. M. (2005). Apolipoprotein E4 enhances brain inflammation by modulation of the NF-κB signaling cascade. Neurobiology of Disease, 20(3), 709–718. https://doi.org/10.1016/j.nbd.2005.05.002

Orchanian, S. B., Still, K., Harris, T. H., & Lodoen, M. B. (2024). Deficiency in astrocyte CCL2 production reduces neuroimmune control of Toxoplasma gondii infection. PLOS Pathogens, 20(1), e1011710. https://doi.org/10.1371/journal.ppat.1011710

O'Regan, G. C., Farag, S. H., Casey, C. S., Wood-Kaczmar, A., Pocock, J. M., Tabrizi, S. J., & Andre, R. (2021). Human Huntington's disease pluripotent stem cell-derived microglia develop normally but are abnormally hyper-reactive and release elevated levels of reactive oxygen species. Journal of Neuroinflammation, 18(1), 94. https://doi.org/10.1186/s12974-021-02147-6

Osman, E. E. A., & Neamati, N. (2024). Ironing Out the Mechanism of gp130 Signaling. Pharmacological Reviews, 76(6), 1399–1443. https://doi.org/10.1124/pharmrev.124.001245

Otani, T., Nguyen, T. P., Tokuda, S., Sugihara, K., Sugawara, T., Furuse, K., Miura, T., Ebnet, K., & Furuse, M. (2019). Claudins and JAM-A coordinately regulate tight junction formation and epithelial polarity. Journal of Cell Biology, 218(10), 3372–3396. https://doi.org/10.1083/jcb.201812157

Ouweneel, A. B., Thomas, M. J., & Sorci-Thomas, M. G. (2020). The ins and outs of lipid rafts: Functions in intracellular cholesterol homeostasis, microparticles, and cell membranes. Journal of Lipid Research, 61(5), 676–686. https://doi.org/10.1194/jlr.TR119000383

Palhol, J. S. C., Balia, M., Sánchez-Román Terán, F., Labarchède, M., Gontier, E., & Battefeld, A. (2023). Direct association with the vascular basement membrane is a frequent feature of myelinating oligodendrocytes in the neocortex. Fluids and Barriers of the CNS, 20(1), 24. https://doi.org/10.1186/s12987-023-00425-4

Palma, L. G., Alvarez-Villanueva, D., Maqueda, M., Barrero, M., Iglesias, A., Bertran, J., Alvarez, D., Garcia-Prieto, C. A., Ballare, C., Rodriguez-Cortez, V., Bueno, C., Vidal, A., Villanueva, A., Menendez, P., Stik, G., Di Croce, L., Payer, B., Esteller, M., Espinosa, L., & Bigas, A. (2025). Chromatin activity of IκBα mediates the exit from naïve pluripotency. eLife, 14, RP102784. https://doi.org/10.7554/eLife.102784.3

Pamies, D., Sartori, C., Schvartz, D., González-Ruiz, V., Pellerin, L., Nunes, C., Tavel, D., Maillard, V., Boccard, J., Rudaz, S., Sanchez, J.-C., & Zurich, M.-G. (2021). Neuroinflammatory Response to TNFα and IL1β Cytokines Is Accompanied by an Increase in Glycolysis in Human Astrocytes In Vitro. International Journal of Molecular Sciences, 22(8), 4065. https://doi.org/10.3390/ijms22084065

Pan, B.-T., & Johnstone, R. M. (1983). Fate of the transferrin receptor during maturation of sheep reticulocytes in vitro: Selective externalization of the receptor. Cell, 33(3), 967–978. https://doi.org/10.1016/0092-8674(83)90040-5

Pan, J.-J., Qi, L., Wang, L., Liu, C., Song, Y., Mamtilahun, M., Hu, X., Li, Y., Chen, X., Khan, H., Xu, Q., Wang, Y., Tang, Y., Yang, G.-Y., & Zhang, Z. (2024). M2 Microglial Extracellular Vesicles Attenuated Blood-brain Barrier Disruption via MiR-23a-5p in Cerebral Ischemic Mice. Aging and Disease, 15(3), 1344–1356. https://doi.org/10.14336/AD.2023.0714

Pan, S., Mayoral, S. R., Choi, H. S., Chan, J. R., & Kheirbek, M. A. (2020). Preservation of a remote fear memory requires new myelin formation. Nature Neuroscience, 23(4), 487–499. https://doi.org/10.1038/s41593-019-0582-1

Pan, Z., Zhao, R., Li, B., Qi, Y., Qiu, W., Guo, Q., Zhang, S., Zhao, S., Xu, H., Li, M., Gao, Z., Fan, Y., Xu, J., Wang, H., Wang, S., Qiu, J., Wang, Q., Guo, X., Deng, L., … Li, G. (2022). EWSR1-induced circNEIL3 promotes glioma progression and exosome-mediated macrophage immunosuppressive polarization via stabilizing IGF2BP3. Molecular Cancer, 21(1), 16. https://doi.org/10.1186/s12943-021-01485-6

Paolicelli, R. C., Sierra, A., Stevens, B., Tremblay, M.-E., Aguzzi, A., Ajami, B., Amit, I., Audinat, E., Bechmann, I., Bennett, M., Bennett, F., Bessis, A., Biber, K., Bilbo, S., Blurton-Jones, M., Boddeke, E., Brites, D., Brône, B., Brown, G. C., … Wyss-Coray, T. (2022). Microglia states and nomenclature: A field at its crossroads. Neuron, 110(21), 3458–3483. https://doi.org/10.1016/j.neuron.2022.10.020

Parenti, A., Titi, C., Brovero, A., Blua, F., Boccato, F., Silvano, A., Fedele, F., Mattioli, A. V., Bertinaria, M., Pagliaro, P., & Penna, C. (2026). NLRP3 inhibition protects human coronary endothelial cells from oxidative and lipotoxic stress. Biochemical Pharmacology, 244, 117615. https://doi.org/10.1016/j.bcp.2025.117615

Park, J. S., Choe, K., Khan, A., Jo, M. H., Park, H. Y., Kang, M. H., Park, T. J., & Kim, M. O. (2023). Establishing Co-Culture Blood–Brain Barrier Models for Different Neurodegeneration Conditions to Understand Its Effect on BBB Integrity. International Journal of Molecular Sciences, 24(6), 5283. https://doi.org/10.3390/ijms24065283

Park, J. Y., Lee, K.-H., Park, H. S., & Choi, S. J. (2017). LPS Sensing Mechanism of Human Astrocytes: Evidence of Functional TLR4 Expression and Requirement of Soluble CD14. Journal of Bacteriology and Virology, 47(4), 189. https://doi.org/10.4167/jbv.2017.47.4.189

Park, S., Patel, S. A., Torr, E. E., Dureke, A.-G. N., McIntyre, A. M., & Skop, A. R. (2023). A protocol for isolating and imaging large extracellular vesicles or midbody remnants from mammalian cell culture. STAR Protocols, 4(4), 102562. https://doi.org/10.1016/j.xpro.2023.102562

Park, S. Y., Ha, B. G., Choi, G. H., Ryu, J., Kim, B., Jung, C. Y., & Lee, W. (2004). EHD2 Interacts with the Insulin-Responsive Glucose Transporter (GLUT4) in Rat Adipocytes and May Participate in Insulin-Induced GLUT4 Recruitment. Biochemistry, 43(23), 7552–7562. https://doi.org/10.1021/bi049970f

Patel, G. K., Khan, M. A., Bhardwaj, A., Srivastava, S. K., Zubair, H., Patton, M. C., Singh, S., Khushman, M., & Singh, A. P. (2017). Exosomes confer chemoresistance to pancreatic cancer cells by promoting ROS detoxification and miR-155-mediated suppression of key gemcitabine-metabolising enzyme, DCK. British Journal of Cancer, 116(5), 609–619. https://doi.org/10.1038/bjc.2017.18

Patel, M. R., & Weaver, A. M. (2021). Astrocyte-derived small extracellular vesicles promote synapse formation via fibulin-2-mediated TGF-β signaling. Cell Reports, 34(10), 108829. https://doi.org/10.1016/j.celrep.2021.108829

Pearson, A. C., Shrestha, K., Curry, T. E., & Duffy, D. M. (2024). Neurotensin modulates ovarian vascular permeability via adherens junctions. The FASEB Journal, 38(7), e23602. https://doi.org/10.1096/fj.202302652RR

Peche, V. S., Pietka, T. A., Jacome-Sosa, M., Samovski, D., Palacios, H., Chatterjee-Basu, G., Dudley, A. C., Beatty, W., Meyer, G. A., Goldberg, I. J., & Abumrad, N. A. (2023). Endothelial cell CD36 regulates membrane ceramide formation, exosome fatty acid transfer and circulating fatty acid levels. Nature Communications, 14(1), 4029. https://doi.org/10.1038/s41467-023-39752-3

Pei, X., Li, Y., Zhu, L., & Zhou, Z. (2019). Astrocyte-derived exosomes suppress autophagy and ameliorate neuronal damage in experimental ischemic stroke. Experimental Cell Research, 382(2), 111474. https://doi.org/10.1016/j.yexcr.2019.06.019

Pekar, O., Benjamin, S., Weidberg, H., Smaldone, S., Ramirez, F., & Horowitz, M. (2012). EHD2 shuttles to the nucleus and represses transcription. Biochemical Journal, 444(3), 383–394. https://doi.org/10.1042/BJ20111268

Pelkmans, W., Shekari, M., Brugulat-Serrat, A., Sánchez-Benavides, G., Minguillón, C., Fauria, K., Molinuevo, J. L., Grau-Rivera, O., González Escalante, A., Kollmorgen, G., Carboni, M., Ashton, N. J., Zetterberg, H., Blennow, K., Suarez-Calvet, M., Gispert, J. D., & for the ALFA study. (2024). Astrocyte biomarkers GFAP and YKL-40 mediate early Alzheimer's disease progression. Alzheimer's & Dementia, 20(1), 483–493. https://doi.org/10.1002/alz.13450

Pellerin, L., & Magistretti, P. J. (1994). Glutamate uptake into astrocytes stimulates aerobic glycolysis: A mechanism coupling neuronal activity to glucose utilization. Proceedings of the National Academy of Sciences, 91(22), 10625–10629. https://doi.org/10.1073/pnas.91.22.10625

Peng, G., Liao, Y., & Shen, C. (2017). miRNA-429 Inhibits Astrocytoma Proliferation and Invasion by Targeting BMI1. Pathology & Oncology Research, 23(2), 369–376. https://doi.org/10.1007/s12253-016-0113-2

Perez, G., Barber, G. P., Benet-Pages, A., Casper, J., Clawson, H., Diekhans, M., Fischer, C., Gonzalez, J. N., Hinrichs, A. S., Lee, C. M., Nassar, L. R., Raney, B. J., Speir, M. L., van Baren, M. J., Vaske, C. J., Haussler, D., Kent, W. J., & Haeussler, M. (2025). The UCSC Genome Browser database: 2025 update. Nucleic Acids Research, 53(D1), D1243–D1249. https://doi.org/10.1093/nar/gkae974

Pérez, L. A., Palacios, E., González, M. F., Leyton-Rivera, I., Martínez-Meza, S., Pérez-Núñez, R., Jeldes, E., Avalos, A. M., Díaz, J., & Leyton, L. (2024). A Pro-Inflammatory Stimulus versus Extensive Passaging of DITNC1 Astrocyte Cultures as Models to Study Astrogliosis. International Journal of Molecular Sciences, 25(17), 9454. https://doi.org/10.3390/ijms25179454

Pérez-Rodriguez, S., Ramírez, O. T., Trujillo-Roldán, M. A., & Valdez-Cruz, N. A. (2020). Comparison of protein precipitation methods for sample preparation prior to proteomic analysis of Chinese hamster ovary cell homogenates. Electronic Journal of Biotechnology, 48, 86–94. https://doi.org/10.1016/j.ejbt.2020.09.006

Perrin, S. (2014). Preclinical research: Make mouse studies work. Nature, 507(7493), 423–425. https://doi.org/10.1038/507423a

Perrot, C. Y., Herrera, J. L., Fournier-Goss, A. E., & Komatsu, M. (2020). Prostaglandin E2 breaks down pericyte–endothelial cell interaction via EP1 and EP4-dependent downregulation of pericyte N-cadherin, connexin-43, and R-Ras. Scientific Reports, 10(1), 11186. https://doi.org/10.1038/s41598-020-68019-w

Pfeiffer, F., Schäfer, J., Lyck, R., Makrides, V., Brunner, S., Schaeren-Wiemers, N., Deutsch, U., & Engelhardt, B. (2011). Claudin-1 induced sealing of blood–brain barrier tight junctions ameliorates chronic experimental autoimmune encephalomyelitis. Acta Neuropathologica, 122(5), 601–614. https://doi.org/10.1007/s00401-011-0883-2

Pham, C. V., Midge, S., Barua, H., Zhang, Y., Ngoc-Gia Nguyen, T., Barrero, R. A., Duan, A., Yin, W., Jiang, G., Hou, Y., Zhou, S., Wang, Y., Xie, X., Tran, P. H. L., Xiang, D., & Duan, W. (2021). Bovine extracellular vesicles contaminate human extracellular vesicles produced in cell culture conditioned medium when 'exosome-depleted serum' is utilised. Archives of Biochemistry and Biophysics, 708, 108963. https://doi.org/10.1016/j.abb.2021.108963

Pisitkun, T., Shen, R.-F., & Knepper, M. A. (2004). Identification and proteomic profiling of exosomes in human urine. Proceedings of the National Academy of Sciences, 101(36), 13368–13373. https://doi.org/10.1073/pnas.0403453101

Pols, M. S., & Klumperman, J. (2009). Trafficking and function of the tetraspanin CD63. Experimental Cell Research, 315(9), 1584–1592. https://doi.org/10.1016/j.yexcr.2008.09.020

Pons-Espinal, M., Blasco-Agell, L., Fernandez-Carasa, I., Andrés-Benito, P., Di Domenico, A., Richaud-Patin, Y., Baruffi, V., Marruecos, L., Espinosa, L., Garrido, A., Tolosa, E., Edel, M. J., Otero, M. J., Mosquera, J. L., Ferrer, I., Raya, A., & Consiglio, A. (2024). Blocking IL-6 signaling prevents astrocyte-induced neurodegeneration in an iPSC-based model of Parkinson's disease. JCI Insight, 9(3), e163359. https://doi.org/10.1172/jci.insight.163359

Pöschl, E., Schlötzer-Schrehardt, U., Brachvogel, B., Saito, K., Ninomiya, Y., & Mayer, U. (2004). Collagen IV is essential for basement membrane stability but dispensable for initiation of its assembly during early development. Development, 131(7), 1619–1628. https://doi.org/10.1242/dev.01037

Posey, J. N., Jordan, M., Lewis, C. V., Sul, C., Dobrinskikh, E., Swindle, D., Denorme, F., Irwin, D., Di Paola, J., Stenmark, K., Nozik, E. S., & Delaney, C. (2025). Nbeal2 knockout mice are not protected against hypoxia-induced pulmonary vascular remodeling and pulmonary hypertension. Blood Advances, 9(7), 1571–1584. https://doi.org/10.1182/bloodadvances.2024013880

Poskanzer, K. E., & Yuste, R. (2016). Astrocytes regulate cortical state switching in vivo. Proceedings of the National Academy of Sciences, 113(19). https://doi.org/10.1073/pnas.1520759113

Postma, R. J., Fischer, S. E., Bijkerk, R., & Van Zonneveld, A. J. (2025). Unveiling endothelial cell border heterogeneity: VE-cadherin adherens junction stratification by deep convolutional neural networks. PLOS ONE, 20(1), e0317110. https://doi.org/10.1371/journal.pone.0317110

Prada, I., Gabrielli, M., Turola, E., Iorio, A., D'Arrigo, G., Parolisi, R., De Luca, M., Pacifici, M., Bastoni, M., Lombardi, M., Legname, G., Cojoc, D., Buffo, A., Furlan, R., Peruzzi, F., & Verderio, C. (2018). Glia-to-neuron transfer of miRNAs via extracellular vesicles: A new mechanism underlying inflammation-induced synaptic alterations. Acta Neuropathologica, 135(4), 529–550. https://doi.org/10.1007/s00401-017-1803-x

Prada, I., & Meldolesi, J. (2016). Binding and Fusion of Extracellular Vesicles to the Plasma Membrane of Their Cell Targets. International Journal of Molecular Sciences, 17(8), 1296. https://doi.org/10.3390/ijms17081296

Prah, J., Winters, A., Chaudhari, K., Hersh, J., Liu, R., & Yang, S.-H. (2019). A novel serum free primary astrocyte culture method that mimic quiescent astrocyte phenotype. Journal of Neuroscience Methods, 320, 50–63. https://doi.org/10.1016/j.jneumeth.2019.03.013

Prieto-Vila, M., Yoshioka, Y., & Ochiya, T. (2021). Biological Functions Driven by mRNAs Carried by Extracellular Vesicles in Cancer. Frontiers in Cell and Developmental Biology, 9, 620498. https://doi.org/10.3389/fcell.2021.620498

Profaci, C. P., Harvey, S. S., Bajc, K., Zhang, T. Z., Jeffrey, D. A., Zhang, A. Z., Nemec, K. M., Davtyan, H., O'Brien, C. A., McKinsey, G. L., Longworth, A., McMullen, T. P., Capocchi, J. K., Gonzalez, J. G., Lawson, D. A., Arnold, T. D., Davalos, D., Blurton-Jones, M., Dabertrand, F., … Daneman, R. (2024). Microglia are not necessary for maintenance of blood-brain barrier properties in health, but PLX5622 alters brain endothelial cholesterol metabolism. Neuron, 112(17), 2910-2921.e7. https://doi.org/10.1016/j.neuron.2024.07.015

Proia, P., Schiera, G., Mineo, M., Ingrassia, A. M. R., Santoro, G., Savettieri, G., & Di Liegro, I. (2008). Astrocytes shed extracellular vesicles that contain fibroblast growth factor-2 and vascular endothelial growth factor. International Journal of Molecular Medicine, 21(1), 63–67.

Propson, N. E., Roy, E. R., Litvinchuk, A., Köhl, J., & Zheng, H. (2021). Endothelial C3a receptor mediates vascular inflammation and blood-brain barrier permeability during aging. Journal of Clinical Investigation, 131(1), e140966. https://doi.org/10.1172/JCI140966

Puhm, F., Afonyushkin, T., Resch, U., Obermayer, G., Rohde, M., Penz, T., Schuster, M., Wagner, G., Rendeiro, A. F., Melki, I., Kaun, C., Wojta, J., Bock, C., Jilma, B., Mackman, N., Boilard, E., & Binder, C. J. (2019). Mitochondria Are a Subset of Extracellular Vesicles Released by Activated Monocytes and Induce Type I IFN and TNF Responses in Endothelial Cells. Circulation Research, 125(1), 43–52. https://doi.org/10.1161/CIRCRESAHA.118.314601

Pulido, R. S., Munji, R. N., Chan, T. C., Quirk, C. R., Weiner, G. A., Weger, B. D., Rossi, M. J., Elmsaouri, S., Malfavon, M., Deng, A., Profaci, C. P., Blanchette, M., Qian, T., Foreman, K. L., Shusta, E. V., Gorman, M. R., Gachon, F., Leutgeb, S., & Daneman, R. (2020). Neuronal Activity Regulates Blood-Brain Barrier Efflux Transport through Endothelial Circadian Genes. Neuron, 108(5), 937-952.e7. https://doi.org/10.1016/j.neuron.2020.09.002

Qian, B.-Z., Li, J., Zhang, H., Kitamura, T., Zhang, J., Campion, L. R., Kaiser, E. A., Snyder, L. A., & Pollard, J. W. (2011). CCL2 recruits inflammatory monocytes to facilitate breast-tumour metastasis. Nature, 475(7355), 222–225. https://doi.org/10.1038/nature10138

Qie, S., Ran, Y., Lu, X., Su, W., Li, W., Xi, J., Gong, W., & Liu, Z. (2020). Candesartan modulates microglia activation and polarization via NF-κB signaling pathway. International Journal of Immunopathology and Pharmacology, 34, 2058738420974900. https://doi.org/10.1177/2058738420974900

Qin, H., Buckley, J. A., Li, X., Liu, Y., Fox, T. H., Meares, G. P., Yu, H., Yan, Z., Harms, A. S., Li, Y., Standaert, D. G., & Benveniste, E. N. (2016). Inhibition of the JAK/STAT Pathway Protects Against α-Synuclein-Induced Neuroinflammation and Dopaminergic Neurodegeneration. The Journal of Neuroscience, 36(18), 5144–5159. https://doi.org/10.1523/JNEUROSCI.4658-15.2016

Qin, J., Ma, Z., Chen, X., & Shu, S. (2023). Microglia activation in central nervous system disorders: A review of recent mechanistic investigations and development efforts. Frontiers in Neurology, 14, 1103416. https://doi.org/10.3389/fneur.2023.1103416

Qin, X., Zhang, K., Qiu, J., Wang, N., Qu, K., Cui, Y., Huang, J., Luo, L., Zhong, Y., Tian, T., Wu, W., Wang, Y., & Wang, G. (2022). Uptake of oxidative stress-mediated extracellular vesicles by vascular endothelial cells under low magnitude shear stress. Bioactive Materials, 9, 397–410. https://doi.org/10.1016/j.bioactmat.2021.10.038

Qin, Z., Shi, D.-D., Li, W., Cheng, D., Zhang, Y.-D., Zhang, S., Tsoi, B., Zhao, J., Wang, Z., & Zhang, Z.-J. (2023). Berberine ameliorates depression-like behaviors in mice via inhibiting NLRP3 inflammasome-mediated neuroinflammation and preventing neuroplasticity disruption. Journal of Neuroinflammation, 20(1), 54. https://doi.org/10.1186/s12974-023-02744-7

Quraishe, S., Asuni, A., Boelens, W. C., O'Connor, V., & Wyttenbach, A. (2008). Expression of the small heat shock protein family in the mouse CNS: Differential anatomical and biochemical compartmentalization. Neuroscience, 153(2), 483–491. https://doi.org/10.1016/j.neuroscience.2008.01.058

Raff, M. C., Miller, R. H., & Noble, M. (1983). A glial progenitor cell that develops in vitro into an astrocyte or an oligodendrocyte depending on culture medium. Nature, 303(5916), 390–396. https://doi.org/10.1038/303390a0

Rajan, A. M., Ma, R. C., Kocha, K. M., Zhang, D. J., & Huang, P. (2020). Dual function of perivascular fibroblasts in vascular stabilization in zebrafish. PLOS Genetics, 16(10), e1008800. https://doi.org/10.1371/journal.pgen.1008800

Ramilowski, J. A., Goldberg, T., Harshbarger, J., Kloppmann, E., Lizio, M., Satagopam, V. P., Itoh, M., Kawaji, H., Carninci, P., Rost, B., & Forrest, A. R. R. (2015). A draft network of ligand–receptor-mediated multicellular signalling in human. Nature Communications, 6(1), 7866. https://doi.org/10.1038/ncomms8866

Randles, M. J., Lausecker, F., Humphries, J. D., Byron, A., Clark, S. J., Miner, J. H., Zent, R., Humphries, M. J., & Lennon, R. (2020). Basement membrane ligands initiate distinct signalling networks to direct cell shape. Matrix Biology, 90, 61–78. https://doi.org/10.1016/j.matbio.2020.02.005

Ransohoff, R. M. (2016). A polarizing question: Do M1 and M2 microglia exist? Nature Neuroscience, 19(8), 987–991. https://doi.org/10.1038/nn.4338

Rao, R., Redha, R., Macias-Perez, I., Su, Y., Hao, C., Zent, R., Breyer, M. D., & Pozzi, A. (2007). Prostaglandin E2-EP4 Receptor Promotes Endothelial Cell Migration via ERK Activation and Angiogenesis in Vivo. Journal of Biological Chemistry, 282(23), 16959–16968. https://doi.org/10.1074/jbc.M701214200

Raposo, G., Nijman, H. W., Stoorvogel, W., Liejendekker, R., Harding, C. V., Melief, C. J., & Geuze, H. J. (1996). B lymphocytes secrete antigen-presenting vesicles. The Journal of Experimental Medicine, 183(3), 1161–1172. https://doi.org/10.1084/jem.183.3.1161

Ratajczak, J., Miekus, K., Kucia, M., Zhang, J., Reca, R., Dvorak, P., & Ratajczak, M. Z. (2006). Embryonic stem cell-derived microvesicles reprogram hematopoietic progenitors: Evidence for horizontal transfer of mRNA and protein delivery. Leukemia, 20(5), 847–856. https://doi.org/10.1038/sj.leu.2404132

Ravasi, T., Suzuki, H., Pang, K. C., Katayama, S., Furuno, M., Okunishi, R., Fukuda, S., Ru, K., Frith, M. C., Gongora, M. M., Grimmond, S. M., Hume, D. A., Hayashizaki, Y., & Mattick, J. S. (2006). Experimental validation of the regulated expression of large numbers

of non-coding RNAs from the mouse genome. Genome Research, 16(1), 11–19. https://doi.org/10.1101/gr.4200206

Reese, T. S., & Karnovsky, M. J. (1967). Fine Structural Localization of a Blood-Brain Barrier To Exogenous Peroxidase. The Journal of Cell Biology, 34(1), 207–217. https://doi.org/10.1083/jcb.34.1.207

Regalia, M. (2002). Prediction of signal recognition particle RNA genes. Nucleic Acids Research, 30(15), 3368–3377. https://doi.org/10.1093/nar/gkf468

Ren, C., Li, N., Wang, B., Yang, Y., Gao, J., Li, S., Ding, Y., Jin, K., & Ji, X. (2015). Limb Ischemic Perconditioning Attenuates Blood-Brain Barrier Disruption by Inhibiting Activity of MMP-9 and Occludin Degradation after Focal Cerebral Ischemia. Aging and Disease, 6(6), 406–417. https://doi.org/10.14336/AD.2015.0812

Ren, Y., Yang, J., Xie, R., Gao, L., Yang, Y., Fan, H., & Qian, K. (2011). Exosomal-like vesicles with immune-modulatory features are present in human plasma and can induce CD4+ T-cell apoptosis in vitro. Transfusion, 51(5), 1002–1011. https://doi.org/10.1111/j.1537-2995.2010.02909.x

Reseco, L., Molina-Crespo, A., Atienza, M., Gonzalez, E., Falcon-Perez, J. M., & Cantero, J. L. (2024). Characterization of Extracellular Vesicles from Human Saliva: Effects of Age and Isolation Techniques. Cells, 13(1), 95. https://doi.org/10.3390/cells13010095

Rho, S.-S., Choi, H.-J., Min, J.-K., Lee, H.-W., Park, H., Park, H., Kim, Y.-M., & Kwon, Y.-G. (2011). Clec14a is specifically expressed in endothelial cells and mediates cell to cell adhesion. Biochemical and Biophysical Research Communications, 404(1), 103–108. https://doi.org/10.1016/j.bbrc.2010.11.075

Ribeiro, E., Gatchoff, P., Nouh, C. D., & Moon, J.-S. (2023). Severe Hypoglycemic Brain Injury Associated with Diffuse Restricted Diffusion on MRI Brain Sparing Cerebellar Lobes (P10-7.006). Neurology, 100(17_supplement_2), 2836. https://doi.org/10.1212/WNL.0000000000202832

Richards, M. H., Narasipura, S. D., Kim, S., Seaton, M. S., Lutgen, V., & Al-Harthi, L. (2015). Dynamic interaction between astrocytes and infiltrating PBMC s in context of neuro AIDS. Glia, 63(3), 441–451. https://doi.org/10.1002/glia.22763

Rider, M. A., Hurwitz, S. N., & Meckes, D. G. (2016). ExtraPEG: A Polyethylene Glycol-Based Method for Enrichment of Extracellular Vesicles. Scientific Reports, 6(1), 23978. https://doi.org/10.1038/srep23978

Riederer, M., Lechleitner, M., Hrzenjak, A., Koefeler, H., Desoye, G., Heinemann, A., & Frank, S. (2011). Endothelial lipase (EL) and EL-generated lysophosphatidylcholines promote IL-8 expression in endothelial cells. Atherosclerosis, 214(2), 338–344. https://doi.org/10.1016/j.atherosclerosis.2010.11.007

Riese, M. J., Grewal, J., Das, J., Zou, T., Patil, V., Chakraborty, A. K., & Koretzky, G. A. (2011). Decreased Diacylglycerol Metabolism Enhances ERK Activation and Augments CD8+ T Cell Functional Responses. Journal of Biological Chemistry, 286(7), 5254–5265. https://doi.org/10.1074/jbc.M110.171884

Río-Hortega, P. (1919a). El “Tercer Elemento” de los Centros Nerviosos. I. La Microglía en Estado Normal, Boletín de la Sociedad Española de Biología VIII. Boletín de La Sociedad Española de Biología VIII, 67–82.

Río-Hortega, P. (1919b). El ‘Tercer Elemento de los Centros Nerviosos’. II. Intervención de la Microglía en los Procesos Patológicos (Células en Bastoncito y Cuerpos Gránuloadiposos). Boletín de La Sociedad Española de Biología VIII, 91–103.

Río-Hortega, P. (1919c). El “Tercer Elemento” de los Centros Nerviosos. III. Naturaleza Probable de la Microglía. Boletín de La Sociedad Española de Biología VIII, 108–121.

Río-Hortega, P. (1919d). El" Tercer Elemento" de los Centros Nerviosos. IV. Poder Fagocitario y Movilidad de la Microglía. Boletín de La Sociedad Española de Biología VIII, 154–171.

Robinson, M. D., McCarthy, D. J., & Smyth, G. K. (2010). edgeR: A Bioconductor package for differential expression analysis of digital gene expression data. Bioinformatics, 26(1), 139–140. https://doi.org/10.1093/bioinformatics/btp616

Rochfort, K. D., Collins, L. E., Murphy, R. P., & Cummins, P. M. (2014). Downregulation of Blood-Brain Barrier Phenotype by Proinflammatory Cytokines Involves NADPH Oxidase-Dependent ROS Generation: Consequences for Interendothelial Adherens and Tight Junctions. PLoS ONE, 9(7), e101815. https://doi.org/10.1371/journal.pone.0101815

Rodrigues-Junior, D. M., Tan, S. S., De Souza Viana, L., Carvalho, A. L., Lim, S. K., Iyer, N. G., & Vettore, A. L. (2019). A preliminary investigation of circulating extracellular vesicles and biomarker discovery associated with treatment response in head and neck squamous cell carcinoma. BMC Cancer, 19(1), 373. https://doi.org/10.1186/s12885-019-5565-9

Rogalska, M. E., Mancini, E., Bonnal, S., Gohr, A., Dunyak, B. M., Arecco, N., Smith, P. G., Vaillancourt, F. H., & Valcárcel, J. (2024). Transcriptome-wide splicing network reveals specialized regulatory functions of the core spliceosome. Science, 386(6721), 551–560. https://doi.org/10.1126/science.adn8105

Rojo Pulido, I., Nightingale, T. D., Darchen, F., Seabra, M. C., Cutler, D. F., & Gerke, V. (2011). Myosin Va Acts in Concert with Rab27a and MyRIP to Regulate Acute Von-Willebrand Factor Release from Endothelial Cells. Traffic, 12(10), 1371–1382. https://doi.org/10.1111/j.1600-0854.2011.01248.x

Rong, Y., Ji, C., Wang, Z., Ge, X., Wang, J., Ye, W., Tang, P., Jiang, D., Fan, J., Yin, G., Liu, W., & Cai, W. (2021). Small extracellular vesicles encapsulating CCL2 from activated astrocytes induce microglial activation and neuronal apoptosis after traumatic spinal cord injury. Journal of Neuroinflammation, 18(1), 196. https://doi.org/10.1186/s12974-021-02268-y

Rothhammer, V., Mascanfroni, I. D., Bunse, L., Takenaka, M. C., Kenison, J. E., Mayo, L., Chao, C.-C., Patel, B., Yan, R., Blain, M., Alvarez, J. I., Kébir, H., Anandasabapathy, N., Izquierdo, G., Jung, S., Obholzer, N., Pochet, N., Clish, C. B., Prinz, M., … Quintana, F. J. (2016). Type I interferons and microbial metabolites of tryptophan modulate astrocyte activity and central nervous system inflammation via the aryl hydrocarbon receptor. Nature Medicine, 22(6), 586–597. https://doi.org/10.1038/nm.4106

Rouget, C. (1873). Mémoire sur le développement, la structure et les propriétés physiologiques des capillaires sanguins et lymphatiques. Archives de Physiologie Normale et Pathologique (Arch Physiol Norm Path), 5, 603–663.

Roy, S., Hochberg, F. H., & Jones, P. S. (2018). Extracellular vesicles: The growth as diagnostics and therapeutics; a survey. Journal of Extracellular Vesicles, 7(1), 1438720. https://doi.org/10.1080/20013078.2018.1438720

Royse, M. K., Fowler, M., Mai, A. K., He, Y., Durante, M. R., Buist, N., Procopio, A., Xu, J., & Veiseh, O. (2024). Development of a 3D printed perfusable in vitro blood–brain barrier model for use as a scalable screening tool. Biomaterials Science, 12(17), 4363–4375. https://doi.org/10.1039/D4BM00663A

Ruan, Z., Pathak, D., Venkatesan Kalavai, S., Yoshii-Kitahara, A., Muraoka, S., Bhatt, N., Takamatsu-Yukawa, K., Hu, J., Wang, Y., Hersh, S., Ericsson, M., Gorantla, S., Gendelman, H. E., Kayed, R., Ikezu, S., Luebke, J. I., & Ikezu, T. (2021). Alzheimer's disease brain-derived extracellular vesicles spread tau pathology in interneurons. Brain, 144(1), 288–309. https://doi.org/10.1093/brain/awaa376

Ruff, C. T., Koren, M. J., Grimsby, J., Rosenbaum, A. I., Tu, X., Karathanasis, S. K., Falloon, J., Hsia, J., Guan, Y., Conway, J., Tsai, L.-F., Hummer, B. T., Hirshberg, B., Kuder, J. F., Murphy, S. A., George, R. T., & Sabatine, M. S. (2021). LEGACY: Phase 2a Trial to Evaluate the Safety, Pharmacokinetics, and Pharmacodynamic Effects of the Anti-EL (Endothelial Lipase) Antibody MEDI5884 in Patients With Stable Coronary Artery Disease. Arteriosclerosis, Thrombosis, and Vascular Biology, 41(12), 3005–3014. https://doi.org/10.1161/ATVBAHA.120.315757

Rupnick, M. A., Carey, A., & Williams, S. K. (1988). Phenotypic diversity in cultured cerebral microvascular endothelial cells. In Vitro Cellular & Developmental Biology, 24(5), 435–444. https://doi.org/10.1007/BF02628495

Russo, M. V., & McGavern, D. B. (2015). Immune Surveillance of the CNS following Infection and Injury. Trends in Immunology, 36(10), 637–650. https://doi.org/10.1016/j.it.2015.08.002

Ryu, Y., Son, H.-J., Hwang, J. S., Noh, K. B., Oh, S.-H., Choi, E.-K., & Shin, Y. J. (2025). AMF30a promotes survival and function of human corneal endothelial cells by regulating TGF-β/ROCK/HIPPO pathway. Scientific Reports, 15(1), 28271. https://doi.org/10.1038/s41598-025-13656-2

Sackmann-Sala, L., Berryman, D. E., Lubbers, E. R., Zhang, H., Vesel, C. B., Troike, K. M., Gosney, E. S., List, E. O., & Kopchick, J. J. (2014). Age-Related and Depot-Specific Changes in White Adipose Tissue of Growth Hormone Receptor-Null Mice. The Journals of Gerontology: Series A, 69(1), 34–43. https://doi.org/10.1093/gerona/glt110

Saito, A. C., Higashi, T., Fukazawa, Y., Otani, T., Tauchi, M., Higashi, A. Y., Furuse, M., & Chiba, H. (2021). Occludin and tricellulin facilitate formation of anastomosing tight-junction strand network to improve barrier function. Molecular Biology of the Cell, 32(8), 722–738. https://doi.org/10.1091/mbc.E20-07-0464

Saitou, M., Furuse, M., Sasaki, H., Schulzke, J.-D., Fromm, M., Takano, H., Noda, T., & Tsukita, S. (2000). Complex Phenotype of Mice Lacking Occludin, a Component of Tight Junction Strands. Molecular Biology of the Cell, 11(12), 4131–4142.

Sakamoto, T., Koya, T., Togi, M., Yoshida, K., Kato, T., Ishigaki, Y., & Shimodaira, S. (2022). Different In Vitro-Generated MUTZ-3-Derived Dendritic Cell Types Secrete Dexosomes with Distinct Phenotypes and Antigen Presentation Potencies. International Journal of Molecular Sciences, 23(15), 8362. https://doi.org/10.3390/ijms23158362

Sansone, P., Savini, C., Kurelac, I., Chang, Q., Amato, L. B., Strillacci, A., Stepanova, A., Iommarini, L., Mastroleo, C., Daly, L., Galkin, A., Thakur, B. K., Soplop, N., Uryu, K., Hoshino, A., Norton, L., Bonafé, M., Cricca, M., Gasparre, G., … Bromberg, J. (2017). Packaging and transfer of mitochondrial DNA via exosomes regulate escape from dormancy in hormonal therapy-resistant breast cancer. Proceedings of the National Academy of Sciences, 114(43). https://doi.org/10.1073/pnas.1704862114

Santana, S. M., Antonyak, M. A., Cerione, R. A., & Kirby, B. J. (2014). Microfluidic isolation of cancer-cell-derived microvesicles from hetergeneous extracellular shed vesicle populations. Biomedical Microdevices, 16(6), 869–877. https://doi.org/10.1007/s10544-014-9891-z

Santavanond, J. P., Rutter, S. F., Atkin-Smith, G. K., & Poon, I. K. H. (2021). Apoptotic Bodies: Mechanism of Formation, Isolation and Functional Relevance. In S. Mathivanan, P. Fonseka, C. Nedeva, & I. Atukorala (Eds), New Frontiers: Extracellular Vesicles (Vol. 97, pp. 61–88). Springer International Publishing. https://doi.org/10.1007/978-3-030-67171-6_4

Sapoń, K., Mańka, R., Janas, T., & Janas, T. (2023). The role of lipid rafts in vesicle formation. Journal of Cell Science, 136(9), jcs260887. https://doi.org/10.1242/jcs.260887

Saunders, N. R., Dreifuss, J.-J., Dziegielewska, K. M., Johansson, P. A., Habgood, M. D., MÃ¸llgÃ¥rd, K., & Bauer, H.-C. (2014). The rights and wrongs of blood-brain barrier permeability studies: A walk through 100 years of history. Frontiers in Neuroscience, 8. https://doi.org/10.3389/fnins.2014.00404

Savettieri, G., Liegro, I. D., Catania, C., Licata, L., Pitarresi, G. L., D'Agostino, S., Schiera, G., De Caro, V., Giandalia, G., Giannola, L. I., & Cestelli, A. (2000). Neurons and ECM regulate occludin localization in brain endothelial cells: NeuroReport, 11(5), 1081–1084. https://doi.org/10.1097/00001756-200004070-00035

Sawada, R., Lowe, J. B., & Fukuda, M. (1993). E-selectin-dependent adhesion efficiency of colonic carcinoma cells is increased by genetic manipulation of their cell surface lysosomal membrane glycoprotein-1 expression levels. The Journal of Biological Chemistry, 268(17), 12675–12681.

Sayed, N., Liu, C., Ameen, M., Himmati, F., Zhang, J. Z., Khanamiri, S., Moonen, J.-R., Wnorowski, A., Cheng, L., Rhee, J.-W., Gaddam, S., Wang, K. C., Sallam, K., Boyd, J. H., Woo, Y. J., Rabinovitch, M., & Wu, J. C. (2020). Clinical trial in a dish using iPSCs shows lovastatin improves endothelial dysfunction and cellular cross-talk in LMNA cardiomyopathy. Science Translational Medicine, 12(554), eaax9276. https://doi.org/10.1126/scitranslmed.aax9276

Schafer, D. P., Lehrman, E. K., Kautzman, A. G., Koyama, R., Mardinly, A. R., Yamasaki, R., Ransohoff, R. M., Greenberg, M. E., Barres, B. A., & Stevens, B. (2012). Microglia Sculpt Postnatal Neural Circuits in an Activity and Complement-Dependent Manner. Neuron, 74(4), 691–705. https://doi.org/10.1016/j.neuron.2012.03.026

Scheld, M., Jülich, N., Vöhringer, K., Zendedel, A., Beyer, C., Kant, S., Tillmann, N., & Sanadgol, N. (2026). Activated Microglia-Derived Extracellular Vesicles Elicit a Pro-Inflammatory Astrocytic Response via Cargo-Dependent Mechanisms. Biomolecules, 16(2), 224. https://doi.org/10.3390/biom16020224

Schiera, G., Sala, S., Gallo, A., Raffa, M. P., Pitarresi, G. L., Savettieri, G., & Liegro, I. D. (2005). Permeability properties of a three-cell type in vitro model of blood-brain barrier. Journal of Cellular and Molecular Medicine, 9(2), 373–379. https://doi.org/10.1111/j.1582-4934.2005.tb00362.x

Schinzari, F., Veneziani, A., Mores, N., Barini, A., Di Daniele, N., Cardillo, C., & Tesauro, M. (2017). Beneficial Effects of Apelin on Vascular Function in Patients With Central Obesity. Hypertension, 69(5), 942–949. https://doi.org/10.1161/HYPERTENSIONAHA.116.08916

Schrade, A., Sade, H., Couraud, P.-O., Romero, I. A., Weksler, B. B., & Niewoehner, J. (2012). Expression and localization of claudins-3 and -12 in transformed human brain endothelium. Fluids and Barriers of the CNS, 9(1), 6. https://doi.org/10.1186/2045-8118-9-6

Schreiner, B., Romanelli, E., Liberski, P., Ingold-Heppner, B., Sobottka-Brillout, B., Hartwig, T., Chandrasekar, V., Johannssen, H., Zeilhofer, H. U., Aguzzi, A., Heppner, F., Kerschensteiner, M., & Becher, B. (2015). Astrocyte Depletion Impairs Redox Homeostasis and Triggers Neuronal Loss in the Adult CNS. Cell Reports, 12(9), 1377–1384. https://doi.org/10.1016/j.celrep.2015.07.051

Schroeder, A., Mueller, O., Stocker, S., Salowsky, R., Leiber, M., Gassmann, M., Lightfoot, S., Menzel, W., Granzow, M., & Ragg, T. (2006). The RIN: An RNA integrity number for assigning integrity values to RNA measurements. BMC Molecular Biology, 7(1), 3. https://doi.org/10.1186/1471-2199-7-3

Schroer, A. B., Ventura, P. B., Sucharov, J., Misra, R., Chui, M. K. K., Bieri, G., Horowitz, A. M., Smith, L. K., Encabo, K., Tenggara, I., Couthouis, J., Gross, J. D., Chan, J. M., Luke, A., & Villeda, S. A. (2023). Platelet factors attenuate inflammation and rescue cognition in ageing. Nature, 620(7976), 1071–1079. https://doi.org/10.1038/s41586-023-06436-3

Schumacher, S., Tahiri, H., Ezan, P., Rouach, N., Witschas, K., & Leybaert, L. (2024). Inhibiting astrocyte connexin-43 hemichannels blocks radiation-induced vesicular VEGF-A release and blood–brain barrier dysfunction. Glia, 72(1), 34–50. https://doi.org/10.1002/glia.24460

Selig, E. E., Zlatic, C. O., Cox, D., Mok, Y.-F., Gooley, P. R., Ecroyd, H., & Griffin, M. D. W. (2020). N- and C-terminal regions of αB-crystallin and Hsp27 mediate inhibition of amyloid nucleation, fibril binding, and fibril disaggregation. Journal of Biological Chemistry, 295(29), 9838–9854. https://doi.org/10.1074/jbc.RA120.012748

Sena, G., & Smith, A. (2022). smithlabcode/falco: V1.2.1 - 9/15/2022 (Version v1.2.1) [Computer software]. Zenodo. https://doi.org/10.5281/ZENODO.7083534

Seo, J. H., Maki, T., Maeda, M., Miyamoto, N., Liang, A. C., Hayakawa, K., Pham, L.-D. D., Suwa, F., Taguchi, A., Matsuyama, T., Ihara, M., Kim, K.-W., Lo, E. H., & Arai, K. (2014). Oligodendrocyte Precursor Cells Support Blood-Brain Barrier Integrity via TGF-β Signaling. PLoS ONE, 9(7), e103174. https://doi.org/10.1371/journal.pone.0103174

Seo, J. H., Miyamoto, N., Hayakawa, K., Pham, L.-D. D., Maki, T., Ayata, C., Kim, K.-W., Lo, E. H., & Arai, K. (2013). Oligodendrocyte precursors induce early blood-brain barrier opening after white matter injury. Journal of Clinical Investigation, JCI65863. https://doi.org/10.1172/JCI65863

Shan, C., Zhang, C., & Zhang, C. (2024). The Role of IL-6 in Neurodegenerative Disorders. Neurochemical Research, 49(4), 834–846. https://doi.org/10.1007/s11064-023-04085-6

Shan, R., Liu, N., Yan, Y., & Liu, B. (2021). Apoptosis, autophagy and atherosclerosis: Relationships and the role of Hsp27. Pharmacological Research, 166, 105169. https://doi.org/10.1016/j.phrs.2020.105169

Shan, S., Zhang, Y., Zhao, H., Zeng, T., & Zhao, X. (2022). Polystyrene nanoplastics penetrate across the blood-brain barrier and induce activation of microglia in the brain of mice. Chemosphere, 298, 134261. https://doi.org/10.1016/j.chemosphere.2022.134261

Shao, J., Meng, Y., Yuan, K., Wu, Q., Zhu, S., Li, Y., Wu, P., Zheng, J., & Shi, H. (2023). RU.521 mitigates subarachnoid hemorrhage-induced brain injury via regulating microglial polarization and neuroinflammation mediated by the cGAS/STING/NF-κB pathway. Cell Communication and Signaling, 21(1), 264. https://doi.org/10.1186/s12964-023-01274-2

Shen, F., Walker, E. J., Jiang, L., Degos, V., Li, J., Sun, B., Heriyanto, F., Young, W. L., & Su, H. (2011). Coexpression of Angiopoietin-1 with VEGF Increases the Structural Integrity of the Blood–Brain Barrier and Reduces Atrophy Volume. Journal of Cerebral Blood Flow & Metabolism, 31(12), 2343–2351. https://doi.org/10.1038/jcbfm.2011.97

Shepro, D., & Morel, N. M. L. (1993). Pericyte physiology. The FASEB Journal, 7(11), 1031–1038. https://doi.org/10.1096/fasebj.7.11.8370472

Sherwood, D. R. (2021). Basement membrane remodeling guides cell migration and cell morphogenesis during development. Current Opinion in Cell Biology, 72, 19–27. https://doi.org/10.1016/j.ceb.2021.04.003

Shi, F.-D., & Yong, V. W. (2025). Neuroinflammation across neurological diseases. Science, 388(6753), eadx0043. https://doi.org/10.1126/science.adx0043

Shi, J.-M., Liu, H., Cai, L., Guo, Y.-B., Ma, H., Li, Y.-S., Li, S.-D., Zhang, Z.-Y., Ma, Y.-D., & Guo, C.-H. (2023). Identification and functional comparison of primary astrocytes and microglia. Journal of Neuroscience Methods, 383, 109731. https://doi.org/10.1016/j.jneumeth.2022.109731

Shi, Y., Jiang, X., Zhang, L., Pu, H., Hu, X., Zhang, W., Cai, W., Gao, Y., Leak, R. K., Keep, R. F., Bennett, M. V. L., & Chen, J. (2017). Endothelium-targeted overexpression of heat shock protein 27 ameliorates blood–brain barrier disruption after ischemic brain injury. Proceedings of the National Academy of Sciences, 114(7). https://doi.org/10.1073/pnas.1621174114

Shigemoto-Mogami, Y., Hoshikawa, K., & Sato, K. (2018). Activated Microglia Disrupt the Blood-Brain Barrier and Induce Chemokines and Cytokines in a Rat in vitro Model. Frontiers in Cellular Neuroscience, 12, 494. https://doi.org/10.3389/fncel.2018.00494

Shigetomi, K., Ono, Y., Inai, T., & Ikenouchi, J. (2018). Adherens junctions influence tight junction formation via changes in membrane lipid composition. Journal of Cell Biology, 217(7), 2373–2381. https://doi.org/10.1083/jcb.201711042

Shimojima, N., Eckman, C. B., McKinney, M., Sevlever, D., Yamamoto, S., Lin, W., Dickson, D. W., & Nguyen, J. H. (2008). Altered Expression of Zonula Occludens-2 Precedes Increased Blood-Brain Barrier Permeability in a Murine Model of Fulminant Hepatic Failure. Journal of Investigative Surgery : The Official Journal of the Academy of Surgical Research, 21(3), 101–108. https://doi.org/10.1080/08941930802043565

Shioya, M., Nishida, A., Yagi, Y., Ogawa, A., Tsujikawa, T., Kim-Mitsuyama, S., Takayanagi, A., Shimizu, N., Fujiyama, Y., & Andoh, A. (2007). Epithelial overexpression of interleukin-32α in inflammatory bowel disease. Clinical and Experimental Immunology, 149(3), 480–486. https://doi.org/10.1111/j.1365-2249.2007.03439.x

Shpakovski, D. G., Shematorova, E. K., & Shpakovski, G. V. (2004). New Genes on Human Chromosome 7: Bioinformation Analysis of a Cluster of Genes from the POLR2J Family. Russian Journal of Bioorganic Chemistry, 30(6), 561–565. https://doi.org/10.1023/B:RUBI.0000049773.14555.4c

Shurer, C. R., Kuo, J. C.-H., Roberts, L. M., Gandhi, J. G., Colville, M. J., Enoki, T. A., Pan, H., Su, J., Noble, J. M., Hollander, M. J., O'Donnell, J. P., Yin, R., Pedram, K., Möckl, L., Kourkoutis, L. F., Moerner, W. E., Bertozzi, C. R., Feigenson, G. W., Reesink, H. L., & Paszek, M. J. (2019). Physical Principles of Membrane Shape Regulation by the Glycocalyx. Cell, 177(7), 1757-1770.e21. https://doi.org/10.1016/j.cell.2019.04.017

Siddharthan, V., Kim, Y. V., Liu, S., & Kim, K. S. (2007). Human astrocytes/astrocyte-conditioned medium and shear stress enhance the barrier properties of human brain microvascular endothelial cells. Brain Research, 1147, 39–50. https://doi.org/10.1016/j.brainres.2007.02.029

Siddiqui, M. R., Mayanil, C. S., Kim, K. S., & Tomita, T. (2015). Angiopoietin-1 Regulates Brain Endothelial Permeability through PTPN-2 Mediated Tyrosine Dephosphorylation of Occludin. PLOS ONE, 10(6), e0130857. https://doi.org/10.1371/journal.pone.0130857

Sierra, A., De Castro, F., Del Río-Hortega, J., Rafael Iglesias-Rozas, J., Garrosa, M., & Kettenmann, H. (2016). The "Big-Bang" for modern glial biology: Translation and comments on Pío del Río-Hortega 1919 series of papers on microglia. Glia, 64(11), 1801–1840. https://doi.org/10.1002/glia.23046

Silachev, D., Goryunov, K., Shpilyuk, M., Beznoschenko, O., Morozova, N., Kraevaya, E., Popkov, V., Pevzner, I., Zorova, L., Evtushenko, E., Starodubtseva, N., Kononikhin, A., Bugrova, A., Evtushenko, E., Plotnikov, E., Zorov, D., & Sukhikh, G. (2019). Effect of MSCs and MSC-Derived Extracellular Vesicles on Human Blood Coagulation. Cells, 8(3), 258. https://doi.org/10.3390/cells8030258

Silva, A. C., Lee, S.-P., Iadecola, C., & Kim, S.-G. (2000). Early Temporal Characteristics of Cerebral Blood Flow and Deoxyhemoglobin Changes during Somatosensory Stimulation. Journal of Cerebral Blood Flow & Metabolism, 20(1), 201–206. https://doi.org/10.1097/00004647-200001000-00025

Simard, M., Arcuino, G., Takano, T., Liu, Q. S., & Nedergaard, M. (2003). Signaling at the Gliovascular Interface. The Journal of Neuroscience, 23(27), 9254–9262. https://doi.org/10.1523/JNEUROSCI.23-27-09254.2003

Sims, M. A., Field, S. D., Barnes, M. R., Shaikh, N., Ellington, K., Murphy, K. E., Spurr, N., & Campbell, D. A. (2000). Cloning and characterisation of ITGAV, the genomic sequence for human cell adhesion protein (vitronectin) receptor alpha subunit, CD51. Cytogenetic and Genome Research, 89(3–4), 268–271. https://doi.org/10.1159/000015631

Singh, B. K., Cooney, A. L., Krishnamurthy, S., & Sinn, P. L. (2020). Extracellular Vesicle-Mediated siRNA Delivery, Protein Delivery, and CFTR Complementation in Well-Differentiated Human Airway Epithelial Cells. Genes, 11(4), 351. https://doi.org/10.3390/genes11040351

Singh, M., Hunt, C. R., Pandita, R. K., Kumar, R., Yang, C.-R., Horikoshi, N., Bachoo, R., Serag, S., Story, M. D., Shay, J. W., Powell, S. N., Gupta, A., Jeffery, J., Pandita, S., Chen, B. P. C., Deckbar, D., Löbrich, M., Yang, Q., Khanna, K. K., … Pandita, T. K. (2013). Lamin A/C Depletion Enhances DNA Damage-Induced Stalled Replication Fork Arrest. Molecular and Cellular Biology, 33(6), 1210–1222. https://doi.org/10.1128/MCB.01676-12

Singh, N. R., Gromnicova, R., Brachner, A., Kraev, I., Romero, I. A., Neuhaus, W., & Male, D. (2023). A hydrogel model of the human blood-brain barrier using differentiated stem cells. PloS One, 18(4), e0283954. https://doi.org/10.1371/journal.pone.0283954

Sixt, M., Engelhardt, B., Pausch, F., Hallmann, R., Wendler, O., & Sorokin, L. M. (2001). Endothelial Cell Laminin Isoforms, Laminins 8 and 10, Play Decisive Roles in T Cell Recruitment across the Blood–Brain Barrier in Experimental Autoimmune Encephalomyelitis. The Journal of Cell Biology, 153(5), 933–946. https://doi.org/10.1083/jcb.153.5.933

Skog, J., Würdinger, T., Van Rijn, S., Meijer, D. H., Gainche, L., Curry, W. T., Carter, B. S., Krichevsky, A. M., & Breakefield, X. O. (2008). Glioblastoma microvesicles transport RNA and proteins that promote tumour growth and provide diagnostic biomarkers. Nature Cell Biology, 10(12), 1470–1476. https://doi.org/10.1038/ncb1800

Skrika-Alexopoulos, E., & Mark Smales, C. (2023). Isolation and characterisation of exosomes from Chinese hamster ovary (CHO) cells. Biotechnology Letters, 45(4), 425–437. https://doi.org/10.1007/s10529-023-03353-3

Sladojevic, N., Stamatovic, S. M., Johnson, A. M., Choi, J., Hu, A., Dithmer, S., Blasig, I. E., Keep, R. F., & Andjelkovic, A. V. (2019). Claudin-1-Dependent Destabilization of the Blood–Brain Barrier in Chronic Stroke. The Journal of Neuroscience, 39(4), 743–757. https://doi.org/10.1523/JNEUROSCI.1432-18.2018

Smolders, S. M., Swinnen, N., Kessels, S., Arnauts, K., Smolders, S., Le Bras, B., Rigo, J., Legendre, P., & Brône, B. (2017). Age-specific function of α5β1 integrin in microglial migration during early colonization of the developing mouse cortex. Glia, 65(7), 1072–1088. https://doi.org/10.1002/glia.23145

Smyth, L. C. D., Highet, B., Jansson, D., Wu, J., Rustenhoven, J., Aalderink, M., Tan, A., Li, S., Johnson, R., Coppieters, N., Handley, R., Narayan, P., Singh-Bains, M. K., Schweder, P., Turner, C., Mee, E. W., Heppner, P., Correia, J., Park, T. I.-H., … Dragunow, M. (2022). Characterisation of PDGF-BB:PDGFRβ signalling pathways in human brain pericytes: Evidence of disruption in Alzheimer's disease. Communications Biology, 5(1), 235. https://doi.org/10.1038/s42003-022-03180-8

Smyth, N., Seda Vatansever, H., Meyer, M., Frie, C., Paulsson, M., & Edgar, D. (1998). The Targeted Deletion of the LAMC1 Gene. Annals of the New York Academy of Sciences, 857(1), 283–286. https://doi.org/10.1111/j.1749-6632.1998.tb10133.x

Sofroniew, M. V. (2015). Astrogliosis. Cold Spring Harbor Perspectives in Biology, 7(2), a020420. https://doi.org/10.1101/cshperspect.a020420

Soliman, Y., Al-khodor, J., Yildirim Köken, G., & Mustafaoglu, N. (2025). A guide for blood–brain barrier models. FEBS Letters, 599(5), 599–644. https://doi.org/10.1002/1873-3468.15053

Solmonson, A., Faubert, B., Gu, W., Rao, A., Cowdin, M. A., Menendez-Montes, I., Kelekar, S., Rogers, T. J., Pan, C., Guevara, G., Tarangelo, A., Zacharias, L. G., Martin-Sandoval, M. S., Do, D., Pachnis, P., Dumesnil, D., Mathews, T. P., Tasdogan, A., Pham, A., … DeBerardinis, R. J. (2022). Compartmentalized metabolism supports midgestation mammalian development. Nature, 604(7905), 349–353. https://doi.org/10.1038/s41586-022-04557-9

Somiya, M., & Kuroda, S. (2021). Real-Time Luminescence Assay for Cytoplasmic Cargo Delivery of Extracellular Vesicles. Analytical Chemistry, 93(13), 5612–5620. https://doi.org/10.1021/acs.analchem.1c00339

Song, C., Fang, X., Fang, N., & Hu, F. (2024). Buyang Huanwu Decoction suppresses ischemic stroke by suppressing glycolysis and cell apoptosis in rat brain microvascular endothelial cells. Brain Research Bulletin, 215, 111032. https://doi.org/10.1016/j.brainresbull.2024.111032

Song, K., Yang, X., An, G., Xia, X., Zhao, J., Xu, X., Wan, C., Liu, T., Zheng, Y., Ren, S., Wang, M., Chang, G., Cronin, S. J. F., Penninger, J. M., Jing, T., Ou, X., Rao, S., Liu, Z., & Zhao, X.-Y. (2022). Targeting APLN/APJ restores blood-testis barrier and improves spermatogenesis in murine and human diabetic models. Nature Communications, 13(1), 7335. https://doi.org/10.1038/s41467-022-34990-3

Song, M., Xu, J., Gui, Z., Wu, Y., Wang, F., Sheng, H., Huang, X., Qian, J., Qin, H., & Wang, Y. (2025). Characterization of lysine crotonylation-related lncRNAs for prognostic assessment and immune response in glioma. Frontiers in Pharmacology, 16, 1573694. https://doi.org/10.3389/fphar.2025.1573694

Song, Q., Wang, X.-Q., Holmes, T. R., Bonkowski, M., Roth, E. W., Ponedal, A., Mirkin, C., & Paller, A. S. (2021). Epidermal SR-A Complexes Are Lipid Raft Based and Promote Nucleic Acid Nanoparticle Uptake. Journal of Investigative Dermatology, 141(6), 1428-1437.e8. https://doi.org/10.1016/j.jid.2020.10.027

Soni, S., O'Dea, K. P., Abe, E., Khamdan, M., Shah, S. V., Sarathchandra, P., Wilson, M. R., & Takata, M. (2022). Microvesicle-Mediated Communication Within the Alveolar Space: Mechanisms of Uptake by Epithelial Cells and Alveolar Macrophages. Frontiers in Immunology, 13, 853769. https://doi.org/10.3389/fimmu.2022.853769

Sorice, M. (2022). Crosstalk of Autophagy and Apoptosis. Cells, 11(9), 1479. https://doi.org/10.3390/cells11091479

Sork, H., Conceicao, M., Corso, G., Nordin, J., Lee, Y. X. F., Krjutskov, K., Orzechowski Westholm, J., Vader, P., Pauwels, M., Vandenbroucke, R. E., Wood, M. J., El Andaloussi, S., & Mäger, I. (2021). Profiling of Extracellular Small RNAs Highlights a Strong Bias towards Non-Vesicular Secretion. Cells, 10(6), 1543. https://doi.org/10.3390/cells10061543

Sorokin, L. M., Pausch, F., Frieser, M., Kröger, S., Ohage, E., & Deutzmann, R. (1997). Developmental Regulation of the Laminin α5 Chain Suggests a Role in Epithelial and Endothelial Cell Maturation. Developmental Biology, 189(2), 285–300. https://doi.org/10.1006/dbio.1997.8668

Srinivasan, B., Kolli, A. R., Esch, M. B., Abaci, H. E., Shuler, M. L., & Hickman, J. J. (2015). TEER Measurement Techniques for In Vitro Barrier Model Systems. SLAS Technology, 20(2), 107–126. https://doi.org/10.1177/2211068214561025

Stael, S., Miller, L. P., Fernández-Fernández, Á. D., & Van Breusegem, F. (2022). Detection of Damage-Activated Metacaspase Activity by Western Blot in Plants. In M. Klemenčič, S. Stael, & P. F. Huesgen (Eds), Plant Proteases and Plant Cell Death (Vol. 2447, pp. 127–137). Springer US. https://doi.org/10.1007/978-1-0716-2079-3_11

Stafford, P., Mitra, S., Debot, M., Lutz, P., Stem, A., Hadley, J., Hom, P., Schaid, T. R., & Cohen, M. J. (2022). Astrocytes and pericytes attenuate severely injured patient plasma mediated expression of tight junction proteins in endothelial cells. PLOS ONE, 17(7), e0270817. https://doi.org/10.1371/journal.pone.0270817

Stamatovic, S. M., Dimitrijevic, O. B., Keep, R. F., & Andjelkovic, A. V. (2006). Protein Kinase Cα-RhoA Cross-talk in CCL2-induced Alterations in Brain Endothelial Permeability. Journal of Biological Chemistry, 281(13), 8379–8388. https://doi.org/10.1074/jbc.M513122200

Stamatovic, S. M., Johnson, A. M., Keep, R. F., & Andjelkovic, A. V. (2016). Junctional proteins of the blood-brain barrier: New insights into function and dysfunction. Tissue Barriers, 4(1), e1154641. https://doi.org/10.1080/21688370.2016.1154641

Stamatovic, S. M., Shakui, P., Keep, R. F., Moore, B. B., Kunkel, S. L., Van Rooijen, N., & Andjelkovic, A. V. (2005). Monocyte Chemoattractant Protein-1 Regulation of Blood–Brain Barrier Permeability. Journal of Cerebral Blood Flow & Metabolism, 25(5), 593–606. https://doi.org/10.1038/sj.jcbfm.9600055

Staufer, O., Hernandez Bücher, J. E., Fichtler, J., Schröter, M., Platzman, I., & Spatz, J. P. (2022). Vesicle Induced Receptor Sequestration: Mechanisms behind Extracellular Vesicle-Based Protein Signaling. Advanced Science, 9(13), 2200201. https://doi.org/10.1002/advs.202200201

Steiner, E., Enzmann, G. U., Lyck, R., Lin, S., Rüegg, M. A., Kröger, S., & Engelhardt, B. (2014). The heparan sulfate proteoglycan agrin contributes to barrier properties of mouse brain endothelial cells by stabilizing adherens junctions. Cell and Tissue Research, 358(2), 465–479. https://doi.org/10.1007/s00441-014-1969-7

Stenman, J. M., Rajagopal, J., Carroll, T. J., Ishibashi, M., McMahon, J., & McMahon, A. P. (2008). Canonical Wnt Signaling Regulates Organ-Specific Assembly and Differentiation of CNS Vasculature. Science, 322(5905), 1247–1250. https://doi.org/10.1126/science.1164594

Stern, L. (1934). A propos de la méthod d'investigation du fonctionnement de la barrière hémato-encéphalique. CR Soc. Biol, 115, 1059–1061.

Stern, L., & Gautier, R. (1918). Le passage dans le liquide céphalo-rachidien de substances introduites dans la circulation et leur action sur le système nerveux central chez les différentes espèces animale. S. R. C. R. d. Ia Soc. de Phys. et d'hist. Natur. de Genève, 35, 91–94.

Stern, L., & Gautier, R. (1921). Recherches Sur Le Liquide CÉphalo-Rachidien: I.–Les Rapports Entre Le Liquide CÉphalo-Rachidien et la Circulation Sanguine. Archives Internationales de Physiologie, 17(2), 138–192. https://doi.org/10.3109/13813452109146211

Stewart, P. A., & Wiley, M. J. (1981). Developing nervous tissue induces formation of blood-brain barrier characteristics in invading endothelial cells: A study using quail-chick

transplantation chimeras. Developmental Biology, 84(1), 183–192. https://doi.org/10.1016/0012-1606(81)90382-1

Stogsdill, J. A., Harwell, C. C., & Goldman, S. A. (2023). Astrocytes as master modulators of neural networks: Synaptic functions and disease-associated dysfunction of astrocytes. Annals of the New York Academy of Sciences, 1525(1), 41–60. https://doi.org/10.1111/nyas.15004

Stokum, J. A., Shim, B., Huang, W., Kane, M., Smith, J. A., Gerzanich, V., & Simard, J. M. (2021). A large portion of the astrocyte proteome is dedicated to perivascular endfeet, including critical components of the electron transport chain. Journal of Cerebral Blood Flow & Metabolism, 41(10), 2546–2560. https://doi.org/10.1177/0271678X211004182

Stone, N. L., England, T. J., & O'Sullivan, S. E. (2019). A Novel Transwell Blood Brain Barrier Model Using Primary Human Cells. Frontiers in Cellular Neuroscience, 13, 230. https://doi.org/10.3389/fncel.2019.00230

Strazza, M., Maubert, M. E., Pirrone, V., Wigdahl, B., & Nonnemacher, M. R. (2016). Co-culture model consisting of human brain microvascular endothelial and peripheral blood mononuclear cells. Journal of Neuroscience Methods, 269, 39–45. https://doi.org/10.1016/j.jneumeth.2016.05.016

Strieter, R. M., Wiggins, R., Phan, S. H., Wharram, B. L., Showell, H. J., Remick, D. G., Chensue, S. W., & Kunkel, S. L. (1989). Monocyte chemotactic protein gene expression by cytokine-treated human fibroblasts and endothelial cells. Biochemical and Biophysical Research Communications, 162(2), 694–700. https://doi.org/10.1016/0006-291X(89)92366-8

Su, C., Shi, K., Cheng, X., Han, Y., Li, Y., Yu, D., & Liu, Z. (2019). Methylation of CLEC14A is associated with its expression and lung adenocarcinoma progression. Journal of Cellular Physiology, 234(3), 2954–2962. https://doi.org/10.1002/jcp.27112

Su, Y., Wang, X., Yang, Y., Chen, L., Xia, W., Hoi, K. K., Li, H., Wang, Q., Yu, G., Chen, X., Wang, S., Wang, Y., Xiao, L., Verkhratsky, A., Fancy, S. P. J., Yi, C., & Niu, J. (2023). Astrocyte endfoot formation controls the termination of oligodendrocyte precursor cell perivascular migration during development. Neuron, 111(2), 190-201.e8. https://doi.org/10.1016/j.neuron.2022.10.032

Sugiyama, S., Sasaki, T., Tanaka, H., Yan, H., Ikegami, T., Kanki, H., Nishiyama, K., Beck, G., Gon, Y., Okazaki, S., Todo, K., Tamura, A., Tsukita, S., & Mochizuki, H. (2023). The tight junction protein occludin modulates blood–brain barrier integrity and neurological function after ischemic stroke in mice. Scientific Reports, 13, 2892. https://doi.org/10.1038/s41598-023-29894-1

Sun, J., Ou, W., Han, D., Paganini-Hill, A., Fisher, M. J., & Sumbria, R. K. (2022). Comparative studies between the murine immortalized brain endothelial cell line (bEnd.3) and induced pluripotent stem cell-derived human brain endothelial cells for paracellular transport. PloS One, 17(5), e0268860. https://doi.org/10.1371/journal.pone.0268860

Sun, L., Li, Y., Jia, X., Wang, Q., Li, Y., Hu, M., Tian, L., Yang, J., Xing, W., Zhang, W., Wang, J., Xu, H., Wang, L., Zhang, D., & Ren, H. (2017). Neuroprotection by IFN-γ via astrocyte-secreted IL-6 in acute neuroinflammation. Oncotarget, 8(25), 40065–40078. https://doi.org/10.18632/oncotarget.16990

Sun, L.-H., Lange, C. M., Hansen, M., & Kumsta, C. (2024). Neuronal waste management: New roles for autophagy genes in the extrusion of protein aggregates and in longevity. Autophagy, 20(7), 1681–1683. https://doi.org/10.1080/15548627.2024.2322420

Sun, R., Liao, W., Lang, T., Qin, K., Jiao, K., Shao, L., Deng, C., & She, Y. (2024). Astrocyte-derived exosomal miR-378a-5p mitigates cerebral ischemic neuroinflammation by modulating NLRP3-mediated pyroptosis. Frontiers in Immunology, 15, 1454116. https://doi.org/10.3389/fimmu.2024.1454116

Sun-Wada, G.-H., Tabata, H., Kawamura, N., Aoyama, M., & Wada, Y. (2009). Direct recruitment of H+-ATPase from lysosomes for phagosomal acidification. Journal of Cell Science, 122(14), 2504–2513. https://doi.org/10.1242/jcs.050443

Suresh, P. S., & Zhang, Q. (2025). Comprehensive Comparison of Methods for Isolation of Extracellular Vesicles from Human Plasma. Journal of Proteome Research, 24(6), 2956–2967. https://doi.org/10.1021/acs.jproteome.5c00149

Suzuki, N., Sekimoto, K., Hayashi, C., Mabuchi, Y., Nakamura, T., & Akazawa, C. (2017). Differentiation of Oligodendrocyte Precursor Cells from Sox10-Venus Mice to Oligodendrocytes and Astrocytes. Scientific Reports, 7(1), 14133. https://doi.org/10.1038/s41598-017-14207-0

Svensson, K. J., Christianson, H. C., Wittrup, A., Bourseau-Guilmain, E., Lindqvist, E., Svensson, L. M., Mörgelin, M., & Belting, M. (2013). Exosome Uptake Depends on ERK1/2-Heat Shock Protein 27 Signaling and Lipid Raft-mediated Endocytosis Negatively Regulated by Caveolin-1. Journal of Biological Chemistry, 288(24), 17713–17724. https://doi.org/10.1074/jbc.m112.445403

Swinnen, N., Smolders, S., Avila, A., Notelaers, K., Paesen, R., Ameloot, M., Brône, B., Legendre, P., & Rigo, J. (2013). Complex invasion pattern of the cerebral cortex bymicroglial cells during development of the mouse embryo. Glia, 61(2), 150–163. https://doi.org/10.1002/glia.22421

Szpakowski, P., Ksiazek-Winiarek, D., Turniak-Kusy, M., Pacan, I., & Glabinski, A. (2022). Human Primary Astrocytes Differently Respond to Pro- and Anti-Inflammatory Stimuli. Biomedicines, 10(8), 1769. https://doi.org/10.3390/biomedicines10081769

Taban, Q., Mumtaz, P. T., Masoodi, K. Z., Haq, E., & Ahmad, S. M. (2022). Scavenger receptors in host defense: From functional aspects to mode of action. Cell Communication and Signaling, 20(1), 2. https://doi.org/10.1186/s12964-021-00812-0

Taddei, A., Giampietro, C., Conti, A., Orsenigo, F., Breviario, F., Pirazzoli, V., Potente, M., Daly, C., Dimmeler, S., & Dejana, E. (2008). Endothelial adherens junctions control tight junctions by VE-cadherin-mediated upregulation of claudin-5. Nature Cell Biology, 10(8), 923–934. https://doi.org/10.1038/ncb1752

Takahashi, T., & Shirasaw, T. (1994). Molecular cloning of rat JAK3, a novel member of the JAK family of protein tyrosine kinases. FEBS Letters, 342(2), 124–128. https://doi.org/10.1016/0014-5793(94)80485-0

Takami, K., Okamoto, K., Etani, Y., Hirao, M., Miyama, A., Okamura, G., Goshima, A., Miura, T., Kurihara, T., Fukuda, Y., Kanamoto, T., Nakata, K., Okada, S., & Ebina, K. (2023). Anti–NF-κB peptide derived from nuclear acidic protein attenuates ovariectomy-

induced osteoporosis in mice. JCI Insight, 8(22), e171962. https://doi.org/10.1172/jci.insight.171962

Takeshita, Y., Obermeier, B., Cotleur, A. C., Spampinato, S. F., Shimizu, F., Yamamoto, E., Sano, Y., Kryzer, T. J., Lennon, V. A., Kanda, T., & Ransohoff, R. M. (2017). Effects of neuromyelitis optica–IgG at the blood–brain barrier in vitro. Neurology Neuroimmunology & Neuroinflammation, 4(1), e311. https://doi.org/10.1212/NXI.0000000000000311

Tanaka, K., Masu, M., & Nakanishi, S. (1990). Structure and functional expression of the cloned rat neurotensin receptor. Neuron, 4(6), 847–854. https://doi.org/10.1016/0896-6273(90)90137-5

Tang, J., Kang, Y., Zhou, Y., Shang, N., Li, X., Wang, H., Lan, J., Wang, S., Wu, L., & Peng, Y. (2023). TIMP2 ameliorates blood-brain barrier disruption in traumatic brain injury by inhibiting Src-dependent VE-cadherin internalization. Journal of Clinical Investigation, 134(3), e164199. https://doi.org/10.1172/JCI164199

Tangwattanachuleeporn, M., Muanwien, P., Teethaisong, Y., & Somparn, P. (2022). Optimizing Concentration of Polyethelene Glycol for Exosome Isolation from Plasma for Downstream Application. Medicina (Kaunas, Lithuania), 58(11), 1600. https://doi.org/10.3390/medicina58111600

Tankov, S., Petrovic, M., Lecoultre, M., Espinoza, F., El-Harane, N., Bes, V., Chliate, S., Bedoya, D. M., Jordan, O., Borchard, G., Migliorini, D., Dutoit, V., & Walker, P. R. (2024). Hypoxic glioblastoma-cell-derived extracellular vesicles impair cGAS-STING activity in macrophages. Cell Communication and Signaling, 22(1), 144. https://doi.org/10.1186/s12964-024-01523-y

Tannahill, G. M., Curtis, A. M., Adamik, J., Palsson-McDermott, E. M., McGettrick, A. F., Goel, G., Frezza, C., Bernard, N. J., Kelly, B., Foley, N. H., Zheng, L., Gardet, A., Tong, Z., Jany, S. S., Corr, S. C., Haneklaus, M., Caffrey, B. E., Pierce, K., Walmsley, S., … O'Neill, L. A. J. (2013). Succinate is an inflammatory signal that induces IL-1β through HIF-1α. Nature, 496(7444), 238–242. https://doi.org/10.1038/nature11986

Tao, Y., Zhang, H., Huang, S., Pei, L., Feng, M., Zhao, X., Ouyang, Z., Yao, S., Jiang, R., & Wei, K. (2019). miR-199a-3p promotes cardiomyocyte proliferation by inhibiting Cd151 expression. Biochemical and Biophysical Research Communications, 516(1), 28–36. https://doi.org/10.1016/j.bbrc.2019.05.174

Tarassishin, L., Suh, H., & Lee, S. C. (2014). LPS and IL-1 differentially activate mouse and human astrocytes: Role of CD14. Glia, 62(6), 999–1013. https://doi.org/10.1002/glia.22657

Tatematsu, S., Francis, S. A., Natarajan, P., Rader, D. J., Saghatelian, A., Brown, J. D., Michel, T., & Plutzky, J. (2013). Endothelial Lipase Is a Critical Determinant of High-Density Lipoprotein–Stimulated Sphingosine 1-Phosphate–Dependent Signaling in Vascular Endothelium. Arteriosclerosis, Thrombosis, and Vascular Biology, 33(8), 1788–1794. https://doi.org/10.1161/ATVBAHA.113.301300

Taylor, A. R., Robinson, M. B., Gifondorwa, D. J., Tytell, M., & Milligan, C. E. (2007). Regulation of heat shock protein 70 release in astrocytes: Role of signaling kinases. Developmental Neurobiology, 67(13), 1815–1829. https://doi.org/10.1002/dneu.20559

The Gene Ontology Consortium, Aleksander, S. A., Balhoff, J., Carbon, S., Cherry, J. M., Drabkin, H. J., Ebert, D., Feuermann, M., Gaudet, P., Harris, N. L., Hill, D. P., Lee, R., Mi, H., Moxon, S., Mungall, C. J., Muruganugan, A., Mushayahama, T., Sternberg, P. W., Thomas, P. D., … Westerfield, M. (2023). The Gene Ontology knowledgebase in 2023. GENETICS, 224(1), iyad031. https://doi.org/10.1093/genetics/iyad031

Theodoraki, M.-N., Laban, S., Jackson, E. K., Lotfi, R., Schuler, P. J., Brunner, C., Hoffmann, T. K., Whiteside, T. L., & Hofmann, L. (2021). Changes in circulating exosome molecular profiles following surgery/(chemo)radiotherapy: Early detection of response in head and neck cancer patients. British Journal of Cancer, 125(12), 1677–1686. https://doi.org/10.1038/s41416-021-01567-8

Théry, C., Amigorena, S., Raposo, G., & Clayton, A. (2006). Isolation and Characterization of Exosomes from Cell Culture Supernatants and Biological Fluids. Current Protocols in Cell Biology, 30(1). https://doi.org/10.1002/0471143030.cb0322s30

Théry, C., Witwer, K. W., Aikawa, E., Alcaraz, M. J., Anderson, J. D., Andriantsitohaina, R., Antoniou, A., Arab, T., Archer, F., Atkin-Smith, G. K., Ayre, D. C., Bach, J.-M., Bachurski, D., Baharvand, H., Balaj, L., Baldacchino, S., Bauer, N. N., Baxter, A. A., Bebawy, M., … Zuba-Surma, E. K. (2018). Minimal information for studies of extracellular vesicles 2018 (MISEV2018): A position statement of the International Society for Extracellular Vesicles and update of the MISEV2014 guidelines. Journal of Extracellular Vesicles, 7(1), 1535750. https://doi.org/10.1080/20013078.2018.1535750

Thomas, M. A., Fahey, M. J., Pugliese, B. R., Irwin, R. M., Antonyak, M. A., & Delco, M. L. (2022). Human mesenchymal stromal cells release functional mitochondria in extracellular vesicles. Frontiers in Bioengineering and Biotechnology, 10, 870193. https://doi.org/10.3389/fbioe.2022.870193

Thomis, D. C., Gurniak, C. B., Tivol, E., Sharpe, A. H., & Berg, L. J. (1995). Defects in B Lymphocyte Maturation and T Lymphocyte Activation in Mice Lacking Jak3. Science, 270(5237), 794–797. https://doi.org/10.1126/science.270.5237.794

Tian, M., Kawaguchi, R., Shen, Y., Machnicki, M., Villegas, N. G., Cooper, D. R., Montgomery, N., Cai, Y., Haring, J., Lan, R., Yuan, A. H., Williams, C. K., Magaki, S., Vinters, H. V., Zhang, Y., De Biase, L. M., Silva, A. J., & Carmichael, S. T. (2025). Deconstructing the intercellular interactome in vascular dementia with focal ischemia for therapeutic applications. Cell, 188(19), 5157-5174.e20. https://doi.org/10.1016/j.cell.2025.06.002

Tian, X., Zhao, L., Song, X., Yan, Y., Liu, N., Li, T., Yan, B., & Liu, B. (2016). HSP27 Inhibits Homocysteine-Induced Endothelial Apoptosis by Modulation of ROS Production and Mitochondrial Caspase-Dependent Apoptotic Pathway. BioMed Research International, 2016, 1–9. https://doi.org/10.1155/2016/4847874

Tilling, T., Korte, D., Hoheisel, D., & Galla, H. (1998). Basement Membrane Proteins Influence Brain Capillary Endothelial Barrier Function In Vitro. Journal of Neurochemistry, 71(3), 1151–1157. https://doi.org/10.1046/j.1471-4159.1998.71031151.x

Tipnis, S. R., Hooper, N. M., Hyde, R., Karran, E., Christie, G., & Turner, A. J. (2000). A Human Homolog of Angiotensin-converting Enzyme. Journal of Biological Chemistry, 275(43), 33238–33243. https://doi.org/10.1074/jbc.M002615200

Tkach, M., Kowal, J., Zucchetti, A. E., Enserink, L., Jouve, M., Lankar, D., Saitakis, M., Martin-Jaular, L., & Théry, C. (2017). Qualitative differences in T-cell activation by dendritic cell-derived extracellular vesicle subtypes. The EMBO Journal, 36(20), 3012–3028. https://doi.org/10.15252/embj.201696003

Tognoli, M. L., Dancourt, J., Bonsergent, E., Palmulli, R., De Jong, O. G., Van Niel, G., Rubinstein, E., Vader, P., & Lavieu, G. (2023). Lack of involvement of CD63 and CD9 tetraspanins in the extracellular vesicle content delivery process. Communications Biology, 6(1), 532. https://doi.org/10.1038/s42003-023-04911-1

Togre, N. S., Mekala, N., Bhoj, P. S., Mogadala, N., Winfield, M., Trivedi, J., Grove, D., Kotnala, S., Rom, S., Sriram, U., & Persidsky, Y. (2024). Neuroinflammatory responses and blood–brain barrier injury in chronic alcohol exposure: Role of purinergic P2 × 7 Receptor signaling. Journal of Neuroinflammation, 21(1), 244. https://doi.org/10.1186/s12974-024-03230-4

Tong, B., Zhang, X., Zhu, D., Wang, Y., Wei, J., Ou, Z., Liang, H., Xu, H., Zhang, Z., Lei, J., Zhou, X., Wu, D., Song, Y., Wang, K., Feng, X., Tan, L., Liao, Z., & Yang, C. (2026). Extracellular vesicle-based targeted protein degradation platform for multiple extracellular proteins. EMBO Molecular Medicine, 18(2), 759–794. https://doi.org/10.1038/s44321-025-00371-8

Tong, L., Zhang, S., Liu, Q., Huang, C., Hao, H., Tan, M. S., Yu, X., Lou, C. K. L., Huang, R., Zhang, Z., Liu, T., Gong, P., Ng, C. H., Muthiah, M., Pastorin, G., Wacker, M. G., Chen, X., Storm, G., Lee, C. N., … Wang, J.-W. (2023). Milk-derived extracellular vesicles protect intestinal barrier integrity in the gut-liver axis. Science Advances, 9(15), eade5041. https://doi.org/10.1126/sciadv.ade5041

Török, M., Huwyler, J., Gutmann, H., Fricker, G., & Drewe, J. (2003). Modulation of transendothelial permeability and expression of ATP-binding cassette transporters in cultured brain capillary endothelial cells by astrocytic factors and cell-culture conditions. Experimental Brain Research, 153(3), 356–365. https://doi.org/10.1007/s00221-003-1620-4

Török, O., Schreiner, B., Schaffenrath, J., Tsai, H.-C., Maheshwari, U., Stifter, S. A., Welsh, C., Amorim, A., Sridhar, S., Utz, S. G., Mildenberger, W., Nassiri, S., Delorenzi, M., Aguzzi, A., Han, M. H., Greter, M., Becher, B., & Keller, A. (2021). Pericytes regulate vascular immune homeostasis in the CNS. Proceedings of the National Academy of Sciences, 118(10), e2016587118. https://doi.org/10.1073/pnas.2016587118

Torres, E., Pellegrino, G., Granados-Rodríguez, M., Fuentes-Fayos, A. C., Velasco, I., Coutteau-Robles, A., Legrand, A., Shanabrough, M., Perdices-Lopez, C., Leon, S., Yeo, S. H., Manchishi, S. M., Sánchez-Tapia, M. J., Navarro, V. M., Pineda, R., Roa, J., Naftolin, F., Argente, J., Luque, R. M., … Romero-Ruiz, A. (2024). Kisspeptin signaling in astrocytes modulates the reproductive axis. Journal of Clinical Investigation, 134(15), e172908. https://doi.org/10.1172/JCI172908

Torrino, S., Shen, W.-W., Blouin, C. M., Mani, S. K., Viaris De Lesegno, C., Bost, P., Grassart, A., Köster, D., Valades-Cruz, C. A., Chambon, V., Johannes, L., Pierobon, P., Soumelis, V., Coirault, C., Vassilopoulos, S., & Lamaze, C. (2018). EHD2 is a mechanotransducer connecting caveolae dynamics with gene transcription. Journal of Cell Biology, 217(12), 4092–4105. https://doi.org/10.1083/jcb.201801122

Tosar, J. P., Cayota, A., & Witwer, K. (2022). Exomeres and supermeres: Monolithic or diverse? Journal of Extracellular Biology, 1(6), e45. https://doi.org/10.1002/jex2.45

Trajkovic, K., Hsu, C., Chiantia, S., Rajendran, L., Wenzel, D., Wieland, F., Schwille, P., Brügger, B., & Simons, M. (2008). Ceramide Triggers Budding of Exosome Vesicles into Multivesicular Endosomes. Science, 319(5867), 1244–1247. https://doi.org/10.1126/science.1153124

Trams, E. G., Lauter, C. J., Norman Salem, Jr., & Heine, U. (1981). Exfoliation of membrane ecto-enzymes in the form of micro-vesicles. Biochimica et Biophysica Acta (BBA) - Biomembranes, 645(1), 63–70. https://doi.org/10.1016/0005-2736(81)90512-5

Trindade, P., Loiola, E. C., Gasparotto, J., Ribeiro, C. T., Cardozo, P. L., Devalle, S., Salerno, J. A., Ornelas, I. M., Ledur, P. F., Ribeiro, F. M., Ventura, A. L. M., Moreira, J. C. F., Gelain, D. P., Porciúncula, L. O., & Rehen, S. K. (2020). Short and long TNF-alpha exposure recapitulates canonical astrogliosis events in human-induced pluripotent stem cells-derived astrocytes. Glia, 68(7), 1396–1409. https://doi.org/10.1002/glia.23786

Tripathi, K., Bandari, S. K., & Sanderson, R. D. (2023). Extracellular vesicles released during hypoxia transport heparanase and enhance macrophage migration, endothelial tube formation and cancer cell stemness. Proteoglycan Research, 1(1), e1. https://doi.org/10.1002/pgr2.1

Tripathi, R. B., Jackiewicz, M., McKenzie, I. A., Kougioumtzidou, E., Grist, M., & Richardson, W. D. (2017). Remarkable Stability of Myelinating Oligodendrocytes in Mice. Cell Reports, 21(2), 316–323. https://doi.org/10.1016/j.celrep.2017.09.050

Tsai, H.-H., Li, H., Fuentealba, L. C., Molofsky, A. V., Taveira-Marques, R., Zhuang, H., Tenney, A., Murnen, A. T., Fancy, S. P. J., Merkle, F., Kessaris, N., Alvarez-Buylla, A., Richardson, W. D., & Rowitch, D. H. (2012). Regional Astrocyte Allocation Regulates CNS Synaptogenesis and Repair. Science, 337(6092), 358–362. https://doi.org/10.1126/science.1222381

Tsai, H.-H., Niu, J., Munji, R., Davalos, D., Chang, J., Zhang, H., Tien, A.-C., Kuo, C. J., Chan, J. R., Daneman, R., & Fancy, S. P. J. (2016). Oligodendrocyte precursors migrate along vasculature in the developing nervous system. Science, 351(6271), 379–384. https://doi.org/10.1126/science.aad3839

Tsai, P. S., Kaufhold, J. P., Blinder, P., Friedman, B., Drew, P. J., Karten, H. J., Lyden, P. D., & Kleinfeld, D. (2009). Correlations of Neuronal and Microvascular Densities in Murine Cortex Revealed by Direct Counting and Colocalization of Nuclei and Vessels. The Journal of Neuroscience, 29(46), 14553–14570. https://doi.org/10.1523/JNEUROSCI.3287-09.2009

Tsukuda, S., Tamura, A., Matsumoto, K., Fujita, Y., Nakata, S., Kaneko, T., Nakayama, A., Nakagawa, H., & Terasaki, A. G. (2019). In Vitro Differentiation of Chicken Astrocytes: Growth, Morphology, and Protein Expression of Astrocytes in Primary Cultures. Zoological Science, 36(6), 458. https://doi.org/10.2108/zs180102

Tu, H., Wang, H., & Cai, H. (2025). Macropinocytosis: Molecular mechanisms and regulation. Current Opinion in Cell Biology, 95, 102563. https://doi.org/10.1016/j.ceb.2025.102563

Tugues, S., Honjo, S., König, C., Padhan, N., Kroon, J., Gualandi, L., Li, X., Barkefors, I., Thijssen, V. L., Griffioen, A. W., & Claesson-Welsh, L. (2013). Tetraspanin CD63 Promotes Vascular Endothelial Growth Factor Receptor 2-β1 Integrin Complex Formation, Thereby Regulating Activation and Downstream Signaling in Endothelial Cells in Vitro and in Vivo. Journal of Biological Chemistry, 288(26), 19060–19071. https://doi.org/10.1074/jbc.M113.468199

Turek, M., Banasiak, K., Piechota, M., Shanmugam, N., Macias, M., Śliwińska, M. A., Niklewicz, M., Kowalski, K., Nowak, N., Chacinska, A., & Pokrzywa, W. (2021). Muscle-derived exophers promote reproductive fitness. EMBO Reports, 22(8), e52071. https://doi.org/10.15252/embr.202052071

Turelli, P., Playfoot, C., Grun, D., Raclot, C., Pontis, J., Coudray, A., Thorball, C., Duc, J., Pankevich, E. V., Deplancke, B., Busskamp, V., & Trono, D. (2020). Primate-restricted KRAB zinc finger proteins and target retrotransposons control gene expression in human neurons. Science Advances, 6(35), eaba3200. https://doi.org/10.1126/sciadv.aba3200

Turner, C. J., Badu-Nkansah, K., & Hynes, R. O. (2017). Endothelium-derived fibronectin regulates neonatal vascular morphogenesis in an autocrine fashion. Angiogenesis, 20(4), 519–531. https://doi.org/10.1007/s10456-017-9563-8

Turovsky, E. A., Golovicheva, V. V., Varlamova, E. G., Danilina, T. I., Goryunov, K. V., Shevtsova, Y. A., Pevzner, I. B., Zorova, L. D., Babenko, V. A., Evtushenko, E. A., Zharikova, A. A., Khutornenko, A. A., Kovalchuk, S. I., Plotnikov, E. Y., Zorov, D. B., Sukhikh, G. T., & Silachev, D. N. (2022). Mesenchymal stromal cell-derived extracellular vesicles afford neuroprotection by modulating PI3K/AKT pathway and calcium oscillations. International Journal of Biological Sciences, 18(14), 5345–5368. https://doi.org/10.7150/ijbs.73747

Ulrich, F., Carretero-Ortega, J., Menéndez, J., Narvaez, C., Sun, B., Lancaster, E., Pershad, V., Trzaska, S., Véliz, E., Kamei, M., Prendergast, A., Kidd, K. R., Shaw, K. M., Castranova, D. A., Pham, V. N., Lo, B. D., Martin, B. L., Raible, D. W., Weinstein, B. M., & Torres-Vázquez, J. (2016). Reck enables cerebrovascular development by promoting canonical Wnt signaling. Development, 143(6), 1055–1055. https://doi.org/10.1242/dev.136507

Umeda, K., Ikenouchi, J., Katahira-Tayama, S., Furuse, K., Sasaki, H., Nakayama, M., Matsui, T., Tsukita, S., Furuse, M., & Tsukita, S. (2006). ZO-1 and ZO-2 Independently Determine Where Claudins Are Polymerized in Tight-Junction Strand Formation. Cell, 126(4), 741–754. https://doi.org/10.1016/j.cell.2006.06.043

Upadhya, R., Madhu, L. N., Attaluri, S., Gitaí, D. L. G., Pinson, M. R., Kodali, M., Shetty, G., Zanirati, G., Kumar, S., Shuai, B., Weintraub, S. T., & Shetty, A. K. (2020). Extracellular vesicles from human iPSC-derived neural stem cells: miRNA and protein signatures, and anti-inflammatory and neurogenic properties. Journal of Extracellular Vesicles, 9(1), 1809064. https://doi.org/10.1080/20013078.2020.1809064

Upadhya, R., Zingg, W., Shetty, S., & Shetty, A. K. (2020). Astrocyte-derived extracellular vesicles: Neuroreparative properties and role in the pathogenesis of neurodegenerative disorders. Journal of Controlled Release, 323, 225–239. https://doi.org/10.1016/j.jconrel.2020.04.017

Valadi, H., Ekström, K., Bossios, A., Sjöstrand, M., Lee, J. J., & Lötvall, J. O. (2007). Exosome-mediated transfer of mRNAs and microRNAs is a novel mechanism of genetic exchange between cells. Nature Cell Biology, 9(6), 654–659. https://doi.org/10.1038/ncb1596

Valentin-Torres, A., Savarin, C., Barnett, J., & Bergmann, C. C. (2018). Blockade of sustained tumor necrosis factor in a transgenic model of progressive autoimmune encephalomyelitis limits oligodendrocyte apoptosis and promotes oligodendrocyte maturation. Journal of Neuroinflammation, 15(1), 121. https://doi.org/10.1186/s12974-018-1164-y

Vallet, S. D., Davis, M. N., Barqué, A., Thahab, A. H., Ricard-Blum, S., & Naba, A. (2021). Computational and experimental characterization of the novel ECM glycoprotein SNED1 and prediction of its interactome. Biochemical Journal, 478(7), 1413–1434. https://doi.org/10.1042/BCJ20200675

Van Horssen, J., Bö, L., Vos, C. M. P., Virtanen, I., & De Vries, H. E. (2005). Basement Membrane Proteins in Multiple Sclerosis-Associated Inflammatory Cuffs: Potential Role in Influx and Transport of Leukocytes: Journal of Neuropathology and Experimental Neurology, 64(8), 722–729. https://doi.org/10.1097/01.jnen.0000173894.09553.13

Van Kralingen, C., Kho, D. T., Costa, J., Angel, C. E., & Graham, E. S. (2013). Exposure to Inflammatory Cytokines IL-1β and TNFα Induces Compromise and Death of Astrocytes; Implications for Chronic Neuroinflammation. PLoS ONE, 8(12), e84269. https://doi.org/10.1371/journal.pone.0084269

Vanacker, C., Defazio, R. A., Sykes, C. M., & Moenter, S. M. (2021). A role for glial fibrillary acidic protein (GFAP)-expressing cells in the regulation of gonadotropin-releasing hormone (GnRH) but not arcuate kisspeptin neuron output in male mice. eLife, 10, e68205. https://doi.org/10.7554/eLife.68205

Vanlandewijck, M., He, L., Mäe, M. A., Andrae, J., Ando, K., Del Gaudio, F., Nahar, K., Lebouvier, T., Laviña, B., Gouveia, L., Sun, Y., Raschperger, E., Räsänen, M., Zarb, Y., Mochizuki, N., Keller, A., Lendahl, U., & Betsholtz, C. (2018). A molecular atlas of cell types and zonation in the brain vasculature. Nature, 554(7693), 475–480. https://doi.org/10.1038/nature25739

Varcianna, A., Myszczynska, M. A., Castelli, L. M., O'Neill, B., Kim, Y., Talbot, J., Nyberg, S., Nyamali, I., Heath, P. R., Stopford, M. J., Hautbergue, G. M., & Ferraiuolo, L. (2019). Micro-RNAs secreted through astrocyte-derived extracellular vesicles cause neuronal network degeneration in C9orf72 ALS. EBioMedicine, 40, 626–635. https://doi.org/10.1016/j.ebiom.2018.11.067

Vazquez-Liebanas, E., Nahar, K., Bertuzzi, G., Keller, A., Betsholtz, C., & Mäe, M. A. (2022). Adult-induced genetic ablation distinguishes PDGFB roles in blood-brain barrier maintenance and development. Journal of Cerebral Blood Flow & Metabolism, 42(2), 264–279. https://doi.org/10.1177/0271678X211056395

Veerman, R. E., Teeuwen, L., Czarnewski, P., Güclüler Akpinar, G., Sandberg, A., Cao, X., Pernemalm, M., Orre, L. M., Gabrielsson, S., & Eldh, M. (2021). Molecular evaluation of five different isolation methods for extracellular vesicles reveals different clinical applicability and subcellular origin. Journal of Extracellular Vesicles, 10(9), e12128. https://doi.org/10.1002/jev2.12128

Ventura-Antunes, aLissa, & Herculano-Houzel, S. (2022). Energy supply per neuron is constrained by capillary density in the mouse brain. Frontiers in Integrative Neuroscience, 16, 760887. https://doi.org/10.3389/fnint.2022.760887

Verkhratsky, A., Untiet, V., & Rose, C. R. (2020). Ionic signalling in astroglia beyond calcium. The Journal of Physiology, 598(9), 1655–1670. https://doi.org/10.1113/JP277478

Vicente Miranda, H., Chegão, A., Oliveira, M. S., Fernandes Gomes, B., Enguita, F. J., & Outeiro, T. F. (2020). Hsp27 reduces glycation-induced toxicity and aggregation of alpha-synuclein. The FASEB Journal, 34(5), 6718–6728. https://doi.org/10.1096/fj.201902936R

Vilaça, A., Jesus, C., Lino, M., Hayman, D., Emanueli, C., Terracciano, C. M., Fernandes, H., De Windt, L. J., & Ferreira, L. (2024). Extracellular vesicle transfer of lncRNA H19 splice variants to cardiac cells. Molecular Therapy - Nucleic Acids, 35(3), 102233. https://doi.org/10.1016/j.omtn.2024.102233

Von Bartheld, C. S., Bahney, J., & Herculano-Houzel, S. (2016). The search for true numbers of neurons and glial cells in the human brain: A review of 150 years of cell counting. Journal of Comparative Neurology, 524(18), 3865–3895. https://doi.org/10.1002/cne.24040

Vorländer, M. K., Rothe, P., Kleifeld, J., Cormack, E. D., Veleti, L., Riabov-Bassat, D., Fin, L., Phillips, A. W., Cochella, L., & Plaschka, C. (2024). Mechanism for the initiation of spliceosome disassembly. Nature, 632(8024), 443–450. https://doi.org/10.1038/s41586-024-07741-1

Wada, M., Tamura, A., Takahashi, N., & Tsukita, S. (2013). Loss of Claudins 2 and 15 From Mice Causes Defects in Paracellular Na+ Flow and Nutrient Transport in Gut and Leads to Death from Malnutrition. Gastroenterology, 144(2), 369–380. https://doi.org/10.1053/j.gastro.2012.10.035

Walsh, T. G., Murphy, R. P., Fitzpatrick, P., Rochfort, K. D., Guinan, A. F., Murphy, A., & Cummins, P. M. (2011). Stabilization of brain microvascular endothelial barrier function by shear stress involves VE-cadherin signaling leading to modulation of pTyr-occludin levels. Journal of Cellular Physiology, 226(11), 3053–3063. https://doi.org/10.1002/jcp.22655

Wang, C., & Li, L. (2023). The critical role of KLF4 in regulating the activation of A1/A2 reactive astrocytes following ischemic stroke. Journal of Neuroinflammation, 20(1), 44. https://doi.org/10.1186/s12974-023-02742-9

Wang, D., Duan, H., Feng, J., Xiang, J., Feng, L., Liu, D., Chen, X., Jing, L., Liu, Z., Zhang, D., Hao, H., & Yan, X. (2020). Soluble CD146, a cerebrospinal fluid marker for neuroinflammation, promotes blood-brain barrier dysfunction. Theranostics, 10(1), 231–246. https://doi.org/10.7150/thno.37142

Wang, F., Ren, S.-Y., Chen, J.-F., Liu, K., Li, R.-X., Li, Z.-F., Hu, B., Niu, J.-Q., Xiao, L., Chan, J. R., & Mei, F. (2020). Myelin degeneration and diminished myelin renewal contribute to age-related deficits in memory. Nature Neuroscience, 23(4), 481–486. https://doi.org/10.1038/s41593-020-0588-8

Wang, G., Li, J., Bojmar, L., Chen, H., Li, Z., Tobias, G. C., Hu, M., Homan, E. A., Lucotti, S., Zhao, F., Posada, V., Oxley, P. R., Cioffi, M., Kim, H. S., Wang, H., Lauritzen, P., Boudreau, N., Shi, Z., Burd, C. E., … Lyden, D. (2023). Tumour extracellular vesicles and

particles induce liver metabolic dysfunction. Nature, 618(7964), 374–382. https://doi.org/10.1038/s41586-023-06114-4

Wang, J., Li, L., Zhang, Z., Zhang, X., Zhu, Y., Zhang, C., & Bi, Y. (2022). Extracellular vesicles mediate the communication of adipose tissue with brain and promote cognitive impairment associated with insulin resistance. Cell Metabolism, 34(9), 1264-1279.e8. https://doi.org/10.1016/j.cmet.2022.08.004

Wang, J., Yu, Q., Ma, X., Yuan, Z., & Mao, J. (2022). Hutchinson-Gilford progeria syndrome complicated with stroke: A report of 2 cases and literature review. Frontiers in Pediatrics, 10, 1056225. https://doi.org/10.3389/fped.2022.1056225

Wang, J.-H., Forterre, A. V., Zhao, J., Frimannsson, D. O., Delcayre, A., Antes, T. J., Efron, B., Jeffrey, S. S., Pegram, M. D., & Matin, A. C. (2018). Anti-HER2 scFv-Directed Extracellular Vesicle-Mediated mRNA-Based Gene Delivery Inhibits Growth of HER2-Positive Human Breast Tumor Xenografts by Prodrug Activation. Molecular Cancer Therapeutics, 17(5), 1133–1142. https://doi.org/10.1158/1535-7163.MCT-17-0827

Wang, K., Qu, H., Hu, R., Lassègue, B., Eaton, D. C., Song, C., Mu, J., Griendling, K. K., & Hernandes, M. S. (2025). Polymerase delta-interacting protein 2 mediates brain vascular permeability by regulating ROS-mediated ZO-1 phosphorylation and localization at the interendothelial border. Cell Communication and Signaling: CCS, 23(1), 9. https://doi.org/10.1186/s12964-024-01982-3

Wang, L., Geng, J., Qu, M., Yuan, F., Wang, Y., Pan, J., Li, Y., Ma, Y., Zhou, P., Zhang, Z., & Yang, G.-Y. (2020). Oligodendrocyte precursor cells transplantation protects blood–brain barrier in a mouse model of brain ischemia via Wnt/β-catenin signaling. Cell Death & Disease, 11(1), 9. https://doi.org/10.1038/s41419-019-2206-9

Wang, P., Jin, L., Zhang, M., Wu, Y., Duan, Z., Guo, Y., Wang, C., Guo, Y., Chen, W., Liao, Z., Wang, Y., Lai, R., Lee, L. P., & Qin, J. (2023). Blood–brain barrier injury and neuroinflammation induced by SARS-CoV-2 in a lung–brain microphysiological system. Nature Biomedical Engineering, 8(8), 1053–1068. https://doi.org/10.1038/s41551-023-01054-w

Wang, P., Lan, G., Xu, B., Yu, Z., Tian, C., Lei, X., Meissner, W. G., Feng, T., Yang, Y., & Zhang, J. (2023). α-Synuclein-carrying astrocytic extracellular vesicles in Parkinson pathogenesis and diagnosis. Translational Neurodegeneration, 12(1), 40. https://doi.org/10.1186/s40035-023-00372-y

Wang, S., Cesca, F., Loers, G., Schweizer, M., Buck, F., Benfenati, F., Schachner, M., & Kleene, R. (2011). Synapsin I is an oligomannose-carrying glycoprotein, acts as an oligomannose-binding lectin, and promotes neurite outgrowth and neuronal survival when released via glia-derived exosomes. The Journal of Neuroscience: The Official Journal of the Society for Neuroscience, 31(20), 7275–7290. https://doi.org/10.1523/JNEUROSCI.6476-10.2011

Wang, S., Wang, Y.-J., Su, Y., Zhou, W., Yang, S., Zhang, R., Zhao, M., Li, Y., Zhang, Z., Zhan, D., & Liu, R. (2012). Rutin inhibits β-amyloid aggregation and cytotoxicity, attenuates oxidative stress, and decreases the production of nitric oxide and proinflammatory cytokines. NeuroToxicology, 33(3), 482–490. https://doi.org/10.1016/j.neuro.2012.03.003

Wang, S., Zhang, H., Li, R., Liu, Z., & Xiang, D. (2025). Altered Neuroplasticity in Epilepsy is Associated with Neuroinflammation and Oxidative Stress: In vivo Evidence of Brain-Derived Extracellular Vesicles. International Journal of Nanomedicine, Volume 20, 7185–7197. https://doi.org/10.2147/IJN.S514559

Wang, W., Wang, Y., Su, L., Zhang, M., Zhang, T., Zhao, J., Ma, H., Zhang, D., Ji, F., Jiao, R. D., Li, H., Xu, Y., Chen, L., & Jiao, J. (2024). Endothelial Cells Mediated by STING Regulate Oligodendrogenesis and Myelination During Brain Development. Advanced Science, 11(38), 2308508. https://doi.org/10.1002/advs.202308508

Wang, X., Fang, L., Xiao, L., Zhong, G., Han, M., Wang, B., Ren, J., & Zang, Y. (2024). Research on the effect of LAMP1 in the development and progression of ccRCC and its potential mechanism with LC3C-mediated autophagy. Frontiers in Immunology, 15, 1494005. https://doi.org/10.3389/fimmu.2024.1494005

Wang, Y., Cho, C., Williams, J., Smallwood, P. M., Zhang, C., Junge, H. J., & Nathans, J. (2018). Interplay of the Norrin and Wnt7a/Wnt7b signaling systems in blood–brain barrier and blood–retina barrier development and maintenance. Proceedings of the National Academy of Sciences, 115(50). https://doi.org/10.1073/pnas.1813217115

Wang, Y., Huang, L., Zhu, J., Zhang, W., Tang, Y., Yang, C., Lin, Y., Wang, Y., & Xiang, H. (2025). LIPG-mediated regulation of lipid deposition and proliferation in goat intramuscular preadipocytes involves the PPARα signaling pathway. PLOS ONE, 20(2), e0317953. https://doi.org/10.1371/journal.pone.0317953

Wang, Y., Jin, S., Sonobe, Y., Cheng, Y., Horiuchi, H., Parajuli, B., Kawanokuchi, J., Mizuno, T., Takeuchi, H., & Suzumura, A. (2014). Interleukin-1β Induces Blood–Brain Barrier Disruption by Downregulating Sonic Hedgehog in Astrocytes. PLoS ONE, 9(10), e110024. https://doi.org/10.1371/journal.pone.0110024

Wang, Y., Sabbagh, M. F., Gu, X., Rattner, A., Williams, J., & Nathans, J. (2019). Beta-catenin signaling regulates barrier-specific gene expression in circumventricular organ and ocular vasculatures. eLife, 8, e43257. https://doi.org/10.7554/eLife.43257

Wang, Y., Zhou, L., Wang, N., Qiu, B., Yao, D., Yu, J., He, M., Li, T., Xie, Y., Yu, X., Bi, Z., Sun, X., Ji, X., Li, Z., Mo, D., & Ge, W. (2025). Comprehensive characterization of metabolic consumption and production by the human brain. Neuron, 113(11), 1708-1722.e5. https://doi.org/10.1016/j.neuron.2025.03.003

Wang, Y.-Z., Castillon, C. C. M., Gebis, K. K., Bartom, E. T., d'Azzo, A., Contractor, A., & Savas, J. N. (2024). Notch receptor-ligand binding facilitates extracellular vesicle-mediated neuron-to-neuron communication. Cell Reports, 43(2), 113680. https://doi.org/10.1016/j.celrep.2024.113680

Wang, Z., He, Z., Liang, S., Yang, Q., Cheng, P., & Chen, A. (2020). Comprehensive proteomic analysis of exosomes derived from human bone marrow, adipose tissue, and umbilical cord mesenchymal stem cells. Stem Cell Research & Therapy, 11(1), 511. https://doi.org/10.1186/s13287-020-02032-8

Warashina, S., Zouda, M., Mohri, K., Wada, Y., Maeda, K., Watanabe, Y., & Mukai, H. (2022). 64Cu-labeling of small extracellular vesicle surfaces via a cross-bridged macrocyclic chelator for pharmacokinetic study by positron emission tomography imaging. International Journal of Pharmaceutics, 624, 121968. https://doi.org/10.1016/j.ijpharm.2022.121968

Wardlaw, J. M., Doubal, F., Armitage, P., Chappell, F., Carpenter, T., Muñoz Maniega, S., Farrall, A., Sudlow, C., Dennis, M., & Dhillon, B. (2009). Lacunar stroke is associated with diffuse blood–brain barrier dysfunction. Annals of Neurology, 65(2), 194–202. https://doi.org/10.1002/ana.21549

Watabe-Uchida, M., Uchida, N., Imamura, Y., Nagafuchi, A., Fujimoto, K., Uemura, T., Vermeulen, S., Van Roy, F., Adamson, E. D., & Takeichi, M. (1998). α-Catenin-Vinculin Interaction Functions to Organize the Apical Junctional Complex in Epithelial Cells. The Journal of Cell Biology, 142(3), 847–857. https://doi.org/10.1083/jcb.142.3.847

Webb, A. M., Francis, C. R., Judson, R. J., Kincross, H., Lundy, K. M., Westhoff, D. E., Meadows, S. M., & Kushner, E. J. (2022). EHD2 modulates Dll4 endocytosis during blood vessel development. Microcirculation, 29(1), e12740. https://doi.org/10.1111/micc.12740

Webber, A. J., & Johnson, S. A. (1970). Platelet participation in blood coagulation aspects of hemostasis. The American Journal of Pathology, 60(1), 19–42.

Wei, F., Ma, C., Zhou, T., Dong, X., Luo, Q., Geng, L., Ding, L., Zhang, Y., Zhang, L., Li, N., Li, Y., & Liu, Y. (2017). Exosomes derived from gemcitabine-resistant cells transfer malignant phenotypic traits via delivery of miRNA-222-3p. Molecular Cancer, 16(1), 132. https://doi.org/10.1186/s12943-017-0694-8

Wei, H., Yu, C., Zhang, C., Ren, Y., Guo, L., Wang, T., Chen, F., Li, Y., Zhang, X., Wang, H., & Liu, J. (2023). Butyrate ameliorates chronic alcoholic central nervous damage by suppressing microglia-mediated neuroinflammation and modulating the microbiome-gut-brain axis. Biomedicine & Pharmacotherapy, 160, 114308. https://doi.org/10.1016/j.biopha.2023.114308

Wei, W., Cardes, F., Hierlemann, A., & Modena, M. M. (2023). 3D In Vitro Blood-Brain-Barrier Model for Investigating Barrier Insults. Advanced Science, 10(11), 2205752. https://doi.org/10.1002/advs.202205752

Wei, X., Jiang, W., Zeng, J., Huang, L., Ding, H., Jing, Y., Han, Y., Li, Y., & Chen, S. (2022). Exosome-Derived lncRNA NEAT1 Exacerbates Sepsis-Associated Encephalopathy by Promoting Ferroptosis Through Regulating miR-9-5p/TFRC and GOT1 Axis. Molecular Neurobiology, 59(3), 1954–1969. https://doi.org/10.1007/s12035-022-02738-1

Wei, Z.-X., Cai, X.-X., Fei, Y.-D., Wang, Q., Hu, X.-L., Li, C., Hou, J.-W., Yang, Y.-L., Wang, Y.-P., & Li, Y.-G. (2024). Ntsr1 contributes to pulmonary hypertension by enhancing endoplasmic reticulum stress via JAK2-STAT3-Thbs1 signaling. Translational Research, 269, 64–75. https://doi.org/10.1016/j.trsl.2024.02.002

Welsh, J. A., Goberdhan, D. C. I., O'Driscoll, L., Buzas, E. I., Blenkiron, C., Bussolati, B., Cai, H., Di Vizio, D., Driedonks, T. A. P., Erdbrügger, U., Falcon-Perez, J. M., Fu, Q., Hill, A. F., Lenassi, M., Lim, S. K., Mahoney, M. G., Mohanty, S., Möller, A., Nieuwland, R., … Witwer, K. W. (2024). Minimal information for studies of extracellular vesicles (MISEV2023): From basic to advanced approaches. Journal of Extracellular Vesicles, 13(2). https://doi.org/10.1002/jev2.12404

Weng, Y., Chen, N., Zhang, R., He, J., Ding, X., Cheng, G., Bi, Q., Lu, Y., Shen, X. Z., Wan, S., & Shi, P. (2024). An integral blood–brain barrier in adulthood relies on microglia-derived PDGFB. Brain, Behavior, and Immunity, 115, 705–717. https://doi.org/10.1016/j.bbi.2023.11.023

Wheeler, M. A., Jaronen, M., Covacu, R., Zandee, S. E. J., Scalisi, G., Rothhammer, V., Tjon, E. C., Chao, C.-C., Kenison, J. E., Blain, M., Rao, V. T. S., Hewson, P., Barroso, A., Gutiérrez-Vázquez, C., Prat, A., Antel, J. P., Hauser, R., & Quintana, F. J. (2019). Environmental Control of Astrocyte Pathogenic Activities in CNS Inflammation. Cell, 176(3), 581-596.e18. https://doi.org/10.1016/j.cell.2018.12.012

White, K. E., Bailey, H. L., Shaw, B. S., Geiszler, P. C., Mesquita-Ribeiro, R., Scott, D., Layfield, R., & Serres, S. (2024). A convenient model of serum-induced reactivity of human astrocytes to investigate astrocyte-derived extracellular vesicles. Frontiers in Cellular Neuroscience, 18, 1414142. https://doi.org/10.3389/fncel.2024.1414142

Wiesolek, H. L., Bui, T. M., Lee, J. J., Dalal, P., Finkielsztein, A., Batra, A., Thorp, E. B., & Sumagin, R. (2020). Intercellular Adhesion Molecule 1 Functions as an Efferocytosis Receptor in Inflammatory Macrophages. The American Journal of Pathology, 190(4), 874–885. https://doi.org/10.1016/j.ajpath.2019.12.006

Wiley, S. R., Schooley, K., Smolak, P. J., Din, W. S., Huang, C.-P., Nicholl, J. K., Sutherland, G. R., Smith, T. D., Rauch, C., Smith, C. A., & Goodwin, R. G. (1995). Identification and characterization of a new member of the TNF family that induces apoptosis. Immunity, 3(6), 673–682. https://doi.org/10.1016/1074-7613(95)90057-8

Wilke, S., Krausze, J., & Büssow, K. (2012). Crystal structure of the conserved domain of the DC lysosomal associated membrane protein: Implications for the lysosomal glycocalyx. BMC Biology, 10(1), 62. https://doi.org/10.1186/1741-7007-10-62

Williams, S., Fernandez-Rhodes, M., Law, A., Peacock, B., Lewis, M. P., & Davies, O. G. (2023). Comparison of extracellular vesicle isolation processes for therapeutic applications. Journal of Tissue Engineering, 14, 20417314231174609. https://doi.org/10.1177/20417314231174609

Williamson, M. R., Fuertes, C. J. A., Dunn, A. K., Drew, M. R., & Jones, T. A. (2021). Reactive astrocytes facilitate vascular repair and remodeling after stroke. Cell Reports, 35(4). https://doi.org/10.1016/j.celrep.2021.109048

Willis, C. M., Nicaise, A. M., Bongarzone, E. R., Givogri, M., Reiter, C. R., Heintz, O., Jellison, E. R., Sutter, P. A., TeHennepe, G., Ananda, G., Vella, A. T., & Crocker, S. J. (2020). Astrocyte Support for Oligodendrocyte Differentiation can be Conveyed via Extracellular Vesicles but Diminishes with Age. Scientific Reports, 10, 828. https://doi.org/10.1038/s41598-020-57663-x

Witwer, K. W., Buzás, E. I., Bemis, L. T., Bora, A., Lässer, C., Lötvall, J., Nolte-'t Hoen, E. N., Piper, M. G., Sivaraman, S., Skog, J., Théry, C., Wauben, M. H., & Hochberg, F. (2013). Standardization of sample collection, isolation and analysis methods in extracellular vesicle research. Journal of Extracellular Vesicles, 2(1), 20360. https://doi.org/10.3402/jev.v2i0.20360

Wolburg, H., Wolburg-Buchholz, K., Kraus, J., Rascher-Eggstein, G., Liebner, S., Hamm, S., Duffner, F., Grote, E.-H., Risau, W., & Engelhardt, B. (2003). Localization of claudin-3 in tight junctions of the blood-brain barrier is selectively lost during experimental autoimmune encephalomyelitis and human glioblastoma multiforme. Acta Neuropathologica, 105(6), 586–592. https://doi.org/10.1007/s00401-003-0688-z

Wolf, P. (1967). The Nature and Significance of Platelet Products in Human Plasma. British Journal of Haematology, 13(3), 269–288. https://doi.org/10.1111/j.1365-2141.1967.tb08741.x

Wolfes, A. C., Ahmed, S., Awasthi, A., Stahlberg, M. A., Rajput, A., Magruder, D. S., Bonn, S., & Dean, C. (2017). A novel method for culturing stellate astrocytes reveals spatially distinct Ca2+ signaling and vesicle recycling in astrocytic processes. Journal of General Physiology, 149(1), 149–170. https://doi.org/10.1085/jgp.201611607

Woo, H.-K., Ahn, H.-S., Park, J., Bae, J., Kim, B., Yu, J., Seo, J. K., Kim, K., & Cho, Y.-K. (2025). Size-Dependent Separation of Extracellular Vesicle Subtypes with Exodisc Enabling Proteomic Analysis in Prostate Cancer. Journal of Proteome Research, 24(2), 861–870. https://doi.org/10.1021/acs.jproteome.4c00945

Wright, A., Snyder, O. L., Christenson, L. K., He, H., & Weiss, M. L. (2022). Effect of Pre-Processing Storage Condition of Cell Culture-Conditioned Medium on Extracellular Vesicles Derived from Human Umbilical Cord-Derived Mesenchymal Stromal Cells. International Journal of Molecular Sciences, 23(14), 7716. https://doi.org/10.3390/ijms23147716

Wu, D., Xu, Y., Ding, T., Zu, Y., Yang, C., & Yu, L. (2017). Pairing of integrins with ECM proteins determines migrasome formation. Cell Research, 27(11), 1397–1400. https://doi.org/10.1038/cr.2017.108

Wu, L., Deng, L., Xu, X., Chang, H., Liu, C., Wu, J., Zhang, C., Wang, R., Gao, R., Chen, H., Ye-Lehmann, S., Zhang, Z., Zhu, T., & Chen, C. (2025). Astrocyte-derived extracellular vesicular NFIA mediates obesity-associated cognitive impairment. Journal of Neuroinflammation, 22(1), 145. https://doi.org/10.1186/s12974-025-03473-9

Wu, L., Liu, Y., He, Q., Ao, G., Xu, N., He, W., Liu, X., Huang, L., Yu, Q., Kanamaru, H., Dong, S., Zhu, S., Yuan, Y., Han, M., Ling, Y., Liu, L., Wu, C., Zhou, Y., Sherchan, P., … Zhang, J. H. (2024). PEDF-34 attenuates neurological deficit and suppresses astrocyte-dependent neuroinflammation by modulating astrocyte polarization via 67LR/JNK/STAT1 signaling pathway after subarachnoid hemorrhage in rats. Journal of Neuroinflammation, 21(1), 178. https://doi.org/10.1186/s12974-024-03171-y

Wu, L., Ye, Z., Pan, Y., Li, X., Fu, X., Zhang, B., Li, Y., Lin, W., Li, X., & Gao, Q. (2018). Vascular endothelial growth factor aggravates cerebral ischemia and reperfusion-induced blood-brain-barrier disruption through regulating LOC102640519/HOXC13/ZO-1 signaling. Experimental Cell Research, 369(2), 275–283. https://doi.org/10.1016/j.yexcr.2018.05.029

Wu, S., Luo, M., To, K. K. W., Zhang, J., Su, C., Zhang, H., An, S., Wang, F., Chen, D., & Fu, L. (2021). Intercellular transfer of exosomal wild type EGFR triggers osimertinib resistance in non-small cell lung cancer. Molecular Cancer, 20(1), 17. https://doi.org/10.1186/s12943-021-01307-9

Wu, T., Han, N., Zhao, C., Huang, X., Su, P., & Li, X. (2022). The long non-sacoding RNA TMEM147-AS1/miR-133b/ ZNF587 axis regulates the Warburg effect and promotes prostatic carcinoma invasion and proliferation. The Journal of Gene Medicine, 24(11), e3453. https://doi.org/10.1002/jgm.3453

Wu, W., Sui, J., Liu, T., Yang, S., Xu, S., Zhang, M., Huang, S., Yin, L., Pu, Y., & Liang, G. (2019). Integrated analysis of two-lncRNA signature as a potential prognostic biomarker

in cervical cancer: A study based on public database. PeerJ, 7, e6761. https://doi.org/10.7717/peerj.6761

Wu, X., Ren, Y., Yao, R., Zhou, L., & Fan, R. (2021). Circular RNA circ-MMP11 Contributes to Lapatinib Resistance of Breast Cancer Cells by Regulating the miR-153-3p/ANLN Axis. Frontiers in Oncology, 11, 639961. https://doi.org/10.3389/fonc.2021.639961

Wu, Y., Hu, X., Wei, Z., & Lin, Q. (2024). Cellular Regulation of Macropinocytosis. International Journal of Molecular Sciences, 25(13), 6963. https://doi.org/10.3390/ijms25136963

Xia, K., Zhang, S., Peng, H., Chen, H., Yang, C., Yu, J., Luo, P., Lu, Q., Chen, H., Huang, L., Xiong, Y., Zhao, L., Jia, L., Li, L., Qiu, Y., Guo, Y., Liu, C., Fan, H., Dai, Z., … Xiang, A. P. (2026). An extracellular vesicle-mediated mitochondrial transfer network critical for testosterone synthesis. Nature Cell Biology, 28(4), 707–724. https://doi.org/10.1038/s41556-026-01896-x

Xia, Y., He, Q., Li, Y., Chen, S., Huang, M., Wang, Y., Gao, Y., Huang, Y., Wang, M., Mao, L., & Hu, B. (2013). Recombinant Human Sonic Hedgehog Protein Regulates the Expression of ZO-1 and Occludin by Activating Angiopoietin-1 in Stroke Damage. PLoS ONE, 8(7), e68891. https://doi.org/10.1371/journal.pone.0068891

Xie, X., Song, Q., Dai, C., Cui, S., Tang, R., Li, S., Chang, J., Li, P., Wang, J., Li, J., Gao, C., Chen, H., Chen, S., Ren, R., Gao, X., & Wang, G. (2023). Clinical safety and efficacy of allogenic human adipose mesenchymal stromal cells-derived exosomes in patients with mild to moderate Alzheimer's disease: A phase I/II clinical trial. General Psychiatry, 36(5), e101143. https://doi.org/10.1136/gpsych-2023-101143

Xie, Y., Kuan, A. T., Wang, W., Herbert, Z. T., Mosto, O., Olukoya, O., Adam, M., Vu, S., Kim, M., Tran, D., Gómez, N., Charpentier, C., Sorour, I., Lacey, T. E., Tolstorukov, M. Y., Sabatini, B. L., Lee, W.-C. A., & Harwell, C. C. (2022). Astrocyte-neuron crosstalk through Hedgehog signaling mediates cortical synapse development. Cell Reports, 38(8), 110416. https://doi.org/10.1016/j.celrep.2022.110416

Xie, Y., Xu, Z., Wu, C., Zhou, C., Zhang, X., Gu, T., Yang, J., Yang, H., Zheng, E., Xu, Z., Cai, G., Li, Z., Liu, D., Wu, Z., & Hong, L. (2022). Extracellular vesicle-encapsulated miR-21-5p in seminal plasma prevents sperm capacitation via Vinculin inhibition. Theriogenology, 193, 103–113. https://doi.org/10.1016/j.theriogenology.2022.09.014

Xing, C., Li, W., Deng, W., Ning, M., & Lo, E. H. (2018). A potential gliovascular mechanism for microglial activation: Differential phenotypic switching of microglia by endothelium versus astrocytes. Journal of Neuroinflammation, 15(1), 143. https://doi.org/10.1186/s12974-018-1189-2

Xing, Y., Zhang, F., Ji, P., Wei, M., Yin, C., Yang, A., Yang, G., & Zhao, J. (2023). Efficient Delivery of GSDMD-N mRNA by Engineered Extracellular Vesicles Induces Pyroptosis for Enhanced Immunotherapy. Small, 19(20), 2204031. https://doi.org/10.1002/smll.202204031

Xingi, E., Koutsoudaki, P. N., Thanou, I., Phan, M.-S., Margariti, M., Scheller, A., Tinevez, J.-Y., Kirchhoff, F., & Thomaidou, D. (2023). LPS-Induced Systemic Inflammation Affects the Dynamic Interactions of Astrocytes and Microglia with the Vasculature of the Mouse Brain Cortex. Cells, 12(10), 1418. https://doi.org/10.3390/cells12101418

Xiong, R., Zhou, X., Tang, Y., Wu, J., Sun, Y., Teng, J., Pan, R., Law, B. Y., Zhao, Y., Qiu, W., Wang, X., Liu, S., Wang, Y., Yu, L., Yu, C., Mei, Q., Qin, D., & Wu, A. (2021). Lychee seed polyphenol protects the BLOOD–BRAIN barrier through inhibiting Aβ(25–35)-induced NLRP3 inflammasome activation via the AMPK / MTOR / ULK1-MEDIATED autophagy in BEND .3 cells and APP / PS1 mice. Phytotherapy Research, 35(2), 954–973. https://doi.org/10.1002/ptr.6849

Xu, B., Zhang, Y., Du, X.-F., Li, J., Zi, H.-X., Bu, J.-W., Yan, Y., Han, H., & Du, J.-L. (2017). Neurons secrete miR-132-containing exosomes to regulate brain vascular integrity. Cell Research, 27(7), 882–897. https://doi.org/10.1038/cr.2017.62

Xu, F., Han, L., Wang, Y., Deng, D., Ding, Y., Zhao, S., Zhang, Q., Ma, L., & Chen, X. (2023). Prolonged anesthesia induces neuroinflammation and complement-mediated microglial synaptic elimination involved in neurocognitive dysfunction and anxiety-like behaviors. BMC Medicine, 21(1), 7. https://doi.org/10.1186/s12916-022-02705-6

Xu, L., Cao, H., Xie, Y., Zhang, Y., Du, M., Xu, X., Ye, R., & Liu, X. (2019). Exosome-shuttled miR-92b-3p from ischemic preconditioned astrocytes protects neurons against oxygen and glucose deprivation. Brain Research, 1717, 66–73. https://doi.org/10.1016/j.brainres.2019.04.009

Xu, R., Greening, D. W., Rai, A., Ji, H., & Simpson, R. J. (2015). Highly-purified exosomes and shed microvesicles isolated from the human colon cancer cell line LIM1863 by sequential centrifugal ultrafiltration are biochemically and functionally distinct. Methods, 87, 11–25. https://doi.org/10.1016/j.ymeth.2015.04.008

Ya, J., & Bayraktutan, U. (2025). Donor Variability Alters the Characteristics of Human Brain Microvascular Endothelial Cells. Current Issues in Molecular Biology, 47(2), 73. https://doi.org/10.3390/cimb47020073

Yamamoto, M., Ramirez, S. H., Sato, S., Kiyota, T., Cerny, R. L., Kaibuchi, K., Persidsky, Y., & Ikezu, T. (2008). Phosphorylation of Claudin-5 and Occludin by Rho Kinase in Brain Endothelial Cells. The American Journal of Pathology, 172(2), 521–533. https://doi.org/10.2353/ajpath.2008.070076

Yang, A. C., Vest, R. T., Kern, F., Lee, D. P., Agam, M., Maat, C. A., Losada, P. M., Chen, M. B., Schaum, N., Khoury, N., Toland, A., Calcuttawala, K., Shin, H., Pálovics, R., Shin, A., Wang, E. Y., Luo, J., Gate, D., Schulz-Schaeffer, W. J., … Wyss-Coray, T. (2022). A human brain vascular atlas reveals diverse mediators of Alzheimer's risk. Nature, 603(7903), 885–892. https://doi.org/10.1038/s41586-021-04369-3

Yang, B., Fang, L., Gao, Q., Xu, C., Xu, J., Chen, Z.-X., Wang, Y., & Yang, P. (2022). Species-specific KRAB-ZFPs function as repressors of retroviruses by targeting PBS regions. Proceedings of the National Academy of Sciences, 119(11), e2119415119. https://doi.org/10.1073/pnas.2119415119

Yang, C., Wang, X., To, K. K. W., Cui, C., Luo, M., Wu, S., Huang, L., Fu, K., Pan, C., Liu, Z., Fan, T., Yang, C., Wang, F., & Fu, L. (2024). Circulating tumor cells shielded with extracellular vesicle-derived CD45 evade T cell attack to enable metastasis. Signal Transduction and Targeted Therapy, 9(1), 84. https://doi.org/10.1038/s41392-024-01789-1

Yang, K., Fan, M., Wang, X., Xu, J., Wang, Y., Tu, F., Gill, P. S., Ha, T., Liu, L., Williams, D. L., & Li, C. (2022). Lactate promotes macrophage HMGB1 lactylation, acetylation, and

exosomal release in polymicrobial sepsis. Cell Death & Differentiation, 29(1), 133–146. https://doi.org/10.1038/s41418-021-00841-9

Yang, L., Lin, Z., Mu, R., Wu, W., Zhi, H., Liu, X., Yang, H., & Liu, L. (2024). Neurons enhance blood–brain barrier function via upregulating claudin-5 and VE-cadherin expression due to glial cell line-derived neurotrophic factor secretion. eLife, 13, RP96161. https://doi.org/10.7554/eLife.96161.3

Yang, T., Tang, Y., Liu, X., Gong, S., & Yao, E. (2024). Microglia synchronizes with the circadian rhythm of the glymphatic system and modulates glymphatic system function. IUBMB Life, 76(12), 1209–1222. https://doi.org/10.1002/iub.2903

Yang, X., Ren, H., Yao, L., Chen, X., & He, A. (2015). Role of EHD2 in migration and invasion of human breast cancer cells. Tumor Biology, 36(5), 3717–3726. https://doi.org/10.1007/s13277-014-3011-9

Yang, Y., Arnold, M. L., Lange, C. M., Sun, L.-H., Broussalian, M., Doroodian, S., Ebata, H., Choy, E. H., Poon, K., Moreno, T. M., Singh, A., Driscoll, M., Kumsta, C., & Hansen, M. (2024). Autophagy protein ATG-16.2 and its WD40 domain mediate the beneficial effects of inhibiting early-acting autophagy genes in C. elegans neurons. Nature Aging, 4(2), 198–212. https://doi.org/10.1038/s43587-023-00548-1

Yang, Y., Estrada, E. Y., Thompson, J. F., Liu, W., & Rosenberg, G. A. (2007). Matrix metalloproteinase-mediated disruption of tight junction proteins in cerebral vessels is reversed by synthetic matrix metalloproteinase inhibitor in focal ischemia in rat. Journal of Cerebral Blood Flow and Metabolism: Official Journal of the International Society of Cerebral Blood Flow and Metabolism, 27(4), 697–709. https://doi.org/10.1038/sj.jcbfm.9600375

Yao, Q., Wang, B., Jia, X., Li, Q., Yao, W., & Zhang, J. (2019). Increased Human Interleukin-32 Expression Is Related to Disease Activity of Graves' Disease. Frontiers in Endocrinology, 10, 613. https://doi.org/10.3389/fendo.2019.00613

Yao, X., Dai, W., Yang, S., Wang, Z., Zhang, Q., Meng, Q., & Zhang, T. (2023). Synergistic Effect of Treatment with Highly Pathogenic Porcine Reproductive and Respiratory Syndrome Virus and Lipopolysaccharide on the Inflammatory Response of Porcine Pulmonary Microvascular Endothelial Cells. Viruses, 15(7), 1523. https://doi.org/10.3390/v15071523

Yao, Y., Chen, Z.-L., Norris, E. H., & Strickland, S. (2014). Astrocytic laminin regulates pericyte differentiation and maintains blood brain barrier integrity. Nature Communications, 5(1), 3413. https://doi.org/10.1038/ncomms4413

Yao, Y., & Tsirka, S. E. (2011). Truncation of monocyte chemoattractant protein 1 by plasmin promotes blood–brain barrier disruption. Journal of Cell Science, 124(9), 1486–1495. https://doi.org/10.1242/jcs.082834

Yao, Z., Qiao, Y., Li, X., Chen, J., Ding, J., Bai, L., Shen, F., Shi, B., Liu, J., Peng, L., Li, J., & Yuan, Z. (2018). Exosomes Exploit the Virus Entry Machinery and Pathway To Transmit Alpha Interferon-Induced Antiviral Activity. Journal of Virology, 92(24), e01578-18. https://doi.org/10.1128/JVI.01578-18

Yao, Z., Van Velthoven, C. T. J., Kunst, M., Zhang, M., McMillen, D., Lee, C., Jung, W., Goldy, J., Abdelhak, A., Aitken, M., Baker, K., Baker, P., Barkan, E., Bertagnolli, D.,

Bhandiwad, A., Bielstein, C., Bishwakarma, P., Campos, J., Carey, D., … Zeng, H. (2023). A high-resolution transcriptomic and spatial atlas of cell types in the whole mouse brain. Nature, 624(7991), 317–332. https://doi.org/10.1038/s41586-023-06812-z

Ye, X., Smallwood, P., & Nathans, J. (2011). Expression of the Norrie disease gene (Ndp) in developing and adult mouse eye, ear, and brain. Gene Expression Patterns, 11(1–2), 151–155. https://doi.org/10.1016/j.gep.2010.10.007

Yeung, M. S. Y., Zdunek, S., Bergmann, O., Bernard, S., Salehpour, M., Alkass, K., Perl, S., Tisdale, J., Possnert, G., Brundin, L., Druid, H., & Frisén, J. (2014). Dynamics of Oligodendrocyte Generation and Myelination in the Human Brain. Cell, 159(4), 766–774. https://doi.org/10.1016/j.cell.2014.10.011

Yogalingam, G., Bonten, E. J., Van De Vlekkert, D., Hu, H., Moshiach, S., Connell, S. A., & d'Azzo, A. (2008). Neuraminidase 1 Is a Negative Regulator of Lysosomal Exocytosis. Developmental Cell, 15(1), 74–86. https://doi.org/10.1016/j.devcel.2008.05.005

Young, M. D., Wakefield, M. J., Smyth, G. K., & Oshlack, A. (2010). Gene ontology analysis for RNA-seq: Accounting for selection bias. Genome Biology, 11(2), R14. https://doi.org/10.1186/gb-2010-11-2-r14

Yu, B., Tang, Y., & Cai, D. (2020). Brain is an endocrine organ through secretion and nuclear transfer of parathymosin. Life Science Alliance, 3(12), e202000917. https://doi.org/10.26508/lsa.202000917

Yu, D., Mei, Y., Wang, L., Zhao, Y., Fan, X., Liang, D., Li, L., Zhu, J., Bi, S., Wang, X., Qi, Z., Zhu, L., & Wang, Y. (2023). Nano-seq analysis reveals different functional tendency between exosomes and microvesicles derived from hUMSC. Stem Cell Research & Therapy, 14(1), 272. https://doi.org/10.1186/s13287-023-03491-5

Yu, H., Xu, Z., Qu, G., Wang, H., Lin, L., Li, X., Xie, X., Lei, Y., He, X., Chen, Y., & Li, Y. (2021). Hypoxic Preconditioning Enhances the Efficacy of Mesenchymal Stem Cells-Derived Conditioned Medium in Switching Microglia toward Anti-inflammatory Polarization in Ischemia/Reperfusion. Cellular and Molecular Neurobiology, 41(3), 505–524. https://doi.org/10.1007/s10571-020-00868-5

Yu, L., Zhu, G., Zhang, Z., Yu, Y., Zeng, L., Xu, Z., Weng, J., Xia, J., Li, J., & Pathak, J. L. (2023). Apoptotic bodies: Bioactive treasure left behind by the dying cells with robust diagnostic and therapeutic application potentials. Journal of Nanobiotechnology, 21(1), 218. https://doi.org/10.1186/s12951-023-01969-1

Yu, Y., Su, Y., Wang, G., Lan, M., Liu, J., Garcia Martin, R., Brandao, B. B., Lino, M., Li, L., Liu, C., Kahn, C. R., & Meng, Q. (2024). Reciprocal communication between FAPs and muscle cells via distinct extracellular vesicle miRNAs in muscle regeneration. Proceedings of the National Academy of Sciences, 121(11), e2316544121. https://doi.org/10.1073/pnas.2316544121

Yu, Z., Fang, X., Liu, W., Sun, R., Zhou, J., Pu, Y., Zhao, M., Sun, D., Xiang, Z., Liu, P., Ding, Y., Cao, L., & He, C. (2022). Microglia Regulate Blood–Brain Barrier Integrity via MiR-126a-5p/MMP9 Axis during Inflammatory Demyelination. Advanced Science, 9(24), 2105442. https://doi.org/10.1002/advs.202105442

Yuan, H., Sun, D., Ji, Y., Meng, B., Lu, B., Liu, R., Xing, X., Wang, R., & Chen, J. (2023). Pericyte loss impairs the blood–brain barrier and cognitive function in aged mice after

anesthesia/surgery. Brain Research Bulletin, 204, 110799. https://doi.org/10.1016/j.brainresbull.2023.110799

Yue, K.-Y., Zhang, P.-R., Zheng, M.-H., Cao, X.-L., Cao, Y., Zhang, Y.-Z., Zhang, Y.-F., Wu, H.-N., Lu, Z.-H., Liang, L., Jiang, X.-F., & Han, H. (2019). Neurons can upregulate Cav-1 to increase intake of endothelial cells-derived extracellular vesicles that attenuate apoptosis via miR-1290. Cell Death & Disease, 10(12), 869. https://doi.org/10.1038/s41419-019-2100-5

Yuen, T. J., Silbereis, J. C., Griveau, A., Chang, S. M., Daneman, R., Fancy, S. P. J., Zahed, H., Maltepe, E., & Rowitch, D. H. (2014). Oligodendrocyte-Encoded HIF Function Couples Postnatal Myelination and White Matter Angiogenesis. Cell, 158(2), 383–396. https://doi.org/10.1016/j.cell.2014.04.052

Zamanian, J. L., Xu, L., Foo, L. C., Nouri, N., Zhou, L., Giffard, R. G., & Barres, B. A. (2012). Genomic Analysis of Reactive Astrogliosis. The Journal of Neuroscience, 32(18), 6391–6410. https://doi.org/10.1523/JNEUROSCI.6221-11.2012

Zamproni, L. N., Gökçe, B., Venckute Larsson, J., Ceballos-Torres, A., Gram, M., Porcionatto, M. A., & Herland, A. (2025). Unraveling the influence of astrocytes on endothelial cell transcription: Towards understanding blood-brain barrier in vitro models' dynamics. Brain Research Bulletin, 224, 111328. https://doi.org/10.1016/j.brainresbull.2025.111328

Zeisberg, E. M., Tarnavski, O., Zeisberg, M., Dorfman, A. L., McMullen, J. R., Gustafsson, E., Chandraker, A., Yuan, X., Pu, W. T., Roberts, A. B., Neilson, E. G., Sayegh, M. H., Izumo, S., & Kalluri, R. (2007). Endothelial-to-mesenchymal transition contributes to cardiac fibrosis. Nature Medicine, 13(8), 952–961. https://doi.org/10.1038/nm1613

Zeng, H., Liu, N., Yang, Y., Xing, H., Liu, X., Li, F., La, G., Huang, M., & Zhou, M. (2019). Lentivirus-mediated downregulation of α-synuclein reduces neuroinflammation and promotes functional recovery in rats with spinal cord injury. Journal of Neuroinflammation, 16(1), 283. https://doi.org/10.1186/s12974-019-1658-2

Zhang, A. Y., Elias, E., White, A. G., Jones, L. G., Hamad, T., & Manners, M. T. (2025). Microglia reactivity is brain region and sex specific in the context of chronic stress. Scientific Reports, 15(1), 33285. https://doi.org/10.1038/s41598-025-18000-2

Zhang, C., & Harder, D. R. (2002). Cerebral Capillary Endothelial Cell Mitogenesis and Morphogenesis Induced by Astrocytic Epoxyeicosatrienoic Acid. Stroke, 33(12), 2957–2964. https://doi.org/10.1161/01.STR.0000037787.07479.9A

Zhang, D., Ruan, J., Peng, S., Li, J., Hu, X., Zhang, Y., Zhang, T., Ge, Y., Zhu, Z., Xiao, X., Zhu, Y., Li, X., Li, T., Zhou, L., Gao, Q., Zheng, G., Zhao, B., Li, X., Zhu, Y., … Jia, J.-M. (2024). Synaptic-like transmission between neural axons and arteriolar smooth muscle cells drives cerebral neurovascular coupling. Nature Neuroscience, 27(2), 232–248. https://doi.org/10.1038/s41593-023-01515-0

Zhang, D., Yang, S., Toledo, E. M., Gyllborg, D., Saltó, C., Carlos Villaescusa, J., & Arenas, E. (2017). Niche-derived laminin-511 promotes midbrain dopaminergic neuron survival and differentiation through YAP. Science Signaling, 10(493), eaal4165. https://doi.org/10.1126/scisignal.aal4165

Zhang, G., Zhang, X., Zhou, K., Ling, X., Zhang, J., Wu, P., Zhang, T., Xie, K., & Dai, G. (2022). miRNA-10a-5p Targeting the BCL6 Gene Regulates Proliferation, Differentiation and Apoptosis of Chicken Myoblasts. International Journal of Molecular Sciences, 23(17), 9545. https://doi.org/10.3390/ijms23179545

Zhang, H., Freitas, D., Kim, H. S., Fabijanic, K., Li, Z., Chen, H., Mark, M. T., Molina, H., Martin, A. B., Bojmar, L., Fang, J., Rampersaud, S., Hoshino, A., Matei, I., Kenific, C. M., Nakajima, M., Mutvei, A. P., Sansone, P., Buehring, W., … Lyden, D. (2018). Identification of distinct nanoparticles and subsets of extracellular vesicles by asymmetric flow field-flow fractionation. Nature Cell Biology, 20(3), 332–343. https://doi.org/10.1038/s41556-018-0040-4

Zhang, L., Graf, I., Kuang, Y., Zheng, X., Haupt, M., Majid, A., Kilic, E., Hermann, D. M., Psychogios, M.-N., Weber, M. S., Ochs, J., Bähr, M., & Doeppner, T. R. (2021). Neural Progenitor Cell-Derived Extracellular Vesicles Enhance Blood-Brain Barrier Integrity by NF-κB (Nuclear Factor-κB)-Dependent Regulation of ABCB1 (ATP-Binding Cassette Transporter B1) in Stroke Mice. Arteriosclerosis, Thrombosis, and Vascular Biology, 41(3), 1127–1145. https://doi.org/10.1161/ATVBAHA.120.315031

Zhang, L., Tang, S., Ma, Y., Liu, J., Monnier, P., Li, H., Zhang, R., Yu, G., Zhang, M., Li, Y., Feng, J., & Qin, X. (2022). RGMa Participates in the Blood–Brain Barrier Dysfunction Through BMP/BMPR/YAP Signaling in Multiple Sclerosis. Frontiers in Immunology, 13. https://doi.org/10.3389/fimmu.2022.861486

Zhang, Q., Higginbotham, J. N., Jeppesen, D. K., Yang, Y.-P., Li, W., McKinley, E. T., Graves-Deal, R., Ping, J., Britain, C. M., Dorsett, K. A., Hartman, C. L., Ford, D. A., Allen, R. M., Vickers, K. C., Liu, Q., Franklin, J. L., Bellis, S. L., & Coffey, R. J. (2019). Transfer of Functional Cargo in Exomeres. Cell Reports, 27(3), 940-954.e6. https://doi.org/10.1016/j.celrep.2019.01.009

Zhang, Q., Jeppesen, D. K., Higginbotham, J. N., Graves-Deal, R., Trinh, V. Q., Ramirez, M. A., Sohn, Y., Neininger, A. C., Taneja, N., McKinley, E. T., Niitsu, H., Cao, Z., Evans, R., Glass, S. E., Ray, K. C., Fissell, W. H., Hill, S., Rose, K. L., Huh, W. J., … Coffey, R. J. (2021). Supermeres are functional extracellular nanoparticles replete with disease biomarkers and therapeutic targets. Nature Cell Biology, 23(12), 1240–1254. https://doi.org/10.1038/s41556-021-00805-8

Zhang, R., Wu, Y., Xie, F., Zhong, Y., Wang, Y., Xu, M., Feng, J., Charish, J., Monnier, P. P., & Qin, X. (2018). RGMa mediates reactive astrogliosis and glial scar formation through TGFβ1/Smad2/3 signaling after stroke. Cell Death & Differentiation, 25(8), 1503–1516. https://doi.org/10.1038/s41418-018-0058-y

Zhang, S., Liao, X., Chen, S., Qian, W., Li, M., Xu, Y., Yang, M., Li, X., Mo, S., Tang, M., Wu, X., Hu, Y., Li, Z., Yu, R., Abudourousuli, A., Song, L., & Li, J. (2022). Large Oncosome-Loaded VAPA Promotes Bone-Tropic Metastasis of Hepatocellular Carcinoma Via Formation of Osteoclastic Pre-Metastatic Niche. Advanced Science, 9(31), 2201974. https://doi.org/10.1002/advs.202201974

Zhang, W., Xiao, D., Mao, Q., & Xia, H. (2023). Role of neuroinflammation in neurodegeneration development. Signal Transduction and Targeted Therapy, 8(1), 267. https://doi.org/10.1038/s41392-023-01486-5

Zhang, W., Yang, X., Liu, J., Pan, Y., Zhang, M., & Chen, L. (2022). Senescent Phenotype of Astrocytes Leads to Activation of BV2 Microglia and N2a Neuronal Cells Death. Molecules, 27(18), 5925. https://doi.org/10.3390/molecules27185925

Zhang, Y., Sloan, S. A., Clarke, L. E., Caneda, C., Plaza, C. A., Blumenthal, P. D., Vogel, H., Steinberg, G. K., Edwards, M. S. B., Li, G., Duncan, J. A., Cheshier, S. H., Shuer, L. M., Chang, E. F., Grant, G. A., Gephart, M. G. H., & Barres, B. A. (2016). Purification and Characterization of Progenitor and Mature Human Astrocytes Reveals Transcriptional and Functional Differences with Mouse. Neuron, 89(1), 37–53. https://doi.org/10.1016/j.neuron.2015.11.013

Zhang, Y.-S., Liu, Z.-Y., Lin, L.-C., Tu, B., Mao, S., Song, K., Liu, P., Yang, J.-J., Chen, Q., Zhao, J.-Y., & Tao, H. (2025). Epigenetic blockade of SOD2 boosts mitochondria ROS and cytoskeleton remodeling in cardiac fibrosis. Cardiovascular Research, cvaf257. https://doi.org/10.1093/cvr/cvaf257

Zhang, Z., Lin, W., Gan, Q., Lei, M., Gong, B., Zhang, C., Henrique, J. S., Han, J., Tian, H., Tao, Q., Potempa, L. A., Stein, T. D., Emili, A., & Qiu, W. Q. (2024). The influences of ApoE isoforms on endothelial adherens junctions and actin cytoskeleton responding to mCRP. Angiogenesis, 27(4), 861–881. https://doi.org/10.1007/s10456-024-09946-4

Zhang, Z., Liu, X., Yang, X., Jiang, Y., Li, A., Cong, J., Li, Y., Xie, Q., Xu, C., & Liu, D. (2023). Identification of faecal extracellular vesicles as novel biomarkers for the non-invasive diagnosis and prognosis of colorectal cancer. Journal of Extracellular Vesicles, 12(1), 12300. https://doi.org/10.1002/jev2.12300

Zhang, Z., Zhang, Z., Lu, H., Yang, Q., Wu, H., & Wang, J. (2017). Microglial Polarization and Inflammatory Mediators After Intracerebral Hemorrhage. Molecular Neurobiology, 54(3), 1874–1886. https://doi.org/10.1007/s12035-016-9785-6

Zhang, Z.-Z., Wang, W., Jin, H.-Y., Chen, X., Cheng, Y.-W., Xu, Y.-L., Song, B., Penninger, J. M., Oudit, G. Y., & Zhong, J.-C. (2017). Apelin Is a Negative Regulator of Angiotensin II–Mediated Adverse Myocardial Remodeling and Dysfunction. Hypertension, 70(6), 1165–1175. https://doi.org/10.1161/HYPERTENSIONAHA.117.10156

Zhao, D., Wu, Y., Zhao, H., Zhang, F., Wang, J., Liu, Y., Lin, J., Huang, Y., Pan, W., Qi, J., Chen, N., Yang, X., Xu, W., Tong, Z., & Cheng, J. (2024). Midbrain FA initiates neuroinflammation and depression onset in both acute and chronic LPS-induced depressive model mice. Brain, Behavior, and Immunity, 117, 356–375. https://doi.org/10.1016/j.bbi.2024.02.004

Zhao, S., Mi, Y., Guan, B., Zheng, B., Wei, P., Gu, Y., Zhang, Z., Cai, S., Xu, Y., Li, X., He, X., Zhong, X., Li, G., Chen, Z., & Li, D. (2020). Tumor-derived exosomal miR-934 induces macrophage M2 polarization to promote liver metastasis of colorectal cancer. Journal of Hematology & Oncology, 13(1), 156. https://doi.org/10.1186/s13045-020-00991-2

Zhao, S., Mi, Y., Zheng, B., Wei, P., Gu, Y., Zhang, Z., Xu, Y., Cai, S., Li, X., & Li, D. (2022). Highly-metastatic colorectal cancer cell released miR-181a-5p-rich extracellular vesicles promote liver metastasis by activating hepatic stellate cells and remodelling the tumour microenvironment. Journal of Extracellular Vesicles, 11(1), e12186. https://doi.org/10.1002/jev2.12186

Zhao, X., Lu, J., Zhang, J., Liu, C., Wang, H., Wang, Y., & Du, Q. (2024). Sleep restriction promotes brain oxidative stress and inflammation, and aggravates cognitive impairment in insulin-resistant mice. Psychoneuroendocrinology, 166, 107065. https://doi.org/10.1016/j.psyneuen.2024.107065

Zhen, H., Zhao, L., Ling, Z., Kuo, L., Xue, X., & Feng, J. (2018). Wip1 regulates blood-brain barrier function and neuro-inflammation induced by lipopolysaccharide via the sonic hedgehog signaling signaling pathway. Molecular Immunology, 93, 31–37. https://doi.org/10.1016/j.molimm.2017.09.020

Zhou, X., Franklin, R. A., Adler, M., Jacox, J. B., Bailis, W., Shyer, J. A., Flavell, R. A., Mayo, A., Alon, U., & Medzhitov, R. (2018). Circuit Design Features of a Stable Two-Cell System. Cell, 172(4), 744-757.e17. https://doi.org/10.1016/j.cell.2018.01.015

Zhou, Y., Zhang, Y.-X., Yang, K.-L., Liu, Y.-L., Wu, F.-H., Gao, Y.-R., & Liu, W. (2022). Connexin 43 Mediated the Angiogenesis of Buyang Huanwu Decoction via Vascular Endothelial Growth Factor and Angiopoietin-1 after Ischemic Stroke. Chinese Journal of Physiology, 65(2), 72–79. https://doi.org/10.4103/cjp.cjp_94_21

Zhou, Z., Wang, H., Zhang, X., Song, M., Yao, S., Jiang, P., Liu, D., Wang, Z., Lv, H., Li, R., Hong, Y., Dai, J., Hu, Y., & Zhao, G. (2022). Defective autophagy contributes to endometrial epithelial-mesenchymal transition in intrauterine adhesions. Autophagy, 18(10), 2427–2442. https://doi.org/10.1080/15548627.2022.2038994

Zhu, M., Zou, Q., Huang, R., Li, Y., Xing, X., Fang, J., Ma, L., Li, L., Yang, X., & Yu, L. (2021). Lateral transfer of mRNA and protein by migrasomes modifies the recipient cells. Cell Research, 31(2), 237–240. https://doi.org/10.1038/s41422-020-00415-3

Zhu, Y., Chen, X., & Liao, Y. (2023). Mesenchymal Stem Cells-Derived Apoptotic Extracellular Vesicles (ApoEVs): Mechanism and Application in Tissue Regeneration. Stem Cells, 41(9), 837–849. https://doi.org/10.1093/stmcls/sxad046

Zhu, Y., Webster, M. J., Mendez Victoriano, G., Middleton, F. A., Massa, P. T., & Weickert, C. S. (2025). Molecular Evidence for Altered Angiogenesis in Neuroinflammation-Associated Schizophrenia and Bipolar Disorder Implicate an Abnormal Midbrain Blood-Brain Barrier. Schizophrenia Bulletin, 51(4), 1146–1161. https://doi.org/10.1093/schbul/sbae184

Zhuang, J., Chen, H., Gao, N., Sun, R., Xiao, C., Zeng, D., Yu, Z., Peng, J., & Xia, Y. (2023). CircUCK2 regulates HECTD1-mediated endothelial-mesenchymal transition inhibition by interacting with FUS and protects the blood-brain barrier in ischemic stroke. The Kaohsiung Journal of Medical Sciences, 39(1), 40–51. https://doi.org/10.1002/kjm2.12611

Zhuang, X., Cross, D., Heath, V. L., & Bicknell, R. (2011). Shear stress, tip cells and regulators of endothelial migration. Biochemical Society Transactions, 39(6), 1571–1575. https://doi.org/10.1042/BST20110746

Zimmer, O., & Goepferich, A. (2023). How clathrin-coated pits control nanoparticle avidity for cells. Nanoscale Horizons, 8(2), 256–269. https://doi.org/10.1039/D2NH00543C

Zlokovic, B. V. (2005). Neurovascular mechanisms of Alzheimer's neurodegeneration. Trends in Neurosciences, 28(4), 202–208. https://doi.org/10.1016/j.tins.2005.02.001

Zlokovic, B. V. (2008). The Blood-Brain Barrier in Health and Chronic Neurodegenerative Disorders. Neuron, 57(2), 178–201. https://doi.org/10.1016/j.neuron.2008.01.003

Zobel, K., Hansen, U., & Galla, H.-J. (2016). Blood-brain barrier properties in vitro depend on composition and assembly of endogenous extracellular matrices. Cell and Tissue Research, 365(2), 233–245. https://doi.org/10.1007/s00441-016-2397-7

Zong, H., Yu, W., Lai, H., Chen, B., Zhang, H., Zhao, J., Huang, S., & Li, Y. (2023). Extracellular vesicles long RNA profiling identifies abundant mRNA, circRNA and lncRNA in human bile as potential biomarkers for cancer diagnosis. Carcinogenesis, 44(8–9), 671–681. https://doi.org/10.1093/carcin/bgad063

Zong, P., Feng, J., Li, C. X., Jellison, E. R., Yue, Z., Miller, B., & Yue, L. (2024). Activation of endothelial TRPM2 exacerbates blood–brain barrier degradation in ischemic stroke. Cardiovascular Research, 120(2), 188–202. https://doi.org/10.1093/cvr/cvad126

Zou, L., Tian, Y., Wang, Y., Chen, D., Lu, X., Zeng, Z., Chen, Z., Lin, C., & Liang, Y. (2023). High-cholesterol diet promotes depression- and anxiety-like behaviors in mice by impact gut microbe and neuroinflammation. Journal of Affective Disorders, 327, 425–438. https://doi.org/10.1016/j.jad.2023.01.122

Appendix

Table of Contents

Chapter 3

The effect of astrocyte conditioned media on cell adhesion……..303

Chapter 4

Comparison of EV RNA isolated via ExtraPEG isolation using frozen vs non-frozen ACM ……..……..304

Chapter 6

Total RNA quality analysis of HBMvECs treated with control, EV_H, and EV_{INF} after isolation……305

Total RNA quality analysis of HBMvECs treated with control (A), EV_H (B), and EV_{INF} (C) after library preparation……..……..…306

Volcano plot of differential gene expression of HBMvECs treated with EV_H ….307

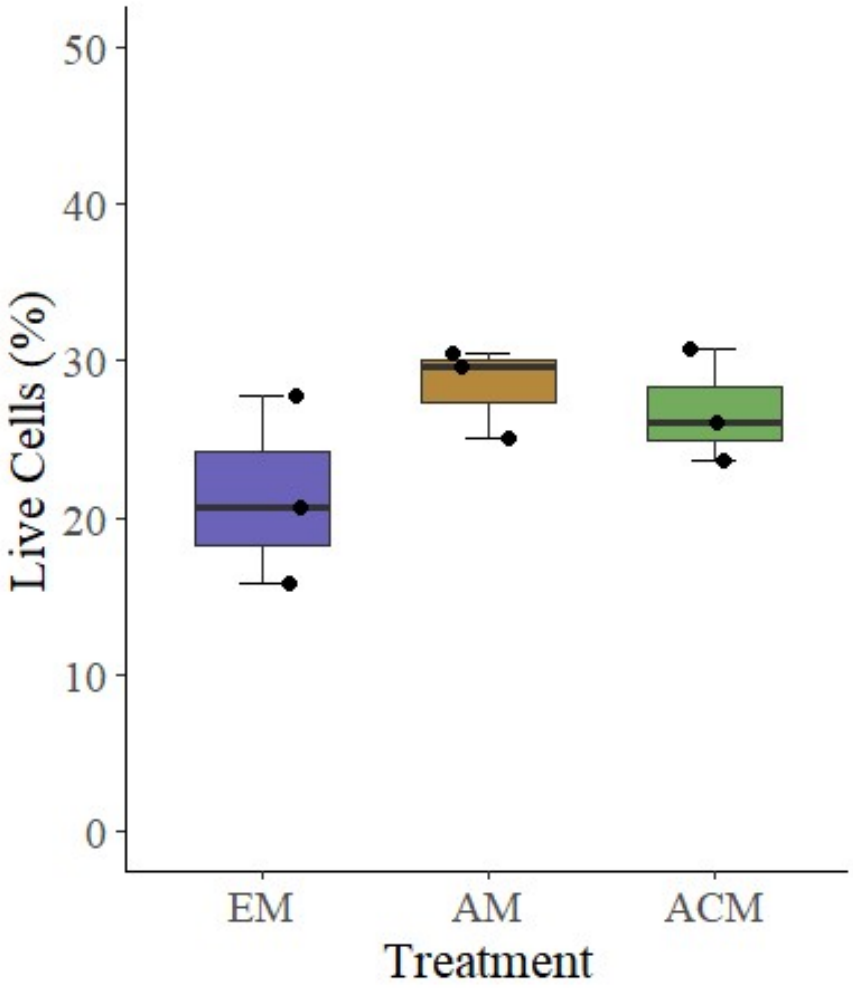


Figure A.1: ***The effect of astrocyte conditioned media on cell adhesion.*** *HBMvECs were seeded to confluency in 6-well transwells and treated basolaterally with undiluted AM and ACM for 48 hours. After this timepoint, the media in apical chamber was collected. 1 part 0.4% trypan blue was added 9 parts collected media. 10 μL of this solution was loaded onto a haemocytometer and the number of live cells (unstained) and dead cells (stained) were counted. The number of live cells is represented above as a percentage of total cells counted. Black dots signify individual data points. Results analysed via one-way ANOVA. p = 0.207.*

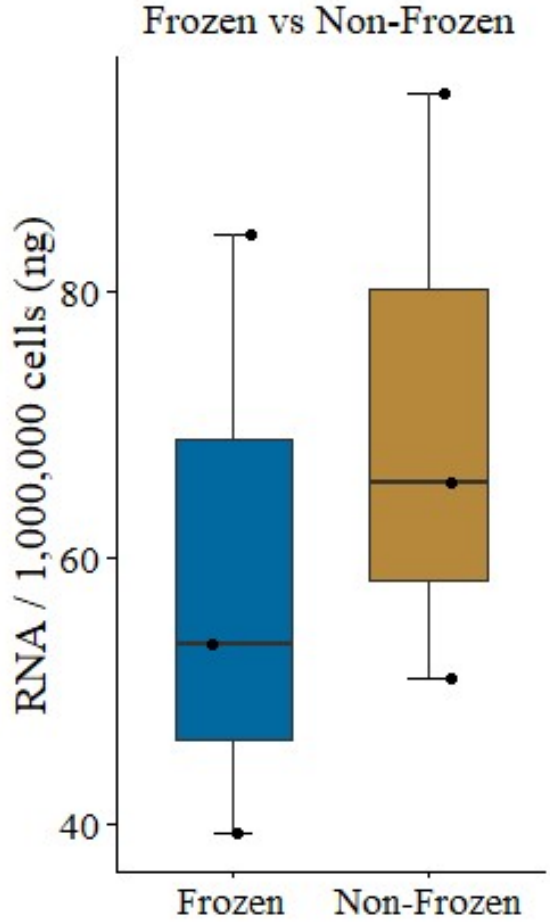


Figure A.*2*: *Comparison of EV RNA isolated via ExtraPEG isolation using frozen vs non-frozen ACM.* *Media conditioned on astrocytes for 48-72 hours was centrifuged at 1500 x g for 15 minutes immediately after collection. Some media was frozen previously and then thawed at room temperature before being processed ("Frozen" media). "Non-frozen" media was processed as described but not frozen before ExtraPEG isolation began. Frozen and non-frozen media was matched as close as possible to passage number and confluency before processing on the same day. Frozen media used was between 2 and 60 days old. RNA was isolated from the generated EV pellets and the The total amount of RNA isolated was normalised to RNA isolated per 1,000,000 cells. This was approximated using the confluency and the number of plates at the time of collection. Isolating EVs from frozen media resulted in a mean of 58.95 ± 22.37 ng per 1,000,000 cells. Non-frozen media resulted in a mean of 70.47 ± 23.04 ng of RNA isolated per 1,000,000 cells. Black dots signify individual data points. Analysis using Welch's Two Sample t-test revealed that there was no significant difference between EV RNA amount isolated from frozen media in comparison to non-frozen media (p = 0.568)*

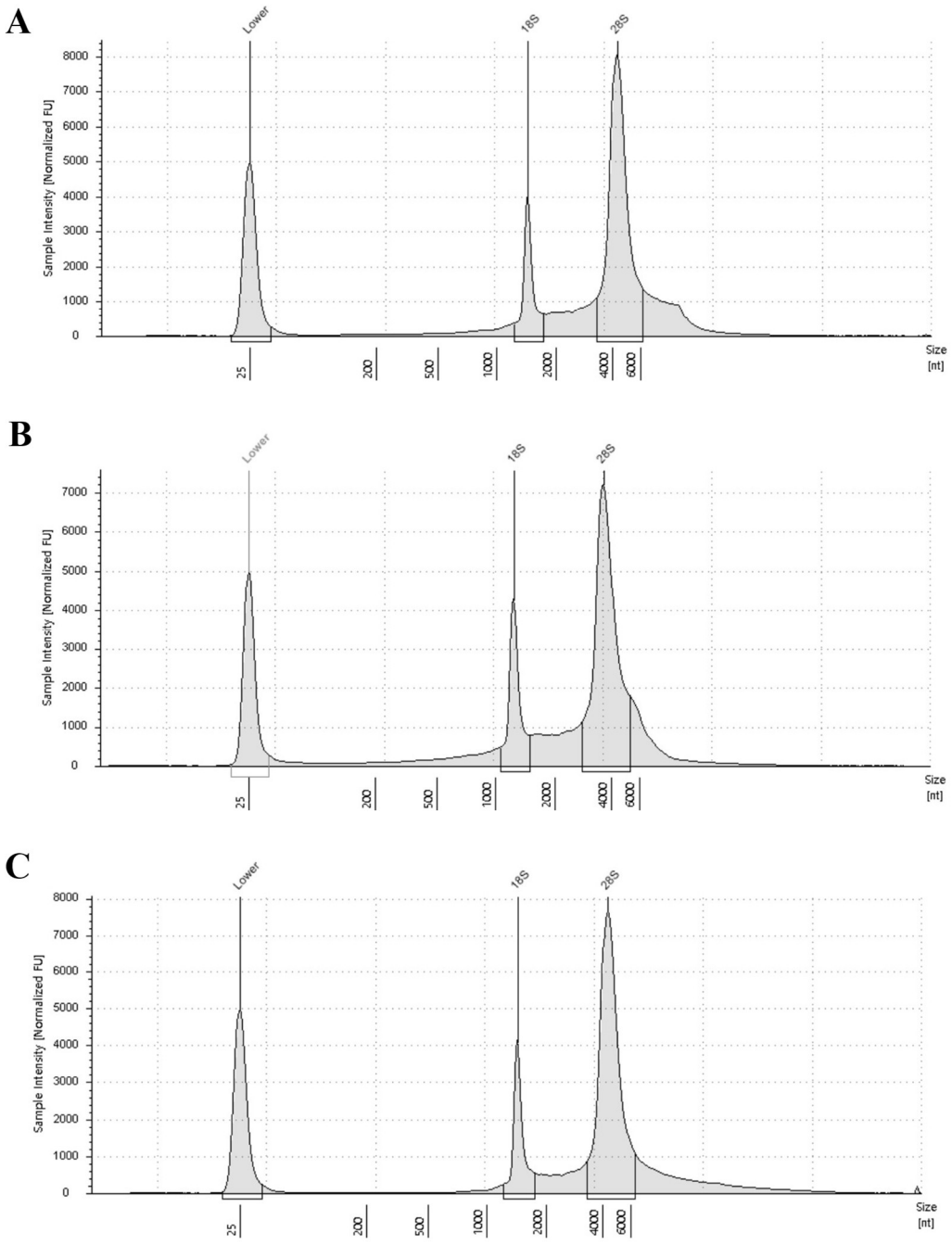


Figure A.3 ***Total RNA quality analysis of HBMvECs treated with control (A), EV_H (B), and EV_{INF} (C) after isolation*** *via BioAnalyser. Representative electropherograms and gel-like images from preparations using the RNA 6000 Pico Chip kit run on the 2100 BioAnalyzer Instrument by Macrogen. n = 2.*

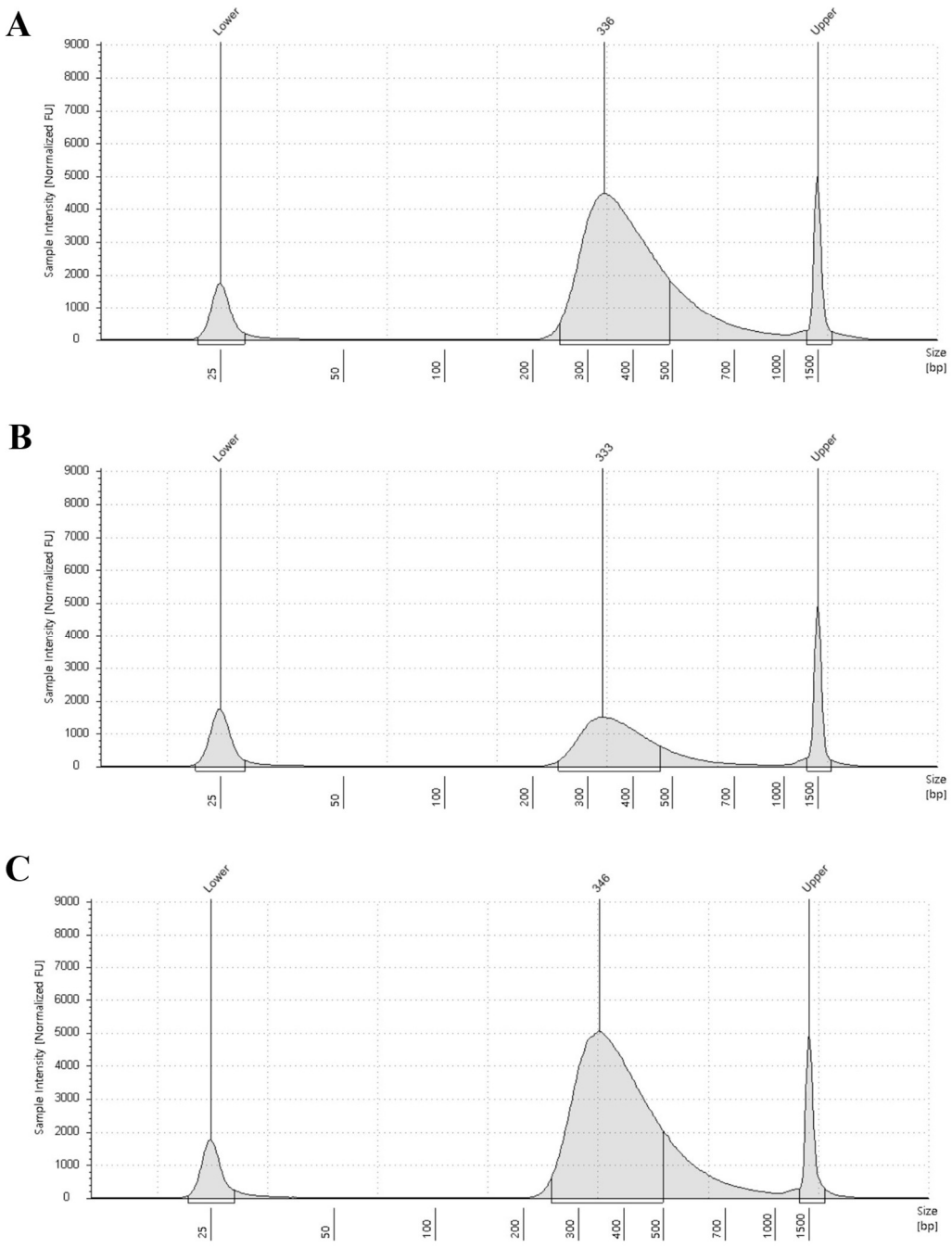


Figure A.4 ***Total RNA quality analysis of HBMvECs treated with control (A), EV_H (B), and EV_{INF} (C) after library preparation*** *via BioAnalyser. Representative electropherograms and gel-like images from preparations using the RNA 6000 Pico Chip kit run on the 2100 Bioanalyzer Instrument by Macrogen. n = 2.*

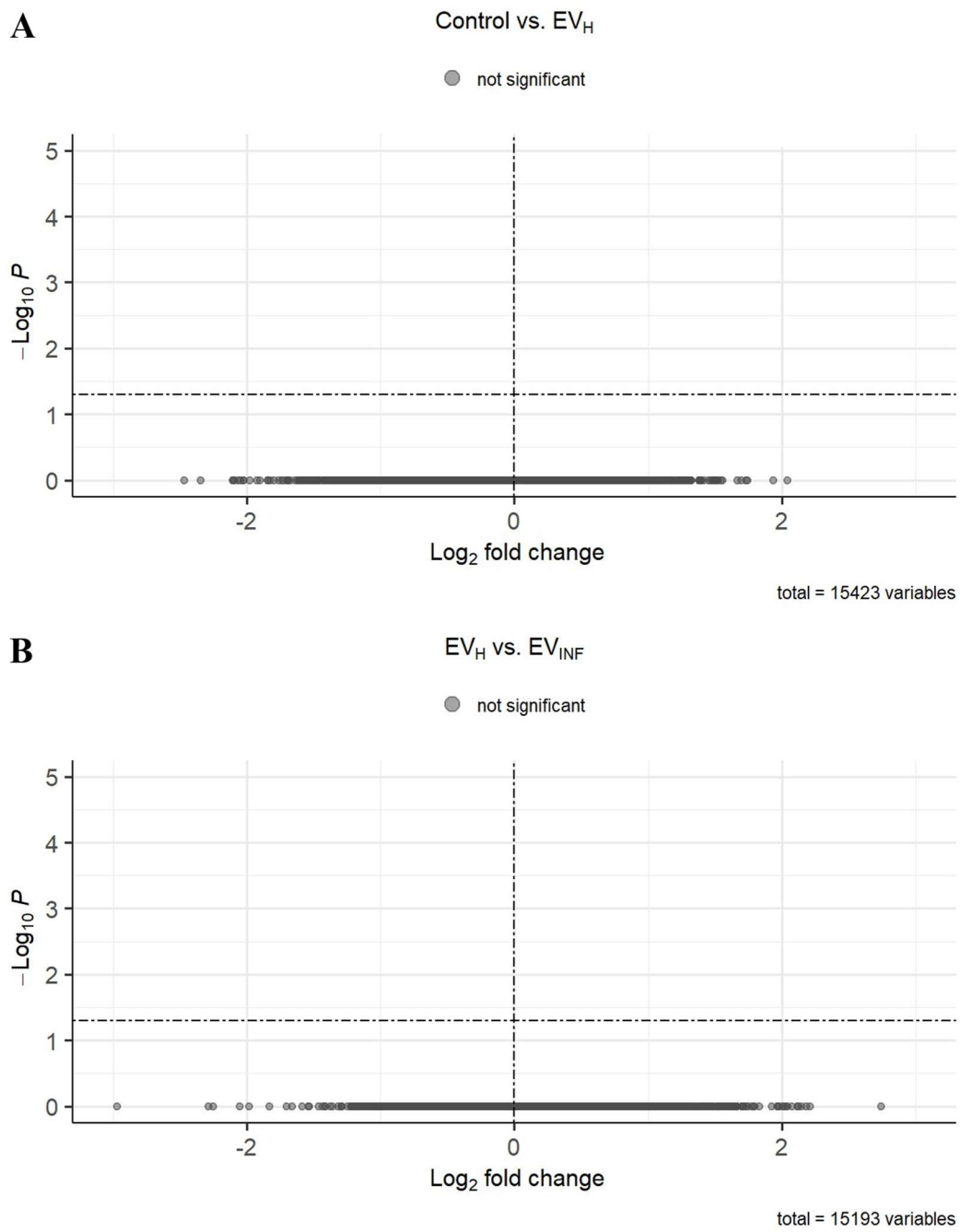


Figure A.5 ***Volcano plot of differential gene expression of HBMvECs treated with EV_H*** *vs control (A) and EV_H vs EV_{INF} (B). Each point represents the average value of one transcript in 2 replicate experiments. X-axis shows the log_2 fold change value. Y-axis shows the value of log_{10} (P value). The expression difference is considered significant for a non-zero log_2 fold change in gene expression (threshold denoted by vertical d*